IMMUNOTHERAPEUTIC AND IMMUNOPROPHYLACTIC STRATEGIES FOR INFECTIOUS DISEASES

EDITED BY: Giuseppe Andrea Sautto and Roberta Antonia Diotti
PUBLISHED IN: Frontiers in Immunology

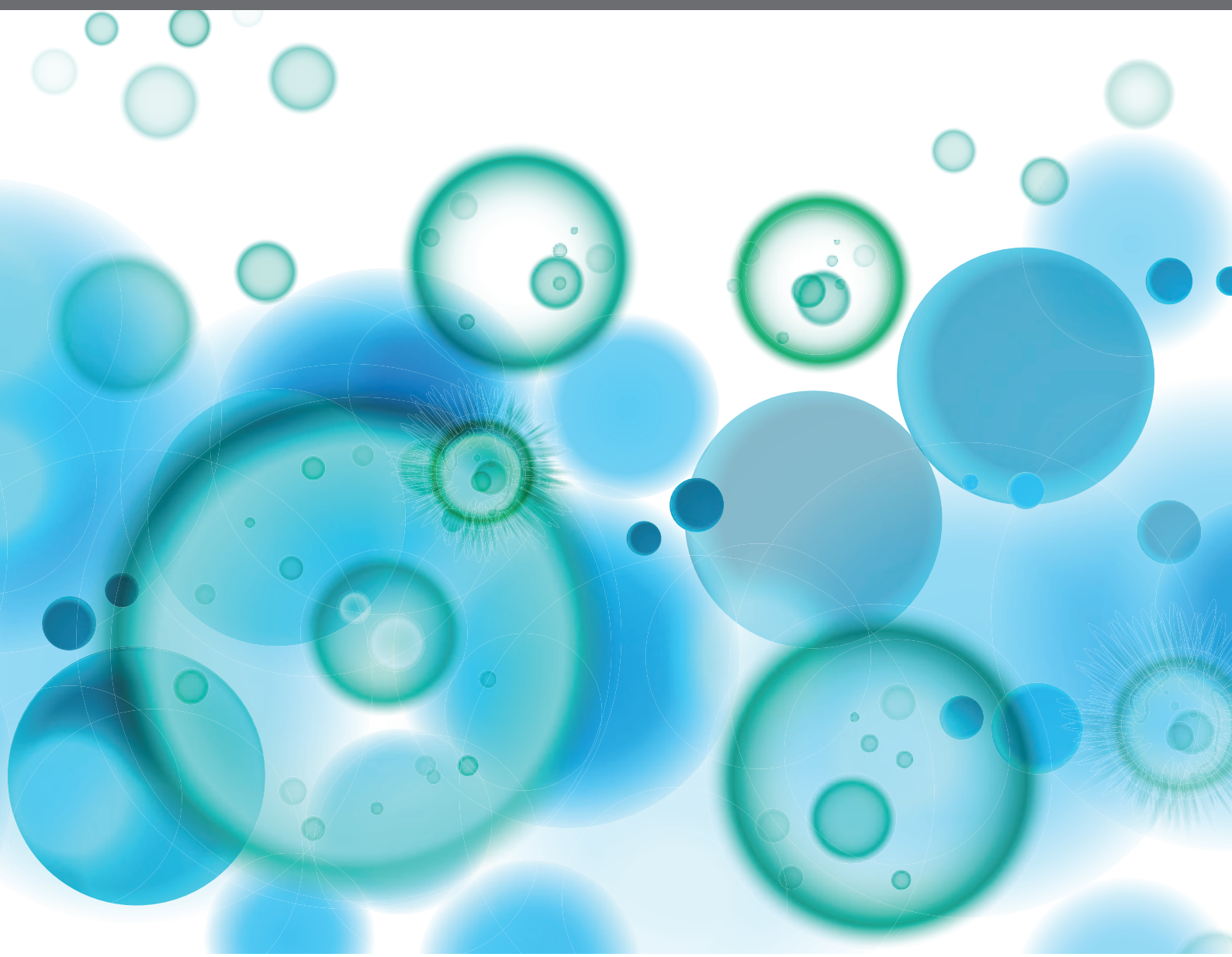

frontiers Research Topics

frontiers

ISSN 1664-8714
ISBN 978-2-88966-009-4
DOI 10.3389/978-2-88966-009-4

About Frontiers

Frontiers is more than just an open-access publisher of scholarly articles: it is a pioneering approach to the world of academia, radically improving the way scholarly research is managed. The grand vision of Frontiers is a world where all people have an equal opportunity to seek, share and generate knowledge. Frontiers provides immediate and permanent online open access to all its publications, but this alone is not enough to realize our grand goals.

Frontiers Journal Series

The Frontiers Journal Series is a multi-tier and interdisciplinary set of open-access, online journals, promising a paradigm shift from the current review, selection and dissemination processes in academic publishing. All Frontiers journals are driven by researchers for researchers; therefore, they constitute a service to the scholarly community. At the same time, the Frontiers Journal Series operates on a revolutionary invention, the tiered publishing system, initially addressing specific communities of scholars, and gradually climbing up to broader public understanding, thus serving the interests of the lay society, too.

Dedication to Quality

Each Frontiers article is a landmark of the highest quality, thanks to genuinely collaborative interactions between authors and review editors, who include some of the world's best academicians. Research must be certified by peers before entering a stream of knowledge that may eventually reach the public - and shape society; therefore, Frontiers only applies the most rigorous and unbiased reviews.
Frontiers revolutionizes research publishing by freely delivering the most outstanding research, evaluated with no bias from both the academic and social point of view. By applying the most advanced information technologies, Frontiers is catapulting scholarly publishing into a new generation.

What are Frontiers Research Topics?

Frontiers Research Topics are very popular trademarks of the Frontiers Journals Series: they are collections of at least ten articles, all centered on a particular subject. With their unique mix of varied contributions from Original Research to Review Articles, Frontiers Research Topics unify the most influential researchers, the latest key findings and historical advances in a hot research area! Find out more on how to host your own Frontiers Research Topic or contribute to one as an author by contacting the Frontiers Editorial Office: researchtopics@frontiersin.org

IMMUNOTHERAPEUTIC AND IMMUNOPROPHYLACTIC STRATEGIES FOR INFECTIOUS DISEASES

Topic Editors:
Giuseppe Andrea Sautto, University of Georgia, United States
Roberta Antonia Diotti, Vita-Salute San Raffaele University, Italy

Roberta Antonia Diotti is a staff scientist of Pomona ricerca s.r.l., a company involved in the development and pre-clinical evaluation of monoclonal antibodies.

Citation: Sautto, G. A., Diotti, R. A., eds. (2020). Immunotherapeutic and Immunoprophylactic Strategies for Infectious Diseases. Lausanne: Frontiers Media SA. doi: 10.3389/978-2-88966-009-4

Table of Contents

frontiers in Immunology

EDITORIAL
published: 28 July 2020
doi: 10.3389/fimmu.2020.01670

Editorial: Immunotherapeutic and Immunoprophylactic Strategies for Infectious Diseases

Giuseppe A. Sautto[1]* *and Roberta A. Diotti*[2]

[1] *Center for Vaccines and Immunology, University of Georgia, Athens, GA, United States,* [2] *Microbiology and Virology Unit, "Vita-Salute San Raffaele" University, Milan, Italy*

Keywords: infectious diseases, vaccines, antiviral drugs, monoclonal antibodies, chimeric antigen receptor (CAR)

Editorial on the Research Topic

Immunotherapeutic and Immunoprophylactic Strategies for Infectious Diseases

The necessity of a rapid development of effective therapeutic and prophylactic strategies for infectious diseases has recently gained further attention and importance due to the very recent SARS-CoV-2 pandemic (1). In fact, these countermeasures are of pivotal importance not only and principally for reducing the associated diseases, deaths, and overload of hospitalized patients during the pandemic outbreak, but also in limiting the tremendous impact on the economy and the society.

It is also important to highlight the fact that while COVID-19 is nowadays a central health issue attracting the attention of a significant portion of the scientific community as well as enormous financial aids, other infectious diseases still represent a global burden for the world population. As an example, influenza cases are still characterized by high morbidity (30–50 million cases yearly) and mortality rates. Approximately 3 to 5 million of these cases are characterized by a severe illness and about 290,000 to 650,000 respiratory deaths are reported annually, according to the World Health Organization (WHO). Additionally, the possibility of new influenza pandemic outbreaks aggravating these case numbers still represents a considerable risk.

In this regard, implementing current vaccination strategies, such as in the case of the current Yellow Fever vaccine as described in a paper of this article collection by Campi-Azevedo et al, and designing and developing next-generation vaccines, especially for high-risk populations, like in the case of influenza (Mathew and Angeletti), represent an important goal for the investigators working in this field not only to limit the related diseases but also to alleviate the associated economic burdens.

Importantly, novel immunotherapeutic strategies are also pivotal to reduce the severity and improve the current drug arsenal to combat influenza infections (De Vlieger et al.), which is currently limited to only two main approved antiviral drug categories: the neuraminidase and the M2 ion channel inhibitors.

In addition to influenza, other respiratory pathogens, such as bacteria and viruses, are responsible for a considerable number of infection cases, especially in more vulnerable subjects, such as children, the elderly, and immunocompromised individuals. Among these pathogens, pneumoviruses represent the leading cause of viral bronchiolitis and viral pneumonia in infants and children that can also result in a fatal outcome. It is thus important to improve our knowledge of the molecular mechanisms leading to a successful immune response, such as the studies aimed at dissecting the antibody response to the main pneumovirus surface fusion proteins (Huang et al.). Furthermore, a comprehensive understanding of the immunomodulatory properties exerted by bacterial pathogens, such as *Mycobacterium tuberculosis* (MTB) and *Bordetella* spp., could help in designing and developing more effective therapeutic and prophylactic strategies aimed at

OPEN ACCESS

Edited and reviewed by:
Denise L. Doolan, James Cook University, Australia

***Correspondence:**
Giuseppe A. Sautto
gasautto@uga.edu

Specialty section:
This article was submitted to Vaccines and Molecular Therapeutics, a section of the journal Frontiers in Immunology

Received: *29 May 2020*
Accepted: *22 June 2020*
Published: *28 July 2020*

Citation:
Sautto GA and Diotti RA (2020) Editorial: Immunotherapeutic and Immunoprophylactic Strategies for Infectious Diseases. Front. Immunol. 11:1670. doi: 10.3389/fimmu.2020.01670

eliciting an effective immune response (Gestal et al.). In particular, these studies are also crucial for developing alternative immunotherapeutic strategies as well as for the design of effective vaccines not only for infectious diseases but also for other disorders, such as autoimmune diseases (Takaya et al.).

As far as bacterial respiratory infections, MTB is certainly one of the most diffused respiratory pathogens worldwide, representing one of the top 10 causes of death and the leading cause from a single infectious agent, according to WHO. Developing new therapeutic strategies to overcome the occurrence of multidrug-resistant strains as well as effective vaccines able to prevent and limit the progression of the lung pathology in infected patients, represents a top health priority worldwide, especially for developing countries. As an example, monoclonal antibodies (mAbs) represent a valid immunotherapeutic approach to target multidrug resistant pathogens (2). Importantly, in recent years, the mAb discovery field has encountered an outstanding renovation and innovative development, mainly thanks to the advancement and improvement of next-generation sequencing (NGS) approaches at the single-cell level. In this regard, the "omics" technologies, employing large genomic, transcriptomic, structural, and proteomic datasets and the interpretation of them under a systems biology paradigm (Martín-Galiano and McConnell), allow for the rational identification of rare mAbs along with the deconvolution of their functional profile (3). Importantly, besides the direct use of mAbs as therapeutics, or as recently proposed, as prophylactic molecules to prevent infection in a determined period time, such as during influenza seasons, they can also be utilized as a tool or engineered for the development of prophylactic or cell-mediated anti-infective strategies, respectively (4). In this regard, the success of chimeric antigen receptor (CAR) T cell therapy for the treatment of difficult to eradicate cancers has inspired researchers to develop CARs for the treatment of infectious diseases as a potential therapeutic option for patients who are unresponsive to standard treatments (Seif et al.).

Different prophylactic strategies are currently under development and targeting different antigens expressed at different stages of bacterial (e.g., MTB) (Kwon et al.) as well as parasitic pathogens (e.g., *Plasmodium* and *Trichinella* spp.) (Stachyra et al.). In this regard, a lot of currently under development prophylactic strategies are also designed not only for prevention purposes but have also been proposed as therapeutic vaccines aimed at boosting or eliciting a *de novo* immune response to eradicate or mitigate infections. In this context, vaccines for human papillomavirus (HPV) have been described to be possibly effective also in the treatment of HPV-related lesions and relapse (Garbuglia et al.).

Additionally, developing novel immunotherapeutic and immunoprophylactic approaches that can be possibly delivered at the site of inflammation (Qin et al.; Zhang et al.) or infection, such as through inhalation or oral administration, improving their bioavailability and efficacy characteristics, represent a valid and desirable strategy for respiratory infections, including MTB (Sécher et al.).

As shown in the review and research articles of this collection, as well as in the recent literature, thanks to the new technologies and rapid scientific advancements it is now possible to expedite the research of innovative prophylactic and therapeutic countermeasures, possibly reducing the time of their approval in the clinical practice. This is certainly true in an emergency setting, like in the course of a pandemic event, but it could be applicable in the near future, where personalized, more effective, specific and rapid interventions will be employed in the clinical routine.

AUTHOR CONTRIBUTIONS

All authors listed have made a substantial, direct and intellectual contribution to the work, and approved it for publication.

ACKNOWLEDGMENTS

We wish to convey our appreciation to all the authors who have participated in this Research Topic and the reviewers for their insightful comments.

REFERENCES

1. Cohen J. The race is on for antibodies that stop the new coronavirus. *Science*. (2020) 368:564–5. doi: 10.1126/science.368.6491.564
2. Andreano E, Seubert A, Rappuoli R. Human monoclonal antibodies for discovery, therapy, and vaccine acceleration. *Curr Opin Immunol*. (2019) 59:130–4. doi: 10.1016/j.coi.2019.07.005
3. Setliff I, Shiakolas AR, Pilewski KA, Murji AA, Mapengo RE, Janowska K, et al. High-throughput mapping of B cell receptor sequences to antigen specificity. *Cell*. (2019) 179:1636–46 e15. doi: 10.1016/j.cell.2019.11.003
4. Mancini N, Marrone L, Clementi N, Sautto GA, Clementi M, Burioni R. Adoptive T-cell therapy in the treatment of viral and opportunistic fungal infections. *Future Microbiol*. (2015) 10:665–82. doi: 10.2217/fmb.14.122

Conflict of Interest: The authors declare that the research was conducted in the absence of any commercial or financial relationships that could be construed as a potential conflict of interest.

frontiers in Immunology

ORIGINAL RESEARCH
published: 06 August 2019
doi: 10.3389/fimmu.2019.01841

Design and Development of a Novel Peptide for Treating Intestinal Inflammation

Lulu Zhang[1], Xubiao Wei[1], Rijun Zhang[1], Jim N. Petitte[2], Dayong Si[1], Zhongxuan Li[1], Junhao Cheng[1] and Mengsi Du[1]*

[1] Laboratory of Feed Biotechnology, State Key Laboratory of Animal Nutrition, College of Animal Science and Technology, China Agricultural University, Beijing, China, [2] Prestage Department of Poultry Science, North Carolina State University, Raleigh, NC, United States

Intestinal inflammatory disorders, such as inflammatory bowel disease (IBD), are associated with increased pro-inflammatory cytokine secretion in the intestines. Furthermore, intestinal inflammation increases the risk of enteric cancer, which is a common malignancy globally. Native anti-inflammatory peptides are a class of anti-inflammatory agents that could be used in the treatment of several intestinal inflammation conditions. However, potential cytotoxicity, and poor anti-inflammatory activity have prevented their development as anti-inflammatory agents. Therefore, in this study, we designed and developed a novel hybrid peptide for the treatment of intestinal inflammation. Eight hybrid peptides were designed by combining the active centers of antimicrobial peptides, including LL-37 (13-36), YW12D, innate defense regulator 1, and cathelicidin 2 (1-13) with thymopentin or the active center of thymosin alpha 1 (Tα1) (17-24). The hybrid peptide, LL-37-Tα1 (LTA), had improved anti-inflammatory activity with minimal cytotoxicity. LTA was screened by molecule docking and *in vitro* experiments. Likewise, its anti-inflammatory effects and mechanisms were also evaluated using a lipopolysaccharide (LPS)-induced intestinal inflammation murine model. The results showed that LTA prevented LPS-induced impairment in the jejunum epithelium tissues and infiltration of leukocytes, which are both histological markers of inflammation. Additionally, LTA decreased the levels of tumor necrosis factor-alpha, interferon-gamma, interleukin-6, and interleukin-1β. LTA increased the expression of zonula occludens-1 and occludin, and reduced permeability and apoptosis in the jejunum of LPS-treated mice. Additionally, its anti-inflammatory effect is associated with neutralizing LPS, binding to the Toll-like receptor 4-myeloid differentiation factor 2 (TLR4/MD-2) complex, and modulating the nuclear factor-kappa B signal transduction pathway. The findings of this study suggest that LTA may be an effective therapeutic agent in the treatment of intestinal inflammation.

Keywords: anti-inflammatory activity, toll-like receptor, molecular dynamics simulation, lipopolysaccharide neutralization, intestinal barrier, NF-κB

OPEN ACCESS

Edited by:
Giuseppe Andrea Sautto, University of Georgia, United States

Reviewed by:
Alejandra Gonzalez Loyola, Université de Lausanne, Switzerland
Wayne Robert Thomas, Telethon Kids Institute, Australia

***Correspondence:**
Rijun Zhang
rjzhang@cau.edu.cn

Specialty section:
This article was submitted to Vaccines and Molecular Therapeutics, a section of the journal Frontiers in Immunology

Received: *11 May 2019*
Accepted: *22 July 2019*
Published: *06 August 2019*

Citation:
Zhang L, Wei X, Zhang R, Petitte JN, Si D, Li Z, Cheng J and Du M (2019) Design and Development of a Novel Peptide for Treating Intestinal Inflammation. Front. Immunol. 10:1841. doi: 10.3389/fimmu.2019.01841

INTRODUCTION

Intestinal inflammation is a defensive response against infections and damage caused by microbiological toxins or noxious substances (1). Clinical symptoms of intestinal inflammation include abdominal pain, diarrhea, rectal bleeding, weight loss, malnutrition, and fever (2). Furthermore, intestinal patients, such as those with inflammatory bowel disease (IBD), have an increased risk of developing colorectal and small intestinal cancers (3–5). The mechanisms of intestinal inflammation as well as its progression to intestinal cancer have been extensively studied, focusing on dysregulation within the immune response and breakdown of the mucosal barrier (6).

Intestinal inflammation is treated with corticosteroids, specifically glucocorticoids (7, 8). This treatment can successfully decrease the production of pro-inflammatory cytokines and chemokines, cell adhesion molecules, and other key mediators of inflammation (9); however, prolonged use of corticosteroids is related to side effects, including impaired wound healing, mild hirsutism, linear growth inhibition, myopathy, osteoporosis, osteonecrosis, peptic ulcers, pancreatitis, and candidiasis (10, 11). Therefore, there is a need to identify and develop new drugs that have both the desired efficiency and improved safety.

In recent years, antimicrobial peptides (AMPs) have been reported to have anti-inflammatory effects (12–14). AMPs can not only directly interact with lipopolysaccharide (LPS) to inhibit the release of inflammatory cytokines (15, 16), but can also inhibit the translocation of nuclear factor-kappa B (NF-κB) to dampen the inflammatory response (13). As a result, AMPs are especially appealing candidates for the treatment of inflammatory disorders. LL-37 and YW12D effectively neutralize LPS; consequently, they have considerable potential for the treatment of LPS-induced inflammation (15, 17, 18). Cathelicidin 2 (CATH-2), a highly cationic (11^+) chicken heterophil-derived peptide, inhibits IL-1β, and nitric oxide production in LPS-induced HD11 cells (19). Innate defense regulator (IDR)-1, one type of synthetic innate defense regulators, has protective activity against LPS-induced inflammation mediated by modulating NF-κB and mitogen-activated protein kinase (MAPK) signaling pathways (13, 20). Based on their previous anti-inflammatory activity observed, LL-37, IDR-1, CATH2, and YW12D were selected for further study.

Thymopentin (TP5) is a synthetic peptide consisting of five amino acid residues (21), and thymosin alpha 1 (Tα1) is a 28-amino acid peptide produced by thymic stromal cells (22, 23). Both TP5 and Tα1 exhibit similar immunoregulatory activity. They play an important role in regulating immunity, tolerance, and inflammation (24–26). TP5 and Tα1 exert their immune-modulating effect by interacting with Toll-like receptors (TLRs) and intracellular signaling pathways, such as NF-κB, MAPK, and myeloid differentiation primary response 88 (MyD88) pathways (27–29) Additionally, TP5 and Tα1 can counteract a pro-inflammatory cytokine storm and autoimmunity (24, 30, 31). Overall, TP5 and Tα1 exhibit immunoregulatory activity and low cytotoxicity (30, 32). Thus, they are commonly used in the clinic to treat various types of inflammatory diseases, such as cancer and infectious disease (21, 24, 33, 34).

The development of AMPs as potential anti-inflammatory drugs has faced several obstacles that are mainly attributed to their significant cytotoxicity toward eukaryotic cells, hampering their clinical development (19, 35, 36). In contrast, TP5 and Tα1 exhibit low cytotoxicity but relatively weak anti-inflammatory activity (30, 32). To improve the anti-inflammatory activity and reduce undesirable cytotoxic effects of native peptides, hybridization has been put forward. Hybridization is a simple and effective strategy for developing novel therapeutic peptides that combines the advantages of different native peptides (37). It has been reported that LL-37 (13-36) and CATH2 (1-13), which are the short peptides derived from native AMP, can effectively attenuate antigen- and pathogen-induced inflammation (19, 38, 39). Tα1 (17-24) also exhibited good immunoregulatory activity (40, 41). Thus, in the present study, we designed eight hybrid peptides by combining AMPs, including YW12D and IDR-1, or the active center of AMPs, including LL-37 (13-36) and CATH2 (1-13) with TP5 or the active center of Tα1 (17-24). The hybrid peptides were evaluated based on their anti-inflammatory activity and cytotoxicity. The best hybrid, based on these criteria, was screened by molecule docking and *in vitro* experiments. Likewise, its anti-inflammatory effect and mechanism were also evaluated using an LPS-induced murine model of intestinal inflammation.

Abbreviations: AMPs, antimicrobial peptides; IDR, innate defense regulator; CATH2, cathelicidin 2; TP5, Thymopentin; Tα1, Thymosin alpha 1; LPS, lipopolysaccharide; LTA, LL-37-Tα1; TNF-α, tumor necrosis factor-alpha; IFN-γ, interferon-gamma; IL-6, interleukin-6; TLR4/MD-2, Toll-like receptor 4/myeloid differentiation factor 2; NF-κB, nuclear factor-kappa B; IBD, inflammatory bowel diseases; UJ, ulcerative jejunitis; TLRs, Toll-like receptors; MAPK, mitogen-activated protein kinase; MyD88, myeloid differentiation primary response 88; LTP, LL-37-TP5; YTP, YW12D-TP5; YTA, YW12D-Tα1; ITP, IDR-1-TP5; ITA, IDR-1-Tα1; CTP, CATH2-TP5; CTA, CATH2-Tα1; DMEM, Dulbecco's modified Eagle's medium; FBS, fetal bovine serum; CCK-8, Cell Counting Kit-8; SPF, specific pathogen free; PMB, Polymyxin B; H&E, hematoxylin-eosin; HRP, horse-radish peroxidase; DAB, 3, 3′diaminobenzidine; DAPI, 4,6-diamidino-2-phenylindole; TUNEL, deoxynucleotidyl transferase mediated dUTP nick end labeling; PPs, Peyer's patches; TEM, Transmission electron microscopy; TJ, tight junctions; TEER, transepithelial electrical resistance; PD, potential difference; Isc, short-circuit current; RT, total electrical resistance; MPO, myeloperoxidase; ZO-1, zonula occluden-1; CE TAL, Chromogenic End-point Tachypleus Amebocyte Lysate; MD, Molecular Dynamics; NPT, number, pressure, and temperature; NVT, number, volume, and temperature; MM-PBSA, Poisson-Boltzmann accessible surface area; IBD, inflammatory bowel diseases.

MATERIALS AND METHODS

Hybrid Peptide Design

The hybrid peptides were constructed by combining the active center of LL-37, YW12D, IDR-1, and CATH2 with the TP5 or the active center of Tα1.The amino acid sequences of the parental and hybrid peptides are listed in the **Table 1**.

Sequence Analysis of Hybrid Peptides

The mean hydrophobicity was calculated online using ProParam (ExPASy Proteomics Server: http://www.expasy.org/tools/protparam.html). The 3D structures of hybrid peptides LL-37-TP5 (LTP), LL-37-Tα1 (LTA), YW12D-TP5 (YTP), YW12D-Tα1 (YTA), IDR-1-TP5 (ITP), IDR-1-Tα1 (ITA), CATH2-TP5 (CTP),

TABLE 1 | Key physicochemical parameters of parental and hybrid peptides.

Peptides	Sequence	H[a]
LL-37	LLGDFFRKSKEKIGKEFKRIVQRIKDFLRNLVPRTES	−0.559
YW12D	YVKLWRMIKFLR	0.167
IDR-1	KSRIVPAIPVSLL	1.046
CATH2	RWGRFLRKIRRFRPKVTITIQGSARF	−0.638
TP5	RKDVT	−1.608
Tα1	SDAAVDTSSEITTKDLKEKKEVVEEAEN	−1.029
LTP	IGKEFKRIVQRIKDFLRNLVPRTERKDVT	−0.8
LTA	IGKEFKRIVQRIKDFLRNLVPRTEKEKKEVVE	−0.894
YTP	YVKLWRMIKFLRRKDVT	−0.376
YTA	YVKLWRMIKFLRKEKKEVVE	−0.59
ITP	KSRIVPAIPVSLLRKDVT	0.289
ITA	KSRIVPAIPVSLLKEKKEVVE	−0.09
CTP	RWGRFLRKIRRFRRKDVT	−1.61
CTA	RWGRFLRKIRRFRKEKKEVVE	−1.635

[a] *The mean hydrophobicity (H) is the total hydrophobicity (sum of all residue hydrophobicity indices) divided by the number of residues.*

and CATH2-Tα1 (CTA) were built using I-TASSER (http://zhanglab.ccmb.med.umich.edu/I-TASSER/).

Hybrid Peptides Scan by Molecule Docking

The constructed 3D structures of the hybrid peptides were then subjected to molecular docking. The initial structure for myeloid differentiation factor 2 (MD-2) was extracted from the crystal structure of the TLR4/MD-2 complex (PDB code: 2Z64). The initial MD-2/hybrid peptide complex was generated by ZDOCK3.0.2. For each hybrid peptide, a total of 3600 decoy structures were predicted through the rigid-binding option in ZDOCK; among these, the decoy with the lowest energy was chosen for the following flexible docking study. For each molecule, 100 docking runs were performed by flexpepdock (http://flexpepdock.furmanlab.cs.huji.ac.il/). The most plausible docking confirmation with the lowest score, which is calculated by the total Rosetta energy, was selected for scanning of the hybrid peptide.

Peptides Synthesis

The hybrid peptides, LTP, LTA, CTP, and YTP, which were selected via molecule docking, and their parental peptides, LL-37, CATH2, YW12D, TP5, and Tα1, were synthesized and purified by KangLong Biochemistry (Jiangsu, China). The purity of all peptides was higher than 95%, as determined by high performance liquid chromatography (HPLC) and mass spectrometry. The peptides were dissolved in endotoxin-free water and stored at −80°C.

Cell Culture

Mouse macrophage cell line (RAW264.7) was purchased from the Shanghai Cell Bank, the Institute of Cell Biology, China Academy of Sciences (Shanghai, China). The cells were cultured in Dulbecco's modified Eagle's medium (DMEM; Hyclone) supplemented with 10% (v/v) fetal bovine serum (FBS; Bioscience) and 1% (v/v) penicillin/streptomycin (Hyclone) at 37°C in a moist atmosphere (5% CO_2, 95% air).

Cell Viability Assay

The viability of peptide-treated RAW264.7 cells was determined using the Cell Counting Kit-8 (CCK-8) Assay Kit (Dojindo) (42). RAW264.7 cells were pre-seeded on a 96-well plate at a density of 3×10^4 cells/mL in 100 μL DMEM medium overnight. The cells were either treated with various concentrations of peptides or without peptides at 37°C and 5% CO_2 for 24 h. Each well was incubated with 10 μL CCK-8 solution for 4 h in the darkness. Then, the absorbance at 450 nm was measured using a microplate reader. Cell viability was calculated as:

$$Cell\ viability\ (\%) = (OD450\ (sample)/OD450(control)) \times 100\%$$

where $OD_{450(sample)}$ is the absorbance at 450 nm of the cells with peptides treated and $OD_{450(control)}$ is the absorbance at 450 nm of the cells without peptides treated.

Animal Model

Seventy-two C57/BL6 male mice (6–8 weeks of age) were purchased from Charles River (Beijing, China). Mice were maintained in a specific pathogen free (SPF) environment at 22 ± 1°C with relative 55 ± 10% humidity, and the assays were performed in conformity with the laws and regulations for live animal treatment at China Agricultural University.

The mice were randomly distributed into six groups ($n = 12$ each): control, LPS (*E. coli*, O111:B4, Sigma-Aldrich, USA) treatment, LL-37 pretreatment followed by LPS treatment (LL-37 + LPS), Tα1 pretreatment followed by LPS treatment (Tα1 + LPS), LTA pretreatment followed by LPS treatment (LTA + LPS). Different peptides (10 mg/kg mouse weight) were injected intraperitoneally once daily for 7 days, whereas an equal volume of sterile saline was injected intraperitoneally to the control and LPS-treated groups. On day 7, mice in LPS, LL-37 + LPS, Tα1 + LPS, and LTA + LPS groups were intraperitoneally injected with LPS (10 mg/kg mouse weight) 1h after saline or the peptides treatment, and the control group was intraperitoneally injected with an equal volume of saline. The mice were then euthanized by cervical dislocation 6 h after intraperitoneal injection of LPS or saline, and samples of the intestines were collected for analysis. The body weights of the mice were recorded before and after the experiment.

Histopathology and Immunohistochemistry

Intestinal tissues samples from the jejunum were fixed in 4% paraformaldehyde immediately after the mice were euthanized. After embedding, the tissues were sectioned (5 μm) using an RM2235 microtome (Leica) and stained with hematoxylin-eosin (H&E). Images were acquired using a DM3000 microscope. LPS-induced intestinal injury was evaluated using Chiu's score (43) according to changes of the villus and glands of the jejunal mucosa. Villus height and crypt depth were measured using CaseViewer software.

For immunohistochemical analysis of $CD177^+$, nonspecific binding sites were blocked with PBS containing 1% w/v BSA for 1 h. Anti-$CD177^+$ antibodies (Santa, USA) were added at

a dilution of 1:100 and incubated overnight at 4°C. Samples were washed five times in PBS and treated with horse-radish peroxidase (HRP)-conjugated rabbit anti-goat IgG (JIR, USA) at ratio of 1:100; samples were left to incubate at 4°C for 1 h. After washing with PBS, 3,3′-diaminobenzidine (DAB; DAKO, USA) was added, and the slides were counterstained with Harris hematoxylin. Finally, the samples were dehydrated in an alcohol gradient (70–100%), and cleared in xylene. All slides were mounted in neutral balsam.

The apoptotic cells in the jejunal sections were detected via a commercial the terminal deoxynucleotidyl transferase mediated dUTP nick end labeling (TUNEL) staining kit according to the manufacturer's instruction (Roche, Indianapolis, IN, USA). The sections were co-stained with the DAPI (Servicebio, Wuhan, China). The number of apoptotic cells was counted in four to six randomly selected fields at 200× magnification.

Transmission Electron Microscopy (TEM)

The tight junctions (TJs) between gut epithelial cells were observed by TEM. A jejunum specimen was excised with a scalpel and fixed in 2.5% glutaraldehyde for 4 h at 4°C. Afterwards, the specimens were treated with osmic acid and embedded in epon. Ultrathin sections were acquired using a diamond knife, and stained with uranyl acetate and lead citrate before visualization by TEM (Model H-7650, HITACHI, Japan).

Measurement of Transepithelial Electrical Resistance (TEER)

The TEER values of intestinal membranes were assessed by an *in vitro* diffusion chamber method using stripped mouse jejunal membranes. The underlying muscularis of the jejunal membranes were removed, and the jejunal segments were mounted in a diffusion chamber with an exposed surface area of 1.78 cm^2. Ussing chambers were equipped with two pairs of electrodes connected to the chambers by 3 M KCl/3.5% agar bridges. Each side of the chamber was bubbled with a mixture of 5% CO_2 and 95% O_2 to maintain the viability of the jejunal membranes. The temperature was maintained at 37°C during the experiment by a circulating water bath. The potential difference (PD) and the short-circuit current (Isc) were measured, and then, total electrical resistance (RT) was calculated by Ohm's law, that is RT = PD/Isc (44).

ELISA

RAW264.7 cells were treated with or without 10 μg/mL peptides for 1h before the addition of 100 ng/mL LPS and further incubation for 12 h at 37°C. Levels of tumor necrosis factor-alpha (TNF-α), interleukin-6 (IL-6), and IL-1β were detected in culture supernatant and jejunum, respectively. In addition, the level of interferon-gamma (IFN-γ) was detected in the jejunum. ELISA was performed using a commercial ELISA kit (eBioscience, San Diego, USA).

The activities of myeloperoxidase (MPO) in the jejunum were detected using ELISA kits (Boster Wuhan, China) according to the manufacturer's instructions.

Western Blotting

Whole protein of intestinal tissues was obtained with the whole protein extraction kit (KeyGEN Biotech, Nanjing, China) according to the manufacturer's instructions. The protein concentration was measured via the BCA kit (KeyGEN Biotech, Nanjing, China). Protein samples (40 μg protein/lane) were separated by 10% sodium dodecyl sulfate-polyacrylamide gel electrophoresis (SDS-PAGE) and transferred to polyvinylidene difluoride (PVDF) membranes (Bio-Rad). The membranes were blocked with 5% nonfat dried milk in 0.05% TBST and immunoblotted with primary specific antibodies against inhibitor of κB (IκB)-α, p-IκB-α, IκB kinase (IKK)-β, p-IKK-β, NF-κB (p65), p-NF-κB (p-p65), zonula occluden-1 (ZO-1), occludin, and β-actin (Santa Cruz, CA, USA). After washing with TBST, membranes were incubated with anti-mouse/rabbit HRP-conjugated secondary antibodies (HuaAn, Hangzhou China). The proteins were detected with SuperSignal West Femto maximum sensitivity substrate (Pierce Biotechnology) and

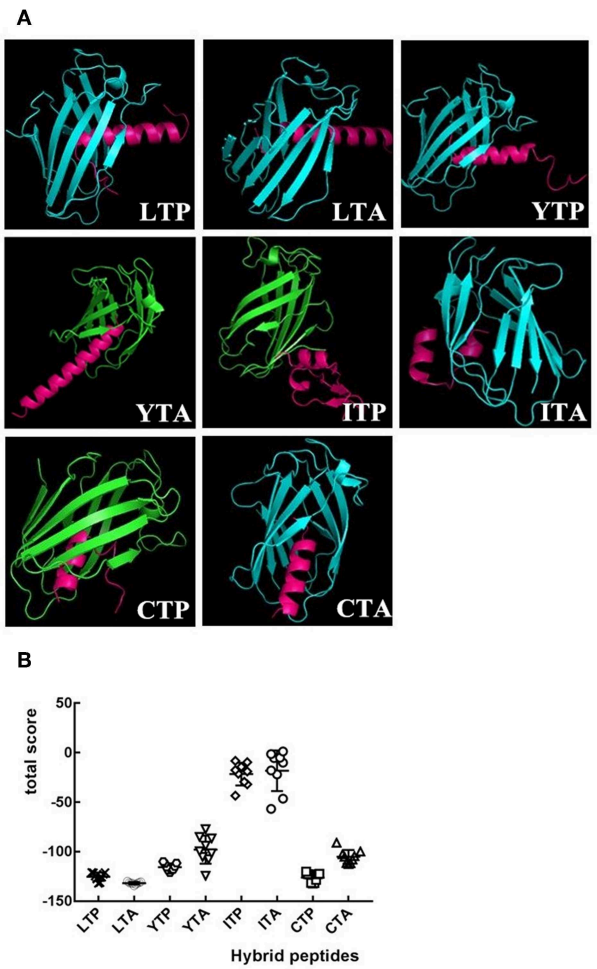

FIGURE 1 | The overall structure of hybrid peptide-MD-2 Complex. **(A)** Shows the views of the hybrid peptides (red) binding to MD-2 (blue or green). **(B)** An energy plot with 10 out of 100 decoy structures from an MD-2 docking study by Flexpepdock. Data are given as mean values ± standard.

visualized using a ChemiDoc MP Imaging System (Bio-Rad, Hercules, CA, USA).

Neutralization of LPS

The neutralization of LPS by the peptides was assessed using a quantitative Chromogenic End-point Tachypleus Amebocyte Lysate (CE TAL) assay via the QCL-1000 kit (Xiamen, China). A constant concentration of LPS (1.0 EU/mL final concentration; *E. coli*, O111:B4, Sigma-Aldrich, USA) was incubated with various concentrations of the peptides or polymyxin B (PMB) (0–64 μg/mL final concentration; Sigma-Aldrich, USA) at 37°C for 15 min in the wells of pyrogenic sterile microliters plates. The 100 μL aliquots concentrate of limulus amebocyte lysate reagent was added and incubated at 37°C for 6 min. On the addition of chromogenic substrate, yellow color appeared. The reactions were stopped by adding 25% HCl, and then the absorbances measured at 540 nm (45).

The level of LPS in the plasma were detected using QCL-1000 kit (Xiamen, China) according to the manufacturer's instructions.

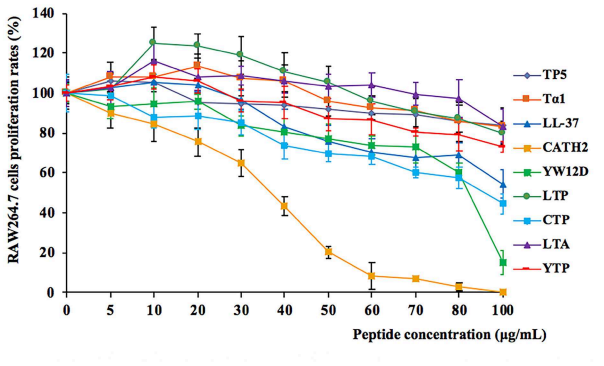

FIGURE 2 | Cell proliferation rates of RAW264.7 cells in the absence or presence of parental peptides and hybrid peptides. RAW264.7 cells were pre-seeded in DMEM medium overnight. The cells were treated with various concentrations of peptides or without peptides at 37°C and 5% CO_2 for 24 h. They were incubated with CCK-8 solution for 4 h, and then, they were measured at 450 nm. Data are given as mean values ± standard deviation from 8 biological replicates.

Molecular Dynamics Simulation

The crystallographic structure of the TLR4/MD-2 complex was taken from PDB bank (PDB code: 2Z64), and the initial structure for MD-2 was extracted from the crystal structure of the TLR4/MD-2 complex. The missing hydrogen atoms were added under pH 7.0 by Maestro (46). The docking pose was determined by RosettaDock (version 3.5), and the pose with the lowest score (total Rosetta energy for this model) was selected for further analysis.

The best binding pose of LTA with MD-2 was refined using a molecular dynamics (MD) simulation with AMBER14 (47, 48). The force fields used for the simulation were GAFF and FF14SB, and the system was solvated with TIP3P water molecules in a cubic box with a minimum distance of 10 Å between the protein

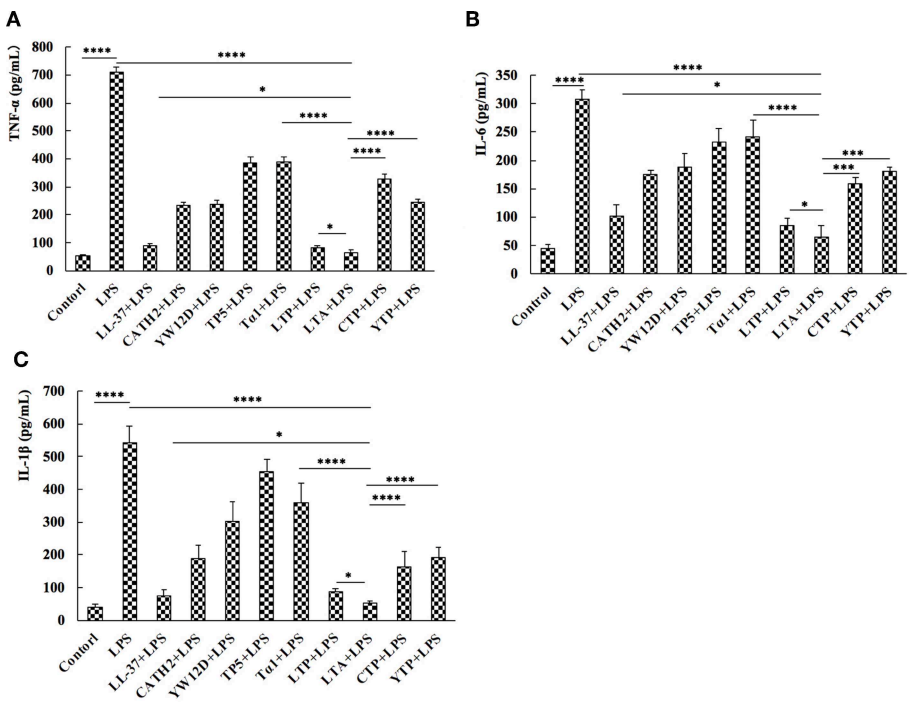

FIGURE 3 | Hybrid peptides suppress the LPS-induced cytokine secretion. 12 h after treatment with 100 ng/mL LPS in the presence or absence of peptides, protein levels of TNF-α **(A)**, IL-6 **(B)**, and IL-1β **(C)** in RAW264.7 cells were quantified by ELISA. Data are given as mean values ± standard deviation from 3 biological replicates. NS: $P > 0.05$, $^{*}P \leq 0.05$, $^{***}P \leq 0.001$, and $^{****}P \leq 0.0001$.

and the edge of the box. Na^+ and Cl^- atoms were added to mimic the physiological conditions and neutralize the system. The system was first minimized with 5000 steps by the conjugate gradient algorithm, following by heating gradually over 100 ps. Subsequently, the volume of the system was adjusted under a constant number, pressure, and temperature (NPT) ensemble. Afterwards, a 60 ns MD simulation was performed under constant number, volume, and temperature (NVT) ensemble.

Based on the 300 snapshots extracted from the last 40 ns of the equilibrated MD simulation, the long-range electrostatic interactions were calculated by the Particle-mesh Ewald (PME) method (49), and the binding energy was calculated by the molecular mechanics Poisson-Boltzmann accessible surface area (MM-PBSA) method (50).

Flow Cytometry

RAW264.7 cells were treated with PBS, anti-mouse mAbTLR4/MD-2 complex (MTS510 Ab) (eBioscience, San Diego, USA) or isotype control (IgG) (eBioscience, San Diego, USA) for 1 h at 4°C before staining with 10 μg/mL N-terminus fluorescein isothiocyanate (FITC)-labeled LTA. The cells were then harvested by trypsin and washed five times with PBS. The average FITC intensity of the cells was measured via flow cytometry.

Analysis of Confocal Laser-Scanning Microscopy

To verify TLR4/MD-2 as the pattern recognition receptor, RAW264.7 cells were treated with PBS, MTS510 Ab or isotype control (IgG) (eBioscience, San Diego, USA) for 1 h at 4°C. Afterwards, RAW264.7 cells were incubated with N-terminus FITC-LTA at 10 μg/mL for 1 h at 4°C in the dark. Then, the cells were washed with PBS, fixed with paraformaldehyde, and rinsed twice with PBS. The cell nuclei were stained with DAPI (diluted 1:500 in PBS) (Sigma, USA) for 5 min, and the cells were rinsed six times with PBS. The above cells were spread on a glass slide, fixed, and observed via a Leica TCA sp5 confocal microscope (Germany).

Statistics

All data are expressed as mean values ± standard deviation from at least 3 independent experiments. Statistical comparisons were carried out by Student's t test and ANOVA test with GraphPad Prism v6 software (La Jolla, California). Significance was claimed with P values ≤ 0.05. NS: $P > 0.05$, $^*P \leq 0.05$, $^{**}P \leq 0.01$, $^{***}P \leq 0.001$, and $^{****}P \leq 0.0001$.

RESULTS

Selection of Anti-inflammatory Peptides by Molecular Docking

As an initial screen of the anti-inflammatory peptides, the binding modes of the eight hybrid peptides to MD-2 were analyzed by molecular docking. As shown in **Figures 1A,B**, of the eight hybrid peptides, LTP, LTA, YTP, and CTP had more favorable docking scores to MD-2, and the total social of them was lower than −100.

Cytotoxicity on RAW264.7 Macrophage Cells

The cytotoxic activity of the peptides on RAW264.7 macrophage cells was evaluated by CCK-8 assay, and the results are shown in **Figure 2**. Among the initial selected hybrid peptides and their parental peptides, LTP, and LTA exhibited the lowest cytotoxic activity, and the cell viability of the lower doses LTP- and LTA-treated cells was greater than 100%. Meanwhile, all the selected hybrid peptides showed lower cytotoxicity than their parental peptides. The cell viability of the peptide-treated RAW264.7 cells was greater than 80%. These data indicated that at a concentration of 10 μg/mL, all of the peptides were minimally cytotoxic to RAW264.7 cells and suitable for the following experiments.

Inhibition of Cytokine Release From LPS-Stimulated RAW264.7 Cells

To evaluate the anti-inflammatory effect of the hybrid peptides, the mouse macrophage cell line, RAW264.7, was used as a model. ELISA results show that all parental peptides and hybrid peptides were potent inhibitors of pro-inflammatory cytokine release (**Figure 3**). LPS caused a significant elevation in TNF-α, IL-6, and IL-1β levels compared to untreated RAW264.7 cells. Compared to the other tested peptides, 10 μg/mL of LTA in the presence of LPS caused a remarkable decrease in the release of TNF-α (**Figure 3A**), IL-6 (**Figure 3B**), and IL-1β (**Figure 3C**). Collectively, these data suggest that LTA is suitable for further anti-inflammatory experiments.

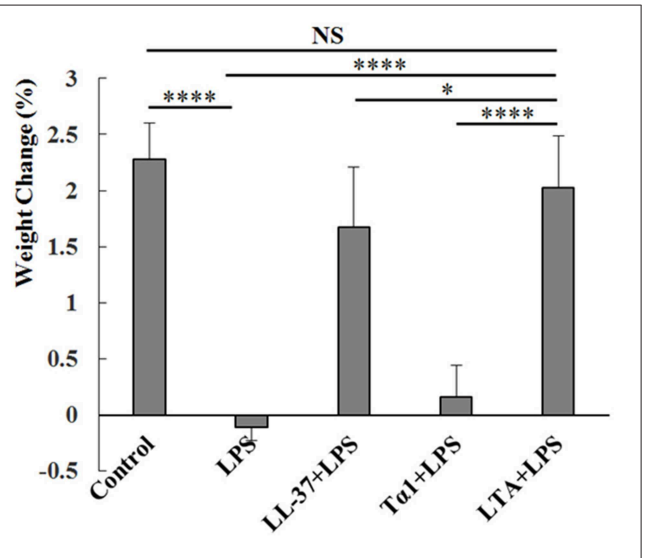

FIGURE 4 | Protective effects of LTA on body weight. Different peptides (10 mg/kg) were injected into the mice once daily for 6 days, whereas the control and LPS-treated groups were injected with an equal volume of sterile saline. On day 6, mice in the LPS and peptide-pretreated groups were injected with LPS (10 mg/kg) 1 h after the peptide or saline treatment. The control group was injected with an equal volume of saline. The body weights of the mice were recorded before and after the experiment. Data are given as mean values ± standard deviation from 12 biological replicates. NS: $P > 0.05$, $^*P \leq 0.05$, and $^{****}P \leq 0.0001$.

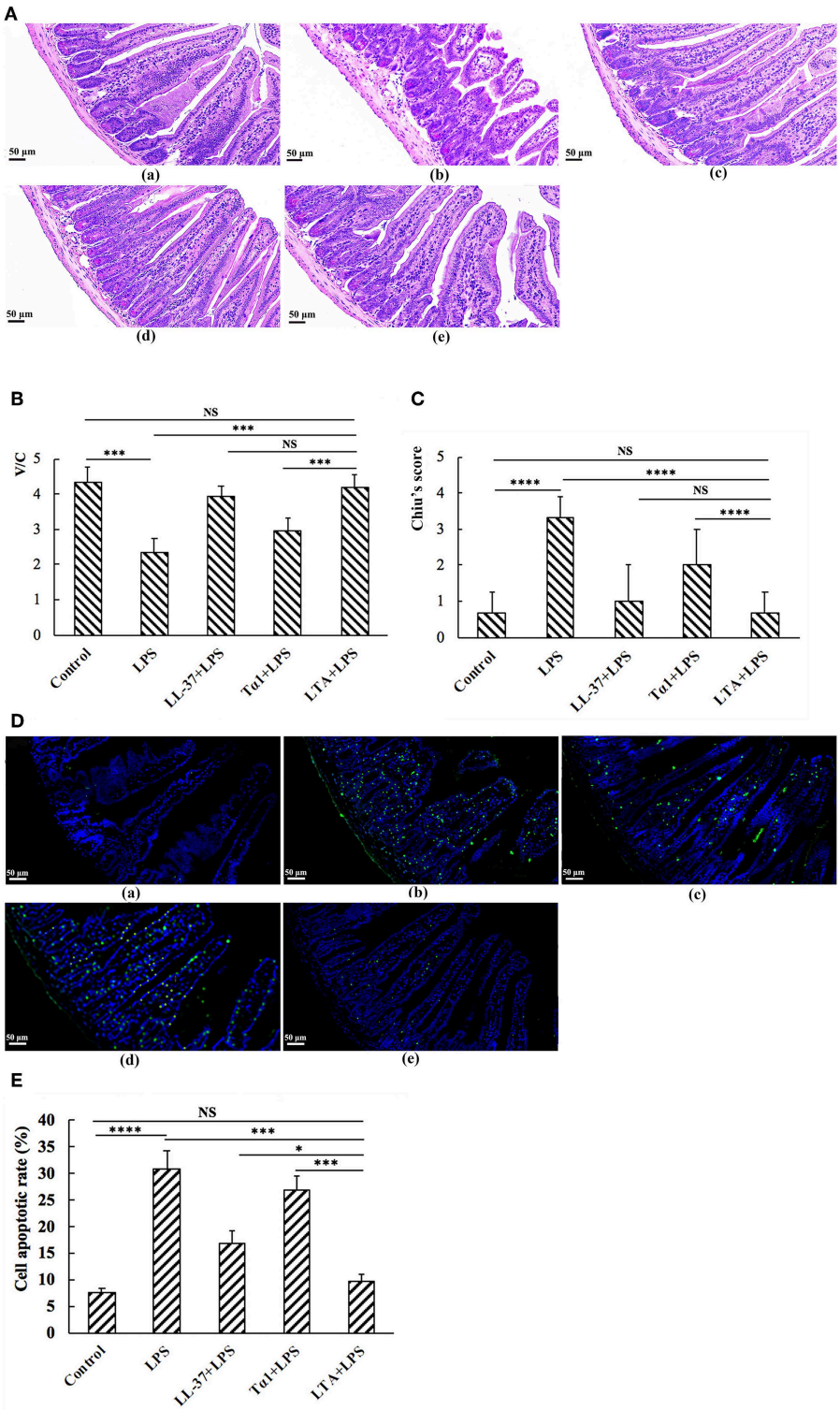

FIGURE 5 | The protective effects of LTA against LPS-induced clinical symptoms in mouse jejunum. Representative H&E-stained sections from (**A**,a) control, (**A**,b) LPS, (**A**,c) LL-37 + LPS, (**A**,d) Tα1 + LPS, (**A**,e) LTA + LPS. Original magnification 200 ×. **(B)** The effect of LTA on Chiu's scores. Chiu's score is comprised of changes of the villus and glands of the jejunal mucosa **(C)** The effect of LTA on the ratio of villus height to crypt depth (V/C) of the jejunum. **(D)** TUNEL staining of jejunal tissues. Original magnification 200 ×. (**D**,a) Control, (**D**,b) LPS, (**D**,c) LL-37 + LPS, (**D**,d) Tα1 + LPS, (**D**,e) LTA + LPS. **(E)** The number of apoptotic cells in 4–6 randomly selected fields was counted according to the number of positive green cells and the average calculated. Data are given as mean values ± standard deviation from 12 biological replicates. NS: $P > 0.05$, $^{*}P \leq 0.05$, $^{***}P \leq 0.001$, and $^{****}P \leq 0.0001$.

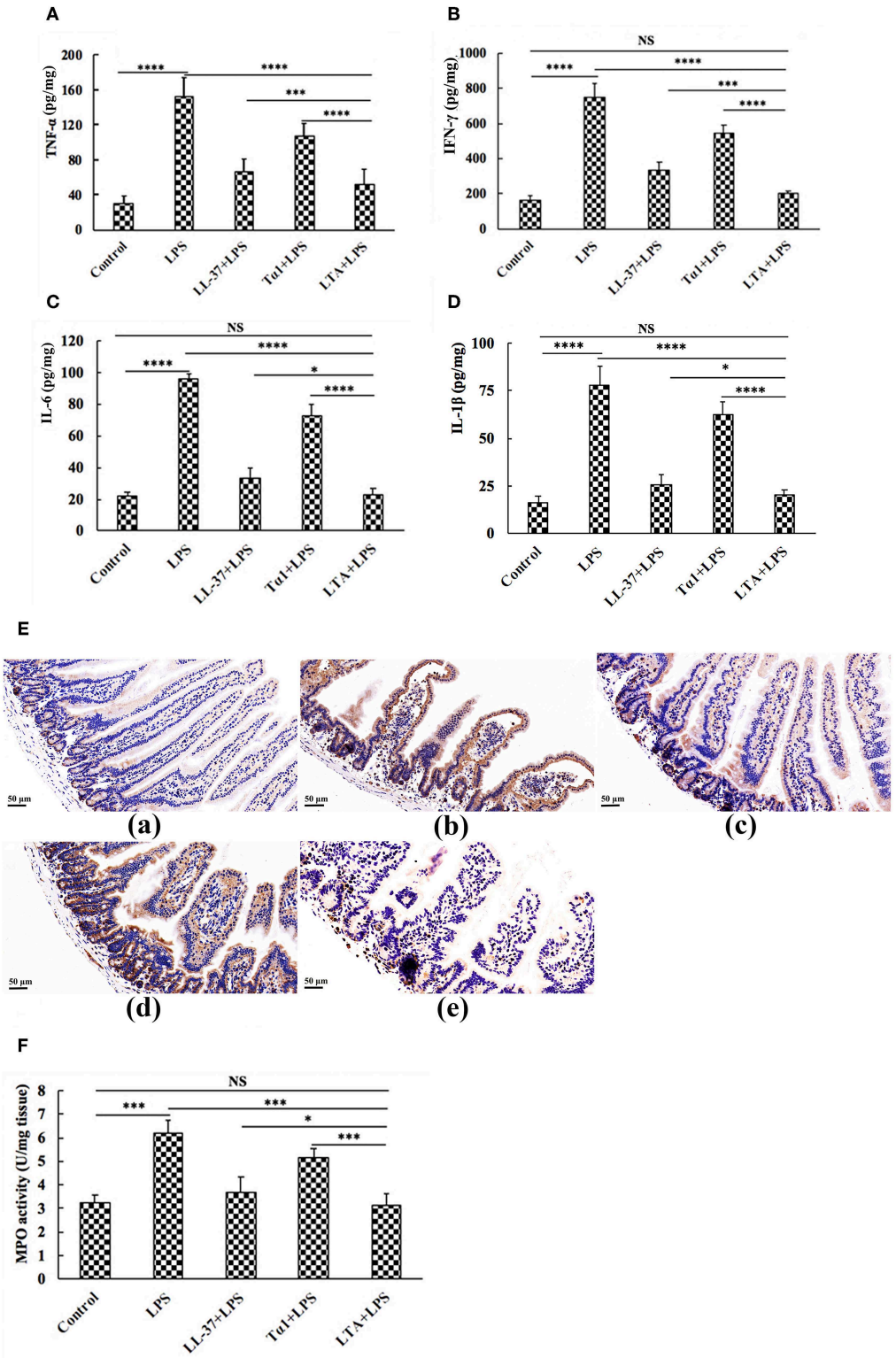

FIGURE 6 | The protective effects of LTA on the inflammatory response. ELISA for TNF-α **(A)**, IFN-γ **(B)**, IL-6 **(C)**, and IL-1β **(D)** in jejunal tissues. **(E)** Representative images of CD177^{+}. Original magnification 400 ×. Formalin-fixed, paraffin-embedded 5-mm cross-sections were stained with a primary Ab to CD177^{+}. (**E**,a) control, (**E**,b) LPS, (**E**,c) LL-37+LPS, (**E**,d) Tα1+LPS, (**E**,e) LTA+LPS. Enzymatic activities of MPO were measured **(F)**. Data are given as mean values ± standard deviation from 12 biological replicates. NS: $P > 0.05$, $^{*}P \leq 0.05$, $^{***}P \leq 0.001$, and $^{****}P \leq 0.0001$.

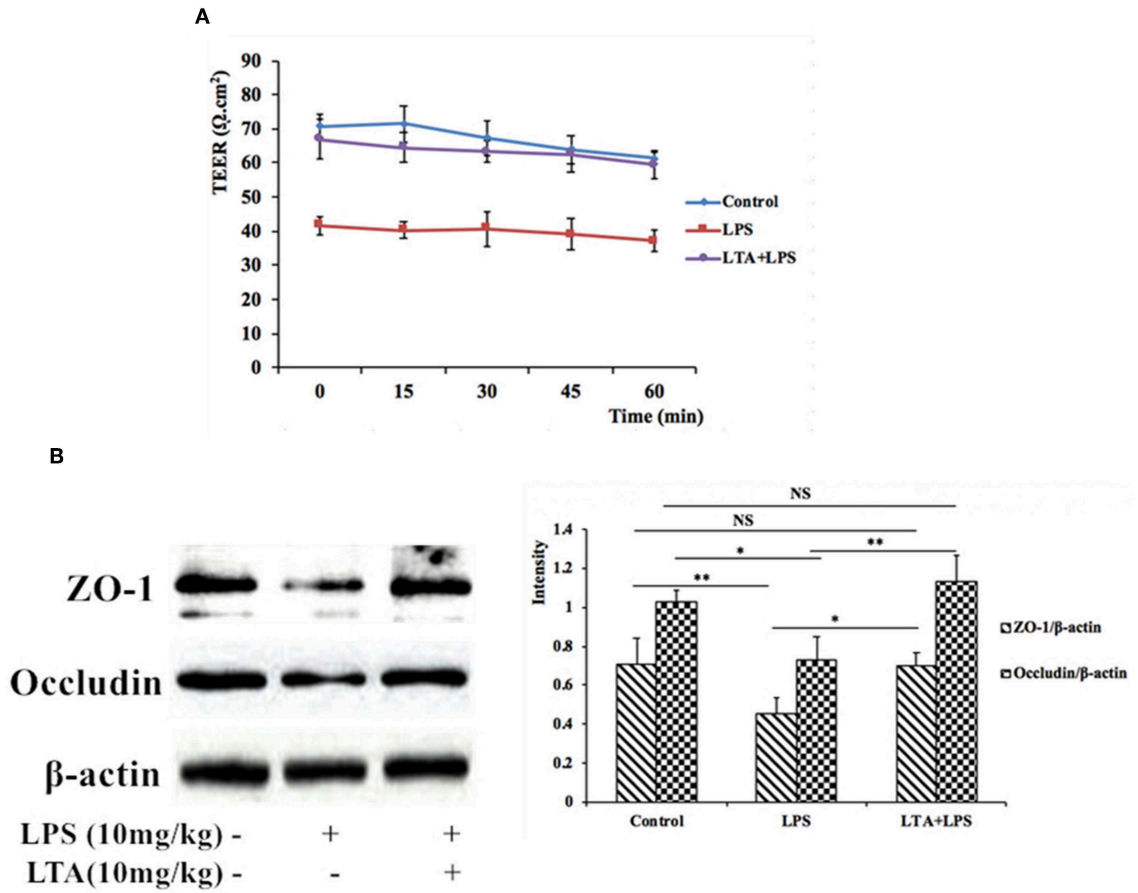

FIGURE 7 | The protective effects of LTA on the intestinal barrier. **(A)** TEER of mouse jejunal epithelium was measured *ex vivo* in Ussing chambers. **(B)** Expression of TJ proteins was determined by western-blot. Data are given as mean values ± standard deviation from at least 3 biological replicates. NS: $P > 0.05$, $^{*}P \leq 0.05$, and $^{**}P \leq 0.01$.

Effect of Hybrid Peptides on Body Weight

As expected, LPS treatment resulted in weight loss. Mice in the LPS-treated group showed significant weight loss compared to the control group. Mice in the LTA-pretreated group recovered their weight loss rapidly (**Figure 4**). Based on the weight-loss recovery, the hybrid peptide, LTA, appears to be more potent than the parental peptides (**Figure 4**).

The Protective Effects of LTA Against LPS-Induced Damage in Jejunum Tissue

Mice in the LPS group had significantly more macroscopic inflammation than those in the control and LTA-pretreated groups. Compared to the control, histological examination of the jejunum tissue in the LPS group showed considerable tissue injury (**Figure 5A**) and a decreased villus height to crypt depth (V/C) ratio (**Figure 5C**). Overall, the LPS-induced intestinal damage was significantly attenuated by LTA pretreatment; Chiu's score was restored from 3.33 ± 0.58 to 0.67 ± 0.58, and the V/C value was restored from 2.35 ± 0.389 to 4.19 ± 0.364 ($p \leq 0.05$) (**Figure 5B**). Based on the Chiu's score, the newly designed hybrid peptide appears to be more potent than the parental peptides (**Figure 5B**). In addition, the V/C value in the LTA-pretreated group was markedly increased compared to that in the Tα1-pretreated group. No statistical significance was found among the LTA-pretreated group compared to the LL-37-pretreated group (**Figure 5C**).

As shown by TUNEL staining, apoptosis of the LPS-treated group was significantly higher than that of the control group, as quantified by the apoptosis index (**Figures 5D,E**). Compared to the LPS-treated group, pretreatment with LTA in LPS-administered mice significantly reduced the apoptosis index (**Figures 5D,E**). In addition, the apoptosis index in the LTA-pretreated group was markedly decreased compared to the parental peptides.

To characterize the protective effect of LTA against inflammation in LPS-induced mice, the secretion of the inflammatory markers, TNF-α, IFN-γ, IL-6, and IL-1β were evaluated by ELISA. Administration of LPS caused a significant elevation of these pro-inflammatory cytokines in the jejunum compared to the control group (**Figures 6A–D**). **Figures 6A–D** shows that all peptides attenuated TNF-α, IFN-γ, IL-6, and IL-1β secretion. Meanwhile, mice in the LTA-pretreated group had

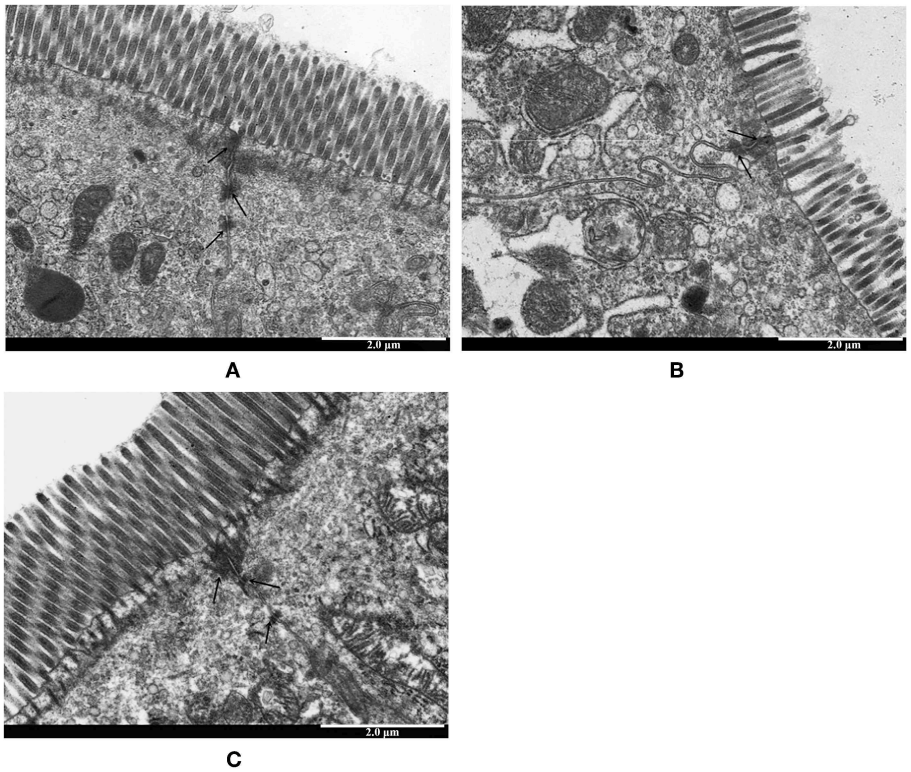

FIGURE 8 | The protective effects of LTA on intestinal TJs structure. TJs structure in the jejunal epithelium was confirmed by transmission electron microscope (TEM). Original magnification 20000 × **(A)** control, **(B)** LPS, **(C)** LTA+LPS. The wider intervals (black arrowheads) between the intestinal epithelial cells are indicated.

significantly lower TNF-α, IFN-γ, IL-6, and IL-1β concentrations than those in the Tα1- or LL-37-pretreated groups.

The infiltration of $CD177^+$ cells into jejunal tissue was detected via immunohistochemistry. In contrast to minimal infiltration of neutrophils into the jejunum of control mice, LPS triggered increased infiltration of $CD177^+$ neutrophils into the jejunal lesion area (**Figure 6E**). Pretreatment with the peptides reduced the infiltration of neutrophils compared to the group treated with LPS alone (**Figure 6E**). LTA, the most active peptide, reduced this effect to the basal level.

MPO (an indicator of jejunal infiltration by leukocytes) activity in the jejunum tissue from LPS treated mice was significantly increased compared to control mice. LTA pretreatment showed markedly decreased MPO activity compared to the LPS-treated group (**Figure 6F**). Moreover, MPO activity in the LTA-pretreated group was markedly decreased compared to Tα1 and LL-37 pretreatment (**Figure 6F**). Collectively, all of these results support the assertion that LTA is the most active peptide against LPS-induced impairment of mice, and it is suitable for further experiments.

LTA Prevented the LPS-Stimulated Disruption of Intestinal TJ Structure and Function

To assess the functional integrity of mouse intestinal epithelium under *ex vivo* conditions, TEER measurements were performed for 60 min. Compared to the control group, the TEER values in the LPS-treated group declined remarkably (**Figure 7A**), indicating an increase in permeability. However, pretreatment with LTA resulted in a significant protective effect; the TEER values in the LTA-pretreated group were similar to those in the control group (**Figure 7A**). These results suggest that LTA minimizes LPS-induced intestinal epithelial hyper permeability.

To investigate the protective effects of LTA on the LPS-stimulated disruption of TJs, TJ marker (ZO-1 and Occludin) levels were determined by western blotting. Compared to control group, the expression of ZO-1 and Occludin was down-regulated in mice treated with LPS alone (**Figure 7B**). However, the expression of these TJ markers in the LTA-pretreated group was significantly higher than that in the LPS-group (**Figure 7B**). These data suggest that LTA maintains the integrity of the junction complex. In addition, TEM, which was used to determine the TJs between gut epithelial cells, supported the protective effect of LTA against LPS-induced damage in jejunum tissues (**Figure 8**).

LTA Effects on the NF-κB Signaling Pathway in LPS-Induced Mice

Next, we investigated the NF-κB signaling pathway in LPS-induced mice pretreated with or without LTA to determine the mechanism by which LTA induces its anti-inflammatory

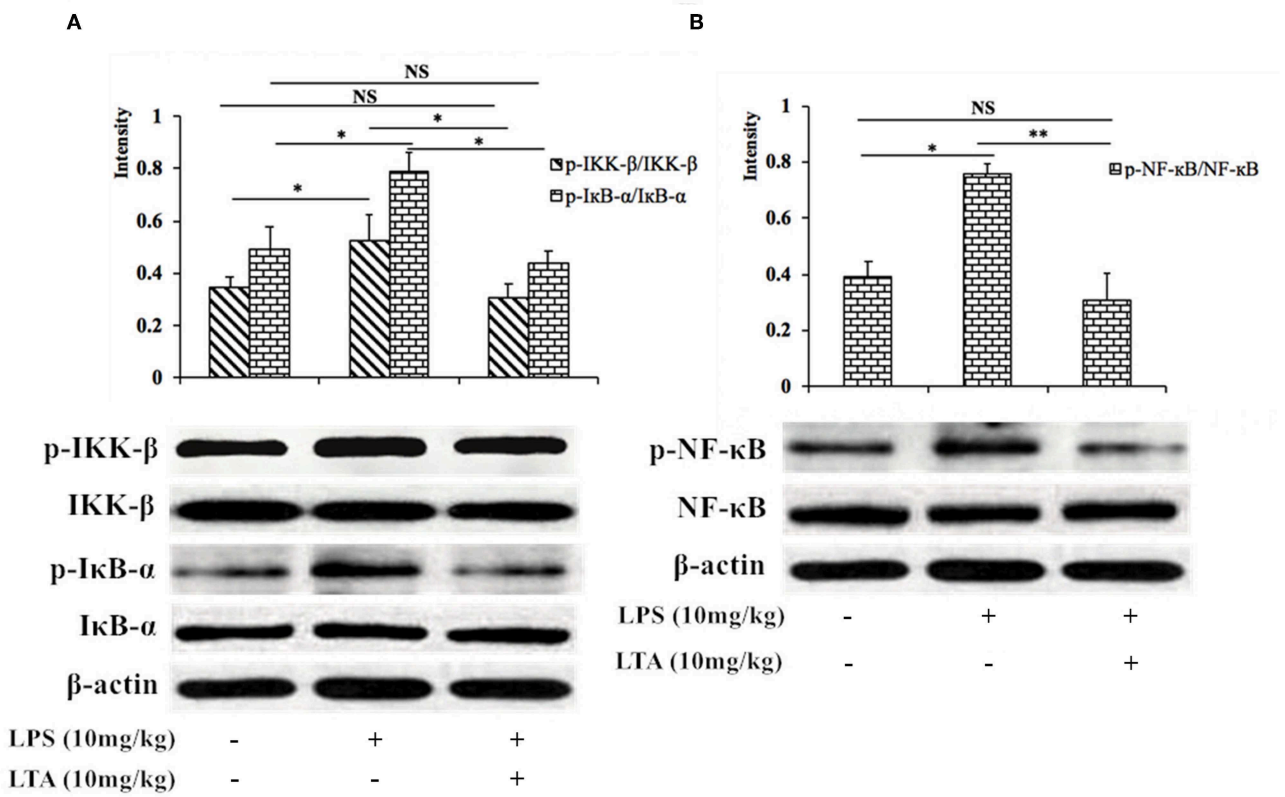

FIGURE 9 | Inhibitory effect of LTA on the NF-κB signaling pathways in mice. Phosphorylated and total protein levels of IKK-β and IκB-α **(A)**, NF-κB **(B)**, and β-actin from jejunal tissues were measured by western blot analyses. Data are given as mean values ± standard deviation from 3 biological replicates. NS: $P > 0.05$, $^{*}P \leq 0.05$, and $^{**}P \leq 0.01$.

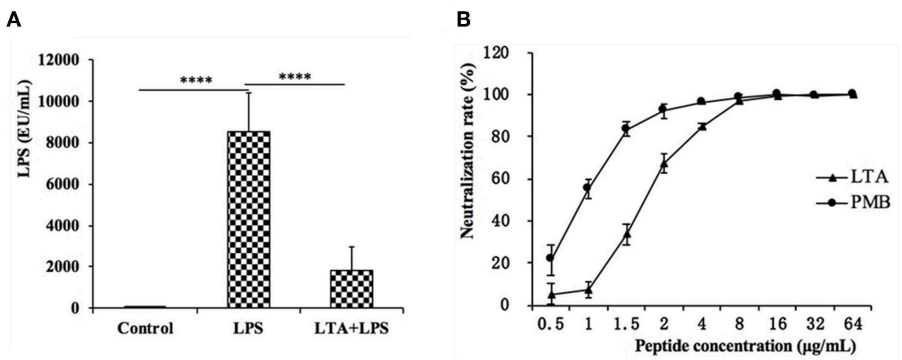

FIGURE 10 | LPS neutralization activity of LTA *in vitro* and *in vivo*. **(A)** The LPS concentration in the mice plasma. **(B)** *In vitro* LPS neutralization by LTA. Binding of LTA (shown as triangles) or PMB (shown as a circle) binding to LPS was determined using the chromogenic *in vitro* TAL assay. Data are given as mean values ± standard deviation from 3 biological replicates. NS: $P > 0.05$, $^{****}P \leq 0.0001$.

activity. The phosphorylation of IKK-β, IκB-α, and NF-κB increased significantly after stimulation with LPS, but the phosphorylation decreased in the group pretreated with LTA (**Figure 9**). These results suggest that one mechanism by which LTA modulates the immune system in mice is via the NF-κB pathway.

LPS Neutralization Activity of LTA *in vitro* and *in vivo*

The plasma LPS concentration in the mice was evaluated by the CE TAL test. In the LPS-treated group, the plasma LPS level sharply increased, but LTA significantly reduced the plasma LPS level (**Figure 10A**).

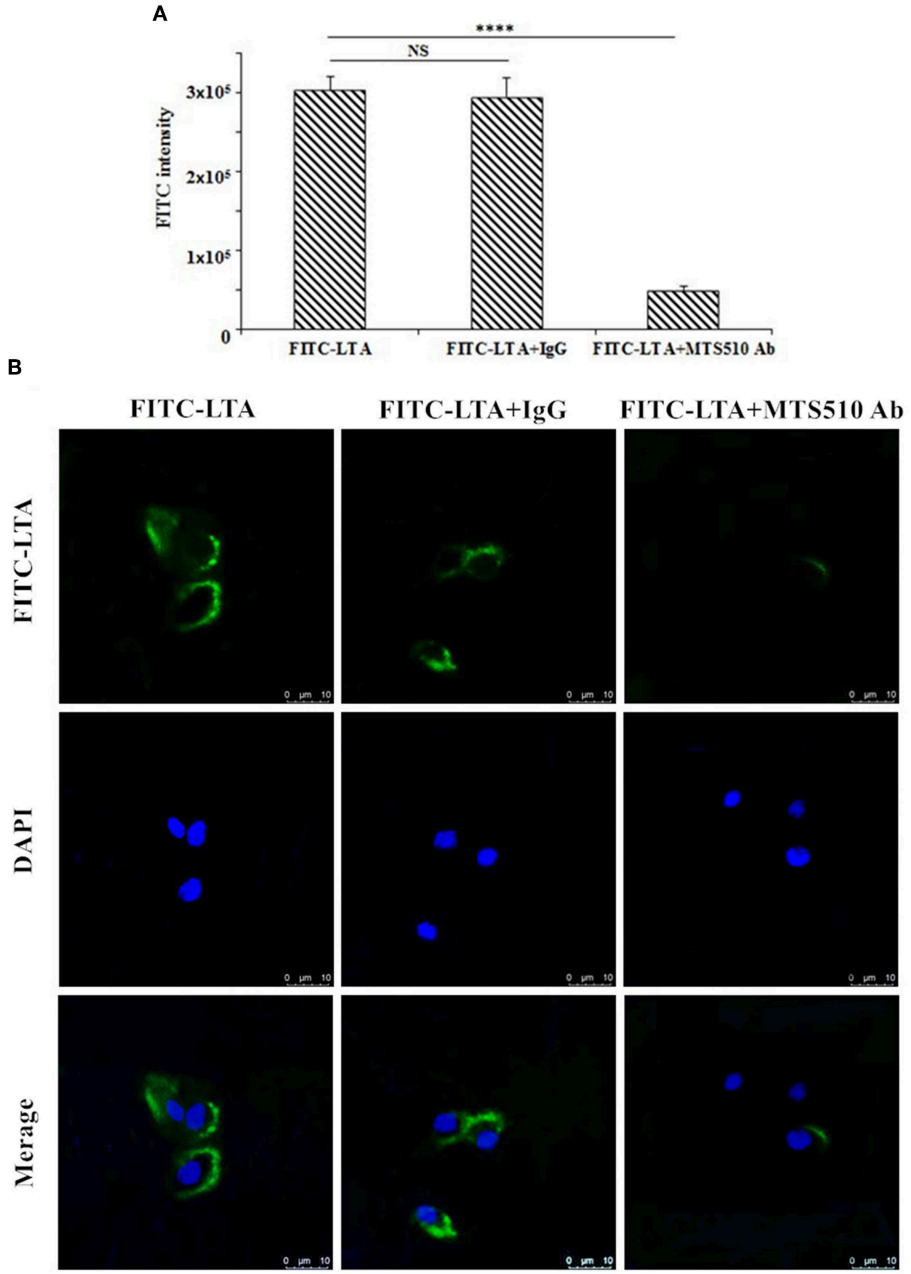

FIGURE 11 | TLR4/MD-2-dependent staining of RAW264.7 cells with FITC-LTA. **(A)** RAW264.7 cells were treated with PBS, anti-mouse mAbTLR4/MD-2 complex (MTS510 Ab) or isotype control (IgG) for 1 h at 4°C before staining with 10 μg/mL. The cells were then harvested by trypsin and washed five times with PBS. The above cells were analyzed by the flow cytometry. **(B)** Cells were treated with PBS, MTS510 Ab, or IgG before FITC-LTA staining for confocal laser scanning microscopy analysis. Bar, 10 μm. Data are given as mean values ± standard deviation from 3 biological replicates. NS: $P > 0.05$, ****$P \leq 0.0001$.

To test whether LTA neutralized LPS, an LPS neutralization activity was performed *in vitro*. As shown in **Figure 10B**, LTA inhibited the activation of tachypleus amebocyte lysate in a dose-dependent manner. The LPS neutralization activity LTA is similar to PMB, a cyclic hydrophobic peptide known to bind LPS (51), and LTA could completely neutralize LPS at 8 ug/mL or more.

The Specific Binding of LTA to TLR4/MD-2

To determine the recognition receptor, a binding assay of LTA to a receptor on the plasma membrane was performed via flow cytometry (**Figure 11A**) and confocal laser-scanning microscopy (**Figure 12B**). FITC-LTA caused a significant increase in the fluorescence intensity of RAW264.7 cells compared to the intensity of cells blocked with an

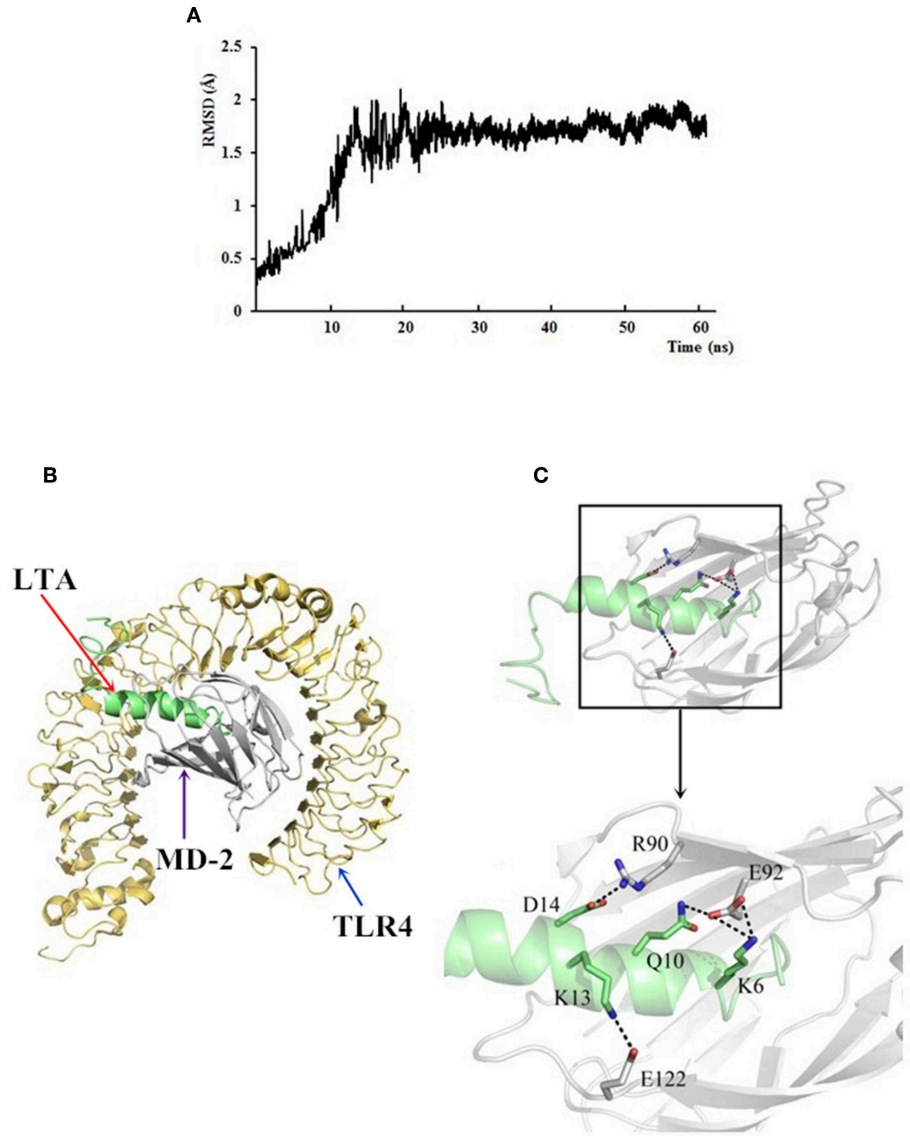

FIGURE 12 | The docking results of LTA to the TLR4/MD-2 complex. **(A)** Time evolution of RMSD during molecular dynamics simulation. **(B)** LTA is bound to the hydrophobic pocket of MD2. The yellow ribbons represented TLR4, gray ribbons represented MD2, and green ribbons represented LTA. **(C)** A close-up view of LTA binding to the MD-2. Residues involved in the interaction between LTA and MD-2 are displayed.

anti-mouse TLR4/MD-2 mAb. Meanwhile, this increased fluorescence intensity was not attenuated by IgG (**Figure 12A**). Similar results were also seen via confocal laser-scanning microscopy (**Figure 11B**).

To further predict binding of LTA to the TLR4/MD-2 complex, MD simulations were performed. Based on the root-mean square deviation (RMSD) values of TLR4/MD-2 (**Figure 12A**), the MD simulation was fully equilibrated during the full 60 ns. A total of 300 snapshots was taken from the last stable 40 ns of the MD simulation. The calculated binding free energy, which was well correlated with the determined binding affinities, is shown in **Table 2**. The binding energy of LTA to MD-2 calculated by MM-PBSA method was −996.2 kJ/mol. The interface of MD-2 that is bound to LPS was compared to that of LTA. There was a common hydrophobic pocket on MD-2 where both LPS (52) and LTA interacted with the protein (**Figures 12B,C**). The interaction between LTA and MD-2 was principally mediated by salt-bridges and hydrogen bonds between Asp14 (LTA) - Arg 90 (MD-2), Lys 6 and Gln 10 (LTA) - Glu 92 (MD-2), and Lys 13 (LTA) – Glu 122 (MD-2) (**Table 3**). This is consistent with the flow cytometry and confocal laser-scanning microscopy results that suggest that LTA blocks LPS binding to TLR4/MD2 complex, resulting in the LPS-antagonizing effects.

TABLE 2 | Key parameters of interactions between LTA and MD-2.

Interaction pair	Number of salt-bridges	Number of hydrogen bonds	Interaction surface (Å^2)	Binding free energy (kj/mol)
MD2…LTA	4	5	343	−996.2

TABLE 3 | Distances and salt-bridges between the binding residues of LTA and MD-2.

Interaction pair MD2…LTA	Distance (Å)	Salt-bridges
R_{90}-NH_2…D_{14}-OD_1	3.30	+
E_{122}-OE_2…K_{13}-NZ	3.00	+
E_{122}-OE_1…K_{13}-NZ	2.94	+
E_{92}-OE_1…Q_{10}-NE_2	3.00	–
E_{92}-OE_1…K_6-NZ	3.03	+
E_{92}-OE_2…K_6-NZ	3.19	+

The distance and salt-bridges of interaction pairs are extrapolated from the LTA/MD-2 molecular dynamics simulation. "+" means existence, and "–" means not determined.

DISCUSSION

LPS, a major component of the cell wall of Gram-negative bacteria, is released by antibiotic intake and can lead to intestinal inflammation. Intestinal inflammation is a chronic inflammatory disease associated with engagement of the immune response by increased pro-inflammatory cytokine secretion in the intestines (53, 54). Historically, intestinal inflammation is more common in western countries than Asia; the increasing incidence in Asia is likely due to the influence of a high-fat diet (55). Notably, intestinal inflammation increases the risk of enteric cancer, which is a commonly malignancy globally (56).

Native anti-inflammatory peptides are a class of anti-inflammatory agents that may be useful in the treatment of a range of inflammatory diseases (13, 18, 25). However, several concerns, such as potential cytotoxicity (35), poor anti-inflammatory activity based on peptide concentration, and weak physiological stability (57), have weakened their development as anti-inflammatory therapeutics. Hybridizing different anti-inflammatory peptides is one of the most successful approaches to obtain a novel anti-inflammatory peptide with increased activity but minimized cytotoxicity (58, 59). Based on previous findings, we designed several hybrid peptides comprising the active center of AMPs, including LL-37 (13-36), YW12D (1-12), IDR-1 (1-13), and CATH2 (1-13), with TP5 or the active center of Tα1 (17-24).

It has been well established that LPS mediates its immune response in macrophages via TLR4 (60). MD-2, an accessory protein of TLR4, is responsible for recognizing LPS; in turn, LPS interacts with the Toll/Interleukin-1 receptor (TIR) domain on TLR4 and induces the inflammatory effects (61, 62). Therefore, targeting MD-2 is an important therapeutic strategy for the attenuation of the inflammatory response (62–64). Initially, molecular docking was used to simply and effectively scan the binding mode of the anti-inflammatory peptides. LTP, LTA, YTP, and CTP were the hybrid peptides selected for further study, and the anti-inflammatory activities of these four hybrid peptides were assessed in RAW264.7 cells. The four hybrid peptides showed higher anti-inflammatory activity than their parental peptides. LTA, the most active peptide, was selected for a comprehensive analysis.

The hybrid peptides designed in our study were aimed to fight inflammatory disorders with reduced cytotoxicity. Because cytotoxicity is often thought to be a bottleneck for the therapeutic use of these peptides, it was important to evaluate toxicity. In this study, the proliferation assays showed that the hybrid peptides had lower cytotoxic than their parental peptides. Presumably, this decreased cytotoxic activity was due to the rational hydrophobicity of these hybrid peptides, which is similar to that described in other studies (59). The low cytotoxic activity at relatively high peptide concentrations combined with modified anti-inflammatory activity is an excellent combination from the parental peptides.

The present study showed that murine models of intestinal inflammation induced by LPS have characteristics similar to human IBD (14, 65), such as weight loss, neutrophil infiltration, histological features of multiple erosions, and inflammatory intestinal mucosal changes, including crypt abscess. However, LTA treatment significantly reverses weight loss and reduce histological damage such as ulceration of the epithelial and decreased villus height to crypt depth ratio, in the LPS-induced intestinal inflammation experimental model. The infiltration of activated neutrophils is one of the most representative histological features observed in intestinal inflammation, because neutrophils generate superoxide anions and other reactive species (66). The infiltration of activated was significantly increased in LPS-treated mice; however, mice pre-treated with LTA did not show the same effect. The activity of MPO is directly proportional to the neutrophil concentration in the inflamed tissue. Therefore, MPO activity is an index of neutrophil infiltration and inflammation (67). Consistent with this, jejunal MPO activity was markedly increased in LPS-treated mice, but pretreatment with LTA significantly reduced this effect. In addition, MPO activity in the LTA-pretreated group was markedly decreased compared to the Tα1 and LL-37 pretreated groups. Apoptosis is one of the ulcerogenic processes associated with intestinal inflammation (68). In this study, TUNEL staining showed that LPS markedly increased the number of apoptotic cells in the jejunal mucosa, while administration of LTA decreased the extent of apoptosis.

Excessive production of inflammatory cytokines, such as TNF-α, which can amplify the inflammatory cascade by triggering the accumulation and activation of leukocytes, is often seen in intestinal inflammation (69). In the present study, we found that pretreatment with LTA reduced the levels of TNF-α, IFN-γ, IL-6, and IL-1β in the jejunum. Moreover, the levels of TNF-α, IFN-γ, IL-6, and IL-1β in LTA-pretreated group were markedly decreased compared to the Tα1- and LL-37-pretreated groups.

Collectively, these results support the deduction that LTA is the most active peptide that prevents LPS-induced impairment

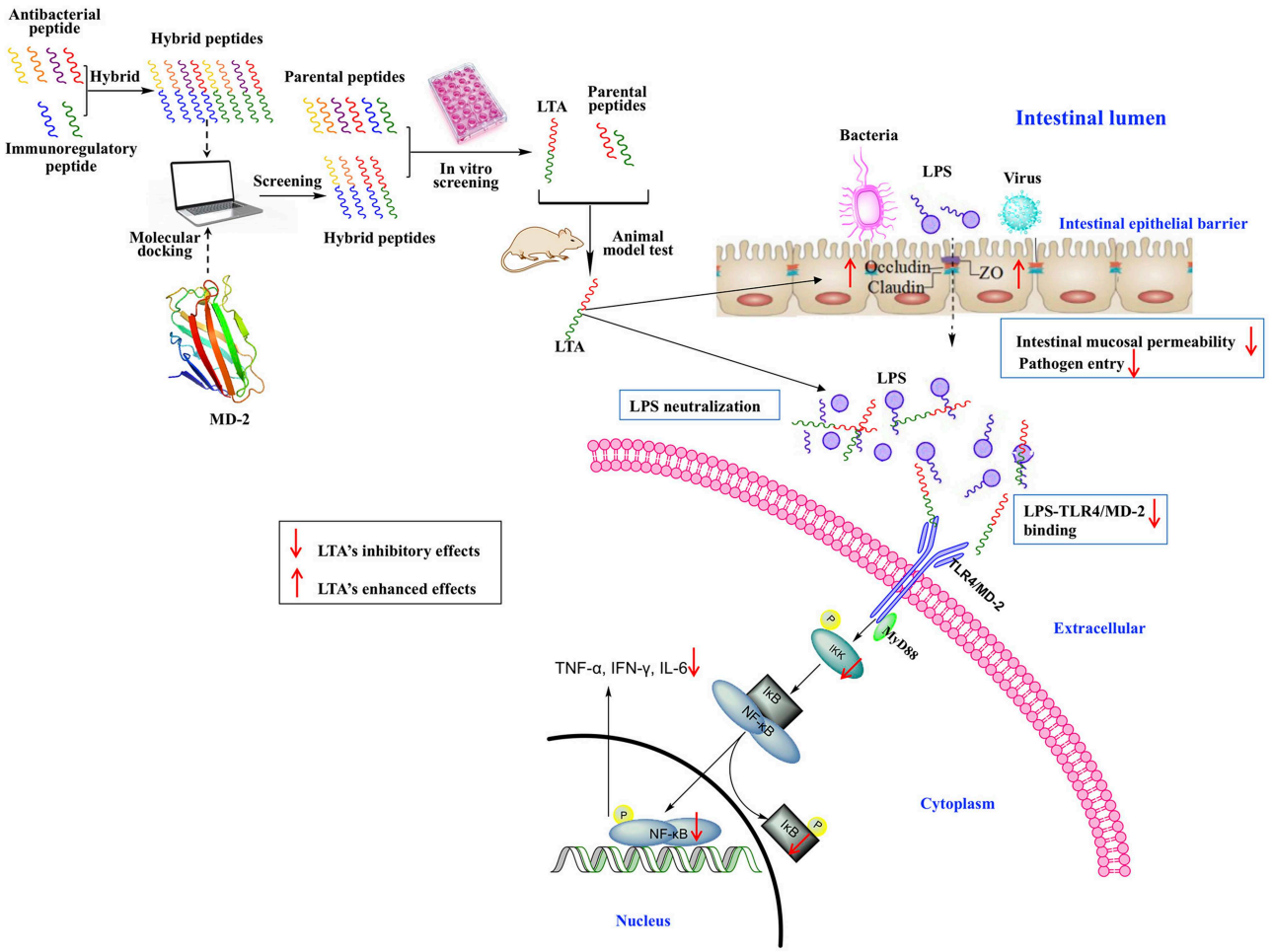

FIGURE 13 | Schematic illustration of design and development of the novel hybrid peptide, LTA for the treatment of intestinal inflammation.

in mice. To identify the mechanisms of the observed anti-inflammatory effects in LPS-treated mice, a comprehensive and detailed analysis was conducted.

LPS can upregulate ∼100 different genes, including pro-inflammatory cytokines, signaling molecules, and transcriptional regulators; thus, it can induce several functional responses that contribute to immunity (70). LPS has high biological activity and plays an important role in the pathogenesis of intestinal inflammation (14). In this study, we found that LTA-pretreated mice had significantly reduced plasma LPS levels compared to the LPS-only treated. *In vitro* experiments showed that LTA can almost completely neutralize LPS at a concentration of 8 μg/mL. By neutralizing LPS, LTA could significantly attenuate the intestinal inflammatory effects by reducing the binding of LPS to the TLR4 receptor in the immune cells *in vivo*.

The intestinal mucosa forms a physical and metabolic barrier against toxins and pathogens from the lumen into the circulatory system (71). Deterioration of the intestinal epithelial barrier increases host susceptibility to luminal pathogens and antigens, leading to the chronic intestinal immune response (72). This deterioration is also a key contributing factor in the pathogenesis of intestinal inflammation (73). First, we evaluated the effect of LTA on gut epithelial barrier function via the TEER tests and the results showed that LTA alleviated LPS-induced permeability. The intestinal epithelial barrier is formed by an interplay between different types of barrier components, such as intercellular TJ proteins (74). TJs are responsible for limiting the paracellular movement of compounds across the intestinal mucosa (75). Regions of increased permeability in the TJs are major sites for both infections and the initiation of inflammation in the gut (76). Our data indicated that the expression of two major TJ proteins, Occludin and ZO-1, was regulated by LTA. In addition, TEM was used to determine the TJs between gut epithelial cells, and its results support the protective effect of LTA against LPS-induced damage in jejunum tissues. The effect of LTA on the epithelial barrier suggests that LTA could protect the host by preventing toxins and luminal antigens from impairing the body's defense mechanism, thereby reducing the severity of intestine inflammation.

The hybrid peptides proposed in this study antagonize the effects of LPS in RAW264.7 cells and in the mouse by binding to the TLR4-MD2 complex. To identify the binding ability of LTA to the TLR4/MD-2 complex, binding assays were performed by flow cytometry and confocal laser-scanning microscopy. The results demonstrated that that LTA competitively blocks LPS binding to the TLR4/MD-2 complex. Consistently, the MD simulation showed that LTA binds to the hydrophobic pocket of MD-2, which partially overlaps with the LPS binding sites on MD-2 (52). This binding mode could be the cause of the LPS-antagonizing effect. Therefore, the present study indicated that LTA confers its anti-inflammatory activity by blocking LPS binding to the TLR4/MD-2 complex.

NF-κB signaling regulates cytokines and cells involved in the inflammatory process (77), and LPS is a strong activator of NF-κB, through its interactions with TLR4. NF-κB is considered to be a crucial initiative factor regulating inflammatory gene expression (78). Thus, we tested the expression of the major proteins involved in the NF-κB pathway to clarify the anti-inflammatory mechanism of LTA in intestinal inflammation. LTA effectively inhibited the activation of NF-κB signaling by suppressing of phosphorylation of IKK-β, IκB-α, and NF-κB.

CONCLUSION

In this study, a feasible approach for the design of anti-inflammatory peptides by the hybridization of different native anti-inflammatory peptides was proposed (**Figure 13**). The anti-inflammatory potency of the peptides was enhanced while cytotoxicity was reduced. Moreover, the different hybrid peptide combinations may provide a range of opportunities for obtaining a more active anti-inflammatory peptide.

One novel hybrid peptide, LTA, was most effective at reducing the LPS-induced inflammatory response. This peptide, which was identified by molecule docking and *in vitro* experiments, had low cytotoxicity. Our study also confirmed that the anti-inflammatory effects of LTA on the LPS-induced murine intestinal inflammation model may be associated with the neutralization of LPS, the maintenance of the TJ network, the binding activity on the TLR4/MD-2 complex, and the inhibition of the NF-κB signal pathway. Thus, LTA is able to modulate TJ proteins, such as Occludin and ZO-1, and inhibit the production of inflammation mediators, such as TNF-α, IFN-γ, IL-6, and IL-1β. As a result of its broad effects against inflammation, LTA exhibits great potential as a useful tool to study or potentially treat inflammatory disorders.

DATA AVAILABILITY

All datasets generated for this study are included in the manuscript and/or the supplementary files.

ETHICS STATEMENT

All of the animal experiments were approved by the Institutional Animal Care and Use Committee of China Agricultural University and were performed in accordance with guidelines set forth by the Care and Use of Laboratory Animals of the Ministry of Science and Technology of China (certificate of the Beijing Laboratory Animal employee, ID: 18086).

AUTHOR CONTRIBUTIONS

LZ, XW, RZ, JP, and DS conceived the project and designed the experiments. LZ, XW, ZL, JC, and MD conducted experiments. LZ and JP wrote the manuscript and analyzed data. All authors read and commented on the manuscript. The authors are in debt to JP for his contribution toward English proficiency.

FUNDING

This work was supported by the National Key Research and Development Program of China (Project No. 2018YFD0500600), National Natural Science Foundation of China (NSFC, 31572442), and National Natural Science Foundation of China (NSFC, 31272476).

REFERENCES

1. Song YS, Lee Y, Kwon TR, Kim YH, Kim BJ. Picrasma quassioides inhibits LPS- and IFN-γ-stimulated nitric oxide production and inflammatory response in RAW264.7 macrophage cells. *Biotechnol Bioproc E.* (2014) 19:404–10. doi: 10.1007/s12257-014-0131-4
2. Burrin DG, Stoll B, Guan XF, Cui LW, Chang XY, Holst JJ. Glucagon-like peptide 2 dose-dependently activates intestinal cell survival and proliferation in neonatal piglets. *Endocrinology.* (2005) 146:22–32. doi: 10.1210/en.2004-1119
3. Gillen CD, Walmsley RS, Prior P, Andrews HA, Allan RN. Ulcerative colitis and Crohn's disease: a comparison of the colorectal cancer risk in extensive colitis. *Gut.* (1994) 35:1590–2. doi: 10.1136/gut.35.11.1590
4. Eaden JA, Abrams KR, Mayberry JF. The risk of colorectal cancer in ulcerative colitis: a meta-analysis. *Gut.* (2001) 48:526–35. doi: 10.1136/gut.48.4.526
5. Bernstein CN, Blanchard JF, Kliewer E, Wajda A. Cancer risk in patients with inflammatory bowel disease - a population-based study. *Cancer.* (2001) 91:854–62. doi: 10.1002/1097-0142(20010215)91:4<;854::AID-CNCR1073>3.0.CO;2-Z
6. Sartor RB. Mechanisms of disease: pathogenesis of Crohn's disease and ulcerative colitis. *Nat Clin Pract Gastr.* (2006) 3:390–407. doi: 10.1038/ncpgasthep0528
7. Boumpas DT, Chrousos GP, Wilder RL, Cupps TR, Balow JE. Glucocorticoid therapy for immune-mediated diseases - basic and clinical correlates. *Ann Intern Med.* (1993) 119:1198–208. doi: 10.7326/0003-4819-119-12-199312150-00007
8. Faubion WA, Loftus EV, Harmsen WS, Zinsmeister AR, Sandborn WJ. The natural history of corticosteroid therapy for inflammatory bowel disease: a population-based study. *Gastroenterology.* (2001) 121:255–60. doi: 10.1053/gast.2001.26279
9. Smoak KA, Cidlowski JA. Mechanisms of glucocorticoid receptor signaling during inflammation. *Mech Ageing Dev.* (2004) 125:697–706. doi: 10.1016/j.mad.2004.06.010
10. Anstead GM. Steroids, retinoids, and wound healing. *Adv Wound Care.* (1998) 11:277–85.
11. Stanbury RM, Graham EM. Systemic corticosteroid therapy - side effects and their management. *Brit J Ophthalmol.* (1998) 82:704–8. doi: 10.1136/bjo.82.6.704

12. Heinbockel L, Weindl G, Martinez-de-Tejada G, Correa W, Sanchez-Gomez S, Barcena-Varela S, et al. Inhibition of lipopolysaccharide- and lipoprotein-induced inflammation by antitoxin peptide pep 19-2.5. *Front Immunol.* (2018) 9:1704. doi: 10.3389/fimmu.2018.01704
13. Wu BC, Lee AHY, Hancock REW. Mechanisms of the innate defense regulator peptide-1002 anti-inflammatory activity in a sterile inflammation mouse model. *J Immunol.* (2017) 199:3592–603. doi: 10.4049/jimmunol.1700985
14. Zong X, Hu WY, Song DG, Li Z, Du HH, Lu ZQ, et al. Porcine lactoferrin-derived peptide LFP-20 protects intestinal barrier by maintaining tight junction complex and modulating inflammatory response. *Biochem Pharmacol.* (2016) 104:74–82. doi: 10.1016/j.bcp.2016.01.009
15. Bhunia A, Chua GL, Domadia PN, Warshakoon H, Cromer JR, David SA, et al. Interactions of a designed peptide with lipopolysaccharide: bound conformation and anti-endotoxic activity. *Biochem Bioph Res Commun.* (2008) 369:853–7. doi: 10.1016/j.bbrc.2008.02.105
16. Mu LX, Zhou L, Yang JJ, Zhuang L, Tang J, Liu T, et al. The first identified cathelicidin from tree frogs possesses anti-inflammatory and partial LPS neutralization activities. *Amino Acids.* (2017) 49:1571–85. doi: 10.1007/s00726-017-2449-7
17. Vandamme D, Landuyt B, Luyten W, Schoofs L. A comprehensive summary of LL-37, the factotum human cathelicidin peptide. *Cell Immunol.* (2012) 280:22–35. doi: 10.1016/j.cellimm.2012.11.009
18. Ishida W, Harada Y, Fukuda K, Fukushima A. Inhibition by the antimicrobial peptide LL37 of lipopolysaccharide-induced innate immune responses in human corneal fibroblasts. *Invest Ophth Vis Sci.* (2016) 57:30–9. doi: 10.1167/ iovs.15-17652
19. van Dijk A, van Eldik M, Veldhuizen EJA, Tjeerdsma-van Bokhoven HLM, de Zoete MR, Bikker FJ, et al. Immunomodulatory and anti-inflammatory activities of chicken cathelicidin-2 derived peptides. *PLoS ONE.* (2016) 11:e0147919. doi: 10.1371/journal.pone.0147919
20. Hou M, Zhang NW, Yang JJ, Meng XY, Yang R, Li J, et al. Antimicrobial peptide LL-37 and IDR-1 ameliorate MRSA pneumonia *in vivo*. *Cell Physiol Biochem.* (2013) 32:614–23. doi: 10.1159/000354465
21. Singh VK, Biswas S, Mathur KB, Haq W, Garg SK, Agarwal SS. Thymopentin and splenopentin as immunomodulators - current status. *Immunol Res.* (1998) 17:345–68. doi: 10.1007/BF02786456
22. Lee HW, Lee JI, Um SH, Ahn SH, Chang HY, Park YK, et al. Combination therapy of thymosin alpha-1 and lamivudine for HBeAg positive chronic hepatitis B: a prospective randomized, comparative pilot study. *J Gastroenterol Hepatol.* (2008) 23:729–35. doi: 10.1111/j.1440-1746.2008.05387.x
23. Low TL, Thurman GB, McAdoo M, McClure J, Rossio JL, Naylor PH, et al. The chemistry and biology of thymosin. I. Isolation, characterization, and biological activities of thymosin alpha1 and polypeptide beta1 from calf thymus. *J Biol Chem.* (1979) 254:981–6.
24. Romani L, Bistoni F, Perruccio K, Montagnoli C, Gaziano R, Bozza S, et al. Thymosin alpha1 activates dendritic cell tryptophan catabolism and establishes a regulatory environment for balance of inflammation and tolerance. *Blood.* (2006) 108:2265–74. doi: 10.1182/blood-2006-02-004762
25. Romani L, Oikonomou V, Moretti S, Iannitti RG, D'Adamo MC, Villella VR, et al. Thymosin α1 represents a potential potent single-molecule-based therapy for cystic fibrosis. *Nat Med.* (2017) 23:590–600. doi: 10.1038/nm.4305
26. Mendling W, Koldovsky U. Investigations by cell-mediated immunologic tests and therapeutic trials with thymopentin in vaginal mycoses. *Infect Dis Obstet Gynecol.* (1996) 4:225–31. doi: 10.1155/S1064744996000439
27. Wang FW, Yu TT, Zheng H, Lao XZ. Thymosin alpha1-fc modulates the immune system and down-regulates the progression of melanoma and breast cancer with a prolonged half-life. *Sci Rep.* (2018) 8:12351. doi: 10.1038/s41598-018-30956-y
28. Zhang P, Chan J, Dragoi AM, Gong X, Ivanov S, Li ZW, et al. Activation of IKK by thymosin alpha 1 requires the TRAF6 signalling pathway. *EMBO Rep.* (2005) 6:531–7. doi: 10.1038/sj.embor.7400433
29. Romani L, Bistoni F, Gaziano R, Bozza S, Montagnoli C, Perruccio K, et al. Thymosin alpha 1 activates dendritic cells for antifungal Th1 resistance through Toll-like receptor signaling. *Blood.* (2004) 103:4232–9. doi: 10.1182/blood-2003-11-4036
30. Romani L, Bistoni F, Montagnoli C, Gaziano R, Bozza S, Bonifazi P, et al. Thymosin alpha1: an endogenous regulator of inflammation, immunity, and tolerance. *Ann N Y Acad Sci.* (2007) 1112:326–38. doi: 10.1196/annals.1415.002
31. Pierluigi B, D'Angelo C, Fallarino F, Moretti S, Zelante T, Bozza S, et al. Thymosin alpha1: the regulator of regulators? *Ann N Y Acad Sci.* (2010) 1194:1–5. doi: 10.1111/j.1749-6632.2010.05465.x
32. Lunin SM, Novoselova TV, Khrenov MO, Glushkova OV, Parfeniuk SB, Smolikhina TI, et al. Immunomodulatory effects of thymopentin under acute and chronic inflammations in mice. *Biofizika.* (2009) 54:182–7. doi: 10.1134/S0006350909020122
33. Goldstein G, Scheid MP, Boyse EA, Schlesinger DH, Vanwauwe J. Synthetic pentapeptide with biological-activity characteristic of the thymic hormone thymopoietin. *Science.* (1979) 204:1309–10. doi: 10.1126/science.451537
34. Goldstein AL, Goldsten AL. From lab to bedside: emerging clinical applications of thymosin alpha(1). *Expert Opin Biol Ther.* (2009) 9:593–608. doi: 10.1517/14712590902911412
35. Anders E, Dahl S, Svensson D, Nilsson BO. LL-37-induced human osteoblast cytotoxicity and permeability occurs independently of cellular LL-37 uptake through clathrin-mediated endocytosis. *Biochem Bioph Res Commun.* (2018) 501:280–5. doi: 10.1016/j.bbrc.2018.04.235
36. Haney EF, Mansour SC, Hilchie AL, de la Fuente-Nunez C, Hancock REW. High throughput screening methods for assessing antibiofilm and immunomodulatory activities of synthetic peptides. *Peptides.* (2015) 71:276–85. doi: 10.1016/j.peptides.2015.03.015
37. Li YQ, Smith C, Wu HF, Teng P, Shi Y, Padhee S, et al. Short antimicrobial lipo-α/γ-AA hybrid peptides. *Chembiochem.* (2014) 15:2275–80. doi: 10.1002/cbic.201402264
38. Nell MJ, Tjabringa GS, Wafelman AR, Verrijk R, Hiemstra PS, Drijfhout JW, et al. Development of novel LL-37 derived antimicrobial peptides with LPS and LTA neutralizing and antimicrobial activities for therapeutic application. *Peptides.* (2006) 27:649–60. doi: 10.1016/j.peptides.2005.09.016
39. Nan YH, Bang JK, Jacob B, Park IS, Shin SY. Prokaryotic selectivity and LPS-neutralizing activity of short antimicrobial peptides designed from the human antimicrobial peptide LL-37. *Peptides.* (2012) 35:239–47. doi: 10.1016/j.peptides.2012.04.004
40. Grottesi A, Sette M, Palamara AT, Rotilio G, Garaci E, Paci M. The conformation of peptide thymosin alpha 1 in solution and in a membrane-like environment by circular dichroism and NMR spectroscopy. A possible model for its interaction with the lymphocyte membrane. *Peptides.* (1998) 19:1731–8. doi: 10.1016/S0196-9781(98)00132-6
41. Mandaliti W, Nepravishta R, Vallebona PS, Pica F, Garaci E, Paci M. Thymosin α1 interacts with exposed phosphatidylserine in membrane models and in cells and uses serum albumin as a carrier. *Biochemistry.* (2016) 55:1462–72. doi: 10.1021/acs.biochem.5b01345
42. Guo ST, Huang YY, Zhang WD, Wang WW, Wei T, Lin DS, et al. Ternary complexes of amphiphilic polycaprolactone-graft-poly (N,N-dimethylaminoethyl methaaylate), DNA and polyglutamic acid-graft-poly (ethylene glycol) for gene delivery. *Biomaterials.* (2011) 32:4283–92. doi: 10.1016/j.biomaterials.2011.02.034
43. Chiu CJ, Scott HJ, Gurd FN. Intestinal mucosal lesion in low-flow states. 2. protective effect of intraluminal glucose as energy substrate. *Arch Surg.* (1970) 101:484–8. doi: 10.1001/archsurg.1970.01340280036010
44. Chen H, Hu YH, Fang Y, Djukic Z, Yamamoto M, Shaheen NJ, et al. Nrf2 deficiency impairs the barrier function of mouse oesophageal epithelium. *Gut.* (2014) 63:711–9. doi: 10.1136/gutjnl-2012-303731
45. Zong X, Song DG, Wang TH, Xia X, Hu WY, Han FF, et al. LFP-20, a porcine lactoferrin peptide, ameliorates LPS-induced inflammation via the MyD88/NF-kappa B and MyD88/MAPK signaling pathways. *Dev Comp Immunol.* (2015) 52:123–31. doi: 10.1016/j.dci.2015.05.006
46. Sastry GM, Adzhigirey M, Day T, Annabhimoju R, Sherman W. Protein and ligand preparation: parameters, protocols, and influence on virtual screening enrichments. *J Comput Aid Mol Des.* (2013) 27:221–34. doi: 10.1007/s10822-013-9644-8
47. Duan Y, Wu C, Chowdhury S, Lee MC, Xiong GM, Zhang W, et al. A point-charge force field for molecular mechanics simulations of proteins based on condensed-phase quantum mechanical calculations. *J Comput Chem.* (2003) 24:1999–2012. doi: 10.1002/jcc.10349
48. Wang JM, Wolf RM, Caldwell JW, Kollman PA, Case DA. Development and testing of a general amber force field. *J Comput Chem.* (2004) 25:1157–74. doi: 10.1002/jcc.20035

49. Darden T, York D, Pedersen L. Particle mesh Ewald - an N.Log(N) method for Ewald sums in large systems. *J Chem Phys.* (1993) 98:10089–92. doi: 10.1063/1.464397
50. Massova I, Kollman PA. Combined molecular mechanical and continuum solvent approach (MM-PBSA/GBSA) to predict ligand binding. *Perspect Drug Discov.* (2000) 18:113–35. doi: 10.1023/A:1008763014207
51. Semple F, MacPherson H, Webb S, Cox SL, Mallin LJ, Tyrrell C, et al. Human β-defensin 3 affects the activity of pro-inflammatory pathways associated with MyD88 and TRIF. *Eur J Immunol.* (2011) 41:3291–300. doi: 10.1002/eji.201141648
52. Garate JA, Oostenbrink C. Lipid a from lipopolysaccharide recognition: Structure, dynamics and cooperativity by molecular dynamics simulations. *Proteins.* (2013) 81:658–74. doi: 10.1002/prot.24223
53. Gibson PR. Increased gut permeability in Crohn's disease: is TNF the link? *Gut.* (2004) 53:1724–5. doi: 10.1136/gut.2004.047092
54. Matricon J. Immunopathogenesis of inflammatory bowel disease. *Med Sci.* (2010) 26:405–10. doi: 10.1051/medsci/2010264405
55. Spiegelman BM, Flier JS. Obesity and the regulation of energy balance. *Cell.* (2001) 104:531–43. doi: 10.1016/S0092-8674(01)00240-9
56. Saleh M, Trinchieri G. Innate immune mechanisms of colitis and colitis-associated colorectal cancer. *Nat Rev Immunol.* (2011) 11:9–20. doi: 10.1038/nri2891
57. DeGraw JI, Almquist RG, Hiebert CK, Colwell WT, Crase J, Hayano T, et al. Stabilized analogs of thymopentin. 1. 4,5-ketomethylene pseudopeptides. *J Med Chem.* (1997) 40:2386–97. doi: 10.1021/jm950803a
58. Liu YF, Xia X, Xu L, Wang YZ. Design of hybrid β-hairpin peptides with enhanced cell specificity and potent anti-inflammatory activity. *Biomaterials.* (2013) 34:237–50. doi: 10.1016/j.biomaterials.2012.09.032
59. Ma Z, Wei DD, Yan P, Zhu X, Shan AS, Bi ZP. Characterization of cell selectivity, physiological stability and endotoxin neutralization capabilities of α-helix-based peptide amphiphiles. *Biomaterials.* (2015) 52:517–30. doi: 10.1016/j.biomaterials.2015.02.063
60. Gangloff M, Gay NJ. MD-2: the Toll 'gatekeeper' in endotoxin signalling. *Trends Biochem Sci.* (2004) 29:294–300. doi: 10.1016/j.tibs.2004.04.008
61. Ohto U, Fukase K, Miyake K, Satow Y. Crystal structures of human MD-2 and its complex with antiendotoxic lipid IVa. *Science.* (2007) 316:1632–4. doi: 10.1126/science.1139111
62. Roh E, Lee HS, Kwak JA, Hong JT, Nam SY, Jung SH, et al. MD-2 as the target of nonlipid chalcone in the inhibition of endotoxin LPS-induced TLR4 activity. *J Infect Dis.* (2011) 203:1012–20. doi: 10.1093/infdis/jiq155
63. Park BS, Song DH, Kim HM, Choi BS, Lee H, Lee JO. The structural basis of lipopolysaccharide recognition by the TLR4-MD-2 complex. *Nature.* (2009) 458:1191–5. doi: 10.1038/nature07830
64. Peri F, Piazza M. Therapeutic targeting of innate immunity with Toll-like receptor 4 (TLR4) antagonists. *Biotechnol Adv.* (2012) 30:251–60. doi: 10.1016/j.biotechadv.2011.05.014
65. Podolsky DK. Inflammatory bowel disease. *N Engl J Med.* (2002) 347:417–29. doi: 10.1056/NEJMra020831
66. Buell MG, Berin MC. Neutrophil-independence of the initiation of colonic injury - comparison of results from 3 models of experimental colitis in the rat. *Digest Dis Sci.* (1994) 39:2575–88. doi: 10.1007/BF02087693
67. Zhang Y, Zhu JL, Guo L, Zou Y, Wang F, Shao H, et al. Cholecystokinin protects mouse liver against ischemia and reperfusion injury. *Int Immunopharmacol.* (2017) 48:180–6. doi: 10.1016/j.intimp.2017.03.028
68. Han FF, Zhang HW, Xia X, Xiong HT, Song DG, Zong X, et al. Porcine β-defensin 2 attenuates inflammation and mucosal lesions in dextran sodium sulfate-induced colitis. *J Immunol.* (2015) 194:1882–93. doi: 10.4049/jimmunol.1402300
69. Raetz CRH, Whitfield C. Lipopolysaccharide endotoxins. *Annu Rev Biochem.* (2002) 71:635–700. doi: 10.1146/annurev.biochem.71.110601.135414
70. Fessler MB, Malcolm KC, Duncan MW, Worthen GS. A genomic and proteomic analysis of activation of the human neutrophil by lipopolysaccharide and its mediation by p38 mitogen-activated protein kinase. *J Biol Chem.* (2002) 277:31291–302. doi: 10.1074/jbc.M200755200
71. Mu XW, Pan C, Zheng SY, Alhamdi Y, Sun BW, Shi QK, et al. Protective effects of carbon monoxide-releasing molecule-2 on the barrier function of intestinal epithelial cells. *PLoS ONE.* (2014) 9:e104032. doi: 10.1371/journal.pone.0104032
72. Park EJ, Thomson ABR, Clandinin MT. Protection of intestinal occludin tight junction protein by dietary gangliosides in lipopolysaccharide-induced acute inflammation. *J Pediatr Gastr Nutr.* (2010) 50:321–8. doi: 10.1097/MPG.0b013e3181ae2ba0
73. Salim SY, Soderholm JD. Importance of disrupted intestinal barrier in inflammatory bowel diseases. *Inflamm Bowel Dis.* (2011) 17:362–81. doi: 10.1002/ibd.21403
74. Turner JR. Intestinal mucosal barrier function in health and disease. *Nat Rev Immunol.* (2009) 9:799–809. doi: 10.1038/nri2653
75. McCall IC, Betanzos A, Weber DA, Nava P, Miller GW, Parkos CA. Effects of phenol on barrier function of a human intestinal epithelial cell line correlate with altered tight junction protein localization. *Toxicol Appl Pharm.* (2009) 241:61–70. doi: 10.1016/j.taap.2009.08.002
76. Qin HL, Zhang ZW, Hang XM, Jiang YQ. L. plantarum prevents enteroinvasive Escherichia coli-induced tight junction proteins changes in intestinal epithelial cells. *BMC Microbiol.* (2009) 9:63. doi: 10.1186/1471-2180-9-63
77. Zhang D, Cheng L, Huang X, Shi W, Xiang J, Gan H. Tetrandrine ameliorates dextran-sulfate-sodium-induced colitis in mice through inhibition of nuclear factor-kappa B activation. *Int J Colorectal Dis.* (2009) 24:5–12. doi: 10.1007/s00384-008-0544-7
78. Hayden MS, Ghosh S. Signaling to NF-kappa B. *Genes Dev.* (2004) 18:2195–224. doi: 10.1101/gad.1228704

Conflict of Interest Statement: The authors declare that the research was conducted in the absence of any commercial or financial relationships that could be construed as a potential conflict of interest.

frontiers in Immunology

ORIGINAL RESEARCH
published: 26 September 2019
doi: 10.3389/fimmu.2019.02192

Short-Lived Immunity After 17DD Yellow Fever Single Dose Indicates That Booster Vaccination May Be Required to Guarantee Protective Immunity in Children

Ana Carolina Campi-Azevedo[1†], Laise Rodrigues Reis[1†], Vanessa Peruhype-Magalhães[1], Jordana Grazziela Coelho-dos-Reis[1], Lis Ribeiro Antonelli[1], Cristina Toscano Fonseca[1], Christiane Costa-Pereira[1], Elaine Maria Souza-Fagundes[2], Ismael Artur da Costa-Rocha[1], Juliana Vaz de Melo Mambrini[1], Jandira Aparecida Campos Lemos[3], José Geraldo Leite Ribeiro[4], Iramaya Rodrigues Caldas[1], Luiz Antônio Bastos Camacho[5], Maria de Lourdes de Sousa Maia[6], Tatiana Guimarães de Noronha[6], Sheila Maria Barbosa de Lima[6], Marisol Simões[6], Marcos da Silva Freire[6], Reinaldo de Menezes Martins[6], Akira Homma[6], Pedro Luiz Tauil[7], Pedro Fernando Costa Vasconcelos[8], Alessandro Pecego Martins Romano[9], Carla Magda Domingues[10], Andréa Teixeira-Carvalho[1] and Olindo Assis Martins-Filho[1*]*

[1] Instituto René Rachou, Fundação Oswaldo Cruz – FIOCRUZ-Minas, Belo Horizonte, Brazil, [2] Departamento de Fisiologia e Biofísica, Universidade Federal de Minas Gerais, Belo Horizonte, Brazil, [3] Secretaria Municipal de Saúde de Belo Horizonte, Belo Horizonte, Brazil, [4] Secretaria do Estado de Saúde de Minas Gerais, Belo Horizonte, Brazil, [5] Escola Nacional de Saúde Pública – FIOCRUZ, Rio de Janeiro, Brazil, [6] Instituto de Tecnologia em Imunobiológicos Bio-Manguinhos – FIOCRUZ, Rio de Janeiro, Brazil, [7] Faculdade de Medicina, Universidade de Brasília, Brasilia, Brazil, [8] Instituto Evandro Chagas, Ananindeua, Brazil, [9] Departamento de Imunização e Doenças Transmissíveis (DEIDT) – Secretaria de Vigilância em Saúde, Ministério da Saúde, Brasilia, Brazil, [10] Programa Nacional de Imunizações – Secretaria de Vigilância em Saúde, Ministério da Saúde, Brasilia, Brazil

OPEN ACCESS

Edited by:
Giuseppe Andrea Sautto, University of Georgia, United States

Reviewed by:
Herwig Kollaritsch, Medical University of Vienna, Austria
Andrea Trevisan, University of Padova, Italy

***Correspondence:**
Ana Carolina Campi-Azevedo
campiazevedo@gmail.com
Olindo Assis Martins-Filho
oamfilho@gmail.com

[†]These authors have contributed equally to this work

Specialty section:
This article was submitted to Vaccines and Molecular Therapeutics, a section of the journal Frontiers in Immunology

Received: *26 June 2019*
Accepted: *30 August 2019*
Published: *26 September 2019*

Citation:
Campi-Azevedo AC, Reis LR, Peruhype-Magalhães V, Coelho-dos-Reis JG, Antonelli LR, Fonseca CT, Costa-Pereira C, Souza-Fagundes EM, Costa-Rocha IAd, Mambrini JVdM, Lemos JAC, Ribeiro JGL, Caldas IR, Camacho LAB, Maia MdLdS, de Noronha TG, de Lima SMB, Simões M, Freire MdS, Martins RdM, Homma A, Tauil PL, Vasconcelos PFC, Romano APM, Domingues CM, Teixeira-Carvalho A and Martins-Filho OA (2019) Short-Lived Immunity After 17DD Yellow Fever Single Dose Indicates That Booster Vaccination May Be Required to Guarantee Protective Immunity in Children. Front. Immunol. 10:2192. doi: 10.3389/fimmu.2019.02192

The Yellow Fever (YF) vaccination is recommended for people living in endemic areas and represents the most effective strategy to reduce the risk of infection. Previous studies have warned that booster regimens should be considered to guarantee the long-term persistence of 17DD-YF-specific memory components in adults living in areas with YF-virus circulation. Considering the lower seroconversion rates observed in children (9–12 months of age) as compared to adults, this study was designed in order to access the duration of immunity in single-dose vaccinated children in a 10-years cross-sectional time-span. The levels of neutralizing antibodies (PRNT) and the phenotypic/functional memory status of T and B-cells were measured at a baseline, 30–45 days, 1, 2, 4, 7, and 10 years following primary vaccination. The results revealed that a single dose induced 85% of seropositivity at 30–45 days and a progressive time-dependent decrease was observed as early as 2 years and declines toward critical values (below 60%) at time-spans of ≥4-years. Moreover, short-lived YF-specific cellular immunity, mediated by memory T and B-cells was also observed after 4-years. Predicted probability and resultant memory analysis emphasize that correlates of protection (PRNT; effector memory $CD8^+$ T-cells; non-classical memory B-cells) wane to critical values within ≥4-years after primary vaccination. Together, these results clearly demonstrate the decline

of 17DD-YF-specific memory response along time in children primarily vaccinated at 9–12 months of age and support the need of booster regimen to guarantee the long-term persistence of memory components for children living in areas with high risk of YF transmission.

Keywords: yellow fever, 17DD vaccine, children, neutralizing antibodies, cellular memory

INTRODUCTION

The Yellow fever (YF) is an acute viral hemorrhagic disease caused by a single-stranded RNA Flavivirus that is endemic in Africa, South America and Central America (1, 2). YF is considered to be a re-emerging public health problem due to increasing number of outbreaks reported in the recent years worldwide (3).

The live attenuated YF vaccine has been an effective and safe control measure available to prevent YF since the 1930s (4). The YF vaccination is recommended for travelers and residents of endemic areas as the most effective strategy to reduce the risk of infection (5). The maintenance of high levels of immunity to YF is necessary to prevent the spread of the disease and large scale access to YF vaccines is critical to establish and maintain high levels of immunity amongst adult and children (3).

According to the World Health Organization, a single dose of YF vaccine is sufficient to provide lifelong protection in the general population (5, 6). However, previous studies have warned that the levels of neutralizing antibodies and the cellular immune responses elicited by YF vaccination decline considerably after primary vaccination (7–14).

Considering that the seroconversion rates observed in children following primary vaccination at 9–12 month of age are already lower than those observed in adults (15), it is expected that the duration of immunity in children would be even shorter as compared to adults. The present study was designed to assess the duration of humoral and cellular immunity following a single dose of 17DD-YF vaccine in children in a 10-year cross-sectional time-span. The quantification of neutralizing antibodies titers (PRNT) and the assessment of phenotypic/functional status of cellular memory were measured at baseline, 30–45 days, 1, 2, 4, 7, and 10 years following primary vaccination. These parameters have been considered relevant proxies of protection and can allow the monitoring of YF-specific immunological memory induced by the 17DD-YF vaccine (16–18).

This study aims to cover the gap in information about the duration of neutralizing antibodies and 17DD-specific T and B-cell memory overtime following the primary vaccination regimen in children. The data presented here bring original insights to support the importance of 17DD-YF booster vaccination in children to restore the YF-specific immune response elicited by primary vaccination.

METHODS

Study Oversight

This study was sponsored by the Programa Nacional de Imunizações-PNI, Ministry of Health, Brazil. The protocol was approved by the research ethics committee at the Escola Nacional de Saúde Pública (CAAE 0014.0.031.000-10, February 20th 2010) as well as at Instituto René Rachou (CAAE 0023.0.245.000-10, February 11th 2011 and CAAE 25315213.6.0000.5091, May 23rd 2015) and registered at the Clinicaltrials.gov (NCT 02990182, January 9th 2015). Written informed consent was obtained from the parents of the participants in this study.

Study Participants and Design

The study population consisted of 673 healthy children, from both genders, with ages ranging from 9 months to 12 years. Participants resided in two municipalities: Contagem and Ribeirão das Neves at Minas Gerais State, Brazil, and these two municipalities had no reports of YF cases for several decades prior the study onset. Moreover, the surveillance for epizootic events had not detected the circulation of YF virus amongst non-human primates in the State of Minas Gerais at the time of the study development. All participants have received, at 9–12 months of age, a single dose of the 17DD-YF substrain vaccine, produced by Instituto de Tecnologia em Imunobiológicos Bio-Manguinhos (FIOCRUZ, Brazil), from the seed lot 993FB013Z. The study was designed and supervised by the authors and structured into "two non-concurrent arms": (i) the first arm was a paired longitudinal analysis to identify early correlates of protection and included two groups, referred as "NV(day 0)"—non-vaccinated children at baseline, $n = 47$ and "PV(day 30–45)"—vaccinees at 30–45 days after primary vaccination, $n = 47$; (ii) the second arm was a cross-sectional analysis comprising of five groups, categorized according to the time after 17DD-YF primary vaccination: "PV(year 1)"—vaccinees at 1 year (8–18 months) after primary vaccination, $n = 141$; "PV(year 2)"—vaccinees at 2 years (19–30 months) after primary vaccination, $n = 114$; "PV(year 4)"—vaccinees at 4 years (31–69 months) after primary vaccination, $n = 128$; "PV(year 7)"—vaccinees at 7 years (75–99 months) after primary vaccination, $n = 116$ and "PV(year 10)"—vaccinees at 10 years (101–142 months) after primary vaccination, $n = 127$.

Heparinized blood samples (7 mL) were collected at health units at Contagem and Ribeirão das Neves (MG, Brazil) and transported to Grupo Integrado de Pesquisas em Biomarcadores at Instituto René Rachou-FIOCRUZ-Minas in Belo Horizonte (MG, Brazil). Blood samples were centrifuged to obtain the plasma that was aliquoted into cryovials and stored at -80°C for further analysis of neutralizing antibodies against yellow fever virus by plaque-reduction neutralization test (PRNT). Mononuclear cells were also isolated to quantify the levels of 17DD-YF specific cellular memory response by *in vitro* phenotypic and functional analyses. In addition to blood collection, a questionnaire was applied to obtain demographic

data. The vaccination status and the date of YF immunization was verified in the vaccination card. Current health status, the use of prescribed medicine, pathological conditions, and any travel history after 17DD-YF vaccination was registered. Eligibility criteria included children of both genders with primary 17DD-YF vaccination at 9–12 months of age, with post-vaccination time ranging from 30–45 days to 10 years. Exclusion criteria encompassed the presence of autoimmune diseases, hemoglobinopathies and transient/permanent immunomodulatory condition. Children with previous history of blood transfusion and therapy based on hyperimmune serum up to 90 days before peripheral blood collection were not recruited to this study. All tests were carried out in a blind fashion without knowing whether the samples were from the first or second arm.

Testing Procedures

YF-Specific Neutralizing Antibodies

Heparin plasma samples were obtained from each volunteer and submitted to Ecteola-cellulose pre-treatment to remove heparin, as previously described by Campi-Azevedo et al. (19), for subsequent use in the PRNT assay. Ecteola-cellulose treated samples were assayed by the micro-$PRNT_{50}$ test according to Simões et al. (20). For the present study, the performances (sensitivity, specificity, and global accuracy) of micro-$PRNT_{50}$ and micro-$PRNT_{90}$ were defined for children samples and the cut-off 1:10 in reciprocal of serum dilution and the micro-$PRNT_{50}$ were selected as the most accurate condition. The micro-$PRNT_{50}$ was performed at the Laboratório de Tecnologia Virológica, Bio-Manguinhos (LATEV, FIOCRUZ-RJ, Brazil). The results were expressed as reverse of sample dilution, considering seropositivity as PRNT titers higher than 1:10 sample dilution.

YF-Specific Phenotypic and Functional Memory

The analysis of 17DD-YF specific cellular memory response was carried out as previously described by Campi-Azevedo et al. (8). Briefly, *in vitro* 17DD-YF-specific peripheral blood lymphoproliferative assay were conducted in two separate batches, referred as: non-stimulated Control Culture and 17DD-YF Culture. After the long-term incubation (144 h), cultured cells were harvested and stained with Live/Dead Dye (Life Technologies, Carlsbad, CA, USA) and a mix of monoclonal antibodies (mAbs) to identify memory T-cell subpopulations (anti-CD4/RPA-T4/FITC; anti-CD8/SK1/PerCP-Cy5.5; anti-CD27/M-T271/PE, and anti-CD45RO/UCHL1/PE-Cy7) and memory B-cell subsets (anti-IgD/IA6-2/FITC, anti-CD27/M-T271/PE, and anti-CD19/HIB19/PerCP). In a parallel, an aliquot of cultured cells were incubated with Live/Dead Dye, labeled with anti-CD8/SK1/PerCP and after pre-fix/permeabilization procedure re-incubated with a cocktail of anti-cytokine mAbs (anti-TNF-α/MAb11/PE-Cy7; anti-IFN-γ/B27/Alexa-Fluor488, and anti-IL-5/JES1-39D10/PE). All monoclonal antibodies were purchased from BD Biosciences (San Jose, CA, USA). Stained cells were washed, fixed and the data was acquired (100,000 lymphocytes/test) on a BD LSRFortessa Flow Cytometer (BD Biosciences, San Diego, CA, USA). FlowJo software (version 9.3.2, TreeStar, San Diego, CA, USA) was used to establish distinct gating strategies to quantify the memory T and B-cells subpopulations as previously described (8), including: "T-cell memory subsets:" Naïve T-cells/(NCD4;NCD8)/$CD27^{+}CD45RO^{-}$; early Effector Memory T-cells/(eEfCD4;eEfCD8)/$CD27^{-}CD45RO^{-}$; Central Memory T-cells/(CMCD4;CMCD8)/$CD27^{+}CD45RO^{+}$ and Effector Memory T-cells/(EMCD4;EMCD8)/$CD27^{-}CD45RO^{+}$ and "B-cell memory subsets:" Naïve B-cells/(NCD19)/$CD27^{-}IgD^{+}$; Non-classical Memory B-cells/(nCMCD19)/$CD27^{+}IgD^{+}$ and Classical Memory B-cells/(CMCD19)/$CD27^{+}IgD^{-}$. The percentage of $cytokine^{+}$ $CD8^{+}$ T-cells was also quantified. The results were reported as 17DD-YF-stimulated Culture/non-stimulated Control Culture Index, calculated as the ratio of results observed in the 17DD-YF-stimulated Cultures divided by the respective non-stimulated Control Culture.

Data Analysis

The GraphPad Prism software, Version 5.0 (San Diego, CA, USA) was employed to perform all statistical analyses. Kolmogorov-Smirnov, D'Agostino and Pearson omnibus and Shapiro-Wilk normality tests were used to check data distribution. Multiple strategies were employed for data analysis. Kruskal-Wallis test followed by Dunn's post-test were employed for intergroup comparative analysis. The Chi-square test was used to compare seropositivity rates, biomarker signatures, descriptive analysis of selected biomarkers and analysis of resultant memory. Spearman's correlation test was carried out to determine the PRNT wane along time continuum. In all cases, significant differences were considered at $p < 0.05$.

Biomarker signature analysis was carried out using the 75th percentile (3rd quartile) values for each biomarker (17DD-YF-stimulated Culture/non-stimulated Control Culture Index) as the cut-off edge to identify subjects with high biomarker levels. Those biomarkers with more than 25% of subjects above the cut-off were considered for comparative analysis amongst groups. Venn diagram analysis (http://bioinformatics.psb.ugent.be/webtools/Venn/) was employed to identify biomarkers observed selectively in PV (days 30–45), referred as correlates of protection. Overlay of ascendant biomarker signatures were employed for comparative analysis of time-depended changes in immunological profile after primary vaccination.

Logistic and multinomial regression models were constructed to evaluate the association between time after vaccination and changes in the biomarker levels. Following this, the fitted regression model was employed to calculate the predicted probabilities for each biomarker (isolated or combined) along time continuum. The Receiver Operating-Characteristic curves (ROC) were was constructed to estimate the capacity of time as a predictor of changes in biomarkers levels to monitor the 17DD-YF memory after primary vaccination in children. The Area Under the ROC Curve (AUC) was used for comparative analysis of predictive capacity amongst biomarkers (isolated or combined).

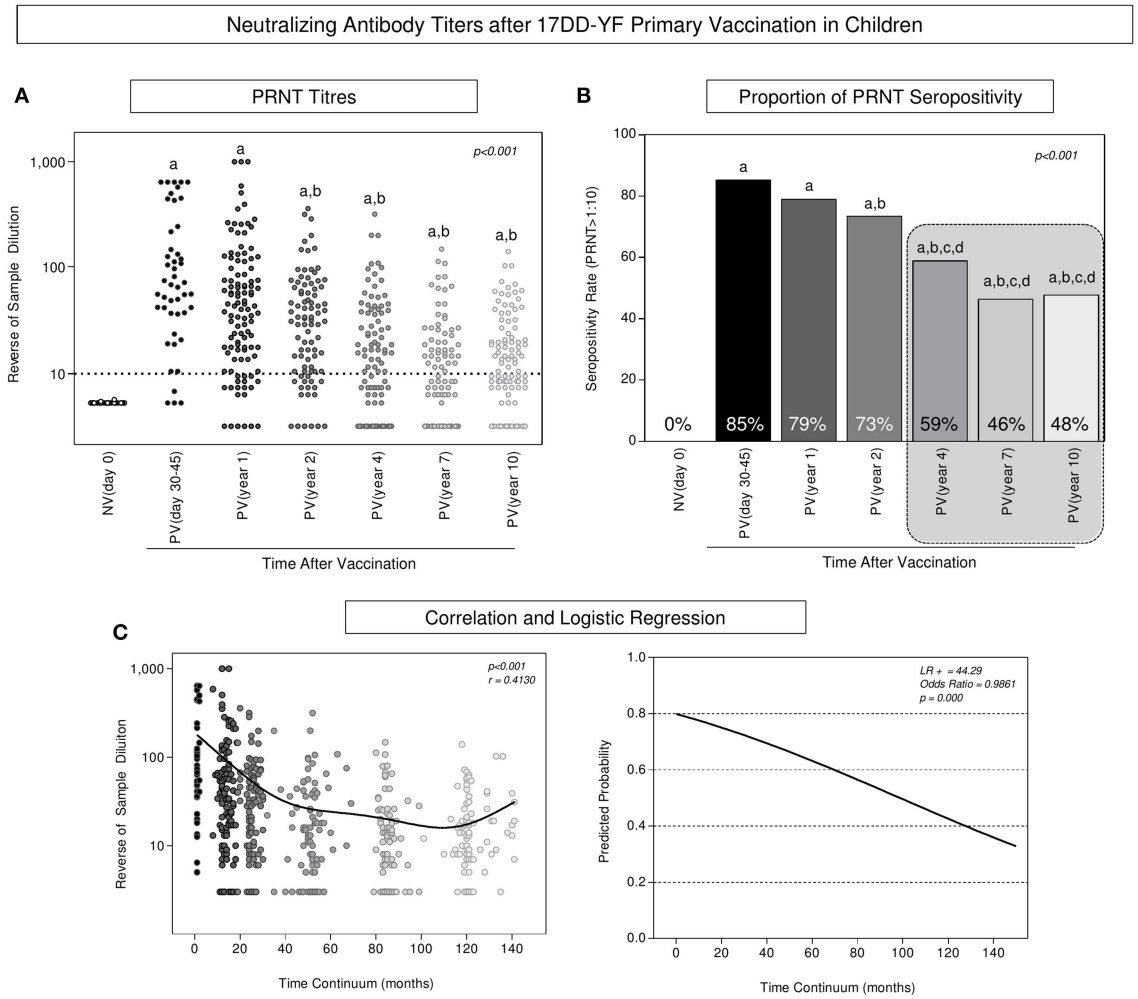

FIGURE 1 | Neutralizing antibody titers after 17DD-YF primary vaccination in children. PRNT titers were measured in Ecteola-treated plasma samples (19) from non-vaccinated children at baseline NV(day 0)/(○, $n = 47$) and at different times after primary vaccination: PV(day 30–45)/(●, $n = 47$), PV(year 1)/(◍, $n = 141$), PV(year 2)/(◍, $n = 114$), PV(year 4)/(◍, $n = 128$), PV(year 7)/(◍, $n = 116$), and PV(year 10)/(◦, $n = 127$), as described previously by Simões et al. (20). **(A)** The PRNT levels were expressed in reverse of serum dilution. **(B)** Proportion of PRNT seropositivity (PRNT>1:10) were calculated for each group and the results expressed as seropositivity rates at baseline NV(day 0) [□] and at different times after primary vaccination: PV(day 30–45) [■], PV(year 1) [▩], PV(year 2) [▩], PV(year 4) [▩], PV(year 7) [▩], and PV(year 10) [▩], considering the serum dilution >1:10 as the cut-off (dashed line). **(C)** Correlation and logistic regression were employed to determine the wane of PRNT levels along time continuum and the results expressed as reverse of serum dilution and predicated probability, respectively. Statistical analysis was carried out as described in Methods. In all cases, significant differences at $p < 0.05$ were underscored by using letters "a," "b," "c," and "d" for comparisons with NV(day 0), PV(day 30–45), PV(year 1), and PV(year 2), respectively and the *p*-values provide in the figure. Spearman correlation indices as well as Likelihood and Odds ratio are provided in the figure. Gray rectangle highlights the critical decrease of PRNT seropositivity rates ≥4 years after primary vaccination.

RESULTS

Progressive Time-Dependent Decrease in Neutralizing Antibody Titers Is Observed After 17DD-YF Primary Vaccination in Children

The levels of neutralizing antibodies, the proportion of PRNT seropositivity along with the correlation between PRNT levels and the logistic regression analysis of PRNT levels along time continuum are presented in the **Figure 1**. Data analysis revealed that primary vaccination induced a significant increase in the PRNT levels (**Figure 1A**) reaching a seropositivity rate of 85% in PV(day 30–45) as compared to NV(day 0) (**Figure 1B**). A progressive decrease in the PRNT levels was observed along time as early as 2 years after primary vaccination as compared to PV(days 30–45) (**Figure 1A**). Critical seropositivity rates (below 60%) were observed amongst vaccinees, particularly ≥4 years after primary vaccination (**Figure 1B**, gray dashed rectangle). Correlation analysis further supports the waning phenomenon observed in the PRNT levels along time after primary vaccination in children (**Figure 1C**). Furthermore, the outstanding likelihood ratio ($LR^+ = 44.29$) and odds

ratio (OR = 0.9861, 95% CI = 0.9819–0.9903) reinforce the abrupt and progressive decline month to month in PRNT levels along time continuum, which reached values of 0.8454, 0.6025, and 0.1865 at 12, 36, and 120 months, respectively (**Figure 1C**).

Primary 17DD-YF Vaccination in Children Elicits Short-Lived YF-Specific Cellular Memory Mediated by Effector CD4$^+$ and CD8$^+$ T-Cells and Non-classical B-Cells

The analysis of YF-specific phenotypic and functional biomarkers was evaluated upon *in vitro* 17DD-YF antigen recall and the results are presented in **Figure 2**. An increase of memory T-cells (eEfCD4, eEfCD8, EMCD4, and EMCD8) as well as nCMCD19 cells along with an up-regulation of TNF-α and IFN-γ produced by CD8$^+$ T-cells is observed in PV(day 30–45) as compared to NV(day 0) (**Figures 2A,B**). Moreover, a significant decrease in these biomarkers occurs along the time, particularly ≥4 years after primary vaccination when almost all these attributes decline as compared to PV(days 30–45) (**Figure 2**).

Biomarker Signatures Emphasize the Short-Term Persistence of Phenotypic Effector Memory and Functional Activity of CD8$^+$ T-Cells

In order to accomplish the characterizing of the duration of phenotypic and functional memory induced by the 17DD-YF primary vaccination in children, the biomarker signatures were built for comparative analyses along time. To accomplish this goal, initially overlaid biomarkers signatures of NV(day 0) vs. PV(days 30–45) were assembled to identify attributes selectively observed in PV(day 30–45), further referred as correlates of protection in children (**Figure 3A**). Venn diagram analysis indicated that besides three common attributes (eEfCD4, eEfCD8, and CMCD19), five biomarkers (EMCD4, EMCD8, nCMCD19, TNFCD8, and IFNCD8) were tagged to be employed as selective correlates of protection for follow-up analysis overtime after primary 17DD-YF vaccination (**Figure 3B**).

Once the correlates of protection for follow-up analysis were selected, overlaid biomarker signatures were constructed to verify changes along time upon 17DD-YF primary vaccination (**Figure 3C**). Data analysis pointed out that all five biomarkers were persistently observed in PV(day 30–45) and PV(year 1). Although some attributes were not observed in PV(year 2), the lack of EMCD8, considered one of the top biomarkers to monitor the immunological memory to 17DD-YF vaccine (9) was noticed in PV(year 4), PV(year 7), and PV(year 10) (**Figure 3C**).

Descriptive Analysis Confirms the Time-Dependent Decrease of Proxies of Protection Upon 17DD-YF Primary Vaccination in Children

The biomarkers tagged as correlates of protection (EMCD4, EMCD8, nCMCD19, TNFCD8, and IFNCD8) were employed together with the neutralizing antibody levels to carry out a descriptive analysis to monitor the YF-specific memory along time after 17DD-YF primary vaccination. For this purpose, the proportion of subjects displaying biomarkers levels above the 75th percentile cut-off and PRNT levels >1:10 were calculated and data reported for each group (**Figure 4A**). Data demonstrated that in NV(day 0) there is a predominance of subjects displaying 0–1 biomarkers above that cut-off. Conversely, in the PV(day 30–45) there is a significantly higher prevalence of subjects displaying 3 biomarkers above that cut-off. In PV(year 1) and PV(year 2) there was a balanced proportion of subjects displaying 1–2 biomarkers above that cut-off. Notably, in PV(year 4), PV(year 7), and PV(year 10) there was a higher prevalence confined in only one biomarker above that cut-off (**Figure 4A**). Complementary analysis further revealed that the median number of biomarkers above that cut-off found in PV(day 30–45), PV(year 1), and PV(year 2) was higher as compared to NV(day 0). Although in PV(year 4), the median value still differed from that observed in NV(day 0), it was lower as compared to PV(days 30–45). Additionally, a critical median number of biomarkers above that cut-off was observed in PV(year 7) and PV(year 10) as compared to PV(days 30–45) that did not differ from those found in NV(day 0) (**Figure 4B**). Based on these findings, the vaccinees were distributed into two major groups referred as PV(≤year 2) and PV(≥year 4). The results showed that both groups presented higher median number of biomarkers above the cut-off as compared to NV(day 0), although the PV(≥year 4) group exhibited lower values as compared to PV(≤year 2) (**Figure 4B**).

Predicted Probability Analysis Emphasizes That Neutralizing Antibody Levels (PRNT), EMCD8, and nCMCD19 Are the Top Biomarkers to Monitor the 17DD-YF Memory After Primary Vaccination in Children

Logistic and multinomial regression models were constructed and the fitted regression model employed to calculate the predicted probabilities for each biomarker previously tagged as correlates of protection (EMCD4, EMCD8, nCMCD19, TNFCD8, and IFNCD8) to monitor the 17DD-YF memory after primary vaccination along time continuum. The ROC curves were constructed for comparative analysis of predicted capacity amongst biomarkers (isolated or combined). Based on the global accuracy (Area Under the ROC Curve—AUC), the neutralizing antibody levels (PRNT), EMCD8, and nCMCD19 presented moderate performance when employed isolated as a single parameter to monitor the 17DD-YF memory after primary vaccination in children (AUC = 0.6777; 0.5601, and 0.5770, respectively) (**Figure 5A**). The combined analysis of neutralizing antibody levels (PRNT), and EMCD8 and nCMCD19 further improved the predictive capacity of using these biomarkers to monitor the 17DD-YF memory after primary vaccination in children (AUC = 0.9201) (**Figure 5B**).

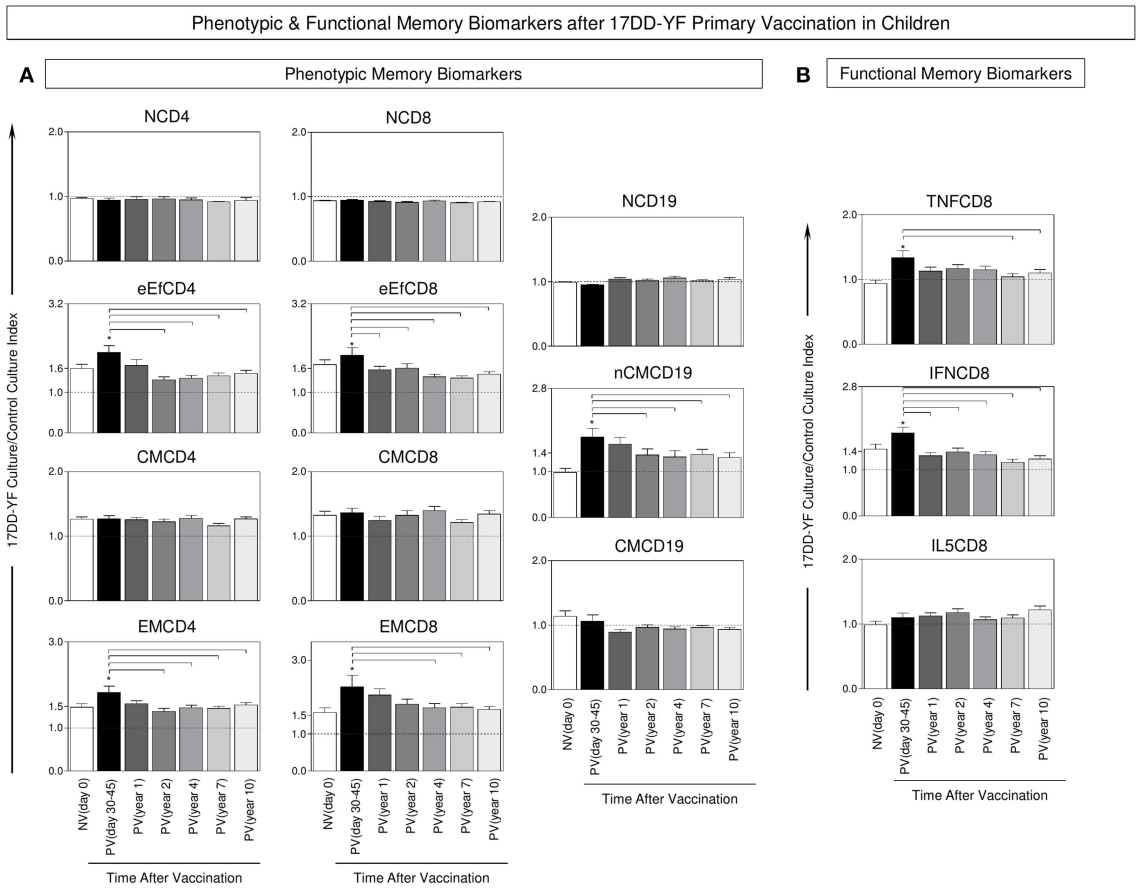

FIGURE 2 | Phenotypic and functional memory biomarkers after 17DD-YF primary vaccination in children. The analysis of 17DD-YF-specific memory was measured upon *in vitro* 17DD-YF antigen recall as described previously by Campi-Azevedo et al. (8) for non-vaccinated children at baseline NV(day 0)/(□, $n = 47$) and at different times after primary vaccination: PV(day 30–45)/(■, $n = 47$), PV(year 1)/(■, $n = 141$), PV(year 2)/(■, $n = 114$), PV(year 4)/(■, $n = 128$), PV(year 7)/(■, $n = 116$), and PV(year 10)/(□, $n = 127$). **(A)** Flow cytometric staining were used to quantify phenotypic features of T-cell memory subsets: Naïve T-cells/(NCD4;NCD8)/$CD27^{+}CD45RO^{-}$; early Effector Memory T-cells/(eEfCD4;eEfCD8)/$CD27^{-}CD45RO^{-}$ Central Memory T-cells/(CMCD4;CMCD8)/$CD27^{+}CD45RO^{+}$ Effector Memory T-cells/(EMCD4;EMCD8)/$CD27^{-}CD45RO^{+}$ and B-cell memory subsets: Naïve B-cells/(NCD19)/$CD27^{-}IgD^{+}$; Non-classical Memory B-cells/(nCMCD19)/$CD27^{+}IgD^{+}$ and Classical Memory B-cells/(CMCD19)/$CD27^{+}IgD^{-}$. **(B)** Flow cytometric staining were also performed to quantity functional $CD8^{+}$ T-cells producing TNF-α, IFN-γ and IL-5. The data were reported as median values ± inter-quartile range for 17DD-YF-stimulated Culture/non-stimulated Control Culture Index as described in Methods, highlighting the equivalence ratio by dashed line (Index = 1.0). Significant differences at $p < 0.05$ were underscored by using asterisk (*) to identify differences between NV(day 0) vs. PV(day 30–45) and intergroup differences identified by connecting lines.

The Resultant Memory (PRNT, EMCD8, or NCMCD19) Wanes Overtime Reaching Critical Values at 4 or More Years After 17DD-YF Primary Vaccination in Children

The results of neutralizing antibody levels (PRNT), EMCD8, and nCMCD19 profiles were combined at individual level to build a memory matrix and calculate the resultant YF-specific memory, comprising of humoral (PRNT) and cell-mediated (EMCD8 or nCMCD19) immunity. Then, each volunteer was classified as they present "None," "PRNT," "EMCD8 and/or nCMCD19," or "Both" attributes above the cut-off threshold, i.e., PRNT positivity at serum dilution >1:10, EMCD8 (17DD-YF-stimulated Culture/non-stimulated Control Culture >2.19) or nCMCD19 (17DD-YF Culture/Control Culture >1.66). The results demonstrated that 17DD-YF primary vaccination was able to guarantee persistent resultant memory in 79% of children included into PV(≤year 2). Conversely, a clear decline in the resultant memory down to 55% was observed into PV(≥year 4). Specifically, the resultant memory initially observed in 96% of children in PV(day 30–45) decrease to 77% in PV(year 1) and 73% in PV(year 2) followed by a marked shift down to 53, 55, and 58% in PV(year 4), PV(year 7) and PV(year 10), respectively (**Figure 6**).

DISCUSSION

The YF vaccination is currently recommended as a single dose for residents of disease risk areas and people traveling from or to those areas, who aged 9 months or older (5, 6,

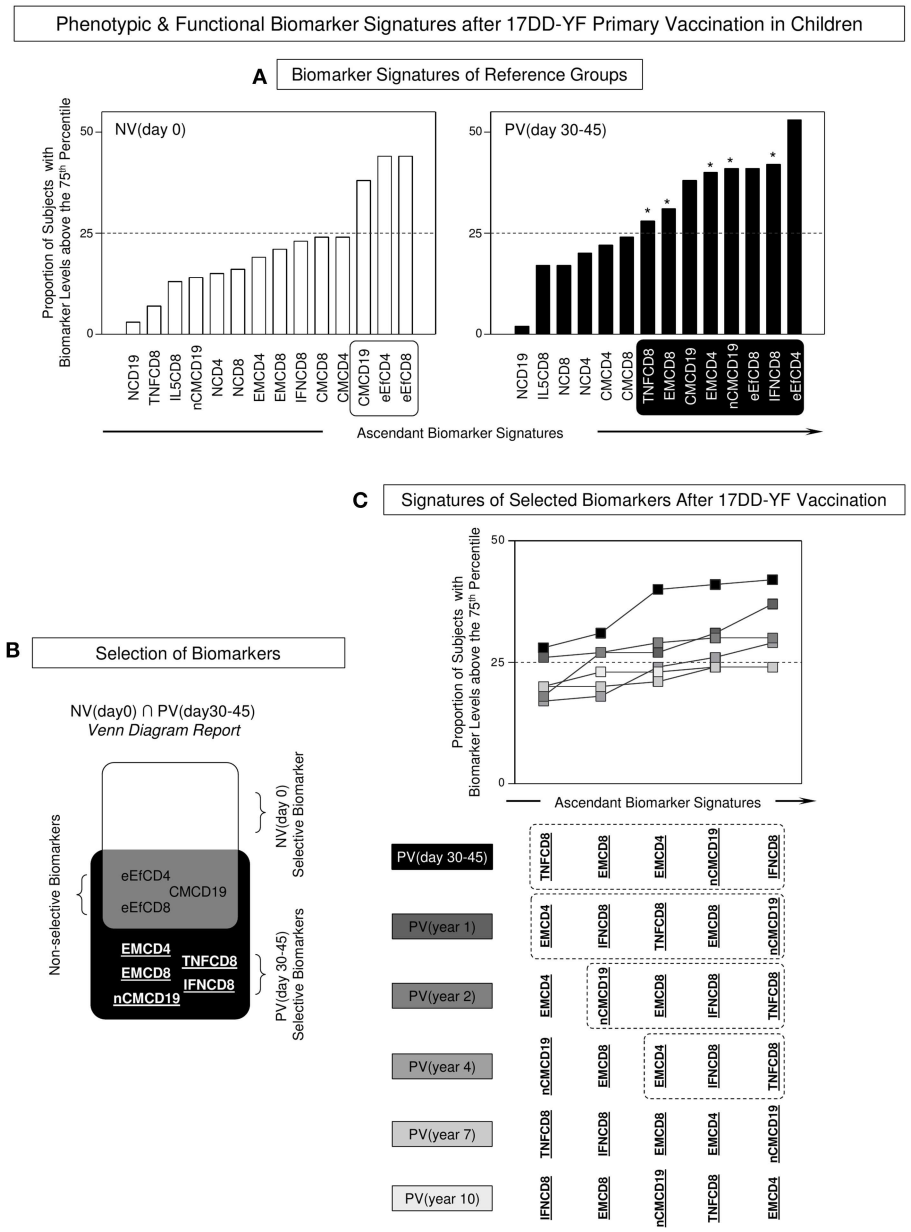

FIGURE 3 | Phenotypic and functional biomarker signatures after 17DD-YF primary vaccination in children. **(A)** Biomarker signatures of reference groups NV(day 0) [□] and PV(day 30–45) [■] were assembled to select biomarkers above the 75th percentile with proportions higher than the 25% in each group (white/black background rectangles). The selected biomarkers were underscored by asterisk (*) to identify differences between NV(day 0) vs. PV(day 30–45). **(B)** Venn diagram report was employed to identify the set of biomarkers selectively increased in [PV(day 30–45) vs. NV(day 0)]. The attributes EMCD4, EMCD8, nCMCD19, TNFCD8, and IFNCD8 were underscored as PV (day 30–45)-selective biomarkers. These attributes were tagged in bold underline format and employed for follow-up analysis overtime after 17DD-YF primary vaccination. Biomarkers with proportion higher than the 25% were underscored by asterisk (*) to identify differences between NV(day 0) vs. PV(day 30–45). **(C)** Overlaid signatures of selected biomarkers were assembled to identify changes in the 17DD-YF specific phenotypic and functional features at different times after primary vaccination: PV(day 30–45) [■], PV(year 1) [■], PV(year 2) [■], PV(year 4) [■], PV(year 7) [■], and PV(year 10) [□]. Dashed rectangles underscore the critical decline of selected biomarkers overtime after primary vaccination with absence of EMCD8 ≥ 4 years after primary vaccination.

21–23). According to the WHO, very few primary vaccine failures following YF vaccination have been reported. It has been proposed that, in addition to neutralizing antibodies, both innate and cell-mediated immunity also contribute to the initial immune response. Defining the parameters that modulate vaccine responses is relevant to increase vaccine effectiveness. It has been proposed that several factors may affect the YF vaccine response including: genetic background, gender,

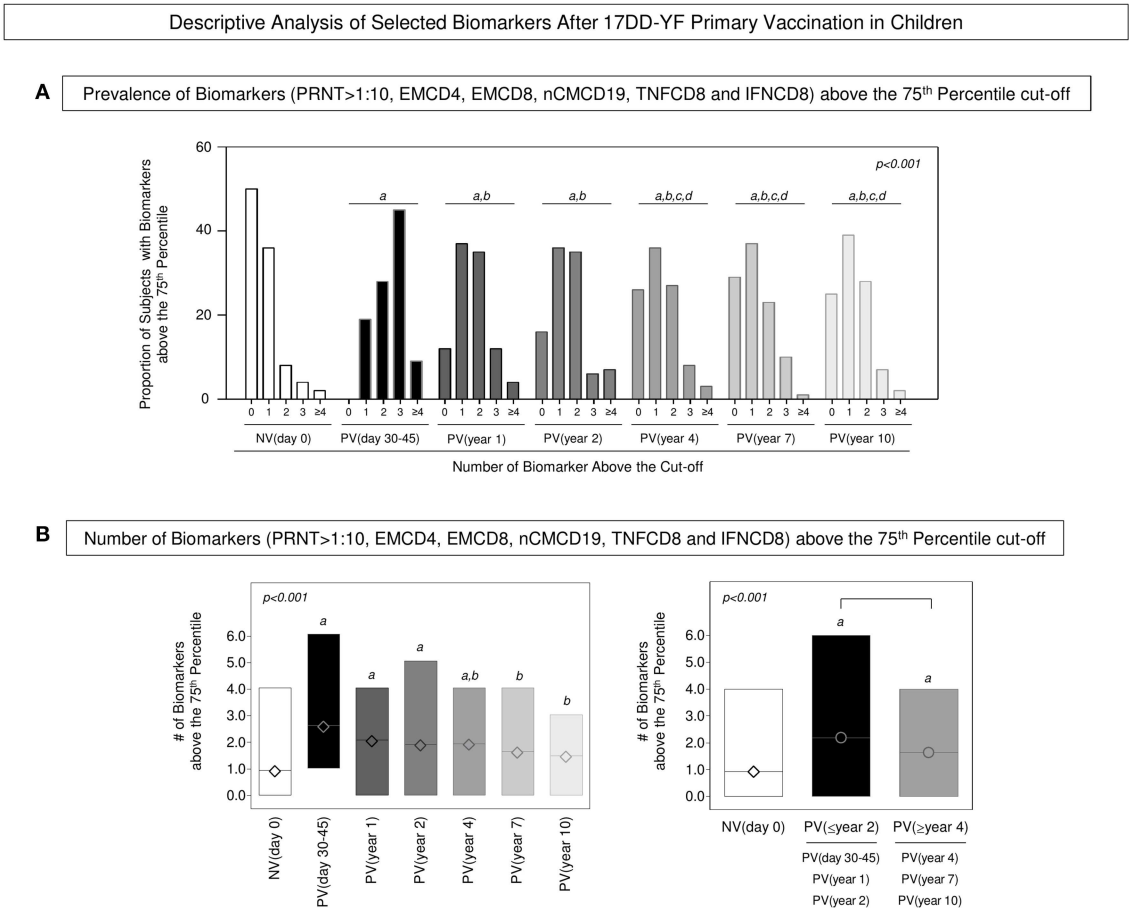

FIGURE 4 | Descriptive analysis of selected biomarkers after 17DD-YF primary vaccination in children. **(A)** Prevalence of Biomarkers (PRNT>1:10, EMCD4, EMCD8, nCMCD19, TNFCD8, and IFNCD8) above the 75th percentile cut-off. Data are presented as proportion of subjects with biomarkers above the cut-off at baseline NV(day 0) [□] and at different times after primary vaccination: PV(day 30–45) [■], PV(year 1) [■], PV(year 2) [■], PV(year 4) [■], PV(year 7) [■], and PV(year 10) [□]. **(B)** Number of Biomarkers (PRNT>1:10, EMCD4, EMCD8, nCMCD19, TNFCD8, and IFNCD8) above the 75th Quartile cut-off. Data are presented as mean (min to max) number of biomarkers above the cut-off at baseline NV(day 0) [◇] and at different times after primary vaccination: PV(day 30–45) [◆], PV(year 1) [◈], PV(year 2) [◈], PV(year 4) [◈], PV(year 7) [◈], and PV(year 10) [◇] as well as PV(≤year 2) [●], PV(≥year 4) [◍]. Significant differences at $p < 0.05$ are underscored by using letters "a," "b," "c," and "d" for comparisons with NV(day 0), PV(day 30–45), PV(year 1), and PV(year 2), respectively. Intergroup differences are identified by connecting lines. The *p*-values are provided in the figure.

age, and environmental differences. Muyanja et al. (24) have proposed that host-specific immune response microenvironment may contribute to the effectiveness of the 17D-YF vaccine. These authors have suggested that an activated immune microenvironment prior to vaccination impedes the efficacy of the 17D-YF vaccine in an African cohort and suggest that booster regimens should be proposed to improve efficient immunity after YF vaccination. Other studies have suggested that the ability of YF-17D vaccine to infect dendritic cells and activate multiple Toll-like receptors seems to be essential for generating a potent immune response after vaccination (17, 25). A distinct hypothesis have been tested to explain the lower seropositivity rates after YF vaccination in children. An observational multicenter study, carried out by the Collaborative Group for Studies on Yellow Fever Vaccines has reported that the 17DD-YF vaccine reached distinct seroconversion rates in children according to the age at vaccination (26). Moreover, it has been demonstrated that simultaneous administration of other viral vaccines reduces significantly the response to YF vaccine in children (15). Conversely, no association between seroconversion rates and the maternal immunity status to YF has been observed (27). Our group have previously observed that children non-responsive to primary 17DD-YF vaccine presented a striking lack of innate immunity pro-inflammatory response, specially low levels of IL-12$^+$ and TNF-α$^+$ neutrophils and monocytes, along with an increased regulatory profile in the adaptive response, including higher levels of IL-4$^+$CD4$^+$ T cells as well as IL-10$^+$ and IL-5$^+$CD8$^+$ T cells (28). Interestingly, the revaccination of children with primary vaccination failure was able to restore the innate and adaptive immunity toward a balanced pro-inflammatory/regulatory profile.

Some studies that investigated the impact of booster doses on the status of YF-specific immune response in adults postulated that booster vaccination did not increase the titers of YF-specific

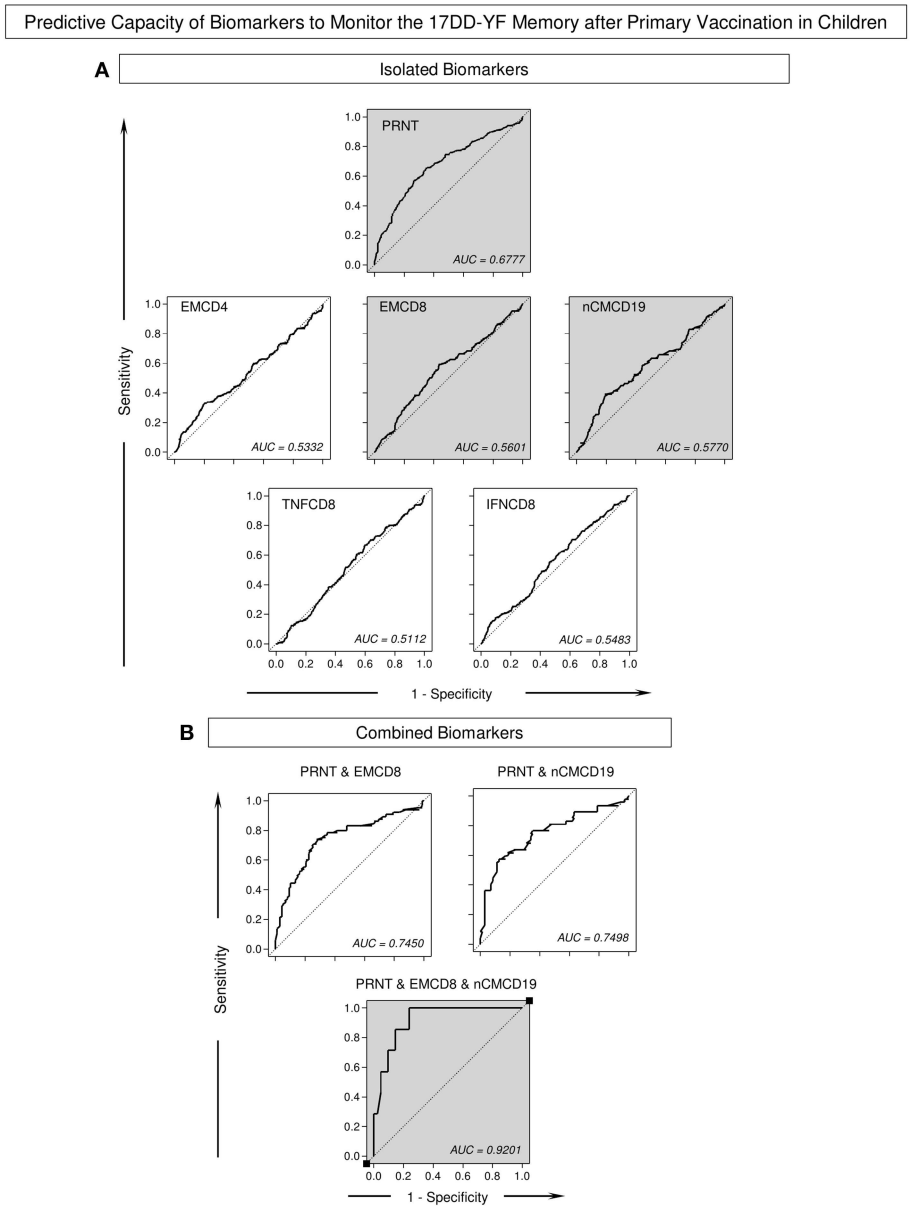

FIGURE 5 | Predictive capacity of biomarkers to monitor the 17DD-YF memory after primary vaccination in children. The Receiver Operating Characteristic (ROC) curves were used to estimate the capacity of time as a predictor of changes in biomarker levels to monitor the 17DD-YF memory after primary vaccination in children. Logistic and multinomial regression models were constructed to evaluate the association between time after vaccination and changes in the biomarker levels. Following, the fitted regression model was employed to calculate the predicted probabilities for each biomarker **(A)** isolated or **(B)** combined along time continuum. The Area Under the ROC Curves (AUC) were employed for comparative analysis of predictive capacity amongst biomarkers and the values provided in the figure. The gray background highlights the top three isolated biomarkers and the best combination of predictor biomarkers to monitor the 17DD-YF memory after primary vaccination in children.

antibodies nor induced or altered the phenotypes of $CD8^+$ T-cells and the immune responses observed following revaccination were reduced compared to primary responses (23, 29, 30). However, other studies have demonstrated that booster doses are relevant to guarantee the long-term persistence of 17DD-YF-specific memory components in travelers (31) and in residents of areas with YF-virus circulation (32, 33). Therefore, the single dose recommendations for YF vaccines have been considered controversial.

The decision to no longer recommend booster vaccination may especially have a direct impact on children, given that besides higher primary vaccination failures (15), there is no evidence for the long-term persistence of protective immunity in primary vaccinated children. Our group has already described the occurrence of time-dependent loss of YF-immunity in primary vaccinated adults (7–9). If this scenario also occurs in children it would contribute to worsening the setting in which a large proportion of individuals would become exposed to potential

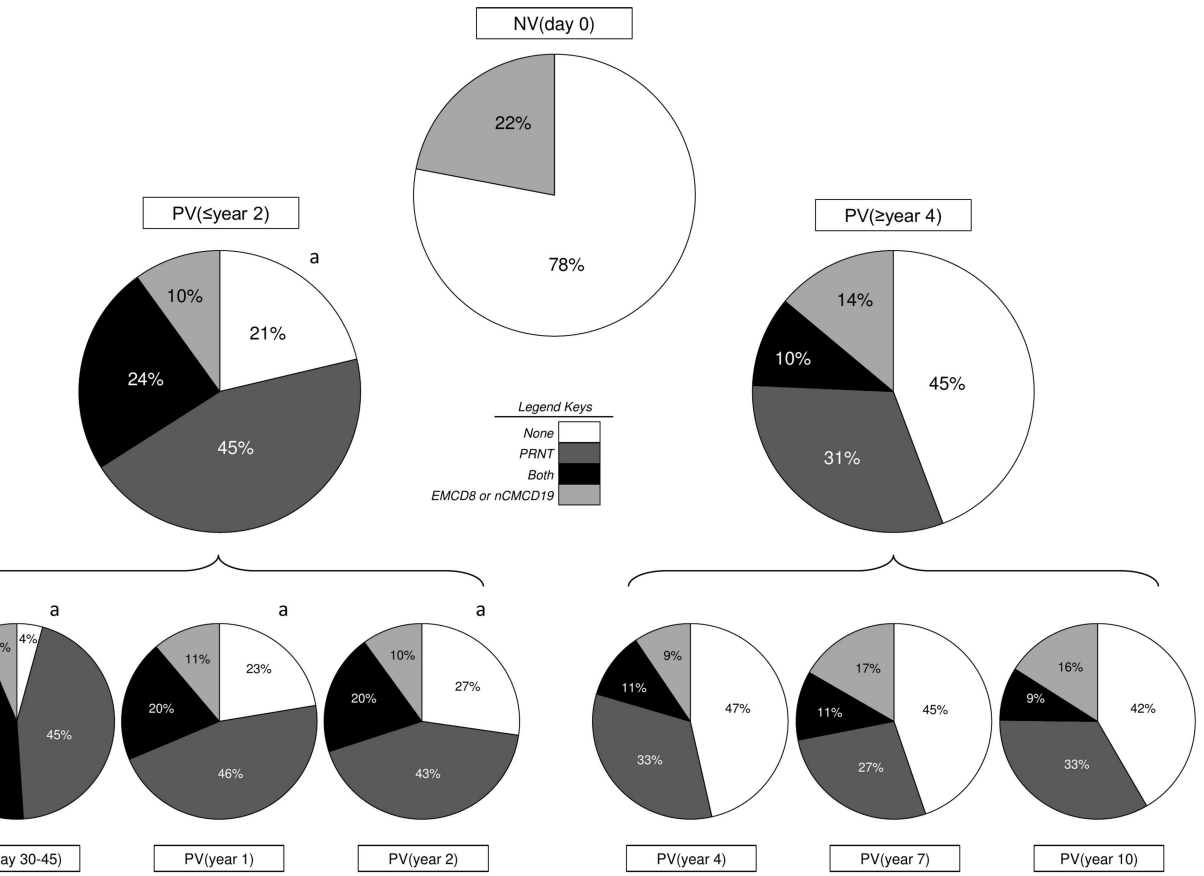

FIGURE 6 | Resultant memory (PRNT, EMCD8, or nCMCD19) after 17DD-YF Primary vaccination in children. The resultant memory status (PRNT, EMCD8, or nCMCD19) were assessed at individual level to define the overall proportion of subjects presenting None (◔), PRNT (◕), cellular memory "EMCD8 and/or nCMCD19" (◔) or both attributes "PRNT and cellular memory" (●) at distinct time-points before/after primary 17DD-YF vaccination, including: NV(day 0), PV(≤year 2), PV(≥year 4) as well as PV(day 30–45), PV(year 1), PV(year 2), PV(year 4), PV(year 7), and PV(year 10). Significant differences ($p < 0.05$) of resultant memory status amongst study groups were assessed by Chi-square test and represented by letter "a" as compared to NV(day 0).

risk of YF infection, especially in endemic areas of high virus circulation. As indicated by the results of the present study, a substantial proportion of children could be susceptible to YF-virus infection, especially in endemic areas.

The studies that evaluated the timeline kinetics of correlates of protection after 17D-YF and 17DD-YF vaccination in adults have demonstrated that both humoral and cellular-mediated YF-specific immunity display a relevant decline overtime in single dose recipients of YF vaccines and that the booster doses efficiently improve the immunological status in re-vaccinated recipients (29–33). Recent studies from our group have shown that secondary or multiple vaccination regimens in adults are able to further improve the immunity parameters triggered by primary 17DD-YF vaccination and restore the resultant YF-specific memory in 100% of the volunteers. Moreover, it was observed that all vaccinees had at least one or both proxy of protection detectable at ≥10 years post-secondary vaccination (33).

Previous studies from our group have compared the cytokine-mediated immune response triggered by 17D-213/77-YF or 17DD-YF vaccines in children submitted to primary vaccination at 9–12 month of age with those non-responders to primary vaccination and also with those that received (28, 34). The results demonstrated that all children that received a booster dose 1 year after primary vaccination failure seroconverted and shifted the overall cytokine signatures toward a balanced pro-inflammatory/regulatory response of innate and adaptive immunity, overcoming the striking lack of innate immunity pro-inflammatory response observed in non-responder children (28, 34). These studies clearly indicated that booster regimens are relevant to guarantee the persistence of long-term immunity in areas with high risk of yellow fever transmission.

Data about the duration of YF-specific immunity in children following primary vaccination is still scarce and can provide supporting evidence to support the public health programs for

YF control worldwide. In this sense, the present investigation was designed to explore the duration of humoral and cellular immunity in primary vaccinated children in a 10-years cross-sectional timeline.

Our findings indicate that a substantial proportion of children lose their antiviral humoral immunity at 4 or more years after 17DD-YF primary vaccination. The PRNT has been considered the classical gold standard to measure post-vaccination immunity to YF for decades and generally regarded as the most appropriate parameter for monitoring protection by YF vaccine (6, 16). Reports from Niedrig et al. (16) regarding the timeline kinetics of YF-neutralizing antibody after 17D-YF vaccination in adults demonstrated that seropositivity rates (>1:10) significantly decrease from 94.0 to 74.5% from 1 to 10 years, respectively. In fact, upon closer inspection, the data clearly showed that antibody titers declined more rapidly during the first 1–4 years after 17D-YF vaccination and that seropositivity rates (>1:10) reached 69% when vaccinees are grouped together from 5 to 35 years post vaccination (13, 16). This rapid decline in neutralizing antibodies early after YF vaccination was also in a study by Hepburn et al. (29), which demonstrated that antibody levels decayed within 3–4 years in approximately half of the adult vaccines, even after booster vaccination.

Short-lived persistence of cell-mediated immunity has also been observed in memory T and B-cells (EMCD4; EMCD8; TNFCD8; IFNCD8; nCMCD19) after 4-years after a 17DD-YF single dose. Complementary predicted probability analysis together with resultant memory assessment highlighted that besides neutralizing antibody levels (PRNT), the levels of EMCD8 and nCMCD19 also decline to critical values at ≥4-years after primary vaccination. Several studies strongly suggested that $CD8^+$T cells are relevant for immune protection upon YF after primary or secondary vaccination (8, 9, 17, 35). The role of nCMCD19 cells has not been completely elucidated in YF-vaccinated recipients. It is known that the maintenance of long-lived plasma cells that secrete antigen-specific antibodies, as well as memory B-cells, is essential for protection against pathogens, and is the basis of successful vaccinations (36). The nCMCD19 cells ($IgD^+CD27^+CD19^+$) are known as unclass-switched cells with similar functions compared to classical switched memory B-cells ($IgD^-CD27^+CD19^+$) and are not in the process of transition from naive to memory B cells. These nCMCD19 cells are believed to play an important role in secondary immune response in early phases of infection (37).

The current study further indicates that booster vaccination regimen may be required to guarantee protective immunity in children. The rapid and expressive loss of humoral and cellular immunity in a subpopulation of primary vaccinated children suggests that the first booster dose of vaccine should be administered within 4–5 years after primary vaccination instead of 10 years after vaccination as proposed previously for adults (32, 33).

The study's limitations include the cross-sectional representation of the average immune status of several birth cohorts, which assumed they differ only in time after vaccination, although this seems a legitimate assumption given that the vaccine and immunization practices have remained unchanged in the time period of those cohorts. Another limitation could be the possibility of booster by natural infections, as those children lived in an area where YF vaccine is recommended. However, it is important to mention that the study participants lived in a metropolitan region where there had been no cases in humans and non human primates.

The inclusion of the YF vaccine into worldwide immunization program for children living in endemic areas represents an important measure to ensure the YF-immunization in infancy and guarantee the effective control of YF expansion. The knowledge about duration of correlates of protection following YF vaccination in children is relevant to support further decisions to be made regarding the need of revaccination and to define the precise time for booster regimens. The results presented here add scientific knowledge about the immune response induced by 17DD-YF vaccine and bring new insights and increase awareness for healthcare workers about the importance of YF vaccination/revaccination in childhood. Moreover, our results may support the revision of the recommendation for a single dose YF-vaccine and will certainly guarantee that a large contingent of children will be revaccinated, improving the prevention of YF. Altogether, these data would be helpful to define targets and indicators for protection and susceptibility, especially in endemic countries with high historical rates of YF virus circulation in continuous expansion.

DATA AVAILABILITY

All datasets generated for this study are included in the manuscript/supplementary files.

ETHICS STATEMENT

This studies involving human participants were reviewed and approved by the research ethics committee at the Escola Nacional de Saúde Pública (CAAE 0014.0.031.000-10, February 20th 2010) as well as at Instituto René Rachou (CAAE 0023.0.245.000-10, February 11th 2011 and CAAE 25315213.6.0000.5091, May 23rd 2015) and registered at the Clinicaltrials.gov (NCT 02990182, January 9th 2015). Written informed consent to participate in this study was provided by the participants' legal guardian/next of kin.

AUTHOR CONTRIBUTIONS

AC-A, IC, LC, MM, MF, RM, AH, PT, PV, AR, CD, AT-C, and OM-F: designing research study. IC, LC, AR, CD, and OM-F: funding acquisition. AC-A, LR, VP-M, JC, LA, CF, CC-P, ES-F, TN, SL, and MS: conducting experiments. JL, JR, and LC: field study. AC-A, LA, SL, and MS: acquiring data. AC-A, LR, VP-M, JC, LA, CF, CC-P, IC-R, and JM:

analyzing data. PT and PV: validation. AH, PT, and PV: advisory committee. AC-A, LR, JC, CC-P, IC-R, AT-C, and OM-F: writing the manuscript.

ACKNOWLEDGMENTS

The authors thank the Program for Technological Development in Tools for Health-RPT-FIOCRUZ for the use of the flow cytometry facility. This study was supported by Fundação de Amparo à Pesquisa do Estado de Minas Gerais (FAPEMIG), BioManguinhos/FIOCRUZ, PROEP/IRR/FIOCRUZ, Conselho Nacional de Desenvolvimento Científico e Tecnológico-CNPq, Programa Nacional de Imunizações (PNI), and Secretaria de Vigilância em Saúde (SVS)-Ministério da Saúde, Brazil. The authors acknowledge the Programa de Pós-Graduação em Ciências da Saúde do Instituto René Rachou-FIOCRUZ-Minas, supported by the Coordenação de Aperfeiçoamento de Pessoal de Nível Superior (CAPES), and Fundação Carlos Chagas Filho de Amparo à Pesquisa do Estado do Rio de Janeiro (FAPERJ). The authors are thankful to the nursing of Secretaria Estadual de Saúde de Minas Gerais: Velizete de Lima, Alessandra de Souza (in memoriam), Matildes Souza Neto, and Rosangela Azevedo. The authors are thankful to the Programa PRINT-FIOCRUZ-CAPES. LA, CF, ES-F, LC, PV, AT-C, and OM-F received fellowships from CNPq.

REFERENCES

1. *Areas with Risk of Yellow fever Virus Transmission in Africa and South America*. (2019). Available online at: https://www.cdc.gov/yellowfever/maps/index.html
2. World Health Organization. *Yellow Fever Fact Sheet*. (2019). Available online at: https://www.who.int/en/news-room/fact-sheets/detail/yellow-fever
3. The Lancet. Yellow fever: a major threat to public health. *Lancet*. (2018) 391:402. doi: 10.1016/S0140-6736(18)30152-1
4. World Health Organization. *Eliminate Yellow fever Epidemics (EYE): A Global Strategy 2017–2026*. (2017). Available online at: https://apps.who.int/iris/handle/10665/255703
5. World Health Organization. Vaccines and vaccination against yellow fever. WHO position paper – June 2013. *Wkly Epidemiol Record*. (2013) 88:269–83.
6. World Health Organization. Background paper on yellow fever vaccine. In: *Vaccine Position Papers*. Geneva, SAGE Working Group (2013).
7. Caldas IR, Camacho LA, Martins-Filho OA, Maia M de L, Freire M da S, Torres C de R, et al. Duration of post-vaccination immunity against yellow fever in adults. *Vaccine*. (2014) 32:4977–84. doi: 10.1016/j.vaccine.2014.07.021
8. Campi-Azevedo AC, Costa-Pereira C, Antonelli LR, Fonseca CT, Teixeira-Carvalho A, Villela-Rezende G, et al. Booster dose after 10 years is recommended following 17DD-YF primary vaccination. *Hum Vaccin Immunother*. (2016) 12:491–502. doi: 10.1080/21645515.2015.1082693
9. Costa-Pereira C, Campi-Azevedo AC, Coelho-dos-Reis JG, Peruhype-Magalhães V, Araújo MSS, Antonelli LRV, et al. Multi-parameter approach to evaluate the timing of memory status after primary 17DD-YF vaccination. *PLoS Neglec Trop Dis*. (2018) 12:e0006462. doi: 10.1371/journal.pntd.0006462
10. Vasconcelos PF. Single shot of 17D vaccine may not confer life-long protection against yellow fever. *Mem Inst Oswaldo Cruz*. (2018) 113:135–7. doi: 10.1590/0074-02760170347
11. Patel D, Simons H. Yellow fever vaccination: is one dose always enough? *Travel Med Infect Dis*. (2013) 11:266–73. doi: 10.1016/j.tmaid.2013.08.007
12. Grobusch MP, Goorhuis A, Wieten RW, Verberk JD, Jonker EF, van Genderen PJ, et al. Yellow fever revaccination guidelines change – a decision too feverish? *Clin Microbiol Infect*. (2013) 19:885–6. doi: 10.1111/1469-0691.12332
13. Amanna IJ, Slifka MK. Questions regarding the safety and duration of immunity following live yellow fever vaccination. *Expert Rev Vaccines*. (2016) 15:1519–33. doi: 10.1080/14760584.2016.1198259
14. Estofolete CF e Nogueira ML. Is a dose of 17D vaccine in the current context of Yellow Fever enough? *Braz J Microbiol*. (2018) 49:683–4. doi: 10.1016/j.bjm.2018.02.003
15. Nascimento Silva JR, Camacho LA, Siqueira MM, Freire Mde S, Castro YP, Maia Mde L, et al. Mutual interference on the immune response to yellow fever vaccine and a combined vaccine against measles, mumps and rubella. *Vaccine*. (2011) 29:6327–34. doi: 10.1016/j.vaccine.2011.05.019
16. Niedrig M, Lademann M, Emmerich P, Lafrenz M. Assessment of IgG antibodies against yellow fever virus after vaccination with 17D by different assays: neutralization test, haemagglutination inhibition test, immunofluorescence assay and ELISA. *Trop Med Int Health*. (1999) 4:867–71. doi: 10.1046/j.1365-3156.1999.00496.x
17. Querec TD, Akondy RS, Lee EK, Cao W, Nakaya HI, Teuwen D, et al. Systems biology approach predicts immunogenicity of the yellow fever vaccine in humans. *Nat Immunol*. (2019) 10:116–25. doi: 10.1038/ni.1688
18. Ahmed R, Akondy RS. Insights into human CD8(+) T-cell memory using the yellow fever and smallpox vaccines. *Immunol Cell Biol*. (2011) 89:340–5. doi: 10.1038/icb.2010.155
19. Campi-Azevedo AC, Peruhype-Magalhães V, Coelho-Dos-Reis JG, Costa-Pereira C, Yamamura AY, Lima SMB, et al. Heparin removal by ecteola-cellulose pre-treatment enables the use of plasma samples for accurate measurement of anti-Yellow fever virus neutralizing antibodies. *J Immunol Methods*. (2017) 448:9–20. doi: 10.1016/j.jim.2017.05.002
20. Simões M, Camacho LAB, Yamamura AMY, Miranda EH, Cajaraville ACRA, Freire MS. Evaluation of accuracy and reliability of the plaque reduction neutralization test (micro-PRNT) in detection of yellow fever virus antibodies. *Biologicals*. (2012) 40:399–404. doi: 10.1016/j.biologicals.2012.09.005
21. Poland JD, Calisher CH, Monath TP, Downs WG, Murphy K. Persistence of neutralizing antibody 30–35 years after immunization with 17D yellow fever vaccine. *Bull World Health Organ*. (1981) 59:895–900.
22. Gotuzzo E, Yactayo S, Córdova E. Review article: Efficacy and duration of immunity after yellow fever vaccination: systematic review on the need for a booster every 10 years. *Am J Trop Med Hyg*. (2013) 89:434–44. doi: 10.4269/ajtmh.13-0264
23. Wieten RW, Jonker EF, van Leeuwen EM, Remmerswaal EB, Ten Berge IJ, de Visser AW, et al. A single 17D yellow fever vaccination provides lifelong immunity; characterization of yellow-fever-specific neutralizing antibody and T-cell responses after vaccination. *PLoS One*. (2016) 11:e0149871. doi: 10.1371/journal.pone.0149871
24. Muyanja E, Ssemaganda A, Ngauv P, Cubas R, Perrin H, Srinivasan D, et al. Immune activation alters cellular and humoral responses to yellow fever 17D vaccine. *J Clin Invest*. (2014) 124:3147–58. doi: 10.1172/JCI75429
25. Gaucher D, Therrien R, Kettaf N, Angermann BR, Boucher G, Filali-Mouhim A, et al. Yellow fever vaccine induces integrated multilineage and polyfunctional immune responses. *J Exp Med*. (2008) 205:3119–31. doi: 10.1084/jem.20082292
26. Collaborative Group for Studies with Yellow Fever Vaccine. Randomized, double-blind, multicenter study of the immunogenicity and reactogenicity of 17DD and WHO 17D-213/77 yellow fever vaccines in children: implications for the Brazilian National Immunization Program. *Vaccine*. (2007) 25:3118–23. doi: 10.1016/j.vaccine.2007.01.053
27. Collaborative Group for Studies of Yellow Fever Vaccine. A randomized double-blind clinical trial of two yellow fever vaccines prepared with substrains 17DD and 17D-213/77 in children nine-23 months old. *Mem Inst Oswaldo Cruz*. (2015) 110:771–80. doi: 10.1590/0074-02760150176
28. Luiza-Silva M, Campi-Azevedo AC, Batista MA, Martins MA, Avelar RS, da Silveira Lemos D, et al. Cytokine signatures of innate and adaptive

immunity in 17DD yellow fever vaccinated children and its association with the level of neutralizing antibody. *J Infect Dis*. (2011) 204:873–83. doi: 10.1093/infdis/jir439

29. Hepburn MJ, Kortepeter MG, Pittman PR, Boudreau EF, Mangiafico JA, Buck PA, et al. Neutralizing antibody response to booster vaccination with the 17d yellow fever vaccine. *Vaccine*. (2006) 24:2843–9. doi: 10.1016/j.vaccine.2005.12.055
30. Kongsgaard M, Bassi MR, Rasmussen M, Skjødt K, Thybo S, Gabriel M, et al. Adaptive immune responses to booster vaccination against yellow fever virus are much reduced compared to those after primary vaccination. *Sci Rep*. (2017) 7:662. doi: 10.1038/s41598-017-00798-1
31. Lindsey NP, Horiuchi KA, Fulton C, Panella AJ, Kosoy OI, Velez JO, et al. Persistence of yellow fever virus-specific neutralizing antibodies after vaccination among US travellers. *J Travel Med*. (2018) 25:1–6. doi: 10.1093/jtm/tay108
32. Collaborative group for studies on yellow fever vaccines. Duration of immunity in recipients of two doses of 17DD yellow fever vaccine. *Vaccine*. (2019) 37:5129–35. doi: 10.1016/j.vaccine.2019.05.048
33. Campi-Azevedo AC, Peruhype-Magalhães V, Coelho-dos-Reis JG, Antonelli LRV, Costa-Pereira C, Speziali E, et al. 17DD-Yellow Fever re-vaccination regimens are required for long-term persistence of neutralizing antibodies and memory $CD8^+$ T-cells in populations of endemic areas with high risk of yellow fever transmission. *Emerg Infec Dis*. (2019) 25:1511–21. doi: 10.3201/eid2508.181432
34. Campi-Azevedo AC, de Araújo-Porto LP, Luiza-Silva M, Batista MA, Martins MA, Sathler-Avelar R, et al. 17DD and 17D-213/77 yellow fever substrains trigger a balanced cytokine profile in primary vaccinated children. *PLoS ONE*. (2012) 7:e49828. doi: 10.1371/journal.pone.0049828
35. Reinhardt B, Jaspert R, Niedrig M, Kostner C, L'age-Stehr J. Development of viremia and humoral and cellular parameters of immune activation after vaccination with yellow fever virus strain 17D: a model of human flavivirus infection. *J Med Virol*. (1998) 56:159–67. doi: 10.1002/(SICI)1096-9071(199810)56:2<159::AID-JMV10>3.0.CO;2-B
36. Sarkander J, Hojyo S, Tokoyoda K. Vaccination to gain humoral immune memory. *Clin Transl Immunol*. (2016) 5:e120. doi: 10.1038/cti.2016.81
37. Shi Y, Agematsu K, Ochs HD, Sugane K. Functional analysis of human memory B-cell subpopulations: IgD^+CD27^+ B cells are crucial in secondary immune response by producing high affinity IgM. *Clin Immunol*. (2003) 108:128–37. doi: 10.1016/S1521-6616(03)00092-5

Conflict of Interest Statement: The authors declare that the research was conducted in the absence of any commercial or financial relationships that could be construed as a potential conflict of interest.

frontiers in Immunology

ORIGINAL RESEARCH
published: 11 October 2019
doi: 10.3389/fimmu.2019.02420

The Immunological Properties of Recombinant Multi-Cystatin-Like Domain Protein From *Trichinella Britovi* Produced in Yeast

Anna Stachyra[1], Anna Zawistowska-Deniziak[1], Katarzyna Basałaj[1], Sylwia Grzelak[1], Michał Gondek[2] and Justyna Bień-Kalinowska[1]**

[1] *Witold Stefanski Institute of Parasitology, Polish Academy of Sciences, Warsaw, Poland,* [2] *Department of Food Hygiene of Animal Origin, Faculty of Veterinary Medicine, University of Life Sciences in Lublin, Lublin, Poland*

Trichinellosis is a globally-distributed zoonotic parasitic disease caused by nematode worms of the genus *Trichinella*. One of the most common species of *Trichinella* known to affect human health is *T. britovi*; however, it is relatively poorly investigated. A thorough knowledge of the proteins expressed by *Trichinella* is important when developing immunological detection methods and vaccines and studying its interactions with the host. The present study uses the *Pichia pastoris* expression system to produce a soluble TbCLP antigen which induces strong antibody responses in the host during natural infection. Our results demonstrate the feasibility of TbCLP antigen production in yeasts, which are able to carry out post-translational modifications such as glycosylation and disulfide bond formation; they also indicate that the glycosylated TbCLP antigen had immunogenic effects in the tested mice and induced a mixed Th1/Th2 response, and was associated with a reduced larval burden after challenge with *T. britovi*. Subsequent *in vitro* stimulation of mice splenocytes revealed that TbCLP most likely possesses immunomodulatory properties and may play a significant role in the early phase of infection, affecting host immunological responses.

Keywords: *Trichinella britovi*, cystatin-like protein, *Pichia pastoris*, immunization, immunomodulation

OPEN ACCESS

Edited by:
Giuseppe Andrea Sautto, University of Georgia, United States

Reviewed by:
Byung-Kwon Choi, Entrada Therapeutics, Inc., United States
Chang Li, Academy of Military Medical Sciences (AMMS), China

****Correspondence:***
Anna Stachyra
astachyra@twarda.pan.pl
Justyna Bień-Kalinowska
bien.justyna@hotmail.com

Specialty section:
This article was submitted to Vaccines and Molecular Therapeutics, a section of the journal Frontiers in Immunology

Received: *13 August 2019*
Accepted: *27 September 2019*
Published: *11 October 2019*

Citation:
Stachyra A, Zawistowska-Deniziak A, Basałaj K, Grzelak S, Gondek M and Bień-Kalinowska J (2019) The Immunological Properties of Recombinant Multi-Cystatin-Like Domain Protein From Trichinella Britovi Produced in Yeast. Front. Immunol. 10:2420. doi: 10.3389/fimmu.2019.02420

INTRODUCTION

Trichinellosis is a common food-borne parasitic zoonosis worldwide. Infection occurs through the consumption of raw or inadequately-cooked meat containing *Trichinella* larvae: one of the most widespread intracellular parasitic nematodes affecting vertebrates (1, 2). The entire life cycle of the *Trichinella* parasite takes place in a single host after ingestion of infected muscle tissue. Parasitic infection can be divided into three separate antigenic stages: adult worms (Ad), newborn larvae (NBL), and muscle larvae (ML).

Within the *Trichinella* genus, the most widespread and most widely-investigated species has historically been *T. spiralis*. The parasite mainly occurs in domestic animals, and its circulation is traditionally associated with consumption of pig meat by humans. However, a range of other *Trichinella* species, such as *T. nativa, T. britovi, T. nelsoni, T. murelli,* and *T. pseudospiralis*, also circulate in sylvatic cycles and could also represent an accidental threat for human and domestic animals.

Of these species, *T. britovi* is the most widely distributed (1, 3). It can infect a wide range of mammalian hosts, mostly carnivores such as raccoon dogs, red foxes, and wolves, but is also known to invade various omnivores including wild boars, martens, badgers, and rodents (3–6). Trichinellosis is a widely-known public health hazard, especially in developing countries, but also represents an economic problem in the production of pork products and food safety. In contrast, developed countries tend to have a lower risk of trichinellosis associated with the consumption of pig-based products due to their high biosecurity standards and strict veterinary control in the pig farming and food processing industries. Currently, the most common source of trichinellosis in developed countries is through the consumption of game hunted for recreation: as it is not intended for sale, but only for private consumption, the meat is often not subject to veterinary inspection. Interestingly, while *T. spiralis* was found to predominate in samples of wild boar, a commonly consumed type of meat, *T. britovi* ML were also present in smaller numbers (7, 8). Hence, it is reasonable to assume that some cases of human trichinellosis may be caused by *T. britovi*, and numerous cases have already been confirmed (9–12). Therefore, to better understand the biology of the nematode and the host-parasite relationship, proteomical and immunological studies of *T. britovi* aimed at the identification of active proteins and potent antigens are needed.

Proteomical analysis (13, 14) and immunoscreening of cDNA expression libraries (15, 16) indicate that the multi-cystatin-like domain protein (named MCD or CLP) of *T. spiralis* is a highly antigenic protein. Its expression has been confirmed by RT-PCR in all developmental stages, with the highest level occurring in Ad. The protein was localized in the stichosome of Ad and ML and was also detected as a component of the excretory-secretory antigen (ES) of both Ad and ML (16–18). Hypothetical CLP was also recently detected by immunoblotting of somatic protein extract of *T. britovi* ML (19). Referred studies revealed, that this protein is produced in various stages of the parasite life cycle, after which it accumulates in the stichosome and is later released at specific stages of development as a component of the ES antigen, with its greatest release probably being at the intestinal stage (16).

Cystatins, inhibitors of cysteine proteinases, are a major class of parasitic nematode molecules with immunomodulatory properties that enhance production of the anti-inflammatory IL-10 cytokine and inhibit legumains, thus preventing MHC-II generation (20). Nematode proteinase inhibitors are generally known to play important functions at the host-parasite interface and are targeted by the immunological system. They control their own proteinase activity and that of the host, and weaken the immunological response by influencing antigen processing and presentation, cytokine production, and T-cell proliferation (21, 22).

Interestingly, the *Trichinella* CLP protein most likely has no cysteine protease inhibitory activity, and its function is unknown. The protein is classified within the cystatin superfamily, and demonstrates a similarity to family 3 kininogens: glycosylated and secreted proteins that are of relatively high mass and contain three family 2 cystatin-like domains (23). Robinson et al. (18) report that recombinant TsCLP produced in *E. coli* was not able to inhibit papain *in vitro*; the authors attribute this to the absence of two conserved motifs (QXVXG and PW in each cystatin domain), which are normally present in family 2 cystatins, and which form a structure that blocks the active site of the protease (24, 25). Instead of inhibitory activity, they propose that the protein can undergo self-processing and release single cystatin-like peptides to perform specific functions. Even so, the function of these peptides remains unknown. These low molecular weight isoforms of native CLP were observed in two-dimensional (2-D) analysis of ES antigen; the isoforms were also observed following expression of TsCLP in HeLa cells but not in *E. coli* (14, 16, 18), suggesting that CLP activity requires eukaryotic post-translational modification, such as the formation of disulfide bonds or glycosylation.

Pichia pastoris is a methylotrophic yeast used for expression of recombinant proteins; it is a particularly attractive host for this process due to its potential for methanol-dependent induction, triggered by the tightly-regulated AOX1 promoter (26). The system is useful for both large-scale and laboratory-level production of recombinant proteins, and can produce large amounts of the protein of interest. As a eukaryotic organism, *P. pastoris* ensures that the proteins undergo post-translational modification, and offers very economical handling and propagation. It is therefore an interesting alternative to other expression systems (27). Following eukaryote-specific post-translational modification, the produced recombinant proteins are generally highly similar to native proteins. Their disulfide bonds are correctly formed and preserved (28). The N-glycosylation profile is usually high mannose with no tendency to hyper-glycosylation and the oligosaccharides are often attached at the same positions as in natural glycoproteins (29, 30). A number of pharmacologically-active proteins are commercially produced in this expression system, e.g., hepatitis B vaccine antigen, human serum albumin, human IFNα, anti-RSV antibody and human insulin (source: https://pichia.com/). However, few studies have been published concerning the production of parasitic nematode proteins in this way (31–34), particularly *Trichinella* proteins.

CLP protein was identified as one of the reactive spots in our previous proteomic analysis of *T. britovi* antigens, based on a combination of 2-D immunoblotting of sera from infected pigs followed by LC-MS/MS analysis (19). It was therefore selected as a promising immunoreactive protein for further study, especially that the *T. britovi* homolog of CLP was yet not known. The aim of the present study was to achieve expression of the TbCLP antigen in a eukaryotic system, and to evaluate its potential diagnostic applications and protective efficacy against *T. britovi* infection in a mouse model.

MATERIALS AND METHODS

T. britovi Parasite and Mouse Model

The reference strain of *T. britovi* (ISS002) had been maintained by several passages in male C3H mice at the Institute of Parasitology, PAS. Muscle larvae were used for challenge infection of C3H mice and as a source of genetic material

for cloning. The larvae were recovered from the infected mice by HCl-pepsin digestion (35). The animals were housed in a temperature-controlled environment at 24°C with 12-h day-night cycles, and received food and water *ad libitum*.

Sequence Analysis

The amino acid (aa) sequences were aligned using CLUSTALW. The N-glycosylation sites were predicted using NetNGlyc server (http://www.cbs.dtu.dk/services/NetNGlyc/).

Cloning of Recombinant CLP Gene

T. britovi ML were obtained for total RNA isolation using Total RNA mini Plus kit (A&A Biotechnology). The RNA template was then used for cDNA synthesis with the Maxima First Strand cDNA Synthesis Kit for RT-qPCR (Thermo Scientific) according to the manufacturer's protocol. The cDNA coding the TbCLP gene without its signal peptide was amplified by PCR with CLP-specific primers (Forward: 5′-AGGCATCGATACAGATACTTG GTGAAAC-3′, Reverse: 5′-GCTCTAGAGCACATTCAACAG TTGACTTG-3′). Since the nucleotide sequence of *T. britovi* CLP was not known, primers were designed according to the nucleotide sequence of *T. spiralis* CLP (GenBank no. FR694976), whose amino acid sequence is thought to be very similar to the hypothetical sequence of TbCLP (GenBank no. KRY50178). The cDNA coding for TbCLP was sequenced and subcloned into the yeast expression vector pPICZαC with the His-tag sequence at the C-terminus (Invitrogen/Thermo). The correct reading frame of the recombinant plasmid was confirmed by DNA sequencing using vector flanking primers, 5′AOX1 and 3′AOX1.

Expression and Purification of Recombinant CLP in *P. pastoris*

Pichia pastoris cells (X33 strain) were transformed with recombinant plasmids by electroporation. X33 transformant selection was performed using a medium containing Zeocin, and successful integration of the CLP gene into the *P. pastoris* genome was confirmed by PCR. The recombinant TbCLP with C-terminus His-tag was expressed by induction with 0.5% methanol for 24–72 h in 200 ml of Buffered Methanol-complex Medium (BMMY), and then purified by immobilized metal ion affinity chromatography using Protino Ni-NTA agarose (Macherey-Nagel). The protein samples were analyzed qualitatively by SDS PAGE and Western blotting, and their concentration was measured using Pierce BCA Protein Assay Kit (Thermo Scientific).

Enzymatic Deglycosylation

Samples of recombinant protein purified from medium after 24, 48, and 72 h of induction were digested with Endo H (New England Biolabs) in denaturing conditions, according to the manufacturer's instructions. Deglycosylated rTbCLP were analyzed by SDS-PAGE.

SDS-PAGE and Western Blot Analysis

SDS-PAGE was performed in 10% BisTris polyacrylamide gels. After electrophoresis, the gels were either stained with Coomassie brilliant blue or the proteins were transferred to a nitrocellulose membrane (Bio-Rad) for Western blotting. The recombinant protein was detected using monoclonal Anti-polyHistidine–Peroxidase antibody (diluted 1:4,000; Sigma). The proteins were viewed with Super Signal Western Pico Chemiluminescent Substrate (Thermo Scientific). Alternatively, rTbCLP was detected using sera from immunized or infected mice (1:200) and a secondary anti-mouse IgG antibody conjugated with HRP (1:8,000, Abcam).

Determination of Recombinant Antigen Immunoreactivity by ELISA

A panel of *T. britovi* serum samples stored in our collection were used for testing rTbCLP as an antigen in ELISA; the samples had been obtained from pigs experimentally infected with 5000 *T. britovi* ML. Testing was performed on samples were taken at multiple time points post-infection (−4, 3, 6, 9, 13, 15, 17, 20, 24, 29, 36, 41, 45, 51, 55, 59, 62 days post-infection, dpi). ELISA plates were coated with 2 μg/ml of rTbCLP protein and incubated at 4°C overnight.

The pig serum samples were added at 1:100 dilution and the plates were incubated at 37°C for 1 h. Goat anti-pig IgG conjugated with peroxidase (Sigma) at 1:20,000 dilution was used for detection of CLP-specific antibodies. The enzymatic color reaction was generated using TMB substrate (3,3′,5,5′-Tetramethylbenzidine; Sigma), and the absorbance value was measured at 450 nm using a Synergy HT microplate reader (BioTek). The cut-off value of ELISA was evaluated on the basis of the average OD plus three standard deviations (SD) of *Trichinella*-free serum samples of pigs (36).

Immunization and Challenge Infection

Eight-week old male C3H mice were divided into three groups of 12 animals each. The vaccine group was immunized subcutaneously with 25 μg of rTbCLP emulsified with the adjuvant Alhydrogel (InvivoGen) in a total volume of 100 μl (antigen/Alhydrogel = 75/25 v/v). The mice were boosted with the same dose after 1 week. The control groups were injected with PBS or PBS+Alhydrogel using the same regimen. 1 week after the final vaccination, six mice from each group were sacrificed, and their blood and spleens were harvested for immunological tests. The remaining six mice from each group were challenged orally with 500 *T. britovi* ML. 7 weeks (48 days) after infection, all mice were sacrificed, the blood and spleens were harvested, and the *T. britovi* muscle larvae were recovered by HCl-pepsin digestion. Protective immunity was calculated according to the number of ML recovered from the vaccinated group compared with those from the PBS group. Sera from all mouse blood samples were isolated and frozen at −20°C for further analysis.

Determination of Serum-Specific Antibodies

TbCLP-specific antibodies (IgG as well as subclasses IgG1 and IgG2a) in serum samples of vaccinated mice were measured by indirect ELISA, with rTbCLP as coating antigen, at 1 week after final immunization and 7 weeks after challenge infection. ELISA plates were coated with 2 μg/ml of rTbCLP protein and incubated at 4°C overnight. Following this, mouse serum samples

at 1:200 dilution were added and incubated at 37°C for 1 h. Then, the plates were incubated with HRP-conjugated antibody goat anti-mouse IgG, IgG1, or IgG2a (1:80,000 or 1:60,000, Abcam) for detection of CLP-specific antibodies. The enzymatic color reaction was generated and the cut-off value of ELISA was evaluated as described in the present study.

Cytokine Analysis

To measure the specific cellular response, the spleens were harvested from vaccinated animals 1 week after final immunization and 7 weeks after challenge infection.

The spleens were pooled into pairs taken from two randomly-selected mice within the same group; following this, the splenocytes were disassociated using a 70 μm cell strainer and then suspended in complete RMPI medium (Biowest). In order to lyse the erythrocytes, the splenocytes were incubated in 5 ml RBC lysis buffer (Thermo Scientific) for 10 min. The cell suspension was centrifuged at 250 × g at room temperature for 7 min. The cell pellets were washed in RPMI medium and then resuspended in complete RPMI medium containing 10% FBS and penicillin/streptomycin (Biowest); following this, the cells were then counted.

For the cytokine stimulation assay, the splenocytes were seeded in a 24-well culture plate (Corning) at 5 × 10^6 cells per well in 1,000 μl medium. The cells were stimulated with 15 μg/ml rTbCLP and incubated for 72 h at 37°C in a humidified atmosphere of 5% CO_2. Cells stimulated with 5 ug/mL Concavalin A were included as positive controls. Non-stimulated cells were included as negative controls. After 72 h, the cells were pelleted by centrifugation at 1,000 × g for 10 min and the supernatants were collected to measure cytokine production. Samples containing the supernatant were tested for levels of IL-2, IL-4, IL-10, IFN-γ using a Mouse Th1/Th2 uncoated ELISA kit (Invitrogen/Thermo Scientific).

Statistical Analysis

Statistical analysis was performed using Statistica 6 software (StatSoft). Data were expressed as means ± standard deviation (SD). Differences among groups were analyzed by one-way analysis of variance (ANOVA). A value of $p < 0.05$ was considered significant.

RESULTS

Cloning, Expression, and Characterization of Recombinant TbCLP Protein

Since the nucleotide sequence of *T. britovi* CLP was not known, PCR primers were designed according to nucleotide sequence of *T. spiralis* CLP. TsCLP (GenBank no. CBX25716) shares 91.5% identity with the hypothetical sequence of TbCLP (Genbank no. KRY50178) derived from conceptual translation of genomic data (37). As the amino acids in regions including the primers sequences was found to be identical in TbCLP and TsCLP, the DNA sequence for TbCLP without its signal peptide was successfully amplified and subcloned into the expression vector (**Figure 1**). Sequencing revealed full compatibility between the hypothetical and cloned TbCLP, with regard to the amino acid sequence, and the nucleotide sequence was 96.2% identical with

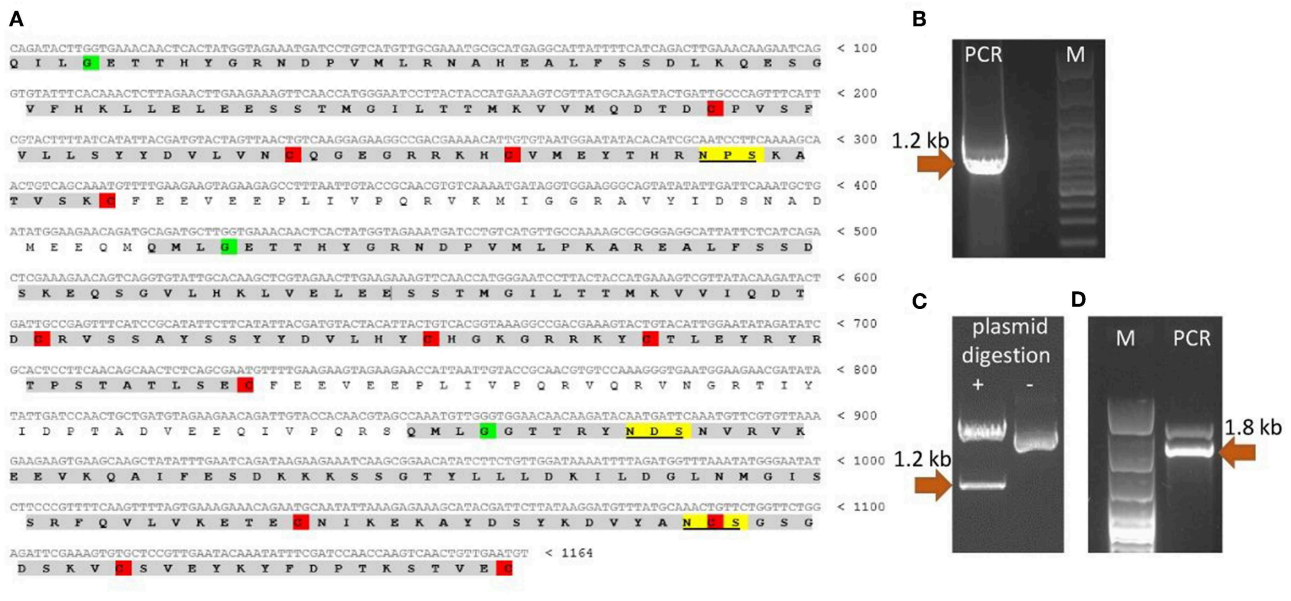

FIGURE 1 | Cloning of TbCLP coding sequence. **(A)** Cloned cDNA sequence and predicted amino acid sequence of TbCLP. Three cystatin-like domains are highlighted in gray [according to Robinson et al. (18)]. Conserved cysteines, that form disulfide bonds are highlighted in red. Conserved glycines are highlighted in green. Predicted N-glycosylation sites are underlined and highlighted in yellow. **(B)** PCR product after amplification of TbCLP cDNA. **(C)** Restriction digestion of recombinant plasmid containing target insert. **(D)** PCR product after screening of *P. pastoris* transformants. Correct DNA fragments are marked with arrows and the molecular mass is indicated.

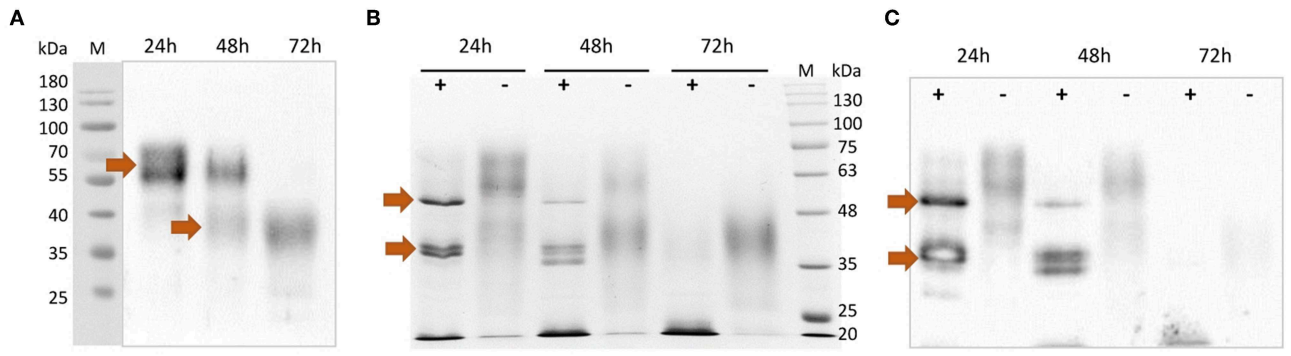

FIGURE 2 | Analysis of purified rTbCLP. **(A)** Anti-His Western blot of protein purified from medium after 24, 48 and 72 h of induction. High molecular weight glycoisoforms (55–70 kDa) and low molecular weight glycoisoforms (35–45 kDa) are marked with arrows. **(B)** SDS PAGE and **(C)** Anti-His Western blot after deglycosylation of rTbCLP with Endo H. Protein samples were incubated with Endo H enzyme (+) or without Endo H (–) in denaturing conditions. Deglycosylated full form rTbCLP (48 kDa) and the shorter isoforms (35–38 kDa) are marked with arrows.

that of the TsCLP gene. The sequence of the cloned TbCLP without the signal peptide is given in **Figure 1A**.

The theoretical molecular weight of the His-tagged TbCLP was predicted as 47.3 kDa, and the molecular weight of a single cystatin-like domain was 12 kDa. NetNGlyc server analysis of the amino acid sequence identified three potential N-glycosylation sites in the protein chain: one in the first cystatin-like domain and another two in the third cystatin-like domain.

CLP gene expression was induced in the X33 *P. pastoris* strain with methanol. In preliminary experiments, 0.5% methanol was added every 24 h until the final time of induction was reached. Further analyses indicated that a single induction with methanol and 24-h cultivation yielded the best rTbCLP level. The recombinant His-tagged protein was purified using affinity chromatography under native conditions.

After purification, the rTbCLP protein appeared to be present as various different glycoisoforms, manifesting as blurred, smear bands with molecular weights of ∼55–70 and 35–45 kDa on Western blot (**Figure 2A**). Interestingly, different protein forms were observed after 24, 48, and 72 h of induction: high molecular weight glycoisoforms were visible after 24 and 48 h of induction, and only low molecular weight glycoisoforms were visible after 72 h of induction. In order to examine the N-glycosylation of recombinant CLP protein, an Endo H digestion procedure was used. Deglycosylation with Endo H reduced the molecular mass of rTbCLP (**Figures 2B,C**) and confirmed that the observed variation in protein masses was caused by changes in glycan content. After the release of N-linked carbohydrates from the protein, the upper band corresponded well with the predicted mass of full length TbCLP (48 kDa), and the lower bands corresponded with the shorter isoforms (35–38 kDa), which may be created by post-translational cleavage events. After 24 and 48 h of induction, the full form of the protein was visible, as well as several shorter forms (**Figures 2B,C**). After 72 h of induction, the full form of protein was no longer visible, and the total amount of protein seemed very low, indicating that the whole pool of rTbCLP expressed in *P. pastoris* had been processed. The protein was taken after 24 h of induction, purified and used in subsequent experiments.

rTbCLP Recognition by Sera From *T. britovi* Infected Pigs

The results in **Figure 3** represent the antibody kinetics in eight pigs that were experimentally infected with 5000 ML *T. britovi* using rTbCLP. The ELISA results demonstrate that seroconversion was detected at 24 days post-infection. The moment of detection was earlier than when using a commercial PrioCHECK® *Trichinella* Antibody ELISA Kit (Thermo Scientific) containing ES *Trichinella* antigen (data not shown). The results confirm the antigenic properties of rTbCLP protein and indicate that rTbCLP is a potential antigen to be used in future experiments for detection of *Trichinella* infection in animals.

Humoral Antibody Response Induced by Immunization of Mice With rTbCLP Formulated With Alhydrogel

Purified rTbCLP was tested for immunogenicity in a mouse model. The total IgG level in serum was first evaluated in immunized and control groups; following this, the humoral antibody responses in the immunized mice were assayed by ELISA, with rTbCLP as a coating antigen (**Figure 4A**).

The results indicate that anti-TbCLP IgG antibodies were elicited by the immunization of mice with rTbCLP+adjuvant. Specific anti-TbCLP IgG were detected in all serum samples from the immunized group; however no anti-TbCLP antibody response was detected in the mice injected with adjuvant or PBS alone. Although anti-TbCLP antibodies were present in sera of all experimental groups after the challenge infection, a significantly higher level of specific anti-TbCLP was observed in the group of mice immunized with rTbCLP+adjuvant than the two control groups.

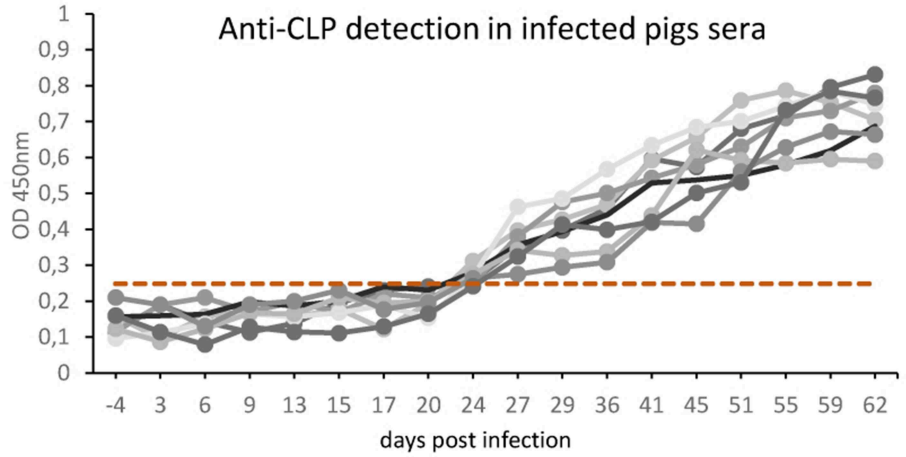

FIGURE 3 | Anti-*Trichinella* IgG levels in pigs infected with *T. britovi* by ELISA with rTbCLP. Pigs ($n = 8$) were experimentally infected with 5,000 ML of *T. britovi* and sera were collected prior to infection (−4 dpi) and 3, 6, 9, 13, 15, 17, 20, 24, 29, 36, 41, 45, 51, 55, 59, 62 dpi. The cut-off value was evaluated on the basis of the average OD plus three SD of *Trichinella*-free serum samples and is marked as a dashed line. All individuals were found positive after 24 days post-infection.

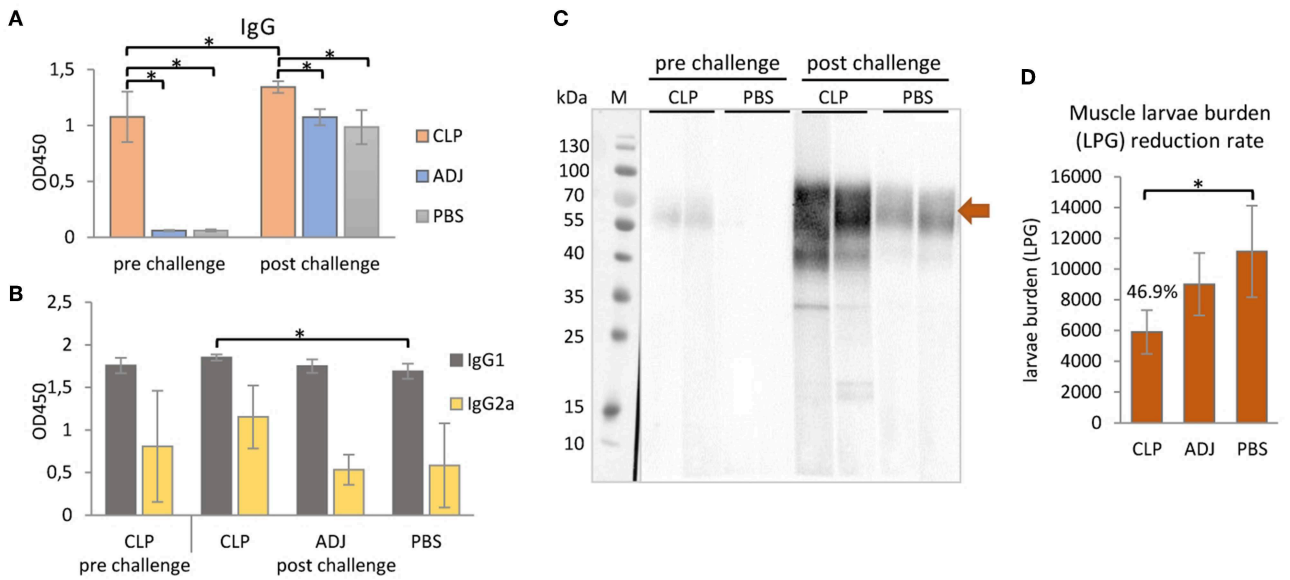

FIGURE 4 | Mouse immune responses to the immunization of rTbCLP. **(A)** Anti-TbCLP total IgG level and **(B)** anti-TbCLP subclasses IgG1 and IgG2a level in sera of immunized mice, measured by ELISA after final immunization and challenge infection, respectively. **(C)** Anti-TbCLP total IgG in sera of experimental mice, detected by Western blot. Two randomly selected sera from each group were used for immunodetection of rTbCLP (3 μg/lane). Specific signal for 55–70 kDa form is marked with arrow. **(D)** Muscle larvae burden reduction rate (%) in three experimental mice groups after challenge infection. Experimental groups: CLP—group injected with rTbCLP+adjuvant, ADJ—group injected with adjuvant, PBS—group injected with PBS. Significant differences are marked with asterisks. Bars represent mean values from six individuals ($n = 6$) ± SD.

A relatively high level of IgG1 and a moderate level of IgG2a were observed following induction by rTbCLP. After the challenge infection with *T. britovi*, all groups demonstrated a high level of IgG1; however, the mice injected with rTbCLP+adjuvant displayed a significantly higher level than the PBS control group. In contrast, moderate levels of anti-TbCLP subclass IgG2a were detected in all tested groups, but no significant differences were detected between groups due to the high level of individual variation (**Figure 4B**). The presence of anti-TbCLP antibodies was also confirmed by Western blot, using sera from the rTbCLP+adjuvant and the PBS control groups after immunization and after challenge infection. Induced IgG were able to give specific signal as showed at **Figure 4C**.

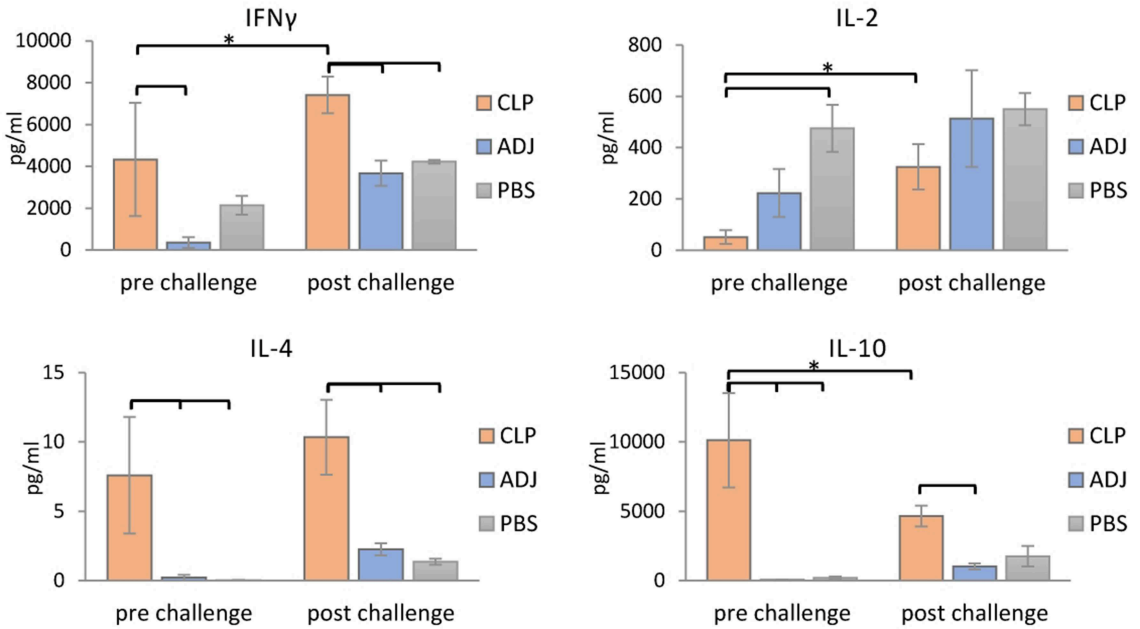

FIGURE 5 | Cytokines detection in supernatants of stimulated splenocytes of the immunized mice. Supernatants harvested after 72 h of incubation were analyzed for detection of secreted cytokines IFNγ, IL-2, IL-4, and IL-10 using Mouse Th1/Th2 uncoated ELISA kit. Experimental groups are indicated as previously described. Immunized groups significantly different from corresponding control groups are marked with empty brackets, while corresponding immunized groups significantly different from each other are marked with asterisks. Bars represent means ± SD from three splenocytes cultures ($n = 3$) each prepared from two pooled spleens from mice from the same group.

Cytokine Profiles of Stimulated Splenocytes From Mice Immunized With rTbCLP

To further confirm that a Th1/Th2 mixed response was induced following rTbCLP vaccination, the levels of selected cytokines (IFNγ, IL-2, IL-4, and IL-10) were measured in the supernatants of stimulated splenocyte cultures. In the case of Th1, higher levels of IFNγ were identified in splenocytes from mice immunized with rTbCLP+adjuvant than controls treated with adjuvant or PBS alone, with significantly lower levels observed in the adjuvant controls. However, after challenge infection with *T. britovi,* significantly higher levels of IFNγ were found in the rTbCLP+adjuvant group than the others (**Figure 5**). In contrast, IL-2 levels were significantly lower in the rTbCLP+adjuvant cultures than the PBS control group. After infection, these levels was still lower in the cultures from immunized mice than controls; however, these differences were not statistically significant.

Clearer differences were visible in case of the Th2 cytokines: the levels of IL-4 and IL-10 were significantly higher in the supernatants of the immunized mice than in the two control groups, in which the cytokine levels were at the limit of detection (**Figure 5**). After infection, the level of IL-4 in the immunized group was at a similar value than before infection, but the level of IL-10 was clearly lower than before infection. These results confirm that immunization with TbCLP triggered a mixed Th1/Th2 response.

Protective Immunity Induced by rTbCLP

The protective response induced by rTbCLP against *T. britovi* infection was investigated in experimental C3H mice. Seven weeks (48 days) after infection, all mice (six per group) were sacrificed and *T. britovi* muscle larvae were recovered from individual mice. The results revealed a significantly different reduction rate (46.9%) between the immunized group and the PBS control group (**Figure 4D**).

DISCUSSION

Multi cystatin-like domain protein (CLP) is promising immunoreactive protein used in studies to control trichinellosis. Although *T. spiralis* CLP has previously been cloned and used for immunization (16, 18, 38), the properties of *T. britovi* CLP are generally unknown, and only genomic data were available of its hypothetical sequence. Our findings indicate a great degree of similarity between the CLP of *T. britovi* and that of *T. spiralis*. Fortunately, the target gene could be successfully amplified by PCR (**Figure 1B**) as the annealing regions in the coding sequences of *T. britovi* and *T. spiralis* were found to share a high degree of similarity. The two nematodes are closely related, and TsCLP and TbCLP share 91.5% identity in their amino acid sequences and 96.2% identity for their nucleotide sequences.

To evaluate the potential of *P. pastoris* as an expression host for production of a recombinant *T. britovi* CLP, the pPICZαC/CLP vector was constructed (**Figures 1C,D**) and

expressed in X33 strain cells. The expressed rTbCLP displayed fuzzy, smear bands on Western blot (**Figure 2A**); it was difficult to precisely determine the mass of the detected protein bands and their mass appeared to vary depending on the duration of induction, i.e., 24, 48, or 72 h. It is known that in some cases protein expression in *P. pastoris* demonstrates heterogenic glycosylation, resulting in its protein population displaying diverse structural heterogeneity (30). Within a cell, two molecules of the same protein may present different oligosaccharide profiles, even when they have been exposed to the same glycosylation machinery. Such variation is typically derived from differences in the type, length and identity of the oligosaccharide at a given glycosylation site. The glycoprotein may also vary with regard to site occupancy.

In case of rTbCLP, great variation can be seen in protein subpopulations. Similar results were previously described by Teh et al. (39), where human erythropoietin (EPO) expressed in the *P. pastoris* system also demonstrated broad smear band in Western blot. EPO is a native glycoprotein (40), as is TbCLP and family 3 cystatins. Fractionation of rEPO followed by PNGase F and Endo H treatment found that the observed variations in molecular mass, manifested as the broad smear observed on the membrane, were caused by variations in glycan content: the deglycosylated protein demonstrated a sharp band with the predicted molecular mass. It is important to emphasize that the recombinant EPO was fully functionally active, despite the observed variation in glycosylation. In our study, deglycosylation with Endo H also resulted in the rTbCLP displaying sharp bands, and revealed the presence of high molecular weight and low molecular weight isoforms (**Figures 2B,C**).

A previous study has found recombinant TsCLP to possess different isoforms (18). Two such isoforms were found to be expressed in Hela cells, one of 49 kDa and another of 38 kDa; these were described respectively, as the full-length protein and the shorter isoform. Subsequent incubation at different pH values revealed that a further two low molecular weight isoforms (35 and 38 kDa) were visible in the pH range 4–8, and these bands were most prominent at pH 5. The authors suggest that the CLP undergoes pH-dependent auto-processing, resulting in the release of individual cystatin-like peptides (18).

This conclusion supports our observation that the amount of full length TbCLP decreases during induction in *P. pastoris*, with only low molecular-weight isoforms being observed after 72 h. It is known that in *Pichia* fermentation, the pH decreases while feeding from a carbon source, as the catabolic activity leads to acid production, potentially resulting in greater processing of the secreted rTbCLP into individual peptides. For this reason, only the protein isolated after 24 h of induction was used in the following experiments. In the future, to scale-up protein expression, it will be necessary to optimize the induction conditions, particularly the control of medium pH, to prevent early processing. Nonetheless, it is important to emphasize that in contrast to the rCLP previously produced in bacteria (16, 18), the *P. pastoris* system yielded an active, functional form of rTbCLP: native CLP is most probably secreted as a glycosylated protein containing disulfide bonds, and the initial full length form is further transformed into the shorter forms, these being the single cystatin-like peptides with specific biological functions, due to post-translational modification.

Our previous 2-D immunoblotting and LS-MS/MS analyses revealed some spots that reacted with the sera of *T. britovi* infected pigs; these were identified as a hypothetical protein highly similar to a multi-cystatin-like domain protein precursor from *Trichinella spiralis*. The molecular mass of the spots ranged from 45 to 50 kDa, which corresponded with the expected mass of CLP (19). To confirm this immunological reactivity, ELISA tests were performed to determine the level of anti-rTbCLP IgG in infected pig sera and seroconversion was detected at 24 dpi (**Figure 3**). However, high background values were observed and further optimization of test procedures is needed before the rTbCLP antigen can be used in diagnostics of anti-*Trichinnella* antibodies in serum samples.

Infection with *Trichinella* is initially characterized by the induction of a Th1 response at the beginning of the intestinal phase; however, the extensive dissemination of newborn larvae results in a shift to a Th2 response. The Th2 state is protective and results in parasite expulsion. *Trichinella* worms rapidly develop to maturity and reproduce before the Th2-mediated expulsion eliminates all adult forms from the gut. Thus, during the intestinal phase, the immune response is mixed, i.e., Th1/Th2, with an initial predominance of the Th1 response shifting to that of the Th2 response (41). In the present study an analysis of mouse humoral immune responses revealed high total IgG levels in serum; in addition, while IgG1 levels were clearly higher than those of IgG2a after vaccination with rTbCLP, IgG2a was also elicited, suggesting that the mixed Th1/Th2 immune response was triggered by immunization with rTbCLP (**Figures 4A,B**). The mixed immune response was further verified by the levels of Th1 (IFN-γ, IL-2) and Th2 cytokines (IL-4, IL-10) observed in the spleen cell cultures of immunized mice following stimulation by rTbCLP protein. Although all tested groups of mice displayed unique cytokine profiles, all cytokines in the immunized cultures were significantly elevated compared to controls, while IL-2 was significantly suppressed (**Figure 5**).

IFNγ is a signature cytokine of the adaptive immune response, and the main cytokine associated with Th1. High levels of IFNγ were detected in samples taken from groups after immunization and after challenge infection; however, the level of IFNγ was almost twice as high in the challenged group. This finding suggests that rTbCLP effectively induced the Th1/cellular response, which was then boosted after infection.

IL-2 plays a dual role in immunological system: it is a potent T cell growth factor associated with protective immune responses, but also influences immune tolerance and the downregulation of inflammation. The function of IL-2 *in vivo* is complex, and its influence on the immune response is not only dependent on its presence or absence, but also the level of IL-2 receptor (IL-2R) signaling that takes place (42, 43). The effect of immunization and splenocyte stimulation on IL-2 production *in vitro* is hard to interpret, but it may be related with CLP possessing certain immunomodulatory properties, which are currently unknown; these could affect IL-2R signaling pathways and the cytokine network in immune cells, resulting in inhibited IL-2 secretion and/or possibly augmented IL-2 consumption. Interestingly, our

results correspond with those of an immune response analysis of *Trichinella* infection described by Yu et al. (44), where IL-2 level was found to be significantly downregulated in mouse sera during the intestinal and larvae migration phases compared to uninfected controls. Other tested cytokines were elevated or unchanged compared to controls during the respective infection phases, and only IL-2 exhibited downregulation during the early phase of infection. Suppression of IL-2 production may also be partially explained by the release of high amounts of IL-10, since IL-10 can inhibit production of IL-2 (45). Interestingly no other cytokine secretion was inhibited in our experiment, indicating that this phenomenon may be somehow related with the dichotomous role played by IL-2 and IL-2R in self-tolerance and immunity.

IL-4 is closely associated with the humoral (Th2) and anti-helminthic responses (46); as it regulates B-cell immunoglobulin secretion, it was not surprising that it was observed at high levels in cultures following immunization compared to naïve controls. In a similar way to IFNγ, the highest level of IL-4 was observed in the immunized and infected group, demonstrating that vaccination very effectively primed Th2 responses against the *T. britovi* parasite; this response was boosted further after infection, and the findings are in agreement with our IgG level analysis. However, the fact that the amounts of IL-4 found in all experimental supernatants were relatively small might be explained by the fact that IL-4 has a short half-life, and the cells were cultured for 72 h (47).

IL-10 is a well-known anti-inflammatory cytokine, and that during parasite infection, it plays a major role in parasite immunomodulation by suppressing immune responses. More interestingly, the main factor inducing the production of IL-10 by APCs, particularly macrophages, during infection are thought to be nematode cystatins (20, 48). Although the exact mechanism by which these cystatins activate IL-10 production in host cells is unknown, it is most probably independent of protease inhibitory activity, and is likely related to their structural features and receptors engagement. TbCLP was previously assumed to lack protease inhibitory activity; therefore, due to its conserved structure, it may modulate the host immune system by inducing the production of anti-inflammatory IL-10. Indeed, our findings indicate the presence of very high amounts of IL-10 in the supernatants of stimulated splenocytes. The level of IL-10 was the highest in the immunized group; however, these levels were significantly lower in the immunized and infected group, suggesting that impact of recombinant protein alone was very strong, but this influence was balanced by the broad immune response to infection. Interestingly, production of IL-4 and IL-10 by splenocytes was much weaker after *T. britovi* infection than after rTbCLP immunization. This could be possibly explained by the fact that the infection was in its late phase: the splenocytes were harvested 48 dpi, when the parasite is at the convalescent phase of the life cycle.

rTbCLP vaccination resulted in a 46.9% larvae reduction (**Figure 4D**); this was a similar benefit to one reported in a previous study of recombinant CLP in *T. spiralis* (16), where mice vaccinated with rTsCLP exhibited a significant reduction in muscle larvae burden. However, the previous experiment was conducted using Freund's Complete Adjuvant (CFA) and the antigen was administered intraperitoneally. These are very harsh immunization conditions, and CFA is known to cause some concerns in animal usage, due to its toxicity and painful reaction; even so, it is often used in mice (49, 50). In contrast, our present study used an alum adjuvant, which is non-toxic and approved for use in humans (51). It obtained good results, suggesting that yeast-derived antigen is superior to bacteria-derived antigens, as the milder immunization conditions yielded a similar immunoprotective effect. It is important to mention that, as far as we are aware, all recombinant *Trichinella* antigens tested so far have been produced in a bacterial expression system and may not have been fully active (52–56). To better characterize the functions of the proteins of interest, a eukaryotic expression system, such as the yeast expression chosen in this study, should be used.

CONCLUSIONS

Immunization with the active full form of rTbCLP resulted in high immunogenicity in tested mice and a significant reduction of larvae burden after experimental infection. The recombinant protein was produced in *Pichia* cells; this approach ensures that the protein is further processed into individual cystatin-like peptides via post-translational modification. Furthermore, it can be assumed that cytokine profiles of the presented splenocytes are both resultants of the immune response against recombinant TbCLP antigen administered as an experimental vaccine, as well as the product of the immunomodulation of immune cells by this antigen, resulting from its biological function. The molecular events triggered by rTbCLP as an antigen, or as a modulator, could be opposing or synergistic. This dichotomy is manifested in the observed imbalance of IL-2 and IL-10, two cytokines involved in immunosuppression (57). However, it should be remembered that our findings illustrate just a small part of the host response to immunization and infection. Future research on the immunomodulatory properties of TbCLP may allow for a better understanding of its function, and further studies on the usage of TbCLP for the purposes of diagnosis and vaccine development would be also desirable.

DATA AVAILABILITY STATEMENT

All datasets generated for this study are included in the manuscript/supplementary files.

ETHICS STATEMENT

The procedures were approved by the First Local Ethical Committee for Scientific Experiments on Animals in Warsaw, Poland (resolution no.: 020/2016, 23 March 2016) and the Second Local Ethical Committee for Scientific Experiments on Animals in Lublin, Poland (resolution no.: 77/2015, 7 July 2015). All efforts were made to minimize suffering. All applicable international, national and/or institutional guidelines for the care and use of animals were followed. In order to collect

material from infected and/or immunized mice, the animals were humanely euthanized by cervical dislocation.

AUTHOR CONTRIBUTIONS

AS and JB-K conceived and designed the experiments and analyzed the data. AS, AZ-D, and KB were involved in cloning. AS performed protein expression and analysis and immunological study. AS, J-BK, and SG participated in mice immunization and *in vitro* experiments. MG supplied the pig sera. AS wrote the manuscript. JB-K, AZ-D, and KB participated in reviewing and editing the manuscript. JB-K supervised the manuscript. All of the authors have read and approved the final manuscript.

FUNDING

Financial support for this study was provided by the National Science Center Poland (grant UMO-2015/18/E/NZ6/00502).

REFERENCES

1. Gottstein B, Pozio E, Nockler K. Epidemiology, diagnosis, treatment, and control of trichinellosis. *Clin Microbiol Rev.* (2009) 22:127. doi: 10.1128/CMR.00026-08
2. Dupouy-Camet J. Trichinellosis: a worldwide zoonosis. *Vet Parasitol.* (2000) 93:191–200. doi: 10.1016/S0304-4017(00)00341-1
3. Pozio E, Zarlenga DS. New pieces of the *Trichinella* puzzle. *Int J Parasitol.* (2013) 43:983–97. doi: 10.1016/j.ijpara.2013.05.010
4. Pozio E, Rinaldi L, Marucci G, Musella V, Galati F, Cringoli G, et al. Hosts and habitats of *Trichinella spiralis* and *Trichinella britovi* in Europe. *Int J Parasitol.* (2009) 39:71–9. doi: 10.1016/j.ijpara.2008.06.006
5. Moskwa B, Gozdzik K, Bien J, Bogdaszewski M, Cabaj W. Molecular identification of *Trichinella britovi* in martens (*Martes martes)* and badgers (*Meles meles*); new host records in Poland. *Acta Parasitol.* (2012) 57:402–5. doi: 10.2478/s11686-012-0054-1
6. Cybulska A, Kornacka A, Moskwa B. The occurrence and muscle distribution of *Trichinella britovi* in raccoon dogs (*Nyctereutes procyonoides*) in wildlife in the Głeboki Bród Forest District, Poland. *Int J Parasitol Parasites Wildl.* (2019) 9:149–53. doi: 10.1016/j.ijppaw.2019.05.003
7. Moskwa B, Cybulska A, Kornacka A, Cabaj W, Bien J. Wild boars meat as a potential source of human trichinellosis in Poland: current data. *Acta Parasitol.* (2015) 60:530–5. doi: 10.1515/ap-2015-0075
8. Bilska-Zajac E, Rózycki M, Chmurzynska E, Marucci G, Cencek T, Karamon J, et al. *Trichinella* species circulating in wild boar (*Sus scrofa*) populations in Poland. *Int J Parasitol Parasites Wildl.* (2013) 2:211–3. doi: 10.1016/j.ijppaw.2013.05.004
9. Akkoc N, Kuruuzum Z, Akar S, Yuce A, Onen F, Yapar N, et al. A large-scale outbreak of trichinellosis caused by *Trichinella britovi* in Turkey. *Zoonoses Public Health.* (2009) 56:65–70. doi: 10.1111/j.1863-2378.2008.01158.x
10. Fichi G, Stefanelli S, Pagani A, Luchi S, De Gennaro M, Gómez-Morales MA, et al. Trichinellosis outbreak caused by meat from a wild boar hunted in an Italian region considered to be at negligible risk for *Trichinella*. *Zoonoses Public Health.* (2015) 62:285–91. doi: 10.1111/zph.12148
11. Gomez-Garcia V, Hernandez-Quero J, Rodriguez-Osorio M. Short report: human infection with *Trichinella britovi* in Granada, Spain. *Am J Trop Med Hyg.* (2003) 68:463–4. doi: 10.4269/ajtmh.2003.68.463
12. Messiaen P, Forier A, Vanderschueren S, Theunissen C, Nijs J, Van Esbroeck M. et al. Outbreak of trichinellosis related to eating imported wild boar meat, Belgium, 2014. *Euro Surveil.* (2016) 21:30341. doi: 10.2807/1560-7917.ES.2016.21.37.30341
13. Liu R, Qi X, Sun G, Jiang P, Zhang X, Wang L. Proteomic analysis of *Trichinella spiralis* adult worm excretory-secretory proteins recognized by early infection sera. *Vet Parasitol.* (2016) 231:43–6. doi: 10.1016/j.vetpar.2016.10.008
14. Robinson M, Connolly B. Proteomic analysis of the excretory-secretory proteins of the *Trichinella spiralis* L1 larva, a nematode parasite of skeletal muscle. *Proteomics.* (2005) 5:4525–32. doi: 10.1002/pmic.200402057
15. Wu X, B. Fu, Wang X, Yu L, Yu S, Deng H, et al. Identification of antigenic genes in *Trichinella spiralis* by immunoscreening of cDNA libraries. *Vet Parasitol.* (2009) 159:272–5. doi: 10.1016/j.vetpar.2008.10.035
16. Tang B, Liu M, Wang L, Yu S, Shi H, Boireau P, et al. Characterisation of a high-frequency gene encoding a strongly antigenic cystatin-like protein from *Trichinella spiralis* at its early invasion stage. *Parasit Vectors.* (2015) 8:78. doi: 10.1186/s13071-015-0689-5
17. Liu R, Wang Z, Wang L, Long S, Ren H, Cui J. Analysis of differentially expressed genes of *Trichinella spiralis* larvae activated by bile and cultured with intestinal epithelial cells using real-time PCR. *Parasitol Res.* (2013) 112:4113–20. doi: 10.1007/s00436-013-3602-1
18. Robinson M, Massie D, Connolly B. Secretion and processing of a novel multi-domain cystatin-like protein by intracellular stages of *Trichinella spiralis*. *Mol Biochem Parasitol.* (2007) 151:9–17. doi: 10.1016/j.molbiopara.2006.09.008
19. Grzelak S, Moskwa B, Bien J. *Trichinella britovi* muscle larvae and adult worms: stage-specific and common antigens detected by two-dimensional gel electrophoresis-based immunoblotting. *Parasit Vectors.* (2018) 11:584. doi: 10.1186/s13071-018-3177-x
20. Hartmann S, Lucius R. Modulation of host immune responses by nematode cystatins. *Int J Parasitol.* (2003) 33:1291–302. doi: 10.1016/S0020-7519(03)00163-2
21. Dzik J. Molecules released by helminth parasites involved in host colonization. *Acta Biochim Pol.* (2006) 53:33–64.
22. Cooper D, Eleftherianos I. Parasitic nematode immunomodulatory strategies: recent advances and perspectives. *Pathogens.* (2016) 5:E58. doi: 10.3390/pathogens5030058
23. Ochieng J, Chaudhuri G. Cystatin superfamily. *J Health Care Poor Underserved.* (2010) 21:51–70. doi: 10.1353/hpu.0.0257
24. Cornwall G, Hsia N. A new subgroup of the family 2 cystatins. *Mol Cell Endocrinol.* (2003) 200:1–8. doi: 10.1016/S0303-7207(02)00408-2
25. Turk V, Bode W. The cystatins - protein inhibitors of cysteine proteinases. *FEBS Lett.* (1991) 285:213–9. doi: 10.1016/0014-5793(91)80804-C
26. Ahmad M, Hirz M, Pichler H, Schwab H. Protein expression in *Pichia pastoris*: recent achievements and perspectives for heterologous protein production. *Appl Microbiol Biotechnol.* (2014) 98:5301–17. doi: 10.1007/s00253-014-5732-5
27. Cereghino G, Cereghino J, Ilgen C, Cregg J. Production of recombinant proteins in fermenter cultures of the yeast *Pichia pastoris*. *Curr Opin Biotechnol.* (2002) 13:329–32. doi: 10.1016/S0958-1669(02)00330-0
28. White C, Kempi N, Komives E. Expression of highly disulfide-bonded proteins in *Pichia pastoris*. *Structure.* (1994) 2:1003–5. doi: 10.1016/S0969-2126(94)00103-0
29. Grinna L, Tschopp J. Size distribution and general structural features on N-linkedoligosaccharides from the methylotrophic yeast, *Pichia pastoris. Yeast.* (1989) 5:107–15. doi: 10.1002/yea.320050206
30. Daly R, Hearn M. Expression of heterologous proteins in *Pichia pastoris*: a useful experimental tool in protein engineering and production. *J Mol Recogn.* (2005) 18:119–38. doi: 10.1002/jmr.687
31. Gonzalez-Hernandez A, Borloo J, Peelaers I, Casaert S, Leclercq G, Claerebout E. Comparative analysis of the immune responses induced by native versus recombinant versions of the ASP-based vaccine against the bovine intestinal parasite *Cooperia oncophora*. *Intl J Parasitol.* (2018) 48:41–9. doi: 10.1016/j.ijpara.2017.07.002
32. Holzhausen J, Haake C, Schicht S, Hinse P, Jordan D, Kremmer E. Biological function of *Dictyocaulus viviparus* asparaginyl peptidase legumain-1 and its suitability as a vaccine target. *Parasitology.* (2018) 145:378–92. doi: 10.1017/S0031182017001573

33. Noon J. Schwarz E, Ostroff G, Aroian R. A highly expressed intestinal cysteine protease of Ancylostoma ceylanicum protects vaccinated hamsters from hookworm infection. *PLoS Negl Trop Dis.* (2019) 13:e0007345. doi: 10.1371/journal.pntd.0007345
34. Wei J, Versteeg L, Liu Z, Keegan B, Gazzinelli-Guimaraes A, Fujiwara R, et al. Yeast-expressed recombinant As16 protects mice against *Ascaris suum* infection through induction of a Th2-skewed immune response. *PLoS Negl Trop Dis.* (2017) 11:e0005769. doi: 10.1371/journal.pntd.0005769
35. Kapel C, Gamble H. Infectivity, persistence, and antibody response to domestic and sylvatic *Trichinella* spp. in experimentally infected pigs. *Int J Parasitol.* (2000) 30:215–21. doi: 10.1016/S0020-7519(99)00202-7
36. Pozio E, Sofronic-Milosavljevic L, Morales M, Boireau P, Nockler K. Evaluation of ELISA and western blot analysis using three antigens to detect anti-*Trichinella* IgG in horses. *Vet Parasitol.* (2002) 108:163–78. doi: 10.1016/S0304-4017(02)00185-1
37. Korhonen PK, Pozio E, La Rosa G, Chang BC, Koehler AV, Hoberg EP. Phylogenomic and biogeographic reconstruction of the *Trichinella* complex. *Nat Commun.* (2016) 7:10513. doi: 10.1038/ncomms10513
38. Tang F, Xu L, Yan R, Song X, Li X. Evaluation of the immune response induced by DNA vaccines expressing MIF and MCD-1 genes of *Trichinella spiralis* in BALB/c mice. *J Helminthol.* (2012) 86:430–9. doi: 10.1017/S0022149X11000654
39. Teh S, Fong M, Mohamed Z. Expression and analysis of the glycosylation properties of recombinant human erythropoietin expressed in *Pichia pastoris*. *Genet Mol Biol.* (2011) 34:464–70. doi: 10.1590/S1415-47572011005000022
40. Jelkmann W. Erythropoietin after a century of research: younger than ever. *Eur J Haematol.* (2007) 78:183–205. doi: 10.1111/j.1600-0609.2007.00818.x
41. Ilic N, Gruden-Movsesijan A, Sofronic-Milosavljevic L. *Trichinella spiralis*: shaping the immune response. *Immunol Res.* (2012) 52:111–9. doi: 10.1007/s12026-012-8287-5
42. Nelson BH. IL-2, regulatory T cells, and tolerance. *J Immunol.* (2004) 172:3983–8. doi: 10.4049/jimmunol.172.7.3983
43. Malek T, Castro I. Interleukin-2 receptor signaling: at the interface between tolerance and immunity. *Immunity.* (2010) 33:153–65. doi: 10.1016/j.immuni.2010.08.004
44. Yu YR, Deng MJ, Lu WW, Jia MZ, Wu W, Qi YF. Systemic cytokine profiles and splenic toll-like receptor expression during *Trichinella spiralis* infection. *Exp Parasitol.* (2013)34:92–101. doi: 10.1016/j.exppara.2013.02.014
45. Couper KN, Blount DG, Riley EM. IL-10: the master regulator of immunity to infection. *J Immunol.* (2008) 180:5771–7. doi: 10.4049/jimmunol.180.9.5771
46. Jankovic D, Sher A, Yap G. Th1/Th2 effector choice in parasitic infection: decision making by committee. *Curr Opin Immunol.* (2001) 13:403–9. doi: 10.1016/S0952-7915(00)00234-X
47. Conlon PJ, Tyler S, Grabstein KH, Morrissey P. Interleukin-4 (B-cell stimulatory factor-1) augments the *in vivo* generation of cytotoxic cells in immunosuppressed animals. *Biotechnol Ther.* (1989) 1:31–41.
48. Klotz C, Ziegler T, Daniłowicz-Luebert E, Hartmann S. Cystatins of parasitic organisms. *Adv Exp Med Biol.* (2011) 12:208–21. doi: 10.1007/978-1-4419-8414-2_13
49. Batista-Duharte A, Martinez DT, Carlos IZ. Efficacy and safety of immunological adjuvants. Where is the cut-off? *Biomed Pharmacother.* (2018) 105:616–24. doi: 10.1016/j.biopha.2018.06.026
50. Martinon S, Cisneros A, Villicana S, Hernandez-Miramontes R, Mixcoha E, Calderon-Vargas P. Chemical and immunological characteristics of aluminum-based, oil-water emulsion, and bacterial-origin adjuvants. *J Immunol Res.* (2019) 2019:3974127. doi: 10.1155/2019/3974127
51. Apostolico J, Lunardelli V, Coirada F, Boscardin S, Rosa D. Adjuvants: classification, modus operandi, and licensing. *J Immunol Res.* (2016) 2016:1459394. doi: 10.1155/2016/1459394
52. Bi K, Yang J, Wang L, Gu Y, Zhan B, Zhu X. Partially protective immunity induced by a 20 kDa protein secreted by *Trichinella spiralis* stichocytes. *PLoS ONE.* (2015) 10:e0136189. doi: 10.1371/journal.pone.0136189
53. Li X, Yao JP, Pan AH, Liu W, Hu XC, Wu ZD et al. An antigenic recombinant serine protease from *Trichinella spiralis* induces protective immunity in BALB/c mice. *Parasitol Res.* (2013) 112:3229–38. doi: 10.1007/s00436-013-3500-6
54. Yang Z, Li W, Yang Z, Pan A, Liao W, Zhou X. A novel antigenic cathepsin B protease induces protective immunity in *Trichinella*-infected mice. *Vaccine.* (2018) 36:248–55. doi: 10.1016/j.vaccine.2017.11.048
55. Sun G, Song Y, Jiang P, Ren H, Yan S, Han Y, et al. Characterization of a *Trichinella spiralis* putative serine protease. Study of its potential as sero-diagnostic tool. *PLoS Negl Trop Dis.* (2018) 12:e0006485. doi: 10.1371/journal.pntd.0006485
56. Xu N, Liu X, Tang B, Wang L, Shi H, Boireau P, et al. Recombinant *Trichinella pseudospiralis* serine protease inhibitors alter macrophage polarization *in vitro*. *Front Microbiol.* (2017) 8:1834. doi: 10.3389/fmicb.2017.01834
57. Höfer T, Krichevsky O, Altan-Bonnet G. Competition for IL-2 between regulatory and effector T cells to chisel immune responses. *Front Immunol.* (2012) 3:268. doi: 10.3389/fimmu.2012.00268

Conflict of Interest: The authors declare that the research was conducted in the absence of any commercial or financial relationships that could be construed as a potential conflict of interest.

frontiers in Immunology

ORIGINAL RESEARCH
published: 29 October 2019
doi: 10.3389/fimmu.2019.02542

B Cell-Based Vaccine Transduced With ESAT6-Expressing Vaccinia Virus and Presenting α-Galactosylceramide Is a Novel Vaccine Candidate Against ESAT6-Expressing Mycobacterial Diseases

*Bo-Eun Kwon[1], Jae-Hee Ahn[1], Eun-Kyoung Park[1], Hyunjin Jeong[1], Hyo-Ji Lee[2], Yu-Jin Jung[2], Sung Jae Shin[3], Hye-Sook Jeong[4], Jung Sik Yoo[4], EunKyoung Shin[4], Sang-Gu Yeo[5], Sun-Young Chang[6] and Hyun-Jeong Ko[1]**

[1] Laboratory of Microbiology and Immunology, College of Pharmacy, Kangwon National University, Chuncheon, South Korea, [2] Department of Biological Sciences, Kangwon National University, Chuncheon, South Korea, [3] Department of Microbiology, Institute for Immunology and Immunological Disease, Brain Korea 21 PLUS Project for Medical Science, Yonsei University College of Medicine, Seoul, South Korea, [4] Division of Vaccine Research, Center for Infectious Disease Research, Korea National Institute of Health (KNIH), Korea Centers for Disease Control and Prevention (KCDC), Cheongju, South Korea, [5] Sejong Institute of Health and Environment, Sejong, South Korea, [6] Laboratory of Microbiology, College of Pharmacy and Research Institute of Pharmaceutical Science and Technology (RIPST), Ajou University, Suwon, South Korea

OPEN ACCESS

Edited by:
Giuseppe Andrea Sautto,
University of Georgia, United States

Reviewed by:
Rodrigo Bessa Abreu,
University of Georgia, United States
Mahavir Singh,
LIONEX GmbH, Germany

***Correspondence:**
Hyun-Jeong Ko
hjko@kangwon.ac.kr

Specialty section:
This article was submitted to Vaccines and Molecular Therapeutics, a section of the journal Frontiers in Immunology

Received: 03 July 2019
Accepted: 14 October 2019
Published: 29 October 2019

Citation:
Kwon B-E, Ahn J-H, Park E-K, Jeong H, Lee H-J, Jung Y-J, Shin SJ, Jeong H-S, Yoo JS, Shin E, Yeo S-G, Chang S-Y and Ko H-J (2019) B Cell-Based Vaccine Transduced With ESAT6-Expressing Vaccinia Virus and Presenting α-Galactosylceramide Is a Novel Vaccine Candidate Against ESAT6-Expressing Mycobacterial Diseases. Front. Immunol. 10:2542. doi: 10.3389/fimmu.2019.02542

Early secretory antigenic target-6 (ESAT6) is a potent immunogenic antigen expressed in *Mycobacterium tuberculosis* as well as in some non-tuberculous mycobacteria (NTM), such as *M. kansasii*. *M. kansasii* is one of the most clinically relevant species of NTM that causes mycobacterial lung disease, which is clinically indistinguishable from tuberculosis. In the current study, we designed a novel cell-based vaccine using B cells that were transduced with vaccinia virus expressing ESAT6 (vacESAT6), and presenting α-galactosylceramide (αGC), a ligand of invariant NKT cells. We found that B cells loaded with αGC had increased levels of CD80 and CD86 after *in vitro* stimulation with NKT cells. Immunization of mice with B/αGC/vacESAT6 induced $CD4^+$ T cells producing TNF-α and IFN-γ in response to heat-killed *M. tuberculosis*. Immunization of mice with B/αGC/vacESAT6 ameliorated severe lung inflammation caused by *M. kansasii* infection. We also confirmed that immunization with B/αGC/vacESAT6 reduced *M. kansasii* bacterial burden in the lungs. In addition, therapeutic administration of B/αGC/vacESAT6 increased IFN-γ^+ $CD4^+$ T cells and inhibited the progression of lung pathology caused by *M. kansasii* infection. Thus, B/αGC/vacESAT6 could be a potent vaccine candidate for the prevention and treatment of ESAT6-expressing mycobacterial infection caused by *M. kansasii*.

Keywords: *Mycobacterium kansasii*, *Mycobacterium tuberculosis*, non-tuberculous mycobacteria, ESAT6, vaccine, α-galactosylceramide

INTRODUCTION

Non-tuberculous mycobacteria (NTM) are one of the mycobacteria species which cause pulmonary disease as a common manifestation (1). *Mycobacterium kansasii* belongs to NTM species and is one of the major causative agent of NTM lung disease (2). Symptoms of *M. kansasii* are mild under single infection, but it is known that more severe symptoms occur when contracted along with other illnesses such as inflammatory pseudotumor (3), sarcoidosis (4), and HIV (5). Especially, it has been reported that in Brazil, most patients who acquire lung disease caused by NTM had previously received tuberculosis treatment (6). These reports implied that NTM was closely associated with other diseases, and therefore is one of the important factors in pulmonary infection.

Bacillus Calmette-Guerin (BCG) is the only approved live attenuated vaccine strain induced from *M. bovis* through multiple sub-culturing for a long period of time (7). The protective efficacy of BCG against tuberculous meningitis and tuberculosis (TB) is well-known in children, however, protection for primary infection or latent infection in adults seems poor (8). Also, BCG vaccination did not provide protection against NTM infection (9). Due to this limitation of BCG, more persistent research is needed to identify novel vaccine candidates.

Early secretory antigenic target-6 (ESAT6) is a protein encoded by a gene located in the region of difference 1, which is expressed in *M. tuberculosis* but not in BCG (10). ESAT6 has sufficient immunogenicity in both humans and mice post *M. tuberculosis* infection (11). Interestingly, some NTM species, including *M. kansasii* also contain genes for ESAT6 homolog. In the present study, we expressed ESAT6 in B cells using ESAT6-expressing vaccinia virus to deliver ESAT6 antigen to B cells, and presented α-galactosylceramide (αGC), an invariant natural killer cell (iNKT) ligand, on CD1d molecule of B cells. Previous studies have suggested that a B cell vaccine which expressed tumor antigen showed potent anti-tumor effect facilitated by activated NKT cells (12, 13).

In the current study, we developed an ESAT6-expressing B cell-based vaccine which was loaded with αGC (B/αGC/vacESAT6) and assessed its preventive and therapeutic effect in a murine model of *M. kansasii* infection.

MATERIALS AND METHODS

Construction of Vaccinia Virus Vector Expressing ESAT6

ESAT6 gene of *M. tuberculosis* strain H37Rv with human optimized codon was synthesized and cloned into vaccinia virus delivery vector PVVT1-C7L (PVVT1-C7L-Tpa-esat6) which contains *tPA* gene for secretion of intracellular signal peptide. Sfi1 restriction enzyme was used for cloning. PVVT1-C7L-Tpa-esat6 was transformed to *E. coli* DH5 competent cells for amplification. The expression of *ESAT6* gene was confirmed by PCR using the following primers; 5′-TTT GAA GCA TTG GAA GCA ACT-3′ (VVTK-F) and 5′-ACGTTGAAATGTCCCATCGACT-3′ (VVTK-R).

Preparation of Recombinant Vaccinia Virus Expressing ESAT6

Vero cells in 12-well plates were infected with vaccinia virus (KCCM11574P) at a multiplicity of infection (MOI) of 0.02 for 2 h, and the infected Vero cells were transfected with PVVT1-C7L-Tpa-esat6 plasmid using Lipofectamine 2000 (Thermo Fisher Scientific, Waltham, MA, USA) transfection reagent for 4 h. Vero cells were incubated for 3–4 days to observe the cytopathic effects, and recombinant viruses were obtained by plaque isolation. For high efficacy and purity, recombinant vaccinia virus expressing ESAT6 (vacESAT6) was concentrated by ultracentrifugation. The expression of ESAT6 protein by Vero cells and isolated B cells after transduction with vacESAT6 was confirmed by confocal microscopy (**Figures 1A,B**, **Supplementary Figure 1**).

Preparation of B Cell-Based Vaccine and Immunization of BCG

$B220^+$ cells were magnetically purified from splenocytes of naïve C57BL/6 mice using CD45R/B220 biotin (BD biosciences, California, USA) and anti-biotin microbeads (Miltenyi Biotec, Bergisch Gladbach, Germany) according to the manufacturer's instructions. Labeled cells were purified through LS column (Miltenyi Biotec, Bergisch Gladbach, Germany). Isolated $B220^+$ cells (2×10^7 cells seeded) were transduced with vacESAT6 (MOI of 1) for 2 h and then loaded with αGC (Enzo life sciences, New York, USA) (1 μg/ml) for 22 h and incubated in a CO_2 incubator. After washing three times with PBS, mice were immunized with cultured cells (B cell-based vaccine) by tail vein injection. As for the comparison group, mice were intramuscularly immunized with BCG (10^5 CFU/mouse).

To confirm preventive effect of Bvac, mice were either immunized with BCG by intramuscular injection at a 10^5 CFU/mouse or administered with Bvac by tail vein injection at day 0 for the priming and day 7 for the boost. At day 14, mice were challenged with 10^7 CFU/mouse of *M. kansasii*. To confirm the therapeutic effect of Bvac, mice were infected with 10^7 CFU of *M. kansasii* per mouse at Day 0, and were administrated with BCG or Bvac at 3 days post-infection. The mice were boosted with Bvac at 7 days post-infection. We analyzed histology, protein levels and bacterial loads from lung and liver after 14 days following *M. kansasii* infection.

Murine Infection Model of *M. kansasii*

C57BL/6 mice were purchased at 6–7 weeks of age from Charles River Laboratories (Orient Bio Inc., Seongnam, Korea). All animal experiments, including the *M. kansasii* challenge experiment, were approved by the Institutional Animal Care and Use Committee of Kangwon National University (Permit Number: KW-160201-4). A hypervirulent *M. kansasii* SM#1 clinical isolate was used for challenge *in vivo* (14). To induce infection, mice were intravenously injected with *M. kansasii* (10^7 CFU/mouse). We checked the bodyweight and survival rate of mice every day following *M. kansasii* infection.

The lungs and liver of infected mice were isolated for determining the bacterial count in these organs at 2 weeks

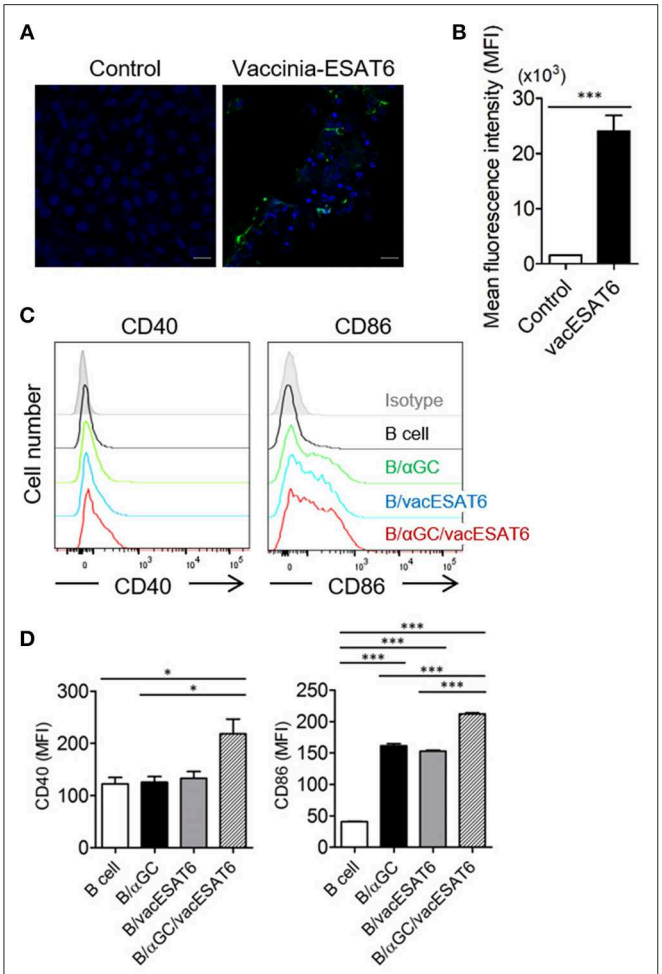

FIGURE 1 | B/αGC/vacESAT6 up-regulates co-stimulatory molecules on B cells. **(A,B)** Vero cells were transduced with vaccinia-ESAT6 (vacESAT6) at a multiplicity of infection (MOI) of 1. Transduced cells were fluorescently stained for ESAT6 (green) and counterstained with DAPI (blue) for nuclei which were analyzed by confocal microscopy to detect the expression of ESAT6 (scale bar = 20 μm). **(A)** Representative confocal images and **(B)** Representation of the evaluation of green fluorescent area. **(C,D)** B220$^+$ cells were isolated from splenocytes of naïve C57BL/6 mice. Isolated B220$^+$ cells were transduced with vacESAT6 at a MOI of 1 and/or loaded with 1 μg/ml of αGC and then co-cultured with naïve splenocytes for 24 h. Incubated cells were stained to examine the expression of B220, CD40, and CD86. Expression levels of CD40 and CD86 in B220$^+$ cells were analyzed by flow cytometry. **(C)** Representative flow cytometry histogram and **(D)** summary of mean fluorescence intensity of CD40 and CD86 expression in B cells. ANOVA. $^*p < 0.05$, $^{***}p < 0.001$.

post *M. kansasii* infection. Lungs were homogenized in 1X PBS containing 0.04% tween 80 and liver was homogenized in 1X PBS containing 1 mM EDTA (125 mg of tissues/ml). The homogenized supernatants were 10-fold serial diluted in Difco™ Middlebrook 7H9 Broth (BD biosciences, California, USA) containing ADC [Sodium Chloride (Duchefa, BH Haarlem, The Nederlands), Dextrose (SHOWA, Gyoda, Japan), Bovine Albumin Fraction V (MPBio, Santa Ana, USA), Catalase (Sigma-Aldrich, St. Louis, USA)] and each diluent was drop cultured in Difco™ Middlebrook 7H10 Agar (BD biosciences, California, USA) containing OADC [Sodium Chloride, Dextrose, Bovine Albumin Fraction V, Catalase, Oleic acid (Sigma-Aldrich, St. Louis, USA)]. Smear plates were cultured in a 37°C incubator and colonies were counted after 2–3 weeks.

Isolation of Cells and Measurement of Co-stimulatory Molecules in B Cells

For the isolation of T cells, splenocytes were labeled with CD8α-PE and anti-PE microbeads (Miltenyi Biotec, Bergisch Gladbach, Germany) according to the manufacturer's instructions. The labeled cells were then purified through LS column (Miltenyi Biotec, Bergisch Gladbach, Germany). CD4$^+$ T cells were isolated by using the mouse CD4$^+$ T cell isolation kit (Miltenyi Biotec, Bergisch Gladbach, Germany). CD11c$^+$ DCs were purified by using CD11c$^+$ microbeads (Miltenyi Biotec, Bergisch Gladbach, Germany). B220$^+$ cells were purified by using CD45R/B220 biotin (BD biosciences, California, USA) and anti-Biotin microbeads (Miltenyi Biotec, Bergisch Gladbach, Germany) from splenocytes of naïve C57BL/6 mice. Purified B cells were transduced with vacESAT6 at a MOI of 1 and/or loaded with 1 μg/ml of αGC and then co-cultured with naïve splenocytes for 24 h. Incubated cells were stained to examine the expression of B220, CD40, and CD86 using antibodies such as APC-conjugated anti-B220 (BD biosciences, California, USA), PE-conjugated isotype control (eBioscience, San Diego, USA), anti-CD40 (Biolegend, San Diego, USA), and anti-CD86 Ab (BD biosciences, California, USA). Cells were analyzed by flow cytometry.

Measurement of Intracellular Cytokines in CD4$^+$ T Cells

For measurement of intracellular cytokines, dendritic cells and CD4$^+$ T cells were co-cultured and stimulated for 3 days with heat-killed H37Rv at 0.1 MOI or overnight with anti-CD3 and anti-CD28 antibody in culture media. H37Rv strain was generously provided by Sang-Nae Cho (Yonsei University). Brefeldin A Solution (1000 x) Thermo Fisher Scientific, Waltham, MA, USA) was added for 4 h before harvest and then harvested cells were stained with PerCP-Cy™5.5 rat anti-mouse CD4 (BD biosciences, California, USA) or PE rat anti-mouse CD8α (BD biosciences, California, USA). Stained cells were permeabilized with IC Fixation Buffer (Thermo Fisher Scientific, Waltham, MA, USA) according to the manufacturer's recommendations. Next, permeabilized cells were stained with TNF-α mAb, APC (Thermo Fisher Scientific, Waltham, MA, USA) and IFN-γ mAb (XMG1.2) PE (Thermo Fisher Scientific, Waltham, MA, USA).

The supernatants of homogenized tissues were analyzed for cytokine production using BD™ Cytometric Bead Array (CBA) Mouse Inflammation kit (BD biosciences, California, USA) according to the manufacturer's instructions.

Western Blotting

Total protein lysates of *M. kansasii* were sonicated with PRO-PREP™ protein extraction solution (iNtRON

Biotechnology, Daejeon, Korea). Lysates were boiled at 100°C and proteins were separated by performing SDS-PAGE. Proteins were transferred onto PVDF membranes (Millipore, Burlington, USA) and then blocked with 5% skim milk in TBS with tween 20. Next, the membranes were incubated with anti-ESAT6 primary antibody [11G4] (Abcam, Cambridge, USA) and proteins were detected using HRP conjugated goat anti-mouse polyclonal antibody (Enzo life sciences, New York, USA). Membranes were developed using femtoLUCENT™ PLUS-HRP chemiluminescence detection system (G-Biosciences, St. Louis, USA).

Flow Cytometry

Cells were collected from spleen and stained with markers such as APC-conjugated anti-B220 (BD biosciences, California, USA) and anti-Ly6C (BD biosciences, California, USA) Ab, FITC-conjugated anti-CD11b Ab (BD biosciences, California, USA), PE-conjugated isotype control (eBioscience, San Diego, USA), anti-CD40 Ab (Biolegend, San Diego, USA), and anti-CD86 (BD biosciences, California, USA) Ab. Flow cytometry was performed on a FACSVerse instrument (BD biosciences, California, USA) and data were analyzed using FlowJo software (Flowjo, San Carlos, USA).

Histology

Mice were sacrificed and lungs were isolated from each group. They were fixed with 4% formalin overnight. Lung tissues were processed using a tissue processor (Leica, Wetzlar, Germany) and then embedded in paraffin. Paraffin-embedded tissue blocks were cut into 5 μm thick sections and stained with hematoxylin and eosin.

Confocal Microscopy

Uninfected or vaccinia virus-infected Vero cells and B cells were cultured in a 37°C incubator for 24 h. Cells were fixed with 4% paraformaldehyde and stained with anti-ESAT6 Ab (Abcam, Cambridge, USA), and further stained with anti-mouse IgG (H+L), $F(ab')_2$ Fragment (Alexa Fluor® 488-conjugated) (Cell signaling, Danvers, USA) or DyLight™ 405 affinipure donkey anti-mouse IgG (H+L) (DyLight™ 405-conjugated). Cells were visualized by confocal microscopy (Carl Zeiss, LSM880 with Airyscan, Zena, Germany).

Statistics

Statistical analysis was conducted with GraphPad Prism 5.0 (GraphPad Software, La Jolla, USA). Differences between groups were assessed by the Student's *t*-test. Comparisons between multiple-groups were carried out by one-way ANOVA analysis of variance followed by the Bonferroni's multiple comparison test. P values < 0.05 were considered as significant at a 95% confidence interval for all analyses.

RESULTS

B/αGC/vacESAT6 Upregulated the Expression of Co-stimulatory Molecules on B Cells

It has been previously reported that αGC-loaded B cell-based vaccines expressing tumor antigens showed significant antitumor effects *in vivo* (15, 16). Thus, we decided to adopt this vaccine strategy for the development of preventive and therapeutic anti-mycobacterial vaccine. B cells were transduced with recombinant vaccinia virus expressing ESAT6 (vacESAT6), and the transduced B cells were loaded with αGC. We found that B cells loaded with αGC/vacESAT6 (B/αGC/vacESAT6) (Bvac) increased the expression of co-stimulatory molecules including CD40 and CD86 when they were co-cultured with splenocytes from naïve C57BL/6 mice for 24 h (**Figures 1C,D**). B cells loaded with αGC or B cells transduced with vacESAT6 increased the expression of CD86, which further increased in B/αGC/vacESAT6 (**Figures 1C,D**). B cells transduced with vacGFP control virus also increased the expression of CD86 (**Supplementary Figure 2**) suggesting that infection of vaccinia virus alone could be stimulatory for B cells. These results suggested that activated NKT cells by αGC on B cells as well as vaccinia virus infection activated the B cells to increase the expression of co-stimulatory molecules including CD40 and CD86, which help B cells to function as professional antigen presenting cells to induce effective T cells.

B/αGC/vacESAT6 Induced $CD4^+$ T Cell Responses Against H37Rv

We next determined whether B/αGC/vacESAT6 induced $CD4^+$ T cell response *in vivo*. Groups of mice were immunized with either saline, BCG or B/αGC/vacESAT6, and mice were sacrificed to obtain splenocytes. We analyzed TNF-α- and IFN-γ-producing $CD4^+$ T cells after 3 days of co-culturing the splenocytes with dendritic cells pulsed with heat-killed H37Rv. As a result, we found that the percentage of $CD4^+$ T cells producing TNF-α^+ and IFN-γ^+ was higher in mice vaccinated with B/αGC/vacESAT6 as compared to control and BCG-immunized mice (**Figures 2A,B**). In addition, IFN-γ production was also increased in the culture supernatant of splenocytes from B/αGC/vacESAT6 group compared to control and BCG group (**Figure 2C**). These results show that B/αGC/vacESAT6 induced the H37Rv-specific $CD4^+$ T cell-mediated cellular immunity which might be critical for the regulation of mycobacterial infection.

Mice Infected With *M. kansasii* Showed Severe Lung Inflammation

M. kansasii is one of the NTM which expresses ESAT6 homolog as a major antigen. We confirmed the expression of ESAT6 in *M. kansasii* by western blotting analysis (**Figure 3A**). We found that the bodyweight of mice significantly decreased with intravenous (i.v) injection of *M. kansasii* (10^7 CFU/mouse). For humane reasons, mice were monitored two times every

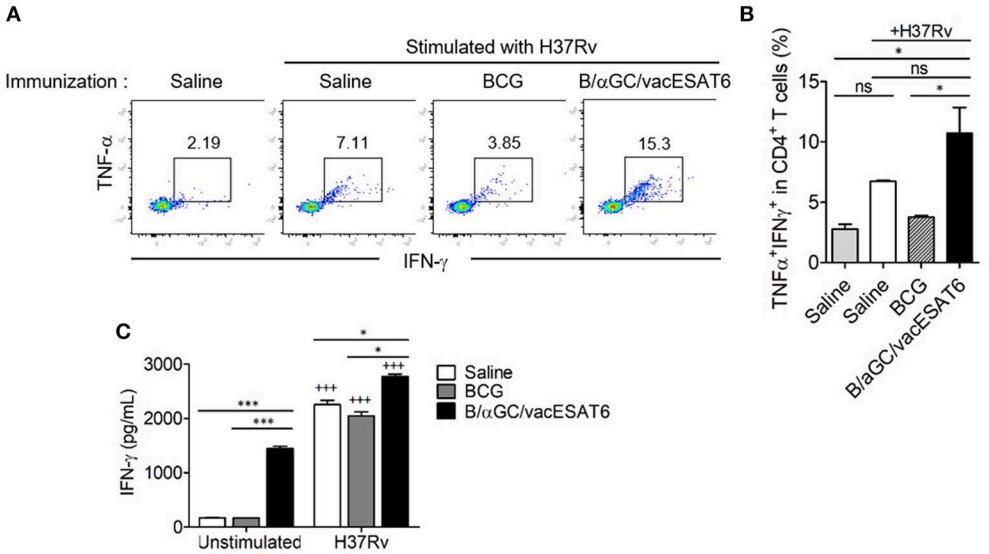

FIGURE 2 | B/αGC/vacESAT6 induced *M. tuberculosis* specific $CD4^+$ T cell response. Splenic $CD4^+$ T cells were isolated from mice which were immunized with BCG (10^5 CFU/mouse) or with B/αGC/vacESAT6 (Bvac), and they were co-cultured with $CD11c^+$ dendritic cells which were stimulated with heat-killed *M. tuberculosis* H37Rv at 0.1 MOI. After 72 h co-culture, $CD4^+$ T cells were analyzed by flow cytometry to detect intracellular TNF-α and IFN-γ production. **(A)** Representative intracellular staining of TNF-α and IFN-γ. **(B)** Summary of TNF-α and IFN-γ secreting $CD4^+$ T cells. **(C)** Secreted IFN-γ levels were measured in culture supernatant by ELISA. ANOVA. $^*p < 0.05$, $^{***}p < 0.001$, $^{+++}p < 0.001$ compared to unstimulated counterpart.

day and sacrificed when they weighed <80% of their initial bodyweight. In addition, there was significant lung injury including infiltration of immune cells around bronchial tubes as well as formation of granuloma-like lesions. We also confirmed the presence of bacteria in lungs of *M. kansasii*-infected mice at 2 weeks after infection. On the contrary, immunization of mice with Bvac ameliorated loss of bodyweight and increased survival rate following *M. kansasii* infection (**Figures 3B,C**). In addition, lungs of mice immunized with Bvac had moderate injury with reduced cell infiltration as compared with non-vaccinated mice after *M. kansasii* infection (**Figures 3D,E**). Bvac also decreased the bacterial burden in the lungs of *M. kansasii*-infected mice (**Figure 3F**). We also analyzed the proportion of NK cells and NKT cells in splenocytes by flow cytometry. We confirmed that Bvac immunization increased the percentage of NKT cells as compared with that of non-vaccinated mice as assessed after *M. kansasii* infection (**Supplementary Figure 3**). We also compared the therapeutic effects of Bvac and BCG vaccine in *M. kansasii*-infected mice. As a result, mice therapeutically treated with BCG and Bvac showed moderate levels of inflammation with reduced cell infiltration and decreased the bacterial burden in the lungs of *M. kansasii*-infected mice (**Supplementary Figures 4A,B**). Intriguingly, however, immunization of mice with Bvac significantly decreased the bacterial burden in the liver than BCG immunization after *M. kansasii* infection (**Supplementary Figures 4C,D**). Collectively, we established a murine model of infection of *M. kansasii* and showed that Bvac had preventive effect against *M. kansasii* expressing ESAT6.

B/αGC/vacESAT6 Had Therapeutic Effects Against *M. kansasii* Infection

We speculated whether B/αGC/vacESAT6 (Bvac) had therapeutic effects against mice infected with *M. kansasii*. To evaluate therapeutic efficacy of Bvac, mice were i.v. challenged with 10^7 CFU/mouse of *M. kansasii*, and 14 days later, they were injected with Bvac at day 3 and 7 post-infection. When we checked the bodyweight, mice administered with Bvac showed alleviation in loss of body weight as compared to mice infected with *M. kansasii* (**Figure 4A**). Further, survival rate increased in mice treated with Bvac (**Figure 4B**). Histological analysis of lungs of infected mice confirmed the therapeutic effects of Bvac against *M. kansasii* infection (**Figures 4C,D**). Bacterial load in the lungs was significantly reduced in mice administered with Bvac as compared to *M. kansasii* infected mice (**Figure 4E**). Also, administered with BCG did not show the therapeutic effect, while Bvac administration reduced bacterial loads in lungs of the infected mice (**Supplementary Figure 5**). Furthermore, production of TNF and IL-6, which were increased in lungs of infected mice following *M. kansasii* infection, were significantly decreased when administered with Bvac (**Figure 5A**). Collectively these results suggested that Bvac had a therapeutic effect in mice infected with *M. kansasii*.

Bvac Increased the Production of IFN-γ in $CD4^+$ T Cells in a Therapeutic Mouse Model

Finally, we assessed the production of intracellular cytokines in $CD4^+$ T cells after therapeutic treatment with Bvac in *M.*

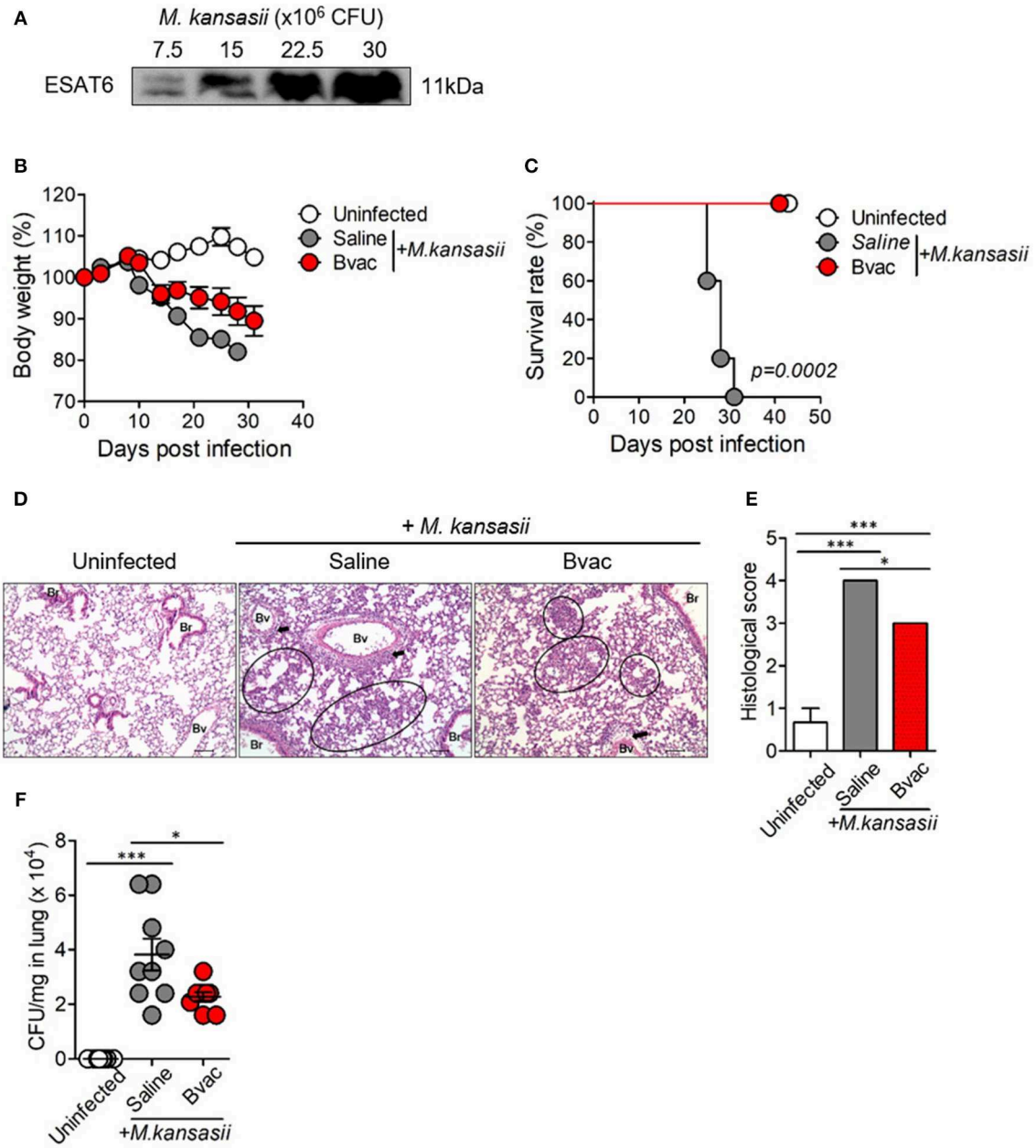

FIGURE 3 | Immunization of mice with Bvac prevented *M. kansasii* infection. **(A)** Expression of 11 kDa ESAT6 obtained from lysates of various CFU of *M. kansasii* by western blotting. **(B–F)** Mice were intravenously immunized with Bvac via tail vein. After 14 days of immunization mice were challenged with *M. kansasii* (10^7 CFU/mouse) ($n = 5$ for uninfected, $n = 6$ for saline and Bvac group). After 14 days following *M. kansasii* infection, histology and bacterial CFU were determined from lungs. **(B)** Bodyweight. ANOVA. $^*p < 0.05$, *M. kansasii* vs. Bvac+ *M. kansasii.* **(C)** Survival rate. Log-rank test. **(D)** Representative hematoxylin and eosin staining of lung sections from each group of mice (scale bar = 100 μm). Bv (Blood vessel), Br (Bronchus), circle indicates interstitial necrotizing inflammatory foci, and arrow is perivascular inflammatory cell infiltration. **(E)** Histological scores of the lung sections. **(F)** CFU of *M. kansasii* from lung homogenates. ANOVA. $^*p < 0.05$, $^{***}p < 0.001$.

kansasii infected mice. IFN-γ-producing T cells are known to play a key role in resistance against various pathogens including *M. tuberculosis* (17). Mice were infected with *M. kansasii* (10^7 CFU/mouse), and i.v. injected with Bvac at day 3 and 7 post infection. After 14 days following *M. kansasii* infection, lung homogenates were analyzed for the production of TNF, IFN-γ, and IL-6. Interestingly, although the levels of TNF, IFN-γ and IL-6, were highly increased in mice infected with *M. kansasii,* the levels of TNF and IL-6 were significantly reduced. When $CD4^+$ T cells obtained from the spleen of the treated mice were analyzed for IFN-γ production, we found that splenocytes of mice administered with Bvac showed increased production of

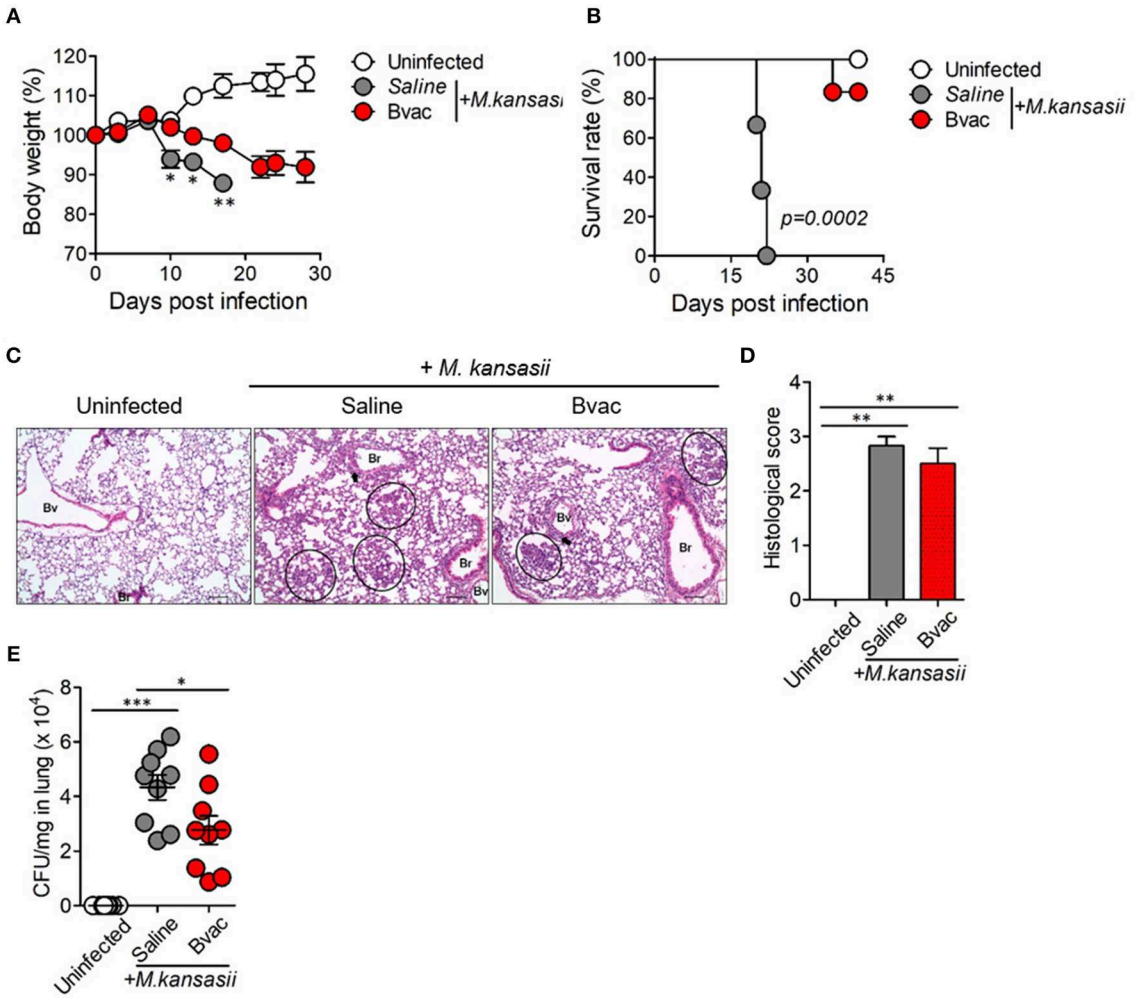

FIGURE 4 | Bvac has therapeutic effect on mice infected with *M. kansasii*. To evaluate therapeutic efficacy of Bvac, mice were infected with 10^7 CFU of *M. kansasii* per mouse, and Bvac was administered via tail vein injection at day 3 and 7 post infection ($n = 5$ for uninfected, $n = 6$ for saline and Bvac group). After 14 days following *M. kansasii* infection, histology and bacterial CFU were determined from lung. **(A)** Body weights of mice are shown, ANOVA. $^*p < 0.05$, $^{**}p < 0.01$, *M. kansasii* vs. Bvac + *M. kansasii*. **(B)** Survival rate. Log-rank test. **(C)** Representative hematoxylin and eosin staining of lung sections from each group of mice (scale bar = 100 μm). Bv (Blood vessel), Br (Bronchus), circle indicates interstitial necrotizing inflammatory foci, and arrow is perivascular inflammatory cell infiltration. **(D)** Histological scores of the lung sections. **(E)** CFU of *M. kansasii* from lung homogenates. ANOVA. $^*p < 0.05$, $^{***}p < 0.001$.

IFN-γ in $CD4^+$ T cells compared to *M. kansasii*-infected mice (**Figure 5B**). Consequently, these results suggest that Bvac could induce IFN-γ-producing $CD4^+$ T cell response, resulting in preventive and therapeutic effects against *M. kansasii* expressing ESAT6 (**Supplementary Figure 6**).

DISCUSSION

Tuberculosis is the most dangerous and incurable disease in the world (18–20). Although most patients with *M. tuberculosis* infection can be cured with appropriate treatment with anti-tuberculosis drugs such as isoniazid, rifampin, pyrazinamide, and ethambutol, it is difficult to treat multidrug resistant tuberculosis (MDR-TB) and extensively drug-resistant tuberculosis (XDR-TB) (21). Novel drugs including bedaquiline and delamanid have been introduced to deal with MDR-TB (22). In addition, drug repositioning approaches have provided linezolid, imatinib, and metformin for the treatment of TB patients (23–27). However, since treatment of MDR-TB requires at least 4 months, studies on the development of new anti-tuberculosis drugs are still needed. In this study, we suggest a novel approach to treat mycobacterial infection including *M. tuberculosis* using a therapeutic vaccine.

Currently, the only licensed vaccine for TB is BCG. BCG is made by attenuating *M. bovis*. However, there are several limitations of BCG as TB vaccine since it cannot prevent the development of primary infection and reactivation of latent pulmonary infection. Besides, the efficacy of BCG vaccine has a broad range and limited efficacy in adults. Due to the limitation of BCG vaccine, there is

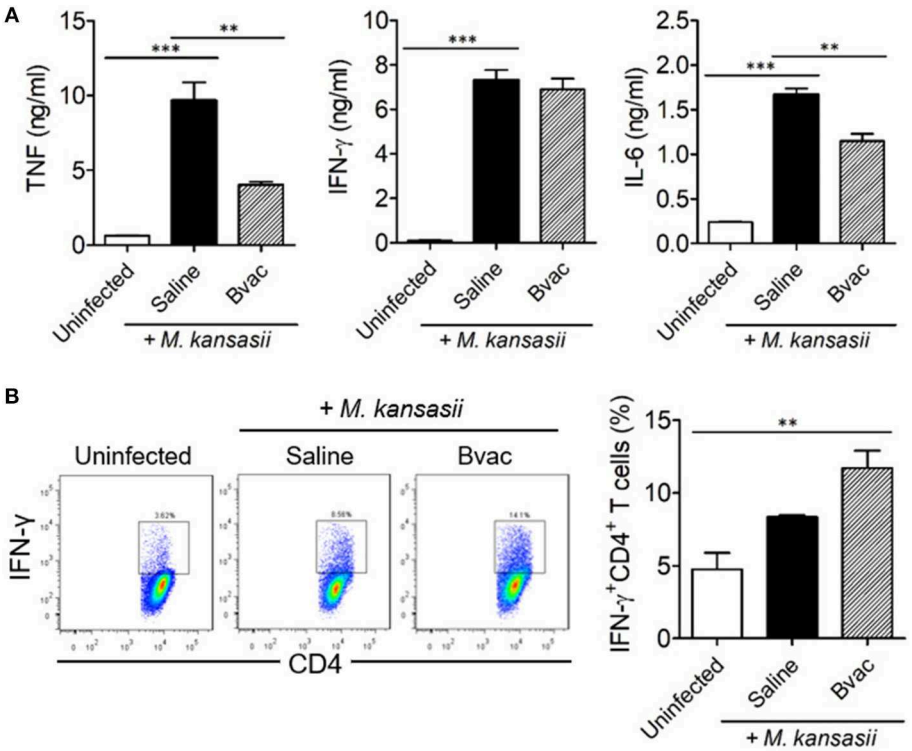

FIGURE 5 | Therapeutic administration of Bvac increased the production of IFN-γ in $CD4^+$ T cells in *M. kansasii*-infected mice. Mice were infected with 10^7 CFU/mouse of *M. kansasii*, and then they were intravenously injected with Bvac at day 3 and 7 post infection. After 14 days following *M. kansasii* infection, lung and spleen were isolated to analyze cytokine production. **(A)** The levels of TNF, IFN-γ, and IL-6 from lung homogenates. **(B)** Splenic $CD4^+$ T cells were analyzed for IFN-γ production after *in vitro* stimulation with plate-coated anti-CD3 and anti-CD28 antibodies. Representative histogram (left) and summary (right) for the percentages of IFN-γ producing $CD4^+$ T cells. ANOVA. $^{**}p < 0.01$, $^{***}p < 0.001$.

an immediate need for further research to develop a novel mycobacterial vaccine.

NTM is another contagious disease-causing pathogen in humans (17). It has been reported that the incidence of multiple NTM infections and NTM-associated mortality rates have dramatically increased in recent times (28, 29). Non-tuberculous mycobacterial pulmonary disease (NTM-PD) is one of the main conditions caused by NTM (30, 31) and the radiological manifestation of NTM-PD is classified as fibrocavitary form (similar to pulmonary tuberculosis) and nodular bronchiectatic form (similar to MAC pulmonary disease) (32, 33). It has been reported that NTM-PD infection increases with age (34), co-infection with chronic obstructive pulmonary disease (COPD) and asthma, in patients (35).

M. kansasii is known as one of the main pathogens causing NTM-PD (36). It has been reported that *M. kansasii*-infected patients are mostly infected with other disorders such as tuberculosis, other types of NTM, and HIV, which are resulting in exacerbated symptoms and weakened immune system (2). Treatment of *M. kansasii* infection is typically by administering rifampin, but sometimes fails due to resistance to rifampin. Ethambutol and isoniazid are also used, but drug resistance against these drugs have also been reported (37, 38). Since NTM-PD is accompanied by other diseases, we presumed that a novel approach using an immunotherapeutic agent or vaccine could be used to treat NTM infection as well as *M. tuberculosis*, which essentially increases host immunity.

To control *M. tuberculosis* or NTM infection, it has been recognized that Th1 response is important. IFN-γ, which is mainly expressed by Th1, supports to activate macrophages and empowers it to successfully degrade invaded bacteria. Additionally, activation of Th1 cells helps B cells to produce antibodies which suppress free bacteria by inducing the formation of immune complexes. However, a recent study reported anomalies of $CD4^+$ T cell physiology in NTM-infected host. NTM infected patients, especially when infected with *M. intracellulare* or *M. avium*, showed reduced $CD4^+$ T cells in PBMC (39). In addition, the importance of IFN-γ production seems controversial in a mouse infection model. A systemic infection model induced by intravenous injection of *M. kansasii* showed $CD4^+$ T cell-dependent reduction of mycobacterial burden in multiple organs. However, intranasal infection revealed no significant alteration of severity between WT and IL-12p40-, CD4-, or IFN-γ- deficient mice, triggered by *M. kansasii* infection (40, 41). These data suggested the restricted contribution of CD4+ T cell function in suppressing *M. kansasii* in intranasally-induced lung infection model. Collectively, these reports imply that the generation

of IFN-γ producing $CD4^+$ T cell response is crucial to control systemic *M. kansasii* infection similar to other species of mycobacterium.

Recently, vaccines using antigen-presenting cells including dendritic cells and B cells have been suggested to induce strong T cell-mediated immunity (11, 15). B cell vaccine is one of the cell-based vaccine approaches developed by using pathogen-specific antigens to induce diverse immune responses including Th1, cytotoxic T cell, and pathogenic antigen-specific antibody response. To augment $CD4^+$ T cell response, αGC, a ligand of NKT cell receptor, was used to load into the CD1d molecules on B cell surface (11).

In the current study, we designed a B cell-based vaccine (B/αGC/vacESAT6), which was transduced by vaccinia virus expressing ESAT6 and loaded with αGC. ESAT6 is a 6 kDa secretory protein and is one of the critical antigens, widely used as a candidate antigen for the development of new TB vaccine. ESAT6 has been shown to have sufficient immunogenicity such as $CD4^+$ T cell and CTL responses in both rodents and humans (42). Although ESAT6 is one of the promising antigen candidates, it might inhibit innate immunity by TLR2 binding, and can also inhibit the function of MHC molecules by the phagosomal rupture. However, we could not find any significant adverse effect after the administration of B/αGC/vacESAT6.

The ESAT6 of *M. bovis* and *M. tuberculosis* is identical (43, 44) and the amino acid sequence of ESAT6 homolog of *M. kansasii* is highly similar to that of *M. bovis*. Thus, we presumed that ESAT6 of *M. tuberculosis* could protect *M. kansasii* infection. In the current study, we confirmed that immunization with B/αGC/vacESAT6 ameliorated pulmonary inflammation caused by *M. kansasii* infection. Especially, therapeutic treatment of B/αGC/vacESAT6 decreased bodyweight loss and bacterial load in the lungs following *M. kansasii* infection, as well as increased the survival rate of *M. kansasii*-infected mice. The therapeutic administration of B/αGC/vacESAT6 increased IFN-γ production by $CD4^+$ T cells. In addition, B/αGC/vacESAT6 altered the composition of other immune cells in lungs such as CD8 T cells and myeloid cells.

Collectively, we developed a αGC-loaded, ESAT6 expressing B-cell based vaccine (B/αGC/vacESAT6) and confirmed the preventive and therapeutic effect of B/αGC/vacESAT6 vaccine in a murine model of *M. kansasii* infection.

DATA AVAILABILITY STATEMENT

All datasets generated for this study are included in the article/**Supplementary Material**.

ETHICS STATEMENT

The animal study was reviewed and approved by Institutional Animal Care and Use Committee of Kangwon National University, Kangwon National University, Chuncheon Gangwon-do 24341, South Korea (Permit Number: KW-160201-4).

AUTHOR CONTRIBUTIONS

B-EK and H-JK designed this study. H-SJ, JY, ES, S-GY, SS, H-JL, and Y-JJ contributed with materials and analysis tools. B-EK performed and analyzed *in vivo* animal experiments together with E-KP and HJ. B-EK and J-HA performed data interpretation and discussion. B-EK, J-HA, S-YC, and H-JK wrote the manuscript. All authors reviewed the manuscript.

FUNDING

This research was supported by a grant from the Korean Health Technology R&D Projects, Ministry of Health & Welfare, Republic of Korea (HI15C0450) and the Basic Science Research Program through the National Research Foundation of Korea (NRF) funded by the Ministry of Science, ICT, and Future Planning (NRF-2017R1A2B2001963, NRF-2017M3A9C8060390).

ACKNOWLEDGMENTS

We thank Byung-Il Yoon, College of Veterinary Medicine and Institute of Veterinary Science at Kangwon National University for providing technical assistance for histopathological examinations.

SUPPLEMENTARY MATERIAL

The Supplementary Material for this article can be found online at: https://www.frontiersin.org/articles/10.3389/fimmu.2019.02542/full#supplementary-material

REFERENCES

1. Kim YJ, Han SH, Kang HW, Lee JM, Kim YS, Seo JH, et al. NKT ligand-loaded, antigen-expressing B cells function as long-lasting antigen presenting cells *in vivo*. *Cell Immunol.* (2011) 270:135–44. doi: 10.1016/j.cellimm.2011.04.006
2. Johnston JC, Chiang L, Elwood K. *Mycobacterium kansasii*. *Microbiol Spectr.* (2017) 5:TNMI7-0011-2016. doi: 10.1128/microbiolspec.TNMI7-0011-2016
3. Marras TK, Daley CL. Epidemiology of human pulmonary infection with nontuberculous mycobacteria. *Clin Chest Med.* (2002) 23:553–67. doi: 10.1016/S0272-5231(02)00019-9
4. Kwon BE, Ahn JH, Min S, Kim H, Seo J, Yeo SG, et al. Development of new preventive and therapeutic vaccines for tuberculosis. *Immune Netw.* (2018) 18:e17. doi: 10.4110/in.2018.18.e17
5. Vynnycky E, Fine PE. The natural history of tuberculosis: the implications of age-dependent risks of disease and the role of reinfection. *Epidemiol Infect.* (1997) 119:183–201. doi: 10.1017/S0950268897007917
6. Al-Zahid S, Wright T, Reece P. Laryngeal inflammatory pseudotumour secondary to *Mycobacterium kansasii*. *Case Rep Pathol.* (2018) 2018:9356243. doi: 10.1155/2018/9356243

7. van Herwaarden N, Bavelaar H, Janssen R, Werre A, Dofferhoff A. Osteomyelitis due to *Mycobacterium kansasii* in a patient with sarcoidosis. *IDCases.* (2017) 9:1–3. doi: 10.1016/j.idcr.2017.04.001
8. Procop GW. HIV and mycobacteria. *Semin Diagn Pathol.* (2017) 34:332–9. doi: 10.1053/j.semdp.2017.04.006
9. Carneiro MDS, Nunes LS, David SMM, Dias CF, Barth AL, Unis G. Nontuberculous mycobacterial lung disease in a high tuberculosis incidence setting in Brazil. *J Bras Pneumol.* (2018) 44:106–11. doi: 10.1590/s1806-37562017000000213
10. Kendall EA, Azman AS, Cobelens FG, Dowdy DW. MDR-TB treatment as prevention: the projected population-level impact of expanded treatment for multidrug-resistant tuberculosis. *PLoS ONE.* (2017) 12:e0172748. doi: 10.1371/journal.pone.0172748
11. Seo H, Jeon I, Kim BS, Park M, Bae EA, Song B, et al. IL-21-mediated reversal of NK cell exhaustion facilitates anti-tumour immunity in MHC class I-deficient tumours. *Nat Commun.* (2017) 8:15776. doi: 10.1038/ncomms15776
12. Mangtani P, Abubakar I, Ariti C, Beynon R, Pimpin L, Fine PE, et al. Protection by BCG vaccine against tuberculosis: a systematic review of randomized controlled trials. *Clin Infect Dis.* (2014) 58:470–80. doi: 10.1093/cid/cit790
13. Zimmermann P, Finn A, Curtis N. Does BCG vaccination protect against nontuberculous mycobacterial infection? A systematic review and meta-analysis. *J Infect Dis.* (2018) 218:679–87. doi: 10.1093/infdis/jiy207
14. Lim YJ, Choi HH, Choi JA, Jeong JA, Cho SN, Lee JH, et al. *Mycobacterium kansasii*-induced death of murine macrophages involves endoplasmic reticulum stress responses mediated by reactive oxygen species generation or calpain activation. *Apoptosis.* (2013) 18:150–9. doi: 10.1007/s10495-012-0792-4
15. Chung Y, Kim BS, Kim YJ, Ko HJ, Ko SY, Kim DH, et al. CD1d-restricted T cells license B cells to generate long-lasting cytotoxic antitumor immunity *in vivo*. *Cancer Res.* (2006) 66:6843–50. doi: 10.1158/0008-5472.CAN-06-0889
16. Kim YJ, Ko HJ, Kim YS, Kim DH, Kang S, Kim JM, et al. alpha-Galactosylceramide-loaded, antigen-expressing B cells prime a wide spectrum of antitumor immunity. *Int J Cancer.* (2008) 122:2774–83. doi: 10.1002/ijc.23444
17. Griffith DE. Nontuberculous mycobacterial lung disease. *Curr Opin Infect Dis.* (2010) 23:185–90. doi: 10.1097/QCO.0b013e328336ead6
18. Havlir DV, Getahun H, Sanne I, Nunn P. Opportunities and challenges for HIV care in overlapping HIV and TB epidemics. *JAMA.* (2008) 300:423–30. doi: 10.1001/jama.300.4.423
19. Lonnroth K, Castro KG, Chakaya JM, Chauhan LS, Floyd K, Glaziou P, et al. Tuberculosis control and elimination 2010-50: cure, care, and social development. *Lancet.* (2010) 375:1814–29. doi: 10.1016/S0140-6736(10)60483-7
20. Rehm J, Samokhvalov AV, Neuman MG, Room R, Parry C, Lonnroth K, et al. The association between alcohol use, alcohol use disorders and tuberculosis (TB). A systematic review. *BMC Public Health.* (2009) 9:450. doi: 10.1186/1471-2458-9-450
21. CDC. Emergence of *Mycobacterium tuberculosis* with extensive resistance to second-line drugs–worldwide, 2000–2004. *MMWR Morb Mortal Wkly Rep.* (2006) 55:301–5.
22. Pontali E, Sotgiu G, D'Ambrosio L, Centis R, Migliori GB. Bedaquiline and multidrug-resistant tuberculosis: a systematic and critical analysis of the evidence. *Eur Respir J.* (2016) 47:394–402. doi: 10.1183/13993003.01891-2015
23. Agyeman AA, Ofori-Asenso R. Efficacy and safety profile of linezolid in the treatment of multidrug-resistant (MDR) and extensively drug-resistant (XDR) tuberculosis: a systematic review and meta-analysis. *Ann Clin Microbiol Antimicrob.* (2016) 15:41. doi: 10.1186/s12941-016-0156-y
24. Bruns H, Stegelmann F, Fabri M, Dohner K, van Zandbergen G, Wagner M, et al. Abelson tyrosine kinase controls phagosomal acidification required for killing of *Mycobacterium tuberculosis* in human macrophages. *J Immunol.* (2012) 189:4069–78. doi: 10.4049/jimmunol.1201538
25. Napier RJ, Norris BA, Swimm A, Giver CR, Harris WA, Laval J, et al. Low doses of imatinib induce myelopoiesis and enhance host anti-microbial immunity. *PLoS Pathog.* (2015) 11:e1004770. doi: 10.1371/journal.ppat.1004770
26. Napier RJ, Rafi W, Cheruvu M, Powell KR, Zaunbrecher MA, Bornmann W, et al. Imatinib-sensitive tyrosine kinases regulate mycobacterial pathogenesis and represent therapeutic targets against tuberculosis. *Cell Host Microbe.* (2011) 10:475–85. doi: 10.1016/j.chom.2011.09.010
27. Singhal A, Jie L, Kumar P, Hong GS, Leow MK, Paleja B, et al. Metformin as adjunct antituberculosis therapy. *Sci Transl Med.* (2014) 6:263ra159. doi: 10.1126/scitranslmed.3009885
28. Cassidy PM, Hedberg K, Saulson A, McNelly E, Winthrop KL. Nontuberculous mycobacterial disease prevalence and risk factors: a changing epidemiology. *Clin Infect Dis.* (2009) 49:e124–9. doi: 10.1086/648443
29. Mirsaeidi M, Machado RF, Garcia JG, Schraufnagel DE. Nontuberculous mycobacterial disease mortality in the United States, 1999-2010: a population-based comparative study. *PLoS ONE.* (2014) 9:e91879. doi: 10.1371/journal.pone.0091879
30. Marras TK, Mendelson D, Marchand-Austin A, May K, Jamieson FB. Pulmonary nontuberculous mycobacterial disease, Ontario, Canada, 1998–2010. *Emerg Infect Dis.* (2013) 19:1889–91. doi: 10.3201/eid1911.130737
31. Strollo SE, Adjemian J, Adjemian MK, Prevots DR. The burden of pulmonary nontuberculous mycobacterial disease in the United States. *Ann Am Thorac Soc.* (2015) 12:1458–64. doi: 10.1513/AnnalsATS.201503-173OC
32. Kwon YS, Koh WJ. Diagnosis and treatment of nontuberculous mycobacterial lung disease. *J Korean Med Sci.* (2016) 31:649–59. doi: 10.3346/jkms.2016.31.5.649
33. Christensen EE, Dietz GW, Ahn CH, Chapman JS, Murry RC, Anderson J, et al. Initial roentgenographic manifestations of pulmonary *Mycobacterium tuberculosis*, *M. kansasii*, and *M. intracellularis* infections. *Chest.* (1981) 80:132–6. doi: 10.1378/chest.80.2.132
34. Marras TK, Mehta M, Chedore P, May K, Al Houqani M, Jamieson F. Nontuberculous mycobacterial lung infections in Ontario, Canada: clinical and microbiological characteristics. *Lung.* (2010) 188:289–99. doi: 10.1007/s00408-010-9241-8
35. Usemann J, Fuchs O, Anagnostopoulou P, Korten I, Gorlanova O, Roosli M, et al. Predictive value of exhaled nitric oxide in healthy infants for asthma at school age. *Eur Respir J.* (2016) 48:925–8. doi: 10.1183/13993003.00439-2016
36. Moon SM, Choe J, Jhun BW, Jeon K, Kwon OJ, Huh HJ, et al. Treatment with a macrolide-containing regimen for *Mycobacterium kansasii* pulmonary disease. *Respir Med.* (2019) 148:37–42. doi: 10.1016/j.rmed.2019.01.012
37. Abate G, Hamzabegovic F, Eickhoff CS, Hoft DF. BCG vaccination induces *M. avium* and *M. abscessus* cross-protective immunity. *Front Immunol.* (2019) 10:234. doi: 10.3389/fimmu.2019.00234
38. Ahn CH, Wallace RJ Jr, Steele LC, Murphy DT. Sulfonamide-containing regimens for disease caused by rifampin-resistant *Mycobacterium kansasii*. *Am Rev Respir Dis.* (1987) 135:10–6.
39. Lim A, Allison C, Tan DB, Oliver B, Price P, Waterer G. Immunological markers of lung disease due to non-tuberculous mycobacteria. *Dis Markers.* (2010) 29:103–9. doi: 10.1155/2010/347142
40. Wieland CW, Florquin S, Pater JM, Weijer S, van der Poll T. CD4+ cells play a limited role in murine lung infection with *Mycobacterium kansasii*. *Am J Respir Cell Mol Biol.* (2006) 34:167–73. doi: 10.1165/rcmb.2005-0198OC
41. Hepper KP, Collins FM. Immune responsiveness in mice heavily infected with *Mycobacterium kansasii*. *Immunology.* (1984) 53:357–64.
42. Pathak SK, Basu S, Basu KK, Banerjee A, Pathak S, Bhattacharyya A, et al. Direct extracellular interaction between the early secreted antigen ESAT-6 of *Mycobacterium tuberculosis* and TLR2 inhibits TLR signaling in macrophages. *Nat Immunol.* (2007) 8:610–8. doi: 10.1038/ni1468
43. Cole ST, Brosch R, Parkhill J, Garnier T, Churcher C, Harris D, et al. Deciphering the biology of *Mycobacterium tuberculosis* from the complete genome sequence. *Nature.* (1998) 393:537–44. doi: 10.1038/24206
44. Garnier T, Eiglmeier K, Camus JC, Medina N, Mansoor H, Pryor M, et al. The complete genome sequence of *Mycobacterium bovis*. *Proc Natl Acad Sci USA.* (2003) 100:7877–82. doi: 10.1073/pnas.1130426100

Conflict of Interest: The authors declare that the research was conducted in the absence of any commercial or financial relationships that could be construed as a potential conflict of interest.

frontiers in Immunology

MINI REVIEW
published: 21 November 2019
doi: 10.3389/fimmu.2019.02711

CAR T Cells Beyond Cancer: Hope for Immunomodulatory Therapy of Infectious Diseases

*Michelle Seif, Hermann Einsele and Jürgen Löffler**

Department of Internal Medicine II, University Hospital Wuerzburg, Würzburg, Germany

Infectious diseases are still a significant cause of morbidity and mortality worldwide. Despite the progress in drug development, the occurrence of microbial resistance is still a significant concern. Alternative therapeutic strategies are required for non-responding or relapsing patients. Chimeric antigen receptor (CAR) T cells has revolutionized cancer immunotherapy, providing a potential therapeutic option for patients who are unresponsive to standard treatments. Recently two CAR T cell therapies, Yescarta® (Kite Pharma/Gilead) and Kymriah® (Novartis) were approved by the FDA for the treatments of certain types of non-Hodgkin lymphoma and B-cell precursor acute lymphoblastic leukemia, respectively. The success of adoptive CAR T cell therapy for cancer has inspired researchers to develop CARs for the treatment of infectious diseases. Here, we review the main achievements in CAR T cell therapy targeting viral infections, including Human Immunodeficiency Virus, Hepatitis C Virus, Hepatitis B Virus, Human Cytomegalovirus, and opportunistic fungal infections such as invasive aspergillosis.

Keywords: infectious diseases, mAb engineering, CAR T cells, HIV, HCV, CMV, invasive aspergillosis, HBV

OPEN ACCESS

Edited by:
Giuseppe Andrea Sautto, University of Georgia, United States

Reviewed by:
Weidong Han, PLA General Hospital, China
Jan Joseph Melenhorst, University of Pennsylvania, United States

***Correspondence:**
Jürgen Löffler
loeffler_j@ukw.de

Specialty section:
This article was submitted to Vaccines and Molecular Therapeutics, a section of the journal Frontiers in Immunology

Received: *17 September 2019*
Accepted: *05 November 2019*
Published: *21 November 2019*

Citation:
Seif M, Einsele H and Löffler J (2019) CAR T Cells Beyond Cancer: Hope for Immunomodulatory Therapy of Infectious Diseases. Front. Immunol. 10:2711. doi: 10.3389/fimmu.2019.02711

INTRODUCTION

Viral and opportunistic fungal infections represent a major threat to chronically infected individuals and immunocompromised patients. Despite the availability of antifungal and antiviral drugs, the mortality rate is still significant in high-risk patients (1–3). Current anti-viral treatments fail to cure chronic viral infections (caused by, e.g., HIV, HBV, and HCV) due to the viral-reservoir composed of infected cells that can stay latent for several years and would restart producing infectious virus at any time (4, 5) and the occurrence of resistance (6, 7). Therapies providing long term control or able to eradicate the viral-reservoir are required.

Pathogen-specific effector T cells play a crucial role in the control of acute viral and fungal infections in immunocompetent individuals (8–12), making adoptive T cell therapy an attractive alternative to currently used anti-infectious therapies. Pathogen-specific T cells occur in low frequencies in the patient's blood, making them difficult to isolate and expand. Moreover, they have exhausted phenotypes and might be rendered inefficient by viral escape mutation mechanisms lowering the major histocompatibility complex (MHC) or mutating the targeted epitope (10, 13–15). Thus, Chimeric antigen receptors (CARs) T cells present an attractive alternative.

CAR T cells are considered as a major scientific breakthrough and an important turning point in cancer immunotherapy (16), especially in the treatment of B cell malignancies. Recently, the US Food and Drug Administration (FDA) then the European Commission have approved two CAR T-cell products, Kymriah® (Novartis) and Yescarta® (Kite Pharma/ Gilead) for the treatment of B-cell precursor acute lymphoblastic leukemia and aggressive B-cell lymphoma, respectively.

CAR T cells are described as having the targeting specificity of a monoclonal antibody combined with the effector functions of a cytotoxic T cell (17). They offer potential advantages over pathogen-specific T cells, the CAR allows antigen recognition independent of the MHC and can be designed to specifically target the conserved and essential epitopes of the antigen, which allows them to overcome pathogen escape mechanisms.

Few anti-infectious CARs were described in the literature so far, most of them targeting HIV. Here we review the progress and discuss the remaining challenges of making CAR T cell therapy a reality for individuals suffering from infectious diseases. The main anti-infectious CAR constructs are summarized in **Table 1**.

CAR T CELLS

CARs are synthetic receptors composed of a targeting element linked by a spacer to a transmembrane domain followed by an intracellular signaling domain. The targeting element is usually, but not exclusively composed by a single-chain variable fragment (scFv) (17). The spacer constitutes mainly of a full-length Fc receptor of an IgG (Hinge-CH_2-CH_3) or shorter parts like the Hinge region only or Hinge-CH_2 (37–40). Furthermore, parts of the extracellular domains of CD28 and CD8α were used as spacers (41, 42). Several transmembrane domains were used to anchor the receptor on the surface of a T cell, mainly derived from CD28, CD8α, or CD4 (42–44). The signaling domain consists of the intracellular part of CD3ζ from the TCR complex (45). Over the years, in order to improve the CAR functionality and persistence, several generations of CARs have been established differing in their intracellular signaling (17). First-generation CARs mediated T-cell activation only through the CD3ζ complex (45, 46). Second-generation CARs include an intracellular costimulatory domain, mainly CD28 or 4-1BB, leading to an enhanced expansion, and functionality (43, 47–52). These second-generation receptors are the origin of the recently approved CAR T-cell therapies (53). Third-generation CARs combine two costimulatory domains, mainly CD28, and 4-1BB (54). Finally, fourth-generation CARs, also called TRUCKs (T-cells redirected for universal cytokine-mediated killing), emerged, including an additional transgene for inducible cytokine secretion upon CAR activation [mainly IL-12 (55)]. Several other strategies for minimizing toxicity and enhancing versatility and control of CAR T cells were reviewed by others (17, 56).

CAR T CELLS SPECIFIC FOR HUMAN IMMUNODEFICIENCY VIRUS (HIV)

Studies on developing CAR T cell therapy to cure HIV infections are ongoing since the early 90th. The first findings were already reviewed by others (57–60). Here we shortly summarize the anti-HIV CAR T cell history and focus on the most recent achievements.

CD4 Based CARs

The concept of CAR T cells was initially described in the 90th when the cytotoxic T cells specificity was redirected toward HIV infected cells. The first CAR was specific for HIV envelope protein (Env) using the CD4 receptor as a targeting element fused to the CD3ζ chain for intracellular signaling (CD4ζCAR) (61, 62). Clinical trials with the CD4ζCAR showed that the concept is feasible and safe, but failed to reduce HIV viral burden permanently (63–66).

To improve the CAR T cell activity and persistence, CD4ζCAR was re-engineered into second-generation and third-generation CARs. While CAR T cells containing CD28 costimulatory domain promoted higher cytokine production and better control over HIV replication *in vitro*, the 4-1BB containing CARs were more potent in controlling HIV infection *in vivo*. When compared to first-generation CAR T cells, second-generation CAR T cells were more potent at suppressing HIV replication *in vitro*. Furthermore, in a humanized mouse model of HIV infection, they preserved the $CD4^+$ T cell count, reduced HIV burden, and expanded to a greater extent than first-generation CAR T cells (20).

However, it was shown that CD4-based CARs render the CAR T cells susceptible to HIV infection (18, 25). To overcome this limitation, CD4ζCAR was equipped with either a viral fusion inhibitor (C46 peptide) (18) or small hairpin RNAs to knock down HIV-1 co-receptor CC-chemokine receptor 5 (CCR5) and degrade viral RNA (19). Both methods successfully rendered CD4ζCAR T resistant to HIV infection and conferred them a long persistence and proper control of HIV infection *in vivo* (18, 19).

Moreover, several genome editing techniques were used to knock out CCR5 in T cells to confer them permanent resistance to HIV infection (67). These include the use of ZFNs (Zinc-finger nucleases) (68), which showed promising results in clinical trials (NCT00842634, NCT01044654, NCT01252641), TALEN (Transcription activator-like nucleases) (69, 70), and CRISPR-CAS 9 (71) in preclinical studies. These endonucleases were already used to produce universal CAR T cells by knocking down the TCR (72–77). It would be useful to test them to knock down CCR5 in HIV-CAR T cells.

scFvs Based CARs

To avoid using the CD4 as targeting element, novel CARs of several generations were designed using single-chain variable fragments (scFv) derived from broadly neutralizing antibodies (bNAbs) targeting Env.

Targets included the CD4-binding site, several antigens of glycoprotein 120 (gp120), the membrane-proximal region of gp41, the mannose-rich region, and variable glycan regions (20, 21, 24, 78).

Second-generation CARs for the different targets enabled the CAR T cells to kill HIV-1-infected cells. However, their antiviral activity was variable according to the virus strain (78). Second-generation anti-glycan CARs, in combination with CCR5 ablation, provided better control of viral replication than the CAR alone (24).

First-generation anti-gp120 CARs induced efficient activation and cytokine secretion by the gene-modified T cells and mediated

TABLE 1 | CAR design of the most promising anti-infectious CAR T-cells.

Pathogen	Targeted antigen	Targeting element	Spacer	Transmembrane domain	Costimulatory domain	Extra modification	References
HIV	CD4 binding site on gp-120	CD4	n.a.	CD4	n.a.	C46 peptide	(18)
	CD4 binding site on gp-120	CD4	n.a.	CD4	n.a.	CCR5 sh 1005; sh 516	(19)
	CD4 binding site on gp-120	CD4	n.a.	CD8α	CD28 or 4-1BB		(20)
	CD4 binding site on gp-120	VRC01-scFv	$(GGGGS)_3$	CD8α or CD28	CD28-4-1BB		(21)
	CD4 binding site on gp-120	105-scFv	CD8 hinge	CD3ζ	n.a.		(22)
	Env/gp120 glycans	CD4/ CRD	CD28	CD28	CD28		(23)
	V1/V2 glycan loop	PGT145-scFv	CD8α Hinge	CD8α	4-1BB	AAV6-CCR5	(24)
	CD4-induced epitope on gp120/CD4 binding site	17b-scFv/CD4	Tripeptide AAA	CD28	CD28		(25)
	CD4-induced epitope on gp120/CD4 binding site	mD1.22-G_4S-m36.4	CD8	CD8	4-1BB	C46 peptide	(26)
HBV	S HBV surface protein	C8-scFv	IgG1 Fc	CD28	CD28		(27–29)
	HBV surface antigen	19.79.6-scFv	IgG4 Fc mutated	CD28	CD28		(30)
HCV	HCV E2 glycoprotein	e137-scFv	IgG Fc	CD28	CD28		(31)
CMV	Glycoprotein B	27-287-scFv	Ig Hinge	CD28	CD28		(32–34)
	Virally encoded FcRs	IgG1 or IgG4 Fc mutated	n.a.	CD28	CD28		(35)
Aspergillus fumigatus	β-glucan	Dectin 1	IgG4 Fc mutated	CD28	CD28		(36)

lysis of envelope-expressing cells and HIV-1-infected $CD4^+$ T-lymphocytes *in vitro* (22). Third generation anti-gp120 CAR-T cells were more efficient than CD4 based CARs in lysing gp120 expressing cells *in vitro*. Furthermore, their interaction with cell-free HIV did not result in their infection. More importantly, they efficiently induced cytolysis of the reactivated HIV reservoir isolated from infected individuals. Thus, anti-gp120 third-generation CAR T cells might be a suitable candidate for therapeutic approaches aiming to eradicate the HIV reservoir (21).

However, one major drawback to developing scFvs-based CAR T cell therapy is the HIV viral escape mutation mechanism that can abrogate the antibody-binding site and render the CAR T cell therapy inefficient.

Bi- and Tri-specific CARs

In order to overcome the HIV mutation escape mechanism, bi-and tri-specific CAR-expressing T cells targeting up to three HIV antigens were designed to increase the specificity and affinity.

The CD4 segment was fused with an scFv specific for a CD4-induced epitope on gp120 (25) or the carbohydrate recognition domain (CRD) of a human C- type lectin binding to conserved glycans on Env (23). The CD4-anti gp120 scFv bispecific CAR had better suppressive activity against HIV than the CD4 alone. CD4-mannose binding lectin (MBL) CARs showed the best potency when compared to both CD4 alone and CD4-anti gp120 (23). However, since C- type lectins can bind glycans which are not specific for HIV infected cells and can be associated with healthy cells, off-targets cannot be excluded.

More recently, T cells were engineered with up to three functionally distinct HIV envelope-binding domains to form bispecific and tri-specific targeting anti-HIV CAR-T cells. These cells carry two distinct CARs expressed on one T cell or one CAR having tow targeting elements linked together. Targets included CD4-binding site on HIV gp120 and CD4-induced (CD4i) epitope on gp120 near the co-receptor binding site. Tri-specific CARs expressed the C46 peptide, which inhibits HIV viral fusion and thus can prevent the infection of CAR T cells. Bi-and tri-specific CAR T cells showed potent *in vitro* and *in vivo* anti-HIV effects, they efficiently killed HIV-infected cells in a humanized mouse model while protecting the CAR- T cells from infection (26).

Despite all the challenges faced, anti-HIV CAR T cell therapy made much progress toward enhancing the CAR T cell antiviral activity, protecting CAR T cells from HIV infection, and overcoming HIV escape mechanisms. Currently, at least two clinical trials are ongoing for latent reservoir eradication, one using a modified bNAb-based CAR-T cell therapy (NCT03240328) and one using CD4-based CAR-T cell therapy with CCR5 ablation (NCT03617198).

CAR T CELLS SPECIFIC FOR HEPATITIS B VIRUS (HBV)

Some preclinical studies are focusing on engineering second-generation CAR T cells to cure chronic hepatitis B and prevent the development of hepatocellular carcinoma (HCC). Cytotoxic T cells were redirected toward HBV surface and secreted antigens.

Second generation CAR T cells were designed to target HBV-surface proteins S and L, which are expressed continuously on the surface of HBV replicating cells. S and L specific CAR T cells were able to recognize soluble HBsAg and HBsAg-positive hepatocytes *in vitro* and subsequently secret IFNγ and IL-2. S-CAR T cells were activated faster and secreted higher cytokine levels than L-CAR T cells. This might be due to the higher expression of the S-protein on the surface of viral and subviral particles when compared with the L-protein (27).

Furthermore, both CAR T cells were able to lyse HBV transfected cells as well as selectively eliminated HBV-infected primary hepatocytes. However, even after the elimination of HBV-infected hepatocytes, HBV core protein and HBV rcDNA remained detectable. It is most probably because HBV rcDNA is localized in viral capsids and thus protected from caspase-activated DNAses (27). The S-CAR construct was tested *in vivo* in an immune-competent HBV transgenic mouse model. $CD8^+$ mouse T cells expressing the human S-CAR localized to the liver and effectively reduced HBV replication, causing only transient liver damage. Furthermore, contact of CAR T cells with circulating viral antigen did not lead to their functional exhaustion or excessive liver damage. However, the survival of the CAR T cells was limited due to the immune response triggered by the human CAR (28). In an immunocompetent mouse model tolerized with a signaling-deficient S-CAR, S-CAR T cells persisted and showed long-lasting antiviral effector function (29). However, the use of a transgene instead of cccDNA to transcribe HBV makes these mouse models unsuitable to judge whether S-CAR T cells can cure HBV infection (28, 29).

More recently, other novel second-generation CARs targeting HBsAg were designed with different spacer length. Only HBs -CAR T-cells equipped with a long spacer (HBs-G4m-CAR) recognized HBV-positive cell lines and HBsAg particles *in vitro* and subsequently produced significant amounts of IFN-γ, IL-2, and TNF-α. However, HBs-G4m-CAR T cells were not capable of killing HBV-positive cell lines *in vitro*. This might be due to HBsAg particles produced by HBV-positive cells that can bind to HBs-G4m-CAR T-cells and potentially inhibit CAR-T targeting or killing of infected cells. In a humanized HBV-infected mouse model, adoptive transfer of HBsAg-CAR T-cells led to the accumulation of the cells in the liver and an important reduction in plasma HBsAg and HBV-DNA levels. Furthermore, the absence of HBV core expression in a portion of human hepatocytes and the unchanged plasma human albumin levels indicated HBV clearance without destruction of the infected hepatocytes. However, no complete elimination of HBV was observed. Despite this limitation, HBs-G4m-CAR T cells had superior anti-HBV activity than HBV entry inhibitors (30).

These studies showed promising results; a direct comparison of S-CAR T cell and HBsAg-CAR T-cell would be interesting to test. Furthermore, a better mouse model more representative of the actual infection should be used to evaluate the CAR activity *in vivo*. Finally, combination therapy using CAR T-cells with reverse transcriptase inhibitors or hepatitis B immunoglobulin might be required to have better control of the HBV infection.

CAR T CELLS SPECIFIC FOR HEPATITIS C VIRUS (HCV)

Very recently, the first two CARs targeting HCV were designed based on a broadly cross-reactive and cross-neutralizing human monoclonal antibody specific for a conserved epitope of the HCV E2 glycoprotein (HCV/E2). Anti-HCV CAR T cells showed good anti-viral activity and lyzed HCV/E2-transfected as well as HCV-infected target cells (31).

This study showed that the concept of CAR T cells might also be suitable for the treatment of HCV. The described CAR should be evaluated *in vivo* in a suitable animal model. Furthermore, since HCV/E2 is the main target of the host immune response and is consequently very susceptible to mutations (32), targeting other conserved, and essential antigens might also be of interest.

CAR T CELLS SPECIFIC FOR HUMAN CYTOMEGALOVIRUS (CMV)

The first CAR targeting CMV was described in 2010 based on the anti-gB antibody. Second generation gB CAR T cells were activated when co-cultured with CMV-infected cells and secreted TNF α and IFN γ and subsequently inhibited CMV replication in infected cells (33–35). Moreover, they eliminated gB transfected cells (33) but were not always able to lyse infected cells, especially at later stages of the replication cycle. This might be due to HCMV-encoded anti-apoptotic proteins that are known to prevent the suicide of infected host cells (34, 35). This CAR T cell therapy was not tested *in vivo* due to the few sequence similarities between the murine CMV gB protein and the human one. An appropriate mouse model using a recombinant MCMV expressing HCMV-gB should be developed (33).

In a later study, it was shown that the long spacer (CH2–CH3 Fc domain from IgG1) usually used in CAR preparation could bind to virally encoded Fc binding receptors on the surface of infected cells and act as a receptor for CMV. The mutated form of the spacer is only recognized by viral FcRs and not the human ones. In this way, the long spacer can act as a receptor for CMV infected cells (35).

The gB-CAR with long and short spacer should be further tested *in vivo* in an appropriate animal model. More targeting elements should be tested. Finally, the combination of new targeting elements with a long spacer might confer a bispecific targeting of CMV infected cells.

CAR T CELLS SPECIFIC FOR EPSTEIN-BARR VIRUS (EBV)

To target Epstein-Barr virus (EBV) associated malignancies, a second-generation CAR specific for the EBV latent membrane protein 1 (LMP1) was described. EBV-CAR T cells were activated *in vitro* in co-culture with nasopharyngeal carcinoma cells overexpressing LMP1

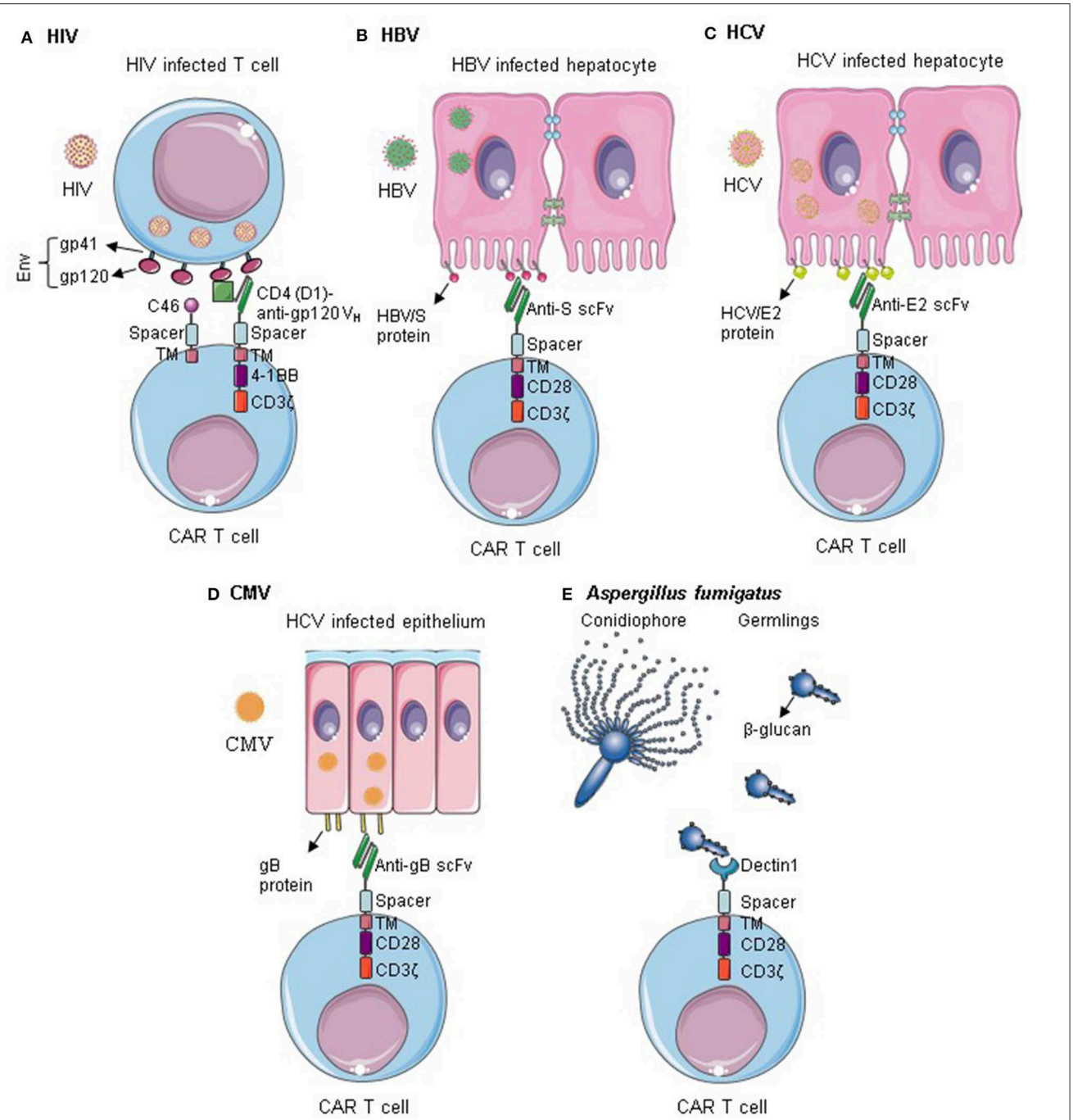

FIGURE 1 | CAR T cells targeting infectious diseases. **(A)** T cells are redirected against HIV by the expression of Env-specific CARs on their surface. Additionally, they are rendered resistant to HIV infection by expression of an anti-fusion peptide. Anti-HIV CAR T cells can successfully kill HIV infected cells and control HIV infection. **(B–D)** CAR T cells specific for HBV S protein, HCV/E2, or gB can recognize cells infected by HBV, HCV, and CMV, respectively. They can selectively kill the infected cells within the epithelium. **(E)** Dectin 1-CAR T cells can directly bind to *Aspergillus fumigatus* germlings and induce hyphal damage. Env, HIV envelope protein; Gp, Glycoprotein; TM, transmembrane; V_H, variable heavy chain; gB, Glycoprotein B. Some illustrations were obtained and modified from Servier Medical Art by Servier, licensed under Creative Commons Attribution 3.0 Unported License.

and subsequently produced IFNɣ and IL-2. Intra-tumoral injection of EBV-CAR T cells in a xenograft mouse model having tumors overexpressing LMP1 reduced tumor growth (79).

CAR-T cell therapy for solid tumors is still facing many challenges, like the inability to reach the tumor and survive in the tumor microenvironment. These challenges and the developed strategies to overcome them were reviewed by others (80).

CAR T CELLS SPECIFIC FOR *Aspergillus fumigatus*

A second-generation CAR using the extracellular domain of Dectin-1 as targeting element called D-CAR was designed to target *Aspergillus fumigatus*. Dectin 1 is a C-type lectin receptor specific for ß-glucan, a motif expressed on the surface of many fungi (81). D-CAR T cells were activated by ß-glucan and subsequently secreted IFNγ and induced hyphal damage *in vitro*. In an immunocompromised invasive aspergillosis mouse model, D-CAR T cells reduced the fungal burden (36).

This study suggested that the application of CAR T cells might extend beyond cancer and chronic viral infections to acute fungal infections. Although promising results were shown for D-CAR T cells, Dectin 1 might not be the best targeting element to redirect the T cell specificity toward *Aspergillus fumigatus*. Since ß-glucans are not specific for *Aspergillus fumigatus* but rather a broad range of commensal and pathogenic microorganisms, off-target activity of the CAR T cells cannot be excluded (82). Using scFvs derived from fungal specific antibodies might provide better specificity and activity of the CAR. Moreover, strategies to significantly shorten the CAR T cell preparation time [currently time from leukapheresis to infusion of the CART product can take up to 3–4 weeks (83)] will be essential to allow their clinical use for acute infections.

CONCLUSION AND PERSPECTIVES

CAR T-cell therapy has gained much interest since its clinical application was approved for cancer immunotherapy. Relying on the knowledge accumulated on CAR T cell engineering in cancer research, many efforts are being made toward developing similar therapies for patients affected by chronical viral and acute invasive fungal infections. While targets are more precise and unique to the pathogen, making it easier to avoid off-targets, pathogen escape mechanisms, and reservoirs are still major obstacles.

Several CARs targeting infectious diseases have been described; the most relevant ones are summarized in **Figure 1** and **Table 1**. Tremendous progress was made in anti-HIV CAR T cell therapy, which reached now clinical trials. CAR T cells targeting other viruses such as HBV, HCV, CMV, and opportunistic fungus are still in their early pre-clinical testing. So far, promising data were observed, providing a proof of concept of CAR T cell application. Nevertheless, considerable optimization work is still required regarding the safety and efficacy of the constructs. More targets should be evaluated *in vitro* and *in vivo* in relevant animal models.

AUTHOR CONTRIBUTIONS

MS wrote the manuscript. JL and HE reviewed and edited the manuscript. All authors approved the manuscript for publication.

FUNDING

This work was funded by the Bundesministerium für Bildung und Forschung (BMBF) (Infect Control 2020—consortium ART4Fun; subproject 2 to HE), the Deutsche Forschungsgemeinschaft (Collaborative Research Center/Transregio 124 Pathogenic fungi and their human host: Networks of interaction—FungiNet; project A2 to HE and JL), and Deutsche Forschungsgemeinschaft (Forschergruppe 2830, Advanced Concepts in Cellular Immune Control of Cytomegalovirus, project 09 to HE).

REFERENCES

1. Heinz WJ, Vehreschild JJ, Buchheidt D. Diagnostic work up to assess early response indicators in invasive pulmonary aspergillosis in adult patients with haematologic malignancies. *Mycoses.* (2019) 62:486–93.doi: 10.1111/myc.12860
2. Green ML. CMV viral load and mortality after hematopoietic cell transplantation: a cohort study in the era of preemptive therapy. *Lancet Haematol.* (2016) 3:e119–27.doi: 10.1016/S2352-3026(15)00289-6
3. Teira P, Battiwalla M, Ramanathan M, Barrett AJ, Ahn KW, Chen M, et al. Early cytomegalovirus reactivation remains associated with increased transplant-related mortality in the current era: a CIBMTR analysis. *Blood.* (2016) 127:2427–38.doi: 10.1182/blood-2015-11-679639
4. Bongiovanni M, Adorni F, Casana M, Tordato F, Tincati C, Cicconi P, et al. Subclinical hypothyroidism in HIV-infected subjects. *J Antimicrob Chemother.* (2006) 58:1086–9.doi: 10.1093/jac/dkl360
5. Wong JK, Hezareh M, Günthard HF, Havlir DV, Ignacio CC, Spina CA, et al. Recovery of replication-competent HIV despite prolonged suppression of plasma viremia. *Science.* (1997) 278:1291–5.doi: 10.1126/science.278.5341.1291
6. Paydary K, Khaghani P, Emamzadeh-Fard S, Alinaghi SAS, Baesi K. The emergence of drug resistant HIV variants and novel anti-retroviral therapy. *Asian Pac J Trop Biomed.* (2013) 3:515–22.doi: 10.1016/S2221-1691(13)60106-9
7. Margeridon-Thermet S, Shafer RW. Comparison of the mechanisms of drug resistance among HIV, hepatitis B, and hepatitis C. *Viruses.* (2010) 2:2696–739.doi: 10.3390/v2122696
8. Neumann-Haefelin C, Thimme R. Adaptive immune responses in hepatitis C virus infection. *Curr Top Microbiol Immunol.* (2013) 369:243–62.doi: 10.1007/978-3-642-27340-7_10
9. Klenerman P, Oxenius A. T cell responses to cytomegalovirus. *Nat Rev Immunol.* (2016) 16:367–77.doi: 10.1038/nri.2016.38
10. Jones RB, Walker BD. Jones, Walker HIV-specific CD8 T cells and HIV eradication. *J Clin Invest.* (2016) 126:455–63.doi: 10.1172/JCI80566
11. Maini MK, Boni C, Ogg GS, King AS, Reignat S, Chun Kyon Lee, et al. Direct *ex vivo* analysis of hepatitis B virus-specific CD8+ T cells associated with the control of infection. *Gastroenterology.* (1999) 117:1386–96.doi: 10.1016/S0016-5085(99)70289-1
12. Kumaresan PR, da Silva TA, Kontoyiannis DP. Methods of controlling invasive fungal infections using CD8 + T cells. *Front Immunol.* (2018) 8:1–14.doi: 10.3389/fimmu.2017.01939
13. Iijima S, Lee Y-J, Ode H, Arold ST, Kimura N, Yokoyama M, et al. A Non-canonical mu-1A-binding motif in the N terminus of HIV-1 nef determines its ability to downregulate major histocompatibility complex class I in T lymphocytes. *J Virol.* (2012) 86:3944–51.doi: 10.1128/JVI.06257-11
14. Boni C, Fisicaro P, Valdatta C, Amadei B, Di Vincenzo P, Giuberti T, et al. Characterization of hepatitis B virus (HBV)-specific T-cell dysfunction in chronic HBV infection. *J Virol.* (2007) 81:4215–25.doi: 10.1128/JVI.02844-06

15. Kurktschiev PD, Raziorrouh B, Schraut W, Backmund M, Wächtler M, Wendtner CM, et al. Dysfunctional CD8$^+$ T cells in hepatitis B and C are characterized by a lack of antigen-specific T-bet induction. *J Exp Med.* (2014) 211:2047–59.doi: 10.1084/jem.20131333
16. Couzin-Frankel J. Cancer immunotherapy. *Crit Rev Clin Lab Sci.* (2016) 8363:167–89.doi: 10.1080/10408360902937809
17. Subklewe M, Von Bergwelt-Baildon M, Humpe A. Chimeric antigen receptor T cells: a race to revolutionize cancer therapy. *Transfus Med Hemotherapy.* (2019) 46:15–24.doi: 10.1159/000496870
18. Zhen A, Peterson CW, Carrillo MA, Reddy SS, Youn CS, Lam BB, et al. Long-term persistence and function of hematopoietic stem cell-derived chimeric antigen receptor T cells in a non-human primate model of HIV/AIDS. *PLoS Pathog.* (2017) 13:e1006753.doi: 10.1371/journal.ppat.1006753
19. Zhen A, Kamata M, Rezek V, Rick J, Levin B, Kasparian S, et al. HIV-specific immunity derived from chimeric antigen receptor-engineered stem cells. *Mol Ther.* (2015) 23:1358–67.doi: 10.1038/mt.2015.102
20. Leibman RS, Richardson MW, Ellebrecht CT, Maldini CR, Glover JA, Secreto AJ, et al. Supraphysiologic control over HIV-1 replication mediated by CD8 T cells expressing a re-engineered CD4-based chimeric antigen receptor. *PLoS Pathog.* (2017) 13:1–30.doi: 10.1371/journal.ppat.1006613
21. Liu B, Zou F, Lu L, Chen C, He D, Zhang X, et al. Chimeric antigen receptor T cells guided by the single-chain Fv of a broadly neutralizing antibody specifically and effectively eradicate virus reactivated from latency in CD4 T lymphocytes isolated from HIV-1- infected individuals receiving suppressive combined antiretroviral therapy. *J Virol.* (2016) 90:9712–24.doi: 10.1128/JVI.00852-16
22. Masiero S, Del Vecchio C, Gavioli R, Mattiuzzo G, Cusi MG, Micheli L, et al. T-cell engineering by a chimeric T-cell receptor with antibody-type specificity for the HIV-1 gp120. *Gene Ther.* (2005) 12:299–310.doi: 10.1038/sj.gt.3302413
23. Ghanem MH, Bolivar-Wagers S, Dey B, Hajduczki A, Vargas-Inchaustegui DA, Danielson DT, et al. Bispecific chimeric antigen receptors targeting the CD4 binding site and high-mannose Glycans of gp120 optimized for anti–human immunodeficiency virus potency and breadth with minimal immunogenicity. *Cytotherapy.* (2018) 20:407–19.doi: 10.1016/j.jcyt.2017.11.001
24. Hale M, Mesojednik T, Ibarra GSR, Sahni J, Bernard A, Sommer K, et al. Engineering HIV-resistant, anti-HIV chimeric antigen receptor T cells. *Mol Ther.* (2017) 25:570–9.doi: 10.1016/j.ymthe.2016.12.023
25. Liu L, Patel B, Ghanem MH, Bundoc V, Zheng Z, Morgan RA, et al. Novel CD4-based bispecific chimeric antigen receptor designed for enhanced anti-HIV potency and absence of HIV entry receptor activity. *J Virol.* (2015) 89:6685–94.doi: 10.1128/JVI.00474-15
26. Anthony-Gonda K, Bardhi A, Ray A, Flerin N, Li M, Chen W, et al. Multispecific anti-HIV duoCAR-T cells display broad *in vitro* antiviral activity and potent *in vivo* elimination of HIV-infected cells in a humanized mouse model. *Sci Transl Med.* (2019) 11:eaav5685.doi: 10.1126/scitranslmed.aav5685
27. Bohne F, Chmielewski M, Ebert G, Wiegmann K, Kürschner T, Schulze A, et al. T cells redirected against hepatitis B virus surface proteins eliminate infected hepatocytes. *Gastroenterology.* (2008) 134:239–47.doi: 10.1053/j.gastro.2007.11.002
28. Krebs K, Böttinger N, Huang LR, Chmielewski M, Arzberger S, Gasteiger G, et al. T cells expressing a chimeric antigen receptor that binds hepatitis B virus envelope proteins control virus replication in mice. *Gastroenterology.* (2013) 145:456–65.doi: 10.1053/j.gastro.2013.04.047
29. Festag MM, Festag J, Fräßle SP, Asen T, Sacherl J, Schreiber S, et al. Evaluation of a fully human, hepatitis B virus-specific chimeric antigen receptor in an immunocompetent mouse model. *Mol Ther.* (2019) 27:947–59.doi: 10.1016/j.ymthe.2019.02.001
30. Kruse RL, Shum T, Tashiro H, Barzi M, Yi Z, Whitten-Bauer C, et al. HBsAg-redirected T cells exhibit antiviral activity in HBV-infected human liver chimeric mice. *Cytotherapy.* (2018) 20:697–705.doi: 10.1016/j.jcyt.2018.02.002
31. Sautto GA, Wisskirchen K, Clementi N, Castelli M, Diotti RA, Graf J, et al. Chimeric antigen receptor (CAR)-engineered t cells redirected against hepatitis C virus (HCV) E2 glycoprotein. *Gut.* (2016) 65:512–23.doi: 10.1136/gutjnl-2014-308316
32. Sautto G, Tarr AW, Mancini N, Clementi M. Structural and antigenic definition of hepatitis C virus E2 glycoprotein epitopes targeted by monoclonal antibodies. *Clin Dev Immunol.* (2013) 2013:450963.doi: 10.1155/2013/450963
33. Full F, Lehner M, Thonn V, Goetz G, Scholz B, Kaufmann KB, et al. T cells engineered with a cytomegalovirus-specific chimeric immunoreceptor. *J Virol.* (2010) 84:4083–8.doi: 10.1128/JVI.02117-09
34. Proff J, Walterskirchen C, Brey C, Geyeregger R, Full F, Ensser A, et al. Cytomegalovirus-infected cells resist T cell mediated killing in an HLA-recognition independent manner. *Front Microbiol.* (2016) 7:1–15.doi: 10.3389/fmicb.2016.00844
35. Proff J, Brey CU, Ensser A, Holter W, Lehner M. Turning the tables on cytomegalovirus : targeting viral Fc receptors by CARs containing mutated CH2 – CH3 IgG spacer domains. *J Transl Med.* (2018) 1–12.doi: 10.1186/s12967-018-1394-x
36. Kumaresan PR, Manuri PR, Albert ND, Maiti S, Singh H, Mi T, et al. Bioengineering T cells to target carbohydrate to treat opportunistic fungal infection. *Proc Natl Acad Sci USA.* (2014) 111:10660–5.doi: 10.1073/pnas.1312789111
37. Hudecek M, Lupo-Stanghellini MT, Kosasih PL, Sommermeyer D, Jensen MC, Rader C, et al. Receptor affinity and extracellular domain modifications affect tumor recognition by ROR1-specific chimeric antigen receptor T cells. *Clin Cancer Res.* (2013) 19:3153–64.doi: 10.1158/1078-0432.CCR-13-0330
38. Hudecek M, Sommermeyer D, Kosasih PL, Silva-Benedict A, Liu L, Rader C, et al. The non-signaling extracellular spacer domain of chimeric antigen receptors is decisive for *in vivo* antitumor activity. *Cancer Immunol Res.* (2015) 3:125–35.doi: 10.1158/2326-6066.CIR-14-0127
39. James SE, Greenberg PD, Jensen MC, Lin Y, Wang J, Till BG, et al. Antigen sensitivity of CD22-specific chimeric TCR is modulated by target epitope distance from the cell membrane. *J Immunol.* (2008) 180:7028–38.doi: 10.4049/jimmunol.180.10.7028
40. Guest RD, Hawkins RE, Kirillova N, Cheadle EJ, Arnold J, O' Neill A, et al. The role of extracellular spacer regions in the optimal design of chimeric immune receptors. *J Immunother.* (2005) 28:203–11.doi: 10.1097/01.cji.0000161397.96582.59
41. Milone MC, Fish JD, Carpenito C, Carroll RG, Binder GK, Teachey D, et al. Chimeric receptors containing CD137 signal transduction domains mediate enhanced survival of T cells and increased antileukemic efficacy *in vivo. Mol Ther.* (2009) 17:1453–64.doi: 10.1038/mt.2009.83
42. Kochenderfer JN, Feldman SA, Zhao Y, Xu H, Black MA, Morgan RA, et al. Construction and preclinical evaluation of an anti-CD19 chimeric antigen receptor. *J Immunother.* (2009) 32:689–702.doi: 10.1097/CJI.0b013e3181ac6138
43. Imai C, Mihara K, Andreansky M, Nicholson IC, Pui CH, Geiger TL, et al. Chimeric receptors with 4-1BB signaling capacity provoke potent cytotoxicity against acute lymphoblastic leukemia. *Leukemia.* (2004) 18:676–84.doi: 10.1038/sj.leu.2403302
44. Jensen M, Tan G, Forman S, Wu AM, Raubitschek A. CD20 is a molecular target for scFvFc:ζ receptor redirected T cells: implications for cellular immunotherapy of CD10+ malignancy. *Biol Blood Marrow Transplant.* (1998) 4:75–83.doi: 10.1053/bbmt.1998.v4.pm9763110
45. Gong MC, Latouche JB, Krause A, Heston WDW, Bander NH, Sadelain M. Cancer patient T cells genetically targeted to prostate-specific membrane antigen specifically lyse prostate cancer cells and release cytokines in response to prostate-specific membrane antigen. *Neoplasia.* (1999) 1:123–7.doi: 10.1038/sj.neo.7900018
46. Brocker T, Karjalainen K. Signals through T cell receptor-ζ chain alone are insufficient to prime resting T lymphocytes. *J Exp Med.* (1995) 181:1653–9.doi: 10.1084/jem.181.5.1653
47. Maher J, Brentjens RJ, Gunset G, Rivière I, Sadelain M. Human T-lymphocyte cytotoxicity and proliferation directed by a single chimeric TCRζ/CD28 receptor. *Nat Biotechnol.* (2002) 20:70–5.doi: 10.1038/nbt0102-70
48. Krause A, Guo HF, Latouche JB, Tan C, Cheung NKV, Sadelain M. Antigen-dependent CD28 signaling selectively enhances survival and proliferation in genetically modified activated human primary T lymphocytes. *J Exp Med.* (1998) 188:619–26.doi: 10.1084/jem.188.4.619
49. Finney HM, Lawson AD, Bebbington CR, Weir AN. Chimeric receptors providing both primary and costimulatory signaling in T cells from a single gene product. *J Immunol.* (1998) 161:2791–7.

50. Finney HM, Akbar AN, Lawson ADG. Activation of resting human primary T cells with chimeric receptors: costimulation from CD28, inducible costimulator, CD134, and CD137 in series with signals from the TCRζ chain. *J Immunol.* (2004) 172:104–13.doi: 10.4049/jimmunol.172.1.104
51. Porter D, Levine BL, Kalos M, Bagg A, June CH. Chimeric antigen receptor–modified T cells in chronic lymphoid leukemia. *N Engl J Med.* (2011) 365:725–33.doi: 10.1056/NEJMoa1103849
52. van der stegen SJC, Hamieh M, Sadelain M. The pharmacology of second-generation chimeric antigen receptors. *Nat Rev Drug Discov.* (2015) 14:499–509.doi: 10.1038/nrd4597
53. Salmikangas P, Kinsella N, Chamberlain P. Chimeric antigen receptor T-cells (CAR T-cells) for cancer immunotherapy – moving target for industry? *Pharm Res*. (2018) 35:1–8.doi: 10.1007/s11095-018-2436-z
54. Wang J, Jensen M, Lin Y, Sui X, Chen E, Lindgren CG, et al. Optimizing adoptive polyclonal T cell immunotherapy of lymphomas, using a chimeric T cell receptor possessing CD28 and CD137 costimulatory domains. *Hum Gene Ther*. (2007) 18:712–25.doi: 10.1089/hum.2007.028
55. Chmielewski M, Abken H. CAR T cells transform to trucks: chimeric antigen receptor-redirected T cells engineered to deliver inducible IL-12 modulate the tumour stroma to combat cancer. *Cancer Immunol Immunother*. (2012) 61:1269–77.doi: 10.1007/s00262-012-1202-z
56. Fesnak AD, June CH, Levine BL. Engineered T cells: the promise and challenges of cancer immunotherapy. *Nat Rev Cancer*. (2016) 16:566–81.doi: 10.1038/nrc.2016.97
57. Maldini CR, Ellis GI, Riley JL. CAR T cells for infection, autoimmunity and allotransplantation. *Nat Rev Immunol.* (2018) 18:605–16.doi: 10.1038/s41577-018-0042-2
58. Wagner TA. Quarter century of Anti-HIV CAR T cells. (2015) 344:1173–8.doi: 10.1007/s11904-018-0388-x
59. Liu B, Zhang W, Zhang H. Development of CAR-T cells for long-term eradication and surveillance of HIV-1 reservoir. *Curr Opin Virol.* (2019) 38:21–30.doi: 10.1016/j.coviro.2019.04.004
60. Kuhlmann AS, Peterson CW, Kiem HP. Chimeric antigen receptor T-cell approaches to HIV cure. *Curr Opin HIV AIDS.* (2018) 13:446–53.doi: 10.1097/COH.0000000000000485
61. Romeo C, Seed B. Cellular immunity to HIV activated by CD4 fused to T cell or Fc receptor polypeptides. *Cell.* (1991) 64:1037–46.doi: 10.1016/0092-8674(91)90327-U
62. Roberts MR, Qin L, Zhang D, Smith DH, Tran AC, Dull TJ, et al. Targeting of human immunodeficiency virus-infected cells by CD8+ T lymphocytes armed with universal T-cell receptors. *Blood*. (1994) 84:2878–89.doi: 10.1182/blood.V84.9.2878.bloodjournal8492878
63. Scholler J, Brady TL, Binder-Scholl G, Hwang WT, Plesa G, Hege K, et al. Decade-long safety and function of retroviral-modified chimeric antigen receptor T-cells. *Sci Transl Med.* (2012) 4:132ra53.doi: 10.1126/scitranslmed.3003761
64. Walker RE, Bechtel CM, Natarajan V, Baseler M, Hege KM, Metcalf JA, et al. Long-term *in vivo* survival of receptor-modified syngeneic T cells in patients with human immunodeficiency virus infection. *Blood*. (2000) 96:467–74. doi: 10.1182/blood.V96.2.467.014k34_467_474
65. Mitsuyasu RT, Anton PA, Deeks SG, Scadden DT, Connick E, Downs MT, et al. Prolonged survival and tissue trafficking following adoptive transfer of CD4ζ gene-modified autologous CD4+ and CD8+ T cells in human immunodeficiency virus-infected subjects. *Blood.* (2000) 96:785–93.doi: 10.1182/blood.V96.3.785.015k10_785_793
66. Deeks SG, Wagner B, Anton PA, Mitsuyasu RT, Scadden DT, Huang C, et al. A phase II randomized study of HIV-specific T-cell gene therapy in subjects with undetectable plasma viremia on combination antiretroviral therapy. *Mol Ther*. (2002) 5:788–97.doi: 10.1006/mthe.2002.0611
67. Kwarteng A, Ahuno ST, Kwakye-Nuako G. The therapeutic landscape of HIV-1 via genome editing. *AIDS Res Ther.* (2017) 14:1–16.doi: 10.1186/s12981-017-0157-8
68. Perez EE, Wang J, Miller JC, Jouvenot Y, Kim KA, Liu O, et al. Establishment of HIV-1 resistance in CD4+ T cells by genome editing using zinc-finger nucleases. *Nat Biotechnol.* (2008) 26:808–16.doi: 10.1038/nbt1410
69. Mock U, MacHowicz R, Hauber I, Horn S, Abramowski P, Berdien B, et al. mRNA transfection of a novel TAL effector nuclease (TALEN) facilitates efficient knockout of HIV co-receptor CCR5. *Nucleic Acids Res.* (2015) 43:5560–71.doi: 10.1093/nar/gkv469
70. Shi B, Li J, Shi X, Jia W, Wen Y, Hu X, et al. TALEN-mediated knockout of CCR5 confers protection against infection of human immunodeficiency virus. *J Acquir Immune Defic Syndr.* (2017) 74:229–41.doi: 10.1097/QAI.0000000000001190
71. Wang W, Ye C, Liu J, Zhang D, Kimata JT, Zhou P. CCR5 gene disruption via lentiviral vectors expressing Cas9 and single guided RNA renders cells resistant to HIV-1 infection. *PLoS ONE.* (2014) 9:1–26.doi: 10.1371/journal.pone.0115987
72. Torikai H, Reik A, Liu PQ, Zhou Y, Zhang L, Maiti S, et al. A foundation for universal T-cell based immunotherapy: T cells engineered to express a CD19-specific chimeric-antigen-receptor and eliminate expression of endogenous TCR. *Blood.* (2012) 119:5697–705.doi: 10.1182/blood-2012-01-405365
73. Qasim W, Zhan H, Samarasinghe S, Adams S, Amrolia P, Stafford S, et al. Molecular remission of infant B-ALL after infusion of universal TALEN gene-edited CAR T cells. *Sci Transl Med.* (2017) 9:1–9.doi: 10.1126/scitranslmed.aaj2013
74. Philip LPB, Schiffer-Mannioui C, Le Clerre D, Chion-Sotinel I, Derniame S, Potrel P, et al. Multiplex genome-edited T-cell manufacturing platform for "off-the-shelf" adoptive T-cell immunotherapies. *Cancer Res.* (2015) 75:3853–64.doi: 10.1158/0008-5472.CAN-14-3321
75. Berdien B, Mock U, Atanackovic D, Fehse B. TALEN-mediated editing of endogenous T-cell receptors facilitates efficient reprogramming of T lymphocytes by lentiviral gene transfer. *Gene Ther.* (2014) 21:539–48.doi: 10.1038/gt.2014.26
76. Ren J, Liu X, Fang C, Jiang S, June CH, Zhao Y. Multiplex genome editing to generate universal CAR T cells resistant to PD1 inhibition. *Clin Cancer Res.* (2017) 23:2255–66.doi: 10.1158/1078-0432.CCR-16-1300
77. Ren J, Zhang X, Liu X, Fang C, Jiang S, June CH, et al. A versatile system for rapid multiplex genome-edited CAR T cell generation. *Oncotarget*. (2017) 8:17002–11.doi: 10.18632/oncotarget.15218
78. Ali A, Kitchen SG, Chen ISY, Ng HL, Zack JA, Yang OO. HIV-1-specific chimeric antigen receptors based on broadly neutralizing antibodies. *J Virol.* (2016) 90:6999–7006.doi: 10.1128/JVI.00805-16
79. Tang X, Zhou Y, Li W, Tang Q, Chen R, Zhu J, et al. T cells expressing a LMP1-specific chimeric antigen receptor mediate antitumor effects against LMP1-positive nasopharyngeal carcinoma cells *in vitro* and *in vivo*. *J Biomed Res.* (2014) 28:468–75.doi: 10.7555/JBR.28.20140066
80. D'Aloia MM, Zizzari IG, Sacchetti B, Pierelli L, Alimandi M. CAR-T cells: the long and winding road to solid tumors review-article. *Cell Death Dis.* (2018) 9:282.doi: 10.1038/s41419-018-0278-6
81. Bowman SM, Free SJ. The structure and synthesis of the fungal cell wall. *BioEssays.* (2006) 28:799–808.doi: 10.1002/bies.20441
82. Iliev ID, Funari VA, Taylor KD, Nguyen Q, Reyes CN, Strom SP, et al. Interactions between commensal fungi and the C-type lectin receptor dectin-1 influence colitis. *Science.* (2012) 336:1314–7.doi: 10.1126/science.1221789
83. Buechner J, Kersten MJ, Fuchs M, Salmon F, Jäger U. Chimeric antigen receptor-T cell therapy: practical considerations for implementation in Europe. *HemaSphere.* (2018) 2:e18.doi: 10.1097/HS9.0000000000000018

Conflict of Interest: The authors declare that the research was conducted in the absence of any commercial or financial relationships that could be construed as a potential conflict of interest.

frontiers in Immunology

MINI REVIEW
published: 29 November 2019
doi: 10.3389/fimmu.2019.02778

Antibody Epitopes of Pneumovirus Fusion Proteins

Jiachen Huang[1,2], *Darren Diaz*[1,2] *and Jarrod J. Mousa*[1,2*]

[1] *Department of Infectious Diseases, College of Veterinary Medicine, University of Georgia, Athens, GA, United States,*
[2] *Center for Vaccines and Immunology, College of Veterinary Medicine, University of Georgia, Athens, GA, United States*

The pneumoviruses respiratory syncytial virus (RSV) and human metapneumovirus (hMPV) are two widespread human pathogens that can cause severe disease in the young, the elderly, and the immunocompromised. Despite the discovery of RSV over 60 years ago, and hMPV nearly 20 years ago, there are no approved vaccines for either virus. Antibody-mediated immunity is critical for protection from RSV and hMPV, and, until recently, knowledge of the antibody epitopes on the surface glycoproteins of RSV and hMPV was very limited. However, recent breakthroughs in the recombinant expression and stabilization of pneumovirus fusion proteins have facilitated in-depth characterization of antibody responses and structural epitopes, and have provided an enormous diversity of new monoclonal antibody candidates for therapeutic development. These new data have primarily focused on the RSV F protein, and have led to a wealth of new vaccine candidates in preclinical and clinical trials. In contrast, the major structural antibody epitopes remain unclear for the hMPV F protein. Overall, this review will cover recent advances in characterizing the antigenic sites on the RSV and hMPV F proteins.

Keywords: RSV, respiratory syncytial virus, human metapneumovirus, hMPV, antibody—antigen complex, X-ray crystallography, pneumovirus infections

OPEN ACCESS

Edited by:
Roberta Antonia Diotti, Vita-Salute San Raffaele University, Italy

Reviewed by:
Bruno Emanuel Correia, École Polytechnique Fédérale de Lausanne, Switzerland
Bert Schepens, VIB-UGent Center for Inflammation Research (IRC), Belgium

***Correspondence:**
Jarrod J. Mousa
jarrod.mousa@uga.edu

Specialty section:
This article was submitted to Vaccines and Molecular Therapeutics, a section of the journal Frontiers in Immunology

Received: *17 September 2019*
Accepted: *13 November 2019*
Published: *29 November 2019*

Citation:
Huang J, Diaz D and Mousa JJ (2019) Antibody Epitopes of Pneumovirus Fusion Proteins. Front. Immunol. 10:2778. doi: 10.3389/fimmu.2019.02778

INTRODUCTION

The recently reclassified *Pneumoviridae* virus family includes the human pathogens respiratory syncytial virus (RSV) and human metapneumovirus (hMPV) (1). These viruses are among the most common causes of childhood respiratory tract infection (2). Severe disease primarily occurs in young children, the elderly, and the immunocompromised, and reinfection can occur throughout childhood and adulthood, as sterilizing immunity is not acquired after infection. Both viruses exhibit genetic stability, with relatively few changes in viral sequences among circulating strains. Despite decades of research, there are no approved vaccines to prevent pneumovirus infection. Fortunately, a wave of new progress in recent years has led to the development of new vaccine candidates and therapeutics, largely due to breakthroughs in structural biology and immunological techniques. This review will cover recent findings on antigenic epitopes of RSV and hMPV fusion glycoproteins.

GLOBAL BURDEN OF PNEUMOVIRUSES

Respiratory Syncytial Virus

RSV is an enveloped, negative-sense, single stranded RNA virus, first isolated in 1955 from chimpanzees with respiratory illness (3), and subsequently isolated from infants with lower respiratory tract infection (4, 5). RSV is the leading cause of viral bronchiolitis and viral pneumonia

in infants and children (6, 7), and nearly all children have been exposed to RSV before the age of 2 (8). RSV infection causes flu-like symptoms, bronchiolitis, and pneumonia that can be fatal to children. In addition, RSV infection poses a substantial threat to elderly populations and immunocompromised adults (9). RSV is highly contagious, and can be transmitted through direct contact or aerosol (10). Although numerous vaccines have undergone clinical trials (11), the monoclonal antibody (mAb) palivizumab remains the only approved therapeutic for RSV infection. Palivizumab has shown moderate efficacy at preventing RSV hospitalizations and intensive care unit admissions (12), however, the drug is only approved for prophylactic use, and in limited cases.

Human Metapneumovirus

hMPV was identified in 2001 in the Netherlands from samples collected from 28 children with respiratory tract infection (13). The clinical features of hMPV infection are virtually identical to RSV, and display as mid-to-upper respiratory tract infection, and can be severe enough to cause life-threatening bronchiolitis and pneumonia. Infants and the elderly are the major groups for which hMPV infection may require hospitalization (14–18). In addition, hMPV infection can be severe in immunocompromised patients such as lung transplant (19) and hematopoietic stem-cell transplant recipients (20–23), and can cause febrile respiratory illness in HIV-infected patients (24) as well as exacerbate chronic obstructive pulmonary disease (25). Nearly 100% of children are seropositive by 5 years of age. There are currently no vaccines to prevent hMPV infection, and unlike the related pathogen respiratory syncytial virus (RSV), for which the prophylactic treatment palivizumab (26) is available for high-risk infants, no treatment or prophylaxis is available for hMPV.

THE PNEUMOVIRUS FUSION PROTEIN

Pneumoviruses have three surface glycoproteins: the (F) fusion, (G) attachment, and small hydrophobic (SH) proteins, and the pneumovirus F protein is absolutely critical for viral infectivity. Antibodies are highly important for pneumovirus immunity (27, 28), and both RSV F and RSV G elicit neutralizing antibodies (29), while only antibodies to hMPV F are neutralizing (30). The pneumovirus F proteins belong to the family of class I viral fusion proteins that mediate the fusion of viral envelope and cell membrane during infection (31). The RSV F protein is first expressed as a F_0 precursor, which is then cleaved at two furin cleavage sites in the trans-Golgi network to become fusion competent, generating the N-terminal F_2 subunit and the C-terminal F_1 subunit, while the p27 fragment in between F_1 and F_2 is removed. In contrast, hMPV F is cleaved at one site by different intracellular enzymes than RSV (32). Cleaved pneumovirus F proteins are anchored on the viral envelope by the trans-membrane domain of F_1. The F_1 and F_2 fragments are covalently linked via two disulfide bonds, and the proteins form a trimeric structure consisting of three of the disulfide-linked fragments. The Pneumovirus F proteins fold into a pre-fusion conformation that contains a buried fusion peptide. Upon activation, the F protein undergoes a series of conformational changes leading to the post-fusion conformation in concert with cell-virus membrane fusion (31). The pre-fusion conformation of the pneumovirus F protein is unstable, and refolding can occur spontaneously or under certain stimuli that irreversibly transform the globular pre-fusion F into the elongated post-fusion formation. During the process of the pre-to-post-fusion conformational change, the highly hydrophobic fusion peptide located at the N terminus of F2 will insert into host cell membrane, forming a hairpin structure that bridges the two membranes together before a refolding event causes membrane fusion.

Until recently, knowledge on the structural aspects of pneumovirus fusion proteins was severely lacking, primarily due to instability of the pre-fusion conformation when recombinantly expressed. An X-ray crystal structure of the post-fusion conformation of RSV F was determined in 2011 by removal of the fusion peptide in the construct used for crystallization (33, 34). A breakthrough in 2013 facilitated structural-determination of the RSV F protein in the pre-fusion conformation by co-expression of RSV F with the mAb Fab fragment D25 to trap the protein in the pre-fusion state (35). This subsequently led to stabilization of the RSV F protein in the pre-fusion conformation by locking the protein in the pre-fusion state via artificial disulfide-bond insertion in addition to cavity-filling mutations (the DS-Cav1 construct) (36). Following this, an additional pre-fusion-stabilized protein was generated in an alternative approach using the substitution of proline residues in the refolding regions and expression of the protein as a single-chain through the introduction of a glycine-serine linker (the SC-TM construct) (37). For hMPV, a partial X-ray crystal structure of hMPV F in the pre-fusion conformation in complex with the neutralizing Fab DS7 was determined in 2012 (38). Following the success with stabilization of pre-fusion RSV F, crystal structures of trimeric hMPV pre-fusion and post-fusion hMPV F were determined (39, 40). Pre-fusion hMPV F was stabilized with proline-substitutions to prevent refolding to the post-fusion conformation, while post-fusion hMPV F required the addition of a trimerization domain. Both hMPV F constructs required cleavage-site modification and co-expression with furin in CV-1 cells to generate fully-cleaved trimeric proteins. In addition to the structures described above, similar strategies were utilized to stabilize the parainfluenza virus fusion proteins, and bovine RSV F in the pre-fusion state (41, 42).

ANTIGENIC DIFFERENCES BETWEEN RSV AND HMPV F

The RSV and hMPV F proteins share ∼30% sequence identify, and among the antigenic sites on RSV F, at least two are shared with hMPV F (antigenic sites III and IV) as a result of this conservation (**Figures 1A,B**). Despite the shared sequence conservation, several distinct features influence the differing antibody response to these viruses. The majority of RSV neutralizing activity in human sera is mediated by pre-fusion-specific RSV F antibodies (43), while the majority of hMPV neutralizing activity is mediated by antibodies recognizing both pre-fusion and post-fusion conformations (40). In addition, vaccination with pre-fusion RSV F induces higher levels of neutralizing IgG than vaccination with post-fusion RSV F (36),

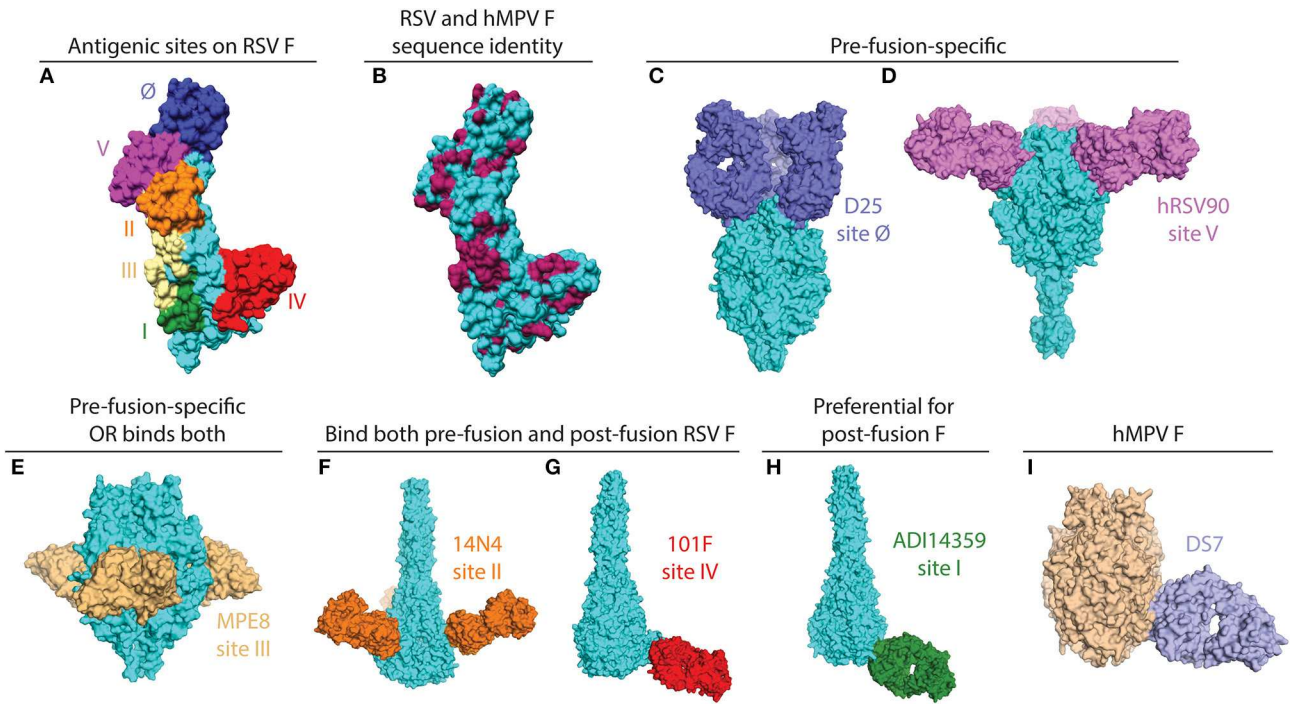

FIGURE 1 | X-ray crystal structures of pneumovirus F proteins alone and in complex monoclonal antibody fragments. **(A)** The main antigenic sites on the RSV F protein are depicted on a monomer of the F protein (PDB ID: 5C6B). **(B)** The same structure as in **(A)** is colored according to sequence conservation with hMPV F. Conserved residues are shown in maroon, and primarily reside within antigenic sites III, IV, and V. Sequences of RSV and hMPV F were derived from PDB IDs: 5C6B and 5WB0. **(C)** The pre-fusion specific antibody D25 binds at the apex of pre-fusion RSV F (PDB ID: 4JHW). **(D)** hRSV90 binds antigenic site V and is pre-fusion-specific (PDB ID: 5TPN). **(E)** MPE8 is pre-fusion-specific and cross-reactive with hMPV F (PDB ID: 5U68). **(F)** 14N4 is a human antibody that targets antigenic site II and binds both pre-fusion and post-fusion RSV F (PDB ID: 5J3D). **(G)** The humanized mouse mAb, 101F, binds at antigenic site IV. For this structure, the crystal structure of 101F binding the site IV peptide (PDB ID: 3O41) was aligned with antigenic site IV of the post-fusion RSV F protein (3RRR). **(H)** The non-neutralizing site I mAb ADI14359 was isolated from an RSV-infected infant, and is preferential for post-fusion RSV F (PDB ID: 6APB). **(I)** DS7 is a hMPV F-specific mAb that was co-crystallized with a fragment of pre-fusion hMPV F. The structure of the DS7-F complex (PDB ID: 4DAG) is overlaid onto the trimeric pre-fusion hMPV F structure (PDB ID: 5WB0). All antibodies are colored in accordance with the text label, the RSV F protein is shown in cyan, and the hMPV F protein is shown in wheat. All figures and alignments were prepared in PyMol and Chimera.

while vaccination with pre-fusion-stabilized hMPV F elicited similar neutralizing IgG titers as vaccination with post-fusion hMPV F (40). These data suggest that pre-fusion-specific RSV F antibodies are more prevalent in infected or vaccinated humans and mice, and pre-fusion-specific hMPV F antibodies are present at low levels as compared to antibodies that recognize both pre-fusion and post-fusion hMPV F. The low level of pre-fusion-specific hMPV F antibodies is likely due to a glycan shield near the corresponding RSV site Ø and site V regions on the head of hMPV F.

ANTIGENIC EPITOPES ON THE RSV F PROTEIN

mAbs binding to the RSV F protein could prevent F protein binding to host cell or hinder the conformational change from pre-fusion to post-fusion, and thus block viral entry into the cell. Due to its sequence conservation, and elicitation of potently neutralizing mAbs, the F protein has become the most popular target for vaccine development. As such, there has been a rapid increase in structural characterization of mAbs in complex with the RSV F protein. Currently available solved structures of mAbs in complex with pneumovirus F proteins are summarized in **Table 1**. To date, multiple antigenic sites targeted by antibodies have been identified on the RSV F protein (**Figure 1**). Based on the secondary structure of the protein, six general regions have been designated as antigenic sites: Ø, I, II, III, IV, and V. Among them, antigenic sites I, II, and IV are quite similar between pre-fusion and post-fusion conformations due to their structural conservation upon transition from pre-fusion to post-fusion F. Antigenic sites Ø and V are only present in the pre-fusion conformation (58), while antigenic site III elicits mAbs that are pre-fusion-specific, such as MPE8, while also eliciting mAbs that bind both conformations, such as 25P13 (50). In addition, more than 60% of the most potent neutralizing mAbs bind to sites Ø and V (59), indicating these areas are crucial for immune system recognition and subsequent virus neutralization.

Antigenic Site Ø

Antigenic site Ø was the first pre-fusion-specific antigenic site identified on the RSV F protein. The methodology for isolating the first site Ø antibodies was crucial as the mAbs were isolated

TABLE 1 | List of structurally-characterized antibodies in complex with pneumovirus F proteins or fragments thereof.

mAb	PDB ID	Origin	Antigenic site	References
RSV F				
motavizumab	3IXT, 3QWO, 4JLR, 6OE5, 4ZYP	Mouse	II	(44)
101F	3O41, 3O45	Mouse	IV	(45)
hRSV90	5TPN	Human	V	(46)
D25	4JHW	Human	Ø	(36)
MEDI8897	5UDC, 5UDD	Human	Ø	(47)
AM22	6DC5, 6APD	Human	Ø	(48)
5C4	5W23	Mouse	Ø	(49)
MPE8	5U68	Human	III	(50)
ADI19425	6APD	Human	III	(51)
CR9501	6OE4/6OE5	Human	V	(52)
AM14	4ZYP	Human	IV, V	(53)
RSD5	6DC3	Human	Ø	(48)
14N4	5J3D	Human	II	(54)
ADI14359	6APD	Human	I	(51)
R4.C6	6CXC	Mouse	II, IV	(55)
RB1	6OUS	Human	IV	(56)
F-VHH-4	5TOJ	Llama	II, III, IV, V	(57)
F-VHH-L66	5TOK	Llama	II, III, IV, V	(57)
hMPV F				
DS7	4DAG	Human	DS7-site	(38)

on the basis of RSV neutralization rather than RSV F protein binding (60). This facilitated the isolation of pre-fusion-specific mAbs without the existence of a pre-fusion RSV F construct. Subsequently, one mAb, D25 (**Figure 1C**), was utilized to lock the RSV F protein in the pre-fusion conformation (35), which then facilitated stabilization of RSV F in the pre-fusion conformation (36). It is now clear that mAbs that target antigenic site Ø are a large portion of the human B cell repertoire (43, 46, 59). 5C4 is a mAb derived from mice immunized with gene-based vectors encoding the F protein, and is 50 times more potent than palivizumab. Human mAbs D25 and AM22, as well as the mouse mAb 5C4 bind to the apex of the pre-fusion F trimer (site Ø) (36). Importantly, a human mAb based on D25, MEDI-8897, is in clinical trials for prevention of RSV disease in infants (61).

Antigenic Site V

Antigenic site V was described recently, based on mAb isolation to new pre-fusion-stabilized constructs (46, 59). hRSV90 (**Figure 1D**) is a site V-targeting human mAb that was found to compete for binding with mAbs that target site II and site Ø. hRSV90 was co-crystallized with the RSV F protein and found to bind just below antigenic site Ø (46). In addition, several site V mAbs were isolated from both adults and infants (51, 59), suggesting these mAbs are prevalent in the human anti-RSV repertoire. CR9501 is a neutralizing mAb isolated from humans, and this mAb was used to demonstrate the dynamic motions of trimeric pre-fusion RSV F protein (52). An antibody that competes for site V of the RSV F protein, MC17, was also shown to cross-react with the hMPV F protein (56).

Antigenic Site III

The prototypical site III mAb MPE8 (**Figure 1E**) is unique as it cross-neutralizes multiple viruses in the *Pneumoviridae* family (62). This broad coverage is related to similar V gene usage and somatic mutations in the variable region based on the isolation of a highly similar human antibody 25P13 (50), as well as several other mAbs from a large panel of anti-RSV F human mAbs (59). In addition, site III-specific mAbs are elicited upon initial RSV infection in infants (51). One mAb, ADI19425, which was isolated from an RSV-infected infant, and is potently neutralizing despite lacking substantial somatic hypermutation, was co-crystallized with pre-fusion RSV F (51).

Antigenic Site II

Palivizumab and motavizumab are the prototypical mAbs to identify antigenic site II on the RSV F protein (26, 44, 63, 64). Targeting antigenic site II of RSV F protein (26), palivizumab is able to neutralize a broad panel of 57 RSV isolates from both subtypes A and B (65). This antigenic site primarily consists of the helix-loop-helix motif of residues 255-275 on the RSV F protein. Several human antibodies have been isolated that bind at antigenic site II (51, 54, 59). The human antibody 14N4 (**Figure 1F**) was co-crystallized in complex with post-fusion RSV F, and primarily focuses on the 255–275 motif. In the same study, a panel of non-neutralizing mAbs was identified that compete with antigenic site II mAbs on post-fusion RSV F, and suggest some limitations of the palivizumab competition assay used in some vaccine efficacy studies (54). The characterization of mAbs to this antigenic site has led to vaccine candidates focused

on antigenic site II (66, 67). Furthermore, serum competition assays with palivizumab have been utilized to characterize vaccine candidates (68). In addition to the mAbs above, nanobodies targeting antigenic site II have been isolated (69, 70), and one nanobody, ALX-0171, has been evaluated as an antiviral therapy to treat RSV infection (71).

Antigenic Site IV

The site IV epitope is epitomized by the humanized mouse mAb 101F (**Figure 1G**) (72), and this epitope is structurally conserved between pre-fusion and post-fusion RSV F. The site IV epitope primarily consists of a linear region based on epitope mapping and structural data (45, 73). In addition, it was recently found that 101F cross-reacts with the hMPV F protein (39), presumably by binding to a conserved region at site IV that is similar between RSV and hMPV F (73). Several human mAbs targeting antigenic site IV have also been isolated (51, 59, 73), and human antibody cross-reactivity with hMPV F was correlated to a specific binding pose (73). In addition to the traditional site IV epitope, a mouse mAb, R4.C6, has been isolated that incorporates site IV as well as site II into its epitope (55). The structure of the R4.C6 Fab-post-fusion RSV F complex obtained by cryo-EM showed that the antibody binds to a cross-protomer area in between site II and IV. Recently, a site IV human antibody, RB1, was co-crystallized in complex with pre-fusion RSV F, and a half-life extended variant of this antibody is in clinical development (74).

Antigenic Site I

The site I epitope on the RSV F protein was identified by the prototypical mouse monoclonal antibody 131-2a (75). Recently, it was determined that human mAbs identified that bind at antigenic site I are weakly or non-neutralizing (51, 54), likely due to insufficient binding to pre-fusion RSV F, as many of these mAbs are post-fusion-specific. The crystal structure of an infant-derived non-neutralizing human mAb, ADI-14359 (**Figure 1H**), in complex with post-fusion RSV F was determined and defined the antigenic surface for site I (51).

Other Epitopes and Antibodies

In addition to the epitopes described above, there are several other antibodies isolated that bind unique regions on the RSV F protein. AM14 is a human mAb that recognizes a quaternary epitope spanning two protomers, suggesting the trimeric F protein has specific antigenic epitopes that are not found on the monomeric F protein (53). Single-domain antibody (VHH) or nanobodies from llama immunization were identified and co-crystallized with the RSV F protein (57). Both F-VHH-4 and F-VHH-L66 bind to a cavity in the intermediate area between antigenic site II of one protomer and antigenic site IV of the neighboring protomer. Intranasal administration of these VHHs significantly reduced viral replication in mice, which provides new therapeutic options for antiviral development.

MABS TARGETING THE HMPV F PROTEIN

The first hMPV F-specific neutralizing mAbs generated were derived from immunization of mice and hamsters with various strains of hMPV (76). Of the 12 mAbs in the study, murine mAbs 234 and 338 were effective as passive prophylaxis, protecting mice from hMPV challenge; mAb 338 was successful in reducing lung viral titers when given both prophylactically or therapeutically (77). By generating monoclonal antibody-resistant mutants of antibodies that neutralize hMPV, six antigenic sites of the hMPV F protein were identified (78). Since then, the terminology regarding pneumovirus antigenic sites for hMPV has followed that for RSV. Antigenic sites IV and III from the RSV F protein have been found to be conserved on hMPV F due to the isolation of cross-reactive mAbs discussed in the RSV section. hMPV F-specific mAbs have shown success in neutralizing hMPV both *in vitro* and *in vivo*.

The DS7-Antigenic Site

A human mAb isolated from a phage display library, termed DS7 (**Figure 1I**), was shown to reduce hMPV lung viral titers when administered therapeutically in cotton rats (79). mAb DS7 was co-crystallized in complex with a fragment of pre-fusion hMPV F (38), and has a unique molecular footprint in the bottom half of the hMPV F protein. Three additional human mAbs, which are naturally-occurring, termed MPV196, MPV201, and MPV314 were recently isolated and compete for binding with DS7, suggesting these mAbs target the same antigenic site (80).

Antigenic Site III

The first mAb identified to bind antigenic site III of hMPV F was the cross-reactive human mAb MPE8 (62). As discussed in the RSV section, MPE8 was co-crystallized with the RSV F protein, and the conserved regions at antigenic site III that facilitate cross-reactivity were also hypothesized (50). A similar mAb, 25P13, also discussed above, neutralized hMPV and RSV and competed for binding at antigenic site III (50). Recently, a human mAb, MPV364, was isolated and this mAb competes for binding at antigenic site III, yet does not cross-react with RSV F (80). MPV364 was shown to effectively limit viral replication in BALB/c mice (80). These data suggest antigenic site III can elicit both virus-specific and cross-reactive mAbs. However, the mechanism behind such mAb induction will require additional structural analysis.

Antigenic Site IV

As discussed earlier, the humanized mouse mAb 101F was identified to cross-react with hMPV F (39). Four human mAbs targeting antigenic site IV of the RSV F protein were isolated, and one mAb, termed 17E10, was identified to also cross-react with hMPV F. This mAb was subjected to peptide mapping and negative-stain microscopy. mAb 17E10 was found to bind a conserved GIIK motif on RSV and hMPV F (39). Furthermore, the binding angle of 17E10 and 101F were shown to be different than non-cross-reactive mAbs, suggesting an altered binding pose is required for cross-reactivity between RSV and hMPV F at antigenic site IV (73).

SUMMARY AND DISCUSSION

In recent years, several breakthroughs have facilitated new knowledge of pneumovirus antibody epitopes. Pre-fusion-stabilized constructs have allowed for isolation of mAbs with optimal neutralization potency, including those binding at antigenic site Ø and V on the RSV F protein. In addition, the use of mAbs to initially lock RSV in the pre-fusion conformation allowed for structure-based design of pre-fusion constructs. While hundreds of mAbs have now been isolated to the RSV F protein, the antigenic epitopes on the hMPV F protein, and related parainfluenza viruses remain unclear. Further studies into antigenic epitopes on these proteins will provide for new insights into pneumovirus immunity and vaccine design. In addition, pre-fusion-stabilized F constructs have now flooded the RSV vaccine field, and there is renewed excitement for the development of an effective RSV vaccine. The field is hopeful that future characterization of mAbs to other pneumovirus surface glycoproteins, as well as assessment of antibody responses to new vaccine candidates will lead to the first safe and effective pneumovirus vaccine.

AUTHOR CONTRIBUTIONS

JH, DD, and JM reviewed the literature, and wrote and edited the manuscript.

FUNDING

This work was supported by the NIH Grant Nos. R01AI143865 and K01OD026569.

REFERENCES

1. Jones HG, Ritschel T, Pascual G, Brakenhoff JPJ, Keogh E, Furmanova-Hollenstein P, et al. Structural basis for recognition of the central conserved region of RSV G by neutralizing human antibodies. *PLoS Pathog*. (2018) 14:e1006935. doi: 10.1371/journal.ppat.1006935
2. Akhras N, Weinberg JB, Newton D. Human metapneumovirus and respiratory syncytial virus: subtle differences but comparable severity. *Infect Dis Rep*. (2010) 2:e12. doi: 10.4081/idr.2010.e12
3. Morris JA, Blount RE, Savage RE. Recovery of cytopathogenic agent from chimpanzees with goryza. *Proc Soc Exp Biol Med*. (1956) 92:544–9. doi: 10.3181/00379727-92-22538
4. Chanock R, Roizman B, Myers R. Recovery from infants with respiratory illness of a virus related to chimpanzee coryza agent (CCA): Isolation, properties and characterization. *Am J Epidemiol*. (1957) 66:291–300. doi: 10.1093/oxfordjournals.aje.a119902
5. Chanock R, Roizman B, Myers R. Recovery from infants with respiratory illness of a virus related to chimpanzee coryza agent (CCA): Isolation, properties and characterization. *Am J Epidemiol*. (1957) 66:281–290. doi: 10.1093/oxfordjournals.aje.a119901
6. Hall CB, Weinberg GA, Poehling KA, Erdman D, Grijalva CG, Zhu Y. The burden of respiratory synctial virus in young children. *N Engl J Med*. (2009) 360:588–98. doi: 10.1056/NEJMoa0804877
7. Shefali-Patel D, Paris MA, Watson F, Peacock JL, Campbell M, Greenough A. RSV hospitalisation and healthcare utilisation in moderately prematurely born infants. *Eur J Pediatr*. (2012) 171:1055–61. doi: 10.1007/s00431-012-1673-0
8. Glezen WP, Taber LH, Frank AL, Kasel JA. Risk of primary infection and reinfection with respiratory syncytial virus. *Am J Dis Child*. (1986) 140:543–6. doi: 10.1001/archpedi.1986.02140200053026
9. Falsey AR, Walsh EE. Respiratory syncytial virus infection in adults. *Clin Microbiol Rev*. (2000) 13:371–84. doi: 10.1128/CMR.13.3.371
10. Grayson SA, Griffiths PS, Perez MK, Piedimonte G. Detection of airborne respiratory syncytial virus in a pediatric acute care clinic. *Pediatr Pulmonol*. (2017) 52:684–8. doi: 10.1002/ppul.23630
11. Higgins D, Trujillo C, Keech C. Advances in RSV vaccine research and development - A global agenda. *Vaccine*. (2016) 34:2870–5. doi: 10.1016/j.vaccine.2016.03.109
12. Anderson EJ, Carosone-Link P, Yogev R, Yi J, Simões EAF. Effectiveness of palivizumab in high-risk infants and children: a propensity score weighted regression analysis. *Pediatr Infect Dis J*. (2017) 36:699–704. doi: 10.1097/INF.0000000000001533
13. van den Hoogen BG, de Jong JC, Groen J, Kuiken T, de Groot R, Fouchier RA, Osterhaus AD. A newly discovered human pneumovirus isolated from young children with respiratory tract disease. *Nat Med*. (2001) 7:719–24. doi: 10.1038/89098
14. Panda S, Mohakud NK, Pena L, Kumar S. Human metapneumovirus: review of an important respiratory pathogen. *Int J Infect Dis*. (2014) 25:45–52. doi: 10.1016/j.ijid.2014.03.1394
15. Falsey AR, Erdman D, Anderson LJ, Walsh EE. Human metapneumovirus infections in young and elderly adults. *J Infect Dis*. (2003) 187:785–90. doi: 10.1086/367901
16. van den Hoogen BG, van Doornum GJ, Fockens JC, Cornelissen JJ, Beyer WE, de Groot R, et al. Prevalence and clinical symptoms of human metapneumovirus infection in hospitalized patients. *J Infect Dis*. (2003) 188:1571–7. doi: 10.1086/379200
17. Madhi SA, Ludewick H, Abed Y, Klugman KP, Boivin G. Human metapneumovirus-associated lower respiratory tract infections among hospitalized human immunodeficiency virus type 1 (HIV-1)-infected and HIV-1-uninfected African infants. *Clin Infect Dis*. (2003) 37:1705–10. doi: 10.1086/379771
18. Haas LEM, Thijsen SFT, van Elden L, Heemstra KA. Human metapneumovirus in adults. *Viruses*. (2013) 5:87–110. doi: 10.3390/v5010087
19. Larcher C, Geltner C, Fischer H, Nachbaur D, Müller LC, Huemer HP. Human metapneumovirus infection in lung transplant recipients: clinical presentation and epidemiology. *J Hear Lung Transpl*. (2005) 24:1891–901. doi: 10.1016/j.healun.2005.02.014
20. Cane PA, van den Hoogen BG, Chakrabarti S, Fegan CD, Osterhaus AD. Human metapneumovirus in a haematopoietic stem cell transplant recipient with fatal lower respiratory tract disease. *Bone Marrow Transplant*. (2003) 31:309–10. doi: 10.1038/sj.bmt.1703849
21. Englund JA, Boeckh M, Kuypers J, Nichols WG, Hackman RC, Morrow RA, et al. Brief communication: fatal human metapneumovirus infection in stem-cell transplant recipients. *Ann Intern Med*. (2013) 144:344–9. doi: 10.7326/0003-4819-144-5-200603070-00010
22. Dokos C, Masjosthusmann K, Rellensmann G, Werner C, Schuler-Lüttmann S, Müller KM, et al. Fatal human metapneumovirus infection following allogeneic hematopoietic stem cell transplantation. *Transpl Infect Dis*. (2013) 15:97–101. doi: 10.1111/tid.12074
23. Shah DP, Shah PK, Azzi JM, El Chaer F, Chemaly RF. Human metapneumovirus infections in hematopoietic cell transplant recipients and hematologic malignancy patients: a systematic review. *Cancer Lett*. (2016) 379:100–6. doi: 10.1016/j.canlet.2016.05.035
24. Klein MB, Yang H, DelBalso L, Carbonneau J, Frost E, Boivin G. Viral pathogens including human metapneumovirus are the primary cause of febrile respiratory illness in HIV-infected adults receiving antiretroviral therapy. *J Infect Dis*. (2010) 201:297–301. doi: 10.1086/649587
25. Kan-o K, Ramirez R, Macdonald MI, Rolph M, Rudd PA, Spann KM, et al. Human metapneumovirus infection in chronic obstructive pulmonary disease: impact of glucocorticosteroids and interferon. *J Infect Dis*. (2018) 215:1536–45. doi: 10.1093/infdis/jix167

26. Group TIm-RS. Palivizumab, a humanized respiratory syncytial virus monoclonal antibody, reduces hospitalization from respiratory syncytial virus infection in high-risk infants. *Pediatrics*. (1998) 102:531–7. doi: 10.1542/peds.102.3.531
27. Domachowske JB, Rosenberg HF. Respiratory syncytial virus infection: immune response, immunopathogenesis, and treatment. *Clin Microbiol Rev*. (1999) 12:298–309. doi: 10.1128/CMR.12.2.298
28. Falsey AR, Hennessey PA, Formica MA, Criddle MM, Biear JM, Walsh EE. Humoral immunity to human metapneumovirus infection in adults. *Vaccine*. (2010) 28:1477–80. doi: 10.1016/j.vaccine.2009.11.063
29. McLellan JS, Ray WC, Peeples ME. Structure and function of RSV surface glycoproteins. *Curr Top Microbiol Immunol*. (2013) 372:83–104. doi: 10.1007/978-3-642-38919-1_4
30. Skiadopoulos MH, Buchholz UJ, Surman SR, Collins PL, Murphy BR. Individual contributions of the human metapneumovirus F, G, and SH surface glycoproteins to the induction of neutralizing antibodies and protective immunity. *Virology*. (2006) 345:492–501. doi: 10.1016/j.virol.2005.10.016
31. White JM, Delos SE, Brecher M, Schornberg K. Structures and mechanisms of viral membrane fusion proteins: multiple variations on a common theme. *Crit Rev Biochem Mol Biol*. (2008) 43:189–219. doi: 10.1080/10409230802058320
32. Schowalter RM, Smith SE, Dutch RE. Characterization of human metapneumovirus F protein-promoted membrane fusion: critical roles for proteolytic processing and low pH. *J Virol*. (2006) 80:10931–41. doi: 10.1128/JVI.01287-06
33. McLellan JS, Yang Y, Graham BS, Kwong PD. Structure of respiratory syncytial virus fusion glycoprotein in the postfusion conformation reveals preservation of neutralizing epitopes. *J Virol*. (2011) 85:7788–96. doi: 10.1128/JVI.00555-11
34. Swanson KA, Settembre EC, Shaw CA, Dey AK, Rappuoli R, Mandl CW, et al. Structural basis for immunization with postfusion respiratory syncytial virus fusion F glycoprotein (RSV F) to elicit high neutralizing antibody titers. *Proc Natl Acad Sci USA*. (2011) 108:9619–24. doi: 10.1073/pnas.1106536108
35. McLellan JS, Chen M, Leung S, Graepel KW, Du X, Yang Y, et al. Structure of RSV fusion glycoprotein trimer bound to a prefusion-specific neutralizing antibody. *Science*. (2013) 340:1113–7. doi: 10.1126/science.1234914
36. McLellan JS, Chen M, Joyce MG, Sastry M, Stewart-Jones GBE, Yang Y, et al. Structure-based design of a fusion glycoprotein vaccine for respiratory syncytial virus. *Science*. (2013) 342:592–8. doi: 10.1126/science.1243283
37. Krarup A, Truan D, Furmanova-Hollenstein P, Bogaert L, Bouchier P, Bisschop IJM, et al. A highly stable prefusion RSV F vaccine derived from structural analysis of the fusion mechanism. *Nat Commun*. (2015) 6:8143. doi: 10.1038/ncomms9143
38. Wen X, Krause JC, Leser GP, Cox RG, Lamb R a, Williams J V, Crowe JE, Jardetzky TS. Structure of the human metapneumovirus fusion protein with neutralizing antibody identifies a pneumovirus antigenic site. *Nat Struc Mol Biol*. (2012) 19:461–3. doi: 10.1038/nsmb.2250
39. Más V, Rodriguez L, Olmedillas E, Cano O, Palomo C, Terrón MC, et al. Engineering, structure and immunogenicity of the human metapneumovirus F protein in the postfusion conformation. *PLoS Pathog*. (2016) 12:e1005859. doi: 10.1371/journal.ppat.1005859
40. Battles MB, Más V, Olmedillas E, Cano O, Vázquez M, Rodríguez L, Melero JA, Mclellan JS. Structure and immunogenicity of pre-fusion-stabilized human metapneumovirus F glycoprotein. *Nat Commun*. (2017) 8:1528. doi: 10.1038/s41467-017-01708-9
41. Stewart-Jones GBE, Chuang G-Y, Xu K, Zhou T, Acharya P, Tsybovsky Y, et al. Structure-based design of a quadrivalent fusion glycoprotein vaccine for human parainfluenza virus types 1–4. *Proc Natl Acad Sci USA*. (2018) 115:12265–70. doi: 10.1073/pnas.1811980115
42. Zhang B, Chen L, Silacci C, Thom M, Boyington JC, Druz A, et al. Protection of calves by a prefusion-stabilized bovine RSV F vaccine. *Nat Struc Mol Biol*. (2017) 2:7. doi: 10.1038/s41541-017-0005-9
43. Ngwuta JO, Chen M, Modjarrad K, Joyce MG, Kanekiyo M, Kumar A, et al. Prefusion F – specific antibodies determine the magnitude of RSV neutralizing activity in human sera. *Sci Transl Med*. (2015) 7:309ra162. doi: 10.1126/scitranslmed.aac4241
44. McLellan JS, Chen M, Kim A, Yang Y, Graham BS, Kwong PD. Structural basis of respiratory syncytial virus neutralization by motavizumab. *Nat Struc Mol Biol*. (2010) 17:248–50. doi: 10.1038/nsmb.1723
45. McLellan JS, Chen M, Chang J-S, Yang Y, Kim A, Graham BS, et al. Structure of a major antigenic site on the respiratory syncytial virus fusion glycoprotein in complex with neutralizing antibody 101F. *J Virol*. (2010) 84:12236–44. doi: 10.1128/JVI.01579-10
46. Mousa JJ, Kose N, Matta P, Gilchuk P, Crowe JE. A novel pre-fusion conformation-specific neutralizing epitope on the respiratory syncytial virus fusion protein. *Nat Microbiol*. (2017) 2:16271. doi: 10.1038/nmicrobiol.2016.271
47. Zhu Q, McLellan JS, Kallewaard NL, Ulbrandt ND, Palaszynski S, Zhang J, et al. A highly potent extended half-life antibody as a potential RSV vaccine surrogate for all infants. *Sci Transl Med*. (2017) 9:1–12. doi: 10.1126/scitranslmed.aaj1928
48. Jones HG, Battles MB, Lin C-C, Bianchi S, Corti D, McLellan JS. Alternative conformations of a major antigenic site on RSV F. *PLoS Pathog*. (2019) 15:e1007944. doi: 10.1371/journal.ppat.1007944
49. Tian D, Battles MB, Moin SM, Chen M, Modjarrad K, Kumar A, et al. Structural basis of respiratory syncytial virus subtype-dependent neutralization by an antibody targeting the fusion glycoprotein. *Nat Commun*. (2017) 8:1877. doi: 10.1038/s41467-017-01858-w
50. Wen X, Mousa JJ, Bates JT, Lamb RA, Crowe JE, Jardetzky TS. Structural basis for antibody cross-neutralization of respiratory syncytial virus and human metapneumovirus. *Nat Microbiol*. (2017) 2:16272. doi: 10.1038/nmicrobiol.2016.272
51. Goodwin E, Gilman MSA, Wrapp D, Graham BS, Mclellan JS, Walker LM. Infants infected with respiratory syncytial virus generate potent neutralizing antibodies that lack somatic hypermutation. *Immunity*. (2018) 48:339–49.e5. doi: 10.1016/j.immuni.2018.01.005
52. Gilman MSA, Furmanova-Hollenstein P, Pascual G, van 't Wout BA, Langedijk JPM, McLellan JS. Transient opening of trimeric prefusion RSV F proteins. *Nat Commun*. (2019) 10:2105. doi: 10.1038/s41467-019-09807-5
53. Gilman MSA, Moin SM, Mas V, Chen M, Patel NK, Kramer K, et al. Characterization of a prefusion-specific antibody that recognizes a quaternary, cleavage-dependent epitope on the RSV fusion glycoprotein. *PLoS Pathog*. (2015) 11:e1005035. doi: 10.1371/journal.ppat.1005035
54. Mousa JJ, Sauer MF, Sevy AM, Finn JA, Bates JT, Alvarado G, et al. Structural basis for nonneutralizing antibody competition at antigenic site II of the respiratory syncytial virus fusion protein. *Proc Natl Acad Sci USA*. (2016) 113:E6849–58. doi: 10.1073/pnas.1609449113
55. Xie Q, Wang Z, Ni F, Chen X, Ma J, Patel N, et al. Structure basis of neutralization by a novel site II/IV antibody against respiratory syncytial virus fusion protein. *PLoS ONE*. (2019) 14:e0210749. doi: 10.1371/journal.pone.0210749
56. Xiao X, Tang A, Cox KS, Wen Z, Callahan C, Sullivan NL, et al. Characterization of potent RSV neutralizing antibodies isolated from human memory B cells and identification of diverse RSV/hMPV cross-neutralizing epitopes. *MAbs*. (2019) 11:1415–27. doi: 10.1080/19420862.2019.1654304
57. Rossey I, Gilman MSA, Kabeche SC, Sedeyn K, Wrapp D, Melero A, et al. Potent single-domain antibodies that arrest respiratory syncytial virus fusion protein in its prefusion state. *Nat Commun*. (2017) 13:14158. doi: 10.1038/ncomms16165
58. Melero JA, Mas V, McLellan JS. Structural, antigenic and immunogenic features of respiratory syncytial virus glycoproteins relevant for vaccine development. *Vaccine*. (2017) 35:461–8. doi: 10.1016/j.vaccine.2016.09.045
59. Gilman MSA, Castellanos CA, Chen M, Ngwuta JO, Goodwin E, Moin SM, et al. Rapid profiling of RSV antibody repertoires from the memory B cells of naturally infected adult donors. *Sci Immunol*. (2016) 1:1–12. doi: 10.1126/sciimmunol.aaj1879
60. Kwakkenbos MJ, Diehl SA, Yasuda E, Bakker AQ, van Geelen CMM, Lukens MV, et al. Generation of stable monoclonal antibody–producing B cell receptor–positive human memory B cells by genetic programming. *Nat Med*. (2010) 16:123–8. doi: 10.1038/nm.2071
61. Domachowske JB, Khan AA, Esser MT, Jensen K, Takas T, Villafana T, et al. Safety, tolerability and pharmacokinetics of MEDI8897, an extended half-life single-dose respiratory syncytial virus prefusion F-targeting monoclonal antibody administered as a single dose to healthy preterm infants. *Pediatr Infect Dis J*. (2018) 37:886–92. doi: 10.1097/INF.0000000000001916

62. Corti D, Bianchi S, Vanzetta F, Minola A, Perez L, Agatic G, et al. Cross-neutralization of four paramyxoviruses by a human monoclonal antibody. *Nature*. (2013) 501:439–43. doi: 10.1038/nature12442
63. Bates JT, Keefer CJ, Slaughter JC, Kulp DW, Schief WR, Crowe JE. Escape from neutralization by the respiratory syncytial virus-specific neutralizing monoclonal antibody palivizumab is driven by changes in on-rate of binding to the fusion protein. *Virology*. (2014) 454–455:139–44. doi: 10.1016/j.virol.2014.02.010
64. Wu H, Pfarr DS, Johnson S, Brewah YA, Woods RM, Patel NK, et al. Development of motavizumab, an ultra-potent antibody for the prevention of respiratory syncytial virus infection in the upper and lower respiratory tract. *J Mol Biol*. (2007) 368:652–65. doi: 10.1016/j.jmb.2007.02.024
65. Johnson S, Oliver C, Prince GA, Hemming VG, Pfarr DS, Want S-C, et al. Development of a humanized monoclonal antibody (Medi-493) with potent *in vitro* and *in vivo* activity against respiratory syncytial virus. *J Infect Dis*. (1997) 17:1215–24. doi: 10.1086/514115
66. Correia BE, Bates JT, Loomis RJ, Baneyx G, Carrico C, Jardine JG, et al. Proof of principle for epitope-focused vaccine design. *Nature*. (2014) 507:201–6. doi: 10.1038/nature12966
67. Luo X, Liu T, Wang Y, Jia H, Zhang Y, Caballero D, et al. An epitope-specific respiratory syncytial virus vaccine based on an antibody scaffold. *Angew Chem Int Ed*. (2015) 54:14531–4. doi: 10.1002/anie.201507928
68. Smith G, Raghunandan R, Wu Y, Liu Y, Massare M, Nathan M, et al. Respiratory syncytial virus fusion glycoprotein expressed in insect cells form protein nanoparticles that induce protective immunity in cotton rats. *PLoS ONE*. (2012) 7:e50852. doi: 10.1371/journal.pone.0050852
69. Detalle L, Stohr T, Palomo C, Piedra PA, Gilbert BE, Mas V, et al. Generation and characterization of ALX-0171, a potent novel therapeutic nanobody for the treatment of respiratory syncytial virus infection. *Antimicrob Agents Chemother*. (2016) 60:6–13. doi: 10.1128/AAC.01802-15
70. Hultberg A, Temperton NJ, Rosseels V, Koenders M, Gonzalez-Pajuelo M, Schepens B, et al. Llama-derived single domain antibodies to build multivalent, superpotent and broadened neutralizing anti-viral molecules. *PLoS ONE*. (2011) 6:e17665. doi: 10.1371/journal.pone.0017665
71. Larios Mora A, Detalle L, Gallup JM, Van Geelen A, Stohr T, Duprez L, et al. Delivery of ALX-0171 by inhalation greatly reduces respiratory syncytial virus disease in newborn lambs. *MAbs*. (2018) 10:778–95. doi: 10.1080/19420862.2018.1470727
72. Wu SJ, Albert Schmidt A, Beil EJ, Day ND, Branigan PJ, Liu C, et al. Characterization of the epitope for anti-human respiratory syncytial virus F protein monoclonal antibody 101F using synthetic peptides and genetic approaches. *J Gen Virol*. (2007) 88:2719–23. doi: 10.1099/vir.0.82753-0
73. Mousa JJ, Binshtein E, Human S, Fong RH, Alvarado G, Doranz BJ, et al. Human antibody recognition of antigenic site IV on Pneumovirus fusion proteins. *PLoS Pathog*. (2018) 14:e1006837. doi: 10.1371/journal.ppat.1006837
74. Tang A, Chen Z, Cox KS, Su H, Callahan C, Fridman A, et al. A potent broadly neutralizing human RSV antibody targets conserved site IV of the fusion glycoprotein. *Nat Commun*. (2019) 10:4153. doi: 10.1038/s41467-019-12137-1
75. Anderson LJ, Hierholzer JC, Stone Y, Tsou C, Fernie BF. Identification of epitopes on respiratory syncytial virus proteins by competitive binding immunoassay. *J Clin Microbiol*. (1986) 23:475–80.
76. Ulbrandt ND, Ji H, Patel NK, Riggs JM, Brewah YA, Ready S, et al. Isolation and characterization of monoclonal antibodies which neutralize human metapneumovirus *in vitro* and *in vivo*. *J Virol*. (2006) 80:7799–806. doi: 10.1128/JVI.00318-06
77. Hamelin ME, Gagnon C, Prince GA, Kiener P, Suzich J, Ulbrandt N, et al. Prophylactic and therapeutic benefits of a monoclonal antibody against the fusion protein of human metapneumovirus in a mouse model. *Antivir Res*. (2010) 88:31–7. doi: 10.1016/j.antiviral.2010.07.001
78. Ulbrandt ND, Ji H, Patel NK, Barnes AS, Wilson S, Kiener PA, et al. Identification of antibody neutralization epitopes on the fusion protein of human metapneumovirus. *J Gen Virol*. (2008) 89:3113–8. doi: 10.1099/vir.0.2008/005199-0
79. Williams JV, Chen Z, Cseke G, Wright DW, Keefer CJ, Tollefson SJ, et al. A recombinant human monoclonal antibody to human metapneumovirus fusion protein that neutralizes virus *in vitro* and is effective therapeutically *in vivo*. *J Virol*. (2007) 81:8315–24. doi: 10.1128/JVI.00106-07
80. Bar-Peled Y, Diaz D, Pena-Briseno A, Murray J, Huang J, Tripp RA, et al. A potent neutralizing site III-specific human antibody neutralizes human metapneumovirus *in vivo*. *J Virol*. (2019) 93:e00342-19. doi: 10.1128/JVI.00342-19

Conflict of Interest: The authors declare that the research was conducted in the absence of any commercial or financial relationships that could be construed as a potential conflict of interest.

frontiers in Immunology

OPINION
published: 29 November 2019
doi: 10.3389/fimmu.2019.02760

Inhalation of Immuno-Therapeutics/-Prophylactics to Fight Respiratory Tract Infections: An Appropriate Drug at the Right Place!

Thomas Sécher[1,2†], *Alexie Mayor*[1,2†] *and Nathalie Heuzé-Vourc'h*[1,2*]

[1] INSERM U1100, Centre d'Etude des Pathologies Respiratoires, Tours, France, [2] Centre d'Etude des Pathologies Respiratoires, Université de Tours, Tours, France

Keywords: respiratory infection, biopharmaceutics, immune-pharmaceutics, topical delivery, inhalation

OPEN ACCESS

Edited by:
Giuseppe Andrea Sautto, University of Georgia, United States

Reviewed by:
Yuan Tian, La Jolla Institute for Immunology (LJI), United States

****Correspondence:***
Nathalie Heuzé-Vourc'h
nathalie.vourch@med.univ-tours.fr

† These authors have contributed equally to this work

Specialty section:
This article was submitted to Vaccines and Molecular Therapeutics, a section of the journal Frontiers in Immunology

Received: *12 September 2019*
Accepted: *12 November 2019*
Published: *29 November 2019*

Citation:
Sécher T, Mayor A and Heuzé-Vourc'h N (2019) Inhalation of Immuno-Therapeutics/-Prophylactics to Fight Respiratory Tract Infections: An Appropriate Drug at the Right Place! Front. Immunol. 10:2760. doi: 10.3389/fimmu.2019.02760

INTRODUCTION

Respiratory tract infections (RTIs) are the third leading cause of morbidity and mortality worldwide, accounting for ∼4.25 million deaths in 2010, in either children, adults or the elderlies. RTIs encompass acute infections of the upper (rhinosinusitis, …) and lower airways (pneumonia, bronchiolitis, …) and are also inherently associated with chronic diseases such as chronic obstructive pulmonary disease (COPD) and cystic fibrosis (CF). In addition to premature mortality, RTIs result in a huge burden on the society considering quality-adjusted life year loss and additional pressure on the overwhelmed healthcare systems, thereby representing a major public health issue.

Antimicrobial chemotherapies (e.g., antibiotics, antivirals) are the standard interventions to prevent and to treat respiratory infections. However, their effectiveness is declining due to increased pathogen resistance, urging alternative or complementary strategies to reinforce the anti-infectious arsenal to fight RTIs. Among those under evaluation, immunomodulatory agents (immunopharmaceutics) like therapeutic antibodies (Ab) or other therapeutic proteins and vaccines may offer novel opportunities for the prevention and treatment of RTIs, by targeting pathogens and boosting the host immune system. When used in a preventive way in patients at risk, or therapeutically to stop or to limit the spread of infection, both immunopropylactics and immunotherapeutics are administered through parenteral routes (including intravenous, subcutaneous, and intramuscular) (**Table 1**). As demonstrated in preclinical studies, parenteral delivery may not be optimal for large molecular weight entities to treat respiratory diseases (1, 2) since they poorly reach the lung compartment. In contrast, inhalation, comprising the intranasal and oral respiratory routes, targets drugs into the respiratory tract. Currently, inhalation is used both for locally- and systemically-acting drugs as it allows a straight delivery to the diseased organ and a portal to the blood circulation, considering the extensive alveolus-capillary interface. By providing a better therapeutic index, inhalation is the gold standard for small molecules, delivered topically as an aerosol, like corticosteroids/steroids, decongestants or bronchodilators for the treatment of asthma, rhinosinusitis or COPD. Besides, it is also indicated for antibiotics (nasal and oral inhalation), a local-acting protein therapeutic—Dornase alpha (Pulmozyme®, oral inhalation), a mucolytic agent for patients with CF and an influenza live vaccine (FluMist® Quadrivalent, nasal inhalation).

LOCAL-ACTING IMMUNOPHARMACEUTICS DELIVERED BY INHALATION

There are accumulating evidences that administration of anti-infectious Abs, protein therapeutics (e.g., cytokines) and vaccines, to the upper and/or lower respiratory tract by inhalation,

with the purpose of inducing a local action, is effective (3). Several preclinical studies showed the superiority of immunopharmaceutics administered topically to the respiratory tract in RTI models, in both therapeutic and prophylactic regimens. For instance, inhalation of anti-infectious Abs in models of pneumonia using *Pseudomonas aeruginosa* or influenza virus conferred higher protection and greater therapeutic response, respectively, compared to parenteral route administration (4, 5). Besides, other immunoprophylactics delivered through the respiratory route such as immunocytokines (e.g., IL-7 Fc) (6) and live-attenuated vaccines (7) showed superior performances over conventional routes against airborne viruses, in mice and non-human primates, respectively. Conversely, restricting the response to the site of action for pleiotropic molecules (e.g., IL-7 Fc), envisioned as adjuvant molecule, may reduce systemic side-effects. As reported for anti-infectious Abs, the inhaled route may also enable a higher efficacy with a lower dose (4). This means that the inhaled route may allow, in the future, to alleviate the financial burden of immunopharmaceutics (in particular Abs), which may exceed the ability of both individual patients and the healthcare systems to sustain them. Additional benefit of the inhaled route includes its non-invasiveness, offering a better comfort for patients, in particular those with chronic respiratory infections, and thus preventing additional healthcare costs. Besides, needle-free vaccination may prevent the risk of cross-contamination and facilitate mass vaccination efforts.

However, beyond clear preclinical proofs of concept and obvious theoretical advantages of the inhalation route for immunotherapeutics and -prophylactics, few of these benefits have materialized in the clinic (**Table 1**). Except for Flumist® Quadrivalent (Astrazeneca), an intranasal live attenuated influenza vaccine, other marketed immunoprophylactics vaccines (including those against *Streptococcus pneumoniae*, *Haemophilus influenza*, *Mycobacterium tuberculosis*, *Bordetella pertussis* or measles and Ab (anti-RSV Pavilizumab)—are administered systemically. Similarly, none of the protein therapeutics is given by inhalation. Recently, Ablynx developed an inhaled anti-RSV trimeric nanobody® (ALX-0171) for therapeutic purposes. Despite promising results in several animal models, the development has been interrupted due to insufficient evidences of efficacy during Phase 2 trial in children (in Japan). In 2019, only one phase 2 trial with an inhaled anti-infectious protein therapeutics is still ongoing (NCT03570359) assessing the efficacy of topical lung delivery of IFN-β1a (SNG001, Synairgen/Astrazeneca), as an immunostimulant to treat COPD exacerbations. Overall, this highlights the complexity of developing inhaled biopharmaceuticals and points out the persisting hurdles (**Figure 1**).

CHALLENGES FOR THE DEVELOPMENT OF INHALED IMMUNE-THERAPEUTICS/PROPHYLACTICS

The instability of immunopharmaceutics and vaccines often emerges as a challenge for inhalation delivery. Therapeutic proteins and vaccines are sensitive to various conditions which may alter their structure, thereby decrease their activity. Delivering a drug through the inhalation route implies either spraying, drying or aerosolizing, which is associated with multiple stresses (shearing, temperature, air/liquid interface, …) potentially deleterious as widely discussed elsewhere (8, 9). To deal with this, both the device used for the generation of the aerosol and the formulation must be adapted, as successfully reported for Ab-based therapeutics (3, 10). However, the excipients must be adapted for respiratory delivery. The choice of mucosal-licensed adjuvants, which should be exempt of intrinsic immune-toxicity, and the instability of the associated carrier [e.g., nanoparticles, liposomes, immune stimulating complexes (ISCOMs)] is particularly challenging for the inhalation delivery of vaccines, especially those of the latest generation (e.g., T, B-epitope-based vaccines). The drug and device combination yields proper aerodynamical properties (particle size, flow rate, …) to achieve the anticipated deposition in the appropriate area of the respiratory tract. Indeed, appropriate deposition to the anatomical site is mandatory to ensure an optimal efficacy. On one hand, this depends on the drug formulation (e.g., surface tension and viscosity for liquid formulation) (11) and device performances to allow the therapeutic agent to reach the site of infection (**Figure 1**), by this means the microbe. For lung infections, most pneumonia consists of an aggregate of trachea-bronchitis and alveolar infections. Theoretically, this clinical condition may benefit from a uniform distribution all over the lungs, with a polydisperse aerosol (ranging 1–5 μm). However, several pathogens are associated with specific anatomic localization, like *S. pneumoniae,* which is mainly found in the alveolar spaces, thereby requiring low-size aerosols (<2–3 μm) to be targeted. On the other hand, delivery to the mucosal-associated lymphoid tissue (MALT), located in the tonsils, would be more adapted for vaccines to induce an adaptive immune response, since MALT plays a central role in the primary respiratory immune defense (**Figure 1**).

Biological barriers are additional hurdles to overcome and apply to all inhaled anti-infectious agents (12). First, a pathogen can "hide" itself inside host cells like *M. tuberculosis* in alveolar macrophages, thus being more difficult to be targeted by immunopharmaceutics. Other pathogens may produce extracellular barriers like the biofilm matrix produced by *P. aeruginosa* in the context of chronic lung infections. This biofilm acts as a diffusion barrier, preventing inhaled immunopharmaceutics from reaching their molecular target. Antibody-based fragments, such as fragment antigen-binding (Fab) and single-chain variable fragments (scFv) might be more efficient in crossing over the biofilm, like they penetrate better solid tumors (13), and eradicate *P. aeruginosa.* Secondly, the host physical defenses, which prevent foreign particles from penetrating into the respiratory tract, may limit the accessibility of inhaled immunopharmaceutics to their target. Among them, the mucus and the mucociliary escalator are highly efficient clearance mechanisms (14, 15). The development of mucoadhesive formulations may be helpful to enhance the bioavailability of inhaled drugs (16). In contrast, anti-adhesive molecules, such as polyethylene glycol may facilitate

TABLE 1 | Marketed immunotherapeutics and immunoprophylactics for infectious diseases.

Target	Product	Category	Sponsors	Administration route	Date of approval	Indication
RSV	Synagis	Monoclonal antibody	MedImmune	IM	1998	Prophylaxis
Influenza	Afluria	Inactivated vaccine Quadrivalent	Seqirus	IM	2007	Prophylaxis
	Fluad	Inactivated vaccine Trivalent	Seqirus	IM	2015	Prophylaxis
	Fluarix	Inactivated vaccine Quadrivalent	GSK	IM	2012	Prophylaxis
	Flublok	Recombinant vaccine Quadrivalent	Protein Sciences Corporation	IM	2013	Prophylaxis
	Flucelvax	Inactivated vaccine Quadrivalent	Seqirus	IM	2012	Prophylaxis
	Pandemic influenza vaccine H5N1	Recombinant vaccine	Medimmune	IN	2016	Prophylaxis
	FluLaval	Inactivated vaccine Quadrivalent	ID Biomedical Corporation of Quebec	IM	2013	Prophylaxis
	FluMist	Live-attenuated vaccine Quadrivalent	MedImmune	IN	2003	Prophylaxis
	Fluzone High Dose	Inactivated vaccine Quadrivalent	Sanofi Pasteur	IM	2014	Prophylaxis
	Fluzone	Inactivated vaccine Quadrivalent	Sanofi Pasteur	IM	2009	Prophylaxis
	Fluvirin	Inactivated vaccine Trivalent	Seqirus	IM	1988	Prophylaxis
Measle	Proquad	Subunit vaccine	Merck	SC	2005	Prophylaxis
	M-M-R II	Subunit vaccine	Merck	SC	2014	Prophylaxis
Smallpox	ACAM2000	Live vaccina virus	Emergent Product Development	Percutaneous	2007	Prophylaxis
Mycobacterium tuberculosis	BCG Vaccine	Live-attenuated vaccine	Organon	Percutaneous	2011	Prophylaxis
Streptococcus pneumoniae	Pneumovax 23	Subunit vaccine	Merck&Co	IM	1983	Prophylaxis
	Prevenar 13	Subunit vaccine	Wyeth Pharmaceuticals	IM	2010	Prophylaxis
Bordetella pertussis	Daptacel	Subunit vaccine	Sanofi Pasteur	IM	2008	Prophylaxis
	Pediarix	Subunit vaccine	GSK	IM	2002	Prophylaxis
	Kinrix	Subunit vaccine	GSK	IM	2008	Prophylaxis
	Quadracel	Subunit vaccine	Sanofi Pasteur	IM	2015	Prophylaxis
	Pentacel	Subunit vaccine	Sanofi Pasteur	IM	2008	Prophylaxis
Haemophilus influenzae	Hiberix	Subunit vaccine	GSK	IM	2009	Prophylaxis
	ActHIB	Subunit vaccine	Sanofi Pasteur	IM	1993	Prophylaxis
	PedvaxHIB	Subunit vaccine	Merck	IM	1989	Prophylaxis
Bordetella pertussis Haemophilus influenzae	Infanrix	Subunit vaccine	GSK	IM	1997	Prophylaxis
	Vaxelis	Subunit vaccine	MCM Vaccine	IM	2018	Prophylaxis
Bacillus anthracis	Anthim	Monoclonal antibody	Elusys Therapeutics	IV	2016	Prophylaxis/Therapy
	Abthrax	Monoclonal antibody	GSK	IV	2012	Prophylaxis/Therapy
	Biothrax	Subunit vaccine	Emergent BioSolutions	IM	2016	Prophylaxis

IM, intramuscular; IN, inhalation (nasal); SC, subcutaneous.

immunopharmaceutics translocation through the mucus blanket, as shown *in vitro* (17) and *in vivo* (18) for other applications. It is noteworthy that, in some pathological conditions (e.g., chronic sinusitis, CF and COPD), the mucus gets thicker. In CF, the mucus exhibited an increased density of disulfide cross-links, further tightening the mucus mesh space, thereby reinforcing its steric barrier potency to immunopharmaceutics (19). To date, overcoming this physical barrier has not been addressed in the design of inhaled immunopharmaceutics. Other biological barriers include alveolar macrophages and the pulmonary surfactant layer in the alveolar region. While the molecular interactions between inhaled particles and

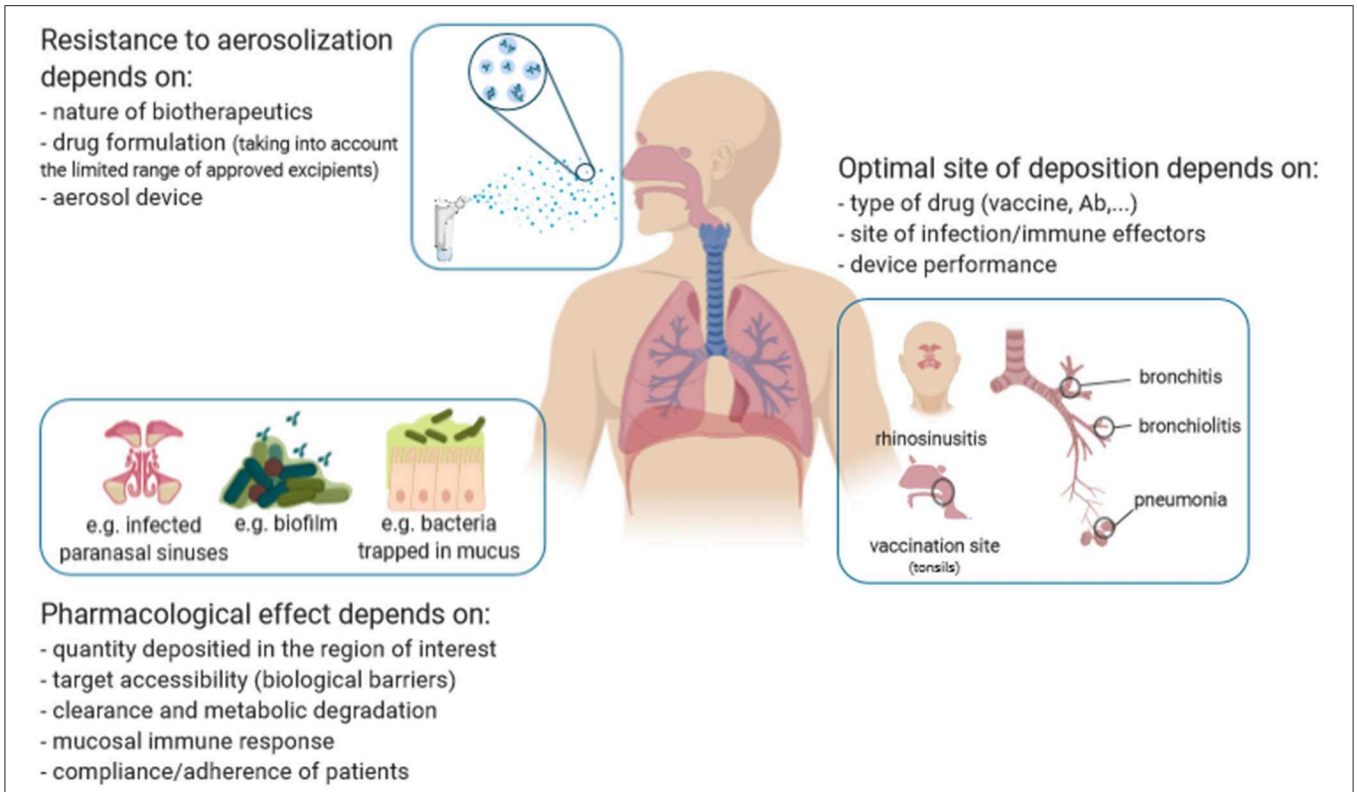

FIGURE 1 | The multifaceted features from the development of inhaled immunopharmaceutics.

the surfactant are largely unknown, some evidences indicate that surfactant proteins may facilitate the uptake of inhaled particles by alveolar macrophages (20). Alveolar macrophages patrol the airways and phagocytose inhaled organic (including pathogens) and inorganic particles ranging between 0.5 and 5μm (21). Interestingly, the size-discriminating property of their phagocytosis potency has led to the development of innovative approaches for inhaled drugs, in which carrier entrapped-particles of smaller or larger size are inhaled to escape the alveolar macrophage phagocytosis and to provide a better controlled drug release [(22, 23); **Figure 1**]. This strategy is investigated for mucosal vaccines to prevent the degradation or denaturation of the peptide/antigen, to sustain its release and favor delivery and adjuvancy (24).

The lung mucosa is a metabolic active environment (25). The presence of proteases [which is more prevalent in the nasal mucosa (26)] may degrade therapeutic proteins before they reach their targets. In addition to host enzymes, bacterial pathogens, like *P. aeruginosa*, release additional proteases, which may metabolize respiratory-delivered drugs (27). In this context, the presence of protease inhibitors in the formulation of inhaled protein therapeutics may improve their pharmacokinetics and efficacy, as previously demonstrated for inhaled peptides such as insulin and calcitonin (28). Furthermore, the encapsulation of protein therapeutics into liposomes may also improve stability and reduce the frequency of dosing (29). This strategy has already been clinically validated for the pulmonary delivery of antibiotics (30). Of note, respiratory diseases are often associated with an impairment of the protease/anti-protease balance. In CF, high levels of proteases are a result of the chronic infection and inflammation induced by *P. aeruginosa* (31). This proteolytic environment self-perpetuates the intensity of inflammation, induces mucus hypersecretion and respiratory tissue damage, which may ultimately affect inhaled immunotherapeutics (**Figure 1**).

CONCLUSION

Compared to the expansion of biopharmaceutics (excluding non-recombinant vaccines) in all medical areas, the field of inhaled protein therapeutics/vaccines has stagnated, with only few drugs approved so far. Despite promising preclinical data and significant advances on macromolecule inhalation, a definitive demonstration that effective and intact inhaled immunopharmaceuticals could be delivered (topically) to humans is still lacking.

Although, we cannot rule out that the recent failures of inhaled biopharmaceutics (Exubera and ALX-0171) make it challenging, to our opinion, it may be time for thinking carefully where inhalation may have the edge over other routes: "finding the right use for this modality!" They may be many possibilities considering the unmet clinical needs for respiratory

diseases and the growing market of immunopharmaceutics. But the inhalation route must be envisioned and integrated early taking into account the disease/population, the target, the drug and the device (**Figure 1**), rather than adapting an approved molecule for the inhalation route. RTIs are undoubtedly an appropriate clinical situation for inhalation, if we consider the importance of matching the delivery of immunoprophylatics or immunotherapeutics to their site of action. Anti-infectious macromolecules may certainly benefit from the success of inhaled antibiotics, but it is critical to remember their precise molecular nature associated with a unique pharmacokinetics profile when considering their development for inhalation. Besides, the recent report of a universal flu vaccine, comprised of Ab-based therapeutics (VHH) produced by an adeno-associated virus delivered intranasally pushed further the boundaries of the potential of the inhalation route for immunoprophylactics (32).

AUTHOR CONTRIBUTIONS

TS, AM, and NH-V participated in the review of research. NH-V prepared figure. TS and AM prepared table. All authors contributed to the manuscript.

FUNDING

This work was supported by the French National Research Agency as part of the Investissements d'Avenir program (LabEx MAbImprove, ANR-10-LABX-53-01), by the Region Centre Val-de-Loire (ARD2020 Biomedicament, PRIMine project/APR IR 2019, Novantinh project), by French Cystic Fibrosis Foundation VLM (Grant No. RF20170502036). TS was funded by a fellowship from ANR-10-LABX-53-01. AM was funded by a CIFRE thesis partnership between the CEPR and Sanofi. Figure was created by BioRender.com.

REFERENCES

1. Dall'Acqua WF, Kiener PA, Wu H. Properties of human IgG1s engineered for enhanced binding to the neonatal Fc receptor (FcRn). *J Biol Chem*. (2006) 281:23514–24. doi: 10.1074/jbc.M604292200
2. Labiris NR, Dolovich MB. Pulmonary drug delivery. Part I: physiological factors affecting therapeutic effectiveness of aerosolized medications. *Br J Clin Pharmacol*. (2003) 56:588–99. doi: 10.1046/j.1365-2125.2003.01892.x
3. Larios Mora A, Detalle L, Gallup JM, Van Geelen A, Stohr T, Duprez L, et al. Delivery of ALX-0171 by inhalation greatly reduces respiratory syncytial virus disease in newborn lambs. *mAbs*. (2018) 10:778–95. doi: 10.1080/19420862.2018.1470727
4. Leyva-Grado VH, Tan GS, Leon PE, Yondola M, Palese P. Direct administration in the respiratory tract improves efficacy of broadly neutralizing anti-influenza virus monoclonal antibodies. *Antimicrob Agents Chemother*. (2015) 59:4162–72. doi: 10.1128/AAC.00290-15
5. Secher T, Dalonneau E, Ferreira M, Parent C, Azzopardi N, Paintaud G, et al. In a murine model of acute lung infection, airway administration of a therapeutic antibody confers greater protection than parenteral administration. *J Control Release*. (2019) 303:24–33. doi: 10.1016/j.jconrel.2019.04.005
6. Kang MC, Choi DH, Choi YW, Park SJ, Namkoong H, Park KS, et al. Intranasal introduction of Fc-fused interleukin-7 provides long-lasting prophylaxis against lethal influenza virus infection. *J Virol*. (2015) 90:2273–84. doi: 10.1128/JVI.02768-15
7. de Swart RL, de Vries RD, Rennick LJ, van Amerongen G, McQuaid S, Verburgh RJ, et al. Needle-free delivery of measles virus vaccine to the lower respiratory tract of non-human primates elicits optimal immunity and protection. *NPJ vaccines*. (2017) 2:22. doi: 10.1038/s41541-017-0022-8
8. Bodier-Montagutelli E, Mayor A, Vecellio L, Respaud R, Heuze-Vourc'h N. Designing inhaled protein therapeutics for topical lung delivery: what are the next steps? *Exp Opin Drug Deliv*. (2018) 15:729–36. doi: 10.1080/17425247.2018.1503251
9. Respaud R, Vecellio L, Diot P, Heuze-Vourc'h N. Nebulization as a delivery method for mAbs in respiratory diseases. *Exp Opin Drug Deliv*. (2015) 12:1027–39. doi: 10.1517/17425247.2015.999039
10. Respaud R, Marchand D, Pelat T, Tchou-Wong KM, Roy CJ, Parent C, et al. Development of a drug delivery system for efficient alveolar delivery of a neutralizing monoclonal antibody to treat pulmonary intoxication to ricin. *J Control Release*. (2016) 234:21–32. doi: 10.1016/j.jconrel.2016.05.018
11. Carvalho TC, McConville JT. The function and performance of aqueous aerosol devices for inhalation therapy. *J Pharm Pharmacol*. (2016) 68:556–78. doi: 10.1111/jphp.12541
12. Ho DK, Nichols BLB, Edgar KJ, Murgia X, Loretz B, Lehr CM. Challenges and strategies in drug delivery systems for treatment of pulmonary infections. *Eur J Pharm Biopharm*. (2019) 144:110–24. doi: 10.1016/j.ejpb.2019.09.002
13. Thurber GM, Schmidt MM, Wittrup KD. Antibody tumor penetration: transport opposed by systemic and antigen-mediated clearance. *Adv Drug Deliv Rev*. (2008) 60:1421–34. doi: 10.1016/j.addr.2008.04.012
14. Geiser M, Cruz-Orive LM, Im Hof V, Gehr P. Assessment of particle retention and clearance in the intrapulmonary conducting airways of hamster lungs with the fractionator. *J Microsc*. (1990) 160(Pt 1):75–88.
15. Gizurarson S. The effect of cilia and the mucociliary clearance on successful drug delivery. *Biol Pharm Bull*. (2015) 38:497–506. doi: 10.1248/bpb.b14-00398
16. Takeuchi H, Yamamoto H, Kawashima Y. Mucoadhesive nanoparticulate systems for peptide drug delivery. *Adv Drug Deliv Rev*. (2001) 47:39–54.doi: 10.1016/s0169-409x(00)00120-4
17. Lai SK, O'Hanlon DE, Harrold S, Man ST, Wang YY, Cone R, et al. Rapid transport of large polymeric nanoparticles in fresh undiluted human mucus. *Proc Natl Acad Sci USA*. (2007) 104:1482–7. doi: 10.1073/pnas.0608611104
18. Muralidharan P, Mallory E, Malapit M, Hayes D Jr, Mansour HM. Inhalable PEGylated phospholipid nanocarriers and PEGylated therapeutics for respiratory delivery as aerosolized colloidal dispersions and dry powder inhalers. *Pharmaceutics*. (2014) 6:333–53. doi: 10.3390/pharmaceutics6020333
19. Yuan S, Hollinger M, Lachowicz-Scroggins ME, Kerr SC, Dunican EM, Daniel BM, et al. Oxidation increases mucin polymer cross-links to stiffen airway mucus gels. *Sci Transl Med*. (2015) 7:276ra27. doi: 10.1126/scitranslmed.3010525
20. Chroneos ZC, Sever-Chroneos Z, Shepherd VL. Pulmonary surfactant: an immunological perspective. *Cell Physiol Biochem*. (2010) 25:13–26. doi: 10.1159/000272047
21. Geiser M. Update on macrophage clearance of inhaled micro- and nanoparticles. *J Aerosol Med Pulm Drug Deliv*. (2010) 23:207–17. doi: 10.1089/jamp.2009.0797
22. Pudlarz AM, Czechowska E, Ranoszek-Soliwoda K, Tomaszewska E, Celichowski G, Grobelny J, et al. Immobilization of recombinant human catalase on gold and silver nanoparticles. *Appl Biochem Biotechnol*. (2018) 185:717–35. doi: 10.1007/s12010-017-2682-2
23. Tsapis N, Bennett D, Jackson B, Weitz DA, Edwards DA. Trojan particles: large porous carriers of nanoparticles for drug delivery. *Proc Natl Acad Sci USA*. (2002) 99:12001–5. doi: 10.1073/pnas.182233999
24. Osman N, Kaneko K, Carini V, Saleem I. Carriers for the targeted delivery of aerosolized macromolecules for pulmonary pathologies. *Exp Opin Drug Deliv*. (2018) 15:821–34. doi: 10.1080/17425247.2018.1502267
25. Candiano G, Bruschi M, Pedemonte N, Musante L, Ravazzolo R, Liberatori S, et al. Proteomic analysis of the airway surface liquid: modulation by

proinflammatory cytokines. *Am J Physiol Lung Cell Mol Physiol*. (2007) 292:L185–98. doi: 10.1152/ajplung.00085.2006
26. Zhou XH. Overcoming enzymatic and absorption barriers to non-parenterally administered protein and peptide drugs. *J Control Release*. (1994) 29:239–52. doi: 10.1016/0168-3659(94)90071-X
27. Gellatly SL, Hancock RE. Pseudomonas aeruginosa: new insights into pathogenesis and host defenses. *Pathogens Dis*. (2013) 67:159–73. doi: 10.1111/2049-632X.12033
28. Hussain A, Arnold JJ, Khan MA, Ahsan F. Absorption enhancers in pulmonary protein delivery. *J Control Release*. (2004) 94:15–24. doi: 10.1016/j.jconrel.2003.10.001
29. Gibbons AM, McElvaney NG, Taggart CC, Cryan SA. Delivery of rSLPI in a liposomal carrier for inhalation provides protection against cathepsin L degradation. *J Microencapsul*. (2009) 26:513–22. doi: 10.1080/02652040802466535
30. Haworth CS, Bilton D, Chalmers JD, Davis AM, Froehlich J, Gonda I, et al. Inhaled liposomal ciprofloxacin in patients with non-cystic fibrosis bronchiectasis and chronic lung infection with Pseudomonas aeruginosa (ORBIT-3 and ORBIT-4): two phase 3, randomised controlled trials. *Lancet Respir Med*. (2019) 7:213–26. doi: 10.1016/S2213-2600(18)30427-2
31. Twigg MS, Brockbank S, Lowry P, FitzGerald SP, Taggart C, Weldon S. The role of serine proteases and antiproteases in the cystic fibrosis lung. *Mediators Inflamm*. (2015) 2015:293053. doi: 10.1155/2015/293053
32. Laursen NS, Friesen RHE, Zhu X, Jongeneelen M, Blokland S, Vermond J, et al. Universal protection against influenza infection by a multidomain antibody to influenza hemagglutinin. *Science*. (2018) 362:598-602. doi: 10.1126/science.aaq0620

Conflict of Interest: The authors declare that the research was conducted in the absence of any commercial or financial relationships that could be construed as a potential conflict of interest.

frontiers in Immunology

MINI REVIEW
published: 10 December 2019
doi: 10.3389/fimmu.2019.02841

Using Omics Technologies and Systems Biology to Identify Epitope Targets for the Development of Monoclonal Antibodies Against Antibiotic-Resistant Bacteria

*Antonio J. Martín-Galiano and Michael J. McConnell**

Intrahospital Infections Laboratory, National Centre for Microbiology, Instituto de Salud Carlos III, Majadahonda, Spain

Over the past few decades, antimicrobial resistance has emerged as an important threat to public health due to the global dissemination of multidrug-resistant strains from several bacterial species. This worrisome trend, in addition to the paucity of new antibiotics with novel mechanisms of action in the development pipeline, warrants the development of non-antimicrobial approaches to combating infection caused by these isolates. Monoclonal antibodies (mAbs) have emerged as highly effective molecules for the treatment of multiple diseases. However, in spite of the fact that antibodies play an important role in protective immunity against bacteria, only three mAb therapies have been approved for clinical use in the treatment of bacterial infections. In the present review, we briefly outline the therapeutic potential of mAbs in the treatment of bacterial diseases and discuss how their development can be facilitated when assisted by "omics" technologies and interpreted under a systems biology paradigm. Specifically, methods employing large genomic, transcriptomic, structural, and proteomic datasets allow for the rational identification of epitopes. Ideally, these include those that are present in the majority of circulating isolates, highly conserved at the amino acid level, surface-exposed, located on antigens essential for virulence, and expressed during critical stages of infection. Therefore, these knowledge-based approaches can contribute to the identification of high-value epitopes for the development of effective mAbs against challenging bacterial clones.

Keywords: monoclonal antibodies, antibiotic resistance, multidrug resistance, systems biology, big data, immunoinformatics, bound rationality

OPEN ACCESS

Edited by:
Giuseppe Andrea Sautto, University of Georgia, United States

Reviewed by:
Walid Mottawea, University of Ottawa, Canada
George Mias, Michigan State University, United States

****Correspondence:***
Michael J. McConnell
michael.mcconnell@isciii.es

Specialty section:
This article was submitted to Vaccines and Molecular Therapeutics, a section of the journal Frontiers in Immunology

Received: *18 September 2019*
Accepted: *19 November 2019*
Published: *10 December 2019*

Citation:
Martín-Galiano AJ and McConnell MJ (2019) Using Omics Technologies and Systems Biology to Identify Epitope Targets for the Development of Monoclonal Antibodies Against Antibiotic-Resistant Bacteria. Front. Immunol. 10:2841. doi: 10.3389/fimmu.2019.02841

DO WE NEED MONOCLONAL ANTIBODIES AGAINST ANTIBIOTIC-RESISTANT BACTERIA?

In recent years, there has been an explosive increase in the emergence and dissemination of antimicrobial resistance. Multiple factors have likely contributed to this phenomenon, including the overuse of existing antibiotics in the clinical setting, non-human use of antibiotics, and increased international travel. A report commissioned by the United Kingdom in 2014 estimated that deaths directly attributable to antimicrobial resistance will increase to 10 million annually by 2050, as compared to the 700,000 deaths currently produced by these infections per year (1).

The predicted economic expense caused by antimicrobial resistance is also significant, as the same study projected that the cumulative worldwide loss of Gross Domestic Product (GDP) between 2014 and 2050 would be higher than the current yearly GDP of all countries combined. Although these extreme scenarios represent projections based on current trends, there is little doubt that antimicrobial resistance will be a major public health threat in the near future. Importantly, the clinical management of multidrug-resistant (MDR) infections is complicated by the lack of currently approved antimicrobials that retain sufficient activity against MDR strains, particularly the so-called ESKAPE microorganisms, which include *Enterococcus faecium*, *Staphylococcus aureus*, *Klebsiella pneumoniae*, *Acinetobacter baumannii*, *Pseudomonas aeruginosa*, and *Enterobacter* spp. (2). Recent sporadic reports from different geographic regions describing pan-drug resistant isolates, with resistance to all clinically-available antibiotics, are cause for particular concern (3–5). In this context, the need to develop new antibiotics, ideally with novel mechanisms of action not affected by cross-resistance to existing mechanisms, is apparent. Unfortunately, while there have been recent approvals of new antibiotics for clinical use, very few antimicrobials with completely novel mechanisms of action have been developed over the last 40 years.

While new antibiotics will be key players in combating resistance, it is likely that treatment and prevention approaches fighting on alternative fronts will need to be explored. In this regard, a recent report summarizing the portfolio of alternatives to antibiotics that are currently under development identified antibody-based therapies, probiotics, phage therapy, immune stimulation, and vaccines as "Tier 1," based on their stage of development and probability of success (6). Among these approaches, therapies based on monoclonal antibodies (mAbs) have a number of characteristics that may make them ideally suited for the treatment and prevention of infections caused by MDR bacteria, including (a) absence of susceptibility to existing resistance mechanisms and lack of selection for resistance to existing antibiotics, (b) facilitating immune-mediated clearance of bacterial pathogens, (c) high specificity and therefore minimal effects on non-target bacteria present in the human microbiota, (d) safety and efficiency in humans, and (e) passive immunization, which, in contrast to active immunization with vaccines, has potential to provide immediate protective immunity against infection, which may be particularly important in critically-ill patients with decreased immune function. In this review, we assess the potential of omics technologies and systems biology approaches to enhance the rational identification of epitopes for the development of mAbs against MDR bacteria.

CHALLENGES TO DEVELOPING MABS FOR RESISTANT BACTERIA

MAbs are highly directed therapeutics that embody the magic bullet ideal of specifically targeting a particular pathogen. However, despite the fact that a large number of therapeutic mAbs have been successfully developed for multiple different human pathologies, most notably for rheumatologic and oncologic diseases, only three mAb therapies have been approved for bacterial infections. Raxibacumab and obiltoxaximab have been developed for inhalational anthrax (7, 8), while bezlotoxumab was recently approved for the prevention of *Clostridium difficile* infection (9). The relative paucity of mAbs for bacterial infections is especially noteworthy given the key role played by antibodies in bacterial clearance during natural infection and vaccine-induced immunity. However, the difference in the rate of increase in approved antibodies for different disease types may be partially due to the fact that the features of the underlying biology being targeted by mAbs for non-infectious diseases are very different from those in pathogenic bacteria. In the former cases, highly conserved human proteins, either cancer antigens or immune effector molecules (e.g., cytokines), are targeted. In stark contrast, antibacterial mAbs target rapidly dividing microorganisms with high genetic plasticity. Bacteria have the ability to downregulate or even completely abolish the expression of molecules containing targeted epitopes, in a process generally known as epitope masking (10). Moreover, these microorganisms can exert epitope switching since they are able to modify and tolerate severe amino acid changes in epitopes that reduce antibody affinity through recombination with externally-acquired DNA or via mutations that do not produce significant changes in virulence and fitness (11, 12). This is a consequence of confronting double Darwinian pressure in search of an equilibrium between keeping important functions for (patho)biology and the evasion of host immunity. By doing so, bacterial pathogens have evolved to avoid detection and neutralization by antibodies.

In the three aforementioned antibacterial mAbs, disease is prevented due to the neutralization of toxins via binding to highly conserved epitopes on toxin subunits. This approach is effective for anthrax and *C. difficile* infection due to the fact that these pathologies are mediated by the action of potent toxins. However, this is not the case for most bacterial pathogens, particularly for MDR-associated species. MAbs for these infections will most likely need to target epitopes present on the bacterial cell and facilitate clearance by the immune system to be effective. In this regard, bacterial epitopes that would be ideal targets for mAbs may need to meet most, if not all, of the following criteria: (a) high conservation between circulating strains, (b) expression during bacterial infection and/or colonization, (c) surface exposure in order to permit antibody binding, and (d) antigenically distinct compared to epitopes on human proteins and the normal human microbiota to prevent cross-reactivity.

The biological function of the molecule containing the targeted epitope may be of particular importance. MAbs that target epitopes on molecules that participate in essential bacterial processes for viability or virulence may be less susceptible to the generation of escape mutants, given that reduced expression or sequence variation in these molecules may be detrimental to bacterial survival. It is worth noting that MDR organisms consist of a series of interacting molecular elements, a functional network, with emergent properties only approachable as a whole by systems biology and high-throughput "omics" techniques (13). One of the emergent properties of

scale-free networks is the tolerance to failures that, in this case, means that many essential bacterial processes are subject to total or partial functional redundancy (14). Bacteria can increase fitness mainly by gathering genes that exert functions efficiently but that can be, at least partially, covered by other means. For example, 30 alternative sugar transporters (15) and seven plasminogen-binding proteins have been identified in *Streptococcus pneumoniae* (16) that ensure that these important tasks required for infection are performed under many conditions. Likewise, antigenic proteins rarely act in isolation but rather as part of functional sub-networks that exert simultaneous or sequential activities leading to colonization and/or disease (13). In this respect, epitope switching by mutation or down-regulation of a single participant targeted by mAbs in one of these pathways may not greatly affect the ability of the bacteria to replicate and produce infection if this change can be adequately compensated for elsewhere in the interactome. Thus, non-overlapping irreplaceable elements of the pathofunctional sub-networks, i.e., virulence hubs, should be prioritized. This may present particular challenges in identifying a single epitope for mAb development that is less susceptible to the generation of escape mutants.

TABLE 1 | Use of omics technologies and systems biology in antibacterial mAb development.

Technology	Use in identifying epitopes/antigens
Comparative genomics	- Identification of epitopes with highly conserved sequences - Identification of epitopes present in the majority of strains within a species - Clonal distribution of epitopes - Avoidance of cross-reaction with microbiota and human proteins
Transcriptomics	- Identification of antigens preferentially expressed during infection
Proteomics	- Identification of antigens highly expressed during infection - Identification of epitopes on the bacterial cell surface
Molecular modeling and dynamics	- Identification of surface-exposed epitopes - Assessment of the stability of surface exposure of the epitope and its binding to the antigen
Interactomics/systems biology	- Identification of optimal synergistic mixtures of epitopes (for use in developing mAb cocktails) - Identification of epitopes/antigens that participate in essential bacterial processes that involve molecular connections

USING OMICS TECHNOLOGY AND SYSTEMS BIOLOGY FOR MAB DEVELOPMENT

Omics Data and Systems Biology Basics

Although there are significant challenges to developing broadly effective mAb-based therapies for bacterial infections, it is conceivable that the availability of multiple large data sets involving genomic sequences and global profiling experiments (e.g., transcriptomics, proteomics, and interactomics; the latter defined as the global pool of physical and/or functional connections between molecules in a cell) may serve as raw material for elucidating high-value epitopes. **Table 1** lists the different omics approaches that are discussed in the sections below and how they can be employed for mAb development. Omics technologies can be considered as those that characterize molecules and their states at a holistic level through the collective characterization of molecular profiles, e.g., transcriptomics, the whole set of transcripts under defined conditions. Omics cover virtually all kinds of biological molecules, and their accumulated outcome volumes approximate to the range of big data, i.e., so massive that they are unable to be stored and managed by ordinary computer users. For instance, central repositories such as the European Bioinformatics Institute store over 160 petabytes of data (17).

While processing large biological data sets could be considered mere brute force, it is important to underscore that the data needed for translational medicine are those that contribute to achieving precise clinical goals, so-called "smart data" (18). Systems biology approaches move in that direction by permitting a more comprehensive and contextual interpretation of the information, given that they can identify not only epitopes meeting certain criteria but also the interplay between different essential criteria (19). The integration of multivariate data for rational vaccine purposes is far from trivial (20); clearly the challenge here is converting large quantities of data into information with biological value that can be used for the development of mAb therapeutics. As data volumes become larger and more varied due to the availability of multi-omics experiments, it is here that systems biology can be of great value in responding to biological problems of great complexity. Systems biology then becomes a natural analysis option that captures emergent properties of bacteria as a whole that cannot be studied by isolated reductionist protocols. The complexity of the immune response to vaccines has been monitored and analyzed through an analogous approach called systems vaccinology, a branch of systems immunology concentrated on the intrinsic responses of the host to vaccines (21). Parallels can be drawn to reverse vaccinology (RV), which employs both genomics and structural biology to reveal the fraction of the molecular space of a pathogen appropriate for vaccine development (22). It is noteworthy that RV has already yielded successes, most notably in the development of a vaccine for *Neisseria meningitidis* (23). In contrast to RV for vaccines, which can operate at the antigen level, omics and computational approaches for mAb development must be performed at the epitope level, potentially adding increased stringency and complexity to the identification process. Thus, RV is confronted with a significant challenge in the design of mAbs, and the question arises of whether such obstacles hamper knowledge-based solutions. This situation evokes the "bounded rationality" idea (24, 25), in which rational approaches are inefficient due to limited understanding of the inherent complexity of the task.

In the following sections, we assess how the availability of huge and variable data sets can be harnessed, together with systems

biology, to enhance RV when oriented to epitope selection for mAb development.

Comparative Genomics: Whole Species and Clone-Specific Epitope Conservation

A common challenge in developing immunoprotective approaches for bacterial infections is that these microorganisms exhibit a high rate of escape from vaccine formulations at the whole species level. Thus, the ideal of identifying immutable antigenic proteins as part of the core proteome of target species and absent from other species is difficult to achieve and may be confined to the aforementioned exotoxins that have already been exploited for mAb development (7–9). Nevertheless, the availability of up to thousands of draft genome sequences for the most important MDR pathogens may enable the assessment of epitope conservation at intra-clonal resolution with sufficient depth (**Figure 1A**). A plausible strategy may be to focus on the development of mAbs tailored to circulating hypervirulent and/or hyperresistant clones for which the recognized epitope is conserved. This is, for instance, the case for mAbs directed against *K. pneumoniae* O-antigen from the ST258 clone, since it is a recurrent infective lineage and a strong producer of this endotoxin (26). In addition, such clonal specificity preserves the microbiota, highlighting one of the advantages of immunological interventions with respect to antibiotics (27).

Identifying Epitopes Highly Expressed During Infection and/or Colonization

Epitopes of interest for mAb development must be expressed during the course of colonization or infection. Rather than

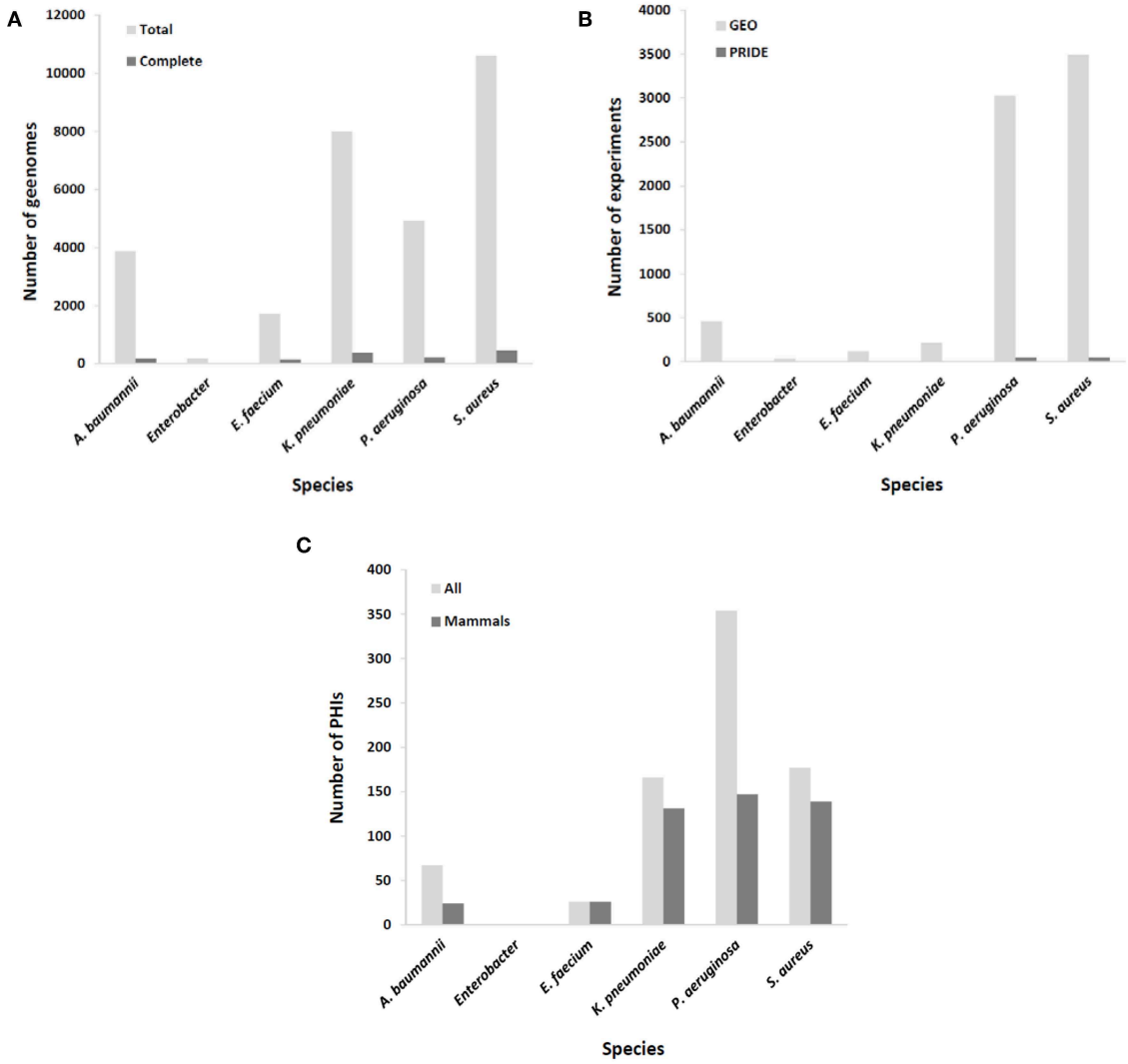

FIGURE 1 | Coverage of ESKAPE organisms by omics databases utilized in rational mAb development. **(A)** Number of available complete and draft/scaffold genomes; **(B)** number of expression experiments, either transcriptomic (GEO database) or proteomic (PRIDE database); **(C)** number of identified molecular interactions between pathogen and host (total and those involving only mammal hosts).

constitutive, the expression of many immunogenic proteins is tightly repressed in order to reduce metabolic expense and overexposure to the host immune system, unless the bacterium senses the right environmental signals for its production (28). To include this important issue in the mAb production pipeline, results from a number of transcriptomic and proteomic experiments stored in databases such as GEO and PRIDE (29), respectively, should be taken into account. MDR microorganisms are well-covered in this respect (**Figure 1B**), including the upregulation of potentially antigenic proteins for mAbs *in vivo* or under *in vitro* conditions that mimic infection, such as bacteremia (30), biofilm (sessile)-to-planktonic transition (31), and iron limitation (32).

Exposure of the Epitope

MAbs must not only fulfill the basic RV principle of being directed against surface or secreted proteins but must also be directed toward epitopes that are exposed on these proteins. This poses a problem on two levels. First, accessible—either secreted or surface—proteins can be detected by the presence of motifs and domains linked to secretion and surface anchoring, in most cases readily detectable by sensitive hidden-Markov models thanks to optimized heuristics adapted to huge protein datasets (33). However, these computational strategies cannot cope with accessible proteins lacking identifiable labels, and must therefore be complemented with experimental high-throughput protein detection on fractionated samples, including cell-free medium for the exoproteome (34) or the outer membrane (35) and cell wall (36) for the surface proteome. On the other hand, the prediction of non-linear epitopes and their location on the solvent-oriented zone of the protein is facilitated by structural information (37). Resolving a structure is labor-intensive, but the combined effort of small scientific groups and large structural genomics consortia (38) has promoted the inclusion of structural biology to the biological pool of large data volumes. The central structural repository, the Protein Data Bank (PDB), currently contains 142,433 proteins (44,971 non-redundant, last accessed: 05/Jul/2019). Likewise, the SwissModel archive reached 1.6 million pre-built structural models (39) covering 62% of *S. aureus* and 72% of *P. aeruginosa* proteins. Once reliable structural information is available for the candidate antigen, epitopes that are highly solvent-accessible can be identified. Dynamic simulations by simulator packages such as GROMACS additionally permit assessment of the dynamic stability of epitope exposure and even of mAb-protein binding when co-crystalized (40).

Design of Anti-virulence mAbs Using Functional Information

As a rational approach, functional information regarding the essentiality of a protein carrying the candidate mAb epitope or its involvement in virulence is invaluable. If these essential/virulence-associated epitopes are not targeted, there is high risk of epitope masking or switching, leading to rapid circumvention of the monoclonal therapy. Specialized resources such as PATRIC, VFDB, and Victors (41–43) compile virulence factors at the species level from dedicated research reports. Laboratory and animal-model screenings, such as signature-tagged mutagenesis (44), permit the explicit detection of potential genes essential for pathogenesis in a high-throughput manner. Such relevant information would be a promising starting point for antigen selection and prioritization to block virulence traits with mAbs in a precise knowledge-based way. Considering that most virulence factors are not essential for fundamental viability, neutralization by mAbs is akin to blocking virulence rather than the viability of the pathogen and follows the anti-virulence drug paradigm, in contrast to lethal antibiotics (45). Currently licensed mAbs that block the activity of exotoxins can be considered virulence-blocking therapies.

Interactomics

According to systems biology principles, the pathogen and host exhibit a dense network of inter-species molecular interactions throughout their relationship (46). The identification of these interactions has permitted the design of protective strategies in viruses (47). This information may be used to design mAbs that impede connections between pathogen and host molecules that are central to infection progression. A proficient resource for this information is the PHI-base database (48), but of the 12,466 interactions included (Last accessed, 5 Sep 2019), only 467 pertain to connections between the six ESKAPE bacteria and mammals, suggesting that the volume of useful information could still be increased to facilitate the prediction of network tolerance in a global manner (**Figure 1C**). A possible exception is those pathogens whose virulence is almost fully dependent upon the activity of potent exotoxins, which indicates that successful mAb strategies at present are those that circumvent the pitfall of pathogenic network tolerance.

OMICS-SYSTEMS BIOLOGY VS. OTHER STRATEGIES

A fundamental controversy may arise when systemic computational approaches in the RV framework are compared to empirical screenings (49) or the low-throughput selection of antigen/epitope targets (50) by microbiology experts. Each of these strategies has advantages and pitfalls based on their underlying assumptions (**Table 2**), but it is worth noting that the only mAb products that have been approved or are in the clinical phases of testing were developed using the latter two approaches. This may call into question the use of rational approaches based on RV strategies for identifying epitopes for mAb development. More empirical approaches may have achieved their previous successes because experimental screenings are better equipped to accommodate the degenerate and flexible nature of the immune system. Nevertheless, massive data and systemic approaches have likely not yet been successful, not because of their lack of potential, but because of the interpretation of results (51, 52). In addition, there is room for improvement for rational approaches through the collection of new data, algorithms, and paradigms, and this is a continuous process, whereas screening and expert selection are probably closer to their respective plateaus. Moreover, different methods of omics data integration

TABLE 2 | Pros and cons of systems biology/big data/reverse vaccinology approaches vs. empirical screening vs. expert selection for mAb development.

Aspects related to mAb development	Omics/systems biology	Empirical screening	Expert selection
Use for mAb cocktail development	++	−	−
Reduced cost	+	−	++
Time required	+	−	++
Focus on clinical clones	++	+	+
Requires bioinformatics expertise	−	++	++
Requires computational infrastructure	−	++	++
Requires experimental infrastructure	++	−	+
Intrinsic experimental validation	−	++	++
Rational selection	++	−	++
Resistance to "bound rationality"	−	++	+
Room for improvement	++	+	+
Scalability to many targets	++	+	−
Species completeness	++	+	+
Systemic view	++	−	−
Transferability to other species	++	−	−

++ Highly efficient.
+ Moderately efficient.
– Low efficiency.

can be developed in order to identify targets for biomedical applications (13). Conceivably, hybrid approaches that combine the strengths of all of these methods may achieve the highest performances. For instance, a list of the candidate mAb epitopes that have a complex list of features could be revealed from large data sets, verified by experts, and then refined by screenings methods.

An option that may also ease the "bound rationality" of RV is the design of mAb cocktails. The advantages of increasing valence by using mAb combinations are multiple: (1) a net increment in the success rate of neutralization of a process by reducing the network tolerance of the pathogen; (2) lower chances of future immune evasion since several concerted epitope switches are exponentially more difficult to achieve than individual ones; (3) the possibility of designing complex blocking strategies concentrated on the same (pathogen siege) or sequential (pathogen exhaustion) stages of infection, thus applying a more comprehensive molecular view of the virulent process. Knowing this, the bottleneck in mAb development against bacteria may not lie in the experimental efficiency of mAb identification but in scaling processes required for the production of a mature pharmaceutical product.

CONCLUSIONS AND FUTURE DIRECTIONS

In contrast to cancer, rheumatologic diseases, and viral infections, the limited use of mAbs for MDR bacterial pathogens may be due to several technical and biological constraints. In this context, rational approaches based on large-scale data/systems biology methodologies may facilitate the identification of high-value epitopes for mAb development, perhaps in concert with traditionally used empirical strategies. The extreme challenge associated with finding ideal, immutable epitopes may support the development of mAb cocktails. This could require improvement in the efficiency (development and scaling) of mAb production, i.e., within a reasonable timeframe and at a reasonable cost, at the service of holistic paradigms that consider the molecular pathobiology of the targeted species. We envisage that the large data/systems biology combination will find its utility in RV approaches applied to mAb development as more information is collected.

AUTHOR CONTRIBUTIONS

MM and AM-G planned the manuscript content, wrote the manuscript, and approved the final version.

FUNDING

This work was supported by grant PI18CIII/00018 from the Instituto de Salud Carlos III/Ministerio de Universidades, Ciencia e Innovación of Spain, awarded to MM. AM-G was supported by the Miguel Servet II Program of the Instituto de Salud Carlos III.

REFERENCES

1. Review on Antimicrobial Resistance. *Antimicrobial Resistance: Tackling A Crisis for the Health and Wealth of Nations*. (2014). Available online at: https://amr-review.org/sites/default/files/AMR%20Review%20Paper%20-%20Tackling%20a%20crisis%20for%20the%20health%20and%20wealth%20of%20nations_1.pdf
2. Boucher HW, Talbot GH, Bradley JS, Edwards JE, Gilbert D, Rice LB, et al. Bad bugs, no drugs: no ESKAPE! An update from the Infectious Diseases Society of America. *Clin Infect Dis*. (2009) 48:1–12. doi: 10.1086/595011
3. Avgoulea K, Di Pilato V, Zarkotou O, Sennati S, Politi L, Cannatelli A, et al. Characterization of extensively drug-resistant or pandrug-resistant sequence Type 147 and 101 OXA-48-producing *Klebsiella pneumoniae* causing bloodstream infections in patients in an intensive care unit. *Antimicrob Agents Chemother*. (2018) 62:e02457-17. doi: 10.1128/AAC.02457-17
4. Brennan-Krohn T, Kirby JE. Synergistic combinations and repurposed antibiotics active against the pandrug-resistant *Klebsiella pneumoniae* nevada strain. *Antimicrob Agents Chemother*. (2019) 63:e01374-19. doi: 10.1128/AAC.01374-19
5. Nowak J, Zander E, Stefanik D, Higgins PG, Roca I, Vila J, et al. High incidence of pandrug-resistant *Acinetobacter baumannii* isolates collected from patients with ventilator-associated pneumonia in Greece, Italy and Spain as part of the MagicBullet clinical trial. *J Antimicrob Chemother*. (2017) 72:3277–82. doi: 10.1093/jac/dkx322
6. Czaplewski L, Bax R, Clokie M, Dawson M, Fairhead H, Fischetti VA, et al. Alternatives to antibiotics-a pipeline portfolio review. *Lancet Infect Dis*. (2016) 16:239–51. doi: 10.1016/S1473-3099(15)00466-1
7. Hou AW, Morrill AM. Obiltoxaximab: adding to the treatment arsenal for bacillus anthracis infection. *Ann Pharmacother*. (2017) 51:908–13. doi: 10.1177/1060028017713029

8. Tsai CW, Morris S. Approval of raxibacumab for the treatment of inhalation anthrax under the US Food and Drug Administration "animal rule." *Front Microbiol.* (2015) 6:1320. doi: 10.3389/fmicb.2015.01320
9. Kufel WD, Devanathan AS, Marx AH, Weber DJ, Daniels LM. Bezlotoxumab: a novel agent for the prevention of recurrent clostridium difficile infection. *Pharmacotherapy.* (2017) 37:1298–308. doi: 10.1002/phar.1990
10. Zhang Q, Wise KS. Coupled phase-variable expression and epitope masking of selective surface lipoproteins increase surface phenotypic diversity in *Mycoplasma hominis*. *Infect Immun.* (2001) 69:5177–81. doi: 10.1128/IAI.69.8.5177-5181.2001
11. Georgieva M, Kagedan L, Lu YJ, Thompson CM, Lipsitch M. Antigenic variation in *Streptococcus pneumoniae* PspC promotes immune escape in the presence of variant-specific immunity. *mBio.* (2018) 9:e00264-18. doi: 10.1128/mBio.00264-18
12. Palmer GH, Bankhead T, Seifert HS. Antigenic variation in bacterial pathogens. *Microbiol Spectr.* (2016) 4. doi: 10.1128/microbiolspec.VMBF-0005-2015
13. Kim CY, Lee M, Lee K, Yoon SS, Lee I. Network-based genetic investigation of virulence-associated phenotypes in methicillin-resistant *Staphylococcus aureus*. *Sci Rep.* (2018) 8:10796. doi: 10.1038/s41598-018-29120-3
14. Albert R, Jeong H, Barabasi AL. Error and attack tolerance of complex networks. *Nature.* (2000) 406:378–82. doi: 10.1038/35019019
15. Bidossi A, Mulas L, Decorosi F, Colomba L, Ricci S, Pozzi G, et al. A functional genomics approach to establish the complement of carbohydrate transporters in *Streptococcus pneumoniae*. *PLoS ONE.* (2012) 7:e33320. doi: 10.1371/journal.pone.0033320
16. Meinel C, Sparta G, Dahse HM, Horhold F, Konig R, Westermann M, et al. *Streptococcus pneumoniae* from patients with hemolytic uremic syndrome binds human plasminogen via the surface protein PspC and uses plasmin to damage human endothelial cells. *J Infect Dis.* (2018) 217:358–70. doi: 10.1093/infdis/jix305
17. Cook CE, Lopez R, Stroe O, Cochrane G, Brooksbank C, Birney E, et al. The European Bioinformatics Institute in 2018: tools, infrastructure and training. *Nucleic Acids Res.* (2019) 47:D15–22. doi: 10.1093/nar/gky1124
18. Geerts H, Dacks PA, Devanarayan V, Haas M, Khachaturian ZS, Gordon MF, et al. Big data to smart data in Alzheimer's disease: the brain health modeling initiative to foster actionable knowledge. *Alzheimer's Dement.* (2016) 12:1014–21. doi: 10.1016/j.jalz.2016.04.008
19. Kitano, H. Systems biology: a brief overview. *Science.* (2002) 295:1662–4. doi: 10.1126/science.1069492
20. Weiner J 3rd, Kaufmann SH, Maertzdorf J. High-throughput data analysis and data integration for vaccine trials. *Vaccine.* (2015) 33:5249–55. doi: 10.1016/j.vaccine.2015.04.096
21. Pulendran B. Learning immunology from the yellow fever vaccine: innate immunity to systems vaccinology. *Nat Rev Immunol.* (2009) 9:741–7. doi: 10.1038/nri2629
22. Rappuoli R, Bottomley MJ, D'Oro U, Finco O, De Gregorio E. Reverse vaccinology 2.0: human immunology instructs vaccine antigen design. *J Exp Med.* (2016) 213:469–81. doi: 10.1084/jem.20151960
23. Parikh SR, Andrews NJ, Beebeejaun K, Campbell H, Ribeiro S, Ward C, et al. Effectiveness and impact of a reduced infant schedule of 4CMenB vaccine against group B meningococcal disease in England: a national observational cohort study. *Lancet.* (2016) 388:2775–82. doi: 10.1016/S0140-6736(16)31921-3
24. Van Regenmortel MH. Basic research in HIV vaccinology is hampered by reductionist thinking. *Front Immunol.* (2012) 3:194. doi: 10.3389/fimmu.2012.00194
25. Van Regenmortel MH. Requirements for empirical immunogenicity trials, rather than structure-based design, for developing an effective HIV vaccine. *Arch Virol.* (2012) 157:1–20. doi: 10.1007/s00705-011-1145-2
26. Szijarto V, Guachalla LM, Hartl K, Varga C, Badarau A, Mirkina I, et al. Endotoxin neutralization by an O-antigen specific monoclonal antibody: a potential novel therapeutic approach against *Klebsiella pneumoniae* ST258. *Virulence.* (2017) 8:1203–15. doi: 10.1080/21505594.2017.1279778
27. Bloom DE, Black S, Salisbury D, Rappuoli R. Antimicrobial resistance and the role of vaccines. *Proc Natl Acad Sci USA.* (2018) 115:12868–71. doi: 10.1073/pnas.1717157115
28. Delaune A, Dubrac S, Blanchet C, Poupel O, Mader U, Hiron A, et al. The WalKR system controls major staphylococcal virulence genes and is involved in triggering the host inflammatory response. *Infect Immun.* (2012) 80:3438–53. doi: 10.1128/IAI.00195-12
29. Vizcaino JA, Csordas A, del-Toro N, Dianes JA, Griss J, Lavidas I, et al. 2016 update of the PRIDE database and its related tools. *Nucleic Acids Res.* (2016) 44:D447–56. doi: 10.1093/nar/gkv1145
30. Murray GL, Tsyganov K, Kostoulias XP, Bulach DM, Powell D, Creek DJ, et al. Global gene expression profile of *Acinetobacter baumannii* during bacteremia. *J Infect Dis.* (2017) 215(Suppl_1):S52–7. doi: 10.1093/infdis/jiw529
31. Guilhen C, Charbonnel N, Parisot N, Gueguen N, Iltis A, Forestier C, et al. Transcriptional profiling of *Klebsiella pneumoniae* defines signatures for planktonic, sessile and biofilm-dispersed cells. *BMC Genom.* (2016) 17:237. doi: 10.1186/s12864-016-2557-x
32. Holden VI, Wright MS, Houle S, Collingwood A, Dozois CM, Adams MD, et al. Iron acquisition and siderophore release by carbapenem-resistant sequence type 258 *Klebsiella pneumoniae*. *mSphere.* (2018) 3:e00125-18. doi: 10.1128/mSphere.00125-18
33. Eddy SR. Accelerated profile HMM searches. *PLoS Comput Biol.* (2011) 7:e1002195. doi: 10.1371/journal.pcbi.1002195
34. Sengupta N, Alam SI, Kumar B, Kumar RB, Gautam V, Kumar S, et al. Comparative proteomic analysis of extracellular proteins of *Clostridium perfringens* type A and type C strains. *Infect Immun.* (2010) 78:3957–68. doi: 10.1128/IAI.00374-10
35. Li H, Zhang DF, Lin XM, Peng XX. Outer membrane proteomics of kanamycin-resistant *Escherichia coli* identified MipA as a novel antibiotic resistance-related protein. *FEMS Microbiol Lett.* (2015) 362:fnv074. doi: 10.1093/femsle/fnv074
36. Wang W, Jeffery CJ. An analysis of surface proteomics results reveals novel candidates for intracellular/surface moonlighting proteins in bacteria. *Mol Biosyst.* (2016) 12:1420–31. doi: 10.1039/C5MB00550G
37. Haste Andersen P, Nielsen M, Lund O. Prediction of residues in discontinuous B-cell epitopes using protein 3D structures. *Protein Sci.* (2006) 15:2558–67. doi: 10.1110/ps.062405906
38. Grabowski M, Niedzialkowska E, Zimmerman MD, Minor W. The impact of structural genomics: the first quindecennial. *J Struct Funct Genom.* (2016) 17:1–16. doi: 10.1007/s10969-016-9201-5
39. Bienert S, Waterhouse A, de Beer TA, Tauriello G, Studer G, Bordoli L, et al. The SWISS-MODEL Repository-new features and functionality. *Nucleic Acids Res.* (2017) 45:D313–9. doi: 10.1093/nar/gkw1132
40. Ebrahimi Z, Asgari S, Ahangari Cohan R, Hosseinzadeh R, Hosseinzadeh G, et al. Rational affinity enhancement of fragmented antibody by ligand-based affinity improvement approach. *Biochem Biophys Res Commun.* (2018) 506:653–9. doi: 10.1016/j.bbrc.2018.10.127
41. Liu B, Zheng D, Jin Q, Chen L, Yang J. VFDB 2019: a comparative pathogenomic platform with an interactive web interface. *Nucleic Acids Res.* (2019) 47:D687–92. doi: 10.1093/nar/gky1080
42. Mao C, Abraham D, Wattam AR, Wilson MJ, Shukla M, Yoo HS, et al. Curation, integration and visualization of bacterial virulence factors in PATRIC. *Bioinformatics.* (2015) 31:252–8. doi: 10.1093/bioinformatics/btu631
43. Sayers S, Li L, Ong E, Deng S, Fu G, Lin Y, et al. Victors: a web-based knowledge base of virulence factors in human and animal pathogens. *Nucleic Acids Res.* (2019) 47:D693–700. doi: 10.1093/nar/gky999
44. Hensel M, Shea JE, Gleeson C, Jones MD, Dalton E, Holden DW. Simultaneous identification of bacterial virulence genes by negative selection. *Science.* (1995) 269:400–3. doi: 10.1126/science.7618105
45. Rasko DA, Sperandio V. Anti-virulence strategies to combat bacteria-mediated disease. *Nat Rev Drug Discov.* (2010) 9:117–28. doi: 10.1038/nrd3013
46. Sen R, Nayak L, De RK. A review on host-pathogen interactions: classification and prediction. *Eur J Clin Microbiol Infect Dis.* (2016) 35:1581–99. doi: 10.1007/s10096-016-2716-7
47. Rahim MN, Klewes L, Zahedi-Amiri A, Mai S, Coombs KM. Global interactomics connect nuclear mitotic apparatus protein NUMA1 to influenza virus maturation. *Viruses.* (2018) 10:731. doi: 10.3390/v10120731
48. Urban M, Cuzick A, Rutherford K, Irvine A, Pedro H, Pant R, et al. PHI-base: a new interface and further additions for the multi-species pathogen-host interactions database. *Nucleic Acids Res.* (2017) 45:D604–10. doi: 10.1093/nar/gkw1089

49. Rossmann FS, Laverde D, Kropec A, Romero-Saavedra F, Meyer-Buehn M, Huebner J. Isolation of highly active monoclonal antibodies against multiresistant gram-positive bacteria. *PLoS ONE.* (2015) 10:e0118405. doi: 10.1371/journal.pone.0118405
50. DiGiandomenico A, Keller AE, Gao C, Rainey GJ, Warrener P, Camara MM, et al. A multifunctional bispecific antibody protects against *Pseudomonas aeruginosa*. *Sci Transl Med.* (2014) 6:262ra155. doi: 10.1126/scitranslmed.3009655
51. Davis MM, Tato CM. Will systems biology deliver its promise and contribute to the development of new or improved vaccines? seeing the forest rather than a few trees. *Cold Spring Harbor Perspect Biol.* (2018) 10:a028886. doi: 10.1101/cshperspect.a028886
52. Van Regenmortel MH. Structure-based reverse vaccinology failed in the case of HIV because it disregarded accepted immunological theory. *Int J Mol Sci.* (2016) 17:E1591. doi: 10.3390/ijms17091591

Conflict of Interest: MM is a founding partner and shareholder in Vaxdyn, a biotechnology spin-off company developing vaccines and antibody-based therapies for antibiotic resistant infections caused by antibiotic resistant bacteria.

The remaining author declares that the research was conducted in the absence of any commercial or financial relationships that could be construed as a potential conflict of interest.

frontiers in Immunology

ORIGINAL RESEARCH
published: 12 December 2019
doi: 10.3389/fimmu.2019.02920

Selective Engagement of FcγRIV by a M2e-Specific Single Domain Antibody Construct Protects Against Influenza A Virus Infection

Dorien De Vlieger[1,2,3], *Katja Hoffmann*[4], *Inge Van Molle*[5,6], *Wim Nerinckx*[1,3], *Lien Van Hoecke*[1,2], *Marlies Ballegeer*[1,2,3], *Sarah Creytens*[1,2,3], *Han Remaut*[5,6], *Hartmut Hengel*[4], *Bert Schepens*[1,2]* *and Xavier Saelens*[1,2,3]*

[1] VIB-UGent Center for Medical Biotechnology, VIB, Ghent, Belgium, [2] Department of Biomedical Molecular Biology, Ghent University, Ghent, Belgium, [3] Department of Biochemistry and Microbiology, Ghent University, Ghent, Belgium, [4] Institute of Virology, Medical Center, Faculty of Medicine, University of Freiburg, Freiburg, Germany, [5] Structural Biology Brussels, Vrije Universiteit Brussel, Brussels, Belgium, [6] VIB-VUB Center for Structural Biology, Brussels, Belgium

Lower respiratory tract infections, such as infections caused by influenza A viruses, are a constant threat for public health. Antivirals are indispensable to control disease caused by epidemic as well as pandemic influenza A. We developed a novel anti-influenza A virus approach based on an engineered single-domain antibody (VHH) construct that can selectively recruit innate immune cells to the sites of virus replication. This protective construct comprises two VHHs. One VHH binds with nanomolar affinity to the conserved influenza A matrix protein 2 (M2) ectodomain (M2e). Co-crystal structure analysis revealed that the complementarity determining regions 2 and 3 of this VHH embrace M2e. The second selected VHH specifically binds to the mouse Fcγ Receptor IV (FcγRIV) and was genetically fused to the M2e-specific VHH, which resulted in a bi-specific VHH-based construct that could be efficiently expressed in *Pichia pastoris*. In the presence of M2 expressing or influenza A virus-infected target cells, this single domain antibody construct selectively activated the mouse FcγRIV. Moreover, intranasal delivery of this bispecific FcγRIV-engaging VHH construct protected wild type but not *FcγRIV*$^{-/-}$ mice against challenge with an H3N2 influenza virus. These results provide proof of concept that VHHs directed against a surface exposed viral antigen can be readily armed with effector functions that trigger protective antiviral activity beyond direct virus neutralization.

Keywords: influenza, matrix protein 2 ectodomain, single domain antibody, Fcγ receptor, effector functions

OPEN ACCESS

Edited by:
Giuseppe Andrea Sautto, University of Georgia, United States

Reviewed by:
Peter Palese, Icahn School of Medicine at Mount Sinai, United States
Gene Tan, J. Craig Venter Institute, United States

***Correspondence:**
Bert Schepens
bert.schepens@vib-ugent.be
Xavier Saelens
xavier.saelens@vib-ugent.be

Specialty section:
This article was submitted to Vaccines and Molecular Therapeutics, a section of the journal Frontiers in Immunology

Received: *16 September 2019*
Accepted: *27 November 2019*
Published: *12 December 2019*

Citation:
De Vlieger D, Hoffmann K, Van Molle I, Nerinckx W, Van Hoecke L, Ballegeer M, Creytens S, Remaut H, Hengel H, Schepens B and Saelens X (2019) Selective Engagement of FcγRIV by a M2e-Specific Single Domain Antibody Construct Protects Against Influenza A Virus Infection. Front. Immunol. 10:2920. doi: 10.3389/fimmu.2019.02920

INTRODUCTION

Influenza A virus infections are a major recurrent cause of seasonal respiratory tract infections. The best way to prevent influenza disease is considered to be vaccination. However due to the accumulation of point mutations in the viral hemagglutinin (HA) and neuraminidase (NA) genes, human influenza vaccines need to be reformulated and administered regularly based on the prediction of the circulating strains (1). The variable effectiveness and the long manufacturing timeline encourage the development of more broadly protective vaccines. Antivirals, such as oseltamivir and baloxavir marboxil, have been licensed for the prophylaxis and treatment of uncomplicated influenza, but the risk of selecting drug resistant viruses limits their widespread use (2, 3).

The 23 amino acid residues long M2 ectodomain (M2e) is highly conserved among the different influenza A virus subtypes and thus represents an attractive target for broadly protective prophylactic vaccine strategies as well as for antibody-based antiviral biologicals [reviewed in Saelens (4)] (4, 5). Various studies using different vaccine formats have demonstrated that M2e-based vaccination can provide broad protection in animal models of influenza A and that this protection is antibody mediated (6–9). Next to vaccines, a therapeutic intervention with an intravenously administered recombinant human IgG1 monoclonal antibody directed against the M2 N-terminus was found to reduce the symptoms in human volunteers that had been infected with an H3N2 virus (10). Furthermore, this phase 2a trial showed that the antibody treatment was associated with a trend toward reduced viral shedding from the nasal mucosa, and no anti-M2e escape mutants could be detected. Finally, intravenous administration of engineered, so called bi-specific T cell engagers that comprise a M2e-specific single chain variable fragment that is linked to a CD3ε-specific single chain variable fragment, could protect mice against an otherwise lethal influenza A virus challenge (11).

Fc gamma receptor (FcγR) interactions are essential for the protective activity of M2e-specific antibodies (12–14). FcγRs are type I membrane proteins that are expressed on different innate immune cells, including macrophages, neutrophils, natural killer cells and dendritic cells (15, 16). In mice, FcγRs are characterized by the presence of an immunoreceptor tyrosine-based activation motif (ITAM) in the cytoplasmic portion of the common γ chain that is associated with the activating FcγRI, FcγRIII and FcγRIV, or by an immunoreceptor tyrosine-based inhibition motif (ITIM) in the cytoplasmic portion of the inhibitory FcγRIIb (17–19). These receptors differ in their affinities for the different IgG isotypes (16, 20). Previously, we have shown that protection by M2e-specific mouse IgG1 requires FcγRIII while IgG2a isotypes can protect by any of the three activating FcγRs (13).

Since the reported discovery of heavy chain-only antibodies in camelids in 1993, recombinant single domain proteins comprising the variable domain of these antibodies (VHHs also known as Nanobodies®) have been used in numerous therapeutic applications (21). In the context of viral infections, various virus-neutralizing VHHs have been described that can interfere with different steps in the viral life cycle (22). Due to their outstanding stability and solubility, as well as their small size (∼15 kDa), ease of production and formatting flexibility, they are highly versatile building blocks for the development of new antivirals. Next to a direct antiviral effect, VHHs can also easily be formatted (e.g., by generating Fc fusions) to recruit host effector functions (23). These features, combined with the possibility to deliver therapeutic VHHs into the lung environment, and maintained stability after prolonged storage, make VHH-based anti-influenza biologicals especially attractive for epidemic as well as pandemic preparedness plans (24–27).

In this study we explored a new strategy to engage host cell effector functions to combat influenza A. This strategy is based on a tail-to-head genetic fusion of two VHHs, one that selectively binds to FcγRIV and a second one that is specific for M2e. The resulting bi-specific construct can be efficiently expressed in *Pichia pastoris* cells and protects mice against an otherwise lethal influenza A virus infection by simple intranasal delivery.

MATERIALS AND METHODS

Cell Lines and Culture Conditions

HEK293T cells (a gift from Dr M. Hall, University of Birmingham, Birmingham, UK) and HEK293T cells stably transfected with influenza M2 (28) were cultured in Dulbecco's modified Eagle's medium supplemented with 10% of fetal calf serum, 2 mM of L-glutamine, 0.4 mM of Na-pyruvate, non-essential amino acids, 100 U/ml of penicillin and 10 μM amantadine for the M2 expressing HEK cells. Madin-Darby canine kidney (MDCK) cells were cultured in Dulbecco's modified Eagle's medium supplemented with 10% of fetal calf serum, 2 mM of L-glutamine, non-essential amino acids and 100 U/ml of penicillin. Mf4/4 cells (an immortalized cell line of spleen macrophages derived from C57BL/6 mice) were grown in RPMI 1640 medium, supplemented with 10% of fetal calf serum, 2 mM of L-glutamine, 0.4 mM of Na-pyruvate, non-essential amino acids, 50 mM 2-mercaptoethanol, 25 mM Hepes and 100 U/ml of penicillin (29). Cloning of Fc***γ***R-ζ constructs, the generation of Fc***γ***R-ζ BW5147 reporter cells and the culture conditions were similar as reported previously (30, 31).

Production of Recombinant Mouse FcγRIV Protein

Recombinant FcγRIV protein was produced by transient transfection of subconfluently grown FreesStyle™293-F cells (ThermoFisher scientific) with pCAGGs expression vectors encoding the ectodomain of FcγRIV (amino acids 1-201) coupled to a C-terminal 6XHis tag. Recombinant FcγRIV protein was purified from the supernatant 6 days after transfection, using a 1 ml HisTrap HP column (GE Healthcare). Fractions containing FcγRIV protein were pooled and concentrated with a Vivaspin column (5 kDa cutoff, GE Healthcare) and then further purified by gel filtration on a Superdex 75 column. Fractions containing FcγRIV protein were pooled and concentrated. Purity was evaluated by SDS-PAGE followed by Coomassie blue staining.

Isolation of M2e-Binding, VHH-Displaying Phages

A llama was immunized 6 times at weekly intervals subcutaneously with 150 μg M2e-tGCN4 (28) in the presence of Gerbu LQ#3000 adjuvant. Immunizations and handling of the llama were performed according to directive 2010/63/EU of the European parliament for the protection of animals used for scientific purposes and approved by the Ethical Committee for Animal Experiments of the Vrije Universiteit Brussel (permit No. 13-601-1). Five days after the last immunization, blood was collected and lymphocytes were prepared. Total RNA was extracted and used as template for the first strand cDNA synthesis with oligodT primer. The VHH encoding sequences were amplified from the cDNA and cloned into the *Pst*I and *Not*I sites of the phagemid vector pMECS. In this vector, the VHH coding sequence is followed by a linker, an HA- and 6xHis tag (AAAYPYDVPDYGSHHHHHH).

Electro-competent *E.coli* TG1 cells were transformed with the recombinant pMECS vector resulting in a VHH library of about 10^8 independent transformants. A library of VHH-presenting phages was obtained after infection with VCS M13 helper phages. Two different panning strategies were used. In the first strategy, phages were added to 20 μg of immobilized M2e-tGCN4 in panning round 1 and 20 μg of human H3N2 peptide (SLLTEVETPIRNEWGCRCNDSSD) in panning round 2. In the second strategy, phages were first added to 25×10^6 HEK293T cells to deplete potential binders to determinants on these cells. The unbound phages were next added to 25×10^6 HEK293T cells stably transfected with influenza M2, to enrich for M2-specific phages. To avoid internalization of the target antigen, all steps were performed at 4°C. After washing, retained phages were eluted by pH elution with TEA-solution (14% triethylamine (Sigma) pH 10) for 10 min. A solution of 1 M Tris-HCl pH 8 was used to lower the pH of the eluted phage solution. The enrichment relative to panning on the negative control antigen, was determined by infecting TG1 cells with 10-fold serial dilutions of the phages after which the bacteria were plated on LB agar plates with 100 μg/ml ampicillin and 1% glucose.

Isolation of FcγRIV-Binding, VHH-Displaying Phages

The FcγRIV specific VHHs were isolated form a library that was part of a study described elsewhere by Deschacht et al. (32). In brief, a llama was immunized six times at weekly intervals with 10^8 immature murine bone marrow-derived dendritic cells. A library of VHH-presenting phages was obtained as described above. FcγRIV specific VHHs were enriched after three panning rounds on 20 μg of immobilized FcγRIV protein.

Periplasmic ELISA Screen to Identify M2e- and FcγRIV-Specific VHHs

After panning, individual pMEC colonies were randomly selected for further analysis by ELISA for the presence of M2e- and FcγRIV-specific VHHs in their periplasm. To prepare periplasmic extract, individual colonies were inoculated in 2 ml of terrific broth (TB) medium with 100 μg/ml ampicillin in 24-well deep well plates. After 5 h incubation isopropyl β-D-1-thiogalactopyranoside (IPTG) (1 mM) was added to induce VHH expression. After overnight incubation at 37°C, bacterial cells were pelleted and resuspended in 200 μl TES buffer (0.2 M Tris-HCl pH 8, 0.5 mM EDTA, 0.5 M sucrose) and incubated at 4°C for 30 min. An osmotic shock was induced by adding 300 μl of water. After 1 h incubation at 4°C followed by centrifugation, the periplasmic extract was collected. VHH-containing periplasmic extracts were then tested for binding to either M2e-tGCN4 (28), human H3N2 M2e peptide (SLLTEVETPIRNEWGCRCNDSSD) or recombinant mouse FcγRIV protein. Briefly, wells of microtiter plates were coated overnight with either 100 ng M2e-tGCN4, 100 ng mouse FcγRIV protein, bovine serum albumin (BSA, Sigma-Aldrich) at 4°C or 100 ng human H3N2 M2e peptide at 37°C. The coated plates were blocked with 5% milk powder in phosphate buffered saline (PBS) and 100 μl of the periplasmic extract was added to the wells. Bound VHHs were detected with anti-HA mAb (1/2000, MMS-101P Biolegend) followed by horseradish peroxidase (HRP)-linked anti-mouse IgG (1/2000, NXA931, GE Healthcare). All periplasmic fractions, which resulted in OD_{450} values of the antigen coated wells that were at least two times higher than the OD_{450} values obtained in BSA coated wells, were selected. DNA of the selected colonies was isolated using the QIAprep Spin Miniprep kit (Qiagen) and sequenced using the primer MP057(5′-TTATGCTTCCGGCTCGTATG-3′).

VHH Expression in *Pichia pastoris*

The VHH encoding sequence was amplified by PCR using the following forward and reverse primer (5′-GGC GGG TAT CTC TCG AGA AAA GGC AGG TGC AGC TGC AGG AGT CTG GG-3′) and (5′- CTA ACT AGT CTA GTG ATG GTG ATG GTG GTG GCT GGA GAC GGT GAC CT GG-3′). The PCR fragments were then cloned between the *Xho*I and *Spe*I sites in the pKai61 expression vector [described by Schoonooghe et al. (33)]. In the vector, the VHHs sequences containing a C-terminal 6XHis tag sequence are under control of the methanol inducible AOX1 promotor and in frame with a modified version of the *S. cerevisiae* α-mating factor prepro signal sequence. The vector contains a Zeocine resistance marker for selection in bacteria as well as in yeast cells. The vectors were linearized by *Pme*I and transformed in the *P. pastoris* strain GS115 using the condensed transformation protocol described by Lin-Cereghino et al. (34) After transformation, the yeast cells were plated on YPD plates (1% (w/v) yeast extract, 2% (w/v) peptone, 2% (w/v) dextrose, and 2% (w/v) agar) supplemented with zeocin (100 μg/ml) for selection.

VHH Production and Purification

The transformed *P. pastoris* clones were first analyzed for VHH expression in 2 ml cultures. On day one, 2–5 clones of each construct were inoculated in 2 ml of YPNG medium (2% pepton, 1% Bacto yeast extract, 1.34% YNB, 0.1 M potassium phosphate pH 6, 1% glycerol) with 100 μg/ml Zeocin (Life Technologies) and incubated at 28°C for 24 h. The next day, the cells were pelleted by centrifugation and the medium was replaced by YPNM medium (2% pepton, 1% Bacto yeast extract, 1.34% YNB, 0.1 M potassium phosphate pH 6.0, 1% methanol). Cultures were incubated at 28°C and 50 μl of 50% methanol was added at 16, 24, and 40 h. After 48 h, the supernatant was collected and the presence of soluble VHHs in the supernatant was verified using SDS-PAGE and subsequent Coomassie Blue staining. Production was scaled up (300 ml) for the transformants with the highest levels of VHH in the medium. Growth and methanol induction conditions and harvesting of medium were similar as mentioned above for the 2 ml cultures. The secreted VHHs in the medium were precipitated by ammonium sulfate $(NH_4)_2SO_4$ precipitation (80% saturation) for 4 h at 4°C. The insoluble fraction was pelleted by centrifugation at 20,000 g and resuspended in 10 ml binding buffer (20 mM NaH_2PO_4 pH 7.5, 0.5M NaCl and 20 mM imidazole pH 7.4). The VHHs were purified from the solution using a 1 ml HisTrap HP column (GE Healthcare). Bound VHHs were eluted with a linear imidazole

gradient starting from 20 mM and ending at 500 mM imidazole in binding buffer over a total volume of 20 ml. VHH containing fractions were pooled and concentrated with a Vivaspin column (5 kDa cutoff, GE Healthcare) and then further purified by gel filtration (Superdex 75) in PBS buffer. Fractions containing VHH were again pooled and concentrated. Purity was evaluated by SDS-PAGE followed by Coomassie blue staining.

Enzyme-Linked Immunosorbent Assay

Wells of microtiter plates were coated overnight with either 100 ng M2e-tGCN4, 100 ng BM2e-tGCN4, 100 ng M2e peptide or 100 ng mouse FcγRIV protein. The coated plates were blocked with 5% milk powder in phosphate buffered saline (PBS) and dilution series of the VHHs were added to the wells. In the M2e ELISA, bound VHHs were detected with mouse anti-Histidine Tag antibody (MCA1396, Abd Serotec) followed by horseradish peroxidase (HRP)-linked anti-mouse IgG (1/2000, NXA931, GE Healthcare). In the ELISA with coated recombinant FcγRIV protein, binding was detected with a HRP conjugated rabbit anti-camelid VHH antibody (A01861-200, GenScript). After washing 50 μl of TMB substrate (Tetramethylbenzidine, BD OptETA) was added to every well. The reaction was stopped by addition of 50 μl of 1M H_2SO_4, after which the absorbance at 450 nM was measured with an iMark Microplate Absorbance Reader (Bio Rad).

Crystallization of M2e-VHH-23m in Complex With M2e Peptide

For crystallization, the purified M2e-VHH-23m was concentrated to 20 mg/ml. The M2e peptide was added in a 1.2 times excess. Crystallization screens were set up in sitting drop vapor diffusion at 20°C. Crystals grown in the Jenna Classic screen, in 30% ethanol, 10% PEG6000, 100 mM Na acetate were cryoprotected using fluorosilicone and flash frozen in liquid nitrogen. X-ray data were collected at the i03 beamline of the Diamond Light Source synchrotron facility and processed using XDS.[47]

The structure of the M2e-VHH-23m-M2e peptide complex was solved using the structure of another nanobody (PDB code 5HGG) as search model for molecular replacement, using the Phaser program from the CCP4 crystallographic software suite (35, 36). The M2e-VHH-23m model was built automatically using Autobuild from the Phenix crystallographic software suite (37). The initial model was further built manually in Coot and refined using phenix.refine and Refmac (38–40). Data collection parameters, as well as processing and refinement statistics are shown in **Table 1**. The crystal structure has been deposited in the Protein Data Bank (PDB) and is available with accession code 6S0Y.

TABLE 1 | Data collection statistics and refinement parameters.

Data collection	
Synchrotron	Diamond Light Source
Beamline	i03
Wavelength, Å	0.97965
Data processing	
Space group	P 21 21 2
Cell parameters, Å ($\alpha=\beta=\gamma=90°$)	57.47 94.76 53.06
Resolution, Å (outer shell) [(c)]	53.06–1.80 (1.83–1.80)
Total reflections	35827 (17918)
No. of unique reflections	27557 (1359)
Completeness	99.97 (100)
Multiplicity	13.0 (13.2)
R_{pim}, %	4.4 (66.6)
$CC_{1/2}$, %	99.8 (57.1)
$<I/\sigma(I)>$	11.0 (1.1)
Mosaicity, °	0.063°
Refinement	
Resolution range, Å	47.38–1.81
No. of reflections	25859
Percentage observed	99.96
R_{cryst},[(a)] %	18.69
R_{free},[(b)] %	22.53
RMS	
Bonds, Å	0.01
Angles, °	1.66
Ramachandran Plot	
Most favored, %	95.28
Additionally allowed, %	4.72
Disallowed, %	0
PDB code	6S0Y

[(a)] *$R_{cryst} = \Sigma(|F_{obs}|-|F_{calc}|)/\Sigma|F_{obs}|$, F_{obs} and F_{calc} are observed and calculated structure factor amplitudes.*
[(b)] *R_{free} as for R_{cryst} using a random subset of the data excluded from the refinement.*
[(c)] *Data in brackets are for the highest resolution shell.*

Docking

All water molecules, the ligand, and chain B of the nanobody crystal structure were manually deleted from the pdb-text file. The emptied structure was subjected to a local minimization with the GROMOS96 (43B1 parameter set) implementation within Swiss-PdbViewer 4.1.0 (41), and polar hydrogens were added. The peptide-ligand VETPIRNEWG was 3D-drawn with Avogadro 1.2.0 (42) and minimized with the built-in united force field. The AutoDockTools 1.5.6 suite (43) was used for pdbqt-format conversions and grid-box determination. The grid-box size was x = 22, y = 30 and z = 20 centered at x = 1.9, y = 9.7 and z = 8.3. Docking was performed with Smina (44, 45) with exhaustiveness set at 128. Visualization was with PyMOL 2.3.0 (46).

Isothermal Titration Calorimetry

M2e-VHH-23m was dialyzed overnight against PBS buffer and concentrated using Amicon Ultra 3 kDa cut off centrifugal filter devices. The M2e peptide was resuspended in PBS at a stock concentration of 3 mM, and diluted in PBS to 300 μM. Titrations comprised 26 × 1.5 μL injections of peptide (300 μM) into the protein (30 μM), with 90 s intervals. An initial injection of ligand (0.5 μL) was made and discarded during data analysis. The data were fitted to a single binding site model using the Microcal LLC ITC_{200} Origin software provided by the manufacturer.

Ala Scan Mutagenesis

HEK293T cells were transiently transfected with Flag-tagged M2 wild type (WT) and M2e Ala scan mutants. 24 h after infection the cells were detached, washed and blocked. Cells were stained with 20 μg/ml M2e VHH-23m or 20 μg/ml F-VHH-4 and subsequently fixed with 2% paraformaldehyde. After permeabilization (10× permeabilization buffer diluted in double-distilled water; eBioscience), cells were stained with mouse anti-Histidine tag antibody (MCA1396, Abd Serotec) and rabbit anti-Flag tag antibody (F7425, Sigma-Aldrich). Binding of the primary antibodies was revealed with donkey anti-mouse IgG coupled to Alexa Fluor 647 (1/600; Invitrogen) and donkey anti-rabbit IgG coupled to Alexa Fluor 488 (1/600; Invitrogen). The median fluorescence intensity (MFI) of the cells was determined with an LSRII HTS flow cytometer (BD) and was calculated by subtracting the median fluorescence of binding of M2e-VHH-23m or F-VHH-4 to transfected cells from the median fluorescence of untransfected cells bound by M2e-VHH-23m or F-VHH-4.

VHH Binding to Influenza A Virus Infected Cells

HEK293T cells were mock-infected or infected with A/Puerto Rico/8/1934 (H1N1), A/X47 (H3N2), A/Udorn/307/1972 (H3N2) or A/Swine/Ontario (H3N3) at a MOI of 1. Twenty-four hours after infection the cells were detached, washed and blocked. Cells were stained with 20 μg/ml M2e VHH-23m, 20 μg/ml F-VHH-4 or 10 μg/ml MAb148. To determine the affinity of M2e-VHH-23m on infected cells, 1/3 dilution series of M2e-VHH-23m or F-VHH4 were applied to A/Puerto Rico/8/1934 (H1N1) infected cells. Subsequently, the cells were fixed with 2% paraformaldehyde and stained with mouse anti-Histidine Tag antibody (MCA1396, Abd Serotec) and goat anti-A/Puerto Rico/8/1934 serum (Biodefense and Emerging Infections Resources Repository, NIAID, NIH, V314-511-157) followed by anti-mouse IgG Alexa 488 (Invitrogen) and anti-goat IgG Alexa 647 (Invitrogen). The median fluorescence intensity (MFI) was measured on the LSRII-tubes flow cytometer (BD) and was calculated by subtracting the median fluorescence of binding of M2e-VHH-23m or F-VHH-4 to infected cells from the median fluorescence of uninfected cells bound by M2e-VHH-23m or F-VHH-4.

Plaque Reduction Assay

Different amounts of M2e-VHH-23m (2.5 μM, 1.25 μM or 0.625 μM), 0.333 μM MAb37 or sera of mice infected with A/Puerto Rico/8/1934 (H1N1) virus were incubated for 1 h at 4°C with 10–20 plaque forming units/well of A/Udorn/307/1972 (H3N2) or A/Puerto Rico/8/1934 (H1N1) virus. After incubation, the mixture was added to MDCK cells, seeded in a flat bottom 24-well plate. After 1 h, the cells were overlaid with an equal volume of 1.2% Avicel RC-591 (FMC Biopolymer) supplemented with 2 μg/ml of TPCK-treated trypsin (Sigma). Infection was allowed for 2 days at 37°C in 5% CO_2. The overlay was subsequently removed and the cells were fixed with 4% paraformaldehyde. Viral plaques were stained with convalescent mouse anti- A/Puerto Rico/8/34 or A/Udorn/307/72 serum followed by horseradish peroxidase (HRP)-linked anti-mouse IgG (NXA931, GE Healthcare). Finally, after washing, the plaques were visualized with TrueBlue peroxidase substrate (KPL, Gaithersburg).

VHH Binding to FcγRs Expressing Cells

Human Embryonic Kidney (HEK) 293T cells were transiently transfected with full length mouse FcγRI (MG50086-CF), FcγRIIb (MG50030-CY, SinoBiological Inc.), FcγRIII (MG50326, SinoBiological Inc.) or FcγRIV (MG50036-CF, SinoBiological Inc.) expression constructs along with the common γ-chain for the activating FcγRs (MG50935-CF) by polyethylenimine (PEI)-based transfection. A GFP-reporter plasmid was co-transfected. FcγRIV-VHH-7m and M2e-VHH-23m were directly labeled with the Alexa Fluor™ 647 antibody labeling kit (A20186, ThermoFisher scientific). Of the labeled VHHs, 0.2 μM or ¼ serial dilution series of the VHHs starting from 0.2 μM were added to the transfected cells or Mf4/4 cells (29). Fluorescence was measured on an LSRII flow cytometer (BD). The median fluorescence intensity (MFI) was calculated by subtracting the median fluorescence of binding of M2e-VHH-23m or FcγRIV-VHH-7m to transfected cells from the median fluorescence of untransfected cells bound by M2e-VHH-23m orFcγRIV-VHH-7m.

Construction of Bispecific VHHs

To construct FcγRIV VHH-M2e VHH, FcγRIV VHH-F VHH, and FcγRIIIa VHH-M2e VHH bispecific VHHs, we made use of a GoldenBraid-based cloning strategy (47). The coding information of FcγRIV-VHH-7m or FcγRIIIa VHH [C28 sdAb, described by Behar et al. (48)] was amplified with the following forward (5′- GCG ATG CAG GGT CTC ACT TCA AGG CAG GTG CAG CTG CAG GAG TC-3′) and reverse primer (5′ GGC GAT GGT GGG TCT CAC TTC ATG AGG AGA CGG TGA CCT GGG-3′) that add specific overhangs for their identity as N-terminal VHH together with a *Bsa*I and *Sap*I restriction site. The C-terminal VHHs, M2e-VHH-23m and F-VHH-4 were amplified with a forward (5′-GCG CGA TGC AGG GTC TCA CTT CAC AGG TGC AGC TGC AGG AG TC-3′) and reverse primer (5′-GGG CGA TGG TGG GTC TCA CTT CAA GTC TAG TGA TGG TGA TGG TGG TGG CTG GAG ACG GTG ACC TG GG-3′) that add specific overhangs for their identity as C-terminal VHH together with a *Bsa*I and *Sap*I restriction site. The 15 amino acid long $(Gly_4Ser)_3$ linker was generated with the following forward (5′- GCG ATG CAG GGT CTC ACT TCA TCA GGC GGA GGC GGT AGT GGC GGA GGT GGA TCT GGA GGC GGC GGT AGT CA GT-3′) and reverse primer (5′-GGC GAT GGT GGG TCT CAC TTC ACT GAC TAC CGC CGC CTC CAG ATC CAC CTC CGC CAC TAC CGC CTC CGC CTG AT-3′) that also add a specific overhang together with a *Bsa*I and *Sap*I restriction site. The PCR amplified fragments were each assembled in a pUPD2 entry vector by a *Bsa*I restriction and ligation reaction. Once stored in the pUPD2 vector, the different parts were assembled together in the pKai61 expression vector using a T4 DNA ligase and a *Sap*I restriction enzyme which recognizes the *Sap*I restriction site which was introduced after ligation into the pUPD2 vector.

In vitro FcγR Activation Assay

FcγR activation by MAbs 37 and 65 as well as by different M2e-specific nanobodies was determined using an *in vitro* FcγR activation assay (13, 30, 31). Cloning of FcγR-ζ constructs and the generation of FcγR-ζ BW5147 reporter cells were performed as reported previously (30, 31). Activation of stably transduced FcγR-ζ BW5147 reporter cells by immune complexes results in the production of mouse interleukin-2 (mIL-2), which was quantified by ELISA (30, 31).

HEK293T cells that were stably transfected with an M2 expression vector (28) were cultured in the presence of 10 μM amantadine. The cells were seeded 1 day before the co-culture experiment in 96-well flat-bottom plates, pre-coated with fibronectin purified from human plasma (4 μg/ml diluted in PBS). The next day, serial dilutions of the respective MAbs or VHH fusion constructs (concentrations as indicated ranging from 4 to 0.0625 μg/ml) were added to the HEK293T-M2 and incubated for 30 min at 37°C, followed by the addition of 1.5×10^5 FcγR-ζ BW5147 reporter cells in a total volume of 200 μl RPMI1640 medium with 10% fetal calf serum per well. Target cells and reporter cells were incubated overnight at 37°C in a 5% CO_2 atmosphere to allow mIL-2 production. Supernatants were analyzed by an anti-mIL-2 sandwich ELISA as described using the capture MAb JES6-1A12 and the biotinylated detection MAb JES6-5H4 (BD Pharmingen™, Belgium) (30, 31).

For infection with influenza A/Puerto Rico/8/1934 virus, Madin-Darby canine kidney (MDCK) cells were seeded in 96-well flat-bottom plates and infected with influenza PR8 virus (multiplicity of infection [MOI], 5). After 1 h of incubation at 37°C, unbound virus particles were removed by washing, and serial dilutions of the respective MAbs or VHHs (concentrations ranging from 4 to 0.0625 μg/ml) were added and incubated for 30 min at 37°C, followed by the addition of 1.5×10^5 FcγR-ζ BW5147 reporter cells in a total volume of 200 μl RPMI1640 medium with 10% fetal calf serum per well. Target cells and reporter cells were incubated overnight at 37°C in a 5% CO_2 atmosphere to allow mIL-2 production. Supernatants were analyzed by an anti-IL-2 sandwich ELISA as described (30, 31). If not indicated otherwise, experiments were performed in triplicates.

Challenge Experiments in Mice

All experiments were approved by and performed according to the guidelines of the animal ethical committee of Ghent University (Ethical applications EC2017-66 and EC2018-12). Female BALB/c mice and male and female C57BL/6 mice were purchased from Charles River (France) and *Fcγ RIV*$^{-/-}$ C57BL/6 mice (49) were bred in-house under specified-pathogen-free conditions. Mice were used at age 6–12 weeks and were SPF-housed with food and water *ad libitum*. Mice were anesthetized with isoflurane for treatment and infection. The mice were treated 4 h before and 24 h after influenza A virus challenge by intranasal administration of 50 μg of the bispecific VHHs in a volume of 50 μl PBS. Mice were challenged with $2xLD_{50}$ of A/X47 (H3N2) influenza virus. Body weight loss was monitored for 14 days. To determine the lung viral titer, complete lungs were harvested on day 6 after infection and homogenized in 1 ml of PBS with a sterile metal bead on the Mixer Mill MM 200 (Retsch). After clearance by centrifugation at 4°C, the lung homogenates were used for virus titration by plaque assay. The plaque assay was performed as described before, plaques were stained using convalescent mouse anti-X47 serum followed by horseradish peroxidase (HRP)-linked anti-mouse IgG (NXA931, GE Healthcare).

Statistical Analysis

Statistical comparison of the differences in body weight loss was analyzed as repeated measurements data using the residual maximum likelihood (REML) as implemented in Genstat v19. Briefly, a linear mixed model (random terms underlined) of the form $y = \mu + \text{experiment} + \text{treatment} + \text{time} + \text{treatment.time} + \text{mouse.time}$ was fitted to the longitudinal data. The term mouse.time represents the residual error term with dependent errors because the repeated measurements are taken in the same individual, causing correlations among observations. Times of measurement were set as equally spaced, and the autoregressive model of order 1 was selected as the best correlation model based on the Aikake Information Coefficient. Significances of treatment effects across time (i.e., treatment.time) and of pairwise differences between treatment effects across time were assessed by an approximate *F*-test, of which the denominator degrees of freedom were calculated using algebraic derivatives as implemented in Genstat v19.

Survival analysis was performed on the right-censored survival data obtained for the five treatment groups. Groups were compared using the nonparametric log-rank test as implemented in Genstat v19. The two independent experiments were set as different groupings for a stratified test.

For the statistical analysis of the differences in lung viral titers a Hierarchical Generalized Linear Mixed Model (HGLMM; fixed model: poisson distribution, log link; random model: gamma distribution, log link) as implemented in Genstat v19 (see ref below), was fitted to the titer data. Treatment, having five levels, was set as fixed term, while replicate was set as random term. T statistics were used to assess the significance of treatment differences compared with the FcγRIV VHH-F VHH set as reference level (on the log-transformed scale). Estimated mean values and standard errors were obtained as predictions from the HGLMM, formed on the original scale of the response variable.

Conservation of the M2 Ectodomain Sequences in Human H3N2 Influenza A Viruses

All complete M2 protein sequences of human H2N2 viruses, human H3N2 viruses and human H1N1 influenza A viruses circulating between 1933 and 2008 were extracted from the Influenza Research Database (http://www.fludb.org/) on 3th May 2019.

RESULTS

Isolation of M2e-Specific VHHs

To generate M2e-specific VHHs a llama was immunized repeatedly with M2e-tGCN4 protein, a soluble recombinant

immunogen that mimics the natural tetrameric M2e conformation, that was previously shown to induce protective M2e-specific IgG antibodies in mice (28, 50). Five days after the last immunization, peripheral blood lymphocytes were isolated from the llama and an immune VHH phagemid library of about 10^8 clones was generated. M2e-specific VHHs were enriched from this library by sequential panning on immobilized M2e-tGCN4 (round 1) and M2e peptide (SLLTEVETPIRNEWGCRCNDSSD, corresponding to M2e of human H3N2 viruses) (round 2). As a second strategy, M2e-specific VHHs were enriched by panning on HEK293T cells that stably express M2. Individual phagemid clones enriched after both panning strategies were randomly selected and tested for binding to M2e-tGCN4 and M2e peptide in ELISA. Sequence analysis of the VHH encoding clones which tested positive for binding to either M2e-tGCN4 or M2e peptide revealed a low sequence diversity. Two clones (M2e-VHH-23m and M2e-VHH-66m) isolated with the first, and one clone (M2e-VHH-10m) isolated with the second panning strategy, were selected for further characterization. These VHHs had a cysteine residue at position 50 in the CDR2 and position 100b in the CDR3 (Kabat numbering), allowing the formation of an additional stabilizing disulfide bound, and were devoid of N-glycosylation sequons (**Figure 1A**) (51). The M2e-specific VHHs and an irrelevant control F-VHH-4 directed against the F protein of human respiratory syncytial virus, were subsequently expressed in *Pichia pastoris* in a secreted format (52). After purification from the yeast medium, the epitope specificity was assessed by ELISA. M2e-VHH-23m and M2e-VHH-66m bound to M2e-tGCN4 with a relatively high affinity, whereas M2e-VHH-10m displayed weaker binding (**Figure 1B**). None of the VHHs bound to purified recombinant influenza B M2 ectodomain fused to tGCN4, suggesting that the VHHs bind to M2e. The three selected VHHs bound to immobilized M2e-peptide in ELISA. Amino-acid residues 10 to 23 of M2(e) display some sequence diversity (50). We therefore tested binding of the VHHs to peptide variants that correspond to M2e from A/Brevig Mission/1918 (H1N1), A/Hong Kong/485/1997 (H5N1) and A/swine/Belgium/1/1998 (H1N1) (**Figure 1B**). None of the purified VHHs bound to these M2e peptides, whereas a control mouse monoclonal antibody (MAb148) that is specific for the extremely conserved amino-terminus of M2 (SLLTEVET) did bind (**Figure 1B**). This indicates that the isolated VHHs can bind to M2 expressed by human H2N2, the majority of human H3N2 strains and the majority of human H1N1 viruses circulating between 1933 and 2008 but are unlikely to recognize M2 of currently circulating human H1N1 viruses or most avian and swine influenza viruses. Remarkably, the isolated VHHs also failed to bind the H1N1 A/Brevig Mission/1/1918 M2e, which suggests that Ile11 in M2e contributes substantially to binding. We selected M2e-VHH-23m to target M2e in the subsequent experiments.

M2e-Specific VHH Clamps M2e Peptide Between Its CDR2 and CDR3

We performed isothermal titration calorimetry (ITC) experiments to determine the binding affinity of M2e-VHH-23m to the human H3N2 M2e peptide. The data revealed a 1:1 biomolecular association between the VHH and the M2e peptide with a K_d value of 730 nM (**Figure 2**). The affinity of the single domain M2e-VHH-23m is thus over a 1,000-fold lower than the previously reported affinities for the M2e-specific mouse monoclonal antibodies MAb65 and MAb37 (13).

To precisely resolve the epitope of M2e-VHH-23m, we determined the crystal structure of this VHH in complex with human H3N2 M2e peptide to 1.81 Å resolution (**Table 1**, PDB code 6S0Y). M2e-VHH-23m binds the M2e N-terminus as a linear epitope (**Figure 3A**, left panel). In the crystal structure, one M2e peptide interacts with three adjacent M2e-VHH-23m molecules at three respective interfaces (**Figure S1**). M2e residues E6 to N13 bind in a shallow groove formed by CDR3, CDR2 and the main body of the VHH formed by β-strands C, C', C", and F (Interface 1; **Figure 3A**). As expected, based on the VHH sequence data, a stabilizing disulfide bridge is observed between the CDR3 and CDR2 (**Figure 3A**). Interface 1 includes hydrogen bonds between the M2e-VHH-23m residues Arg45-Gln46-Gly47 and M2e residues Glu8 and Thr9, M2e-VHH-23m residue Cys100b and M2e residue Ile11, and M2e-VHH-23m residue Glu100 and M2e residues Arg12 and Asn13. In addition, three hydrophobic contacts are formed: (1) M2e residue Val7 binds a shallow pocket lined by residue Phe37, Val100f and Trp103, (2) Pro10 stacks against Tyr100d, and (3) the side chain of M2e residue IIe11 is inserted in a pocket formed by the side chain of IIe58 of the VHH CDR2, and the backbones of Tyr59 (CDR2), Gly47, Val48 and Ser49 (CDR3). De bottom of the latter pocket is formed by the stabilizing disulfide bridge between Cys50 in CDR2 and Cys100b in CDR3 (**Figure 3A**). In interface 2, M2e residues 14 to 19 lie on a surface formed by CDR2 and CDR3. The highly conserved M2e Trp15 side chain is inserted in a deep pocket formed by residues from the 3 CDRs: the side chains of Ile58 and Tyr97, and backbones of Ile51, Gly56, Thr57, Asn98, Val99, and Gly100a. In addition, the imidazole NH of Trp15 is hydrogen bonded to the backbone of Asn98 (Interface 2, **Figure 3B**).

In the crystals, the M2e peptide contacts three adjacent molecules in an interaction reminiscent of domain swapping (53). Closer inspection indeed suggests that ligand swapping occurs between the M2e peptides bound to symmetry related molecules in the crystal (**Figure S2**). Docking experiments using the VETPIRNEWG M2e peptide show that the Interface 1 and 2 regions of the M2e peptide (residues 6–12 and 14–19, respectively) can bind a single M2e-VHH-23m molecule (**Figure 3C**). This is also supported by ITC experiments indicating that in solution M2e-VHH-23m and M2e interact in a 1:1 stoichiometry (**Figure 2**). To validate the relative importance of the two binding interfaces in this interaction, we additionally tested the binding of M2e-VHH-23m to HEK293T cells expressing M2 protein or M2e Ala-mutants by flow cytometry (**Figure 3D**). M2e-VHH-23m did not bind to cell that were transfected with an M2Ile11Ala or M2Trp15Ala expression construct, confirming the involvement of interface 1 and 2 in the interaction with M2e. These findings are also in line with the observation that M2e-VHH-23m fails to bind the H1N1 A/Brevig Mission/1/1918 M2e peptide, which carries a serine instead of an isoleucine residue at position 11 (**Figure 1B**). Reduced binding to cells expressing M2Val7Ala also concurs

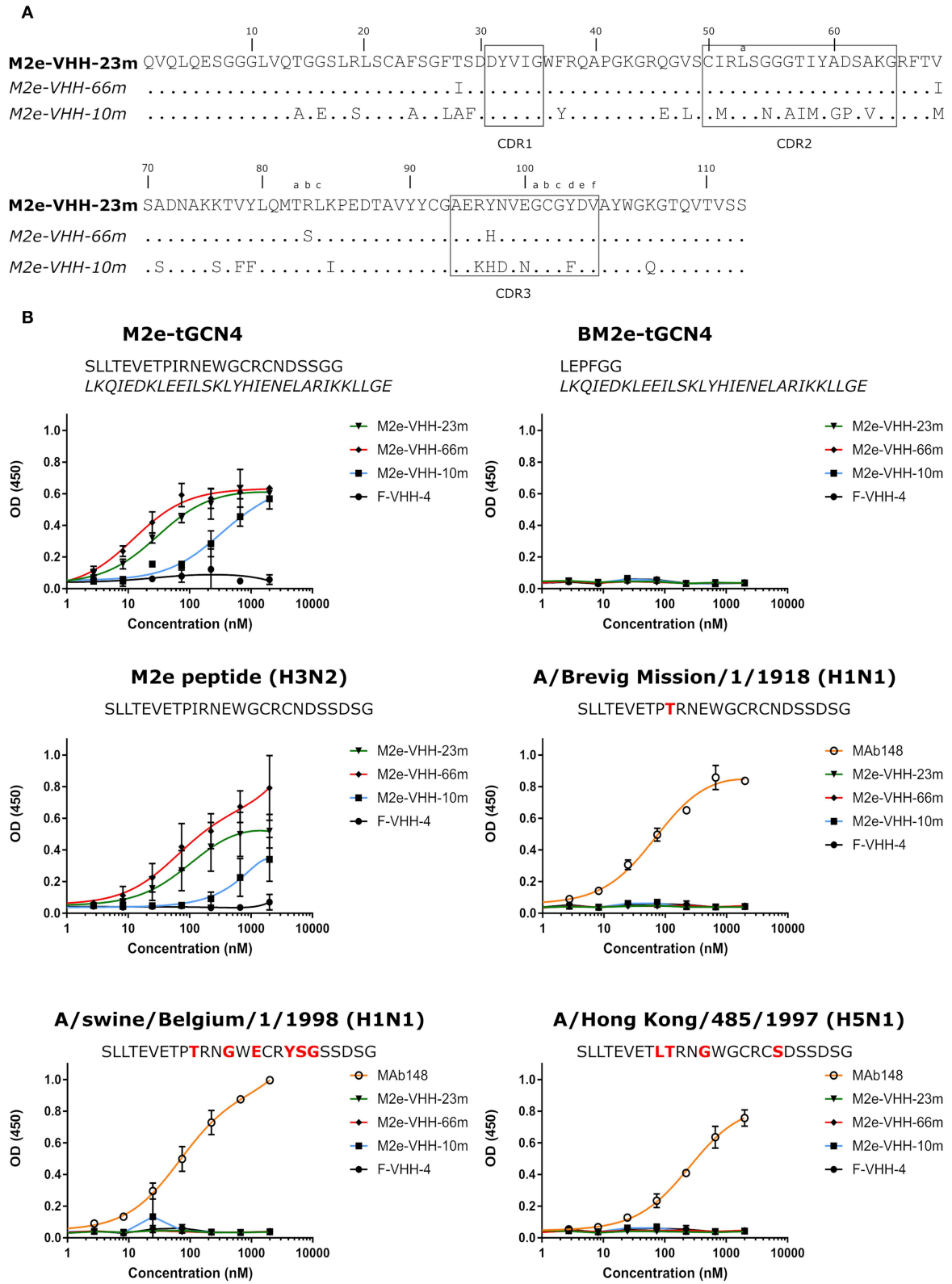

FIGURE 1 | M2e-specific VHHs and their binding specificities. **(A)** Predicted amino acid residue sequences of M2e-VHH-23m and M2e-VHH-66m (isolated after panning on M2e-tGCN4 and human H3N2 M2e peptide) and M2e-VHH-10m (isolated after panning on HEK cells stably expressing M2). Above the sequences the

(Continued)

FIGURE 1 | Kabat numbering is indicated. The complementarity determining regions (CDR) are boxed. **(B)** M2e peptide ELISAs. Wells of microtiter plates were coated with 100 ng M2e-tGCN4, BM2e-tGCN4, or high-performance liquid chromatography (HPLC)-purified M2e peptide. The amino acid residue sequences of the coated proteins or peptides are depicted above the graphs. Amino acid residues that deviate from the consensus human H3N2 M2e sequence are highlighted in red. Dilution series of the indicated VHHs and MAb148 (a mouse monoclonal IgG1 that recognizes the M2e N-terminus) were added to the coated plates. Binding was detected with a mouse anti-His tag MAb, followed by a secondary sheep anti-mouse IgG Ab conjugated to horseradish peroxidase (HRP). Data points represent averages of triplicates and error bars represent standard deviations.

with the co-crystal structure data which show an interaction of M2eVal7 with a shallow hydrophobic pocket on the surface of M1e- VHH-23m (**Figure 3A**).

M2e-VHH-23m Binds to Infected Cells and Does Not Neutralize Influenza A Virus

Next we used flow cytometry to determine if M2e-VHH-m23 could bind to M2e in its natural context, on the surface of influenza A virus infected cells. HEK293T cells were infected with A/Puerto Rico/8/1934 (H1N1) (M2e: SLLTEVETPIRNEWGCRCNGSSD), A/X47 (H3N2) (M2e: SLLTEVETPIRNEWGCRCNDSSD) or A/Udorn/307/1972 (H3N2) (M2e: SLLTEVETPIRNEWGCRCNDSSD) and were subsequently immuno-stained with MAb148, M2e-VHH-23m or F-VHH-4. M2e-VHH-23m could bind to the surface of cells infected with either of the three viruses with a K_d of 13.63 nM for influenza A/Puerto Rico/8/1934 (H1N1) infected cells (**Figure 4A**). In contrast, and as expected, M2e-VHH-23m failed to bind to cells infected with A/Swine/Ontario/42729A/2001 (H3N3) (M2e: SLLTEVETPTRNGWECRCSDSSD) virus. These data confirm that M2e-VHH-23m can bind to M2e sequences that are similar to the H3N2 M2e consensus sequence, recognizes the central part of such M2e sequences and that at least the aspartic acid to glycine substitution at position 21 in A/Puerto Rico/8/1934 M2 is not essential for binding.

It is known that some anti-M2e antibodies can restrict the *in vitro* replication of certain influenza A virus strains such as A/Udorn/307/1972 and A/Hong Kong/8/1968 but not other viruses such as A/Puerto Rico/8/1934 and A/WSN/1933 *in vitro* (54, 55). To address this issue, M2e-VHH-23m or MAb37, a M2e-specific IgG1 antibody with *in vitro* neutralizing activity against A/Udorn/307/1972, were mixed with 10–20 plaque forming units (pfu) of A/Puerto Rico/8/1934 or A/Udorn/307/1972 before infection of MDCK cells (56). As expected, both the plaque size and number of A/Udorn/307/1972, but not of A/Puerto Rico/8/1934 were reduced in the presence of MAb37 (**Figure 4B**). However, unlike MAb37, and even at a concentration of 2.5 μM (30 μg/ml), M2e-VHH-23m did not affect the number and size of A/Udorn/307/1972 plaques (**Figure 4B**).

Isolation of FcγRIV-Specific VHHs

Our next aim was to arm M2e-VHH-23m with a second VHH that targets one of the activating FcγRs such as FcγRIV. We focused on this activating FcγR because of its restricted expression on macrophages, monocytes, neutrophils and dendritic cells but no other myeloid cell population, and because of its very high affinity for IgG2a monoclonal antibodies, which contribute the most protection by non-neutralizing influenza antibodies in the mouse model (13, 20).

To isolate FcγRIV-specific VHHs a phage library obtained from a llama that had been immunized with immature mouse dendritic cells (described by Deschacht *et al.*) was enriched for candidate FcγRIV-specific phagemid clones by three panning rounds using immobilized recombinant mouse FcγRIV extracellular domain protein produced in HEK293T cells (32). Of these candidates, FcγRIV-VHH-7m was selected after a subsequent ELISA screen using the FcγRIV antigen (**Figure 5A**). The binding specificity of purified FcγRIV-VHH-7m was analyzed by flow cytometry using HEK-293 cells that were transiently transfected with GFP and expression vectors coding for mouse FcγRI, FcγRIII or FcγRIV together with a plasmid coding for the common γ-chain, or with an expression vector coding for the inhibitory FcγRIIb. Concentration-dependent binding to cells transfected with the mouse FcγRIV plus the common γ chain was clearly detected (**Figure 5B**). Only at the highest concentration tested, FcγRIV-VHH-7m weakly bound to HEK293T cells that expressed mouse FcγRI, FcγRIIb or FcγRIII (**Figure 5B**). Expression of the FcγRs on the surface of the HEK293T cells was verified by staining with an antibody directed against the tag attached to the FcγRs (**Figure S4**). Clear expression of the mouse FcγRI, FcγRIII and FcγRIV was detected. Expression of the mouse FcγRIIb was less evident, therefore no firm conclusions about the binding of FcγRIV-VHH-7m to the mouse FcγRIIb could be deduced. To evaluate that FcγRIV-VHH-7m was able to bind to cells that express endogenous levels of the mouse FcγRIV, we tested its binding to Mf4/4 cells, a mouse macrophage like cell line (29). Unlike M2e-VHH-M2e, FcγRIV-VHH-7m bound Mf4/4 cells with a deduced K_d value comparable to the K_d value for binding to FcγRIV transfected cells (**Figure 5B**).

Tail-to-Head Fused FcγRIV- and M2e-Specific VHHs Selectively and M2-Dependently Activate FcγRIV

To evaluate the possibility to arm the M2e-specifc VHH with FcγRIV-dependent effector functions, we genetically fused M2e-VHH-23m carboxy-terminal of FcγRIV-VHH-7m by means of a flexible 15 amino acid long $(Gly_4Ser)_3$ linker. As controls M2e-VHH-23m was also fused to a VHH directed against human FcγRIIIa [described by Behar et al. (48)] and FcγRIV-VHH-7m was linked to F-VHH4. The resulting constructs were named FcγRIV VHH-M2e VHH, FcγRIIIa VHH-M2e VHH, and FcγRIV VHH-F VHH, respectively, and were produced in transformed *Pichia pastoris* shake flask cultures (**Figure 6A**). FcγRIV VHH-M2e VHH could bind to M2e peptide and coated soluble FcγRIV protein in ELISA (**Figure 6A**). Next, we evaluated the potency of the bispecific constructs to activate individual

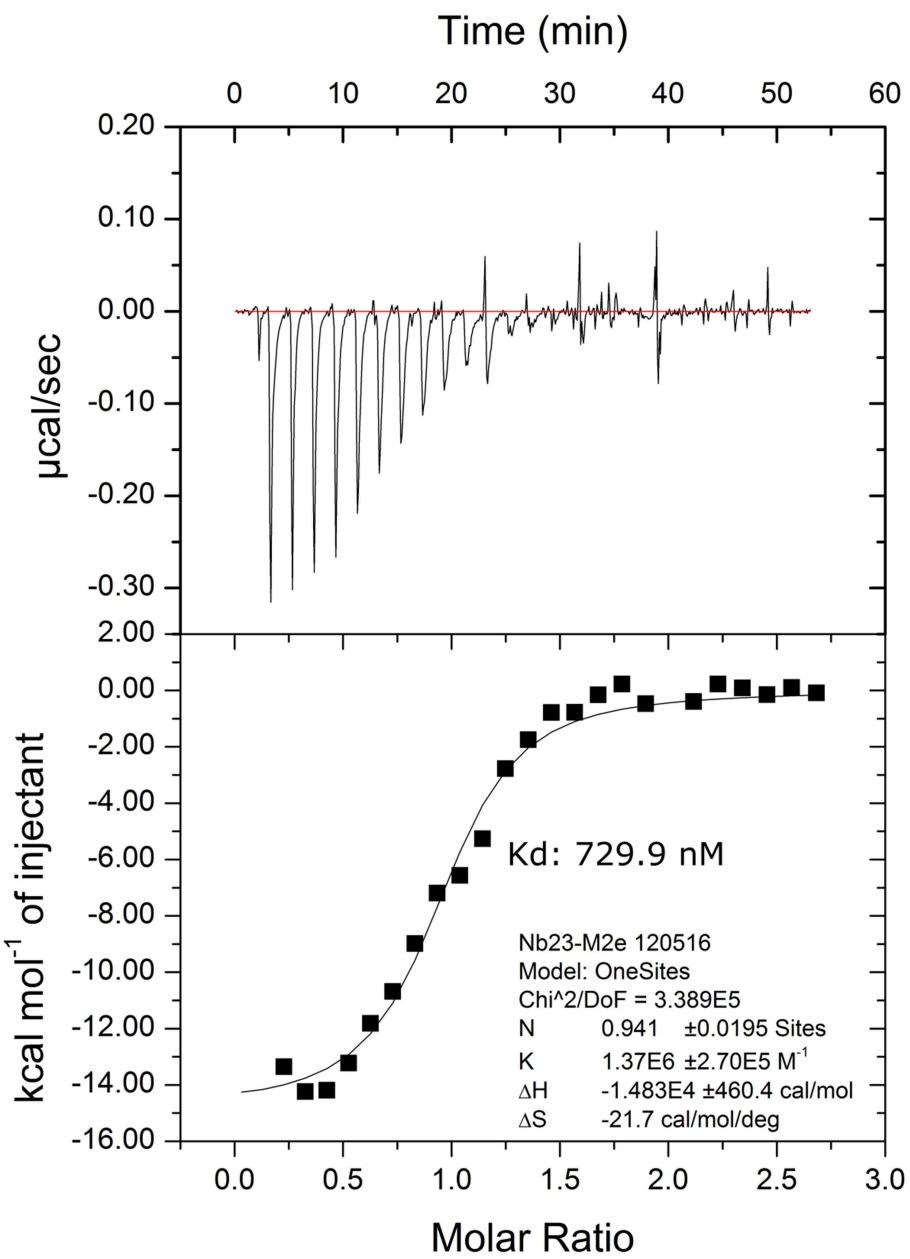

FIGURE 2 | Thermodynamic characterization of the M2e:M2e-VHH-23m interaction. Isothermal titration calorimetry of the Me peptide into M2e-VHH-23m.

FcγRs *in vitro*, by making use of a co-culture of M2-expressing cells and a set of reporter cell transfectants, which produce interleukin 2 upon the activation of a specific FcγR (**Figure 6B**) (30). As controls for FcγR activation, we used mouse M2e-specific MAb 37 (IgG1) and MAb 65 (IgG2a). In the presence of M2-expressing HEK293T cells, MAb 65 dose-dependently activated all mouse FcγRs. This is expected as mouse IgG2a antibodies can bind and activate all mouse FcγRs (16). Only mouse FcγRIIb and -RIII were activated by MAb37, again in line with the known binding specificity of mouse IgG1 antibodies for mouse FcγRs (15). In the presence of M2-expressing cells FcγRIV VHH-M2eVHH potently activated mouse FcγRIV but

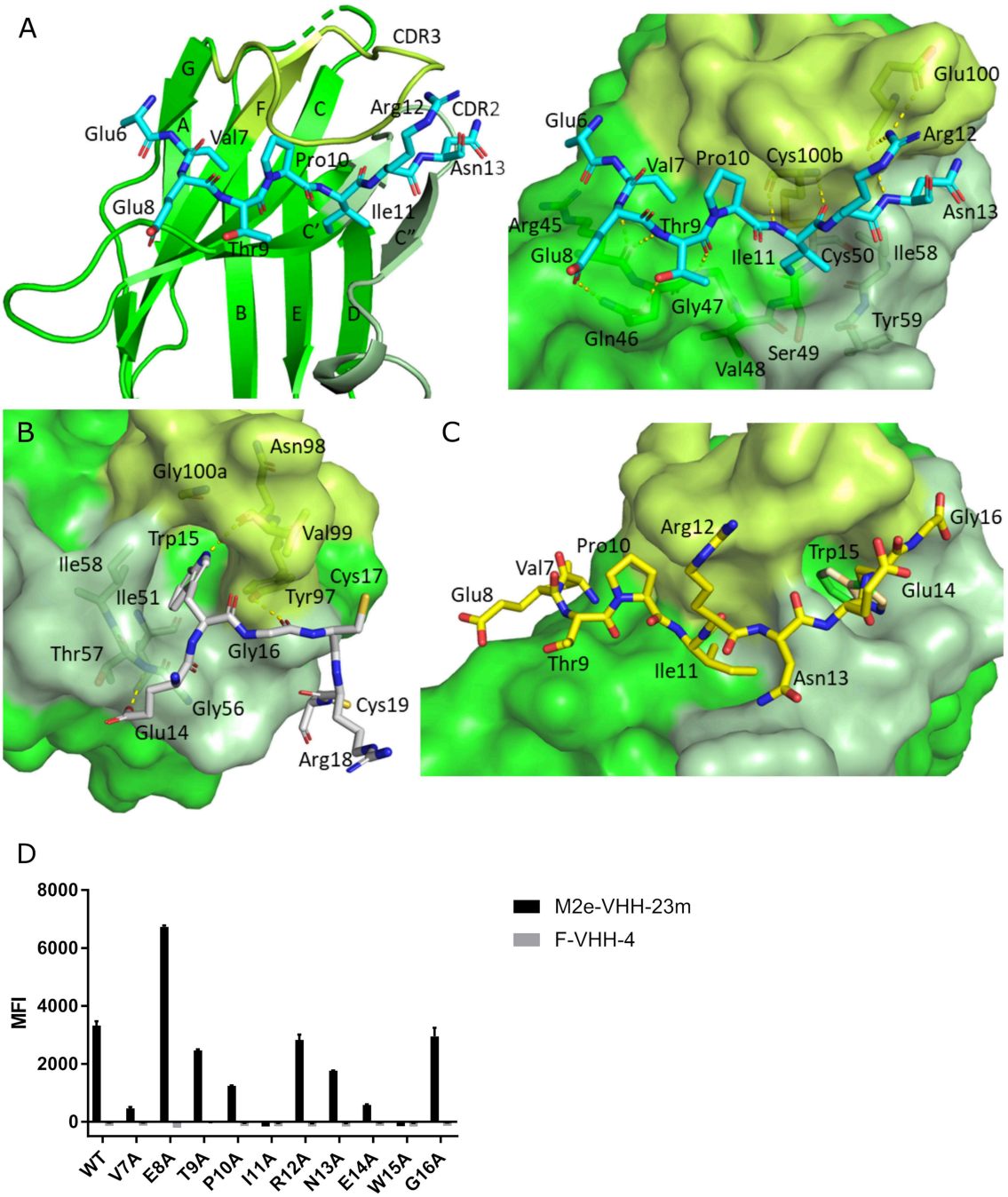

FIGURE 3 | Molecular details of the M2e-VHH-23m: M2e interaction**. (A)** Crystal structure of M2e-VHH-23m in complex with the M2e peptide, showing the linear binding epitope of M2e residues 6–13 binding to a shallow groove on the surface of M2e-VHH-23m (Interface 1). Left: The M2e peptide is shown in cyan stick representation, the M2e-VHH-23m in green cartoon representation. CDR2 and CDR3 are colored pale and lime green, respectively. Right: Details of the interactions between M2e residues 6–13 and the residues making up interface 1 on M2e-VHH-23m. **(B)** Details of the interactions between M2e residues 14–19 and the residues making up interface 2 on M2e-VHH-23m. Coloring of M2e-VHH-23m as in A, M2e shown in gray stick representation. **(C)** Docking of the M2e peptide on the crystal structure of M2e-VHH-23m confirms the ligand swapping hypothesis, showing that M2e binds an extended grove on M2e-VHH-23m comprising both Interface 1 and Interface 2. Coloring of M2e-VHH-23m as in A, M2e shown in yellow stick representation. **(D)** Binding of M2e-VHH-23m to M2e Ala scan mutants. HEK293T cells were transfected with Flag-tagged M2 wild type (WT) and M2e Ala scan mutant expression constructs and subsequently incubated with 20 μg/ml of M2e-VHH-23m or F-VHH-4. After fixation with 2% paraformaldehyde and permeabilization, binding was detected with a mouse anti-Histidine tag antibody and rabbit anti-Fag tag antibody followed by an anti-mouse IgG Alexa 647 and anti-rabbit IgG Alexa 488, respectively. The median fluorescence intensity (MFI) was calculated by subtracting the median fluorescence of binding of M2e-VHH-23m or F-VHH-4 to transfected cells from the median fluorescence of non-transfected cells bound by M2e-VHH-23m or F-VHH-4.

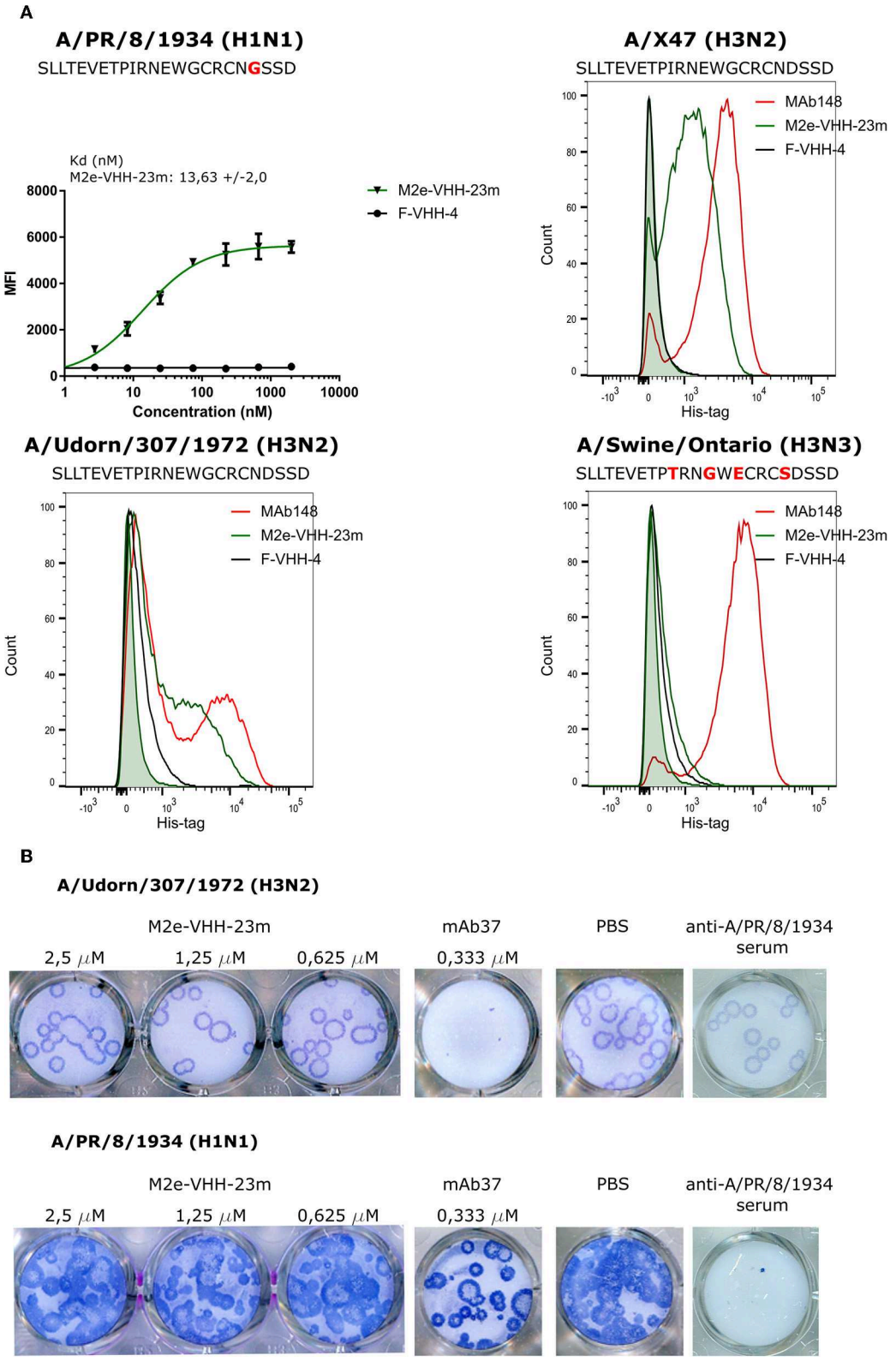

FIGURE 4 | M2e-VHH-23m bind infected cells and lacks *in vitro* antiviral activity. **(A)** HEK293T cells were infected with A/Puerto Rico/8/1934 (H1N1), A/X47 (H3N2), A/Udorn/307/1972 (H3N2) or A/Swine/Ontario (H3N3) virus. The M2e sequences of the different viruses are shown above each graph, residues that differ from the

(Continued)

FIGURE 4 | consensus human H3N2 M2e sequence are colored red. Twenty-four hours after infection, the cells were stained with 20 μg/ml M2e VHH-23m, 20 μg/ml F-VHH-4 or 10 μg/ml MAb148. The A/Puerto Rico/8/1934 (H1N1) infected cells were stained with 1/3 dilution series of M2e-VHH-23m or F-VHH-4. After fixation with 2% paraformaldehyde, infected cells were stained with goat anti-A/Puerto Rico/8/1934 serum followed by anti-goat IgG Alexa 647 and bound VHHs were detected with a mouse anti-Histidine tag antibody followed by anti-mouse IgG Alexa 488. The mean fluorescence intensity (MFI) was calculated by subtracting the median fluorescence of binding of M2e-VHH-23m or F-VHH-4 to infected cells from the median fluorescence of uninfected cells bound by M2e-VHH-23m or F-VHH-4. Data points represent averages of triplicates and error bars represent standard deviations. Results of a representative of 3 repeat experiments is depicted for the binding to the A/Puerto Rico/8/1934 (H1N1) infected cells, the dissociation constant (Kd), is the average of three independent experiments together with the standard deviation. The green shading in the histograms corresponds to the binding of M2e-VHH-23m to mock-infected HEK cells. **(B)** M2e-VHH-23m (2.5, 1.25, or 0.625 μM), 0.333 μM MAb37 or sera of mice infected with A/Puerto Rico/8/1934 (H1N1) virus were incubated with 10 to 20 plaque forming units/well of A/Udorn/307/1972 (H3N2) or A/Puerto Rico/8/1934 (H1N1) virus and then added to MDCK cells. After 1 h, the cells were overlaid with Avicel supplemented with TPCK-treated trypsin. The overlay was removed after 2 days, cells were fixed with paraformaldehyde and viral plaques were stained with convalescent mouse anti- A/Puerto Rico/8/1934 or A/Udorn/307/1972 serum followed by HRP-linked anti-mouse IgG (NXA931, GE Healthcare) and TrueBleu substrate.

not FcγRI, -III, and -IIb. None of the control VHH fusion constructs activated any of the FcγRs, indicating that specificity for both M2e and FcγRIV of the VHH fusion constructs was required. Moreover, activation of the mouse FcγRIV reporter cells by FcγRIV VHH-M2eVHH was only observed in the presence of M2 expressing target cells (**Figure S5**). Potent and dose-dependent activation of mouse FcγRIV by the FcγRIV VHH-M2e VHH fusion was also observed when A/Puerto Rico/8/1934 infected MDCK cells were used as target cells (**Figure 6C**). Finally, FcγRIIIa VHH-M2e VHH, but not FcγRIV VHH-M2eVHH, activated the human FcγRIIIa, the ortholog of mouse FcγRIV, in the presence of A/Puerto Rico/8/1934 infected targeted cells (**Figure 6D**). We conclude that the tail-to-head fusion of the FcγRIV- with the M2e-specific VHHs allows selective, M2-dependent *in vitro* activation of the mouse FcγRIV.

Intranasal Administration of Bispecific FcγRIV VHH-M2e VHH Protects Mice From a Potentially Lethal Influenza A Virus Challenge

In a final set of experiments, we explored the protective potential of FcγRIV VHH-M2e VHH *in vivo*. SPF-housed female BALB/c mice were treated intranasally with 50 μg FcγRIV VHH-M2e VHH 4 h before and 24 h after challenge with $2xLD_{50}$ of A/X47 (H3N2) influenza virus. As controls, mice were treated with PBS, 50 μg of FcγRIIIa VHH-M2e VHH or FcγRIV VHH-F VHH. The mice that had been treated with FcγRIV VHH-M2e VHH were significantly better protected from body weight loss and lethality caused by the influenza virus infection compared, to mice that had been treated with the negative control VHH fusion constructs, which combine targeting of FcγRIIIa with M2e-specificity or targeting of RSV-F with FcγRIII-specificity (**Figure 7A**). In addition, the protection mediated by FcγRIV VHH-M2e VHH was associated with a modest but statistically significant reduction in lung viral titer (**Figure 7B**). To verify if the protection by FcγRIV VHH-M2e VHH was mediated by FcγRIV engagement, wild-type and $Fc\gamma RIV^{-/-}$ C57BL/6 mice were intranasally treated with 50 μg FcγRIV VHH-M2e VHH or FcγRIIIa VHH-M2e VHH, as negative control, 4 h before and 24 h after challenge with $2xLD_{50}$ of A/X47 (H3N2) influenza virus. While treatment with FcγRIV VHH-M2e VHH could protect wild-type mice, $Fc\gamma RIV^{-/-}$ mice and control-treated wild-type mice did not survive the virus challenge (**Figure 7C**). Moreover, body weight loss after challenge was statistically significantly reduced in FcγRIV VHH-M2e VHH treated wild-type mice, compared to $Fc\gamma RIV^{-/-}$ mice ($p < 0.001$). Thus, selective targeting of mouse FcγRIV with the recombinant two-domain construct FcγRIV VHH-M2e VHH, can protect mice against a potentially lethal influenza A virus challenge.

DISCUSSION

Formatting of VHH fragments to develop biologicals to prevent or treat infectious diseases is a powerful and attractive approach to develop biologicals with enhanced specificity, activity, half-life and breadth of protection. Here, VHH formatting was used to test if arming of a virus surface antigen-specific VHH with an artificial and selective FcγR activation function can potentiate its activity to combat viral infections in the absence of direct virus neutralization. To explore this possibility, we focused on influenza A M2e as a viral target. This antigen is conserved among influenza A viruses and is therefore an attractive target to achieve broad protection. M2e-specific VHHs were obtained after immunization of a llama with M2e fused to a heterologous tetramerizing domain, to mimic the natural quaternary structure of M2, followed by panning on M2e peptide or cells that stably express M2. We isolated and characterized in more detail three M2e-specific VHHs. Although several M2e-specific conventional MAbs have been described in recent years, to our knowledge, these are the first reported single domain antibodies that specifically bind to M2e. Recently, a M2-specific VHH was isolated from a synthetic VHH library by Wei et al. (57), however their VHH failed to bind to M2e peptide.

We determined the crystal structure of M2e-VHH-23m in complex with a M2e peptide, that corresponds to the consensus sequence of human H1N1 viruses that circulated between 1933 and 2008, human H2N2 and H3N2 viruses. This structure revealed that the M2e antigen is bound by the VHH in an extended conformation that wraps around two main interfaces on the VHH. A first interface is a shallow groove formed by the CDR2 and CDR3 loops and the C, C', C", and F β-strands (**Figure 3A**). This interface binds the M2e region spanning residues 6–12, where Val7, Pro10 and Ile 11 bind hydrophobic patches on the VHH. In addition to three main chain interactions, the side chains of M2eGlu8 and -Thr9 each go into an H-bond interaction with the VHH. A second binding interface is found on the "back" side of the VHH, interacting with

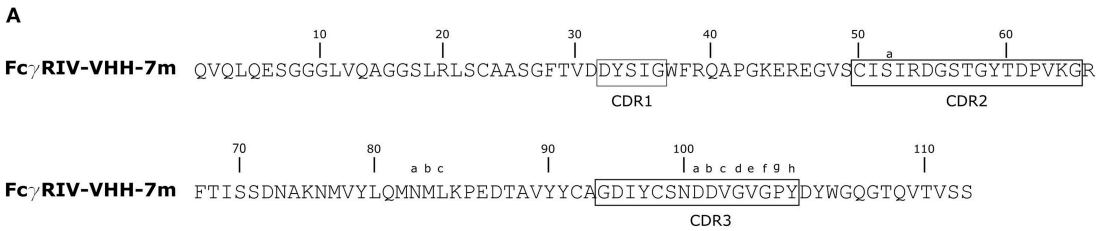

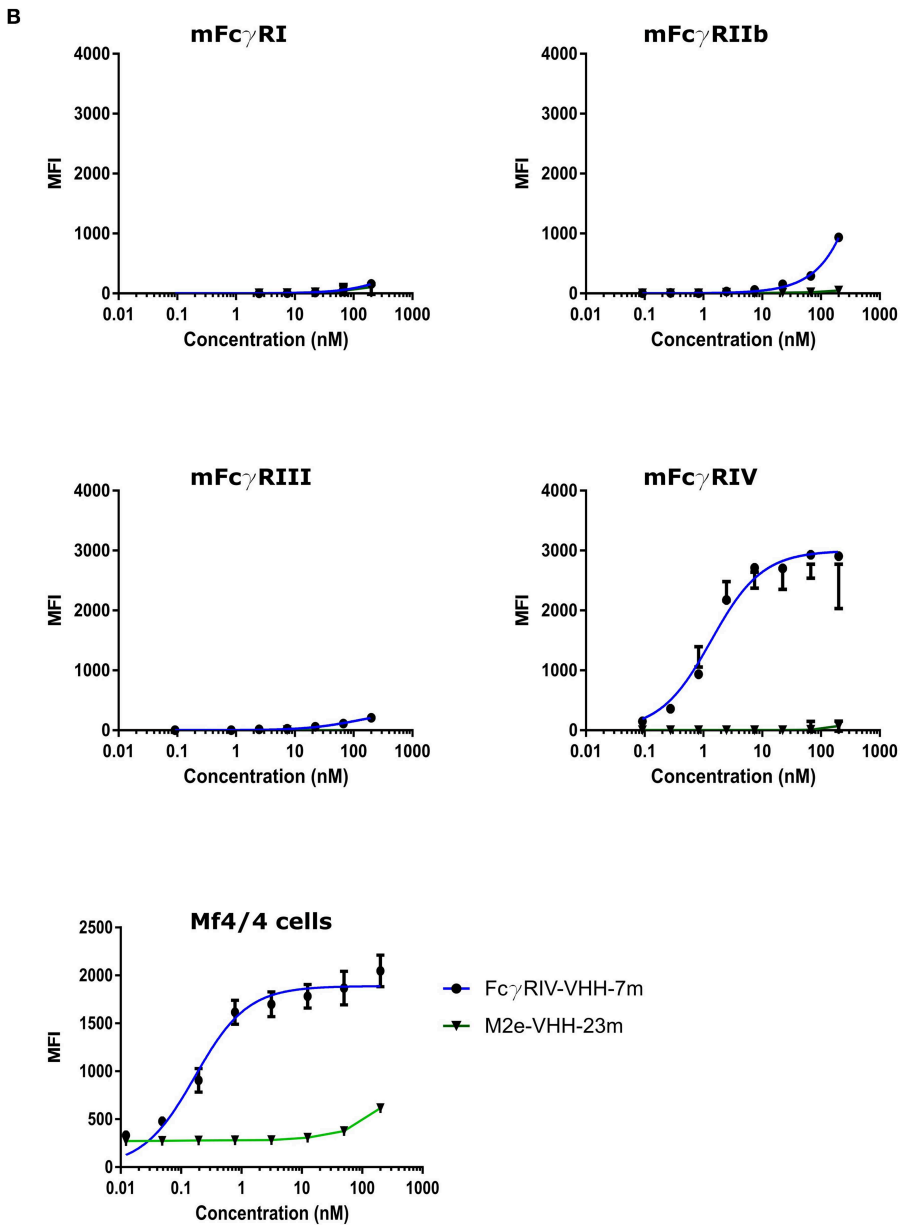

FIGURE 5 | Characterization of the isolated FcγRIV-specific VHH. **(A)** The predicted amino acid residue sequence of FcγRIV-VHH-7m, isolated after panning on recombinant mouse FcγRIV protein of a VHH library derived from a llama immunized with immature mouse dendritic cells. Above the sequences the Kabat numbering is indicated. CDR1, −2, and −3 are boxed. **(B)** Flow cytometric analysis showing binding of FcgRIV-VHH-7m and M2e-VHH-23m to HEK 293T cells transiently transfected with expression vectors coding for mouse FcγRI, FγRIIb, FcγRIII, and FcγRIV along with the common γ-chain for the activating FcγRs and a GFP expression plasmid. The lower graph depicts binding to Mf4/4 cells. The cells were incubated with fourfold serial dilution of Alexa Fluor™ 647 labeled FcγRIV-VHH-7m or M2e-VHH-23m, starting at a concentration of 0.2 μM, binding of the VHHs to the GFP positive cells was analyzed. Data points represent averages of triplicates and error bars standard deviations.

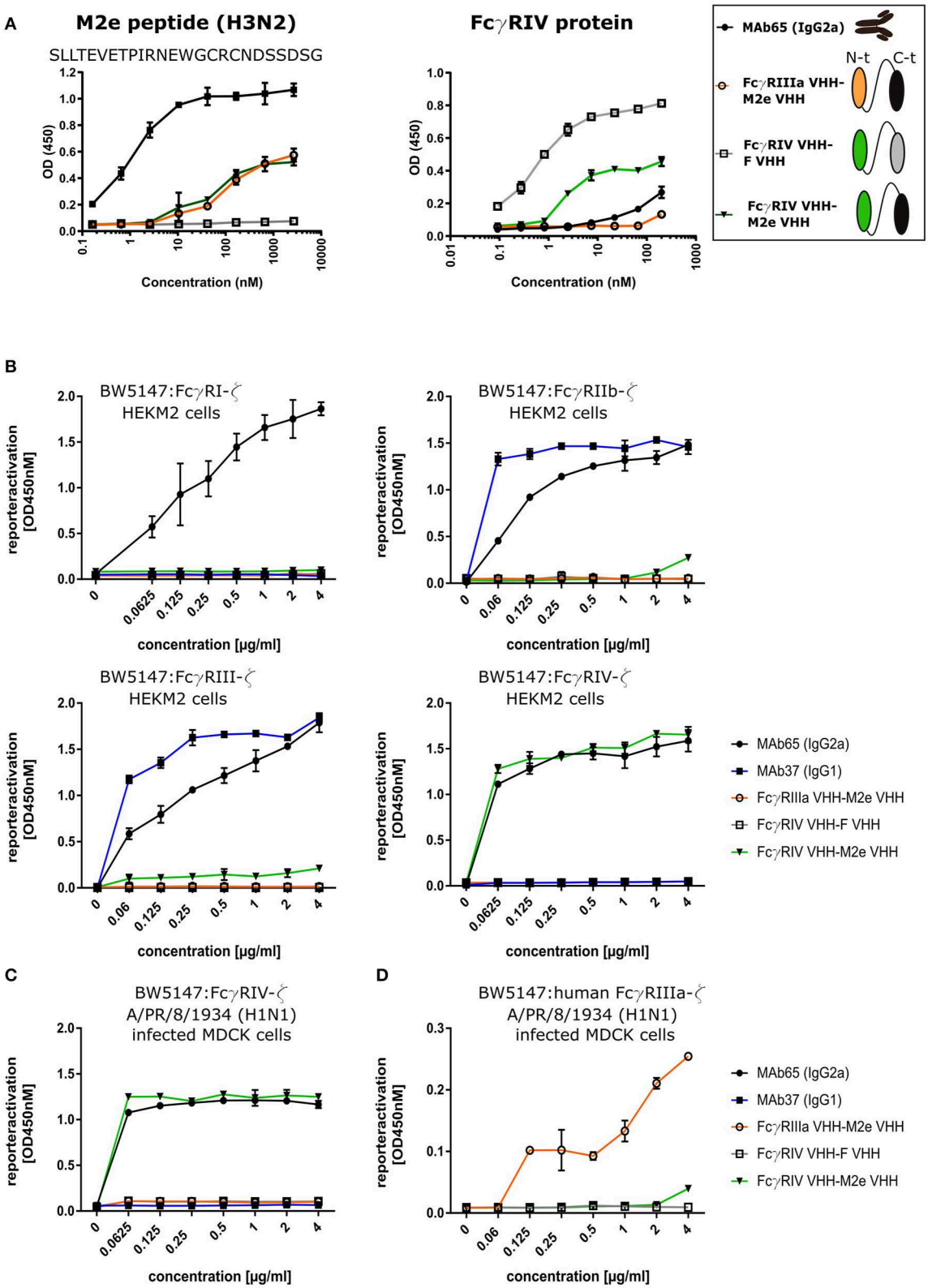

FIGURE 6 | Bispecific fusion construct of anti-mouse FcγRIV VHH with M2e-VHH-23m selectively activates FcγRIV *in vitro*. **(A)** Schematic representation of the bispecific VHHs and ELISA on human H3N2 M2e peptide and recombinant FcγRIV protein is shown on the right. Wells of microtiter plates were coated with 100 ng

(Continued)

FIGURE 6 | peptide or protein. Dilution series of the bispecific VHH fusion constructs were added to the coated plates. Binding was detected with a mouse anti-His tag MAb, followed by a secondary sheep anti-mouse IgG Ab conjugated to HRP for the peptide ELISA. In the ELISA with coated recombinant FcγRIV protein, binding was detected with a HRP-conjugated rabbit anti-camelid VHH antibody. **(B)** Serial dilutions of the bispecific VHH fusion construct or monoclonal antibodies were added to HEK293T cells stably transfected with an influenza M2 expression plasmid. Thirty minutes later, FcγR-ζ BW5147 reporter cells were added to the HEK293T cells. After overnight incubation produced mIL-2 was measured in a sandwich-ELISA, which served as an indicator for the magnitude of FcγR activation. (C) MDCK cells were infected with A/Puerto Rico/8/1934 (H1N1) virus for 1 h. Unbound virus particles were washed away and serial dilutions of the bispecific VHHs or monoclonal antibodies were added and incubated for 30 min, followed by the addition of the FcγRIV-ζ BW5147 reporter cells **(C)** or human FcγRIIIa-ζ BW5147 reporter cells **(D)**. After overnight incubation supernatants were analyzed by an anti mIL-2 sandwich ELISA. Data points represent averages of triplicates and error bars represent standard deviations. The graphs are a representative of one out of three repeat experiments.

residues 14–19 of M2e. This interface contains a well-defined hydrophobic pocket that captures the side chain of the highly conserved Trp15. Most avian and swine influenza A viruses, and, since the 2009 pandemic, also most circulating human H1N1 viruses, have a threonine instead of an isoleucine at position 11 of M2(e). Threonine is not hydrophobic and would be incompatible to the VHH's hydrophobic pocket. This likely explains why M2e-VHH-23m fails to bind to the tested avian and swine M2e peptide variants. In contrast to Ile11, M2e-Trp15, which occupies the second hydrophobic pocket of the VHH, is strictly conserved in all known influenza A viruses. M2e Ala-scan analysis revealed that next to Ile11 and Trp15 also substitution of Val7 or Glu14 considerably impairs binding of M2e-VHH-23m. M2eVal7 is strictly conserved in all influenza A viruses and M2eGlu14 is highly conserved in human influenza A viruses. Since M2eVal7, -Ile11, -Glu14, and -Trp15 are highly conserved in all H3N2 influenza A strains, M2e-VHH-23m might have the potential to recognize the vast majority of these strains. The M2e N-terminus (SLLTEVET) is highly conserved among all influenza A viruses and is recognized by some conventional monoclonal antibodies such as MAb 148 and TCN-032. Despite employing various panning strategies using avian and swine M2e variants, we could not yet isolate a VHH that specifically binds the strictly conserved region in the M2e N-terminus.

Earlier we reported the crystal structures of M2e in complex with the Fab fragment of two different mouse monoclonal antibodies (MAb 65 and MAb 148) that recognize partially overlapping epitopes of M2e (50, 58). In these two crystal structures, M2e adopted two different conformations. The epitopes of the MAb 65 and M2e-VHH-23m are highly similar: they both span the TEVETPIRNEW fragment and in both M2eIle11 and -Trp15 are important for binding. Nevertheless, the conformation of the TEVETPIRNEW part of M2e in complex with M2e-VHH-23m is very different from that in complex with the MAb 65 (**Figure S3**). This indicates that M2e indeed has little intrinsic structure and can adopt multiple conformations dependent on the bound antibody. This flexible nature of the M2e peptide could explain why it appears to be difficult to isolate a VHH that recognizes the N-terminal part of M2e. Moreover, due to the absence of the light chain, VHHs typically bind to concave epitopes rather than to convex or protruding peptide termini (59, 60). Nevertheless a few VHHs directed against linear peptides have been described (61, 62). De Genst et al. reported on a VHH that binds to the C-terminus of the intrinsically disordered a-synuclein protein with nanomolar range affinity (61). The crystal structure revealed that this VHH binds the four C-terminal amino acids of α-synuclein by a narrow pocket formed by its CDR2 and CDR3. This suggests that it may be possible to isolate VHHs that specifically bind the highly conserved N-terminus of M2.

In this study, we also report the isolation of a FcγRIV-specific VHH from a llama that had been immunized with immature mouse dendritic cells. This VHH bound to mouse FcγRIV and showed no cross reactivity with the other FcγRs. To our knowledge, this is the first report of an FcγRIV-specific VHH. A fibronectin scaffold protein that could specifically bind to FcγRIV with high affinity has been reported (63). In addition, this scaffold protein was able to delay tumor growth in a mouse model when linked to an anti-tumor antigen-specific single-chain antibody and mouse serum albumin (to extend the half-life of the fusion construct).

The bivalent VHH comprising the FcγRIV-specific VHH and the M2e-specific VHH, could activate the mouse FcγRIV in the presence of influenza A virus infected cells. Specifically targeting only FcγRIV might be an advantage over conventional antibodies since the activation of the inhibitory FcγRIIb receptor, which dampens the immune cell activation, is circumvented this way. In this context, other strategies such as site-directed mutagenesis, bispecific antibody formats and glycan engineering have been explored to try to increase Fc binding to activating receptors and decrease the interaction with the inhibitory receptor FcγRIIb (64–67). For example, afucosylated antibodies against RSV, Ebola virus and HIV with enhanced FcγR binding showed enhanced efficacy in rodent models (67–69).

When administered 4 h before and 24 h after infection, the bispecific FcγRIV VHH-M2e VHH construct protected wild-type but not *Fcγ RIV*$^{-/-}$ mice against an otherwise lethal influenza A virus challenge. It is well documented that protection by M2e-specifc antibodies is FcγR mediated (6–9). We recently reported that wild type mice treated with an M2e-specific IgG2a showed significantly less body weight loss after infection compared with *Fcγ RIV*-/- mice, suggesting that FcγRIV could contribute to protection by M2e-specific IgG2a (13). Here we show that the selective activation of the mouse FcγRIV with a bispecific VHH fusion that also binds to M2e is sufficient to protect mice against a potentially lethal influenza A virus challenge. Antitumor activity has been reported for bispecific VHH fusion constructs that consist of a VHH directed against the human FcγRIIIa (the ortholog of the mouse FcγRIV), fused to either a VHH directed against carcinoembryonic antigen (CEA) or HER2 (70, 71). In the context of viral infections, it has been reported that selective engagement of human FcγRIIIa could

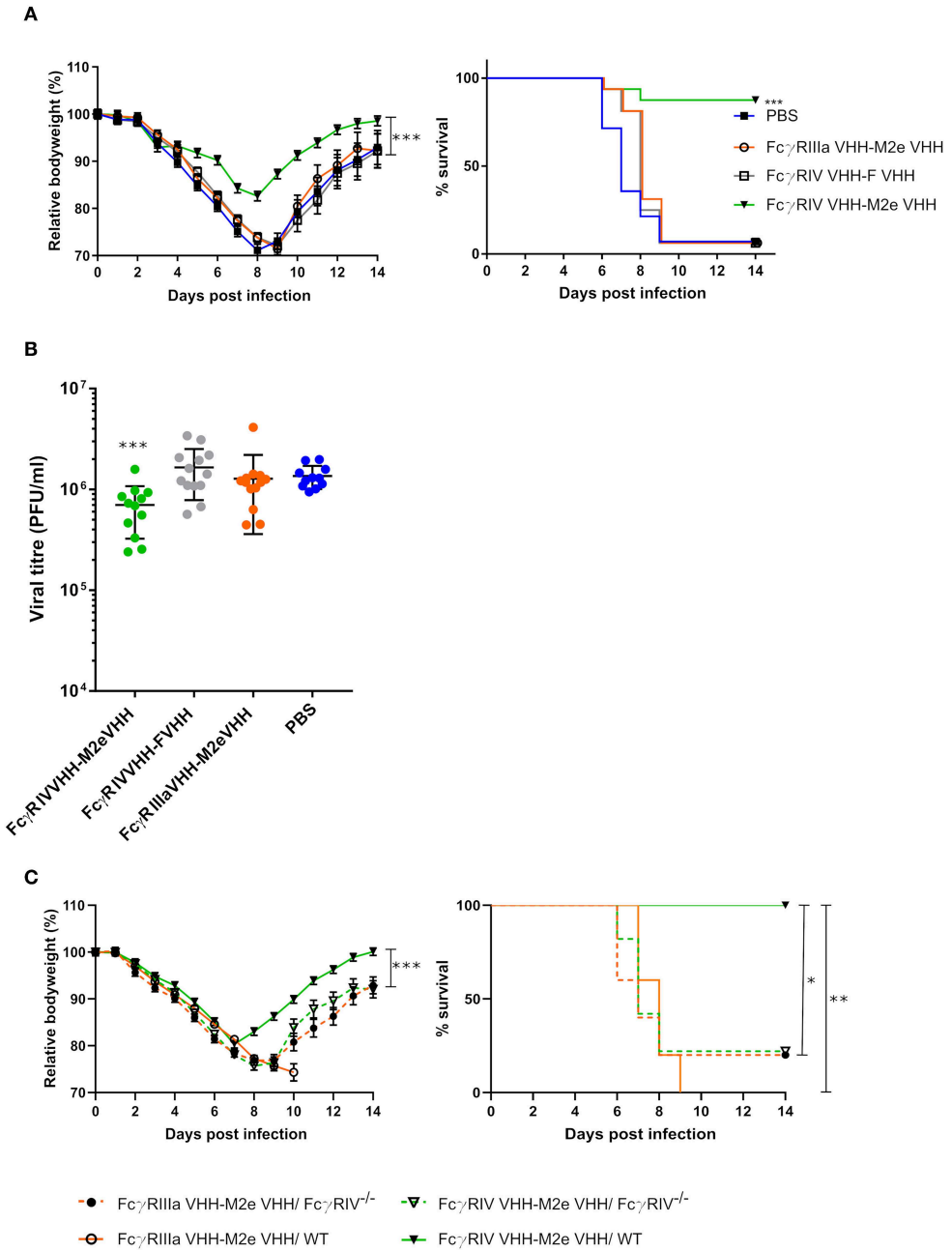

FIGURE 7 | Bispecific fusion construct of a FcγRIV- and M2e-specific VHH protects mice against a potentially lethal influenza A virus infection. **(A)** Groups of 16 (bispecific VHHs) or 14 (PBS) BALB/c mice were intranasally treated with 50 μg of the bispecific VHHs or PBS 4 h before and 24 h after challenge with 2xLD_{50} of A/X47 (H3N2) influenza virus. Body weight change (left) and survival (right) were monitored for 14 days. The mean relative changes in body weight together with their standard errors, are represented. The difference in body weight loss between FcγRIV VHH-M2e VHH and the negative-control groups was statistically significant (***$P < 0.001$, REML variance components analysis). The survival rate of the group receiving FcγRIV VHH-M2e VHH was significantly different from FcγRIV VHH-F VHH control treatment group (***$p < 0.001$, Log-rank test). **(B)** To determine the effect on the viral load in the lungs, groups of 13 (bispecific VHHs) or 11 (PBS) BALB/c mice received 50 μg of the bispecific VHHs or PBS 4 h before and 24 h after viral challenge with 2xLD_{50} of A/X47 (H3N2) influenza virus. On day 6 after infection, the lungs were harvested and the viral titer was determined by plaque assay. The viral titer of mice FcγRIV VHH-M2e VHH was significantly different compared to mice that received the FcγRIV VHH-F VHH control treatment (***$P < 0.001$, unpaired *t*-test). **(C)** Groups of 5 wild-type and *FcγRIV*$^{-/-}$ C57BL/6 mice (male and female mice) were treated with 50 μg of the bispecific VHHs 4 h before and 24 h after viral challenge with 2xLD_{50} of A/X47 (H3N2) influenza virus and body weight (left) and survival (right) were monitored. In the left-hand graph, data points represent means and error bars represent the standard errors of the means. Body weight changes between FcγRIV VHH-M2e VHH treated wild-type and FcγRIV$^{-/-}$ mice were significantly different (***$P < 0.001$, REML variance components analysis). The survival rate of wild-type mice that received FcγRIV VHH-M2e VHH was significantly different from wild-type mice treated with FcγRIIIa VHH-M2e VHH (**$P < 0.01$, REML variance components analysis) and FcγRIV$^{-/-}$ mice treated with FcγRIV VHH-M2e VHH and FcγRIIIa VHH-M2e VHH (*$P < 0.05$, REML variance components analysis). Data in **(A,B)** are pooled from 2 independent experiments.

mediate killing of HIV infected target cells by NK cells (72, 73). It remains to be investigated whether exchanging the mouse FcγRIV specific VHH by a human FcγRIIIa specific VHH in the bispecific fusion construct described here, would be able to protect against influenza A virus infection in the context of a human FcγR repertoire. Moreover, the M2e-specific VHH could be exchanged by a VHH direct against another (conserved) viral target antigen such as the hemagglutinin stalk domain, since FcγRs also seem to play an important role in the protection mediated by anti-stalk antibodies (74, 75).

In summary, we have demonstrated that an intranasally administered, bi-specific VHH fusion construct that selectively binds to and activates FcγRIV with one moiety and M2e as present on infected target cells can protect against influenza A virus challenge. However, the treated mice still showed substantial bodyweight loss following challenge whereas intranasal administration of a M2e-specific IgG2a monoclonal antibody largely controlled the morbidity following challenge of the mice (unpublished result). In future studies one could try to optimize the Fcγ Receptor engaging VHH-fusions by extending their lung retention, and further increasing the affinity for both the viral target and the specific FcγR. Finally, when humanized, formatted M2e-specific VHHs might provide a new treatment option in the battle against influenza A virus infections. This approach could also be of interest for other viral infections. Such VHHs might be especially well suited to prevent or treat respiratory infections because VHHs can be delivered directly to the site of infection as inhaled biotherapeutics by nebulization (27).

DATA AVAILABILITY STATEMENT

All datasets generated for this study are included in the article/**Supplementary Material**, and will also be made available by the authors, without undue reservation, to any qualified researcher.

ETHICS STATEMENT

All mouse experiments complied with national (Belgian Law 14/08/1986 and 22/12/20333, Belgian Royal Decree 06/04/2010) and European legislation (EU Directives 2010/63/EU and 86/609EEG) on animal regulations. All experiments were approved by and performed according to the guidelines of the animal ethical committee of Ghent University (permit number LA1400091, ethical applications EC2017-66 and EC2018-12).

AUTHOR CONTRIBUTIONS

DD, BS, and XS planned the study. DD, KH, IV, WN, LV, MB, SC, and BS performed the research. DD, BS, IV, and XS wrote the manuscript with contributions from KH, WN, HR, and HH. All authors reviewed the manuscript before submission.

FUNDING

DD was supported by an IWT-SB fellowship (B/14438/57) and VIB dotation to the group of Xavier Saelens. BS was a postdoctoral assistant and LV was a junior assistant at the Department for Biomedical Molecular Biology at Ghent University and was also supported by FWO-EOS project Vir-EOS. This research was also supported by research project BOF17-GOA-018 from Ghent University, and FWO-Vlaanderen research projects G0B1917N and G043515N.

ACKNOWLEDGMENTS

We thank the VIB Nanobody Core facility for the llama immunizations and preparation of the VHH phage libraries. We also thank Marnik Vuylsteke for performing the statistical analysis and Geert Raes for providing the phage library of a llama immunized with immature mouse dendritic cells. We thank the beamline scientists at the i03 beamline of the Diamond Light Source synchrotron facility.

SUPPLEMENTARY MATERIAL

The Supplementary Material for this article can be found online at: https://www.frontiersin.org/articles/10.3389/fimmu.2019.02920/full#supplementary-material

REFERENCES

1. Paules CI, Fauci AS. Influenza vaccines: good, but we can do better. *J Infect Dis.* (2019) 219:S1–4. doi: 10.1093/infdis/jiy633
2. Koszalka P, Tilmanis D, Roe M, Vijaykrishna D, Hurt AC. Baloxavir marboxil susceptibility of influenza viruses from the Asia-Pacific, 2012–2018. *Antiviral Res.* (2019) 164:91–6. doi: 10.1016/j.antiviral.2019.02.007
3. Lee N, Hurt AC. Neuraminidase inhibitor resistance in influenza: a clinical perspective. *Curr Opin Infect Dis.* (2018) 31:520–6. doi: 10.1097/QCO.0000000000000498
4. Saelens X. The role of M2e in the development of universal influenza vaccines. *J Infect Dis.* (2019) 219:S68–74. doi: 10.1093/infdis/jiz003
5. Ito T, Gorman OT, Kawaoka Y, Bean WJ, Webster RG. Evolutionary analysis of the influenza A virus M gene with comparison of the M1 and M2 proteins. *J Virol.* (1991) 65:5491–8.
6. Neirynck S, Deroo T, Saelens X, Vanlandschoot P, Jou WM, Fiers W. A universal influenza A vaccine based on the extracellular domain of the M2 protein. *Nat Med.* (1999) 5:1157–63. doi: 10.1038/13484
7. Fan J, Liang X, Horton MS, Perry HC, Citron MP, Heidecker, GJ, et al. Preclinical study of influenza virus A M2 peptide conjugate vaccines in mice, ferrets, and rhesus monkeys. *Vaccine.* (2004) 22:2993–3003. doi: 10.1016/j.vaccine.2004.02.021
8. Turley CB, Rupp RE, Johnson C, Taylor DN, Wolfson J, Tussey L, et al. Safety and immunogenicity of a recombinant M2e-flagellin influenza vaccine (STF2.4xM2e) in healthy adults. *Vaccine.* (2011) 29:5145–52. doi: 10.1016/j.vaccine.2011.05.041
9. Slepushkin VA, Katz JM, Black RA, Gamble WC, Rota PA, Cox NJ. Protection of mice against influenza A virus challenge by vaccination with baculovirus-expressed M2 protein. *Vaccine.* (1995) 13:1399–402. doi: 10.1016/0264-410X(95)92777-Y

10. Ramos EL, Mitcham JL, Koller TD, Bonavia A, Usner DW, Balaratnam G, et al. Efficacy and safety of treatment with an anti-m2e monoclonal antibody in experimental human influenza. *J Infect Dis.* (2015) 211:1038–44. doi: 10.1093/infdis/jiu539
11. Pendzialek J, Roose K, Smet A, Schepens B, Kufer P, Raum T, et al. Bispecific T cell engaging antibody constructs targeting a universally conserved part of the viral M2 ectodomain cure and prevent influenza A virus infection. *Antiviral Res.* (2017) 141:155–64. doi: 10.1016/j.antiviral.2017.02.016
12. El Bakkouri K, Descamps F, De Filette M, Smet A, Festjens E, Birkett A, et al. Universal vaccine based on ectodomain of matrix protein 2 of influenza A: Fc receptors and alveolar macrophages mediate protection. *J Immunol.* (2011) 186:1022–31. doi: 10.4049/jimmunol.0902147
13. Van den Hoecke S, Ehrhardt K, Kolpe A, El Bakkouri K, Deng L, Grootaert H, et al. Hierarchical and redundant roles of activating FcγRs in protection against influenza disease by M2e-specific IgG1 and IgG2a antibodies. *J Virol.* (2017) 91:1–13. doi: 10.1128/JVI.02500-16
14. Song A, Myojo K, Laudenslager J, Harada D, Miura T, Suzuki K, et al. Evaluation of a fully human monoclonal antibody against multiple influenza A viral strains in mice and a pandemic H1N1 strain in nonhuman primates. *Antiviral Res.* (2014) 111:60–8. doi: 10.1016/j.antiviral.2014.08.016
15. Guilliams M, Bruhns P, Saeys Y, Hammad H, Lambrecht BN. The function of Fcγ receptors in dendritic cells and macrophages. *Nat Rev Immunol.* (2014) 14:94–108. doi: 10.1038/nri3582
16. Bruhns P. Properties of mouse and human IgG receptors and their contribution to disease models. *Blood*. (2012) 119:5640–9. doi: 10.1182/blood-2012-01-380121
17. Ra C, Jouvin MH, Blank U, Kinet JP. A macrophage Fc gamma receptor and the mast cell receptor for IgE share an identical subunit. *Nature.* (1989) 341:752–4. doi: 10.1038/341752a0
18. Daëron M, Latour S, Malbec O, Espinosa E, Pina P, Pasmans S, Fridman WH. The same tyrosine-based inhibition motif, in the intracytoplasmic domain of Fc gamma RIIB, regulates negatively BCR-, TCR-, and FcR-dependent cell activation. *Immunity*. (1995) 3:635–46. doi: 10.1016/1074-7613(95)90134-5
19. Cambier JC. New nomenclature for the Reth motif (or ARH1/TAM/ARAM/YXXL). *Immunol Today.* (1995) 16:110. doi: 10.1016/0167-5699(95)80105-7
20. Nimmerjahn F, Bruhns P, Horiuchi K, Ravetch JV. FcgammaRIV: a novel FcR with distinct IgG subclass specificity. *Immunity*. (2005) 23:41–51. doi: 10.1016/j.immuni.2005.05.010
21. Hamers-Casterman C, Atarhouch T, Muyldermans S, Robinson G, Hamers C, Songa EB, et al. Naturally occurring antibodies devoid of light chains. *Nature.* (1993) 363:446–8. doi: 10.1038/363446a0
22. Wu Y, Jiang S, Ying T. Single-domain antibodies as therapeutics against human viral diseases. *Front Immunol.* (2017) 8:1802. doi: 10.3389/fimmu.2017.01802
23. De Vlieger D, Ballegeer M, Rossey I, Schepens B, Saelens X. Single-domain antibodies and their formatting to combat viral infections. *Antibodies.* (2019) 8:1. doi: 10.3390/antib8010001
24. *A Multicentre Study in Otherwise Healthy Infants and Toddlers Hospitalised For and Diagnosed With RSV Lower Respiratory Tract Infection to Evaluate the Safety, Tolerability, and Clinical Activity of ALX-0171 - Full Text View - ClinicalTrials.gov*. Available online at: https://clinicaltrials.gov/ct2/show/NCT02309320 (accessed May 17, 2019).
25. van der Linden RH, Frenken LG, de Geus B, Harmsen MM, Ruuls RC, Stok W, et al. Comparison of physical chemical properties of llama VHH antibody fragments and mouse monoclonal antibodies. *Biochim Biophys Acta.* (1999) 1431:37–46. doi: 10.1016/S0167-4838(99)00030-8
26. Dumoulin M, Conrath K, Van Meirhaeghe A, Meersman F, Heremans K, Frenken LGJ, et al. Single-domain antibody fragments with high conformational stability. *Protein Sci.* (2002) 11:500–15. doi: 10.1110/ps.34602
27. Van Heeke G, Allosery K, De Brabandere V, De Smedt T, Detalle L, de Fougerolles A. Nanobodies® as inhaled biotherapeutics for lung diseases. *Pharmacol Ther.* (2017) 169:47–56. doi: 10.1016/j.pharmthera.2016.06.012
28. De Filette M, Martens W, Roose K, Deroo T, Vervalle F, Bentahir M, et al. An influenza A vaccine based on tetrameric ectodomain of matrix protein 2. *J Biol Chem.* (2008) 283:11382–7. doi: 10.1074/jbc.M800650200
29. Desmedt M, Rottiers P, Dooms H, Fiers W, Grooten J. Macrophages induce cellular immunity by activating Th1 cell responses and suppressing Th2 cell responses. *J Immunol.* (1998) 160:5300–8.
30. Corrales-Aguilar E, Trilling M, Reinhard H, Mercé-Maldonado E, Widera M, Schaal H, et al. A novel assay for detecting virus-specific antibodies triggering activation of Fcγ receptors. *J Immunol Methods.* (2013) 387:21–35. doi: 10.1016/j.jim.2012.09.006
31. Corrales-Aguilar E, Trilling M, Hunold K, Fiedler M, Le VTK, Reinhard H, et al. Human cytomegalovirus Fcγ binding proteins gp34 and gp68 antagonize Fcγ receptors I, II and III. *PLoS Pathog.* (2014) 10:e1004131. doi: 10.1371/journal.ppat.1004131
32. Deschacht N, Groeve KD, Vincke C, Raes G, Baetselier PD, Muyldermans S. A novel promiscuous class of camelid single-domain antibody contributes to the antigen-binding repertoire. *J Immunol.* (2010) 184:5696–704. doi: 10.4049/jimmunol.0903722
33. Schoonooghe S, Kaigorodov V, Zawisza M, Dumolyn C, Haustraete J, Grooten J, et al. Efficient production of human bivalent and trivalent anti-MUC1 Fab-scFv antibodies in Pichia pastoris. *BMC Biotechnol.* (2009) 9:70. doi: 10.1186/1472-6750-9-70
34. Lin-Cereghino J, Wong WW, Xiong S, Giang W, Luong LT, Vu J, et al. Condensed protocol for competent cell preparation and transformation of the methylotrophic yeast Pichia pastoris. *BioTechniques.* (2005) 38:44–8. doi: 10.2144/05381BM04
35. McCoy AJ, Grosse-Kunstleve RW, Adams PD, Winn MD, Storoni LC, Read RJ. Phaser crystallographic software. *J Appl Crystallogr.* (2007) 40:658–74. doi: 10.1107/S0021889807021206
36. Vagin A, Teplyakov A. Molecular replacement with MOLREP. *Acta Crystallogr D Biol Crystallogr.* (2010) 66:22–5. doi: 10.1107/S0907444909042589
37. Adams PD, Afonine PV, Bunkóczi G, Chen VB, Davis IW, Echols N, et al. PHENIX: a comprehensive Python-based system for macromolecular structure solution. *Acta Crystallogr D Biol Crystallogr.* (2010) 66:213–21. doi: 10.1107/S0907444909052925
38. Emsley P, Cowtan K. Coot: model-building tools for molecular graphics. *Acta Crystallogr D Biol Crystallogr.* (2004) 60:2126–32. doi: 10.1107/S0907444904019158
39. Afonine PV, Grosse-Kunstleve RW, Echols N, Headd JJ, Moriarty NW, Mustyakimov M, et al. Towards automated crystallographic structure refinement with phenix.refine. *Acta Crystallogr D Biol Crystallogr.* (2012) 68:352–67. doi: 10.1107/S0907444912001308
40. Murshudov GN, Vagin AA, Dodson EJ. Refinement of macromolecular structures by the maximum-likelihood method. *Acta Crystallogr D Biol Crystallogr.* (1997) 53:240–55. doi: 10.1107/S0907444996012255
41. Guex N, Peitsch MC. SWISS-MODEL and the Swiss-PdbViewer: an environment for comparative protein modeling. *Electrophoresis.* (1997) 18:2714–23. doi: 10.1002/elps.1150181505
42. Hanwell MD, Curtis DE, Lonie DC, Vandermeersch T, Zurek E, Hutchison GR. Avogadro: an advanced semantic chemical editor, visualization, and analysis platform. *J Cheminform.* (2012) 4:17. doi: 10.1186/1758-2946-4-17
43. Morris GM, Huey R, Lindstrom W, Sanner MF, Belew RK, Goodsell DS, et al. AutoDock4 and AutoDockTools4: automated docking with selective receptor flexibility. *J Comput Chem.* (2009) 30:2785–91. doi: 10.1002/jcc.21256
44. Trott O, Olson AJ. AutoDock vina: improving the speed and accuracy of docking with a new scoring function, efficient optimization and multithreading. *J Comput Chem.* (2010) 31:455–61. doi: 10.1002/jcc.21334
45. Koes DR, Baumgartner MP, Camacho CJ. Lessons learned in empirical scoring with smina from the CSAR 2011 benchmarking exercise. *J Chem Inf Model.* (2013) 53:1893–904. doi: 10.1021/ci300604z
46. *PyMOL | pymol.org*. Available online at: https://pymol.org/2/ (accessed July 3, 2019).
47. Sarrion-Perdigones A, Vazquez-Vilar M, Palací J, Castelijns B, Forment J, Ziarsolo P, et al. GoldenBraid 2.0: a comprehensive DNA assembly framework for plant synthetic biology. *Plant Physiol.* (2013) 162:1618–31. doi: 10.1104/pp.113.217661
48. Behar G, Sibéril S, Groulet A, Chames P, Pugnière M, Boix C, et al. Isolation and characterization of anti-FcgammaRIII (CD16) llama single-domain antibodies that activate natural killer cells. *Protein Eng Des Sel.* (2008) 21:1–10. doi: 10.1093/protein/gzm064

49. Nimmerjahn F, Lux A, Albert H, Woigk M, Lehmann C, Dudziak D, et al. FcγRIV deletion reveals its central role for IgG2a and IgG2b activity *in vivo*. *Proc Natl Acad Sci USA*. (2010) 107:19396–401. doi: 10.1073/pnas.1014515107
50. Cho KJ, Schepens B, Seok JH, Kim S, Roose K, Lee J-H, et al. Structure of the extracellular domain of matrix protein 2 of influenza A virus in complex with a protective monoclonal antibody. *J Virol.* (2015) 89:3700–11. doi: 10.1128/JVI.02576-14
51. Kunz P, Zinner K, Mücke N, Bartoschik T, Muyldermans S, Hoheisel JD. The structural basis of nanobody unfolding reversibility and thermoresistance. *Sci Rep.* (2018) 8:7934. doi: 10.1038/s41598-018-26338-z
52. Rossey I, Gilman MSA, Kabeche SC, Sedeyn K, Wrapp D, Kanekiyo M, et al. Potent single-domain antibodies that arrest respiratory syncytial virus fusion protein in its prefusion state. *Nat Commun.* (2017) 8:14158. doi: 10.1038/ncomms14158
53. Liu Y, Eisenberg D. 3D domain swapping: as domains continue to swap. *Protein Sci.* (2002) 11:1285–99. doi: 10.1110/ps.0201402
54. Zebedee SL, Lamb RA. Influenza A virus M2 protein: monoclonal antibody restriction of virus growth and detection of M2 in virions. *J Virol.* (1988) 62:2762–72.
55. Kolpe A, Schepens B, Ye L, Staeheli P, Saelens X. Passively transferred M2e-specific monoclonal antibody reduces influenza A virus transmission in mice. *Antiviral Res.* (2018) 158:244–54. doi: 10.1016/j.antiviral.2018.08.017
56. Kolpe A, Arista-Romero M, Schepens B, Pujals S, Saelens X, Albertazzi L. Super-resolution microscopy reveals significant impact of M2e-specific monoclonal antibodies on influenza A virus filament formation at the host cell surface. *Sci Rep.* (2019) 9:4450. doi: 10.1038/s41598-019-41023-5
57. Wei G, Meng W, Guo H, Pan W, Liu J, Peng T, et al. Potent neutralization of influenza A virus by a single-domain antibody blocking M2 ion channel protein. *PLoS ONE.* (2011) 6:e28309. doi: 10.1371/journal.pone.0028309
58. Cho KJ, Schepens B, Moonens K, Deng L, Fiers W, Remaut H, et al. Crystal structure of the conserved amino terminus of the extracellular domain of matrix protein 2 of influenza A virus gripped by an antibody. *J Virol.* (2015) 90:611–5. doi: 10.1128/JVI.02105-15
59. Pírez-Schirmer M, Rossotti M, Badagian N, Leizagoyen C, Brena BM, González-Sapienza G. Comparison of three antihapten VHH selection strategies for the development of highly sensitive immunoassays for microcystins. *Anal Chem.* (2017) 89:6800–6. doi: 10.1021/acs.analchem.7b01221
60. De Genst E, Silence K, Decanniere K, Conrath K, Loris R, Kinne J, et al. Molecular basis for the preferential cleft recognition by dromedary heavy-chain antibodies. *Proc Natl Acad Sci USA.* (2006) 103:4586–91. doi: 10.1073/pnas.0505379103
61. De Genst EJ, Guilliams T, Wellens J, O'Day EM, Waudby CA, Meehan S, et al. Structure and properties of a complex of α-synuclein and a single-domain camelid antibody. *J Mol Biol.* (2010) 402:326–43. doi: 10.1016/j.jmb.2010.07.001
62. Braun MB, Traenkle B, Koch PA, Emele F, Weiss F, Poetz O, et al. Peptides in headlock – a novel high-affinity and versatile peptide-binding nanobody for proteomics and microscopy. *Sci Rep.* (2016) 6:19211. doi: 10.1038/srep19211
63. Chen TF, Li KK, Zhu EF, Opel CF, Kauke MJ, Kim H, et al. Artificial anti-tumor opsonizing proteins with fibronectin scaffolds engineered for specificity to each of the murine FcγR types. *J Mol Biol.* (2018) 430:1786–98. doi: 10.1016/j.jmb.2018.04.021
64. Shields RL, Namenuk AK, Hong K, Meng YG, Rae J, Briggs J, et al. High resolution mapping of the binding site on human IgG1 for Fc gamma RI, Fc gamma RII, Fc gamma RIII, and FcRn and design of IgG1 variants with improved binding to the Fc gamma R. *J Biol Chem.* (2001) 276:6591–604. doi: 10.1074/jbc.M009483200
65. Mori K, Iida S, Yamane-Ohnuki N, Kanda Y, Kuni-Kamochi R, Nakano R, et al. Non-fucosylated therapeutic antibodies: the next generation of therapeutic antibodies. *Cytotechnology.* (2007) 55:109–14. doi: 10.1007/s10616-007-9103-2
66. Müller D, Karle A, Meissburger B, Höfig I, Stork R, Kontermann RE. Improved pharmacokinetics of recombinant bispecific antibody molecules by fusion to human serum albumin. *J Biol Chem.* (2007) 282:12650–60. doi: 10.1074/jbc.M700820200
67. Hiatt A, Bohorova N, Bohorov O, Goodman C, Kim D, Pauly MH, et al. Glycan variants of a respiratory syncytial virus antibody with enhanced effector function and *in vivo* efficacy. *Proc Natl Acad Sci USA.* (2014) 111:5992–7. doi: 10.1073/pnas.1402458111
68. Bardhi A, Wu Y, Chen W, Li W, Zhu Z, Zheng JH, et al. Potent *in vivo* NK cell-mediated elimination of HIV-1-infected cells mobilized by a gp120-bispecific and hexavalent broadly neutralizing fusion protein. *J Virol.* (2017) 91:1–19. doi: 10.1128/JVI.00937-17
69. Zeitlin L, Pettitt J, Scully C, Bohorova N, Kim D, Pauly M, et al. Enhanced potency of a fucose-free monoclonal antibody being developed as an Ebola virus immunoprotectant. *Proc Natl Acad Sci USA.* (2011) 108:20690–4. doi: 10.1073/pnas.1108360108
70. Rozan C, Cornillon A, Pétiard C, Chartier M, Behar G, Boix C, et al. Single-domain antibody-based and linker-free bispecific antibodies targeting FcγRIII induce potent antitumor activity without recruiting regulatory T cells. *Mol Cancer Ther.* (2013) 12:1481–91. doi: 10.1158/1535-7163.MCT-12-1012
71. Turini M, Chames P, Bruhns P, Baty D, Kerfelec B. A FcγRIII-engaging bispecific antibody expands the range of HER2-expressing breast tumors eligible to antibody therapy. *Oncotarget.* (2014) 5:5304–19. doi: 10.18632/oncotarget.2093
72. Li W, Wu Y, Kong D, Yang H, Wang Y, Shao J, et al. One-domain CD4 fused to human anti-CD16 antibody domain mediates effective killing of HIV-1-infected cells. *Sci Rep.* (2017) 7:9130. doi: 10.1038/s41598-017-07966-3
73. Gleason MK, Verneris MR, Todhunter DA, Zhang B, McCullar V, Zhou SX, et al. Bispecific and trispecific killer cell engagers directly activate human NK cells through CD16 signaling and induce cytotoxicity and cytokine production. *Mol Cancer Ther.* (2012) 11:2674–84. doi: 10.1158/1535-7163.MCT-12-0692
74. DiLillo DJ, Tan GS, Palese P, Ravetch JV. Broadly neutralizing hemagglutinin stalk-specific antibodies require FcγR interactions for protection against influenza virus *in vivo*. *Nat Med.* (2014) 20:143–51. doi: 10.1038/nm.3443
75. Thulin NK, Wang TT. The role of Fc gamma receptors in broad protection against influenza viruses. *Vaccines (Basel).* (2018) 6:36. doi: 10.3390/vaccines6030036

Conflict of Interest: The authors declare that the research was conducted in the absence of any commercial or financial relationships that could be construed as a potential conflict of interest.

frontiers in Immunology

REVIEW
published: 13 December 2019
doi: 10.3389/fimmu.2019.02869

Immunomodulation as a Novel Strategy for Prevention and Treatment of *Bordetella* spp. Infections

Monica C. Gestal, Hannah M. Johnson and Eric T. Harvill**

Department of Infectious Diseases, College of Veterinary Sciences, University of Georgia, Athens, GA, United States

Well-adapted pathogens have evolved to survive the many challenges of a robust immune response. Defending against all host antimicrobials simultaneously would be exceedingly difficult, if not impossible, so many co-evolved organisms utilize immunomodulatory tools to subvert, distract, and/or evade the host immune response. *Bordetella* spp. present many examples of the diversity of immunomodulators and an exceptional experimental system in which to study them. Recent advances in this experimental system suggest strategies for interventions that tweak immunity to disrupt bacterial immunomodulation, engaging more effective host immunity to better prevent and treat infections. Here we review advances in the understanding of respiratory pathogens, with special focus on *Bordetella* spp., and prospects for the use of immune-stimulatory interventions in the prevention and treatment of infection.

Keywords: immunomodulation, *Bordetella*, Toll-receptors, adjuvants, pertussis

OPEN ACCESS

Edited by:
Roberta Antonia Diotti, Vita-Salute San Raffaele University, Italy

Reviewed by:
Rene Raeven, Intravacc, Netherlands
Giorgio Fedele, Istituto Superiore di Sanità (ISS), Italy

****Correspondence:***
Monica C. Gestal
mcarges@gmail.com
Eric T. Harvill
harvill@uga.edu

Specialty section:
This article was submitted to Vaccines and Molecular Therapeutics, a section of the journal Frontiers in Immunology

Received: *16 September 2019*
Accepted: *22 November 2019*
Published: *13 December 2019*

Citation:
Gestal MC, Johnson HM and Harvill ET (2019) Immunomodulation as a Novel Strategy for Prevention and Treatment of Bordetella spp. Infections. Front. Immunol. 10:2869. doi: 10.3389/fimmu.2019.02869

INTRODUCTION TO THE STRATEGY OF IMMUNOMODULATION FOR HEALTH

We are exposed to vast numbers of pathogens during our lifespan, but only a small number manage to cause disease. Invading bacteria face a hostile environment in hosts with arrays of antimicrobial compounds and components of immunity. To persist in such an environment, bacteria must find a way to survive this onslaught of antibacterials. The strategy of resisting them all may be exceedingly challenging or impossible; instead, most of the best-studied pathogens have mechanisms that allow them to evade the full effects of host defenses (1–12). In this review, we will consider examples of novel approaches in vaccine and therapeutic development that have been guided by the better understanding of bacterial immunomodulatory abilities. We will focus on findings with *Bordetella* spp., considering novel adjuvants that enhance host immune response and new immunostimulatory therapies that can augment the most effective aspects of the host immune response. The results highlighted in this review demonstrate that the manipulation and/or disruption of bacterial immunomodulatory properties are providing a highly promising approach that could replace antibiotics in a near future. Understanding the mechanisms that bacteria utilize to manipulate host immune response, as well as the immune signaling pathways that lead to greater protective immunity, can guide the development of targeted interventions that can enhance the host immune response to more effectively kill the bacterial hazard.

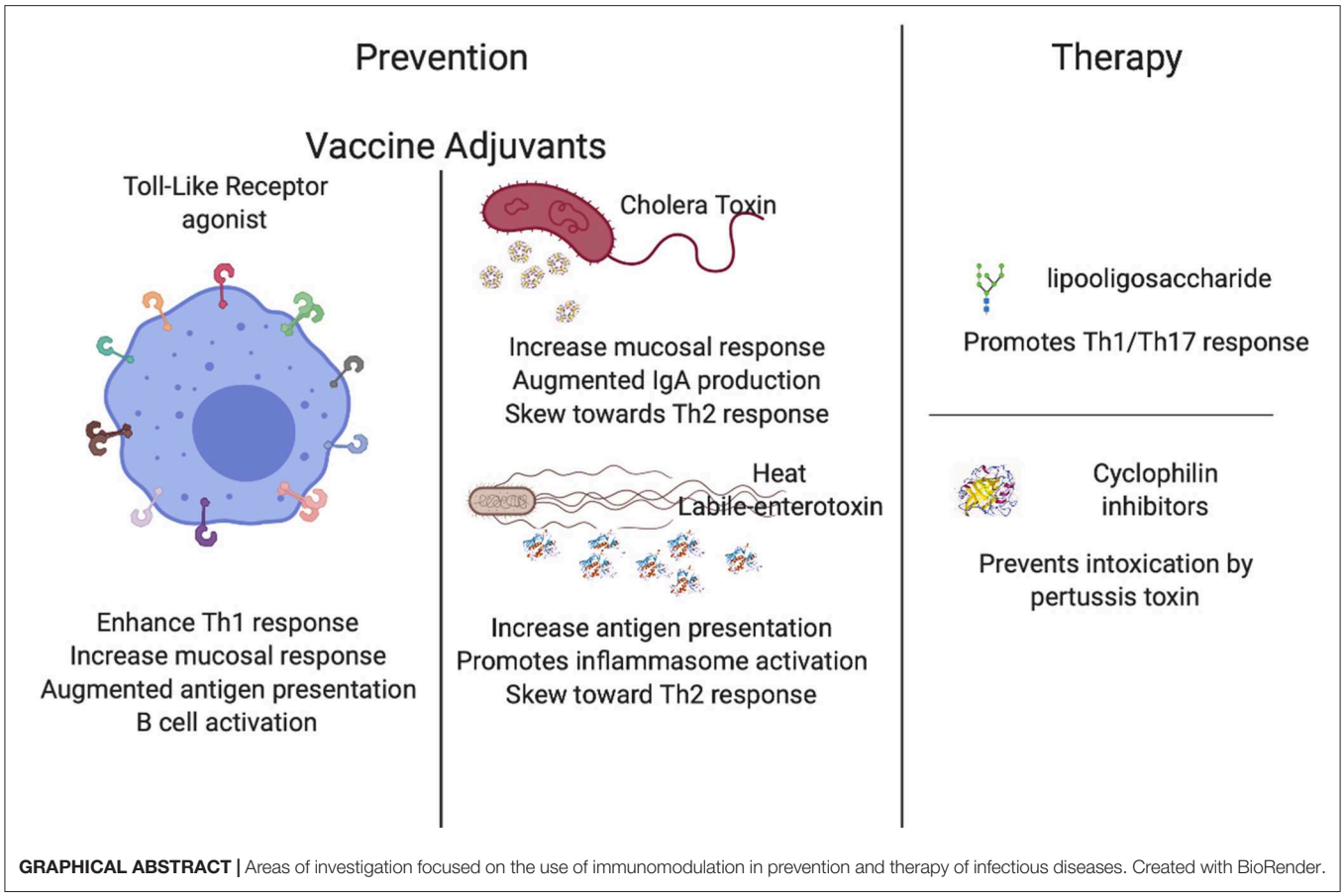

GRAPHICAL ABSTRACT | Areas of investigation focused on the use of immunomodulation in prevention and therapy of infectious diseases. Created with BioRender.

THE BORDETELLAE; BIOLOGY; AND EXPERIMENTAL SYSTEM

Pertussis disease is caused by *B. pertussis*, a highly transmissible human pathogen that causes a respiratory illness also known as the 100-day cough (13). Among the proposed reasons for its resurgence are waning immunity (13), the end of the "honeymoon period" (14), the past vaccination calendar (15), and the failure of the current acellular vaccine to confer sterilizing immunity and long-lasting herd immunity. The increase in the number of cases is associated with more advanced diagnostic tools than ever before, allowing for an increase in the number of identified cases (16–31), but also with increased morbidity and mortality that creates an unambiguous imperative for improved prevention methods.

Vaccination has greatly increased life expectancy by preventing several historically notorious infectious diseases (32–36). However, we are witnessing a rise in several preventable diseases previously thought to be controlled (37), such as pertussis (38). Around 1945, a whole-cell vaccine against *B. pertussis* was introduced, causing an unprecedented decrease in the number of reported pertussis cases. However, due to undesirable adverse effects such as fever, erythema, swelling, drowsiness and others, this was replaced in several industrialized countries by an acellular vaccine that contains between 3 to 5 bacterial proteins (39–44). Despite the fact that both types of vaccines generate antibodies that impede bacterial adhesion and have bactericidal action, these have not been sufficient to halt the increase in the number of cases. In response to this increase a boost was introduced to extend immunological memory, and new vaccination strategies targeted to pregnant women and close family have also been introduced as an attempt to protect highly susceptible newborns (45–48).

As the number of cases continues to increase, the scientific community is working to understand the causes that drive this reemergence (13, 49). Amongst the proposed causes of this increase are, limitation to the protection conferred by the current acellular vaccine. Not only does the acquired anamnestic response wane rapidly (50), but the acellular vaccine still allows for bacterial colonization of the nasal cavity and shedding. Combined, these factors illuminate the fact that the current vaccines used in most industrialized countries still permit transmission of pertussis from host to host (51–54), which has even more significant impacts when considered in tandem with the rise of anti-vaccination movements. Yet another cause for the increase is the differences detected in the immune response triggered by the whole cell vaccine (Th17) vs. the acellular vaccine (Th2) (51, 55–57). It is important to highlight that while neither

whole-cell nor acellular vaccines confer long-lasting immunity, and the merits of both responses have been debated in recent years, the general consensus agrees on advantages to skewing T cell response toward Th1/Th17 immunity (58–61).

The "gold standard" of immunity to pertussis is considered to be the classical Th1/Th17 T cell response induced by convalescent immunity (62); however, there is significant cumulative evidence that infection-induced immunity is imperfect and shorter-lived than it could be (50). Current discoveries contribute to better understanding of the immune response to Bordetellae, and the important role that CD4 resident T cells play in a local memory response has been recently demonstrated (63). Another hypothesis is that Bordetellae are evolving, and due to the genome plasticity and adaptability of this pathogen, current isolates of *B. pertussis* have lost some of the antigens included in the acellular vaccine. This phenomenon is referred to as "vaccine driven evolution," which helps justify why immunity is not as robust as it has previously been (64–67).

These are only some of the potential causes that are currently being considered, and it is most likely an uneven combination of all of them that is truly driving this pertussis resurgence. Although the whole-cell vaccine is still used, the trend is shifting toward a safer acellular vaccine, and efforts on improving their performance and the length of protective memory these generate will be discussed in this manuscript.

The current strategy for the development of vaccines is driven by the hypothesis that antibodies provide strong protection. As a consequence, most of the current acellular vaccines are highly safe and generate a rapid antibody response that is protective, albeit limited (68, 69). Importantly, infection triggers a complex and well-orchestrated sequence of responses involving many interacting components of innate and adaptive immunity, directed by several signaling pathways that present numerable known, and probably many more unknown, opportunities to interfere in the succession of events that can skew the resulting immune response.

Bordetellae harbor multiple mechanisms that allow them to modulate the host immune response (1, 70, 71). Some of the proteins that these organisms utilize to manipulate immune cells include adenylate cyclase toxin (ACT), a pore forming protein that leads to the deregulation of cAMP levels within target cells (72, 73); type 3 secretion system (T3SS), a needle-like structure that injects toxins within mammalian cells (74–76); a type 6 secretion system that uses a phage-like mechanism to inject molecules (77); pertussis toxin (PTX), which prevents G proteins from interacting with G protein-coupled receptors on the cell membrane and therefore interfering with intracellular communication (78–80); and filamentous hemagglutinin (FHA), which binds signaling receptors, enables adhesion to epithelial cells and interferes with cytokine production (81, 82). Based on these studies of various immunomodulators we can now begin to adjust the way we design preventative and responsive medications to fight bacterial infections in more effective ways.

A good understanding of the sequential reactions of the immune response (and bacterial manipulation of them) is key to improving the induction and maintenance of robust long-lasting protective immunity. Some of the *Bordetella* spp. virulence factors are already being investigated for treatments, such as PTX for human immunodeficiency virus (HIV) treatment (83–89). Understanding how we can alter bacterial ability to sense and respond to the host to modulate its response can lead to treatments and therapies that focus on the enhancement of more appropriate and effective host immune responses.

IMMUNOTHERAPY IN PREVENTION

Adjuvants

The *Bordetella pertussis* acellular vaccine has not completely blocked the spread of pertussis because it allows for colonization of the nasal cavity (48) and provides only temporary protection (13). Adjuvants are well-documented for their potential to increase vaccine performance, and some adjuvants such as CpG oligodeoxynuceotides or alum are commonly found in vaccine formulations (90, 91). There are a plethora of adjuvants that can potentiate the performance of a vaccine and can be classified into two main groups: Toll-like receptors agonists (92–94) and mucosal adjuvants (58, 95–97). These two distinct classes have been closely considered for their contributions to pertussis vaccines as well as therapeutics (98–103), yielding highly promising enhancing properties.

Toll-Like Receptors Agonists

Toll-Like Receptors (TLRs) are highly sophisticated sentinels that recognize specific pathogen-associated molecular patterns (PAMPs). The differential activation of TLRs is one of the main determinants for an efficient immune response against pathogens. Under this premise, researchers have been working on the addition of TLR agonists to vaccines with the expectation that activating different TLRs will command the type of T cell response produced (104) and will ultimately enhance host protective immunity (105).

One of the best studied Toll-Like Receptors is TLR2, which recognizes a broad spectrum of bacterial cell wall components, including lipopolypeptides, peptidoglycan, and lipochoic acids, that trigger different signals that shape the immune response against the bacterial threat (106). It has been demonstrated that the use of TLR2 agonists as adjuvants to already developed vaccines increases immunity, especially in neonates (93). This feature is highly relevant to the design of vaccines against diseases that primarily affect newborns and young infants (93). Moreover, TLR2 agonists in combination with the BCG vaccine can enhance protection against *Mycobacterium tuberculosis* (107), skewing the cellular response toward Th1 (100), and resulting in a more robust protective memory response, further promoting its use in vaccinology. TLR2 has been also correlated with an efficient response to *B. pertussis* infections (108), and some preliminary data has revealed that the use of these agonists enhances protection against infection by pertussis (58, 100). Altogether, these data suggest that TLR2 agonists may be promising candidates to combine with current or new vaccines to enhance the protective response.

Similarly, TLR4 appears a good candidate for vaccine enhancement because it recognizes lipopolysaccharide (LPS) molecules, which are commonly present on the surface of

most bacteria. Agonists of TLR4 enhance the performance of several vaccines including viral, bacterial, and even mycobacterial (109–113). One important aspect is its promotion of mucosal immunity (114–116), which is critical for the generation of protection against certain infections including gut and respiratory diseases like pertussis (117–119), although this increase is achieved via mucosal delivery of the vaccine rather than systemic (120). Molecular evidence has revealed that the addition of a TLR4 ligand to the acellular pertussis vaccine resulted in a shift from a Th2-dominant response to additional induction of Th17 (121, 122). The abundant immunological evidence that highlights the role of TLR4 in the immune response to *B. pertussis* (102, 123–130) indicates that TLR4 agonists are promising candidate for the generation of more robust protective immunity.

TLR5 (131) is also a highly plausible candidate to augment vaccine performance since it recognizes flagella, which are present in a multitude of bacterial species. Previous literature has indicated that ectopic expression of flagella in *Bordetella* spp. leads to faster clearance of the infection (132), and it was later revealed that TLR5 activates antigen-presenting cells, increasing T cell response (133) (*manuscript in preparation*), and may ultimately contribute to the more rapid clearance previously reported. In several other microorganisms, the addition of TLR5 agonists have resulted in an increased performance of the vaccine (134–141). Altogether these data suggest that TLR5 agonists could significantly increase the performance of the current acellular pertussis vaccine.

TLR7 recognizes single-stranded RNA (142–153) and has been demonstrated to be a promising vaccine adjuvant for protection against several microorganisms (154, 155). Similar to TLR2, the TLR7 agonist augments immunity in newborns, the most susceptible population (93, 102, 143, 156, 157). The addition of a TLR7 agonist to an alum-adjuvant of pertussis vaccine skewed the immune response toward Th1/Th17 and significantly decreased colonization (98), providing preliminary data to further pursue this agonist in other animal models.

Lastly, TLR9 recognizes unmethylated CpG oligodeoxynucleotides and promotes IL-6 secretion and consequent B cell activation (158–168). It has been demonstrated that enhancement of TLR9 receptors augment activity of antigen-presenting cells in neonates (93, 102, 169). Addition of a TLR9 agonist to the acellular pertussis vaccine resulted in greater stimulation of B and T cells and a shift to Th1, as well as higher antibody titers (81, 170–174), suggesting that an agonist of TLR9 is also a candidate to add to the current pertussis vaccines. These have the potential to be widely used agonists, as most of the current vaccine's efficacy is measured as an increase in antibody titers.

Altogether, these results demonstrate that TLR agonists are great candidates to be used as vaccine adjuvants to increase protective immunity. Interestingly, some of the TLR agonists substantially augment vaccine performance in newborns and infants, which represent the most susceptible population (93, 169) although there are substantial hurdles to applying this knowledge. Moreover, preliminary data obtained with TLR2, and TLR7 agonists demonstrate the improved performance of the current *B. pertussis* vaccine and indicates that the use of adjuvants can feasibly potentiate and augment the generation of protective immunity (58, 98, 100).

Mucosal Adjuvants

Adjuvants have been used to potentiate, enhance, or accelerate vaccine effects since the 1920s (105) and the field has greatly evolved since. Mucosal adjuvants include cholera toxin, heat-labile enterotoxin, and other compounds have been studied for their particular ability to increase protection on mucosal surfaces (175). These are of extreme importance, not only because of the aforementioned increase in vaccine performance, but also because the delivery method involving intranasal vaccination has a lot of potential for improving the delivery of the vaccine and increasing acceptance among needle-phobic population. In the following paragraphs we will detail the mechanisms of action and the data compiled for some of the most promising mucosal adjuvants.

Cholera toxin (CT) and heat-labile enterotoxin of *Escherichia coli* (LT) are highly antigenic; however, due to their toxicity, they are not ideal candidates for human therapies. Recently, safe forms of these toxins created via genetic manipulation have been utilized as adjuvants to enhance the function of mucosal vaccines (103, 176–181). The mechanism behind this augmented immune response induced by CT is an increase in the permeability of the mucosal epithelium, enhanced antigen presentation, the consequent promotion of dendritic cell maturation, increased IgA response, and finally, the generation of complex stimulatory and inhibitory effects on T cell proliferation and cytokine production such as IL-4, IL-5, IL-6, and IL-10 that skew the response toward a Th2-type (177, 182). CTA1 is the subunit responsible for the immunomodulatory activity in conjunction with ERdj5 in the endoplasmic reticulum, which is the target for CT. In the absence of ERdj5, mice failed to produce inflammatory cytokines, indicating that CT action requires ERdj5 (183). Similarly, the calcium-binding protein S100A4 is required for efficient antigen presentation and enhanced activity of CT, as it is necessary for the humoral and cellular response (184). CT has been tested as an adjuvant for pertussis vaccine and preliminary data suggests that it substantially improves mucosal protection by augmenting IgA levels (183, 185), and it has even been suggested that this adjuvant may be safe for use in humans (186, 187). Some studies have revealed that conjugation of CT with pertussis toxoid added to the current acellular vaccine (188) or Fimbriae (Fim2) (189) are highly promising candidates to improve the generation of protective immunity from these vaccines.

Similar to CT, the heat-labile enterotoxin from *E. coli* (LT) promotes an antigen-specific response inducing IgA antibodies, Th17 response, and the enhancement of long-lasting protective immunity (190) while also being safe for use in humans (191). LT promotes maturation of dendritic cells, antigen-specific IL-17 positive cells, and production of IL-1α, IL-1β, and IL-23 by dendritic cells. Trials in animals have revealed the efficacy of this adjuvant at enhancing mucosal response (192). LT promotes dendritic cell maturation enhancing IL-1β production through activation of caspase-1 and the NLRP3 inflammasome complex. Simultaneously, LT enhances LPS-induced IL-1α

and IL-23 expression through activation of ERK MAPK in dendritic cells inducing the development of Th17 T cells (193). Interestingly, LT derivatives LTK63 (non-toxic mutant of LT) and LTR72 (which retains partial enzymatic activity) revealed two distinct phenotypes characterized by stimulation of IL-12 and TNF-α production by macrophages, resulting in enhanced Th1 responses with the LTK63 adjuvants. In contrast, LTR72 suppresses LPS-induced IL-12 production, increases type 2 responses, inhibits Th1 response, and facilitates clearance of bacterial burden (194), demonstrating that both subunits of the toxin have particular activities that can be beneficial for the improvement of the current acellular pertussis vaccine.

Another mucosal adjuvant that is widely investigated is retinoic acid, a powerful immunomodulator that interferes with growth, differentiation, and other aspects of the cell life cycle. Importantly, retinoic acid is also essential in the generation of mucosal immunity, the promotion of tolerogenic effects, the generation of a robust innate and adaptive immune response, and moreover, it also acts as a negative regulator of IgE production (195–197). It has been hypothesized that retinoic acid plays a fundamental role in sustaining mucosal homeostasis by down-regulating IgE levels (197). Its performance as an adjuvant has been studied in several organisms and the plethora of results obtained have revealed that retinoic acid is a promising candidate to use as an adjuvant of mucosal vaccines by itself or encapsulated in nanoparticles (198–203). Unfortunately, its activity in conjunction with the pertussis vaccine has not yet been assessed.

The use of biopolymers in mucosally-administered vaccines has substantially improved the current vaccine formulations and has great potential for the future (204). Some of the presently investigated biopolymers include alginate (205–212) and gellan (213, 214). Although these are still in early stages of study, other biopolymers, such as chitosan (95–97, 215–232), starch (233), and β-glucan (234–241), have already been tested in animal trials with encouraging success. While the use of biopolymers is still rising, this area of investigation is highly promising, especially for enhancement of mucosal protection. Mucosal delivery has been explored for pertussis immunization from different approaches that have resulted in hopeful results in which Th17 response was enhanced and the animals were more robustly protected against challenge (58, 170, 242, 243).

To summarize, several mucosal adjuvants are being investigated, some of which are derived from toxins while still others are derived from biopolymers. Both act to enhance the performance of vaccines, particularly those that can be orally or intranasally delivered, usually in cases in which mucosal protection is a key component of immunity. However, these further demonstrate that different strategies and approaches can be used to improve the performance of the current vaccines to produce and enhance individual and herd immunity.

Novel Vaccination Strategies

The combination of BCG and acellular pertussis vaccination has been shown to reduce the mortality rate of pertussis (244–247). Immunological studies unraveling the underlying mechanism by which protection against pertussis is enhanced are necessary. Some groups have focused on the addition of antigens to the current vaccine in order to improve performance. After demonstrating via *in vitro* experiments that the autotransporter BrkA would be a good candidate to generate antibodies that kill *Bordetella* spp., BrkA has been tested as an adjuvant of the current acellular pertussis vaccine, the results of which revealed robust lung protection against infection with *B. pertussis* (248, 249). Two other autotransporters, Vag8 (250, 251) and SphB1, when added to the current pertussis vaccine resulted in improved protection against *B. pertussis* infection (252). Adenylate cyclase toxin (ACT), when added to a current vaccine formulation significantly decreased inflammation and increased the generation of protective immunity (253, 254). BcfA (colonization factor A) has been used as adjuvant in the current vaccine, and the preliminary data obtained with the murine model reveals that the addition of this adjuvant shifts the T cell response toward Th1/Th17 (255).

Live vaccines have the potential to induce strong mucosal protection, but suffer from concern about their risk. An exciting new vaccine candidate against *B. pertussis* is the live attenuated vaccine, BPZE1, which has been shown to induce a robust local B and T cell response (256–282) despite genetically engineered mutations that render it relatively safe (283, 284). Excitingly, phase I trials demonstrate that the intranasal formulation of the vaccine transiently colonizes the nasal cavity, leading to the generation of stronger immunity (264, 268).

Several groups are currently working on the development of outer membrane vesicles and outer membrane proteins in protection against *B. pertussis* as well as cross-protection against several *Bordetella* spp. and characterizing the immune response as well as protective immunity (285–295). In animal studies, immunization with outer membrane vesicles led to not only better humoral and cellular (Th17) memory, but also to a significant increase in IgA titers, which is one of the major hurdles of current vaccination strategies against this pathogen (296–298). It is important to highlight that the increase in IgA responses upon immunization with outer membrane vesicles is only obtained when these are administrated mucosally (299). The classic delivery for OMV's, which is subcutaneous or intraperitoneal immunization, does not induce IgA responses and this novel delivery method provides a great advance, as it can be administered with more ease and induces an even better immunological response. The increase in mucosal protection has led to efforts toward improved nasal delivery approaches and a thermostable spray containing outer membrane vesicles has been developed. This spray significantly improves delivery and decreases the discomfort other intranasal formulations might cause. Importantly, this delivery method still maintains all the outstanding qualities of the classical delivery of these purified outer membrane vesicles (300).

Finally, another highly promising strategy is focused on the disruption of bacterial ability to manipulate the host immune response. Under the premise that bacteria harbor mechanisms that allow them to sense and respond to host immunity, disrupting these pathways would allow for the generation of more robust protective immunity. A live attenuated vaccine in which immunomodulatory mechanisms are disrupted might confer

cross-protection against classical Bordetellae, which are known to share many antigens. Although this is only the first study for this method of vaccine design (*manuscript in revision*), this novel approach has great potential for the generation of new vaccine candidates and possibly therapeutics.

IMMUNOTHERAPY IN TREATMENT

LOS-Derived Oligosaccharide Glycoconjugates

Pertussis toxin (PTX) in an inactivated form (PTd) functions as a major protective antigen, stimulating production of toxin-neutralizing antibodies which can protect against damage caused by the toxin, but do not target the bacteria itself (301, 302); however, it also demonstrates possible partial reversion back to its toxic active form (303, 304), which may be responsible for the reactogenicity seen in a small percentage of vaccine recipients. It is also a secretory protein, which is only loosely associated with the cell and is therefore not an ideal target for bactericidal antibodies. A more effective target is an abundant surface component such as the endotoxin lipooligosaccharide (LOS), an LPS analog with a complete absence of the O-specific polysaccharide chain that is produced by several varieties of Gram-negative bacteria (305). LOS provides significant adjuvant properties via induction of IL-12 and 1L-1β that promote Th1 and Th17 responses, respectively (306, 307). It also displays pyrogenic, mitogenic, and endotoxic activity that necessitate its conjugation or conversion to a less destructive form prior to its use in a vaccine.

LOS conjugated to protein carriers filamentous hemagglutinin, bovine serum albumin, and tetanus toxoid (TTd) successfully induce a strong bactericidal response specific to LOS presented on the surface of *B. pertussis*, leading to complement-mediated destruction of the cell (90, 308, 309). These protein carriers are also surface components, like LOS, and the resulting surface-associated conjugate acts as a strong target for antibody action directed against *B. pertussis*.

Somewhat surprisingly, another conjugate iteration in which an LOS-derived oligosaccharide is covalently linked with the secretory protein PTX yields a uniquely non-toxic and immunogenic glycoconjugate that retains the antigenic properties of PTX while also inducing the production of bactericidal antibodies. The presumed linkage at the fetuin- and glycoprotein-binding sites of PTX inactivates the enzymatic activity of the protomer A and binding properties of oligomer B, demonstrated using *in vitro* assays (310). Although the use of LOS appears to be highly promising, *in vivo* studies still need to be done to assess pharmacological parameters of safety and biodistribution.

Cyclophilin Inhibitors

PTX is internalized in cells via endocytosis and then follows a retrograde transport system to the endoplasmic reticulum. The enzymatically active (A) subunit of PTX, PTS1, detaches from the rest of the toxin in the ER and unfolds due to its thermal instability. It is then transported into the cytosol with the help of cyclophilin (Cyps), an important protein folding helper enzyme that also is required to facilitate membrane translocation from early endosomes into the cytosol of various ADP-ribosylating toxins (311–313). Inhibiting Cyps activity has been shown to in turn inhibit membrane translocation and protect cells from intoxication with PTX and others (311).

Inhibition can be achieved via the approved immunosuppressive drug cyclosporine A (CsA), which specifically inhibits Cyps activity in mammalian cells by binding directly to Cyps and forming a ternary complex. It has been used as the primary agent in immunosuppressive regimens such as grafts and transplants since the 1980s. It is now suggested that CsA might interfere with the translocation of PTS1 from the ER into the cytosol; it may also play a role in reassembling the unfolded PTS1 subunit (311).

In vitro intoxication assays performed on CHO-K1 cells demonstrated that CsA-treated cells were protected from PTX intoxication. Interestingly, up to 50% of CsA is retained intracellularly, even in the absence of extracellular inhibitor, after 18 h (314). Thus, presumably, intracellular Cyps stay inhibited over a longer period of time, explaining the toxin-resistant phenotype. This is also concomitant with the long retention of CsA in different tissues observed after CsA administration in human patients (315, 316). This inhibitor was delivered orally during trials, but its use in a mucosal spray or as a directly injectable vaccine component has yet to be investigated.

FUTURE DIRECTIONS AND CONCLUSION

Since the years of our notoriously premature celebration of victory over infectious disease, there has been seemingly inexorable retaliation. There is now justifiable concern, shifting toward fear, about the combined threats of increasing antibiotic resistance and the failures of current vaccines due to factors including incomplete vaccine uptake, vaccine-driven evolution and other threats. However, recent advances in our understanding of immunology and the tools to manipulate it present hope for more rational targeted interventions that are focused on enhancing the natural host response. Similarly, improved understanding of strategies and mechanisms by which bacteria modulate the immune response provides new targets for treatment and prevention. In the coming years, we will likely witness an expansion in the field of immunotherapy promoted by a better understanding of the finely tuned interactions of bacteria and host.

AUTHOR CONTRIBUTIONS

MG: original idea of the manuscript, writing, and editing. HJ: writing and editing. EH: editing and final approval.

FUNDING

This work was supported by the National Institutes of Health (NIH) (Grant Nos. R21 AI142678-01, R21AI140399, and RO1GM113681) and by the National Institute of Allergy and

Infectious Diseases. This work has been also supported by the Catalyst Award (American Lung Association). The funders had no role in the study design, data collection, and interpretation, or the decision to submit the work for publication.

ACKNOWLEDGMENTS

The authors would like to acknowledge the members of the EH Lab for helpful and fruitful discussions and brainstorming.

REFERENCES

1. Gestal MC, Whitesides LT, Harvill ET. Integrated signaling pathways mediate *Bordetella* immunomodulation, persistence, and transmission. *Trends Microbiol.* (2019) 27:118–30. doi: 10.1016/j.tim.2018.09.010
2. Hancock RE, Nijnik A, Philpott DJ. Modulating immunity as a therapy for bacterial infections. *Nat Rev Microbiol.* (2012) 10:243–54. doi: 10.1038/nrmicro2745
3. Liu Y, Islam EA, Jarvis GA, Gray-Owen SD, Russell MW. Neisseria gonorrhoeae selectively suppresses the development of Th1 and Th2 cells, and enhances Th17 cell responses, through TGF-β-dependent mechanisms. *Mucosal Immunol.* (2012) 5:320–31. doi: 10.1038/mi.2012.12
4. Wolfe DN, Karanikas AT, Hester SE, Kennett MJ, Harvill ET. IL-10 induction by *Bordetella parapertussis* limits a protective IFN-gamma response. *J Immunol.* (2010) 184:1392–400. doi: 10.4049/jimmunol.0803045
5. Carbonetti NH. Immunomodulation in the pathogenesis of *Bordetella pertussis* infection and disease. *Curr Opin Pharmacol.* (2007) 7:272–8. doi: 10.1016/j.coph.2006.12.004
6. Tateda K, Ishii Y, Horikawa M, Matsumoto T, Miyairi S, Pechere JC, et al. The *Pseudomonas aeruginosa* autoinducer N-3-oxododecanoyl homoserine lactone accelerates apoptosis in macrophages and neutrophils. *Infect Immun.* (2003) 71:5785–93. doi: 10.1128/IAI.71.10.5785-5793.2003
7. Ritchie AJ, Yam AO, Tanabe KM, Rice SA, Cooley MA. Modification of *in vivo* and *in vitro* T- and B-cell-mediated immune responses by the *Pseudomonas aeruginosa* quorum-sensing molecule N-(3-oxododecanoyl)-L-homoserine lactone. *Infect Immun.* (2003) 71:4421–31. doi: 10.1128/IAI.71.8.4421-4431.2003
8. Sperandio V. Pathogens' adaptation to the human host. *Proc Natl Acad Sci USA.* (2018) 115:9342–3. doi: 10.1073/pnas.1813379115
9. Lustri BC, Sperandio, V, and Moreira, CG. Bacterial chat: intestinal metabolites and signals in host-microbiota-pathogen interactions. *Infect Immun.* (2017) 85:e00476-17. doi: 10.1128/IAI.00476-17
10. Bäumler AJ, Sperandio V. Interactions between the microbiota and pathogenic bacteria in the gut. *Nature.* (2016) 535:85–93. doi: 10.1038/nature18849
11. Kendall MM, Sperandio V. What a dinner party! mechanisms and functions of interkingdom signaling in host-pathogen associations. *MBio.* (2016) 7:e01748. doi: 10.1128/mBio.01748-15
12. Curtis MM, Sperandio V. A complex relationship: the interaction among symbiotic microbes, invading pathogens, and their mammalian host. *Mucosal Immunol.* (2011) 4:133–8. doi: 10.1038/mi.2010.89
13. Kilgore PE, Salim AM, Zervos MJ, and Schmitt HJ. Pertussis: microbiology, disease, treatment, and prevention. *Clin Microbiol Rev.* (2016) 29, 449–486. doi: 10.1128/CMR.00083-15
14. Domenech de Cellès M, Magpantay FM, King AA, and Rohani P. The pertussis enigma: reconciling epidemiology, immunology and evolution. *Proc Biol Sci.* (2016) 283:20152309. doi: 10.1098/rspb.2015.2309
15. Broutin H, Viboud C, Grenfell BT, Miller MA, and Rohani P. Impact of vaccination and birth rate on the epidemiology of pertussis: a comparative study in 64 countries. *Proc Biol Sci.* (2010) 277:3239–45. doi: 10.1098/rspb.2010.0994
16. Miyashita N, Akaike H, Teranishi H, Kawai Y, Ouchi K, Kato T, et al. Diagnostic value of symptoms and laboratory data for pertussis in adolescent and adult patients. *BMC Infect Dis.* (2013) 13:129. doi: 10.1186/1471-2334-13-129
17. Subissi L, Rodeghiero C, Martini H, Litzroth A, Huygen K, Leroux-Roels G, et al. Assessment of IgA anti-PT and IgG anti-ACT reflex testing to improve *Bordetella pertussis* serodiagnosis in recently vaccinated subjects. *Clin Microbiol Infect.* (2019) pii: S1198-743X(19)30528-2. doi: 10.1016/j.cmi.2019.10.001
18. Gil-Prieto R, Walter S, San-Román-Montero J, Marín-García P, González-Escalada A, Gil-de-Miguel A. Paediatric hospitalizations due to whooping cough in Spain (1997-2017). *Vaccine.* (2019) 37:6342–7. doi: 10.1016/j.vaccine.2019.09.017
19. Stefanelli P. Pertussis: identification, prevention and control. *Adv Exp Med Biol.* (2019). doi: 10.1007/5584_2019_408
20. Wu DX, Chen Q, Yao KH, Li L, Shi W, Ke JW, et al. Pertussis detection in children with cough of any duration. *BMC Pediatr.* (2019) 19:236. doi: 10.1186/s12887-019-1615-3
21. Rabi A, Rokni T, Bennaoui F, Rada N, El Idrissi Slitine N, Draiss G, et al. Epidemiology of pertussis in Marrakech and contribution of molecular diagnosis. *Infect Dis.* (2019) 51:703–5. doi: 10.1080/23744235.2019.1637537
22. Fumimoto R, Otsuka N, Kamiya H, Sunagawa T, Tanaka-Taya K, Kamachi K, et al. Seroprevalence of IgA and IgM antibodies to *Bordetella pertussis* in healthy Japanese donors: assessment for the serological diagnosis of pertussis. *PLoS ONE.* (2019) 14:e0219255. doi: 10.1371/journal.pone.0219255
23. Dou M, Macias N, Shen F, Bard JD, Domínguez DC, Li X. Rapid and accurate diagnosis of the respiratory disease pertussis on a point-of-care biochip. *EClinicalMedicine.* (2019) 8:72–7. doi: 10.1016/j.eclinm.2019.02.008
24. Dou M, Sanchez J, Tavakoli H, Gonzalez JE, Sun J, Dien Bard J, et al. A low-cost microfluidic platform for rapid and instrument-free detection of whooping cough. *Anal Chim Acta.* (2019) 1065:71–8. doi: 10.1016/j.aca.2019.03.001
25. Markey K, Douglas-Bardsley A, Asokanathan C, Fry NK, Barkoff AM, Bacci S, et al. Improvement in serological diagnosis of pertussis by external quality assessment. *J Med Microbiol.* (2019) 68:741–7. doi: 10.1099/jmm.0.000926
26. Damouni Shalabi R, Srugo I, Golan-Shany O, Kugelman A, Bamberger E. Respiratory viruses frequently mimic pertussis in young infants. *Pediatr Infect Dis J.* (2019) 38:e107–9. doi: 10.1097/INF.0000000000002223
27. Moosa F, du Plessis M, Wolter N, Carrim M, Cohen C, von Mollendorf C, et al. Challenges and clinical relevance of molecular detection of *Bordetella pertussis* in South Africa. *BMC Infect Dis.* (2019) 19:276. doi: 10.1186/s12879-019-3869-7
28. Tascini C, Carannante N, Sodano G, Tiberio C, Atripaldi L, Di Caprio G, et al. Neonatal pertussis diagnosis: low procalcitonin level and high lymphocyte count are able to discriminate pertussis from bacterial and viral infections. *New Microbiol.* (2019) 42:49–51.
29. Choi GS, Huh DH, Han SB, Ahn DH, Kang KR, Kim JA, et al. Enzyme-linked immunosorbent assay for detecting anti-pertussis toxin antibody in mouse. *Clin Exp Vaccine Res.* (2019) 8:64–9. doi: 10.7774/cevr.2019.8.1.64
30. Saiki-Macedo S, Valverde-Ezeta J, Cornejo-Tapia A, Castillo ME, Petrozzi-Helasvuo V., Aguilar-Luis MA, et al. Identfication of viral and bacterial etiologic agents of the pertussis-like syndrome in children under 5 years old hospitalized. *BMC Infect Dis.* (2019) 19:75. doi: 10.1186/s12879-019-3671-6
31. Di Matola T, Miele C, Coppola M, Fumi M, Pancione Y, Sale S, et al. Utility of peripheral blood smear in rapid diagnosis of Pertussis. *Int J Lab Hematol.* (2019) 41:e41–2. doi: 10.1111/ijlh.12947
32. Wadman M, You J. The vaccine wars. *Science.* (2017) 356:364–5. doi: 10.1126/science.356.6336.364
33. Paff ML, Nuismer SL, Ellington A, Molineux IJ, Bull JJ. Virus wars: using one virus to block the spread of another. *PeerJ.* (2016) 4:e2166. doi: 10.7717/peerj.2166
34. De Gregorio E, Rappuoli R. Vaccines for the future: learning from human immunology. *Microb Biotechnol.* (2012) 5:149–55. doi: 10.1111/j.1751-7915.2011.00276.x
35. Frishman WH. Ten secrets to a long life. *Am J Med.* (2019) 132:564–6. doi: 10.1016/j.amjmed.2018.12.020

36. Roush SW, Murphy TV, and Vaccine-Preventable Disease Table Working Group. Historical comparisons of morbidity and mortality for vaccine-preventable diseases in the United States. *JAMA*. (2007) 298:2155–63. doi: 10.1001/jama.298.18.2155
37. McKee M, Middleton J. Information wars: tackling the threat from disinformation on vaccines. *BMJ*. (2019) 365:l2144. doi: 10.1136/bmj.l2144
38. Rohani P, Drake JM. The decline and resurgence of pertussis in the US. *Epidemics*. (2011) 3:183–8. doi: 10.1016/j.epidem.2011.10.001
39. Goezsy B, Kato L. Sensitizing properties of *B. pertussis* in the mouse and rat. *Rev Can Biol*. (1964) 23:427–37.
40. Morrone G, Nunziata B, Picciotto L. [Immunitary response of the infant vaccinated with quadruple DPT-polio vaccine]. *Riv Ist Sieroter Ital*. (1959) 34:321–9.
41. Chen BL, Chou CT, Huang CT, Wang YT, Ko HH, Huang WC, et al. Studies on diphtheria-pertussis-tetanus combined immunization in children. II. Immune responses after the primary vaccination. *J Immunol*. (1957) 79:39–45.
42. Ipsen J, Bowen HE. Effects of routine immunization of children with triple vaccine (diphtheria-tetanus-pertussis). *Am J Public Health Nations Health*. (1955) 45:312–8. doi: 10.2105/AJPH.45.3.312
43. Albkrt A. Diphtheria-pertussis-tetanus immunizing of infants. *J Maine Med Assoc*. (1954) 45:126.
44. Combined immunization against diphtheria tetanus pertussis. *Squibb Memo*. (1947) 26:4–7.
45. Caboré RN, Maertens K, Dobly A, Leuridan E, Van Damme P, and Huygen K. Influence of maternal vaccination against diphtheria, tetanus, and pertussis on the avidity of infant antibody responses to a pertussis containing vaccine in Belgium. *Virulence*. (2017) 8: 1245–54. doi: 10.1080/21505594.2017.1296998
46. Gaillard ME, Bottero D, Zurita ME, Carriquiriborde F, Martin Aispuro P, Bartel E, et al. Pertussis maternal immunization: narrowing the knowledge gaps on the duration of transferred protective immunity and on vaccination frequency. *Front Immunol*. (2017) 8:1099. doi: 10.3389/fimmu.2017.01099
47. Gkentzi D, Katsakiori P, Marangos M, Hsia Y, Amirthalingam G, Heath PT, et al. Maternal vaccination against pertussis: a systematic review of the recent literature. *Arch Dis Child Fetal Neonatal Ed*. (2017) 102:F456–63. doi: 10.1136/archdischild-2016-312341
48. Warfel JM, Papin JF, Wolf RF, Zimmerman LI, Merkel TJ. Maternal and neonatal vaccination protects newborn baboons from pertussis infection. *J Infect Dis*. (2014) 210:604–10. doi: 10.1093/infdis/jiu090
49. Black RE, Cousens S, Johnson HL, Lawn JE, Rudan I, Bassani DG, et al. Global, regional, and national causes of child mortality in 2008: a systematic analysis. *Lancet*. (2010) 375:1969–87. doi: 10.1016/S0140-6736(10)60549-1
50. Wendelboe AM, Van Rie A, Salmaso S, Englund JA. Duration of immunity against pertussis after natural infection or vaccination. *Pediatr Infect Dis J*. (2005) 24:S58–61. doi: 10.1097/01.inf.0000160914.59160.41
51. Warfel JM, Zimmerman LI, Merkel TJ. Acellular pertussis vaccines protect against disease but fail to prevent infection and transmission in a nonhuman primate model. *Proc Natl Acad Sci USA*. (2014) 111:787–92. doi: 10.1073/pnas.1314688110
52. Zhang X, Weyrich LS, Lavine JS, Karanikas AT, Harvill ET. Lack of cross-protection against *Bordetella holmesii* after pertussis vaccination. *Emerg Infect Dis*. (2012) 18:1771–9. doi: 10.3201/eid1811.111544
53. Lavine J, Broutin H, Harvill ET, Bjørnstad ON. Imperfect vaccine-induced immunity and whooping cough transmission to infants. *Vaccine*. (2010) 29:11–6. doi: 10.1016/j.vaccine.2010.10.029
54. Long GH, Karanikas AT, Harvill ET, Read AF, and Hudson PJ. Acellular pertussis vaccination facilitates *Bordetella parapertussis* infection in a rodent model of bordetellosis. *Proc Biol Sci*. (2010) 277:2017–25. doi: 10.1098/rspb.2010.0010
55. Diavatopoulos DA, and Edwards KM. What is wrong with pertussis vaccine immunity? why immunological memory to pertussis is failing. *Cold Spring Harb Perspect Biol*. (2017) 9:a029553. doi: 10.1101/cshperspect.a029553
56. Burdin N, Handy LK, and Plotkin SA. What is wrong with pertussis vaccine immunity? the problem of waning effectiveness of pertussis vaccines. *Cold Spring Harb Perspect Biol*. (2017) 9:a029454. doi: 10.1101/cshperspect.a029454
57. Bancroft T, Dillon MB, da Silva Antunes R, Paul S, Peters B, Crotty S, et al. Th1 versus Th2 T cell polarization by whole-cell and acellular childhood pertussis vaccines persists upon re-immunization in adolescence and adulthood. *Cell Immunol*. (2016) 304–5:35–43. doi: 10.1016/j.cellimm.2016.05.002
58. Allen AC, Wilk MM, Misiak A, Borkner L, Murphy D, and Mills KHG. Sustained protective immunity against *Bordetella pertussis* nasal colonization by intranasal immunization with a vaccine-adjuvant combination that induces IL-17-secreting T_{RM} cells. *Mucosal Immunol*. (2018) 11:1763–76. doi: 10.1038/s41385-018-0080-x
59. Kapil P, Merkel TJ. Pertussis vaccines and protective immunity. *Curr Opin Immunol*. (2019) 59:72–8. doi: 10.1016/j.coi.2019.03.006
60. Lambert EE, Buisman AM, and van Els CACM. Superior *B. pertussis* specific CD4+ T-cell immunity imprinted by natural infection. *Adv Exp Med Biol*. (2019). doi: 10.1007/5584_2019_405
61. Wilk MM, Borkner L, Misiak A, Curham L, Allen AC, and Mills KHG. Immunization with whole cell but not acellular pertussis vaccines primes CD4 T_{RM} cells that sustain protective immunity against nasal colonization with *Bordetella pertussis*. *Emerg Microbes Infect*. (2019) 8:169–85. doi: 10.1080/22221751.2018.1564630
62. Raeven RH, Brummelman J, Pennings JL, Nijst OE, Kuipers B, Blok LE, et al. Molecular signatures of the evolving immune response in mice following a *Bordetella pertussis* infection. *PLoS ONE*. (2014) 9:e104548. doi: 10.1371/journal.pone.0104548
63. Wilk MM, Misiak A, McManus RM, Allen AC, Lynch MA, and Mills KHG. Lung CD4 Tissue-resident memory t cells mediate adaptive immunity induced by previous infection of mice with *Bordetella pertussis*. *J Immunol*. (2017) 199:233–43. doi: 10.4049/jimmunol.1602051
64. Bouchez V, Hegerle N, Strati F, Njamkepo E, Guiso N. New data on vaccine antigen deficient *Bordetella pertussis* isolates. *Vaccines*. (2015) 3:751–70. doi: 10.3390/vaccines3030751
65. Azarian T, Ali A, Johnson JA, Mohr D, Prosperi M, Veras NM, et al. Phylodynamic analysis of clinical and environmental *Vibrio cholerae* isolates from Haiti reveals diversification driven by positive selection. *MBio*. (2014) 5:e01824-14. doi: 10.1128/mBio.01824-14
66. Hegerle N, and Guiso N. Antibody-mediated inhibition of *Bordetella pertussis* adenylate cyclase-haemolysin-induced macrophage cytotoxicity is influenced by variations in the bacterial population. *Microbiology*. (2014) 160(Pt 5):962–9. doi: 10.1099/mic.0.074690-0
67. Octavia S, Maharjan RP, Sintchenko V, Stevenson G, Reeves PR, Gilbert GL, et al. Insight into evolution of *Bordetella pertussis* from comparative genomic analysis: evidence of vaccine-driven selection. *Mol Biol Evol*. (2011) 28:707–15. doi: 10.1093/molbev/msq245
68. Kirimanjeswara GS, Mann PB, Harvill ET. Role of antibodies in immunity to *Bordetella* infections. *Infect Immun*. (2003) 71:1719–24. doi: 10.1128/IAI.71.4.1719-1724.2003
69. Wolfe DN, Goebel EM, Bjornstad ON, Restif O, Harvill ET. The O antigen enables *Bordetella parapertussis* to avoid *Bordetella pertussis*-induced immunity. *Infect Immun*. (2007) 75:4972–9. doi: 10.1128/IAI.00763-07
70. Melvin JA, Scheller EV, Miller JF, Cotter PA. *Bordetella pertussis* pathogenesis: current and future challenges. *Nat Rev Microbiol*. (2014) 12:274–88. doi: 10.1038/nrmicro3235
71. Fedele G, Bianco M, Ausiello CM. The virulence factors of *Bordetella pertussis*: talented modulators of host immune response. *Arch Immunol Ther Exp*. (2013) 61:445–57. doi: 10.1007/s00005-013-0242-1
72. Gorgojo J, Scharrig E, Gómez RM, Harvill ET, Rodríguez ME. *Bordetella parapertussis* circumvents neutrophil extracellular bactericidal mechanisms. *PLoS ONE*. (2017) 12:e0169936. doi: 10.1371/journal.pone.0169936
73. Fedele G, Schiavoni I, Adkins I, Klimova N, and Sebo P. Invasion of dendritic cells, macrophages and neutrophils by the *Bordetella* adenylate cyclase toxin: a subversive move to fool host immunity. *Toxins*. (2017) 9:E293. doi: 10.3390/toxins9100293
74. Nicholson TL, Brockmeier SL, Loving CL, Register KB, Kehrli ME, Shore SM. The *Bordetella bronchiseptica* type III secretion system is required for persistence and disease severity but not transmission in swine. *Infect Immun*. (2014) 82:1092–103. doi: 10.1128/IAI.01115-13
75. Fennelly NK, Sisti F, Higgins SC, Ross PJ, van der Heide H, Mooi FR, et al. *Bordetella pertussis* expresses a functional type III secretion system that

subverts protective innate and adaptive immune responses. *Infect Immun.* (2008) 76:1257–66. doi: 10.1128/IAI.00836-07
76. Skinner JA, Pilione MR, Shen H, Harvill ET, Yuk MH. *Bordetella* type III secretion modulates dendritic cell migration resulting in immunosuppression and bacterial persistence. *J Immunol.* (2005) 175:4647–52. doi: 10.4049/jimmunol.175.7.4647
77. Coulthurst S. The Type VI secretion system: a versatile bacterial weapon. *Microbiology.* (2019) 165:503–15. doi: 10.1099/mic.0.000789
78. Starost LJ, Karassek S, Sano Y, Kanda T, Kim KS, Dobrindt U, et al. Pertussis Toxin Exploits host cell signaling pathways induced by meningitis-causing *E. coli* K1-RS218 and enhances adherence of monocytic THP-1 cells to human cerebral endothelial cells. *Toxins.* (2016) 8:E291. doi: 10.3390/toxins8100291
79. Suh HW, Sim YB, Park SH, Sharma N, Im HJ, Hong JS. Effect of pertussis toxin pretreated centrally on blood glucose level induced by stress. *Korean J Physiol Pharmacol.* (2016) 20:467–76. doi: 10.4196/kjpp.2016.20.5.467
80. Kirimanjeswara GS, Agosto LM, Kennett MJ, Bjornstad ON, Harvill ET. Pertussis toxin inhibits neutrophil recruitment to delay antibody-mediated clearance of *Bordetella pertussis*. *J Clin Invest.* (2005) 115:3594–601. doi: 10.1172/JCI24609
81. Bakhshaei P, Kazemi MH, Golara M, Abdolmaleki S, Khosravi-Eghbal R, Khoshnoodi J, et al. Investigation of the cellular immune response to recombinant fragments of filamentous hemagglutinin and pertactin of *Bordetella pertussis* in BALB/c mice. *J Interferon Cytokine Res.* (2018) 38:161–70. doi: 10.1089/jir.2017.0060
82. Villarino Romero R, Hasan S, Faé K, Holubova J, Geurtsen J, Schwarzer M, et al. *Bordetella pertussis* filamentous hemagglutinin itself does not trigger anti-inflammatory interleukin-10 production by human dendritic cells. *Int J Med Microbiol.* (2016) 306:38–47. doi: 10.1016/j.ijmm.2015.11.003
83. Rizzi C, Crippa MP, Jeeninga RE, Berkhout B, Blasi F, Poli G, et al. Pertussis toxin B-oligomer suppresses IL-6 induced HIV-1 and chemokine expression in chronically infected U1 cells via inhibition of activator protein 1. *J Immunol.* (2006) 176:999–1006. doi: 10.4049/jimmunol.176.2.999
84. Alfano M, Grivel JC, Ghezzi S, Corti D, Trimarchi M, Poli G, et al. Pertussis toxin B-oligomer dissociates T cell activation and HIV replication in CD4 T cells released from infected lymphoid tissue. *AIDS.* (2005) 19:1007–14. doi: 10.1097/01.aids.0000174446.40379.3b
85. Alfano M, Rizzi C, Corti D, Adduce L, Poli G. Bacterial toxins: potential weapons against HIV infection. *Curr Pharm Des.* (2005) 11:2909–26. doi: 10.2174/1381612054546725
86. Lapenta C, Spada M, Santini SM, Racca S, Dorigatti F, Poli G, et al. Pertussis toxin B-oligomer inhibits HIV infection and replication in hu-PBL-SCID mice. *Int Immunol.* (2005) 17:469–75. doi: 10.1093/intimm/dxh226
87. Alfano M, Vallanti G, Biswas P, Bovolenta C, Vicenzi E, Mantelli B, et al. The binding subunit of pertussis toxin inhibits HIV replication in human macrophages and virus expression in chronically infected promonocytic U1 cells. *J Immunol.* (2001) 166:1863–70. doi: 10.4049/jimmunol.166.3.1863
88. Alfano M, Pushkarsky T, Poli G, Bukrinsky M. The B-oligomer of pertussis toxin inhibits human immunodeficiency virus type 1 replication at multiple stages. *J Virol.* (2000) 74:8767–70. doi: 10.1128/JVI.74.18.8767-8770.2000
89. Alfano M, Schmidtmayerova H, Amella CA, Pushkarsky T, Bukrinsky M. The B-oligomer of pertussis toxin deactivates CC chemokine receptor 5 and blocks entry of M-tropic HIV-1 strains. *J Exp Med.* (1999) 190:597–605. doi: 10.1084/jem.190.5.597
90. Robbins JB, Schneerson R, Kubler-Kielb J, Keith JM, Trollfors B, Vinogradov E, et al. Toward a new vaccine for pertussis. *Proc Natl Acad Sci USA.* (2014) 111:3213–6. doi: 10.1073/pnas.1324149111
91. Coffman RL, Sher A, Seder RA. Vaccine adjuvants: putting innate immunity to work. *Immunity.* (2010) 33:492–503. doi: 10.1016/j.immuni.2010.10.002
92. Kumar S, Sunagar R, Gosselin E. Bacterial protein toll-like-receptor agonists: a novel perspective on vaccine adjuvants. *Front Immunol.* (2019) 10:1144. doi: 10.3389/fimmu.2019.01144
93. Surendran N, Simmons A, Pichichero ME. TLR agonist combinations that stimulate Th type I polarizing responses from human neonates. *Innate Immun.* (2018) 24:240–51. doi: 10.1177/1753425918771178
94. Ignacio BJ, Albin TJ, Esser-Kahn AP, Verdoes M. Toll-like receptor agonist conjugation: a chemical perspective. *Bioconjug Chem.* (2018) 29:587–603. doi: 10.1021/acs.bioconjchem.7b00808
95. Sinani G, Sessevmez M, Gök MK, Özgümüş S, Oya Alpar H, and Cevher E. Modified chitosan-based nanoadjuvants enhance immunogenicity of protein antigens after mucosal vaccination. *Int J Pharm.* (2019) 569:118592. doi: 10.1016/j.ijpharm.2019.118592
96. Mehrabi M, Montazeri H, Mohamadpour Dounighi N, Rashti A, Vakili-Ghartavol R. Chitosan-based nanoparticles in mucosal vaccine delivery. *Arch Razi Inst.* (2018) 73:165–76. doi: 10.22092/ari.2017.109235.1101
97. Moran HBT, Turley JL, Andersson M, Lavelle EC. Immunomodulatory properties of chitosan polymers. *Biomaterials.* (2018) 184:1–9. doi: 10.1016/j.biomaterials.2018.08.054
98. Misiak A, Leuzzi R, Allen AC, Galletti B, Baudner BC, D'Oro U, et al. Addition of a TLR7 agonist to an acellular pertussis vaccine enhances Th1 and Th17 responses and protective immunity in a mouse model. *Vaccine.* (2017) 35:5256–63. doi: 10.1016/j.vaccine.2017.08.009
99. Brummelman J, Wilk MM, Han WG, van Els CA, Mills KH. Roads to the development of improved pertussis vaccines paved by immunology. *Pathog Dis.* (2015) 73:ftv067. doi: 10.1093/femspd/ftv067
100. Dunne A, Mielke LA, Allen AC, Sutton CE, Higgs R, Cunningham CC, et al. A novel TLR2 agonist from *Bordetella pertussis* is a potent adjuvant that promotes protective immunity with an acellular pertussis vaccine. *Mucosal Immunol.* (2015) 8:607–17. doi: 10.1038/mi.2014.93
101. Dunne A, Marshall NA, Mills KH. TLR based therapeutics. *Curr Opin Pharmacol.* (2011) 11:404–11. doi: 10.1016/j.coph.2011.03.004
102. Higgins SC, Mills KH. TLR, NLR Agonists, and other immune modulators as infectious disease vaccine adjuvants. *Curr Infect Dis Rep.* (2010) 12:4–12. doi: 10.1007/s11908-009-0080-9
103. Pizza M, Giuliani MM, Fontana MR, Monaci E, Douce G, Dougan G, et al. Mucosal vaccines: non toxic derivatives of LT and CT as mucosal adjuvants. *Vaccine.* (2001) 19:2534–41. doi: 10.1016/S0264-410X(00)00553-3
104. Walsh KP, Mills KH. Dendritic cells and other innate determinants of T helper cell polarisation. *Trends Immunol.* (2013) 34:521–30. doi: 10.1016/j.it.2013.07.006
105. Di Pasquale A, Preiss SF, Tavares Da Silva, Garçon N. Vaccine adjuvants: from 1920 to 2015 and Beyond. *Vaccines.* (2015) 3:320–43. doi: 10.3390/vaccines3020320
106. Guo X, Wu N, Shang Y, Liu X, Wu T, Zhou Y, et al. The novel toll-like receptor 2 agonist SUP3 enhances antigen presentation and T cell activation by dendritic cells. *Front Immunol.* (2017) 8:158. doi: 10.3389/fimmu.2017.00158
107. Jiang L, Liu G, Ni W, Zhang N, Jie J, Xie F, et al. The combination of MBP and BCG-induced dendritic cell maturation through TLR2/TLR4 promotes Th1 activation *in vitro* and *vivo*. *Mediators Inflamm.* (2017) 2017:1953680. doi: 10.1155/2017/1953680
108. Asgarian-Omran H, Amirzargar AA, Zeerleder S, Mahdavi M, van Mierlo G, Solati S, et al. Interaction of *Bordetella pertussis* filamentous hemagglutinin with human TLR2: identification of the TLR2-binding domain. *APMIS.* (2015) 123:156–62. doi: 10.1111/apm.12332
109. Rostamian M, Bahrami F, Niknam HM. Vaccination with whole-cell killed or recombinant leishmanial protein and toll-like receptor agonists against Leishmania tropica in BALB/c mice. *PLoS ONE.* (2018) 13:e0204491. doi: 10.1371/journal.pone.0204491
110. Rostamian M, Niknam HM. Evaluation of the adjuvant effect of agonists of toll-like receptor 4 and 7/8 in a vaccine against leishmaniasis in BALB/c mice. *Mol Immunol.* (2017) 91:202–8. doi: 10.1016/j.molimm.2017.09.010
111. Lebedeva E, Bagaev A, Pichugin A, Chulkina M, Lysenko A, Tutykhina I, et al. The differences in immunoadjuvant mechanisms of TLR3 and TLR4 agonists on the level of antigen-presenting cells during immunization with recombinant adenovirus vector. *BMC Immunol.* (2018) 19:26. doi: 10.1186/s12865-018-0264-x
112. Goff PH, Hayashi T, He W, Yao S, Cottam HB, Tan GS, et al. Synthetic Toll-like receptor 4 (TLR4) and TLR7 ligands work additively via myd88 to induce protective antiviral immunity in mice. *J Virol.* (2017) 91:e01050-17. doi: 10.1128/JVI.01050-17
113. Su Y, Li D, Xing Y, Wang H, Wang J, Yuan J, et al. Subcutaneous immunization with fusion protein DnaJ-ΔA146Ply without additional adjuvants induces both humoral and cellular immunity against Pneumococcal infection partially depending on TLR4. *Front Immunol.* (2017) 8:686. doi: 10.3389/fimmu.2017.00686

114. Shibata N, Kunisawa J, Hosomi K, Fujimoto Y, Mizote K, Kitayama N, et al. Lymphoid tissue-resident Alcaligenes LPS induces IgA production without excessive inflammatory responses via weak TLR4 agonist activity. *Mucosal Immunol.* (2018) 11:693–702. doi: 10.1038/mi.2017.103
115. Reed SG, Hsu FC, Carter D, Orr MT. The science of vaccine adjuvants: advances in TLR4 ligand adjuvants. *Curr Opin Immunol.* (2016) 41:85–90. doi: 10.1016/j.coi.2016.06.007
116. Zaffaroni L, Peri F. Recent advances on Toll-like receptor 4 modulation: new therapeutic perspectives. *Future Med Chem.* (2018) 10:461–76. doi: 10.4155/fmc-2017-0172
117. Rolin O, Smallridge W, Henry M, Goodfield L, Place D, Harvill ET. Toll-like receptor 4 limits transmission of *Bordetella bronchiseptica*. *PLoS ONE.* (2014) 9:e85229. doi: 10.1371/journal.pone.0085229
118. Dadaglio G, Fayolle C, Zhang X, Ryffel B, Oberkampf M, Felix T, et al. Antigen targeting to CD11b+ dendritic cells in association with TLR4/TRIF signaling promotes strong CD8+ T cell responses. *J Immunol.* (2014) 193:1787–98. doi: 10.4049/jimmunol.1302974
119. Fedele G, Spensieri F, Palazzo R, Nasso M, Cheung GY, Coote JG, et al. *Bordetella pertussis* commits human dendritic cells to promote a Th1/Th17 response through the activity of adenylate cyclase toxin and MAPK-pathways. *PLoS ONE.* (2010) 5:e8734. doi: 10.1371/journal.pone.0008734
120. Boehm DT, Wolf MA, Hall JM, Wong TY, Sen-Kilic E, Basinger HD, et al. Intranasal acellular pertussis vaccine provides mucosal immunity and protects mice from. *NPJ Vaccines.* (2019) 4:40. doi: 10.1038/s41541-019-0136-2
121. Brummelman J, Raeven RH, Helm K, Pennings JL, Metz B, van Eden W, et al. Transcriptome signature for dampened Th2 dominance in acellular pertussis vaccine-induced CD4(+) T cell responses through TLR4 ligation. *Sci Rep.* (2016) 6:25064. doi: 10.1038/srep25064
122. Brummelman J, Helm K, Hamstra HJ, van der Ley P, Boog CJ, Han WG, et al. Modulation of the CD4(+) T cell response after acellular pertussis vaccination in the presence of TLR4 ligation. *Vaccine.* (2015) 33:1483–91. doi: 10.1016/j.vaccine.2015.01.063
123. Wolfe DN, Buboltz AM, Harvill ET. Inefficient Toll-like receptor-4 stimulation enables *Bordetella parapertussis* to avoid host immunity. *PLoS ONE.* (2009) 4:e4280. doi: 10.1371/journal.pone.0004280
124. Fedele G, Nasso M, Spensieri F, Palazzo R, Frasca L, Watanabe M, et al. Lipopolysaccharides from *Bordetella pertussis* and *Bordetella parapertussis* differently modulate human dendritic cell functions resulting in divergent prevalence of Th17-polarized responses. *J Immunol.* (2008) 181:208–16. doi: 10.4049/jimmunol.181.1.208
125. MacArthur I, Mann PB, Harvill ET, Preston A. IEIIS Meeting minireview: *Bordetella* evolution: lipid A and Toll-like receptor 4. *J Endotoxin Res.* (2007) 13:243–7. doi: 10.1177/0968051907082609
126. Kirimanjeswara GS, Mann PB, Pilione M, Kennett MJ, Harvill ET. The complex mechanism of antibody-mediated clearance of *Bordetella* from the lungs requires TLR4. *J Immunol.* (2005) 175:7504–11. doi: 10.4049/jimmunol.175.11.7504
127. Mann PB, Wolfe D, Latz E, Golenbock D, Preston A, Harvill ET. Comparative toll-like receptor 4-mediated innate host defense to *Bordetella* infection. *Infect Immun.* (2005) 73:8144–52. doi: 10.1128/IAI.73.12.8144-8152.2005
128. Mann PB, Elder KD, Kennett MJ, Harvill ET. Toll-like receptor 4-dependent early elicited tumor necrosis factor alpha expression is critical for innate host defense against *Bordetella bronchiseptica*. *Infect Immun.* (2004) 72:6650–8. doi: 10.1128/IAI.72.11.6650-6658.2004
129. McKay PF, King DF, Mann JF, Barinaga G, Carter D, Shattock RJ. TLR4 and TLR7/8 adjuvant combinations generate different vaccine antigen-specific immune outcomes in minipigs when administered via the ID or IN routes. *PLoS ONE.* (2016) 11:e0148984. doi: 10.1371/journal.pone.0148984
130. Mann PB, Kennett MJ, Harvill ET. Toll-like receptor 4 is critical to innate host defense in a murine model of bordetellosis. *J Infect Dis.* (2004) 189:833–6. doi: 10.1086/381898
131. Mizel SB, West AP, Hantgan RR. Identification of a sequence in human toll-like receptor 5 required for the binding of Gram-negative flagellin. *J Biol Chem.* (2003) 278:23624–9. doi: 10.1074/jbc.M303481200
132. Akerley BJ, Cotter PA, Miller JF. Ectopic expression of the flagellar regulon alters development of the *Bordetella*-host interaction. *Cell.* (1995) 80:611–20. doi: 10.1016/0092-8674(95)90515-4
133. Tremblay MM, Bilal MY, Houtman JC. Prior TLR5 induction in human T cells results in a transient potentiation of subsequent TCR-induced cytokine production. *Mol Immunol.* (2014) 57:161–70. doi: 10.1016/j.molimm.2013.09.002
134. Bargieri DY, Rosa DS, Braga CJ, Carvalho BO, Costa FT, Espíndola NM, et al. New malaria vaccine candidates based on the *Plasmodium vivax* merozoite surface protein-1 and the TLR-5 agonist Salmonella Typhimurium FliC flagellin. *Vaccine.* (2008) 26:6132–42. doi: 10.1016/j.vaccine.2008.08.070
135. Honko AN, Sriranganathan N, Lees CJ, Mizel SB. Flagellin is an effective adjuvant for immunization against lethal respiratory challenge with *Yersinia pestis*. *Infect Immun.* (2006) 74:1113–20. doi: 10.1128/IAI.74.2.1113-1120.2006
136. Letran SE, Lee SJ, Atif SM, Uematsu S, Akira S, McSorley SJ. TLR5 functions as an endocytic receptor to enhance flagellin-specific adaptive immunity. *Eur J Immunol.* (2011) 41:29–38. doi: 10.1002/eji.201040717
137. Taylor DN, Treanor JJ, Strout C, Johnson C, Fitzgerald T, Kavita U, et al. Induction of a potent immune response in the elderly using the TLR-5 agonist, flagellin, with a recombinant hemagglutinin influenza-flagellin fusion vaccine (VAX125, STF2.HA1 SI). *Vaccine.* (2011) 29:4897–902. doi: 10.1016/j.vaccine.2011.05.001
138. Kinnebrew MA, Ubeda C, Zenewicz LA, Smith N, Flavell RA, Pamer EG. Bacterial flagellin stimulates Toll-like receptor 5-dependent defense against vancomycin-resistant Enterococcus infection. *J Infect Dis.* (2010) 201:534–43. doi: 10.1086/650203
139. Kim JR, Holbrook BC, Hayward SL, Blevins LK, Jorgensen MJ, Kock ND, et al. Inclusion of flagellin during vaccination against influenza enhances recall responses in nonhuman primate neonates. *J Virol.* (2015) 89:7291–303. doi: 10.1128/JVI.00549-15
140. Song H, Xiong D, Wang J, Zhai X, Liang G. A porcine reproductive and respiratory syndrome virus vaccine candidate based on PRRSV glycoprotein 5 and the Toll-like receptor 5 agonist Salmonella typhimurium flagellin. *J Mol Microbiol Biotechnol.* (2015) 25:56–9. doi: 10.1159/000375496
141. Cunningham AL, Dang KM, Yu JJ, Guentzel MN, Heidner HW, Klose KE, et al. Enhancement of vaccine efficacy by expression of a TLR5 ligand in the defined live attenuated *Francisella tularensis* subsp. novicida strain U112ΔiglB::fljB. *Vaccine.* (2014) 32:5234–40. doi: 10.1016/j.vaccine.2014.07.038
142. Dowling DJ. Recent advances in the discovery and delivery of TLR7/8 agonists as vaccine adjuvants. *Immunohorizons.* (2018) 2:185–97. doi: 10.4049/immunohorizons.1700063
143. Dowling DJ, van Haren SD, Scheid A, Bergelson I, Kim D, Mancuso CJ, et al. TLR7/8 adjuvant overcomes newborn hyporesponsiveness to pneumococcal conjugate vaccine at birth. *JCI Insight.* (2017) 2:e91020. doi: 10.1172/jci.insight.91020
144. van Haren SD, Dowling DJ, Foppen W, Christensen D, Andersen P, Reed SG, et al. Age-specific adjuvant synergy: dual TLR7/8 and mincle activation of human newborn dendritic cells enables Th1 polarization. *J Immunol.* (2016) 197:4413–24. doi: 10.4049/jimmunol.1600282
145. van Haren SD, Ganapathi L, Bergelson I, Dowling DJ, Banks M, Samuels RC, et al. *In vitro* cytokine induction by TLR-activating vaccine adjuvants in human blood varies by age and adjuvant. *Cytokine.* (2016) 83:99–109. doi: 10.1016/j.cyto.2016.04.001
146. Ganapathi L, Van Haren S, Dowling DJ, Bergelson I, Shukla NM, Malladi SS, et al. The imidazoquinoline toll-like receptor-7/8 agonist hybrid-2 potently induces cytokine production by human newborn and adult leukocytes. *PLoS ONE.* (2015) 10:e0134640. doi: 10.1371/journal.pone.0134640
147. Wilkinson A, Lattmann E, Roces CB, Pedersen GK, Christensen D, Perrie Y. Lipid conjugation of TLR7 agonist Resiquimod ensures co-delivery with the liposomal Cationic Adjuvant Formulation 01 (CAF01) but does not enhance immunopotentiation compared to non-conjugated Resiquimod+CAF01. *J Control Release.* (2018) 291:1–10. doi: 10.1016/j.jconrel.2018.10.002
148. Collier MA, Junkins RD, Gallovic MD, Johnson BM, Johnson MM, Macintyre AN, et al. Acetalated dextran microparticles for codelivery of STING and TLR7/8 agonists. *Mol Pharm.* (2018) 15:4933–46. doi: 10.1021/acs.molpharmaceut.8b00579

149. McGowan DC, Herschke F, Khamlichi MD, Rosauro ML, Benedicto SMP, Pauwels F, et al. Design and synthesis of tetrahydropyridopyrimidine based toll-like receptor (TLR) 7/8 dual agonists. *Bioorg Med Chem Lett.* (2018) 28:3216–21. doi: 10.1016/j.bmcl.2018.08.015
150. Gadd AJR, Castelletto V, Kabova E, Shankland K, Perrie Y, Hamley I, et al. High potency of lipid conjugated TLR7 agonist requires nanoparticulate or liposomal formulation. *Eur J Pharm Sci.* (2018) 123:268–76. doi: 10.1016/j.ejps.2018.07.048
151. Vo HTM, Baudner BC, Sammicheli S, Iannacone M, D'Oro U, Piccioli D. Alum/toll-like receptor 7 adjuvant enhances the expansion of memory B cell compartment within the draining lymph node. *Front Immunol.* (2018) 9:641. doi: 10.3389/fimmu.2018.00641
152. Carignan D, Herblot S, Laliberté-Gagné M, Bolduc M, Duval M, Savard P, et al. Activation of innate immunity in primary human cells using a plant virus derived nanoparticle TLR7/8 agonist. *Nanomedicine.* (2018) 14:2317–27. doi: 10.1016/j.nano.2017.10.015
153. Van Hoeven N, Fox CB, Granger B, Evers T, Joshi SW, Nana GI, et al. A formulated TLR7/8 agonist is a flexible, highly potent and effective adjuvant for pandemic influenza vaccines. *Sci Rep.* (2017) 7:46426. doi: 10.1038/srep46426
154. Rubtsova K, Rubtsov AV, Halemano K, Li SX, Kappler JW, Santiago ML, et al. T cell production of IFNγ in response to TLR7/IL-12 stimulates optimal B cell responses to viruses. *PLoS ONE.* (2016) 11:e0166322. doi: 10.1371/journal.pone.0166322
155. Hu Y, Cong X, Chen L, Qi J, Wu X, Zhou M, et al. Synergy of TLR3 and 7 ligands significantly enhances function of DCs to present inactivated PRRSV antigen through TRIF/MyD88-NF-κB signaling pathway. *Sci Rep.* (2016) 6:23977. doi: 10.1038/srep23977
156. Aguado-Martínez A, Basto AP, Tanaka S, Ryser LT, Nunes TP, Ortega-Mora LM, et al. Immunization with a cocktail of antigens fused with OprI reduces Neospora caninum vertical transmission and postnatal mortality in mice. *Vaccine.* (2019) 37:473–83. doi: 10.1016/j.vaccine.2018.11.060
157. Buonsanti C, Balocchi C, Harfouche C, Corrente F, Galli Stampino L, Mancini F, et al. Novel adjuvant Alum-TLR7 significantly potentiates immune response to glycoconjugate vaccines. *Sci Rep.* (2016) 6:29063. doi: 10.1038/srep29063
158. Lu F, Mosley YC, Carmichael B, Brown DD, HogenEsch H. Formulation of aluminum hydroxide adjuvant with TLR agonists poly(I:C) and CpG enhances the magnitude and avidity of the humoral immune response. *Vaccine.* (2019) 37:1945–53. doi: 10.1016/j.vaccine.2019.02.033
159. Li N, Zhang L, Zheng B, Li W, Liu J, Zhang H, et al. RSV recombinant candidate vaccine G1F/M2 with CpG as an adjuvant prevents vaccine-associated lung inflammation, which may be associated with the appropriate types of immune memory in spleens and lungs. *Hum Vaccin Immunother.* (2019) 15:2684–94. doi: 10.1080/21645515.2019.1596710
160. Jin JW, Tang SQ, Rong MZ, Zhang MQ. Synergistic effect of dual targeting vaccine adjuvant with aminated β-glucan and CpG-oligodeoxynucleotides for both humoral and cellular immune responses. *Acta Biomater.* (2018) 78:211–23. doi: 10.1016/j.actbio.2018.08.002
161. Guan X, Chen J, Hu Y, Lin L, Sun P, Tian H, et al. Highly enhanced cancer immunotherapy by combining nanovaccine with hyaluronidase. *Biomaterials.* (2018) 171:198–206. doi: 10.1016/j.biomaterials.2018.04.039
162. Alkie TN, Taha-Abdelaziz K, Barjesteh N, Bavananthasivam J, Hodgins DC, Sharif S. Characterization of innate responses induced by PLGA encapsulated- and soluble TLR ligands *in vitro* and *in vivo* in chickens. *PLoS ONE.* (2017) 12:e0169154. doi: 10.1371/journal.pone.0169154
163. Hawksworth D. Advancing Freund's and addaVax adjuvant regimens using CpG oligodeoxynucleotides. *Monoclon Antib Immunodiagn Immunother.* (2018) 37:195–9. doi: 10.1089/mab.2018.0022
164. Lai CY, Yu GY, Luo Y, Xiang R, Chuang TH. Immunostimulatory activities of CpG-oligodeoxynucleotides in teleosts: toll-like receptors 9 and 21. *Front Immunol.* (2019) 10:179. doi: 10.3389/fimmu.2019.00179
165. Akkaya M, Akkaya B, Miozzo P, Rawat M, Pena M, Sheehan PW, et al. B cells produce type 1 IFNs in response to the TLR9 agonist CpG-A conjugated to cationic lipids. *J Immunol.* (2017) 199:931–40. doi: 10.4049/jimmunol.1700348
166. Ye L, Feng Z, Doycheva D, Malaguit J, Dixon B, Xu N, et al. CpG-ODN exerts a neuroprotective effect via the TLR9/pAMPK signaling pathway by activation of autophagy in a neonatal HIE rat model. *Exp Neurol.* (2018) 301(Pt A):70–80. doi: 10.1016/j.expneurol.2017.12.008
167. Zhang H, Yan T, Xu S, Feng S, Huang D, Fujita M, et al. Graphene oxide-chitosan nanocomposites for intracellular delivery of immunostimulatory CpG oligodeoxynucleotides. *Mater Sci Eng C Mater Biol Appl.* (2017) 73:144–51. doi: 10.1016/j.msec.2016.12.072
168. Zhang P, Dong S, Guo J, Yang Y, Liu C, Li B, et al. CpG-oligodeoxynucleotides improved irradiation-induced injuries by G-CSF and IL-6 up-regulation. *Cell Physiol Biochem.* (2017) 44:2368–77. doi: 10.1159/000486153
169. Ramirez A, Co M, Mathew A. CpG improves influenza vaccine efficacy in young adult but not aged mice. *PLoS ONE.* (2016) 11:e0150425. doi: 10.1371/journal.pone.0150425
170. Asokanathan C, Corbel M, Xing D. A CpG-containing oligodeoxynucleotide adjuvant for acellular pertussis vaccine improves the protective response against *Bordetella pertussis*. *Hum Vaccin Immunother.* (2013) 9:325–31. doi: 10.4161/hv.22755
171. Knight JB, Huang YY, Halperin SA, Anderson R, Morris A, Macmillan A, et al. Immunogenicity and protective efficacy of a recombinant filamentous haemagglutinin from *Bordetella pertussis*. *Clin Exp Immunol.* (2006) 144:543–51. doi: 10.1111/j.1365-2249.2006.03097.x
172. Boyd AP, Ross PJ, Conroy H, Mahon N, Lavelle EC, Mills KH. *Bordetella pertussis* adenylate cyclase toxin modulates innate and adaptive immune responses: distinct roles for acylation and enzymatic activity in immunomodulation and cell death. *J Immunol.* (2005) 175:730–8. doi: 10.4049/jimmunol.175.2.730
173. Maletto B, Ropolo A, Morón V, Pistoresi-Palencia MC. CpG-DNA stimulates cellular and humoral immunity and promotes Th1 differentiation in aged BALB/c mice. *J Leukoc Biol.* (2002) 72:447–54.
174. Gracia A, Polewicz M, Halperin SA, Hancock RE, Potter AA, Babiuk LA, et al. Antibody responses in adult and neonatal BALB/c mice to immunization with novel *Bordetella pertussis* vaccine formulations. *Vaccine.* (2011) 29:1595–604. doi: 10.1016/j.vaccine.2010.12.083
175. de Apostólico JS, Lunardelli VA, Coirada FC, Boscardin SB, Rosa DS. Adjuvants: classification, modus operandi, and licensing. *J Immunol Res.* (2016) 2016:1459394. doi: 10.1155/2016/1459394
176. Holmgren J, Adamsson J, Anjuère F, Clemens J, Czerkinsky C, Eriksson K, et al. Mucosal adjuvants and anti-infection and anti-immunopathology vaccines based on cholera toxin, cholera toxin B subunit and CpG DNA. *Immunol Lett.* (2005) 97:181–8. doi: 10.1016/j.imlet.2004.11.009
177. Bromander AK, Kjerrulf M, Holmgren J, Lycke, N. Cholera toxin enhances antigen presentation. *Adv Exp Med Biol.* (1995) 371B:1501–6.
178. Holmgren J, Czerkinsky C, Lycke N, Svennerholm AM. Strategies for the induction of immune responses at mucosal surfaces making use of cholera toxin B subunit as immunogen, carrier, and adjuvant. *Am J Trop Med Hyg.* (1994) 50:42–54.
179. Bromander AK, Kjerrulf M, Holmgren J, Lycke N. Cholera toxin enhances alloantigen presentation by cultured intestinal epithelial cells. *Scand J Immunol.* (1993) 37:452–8. doi: 10.1111/j.1365-3083.1993.tb03318.x
180. Holmgren J, Lycke N, Czerkinsky C. Cholera toxin and cholera B subunit as oral-mucosal adjuvant and antigen vector systems. *Vaccine.* (1993) 11:1179–84. doi: 10.1016/0264-410X(93)90039-Z
181. Holmgren J, Nordqvist S, Blomquist M, Jeverstam F, Lebens M, Raghavan S. Preclinical immunogenicity and protective efficacy of an oral *Helicobacter pylori* inactivated whole cell vaccine and multiple mutant cholera toxin: a novel and non-toxic mucosal adjuvant. *Vaccine.* (2018) 36:6223–30. doi: 10.1016/j.vaccine.2018.07.073
182. Lavelle EC, Jarnicki A, McNeela E, Armstrong ME, Higgins SC, Leavy O, et al. Effects of cholera toxin on innate and adaptive immunity and its application as an immunomodulatory agent. *J Leukoc Biol.* (2004) 75:756–63. doi: 10.1189/jlb.1103534
183. Kim MS, Yi EJ, Kim YI, Kim SH, Jung YS, Kim SR, et al. ERdj5 in innate immune cells is a crucial factor for the mucosal adjuvanticity of cholera toxin. *Front Immunol.* (2019) 10:1249. doi: 10.3389/fimmu.2019.01249
184. Sun JB, Holmgren J, Larena M, Terrinoni M, Fang Y, Bresnick AR, et al. Deficiency in calcium-binding protein S100A4 impairs the adjuvant action of cholera toxin. *Front Immunol.* (2017) 8:1119. doi: 10.3389/fimmu.2017.01119

185. Barati B, Ebrahimi F, Nazarian S. Production of chicken egg yolk antibody (IgY) against recombinant cholera toxin B subunit and evaluation of its prophylaxis potency in mice. *Iran J Immunol.* (2018) 15:47–58.
186. Isaka M, Komiya T, Takahashi M, Yasuda Y, Taniguchi T, Zhao Y, et al. Recombinant cholera toxin B subunit (rCTB) as a mucosal adjuvant enhances induction of diphtheria and tetanus antitoxin antibodies in mice by intranasal administration with diphtheria-pertussis-tetanus (DPT) combination vaccine. *Vaccine.* (2004) 22:3061–8. doi: 10.1016/j.vaccine.2004.02.019
187. Lee SF, Halperin SA, Salloum DF, MacMillan A, Morris A. Mucosal immunization with a genetically engineered pertussis toxin S1 fragment-cholera toxin subunit B chimeric protein. *Infect Immun.* (2003) 71:2272–5. doi: 10.1128/IAI.71.4.2272-2275.2003
188. Isaka M, Yasuda Y, Taniguchi T, Kozuka S, Matano K, Maeyama J, et al. Mucosal and systemic antibody responses against an acellular pertussis vaccine in mice after intranasal co-administration with recombinant cholera toxin B subunit as an adjuvant. *Vaccine.* (2003) 21:1165–73. doi: 10.1016/S0264-410X(02)00516-9
189. Olivera N, Castuma CE, Hozbor D, Gaillard ME, Rumbo M, Gómez RM. Immunization with the recombinant Cholera toxin B fused to Fimbria 2 protein protects against *Bordetella pertussis* infection. *Biomed Res Int.* (2014) 2014:421486. doi: 10.1155/2014/421486
190. Clements JD, Norton EB. The mucosal vaccine adjuvant LT(R192G/L211A) or dmLT. *mSphere.* (2018) 3:e00215-18. doi: 10.1128/mSphere.00215-18
191. Albert MJ, Haridas S, Ebenezer M, Raghupathy R, Khan I. Immunization with a double-mutant (R192G/L211A) of the heat-labile enterotoxin of escherichia coli offers partial protection against campylobacter jejuni in an adult mouse intestinal colonization model. *PLoS ONE.* (2015) 10:e0142090. doi: 10.1371/journal.pone.0142090
192. Chang YC, Chang CY, Tsai PS, Chiou HY, Jeng CR, Pang VF, et al. Efficacy of heat-labile enterotoxin B subunit-adjuvanted parenteral porcine epidemic diarrhea virus trimeric spike subunit vaccine in piglets. *Appl Microbiol Biotechnol.* (2018) 102:7499–507. doi: 10.1007/s00253-018-9110-6
193. Brereton CF, Sutton CE, Ross PJ, Iwakura Y, Pizza M, Rappuoli R, et al. *Escherichia coli* heat-labile enterotoxin promotes protective Th17 responses against infection by driving innate IL-1 and IL-23 production. *J Immunol.* (2011) 186:5896–906. doi: 10.4049/jimmunol.1003789
194. Ryan EJ, McNeela E, Pizza M, Rappuoli R, O'Neill L, Mills KH. Modulation of innate and acquired immune responses by Escherichia coli heat-labile toxin: distinct pro- and anti-inflammatory effects of the nontoxic AB complex and the enzyme activity. *J Immunol.* (2000) 165:5750–9. doi: 10.4049/jimmunol.165.10.5750
195. Coleman MM, Basdeo SA, Coleman AM, Cheallaigh CN, Peral de Castro C, McLaughlin AM, et al. All-trans retinoic acid augments autophagy during intracellular bacterial infection. *Am J Respir Cell Mol Biol.* (2018) 59:548–556. doi: 10.1165/rcmb.2017-0382OC
196. Oliveira LM, Teixeira FME, Sato MN. Impact of retinoic acid on immune cells and inflammatory diseases. *Mediators Inflamm.* (2018) 2018:3067126. doi: 10.1155/2018/3067126
197. Seo GY, Lee JM, Jang YS, Kang SG, Yoon SI, Ko HJ, et al. Mechanism underlying the suppressor activity of retinoic acid on IL4-induced IgE synthesis and its physiological implication. *Cell Immunol.* (2017) 322:49–55. doi: 10.1016/j.cellimm.2017.10.001
198. Bezerra IPS, Costa-Souza BLS, Carneiro G, Ferreira LAM, de Matos Guedes HL, Rossi-Bergmann B. Nanoencapsulated retinoic acid as a safe tolerogenic adjuvant for intranasal vaccination against cutaneous leishmaniasis. *Vaccine.* (2019) 37:3660–7. doi: 10.1016/j.vaccine.2019.05.043
199. Mwanza-Lisulo M, Kelly P. Potential for use of retinoic acid as an oral vaccine adjuvant. *Philos Trans R Soc Lond B Biol Sci.* (2015) 370:20140145. doi: 10.1098/rstb.2014.0145
200. Lisulo MM, Kapulu MC, Banda R, Sinkala E, Kayamba V, Sianongo S, et al. Adjuvant potential of low dose all-trans retinoic acid during oral typhoid vaccination in Zambian men. *Clin Exp Immunol.* (2014) 175:468–75. doi: 10.1111/cei.12238
201. Tan X, Sande JL, Pufnock JS, Blattman JN, Greenberg PD. Retinoic acid as a vaccine adjuvant enhances CD8+ T cell response and mucosal protection from viral challenge. *J Virol.* (2011) 85:8316–27. doi: 10.1128/JVI.00781-11
202. Qiang Y, Xu J, Yan C, Jin H, Xiao T, Yan N, et al. Butyrate and retinoic acid imprint mucosal-like dendritic cell development synergistically from bone marrow cells. *Clin Exp Immunol.* (2017) 189:290–7. doi: 10.1111/cei.12990
203. Raverdeau M, Mills KH. Modulation of T cell and innate immune responses by retinoic acid. *J Immunol.* (2014) 192:2953–8. doi: 10.4049/jimmunol.1303245
204. Torres-Sangiao E, Holban AM, Gestal MC. Advanced nanobiomaterials: vaccines, diagnosis and treatment of infectious diseases. *Molecules.* (2016) 21:E867. doi: 10.3390/molecules21070867
205. Alagpulinsa DA, Cao JJL, Driscoll RK, Sîrbulescu RF, Penson MFE, Sremac M, et al. Alginate-microencapsulation of human stem cell-derived β cells with CXCL12 prolongs their survival and function in immunocompetent mice without systemic immunosuppression. *Am J Transplant.* (2019) 19:1930–40. doi: 10.1111/ajt.15308
206. Ibe MI, Odimegwu DC, Onuigbo EB. Alginate-coated chitosan microparticles encapsulating an oral plasmid-cured live *Salmonella enterica* serovar Gallinarum vaccine cause a higher expression of interferon-gamma in chickens compared to the parenteral live vaccine. *Avian Pathol.* (2019) 48:423–28. doi: 10.1080/03079457.2019.1616673
207. Minakshi P, Ghosh M, Brar B, Kumar R, Lambe UP, Ranjan K, et al. Nano-antimicrobials: a new paradigm for combating mycobacterial resistance. *Curr Pharm Des.* (2019) 25:1554–79. doi: 10.2174/1381612825666190620094041
208. Vaghasiya K, Eram A, Sharma A, Ray E, Adlakha S, Verma RK. Alginate microspheres elicit innate M1-inflammatory response in macrophages leading to bacillary killing. *AAPS PharmSciTech.* (2019) 20:241. doi: 10.1208/s12249-019-1458-0
209. Coelho-Rocha ND, de Castro CP, de Jesus LCL, Leclercq SY, de Cicco Sandes SH, Nunes AC, et al. Microencapsulation of lactic acid bacteria improves the gastrointestinal delivery and *in situ* expression of recombinant fluorescent protein. *Front Microbiol.* (2018) 9:2398. doi: 10.3389/fmicb.2018.02398
210. Kordbacheh E, Nazarian S, Hajizadeh A, Sadeghi D. Entrapment of LTB protein in alginate nanoparticles protects against Enterotoxigenic *Escherichia coli*. *APMIS.* (2018) 126:320–8. doi: 10.1111/apm.12815
211. Lee J, Kim YM, Kim JH, Cho CW, Jeon JW, Park JK, et al. Nasal delivery of chitosan/alginate nanoparticle encapsulated bee (*Apis mellifera*) venom promotes antibody production and viral clearance during porcine reproductive and respiratory syndrome virus infection by modulating T cell related responses. *Vet Immunol Immunopathol.* (2018) 200:40–51. doi: 10.1016/j.vetimm.2018.04.006
212. Yuan J, Guo L, Wang S, Liu D, Qin X, Zheng L, et al. Preparation of self-assembled nanoparticles of ε-polylysine-sodium alginate: a sustained-release carrier for antigen delivery. *Colloids Surf B Biointerfaces.* (2018) 171:406–12. doi: 10.1016/j.colsurfb.2018.07.058
213. Wu H, Bao Y, Wang X, Zhou D, Wu W. Alkyl polyglycoside, a highly promising adjuvant in intranasal split influenza vaccines. *Hum Vaccin Immunother.* (2017) 13:1–9. doi: 10.1080/21645515.2016.1278098
214. Bacon A, Makin J, Sizer PJ, Jabbal-Gill I, Hinchcliffe M, Illum L, et al. Carbohydrate biopolymers enhance antibody responses to mucosally delivered vaccine antigens. *Infect Immun.* (2000) 68:5764–70. doi: 10.1128/IAI.68.10.5764-5770.2000
215. Bagheripour MJ, Ebrahimi F, Hajizade A, Nazarian S. Immunogenicity evaluation of rBoNT/E nanovaccine after mucosal administration. *Iran J Basic Med Sci.* (2019) 22:353–9.
216. Díaz AG, Quinteros DA, Paolicchi FA, Rivero MA, Palma SD, Pardo RP, et al. Mucosal immunization with polymeric antigen BLSOmp31 using alternative delivery systems against *Brucella ovis* in rams. *Vet Immunol Immunopathol.* (2019) 209:70–7. doi: 10.1016/j.vetimm.2019.02.005
217. Ghaffari Marandi BH, Zolfaghari MR, Kazemi R, Motamedi MJ, Amani J. Immunization against *Vibrio cholerae*, ETEC, and EHEC with chitosan nanoparticle containing LSC chimeric protein. *Microb Pathog.* (2019) 134:103600. doi: 10.1016/j.micpath.2019.103600
218. Kole S, Qadiri SSN, Shin SM, Kim WS, Lee J, Jung SJ. Nanoencapsulation of inactivated-viral vaccine using chitosan nanoparticles: evaluation of its protective efficacy and immune modulatory effects in olive flounder (*Paralichthys olivaceus*) against viral haemorrhagic septicaemia virus (VHSV) infection. *Fish Shellfish Immunol.* (2019) 91:136–47. doi: 10.1016/j.fsi.2019.05.017

219. Korupalli C, Pan WY, Yeh CY, Chen PM, Mi FL, Tsai HW, et al. Single-injecting, bioinspired nanocomposite hydrogel that can recruit host immune cells *in situ* to elicit potent and long-lasting humoral immune responses. *Biomaterials.* (2019) 216:119268. doi: 10.1016/j.biomaterials.2019.119268
220. Muralidharan A, Russell MS, Larocque L, Gravel C, Sauvé S, Chen Z, et al. Chitosan alters inactivated respiratory syncytial virus vaccine elicited immune responses without affecting lung histopathology in mice. *Vaccine.* (2019) 37:4031–9. doi: 10.1016/j.vaccine.2019.06.003
221. Senevirathne A, Hewawaduge C, Hajam IA, Lalsiamthara J, Lee JH. Intranasally administered anti-Brucella subunit vaccine formulation induces protective immune responses against nasal Brucella challenge. *Vet Microbiol.* (2019) 228:112–8. doi: 10.1016/j.vetmic.2018.11.022
222. Singh A, Nisaa K, Bhattacharyya S, Mallick AI. Immunogenicity and protective efficacy of mucosal delivery of recombinant hcp of *Campylobacter jejuni* type VI secretion system (T6SS) in chickens. *Mol Immunol.* (2019) 111:182–97. doi: 10.1016/j.molimm.2019.04.016
223. Soh SH, Shim S, Im YB, Park HT, Cho CS, Yoo HS. Induction of Th2-related immune responses and production of systemic IgA in mice intranasally immunized with *Brucella abortus* malate dehydrogenase loaded chitosan nanoparticles. *Vaccine.* (2019) 37:1554–64. doi: 10.1016/j.vaccine.2019.02.005
224. Zhang J, Fu X, Zhang Y, Zhu W, Zhou Y, Yuan G, et al. Chitosan and anisodamine improve the immune efficacy of inactivated infectious spleen and kidney necrosis virus vaccine in Siniperca chuatsi. *Fish Shellfish Immunol.* (2019) 89:52–60. doi: 10.1016/j.fsi.2019.03.040
225. Hojatizade M, Soleymani M, Tafaghodi M, Badiee A, Chavoshian O, Jaafari MR. Chitosan nanoparticles loaded with whole and soluble leishmania antigens, and evaluation of their immunogenecity in a mouse model of leishmaniasis. *Iran J Immunol.* (2018) 15:281–93. doi: 10.22034/IJI.2018.39397
226. Huang T, Song X, Jing J, Zhao K, Shen Y, Zhang X, et al. Chitosan-DNA nanoparticles enhanced the immunogenicity of multivalent DNA vaccination on mice against *Trueperella pyogenes* infection. *J Nanobiotechnol.* (2018) 16:8. doi: 10.1186/s12951-018-0337-2
227. Malik A, Gupta M, Mani R, Gogoi H, Bhatnagar R. Trimethyl chitosan nanoparticles encapsulated protective antigen protects the mice against anthrax. *Front Immunol.* (2018) 9:562. doi: 10.3389/fimmu.2018.00562
228. Sun B, Yu S, Zhao D, Guo S, Wang X, Zhao K. Polysaccharides as vaccine adjuvants. *Vaccine.* (2018) 36:5226–34. doi: 10.1016/j.vaccine.2018.07.040
229. Lebre F, Bento D, Ribeiro J, Colaço M, Borchard G, de Lima MCP, et al. Association of chitosan and aluminium as a new adjuvant strategy for improved vaccination. *Int J Pharm.* (2017) 527:103–14. doi: 10.1016/j.ijpharm.2017.05.028
230. Spinner JL, Oberoi HS, Yorgensen YM, Poirier DS, Burkhart DJ, Plante M, et al. Methylglycol chitosan and a synthetic TLR4 agonist enhance immune responses to influenza vaccine administered sublingually. *Vaccine.* (2015) 33:5845–53. doi: 10.1016/j.vaccine.2015.08.086
231. Torlak E, Sert D. Antibacterial effectiveness of chitosan-propolis coated polypropylene films against foodborne pathogens. *Int J Biol Macromol.* (2013) 60:52–5. doi: 10.1016/j.ijbiomac.2013.05.013
232. Kang ML, Kang SG, Jiang HL, Guo DD, Lee DY, Rayamahji N, et al. Chitosan microspheres containing *Bordetella bronchiseptica* antigens as novel vaccine against atrophic rhinitis in pigs. *J Microbiol Biotechnol.* (2008) 18:1179–85.
233. de Paula Oliveira Santos B, Trentini MM, Machado RB, Rúbia Nunes Celes M, Kipnis A, Petrovsky N, et al. Advax4 delta inulin combination adjuvant together with ECMX, a fusion construct of four protective mTB antigens, induces a potent Th1 immune response and protects mice against *Mycobacterium tuberculosis* infection. *Hum Vaccin Immunother.* (2017) 13:2967–76. doi: 10.1080/21645515.2017.1368598
234. Horst G, Levine R, Chick R, Hofacre C. Effects of beta-1,3-glucan (AletaTM) on vaccination response in broiler chickens. *Poult Sci.* (2019) 98:1643–7. doi: 10.3382/ps/pey523
235. Wang H, Yang B, Wang Y, Liu F, Fernández-Tejada A, Dong S. β-Glucan as an immune activator and a carrier in the construction of a synthetic MUC1 vaccine. *Chem Commun.* (2018) 55:253–6. doi: 10.1039/C8CC07691J
236. Whelan AO, Flick-Smith HC, Homan J, Shen ZT, Carpenter Z, Khoshkenar P, et al. Protection induced by a Francisella tularensis subunit vaccine delivered by glucan particles. *PLoS ONE.* (2018) 13:e0200213. doi: 10.1371/journal.pone.0200213
237. Hung CY, Zhang H, Castro-Lopez N, Ostroff GR, Khoshlenar P, Abraham A, et al. Glucan-chitin particles enhance Th17 response and improve protective efficacy of a multivalent antigen (rCpa1) against pulmonary *Coccidioides posadasii* infection. *Infect Immun.* (2018) 86:e00070-18. doi: 10.1128/IAI.00070-18
238. Bundle DR, Paszkiewicz E, Elsaidi HRH, Mandal SS, Sarkar S. A three component synthetic vaccine containing a β-mannan T-cell peptide epitope and a β-glucan dendritic cell ligand. *Molecules.* (2018) 23:E1961. doi: 10.3390/molecules23081961
239. Ferreira LG, Endrighi M, Lisenko KG, de Oliveira MRD, Damasceno MR, Claudino JA, et al. Oat beta-glucan as a dietary supplement for dogs. *PLoS ONE.* (2018) 13:e0201133. doi: 10.1371/journal.pone.0201133
240. Deepe GS, Buesing WR, Ostroff GR, Abraham A, Specht CA, Huang H, et al. Vaccination with an alkaline extract of Histoplasma capsulatum packaged in glucan particles confers protective immunity in mice. *Vaccine.* (2018) 36:3359–67. doi: 10.1016/j.vaccine.2018.04.047
241. Jin Y, Li P, Wang F. β-glucans as potential immunoadjuvants: a review on the adjuvanticity, structure-activity relationship and receptor recognition properties. *Vaccine.* (2018) 36:5235–44. doi: 10.1016/j.vaccine.2018.07.038
242. Li P, Asokanathan C, Liu F, Khaing KK, Kmiec D, Wei X, et al. PLGA nano/micro particles encapsulated with pertussis toxoid (PTd) enhances Th1/Th17 immune response in a murine model. *Int J Pharm.* (2016) 513:183–90. doi: 10.1016/j.ijpharm.2016.08.059
243. Shi W, Kou Y, Jiang H, Gao F, Kong W, Su W, et al. Novel intranasal pertussis vaccine based on bacterium-like particles as a mucosal adjuvant. *Immunol Lett.* (2018) 198:26–32. doi: 10.1016/j.imlet.2018.03.012
244. Claesson MH. Immunological links to nonspecific effects of DTwP and BCG vaccines on infant mortality. *J Trop Med.* (2011) 2011:706304. doi: 10.1155/2011/706304
245. Nascimento IP, Dias WO, Quintilio W, Hsu T, Jacobs WR, Leite LC. Construction of an unmarked recombinant BCG expressing a pertussis antigen by auxotrophic complementation: protection against *Bordetella pertussis* challenge in neonates. *Vaccine.* (2009) 27:7346–51. doi: 10.1016/j.vaccine.2009.09.043
246. Nascimento IP, Dias WO, Quintilio W, Christ AP, Moraes JF, Vancetto MD, et al. Neonatal immunization with a single dose of recombinant BCG expressing subunit S1 from pertussis toxin induces complete protection against *Bordetella pertussis* intracerebral challenge. *Microbes Infect.* (2008) 10:198–202. doi: 10.1016/j.micinf.2007.10.010
247. Nascimento IP, Dias WO, Mazzantini RP, Miyaji EN, Gamberini M, Quintilio W, et al. Recombinant *Mycobacterium bovis* BCG expressing pertussis toxin subunit S1 induces protection against an intracerebral challenge with live *Bordetella pertussis* in mice. *Infect Immun.* (2000) 68:4877–83. doi: 10.1128/IAI.68.9.4877-4883.2000
248. Cainelli Gebara VC, Risoléo L, Lopes AP, Ferreira VR, Quintilio W, Lépine F, et al. Adjuvant and immunogenic activities of the 73kDa N-terminal alpha-domain of BrkA autotransporter and Cpn60/60kDa chaperonin of *Bordetella pertussis*. *Vaccine.* (2007) 25:621–9. doi: 10.1016/j.vaccine.2006.08.033
249. Oliver DC, Fernandez RC. Antibodies to BrkA augment killing of *Bordetella pertussis*. *Vaccine.* (2001) 20:235–41. doi: 10.1016/S0264-410X(01)00269-9
250. Marr N, Shah NR, Lee R, Kim EJ, Fernandez RC. *Bordetella pertussis* autotransporter Vag8 binds human C1 esterase inhibitor and confers serum resistance. *PLoS ONE.* (2011) 6:e20585. doi: 10.1371/journal.pone.0020585
251. Finn TM, Amsbaugh DF. Vag8, a *Bordetella pertussis* bvg-regulated protein. *Infect Immun.* (1998) 66:3985–9.
252. Suzuki K, Shinzawa N, Ishigaki K, Nakamura K, Abe H, Fukui-Miyazaki A, et al. Protective effects of *in vivo*-expressed autotransporters against *Bordetella pertussis* infection. *Microbiol Immunol.* (2017) 61:371–9. doi: 10.1111/1348-0421.12504
253. Boehm DT, Hall JM, Wong TY, DiVenere AM, Sen-Kilic E, Bevere JR, et al. Evaluation of adenylate cyclase toxoid antigen in acellular pertussis vaccines by using a *Bordetella pertussis* challenge model in mice. *Infect Immun.* (2018) 86:e00857-17. doi: 10.1128/IAI.00857-17
254. Wang X, Gray MC, Hewlett EL, Maynard JA. The *Bordetella* adenylate cyclase repeat-in-toxin (RTX) domain is immunodominant

and elicits neutralizing antibodies. *J Biol Chem.* (2015) 290:23025. doi: 10.1074/jbc.A114.585281
255. Jennings-Gee J, Quataert S, Ganguly T, D'Agostino R, Deora R, Dubey P. The adjuvant *Bordetella* colonization factor A attenuates alum-induced Th2 responses and enhances *Bordetella pertussis* clearance from mouse lungs. *Infect Immun.* (2018) 86:e00935-17. doi: 10.1128/IAI.00935-17
256. Scanlon KM, Skerry C, Carbonetti NH. Novel therapies for the treatment of pertussis disease. *Pathog Dis.* (2015) 73:ftv074. doi: 10.1093/femspd/ftv074
257. Skerry CM, Mahon BP. A live, attenuated *Bordetella pertussis* vaccine provides long-term protection against virulent challenge in a murine model. *Clin Vaccine Immunol.* (2011) 18:187–93. doi: 10.1128/CVI.00371-10
258. Skerry CM, Cassidy JP, English K, Feunou-Feunou P, Locht C, Mahon BP. A live attenuated *Bordetella pertussis* candidate vaccine does not cause disseminating infection in gamma interferon receptor knockout mice. *Clin Vaccine Immunol.* (2009) 16:1344–51. doi: 10.1128/CVI.00082-09
259. Brennan MJ. A new whooping cough vaccine that may prevent colonization and transmission. *Vaccines.* (2017) 5:E43. doi: 10.3390/vaccines5040043
260. Locht C, Papin JF, Lecher S, Debrie AS, Thalen M, Solovay K, et al. Live attenuated pertussis vaccine BPZE1 protects baboons against *Bordetella pertussis* disease and infection. *J Infect Dis.* (2017) 216:117–24. doi: 10.1093/infdis/jix254
261. Locht C. Live pertussis vaccines will they protect against carriage and spread of pertussis? *Clin Microbiol Infect.* (2016) 22(Suppl. 5):S96–102. doi: 10.1016/j.cmi.2016.05.029
262. Locht C. Pertussis: where did we go wrong and what can we do about it? *J Infect.* (2016) 72(Suppl.): S34–40. doi: 10.1016/j.jinf.2016.04.020
263. Feunou PF, Kammoun H, Debrie AS, Locht C. Heterologous prime-boost immunization with live attenuated *B. pertussis* BPZE1 followed by acellular pertussis vaccine in mice. *Vaccine.* (2014) 32:4281–8. doi: 10.1016/j.vaccine.2014.06.019
264. Jahnmatz M, Amu S, Ljungman M, Wehlin L, Chiodi F, Mielcarek N, et al. B-cell responses after intranasal vaccination with the novel attenuated *Bordetella pertussis* vaccine strain BPZE1 in a randomized phase I clinical trial. *Vaccine.* (2014) 32:3350–6. doi: 10.1016/j.vaccine.2014.04.048
265. Lim A, Ng JK, Locht C, Alonso S. Protective role of adenylate cyclase in the context of a live pertussis vaccine candidate. *Microbes Infect.* (2014) 16:51–60. doi: 10.1016/j.micinf.2013.10.002
266. Schiavoni I, Fedele G, Quattrini A, Bianco M, Schnoeller C, Openshaw PJ, et al. Live attenuated *B. pertussis* BPZE1 rescues the immune functions of Respiratory Syncytial virus infected human dendritic cells by promoting Th1/Th17 responses. *PLoS ONE.* (2014) 9:e100166. doi: 10.1371/journal.pone.0100166
267. Schnoeller C, Roux X, Sawant D, Raze D, Olszewska W, Locht C, et al. Attenuated *Bordetella pertussis* vaccine protects against respiratory syncytial virus disease via an IL-17-dependent mechanism. *Am J Respir Crit Care Med.* (2014) 189:194–202. doi: 10.1164/rccm.201307-1227OC
268. Thorstensson R, Trollfors B, Al-Tawil N, Jahnmatz M, Bergström J, Ljungman M, et al. A phase I clinical study of a live attenuated *Bordetella pertussis* vaccine–BPZE1; a single centre, double-blind, placebo-controlled, dose-escalating study of BPZE1 given intranasally to healthy adult male volunteers. *PLoS ONE.* (2014) 9:e83449. doi: 10.1371/journal.pone.0083449
269. Kammoun H, Roux X, Raze D, Debrie AS, De Filette M, Ysenbaert T, et al. Immunogenicity of live attenuated *B. pertussis* BPZE1 producing the universal influenza vaccine candidate M2e. *PLoS ONE.* (2013) 8:e59198. doi: 10.1371/journal.pone.0059198
270. Kammoun H, Feunou PF, Foligne B, Debrie AS, Raze D, Mielcarek N, et al. Dual mechanism of protection by live attenuated *Bordetella pertussis* BPZE1 against *Bordetella bronchiseptica* in mice. *Vaccine.* (2012) 30:5864–70. doi: 10.1016/j.vaccine.2012.07.005
271. Li R, Cheng C, Chong SZ, Lim AR, Goh YF, Locht C, et al. Attenuated *Bordetella pertussis* BPZE1 protects against allergic airway inflammation and contact dermatitis in mouse models. *Allergy.* (2012) 67:1250–8. doi: 10.1111/j.1398-9995.2012.02884.x
272. Fedele G, Bianco M, Debrie AS, Locht C, Ausiello CM. Attenuated *Bordetella pertussis* vaccine candidate BPZE1 promotes human dendritic cell CCL21-induced migration and drives a Th1/Th17 response. *J Immunol.* (2011) 186:5388–96. doi: 10.4049/jimmunol.1003765
273. Li R, Lim A, Alonso S. Attenuated *Bordetella pertussis* BPZE1 as a live vehicle for heterologous vaccine antigens delivery through the nasal route. *Bioeng Bugs.* (2011) 2:315–9. doi: 10.4161/bbug.2.6.18167
274. Li R, Lim A, Ow ST, Phoon MC, Locht C, Chow VT, et al. Development of live attenuated *Bordetella pertussis* strains expressing the universal influenza vaccine candidate M2e. *Vaccine.* (2011) 29:5502–11. doi: 10.1016/j.vaccine.2011.05.052
275. Feunou PF, Bertout J, Locht C. T- and B-cell-mediated protection induced by novel, live attenuated pertussis vaccine in mice. Cross protection against parapertussis. *PLoS ONE.* (2010) 5:e10178. doi: 10.1371/journal.pone.0010178
276. Feunou PF, Kammoun H, Debrie AS, Mielcarek N, Locht C. Long-term immunity against pertussis induced by a single nasal administration of live attenuated *B. pertussis* BPZE1. *Vaccine.* (2010) 28:7047–53. doi: 10.1016/j.vaccine.2010.08.017
277. Kavanagh H, Noone C, Cahill E, English K, Locht C, Mahon BP. Attenuated *Bordetella pertussis* vaccine strain BPZE1 modulates allergen-induced immunity and prevents allergic pulmonary pathology in a murine model. *Clin Exp Allergy.* (2010) 40:933–41. doi: 10.1111/j.1365-2222.2010.03459.x
278. Li R, Lim A, Phoon MC, Narasaraju T, Ng JK, Poh WP, et al. Attenuated *Bordetella pertussis* protects against highly pathogenic influenza A viruses by dampening the cytokine storm. *J Virol.* (2010) 84:7105–13. doi: 10.1128/JVI.02542-09
279. Mielcarek N, Debrie AS, Mahieux S, Locht C. Dose response of attenuated *Bordetella pertussis* BPZE1-induced protection in mice. *Clin Vaccine Immunol.* (2010) 17:317–24. doi: 10.1128/CVI.00322-09
280. Feunou PF, Ismaili J, Debrie AS, Huot L, Hot D, Raze D, et al. Genetic stability of the live attenuated *Bordetella pertussis* vaccine candidate BPZE1. *Vaccine.* (2008) 26:5722–7. doi: 10.1016/j.vaccine.2008.08.018
281. Ho SY, Chua SQ, Foo DG, Locht C, Chow VT, Poh CL, et al. Highly attenuated *Bordetella pertussis* strain BPZE1 as a potential live vehicle for delivery of heterologous vaccine candidates. *Infect Immun.* (2008) 76:111–9. doi: 10.1128/IAI.00795-07
282. Mielcarek N, Debrie AS, Raze D, Bertout J, Rouanet C, Younes AB, et al. Live attenuated B. *pertussis* as a single-dose nasal vaccine against whooping cough. *PLoS Pathog.* (2006) 2:e65. doi: 10.1371/journal.ppat.0020065
283. Debrie AS, Coutte L, Raze D, Mooi F, Alexander F, Gorringe A, et al. Construction and evaluation of *Bordetella pertussis* live attenuated vaccine strain BPZE1 producing Fim3. *Vaccine.* (2018) 36:1345–52. doi: 10.1016/j.vaccine.2018.02.017
284. Solans L, Debrie AS, Borkner L, Aguiló N, Thiriard A, Coutte L, et al. IL-17-dependent SIgA-mediated protection against nasal *Bordetella pertussis* infection by live attenuated BPZE1 vaccine. *Mucosal Immunol.* (2018) 11:1753–62. doi: 10.1038/s41385-018-0073-9
285. Gasperini G, Biagini M, Arato V, Gianfaldoni C, Vadi A, Norais N, et al. Outer Membrane Vesicles (OMV)-based and proteomics-driven antigen selection identifies novel factors contributing to epithelial cells. *Mol Cell Proteomics.* (2018) 17:205–15. doi: 10.1074/mcp.RA117.000045
286. Gasperini G, Biagini M, Arato V, Gianfaldoni C, Vadi A, Norais N, et al. Outer Membrane Vesicles (OMV)-based and proteomics-driven antigen selection identifies novel factors contributing to *Bordetella pertussis* adhesion to epithelial cells. *Mol Cell Proteomics.* (2017) 17:205–15.
287. Saito M, Odanaka K, Otsuka N, Kamachi K, Watanabe M. Development of vaccines against pertussis caused by *Bordetella holmesii* using a mouse intranasal challenge model. *Microbiol Immunol.* (2016) 60:599–608. doi: 10.1111/1348-0421.12409
288. Bottero D, Zurita ME, Gaillard ME, Bartel E, Vercellini C, Hozbor D. Membrane vesicles derived from *Bordetella bronchiseptica*: active constituent of a new vaccine against infections caused by this pathogen. *Appl Environ Microbiol.* (2018) 84:e01877-17. doi: 10.1128/AEM.01877-17
289. Bottero D, Zurita ME, Gaillard ME, Bartel E, Vercellini C, Hozbor D. Membrane vesicles derived from *Bordetella bronchiseptica*: active constituent of a new vaccine against infections caused by this pathogen. *Appl Environ Microbiol.* (2017) 84:e01877-17.
290. Bottero D, Gaillard ME, Zurita E, Moreno G, Martinez DS, Bartel E, et al. Characterization of the immune response induced by pertussis OMVs-based vaccine. *Vaccine.* (2016) 34:3303–9. doi: 10.1016/j.vaccine.2016.04.079

291. Gaillard ME, Bottero D, Errea A, Ormazábal M, Zurita ME, Moreno G, et al. Acellular pertussis vaccine based on outer membrane vesicles capable of conferring both long-lasting immunity and protection against different strain genotypes. *Vaccine.* (2014) 32:931–7. doi: 10.1016/j.vaccine.2013.12.048
292. Ormazábal M, Bartel E, Gaillard ME, Bottero D, Errea A, Zurita ME, et al. Characterization of the key antigenic components of pertussis vaccine based on outer membrane vesicles. *Vaccine.* (2014) 32:6084–90. doi: 10.1016/j.vaccine.2014.08.084
293. Bottero D, Gaillard ME, Errea A, Moreno G, Zurita E, Pianciola L, et al. Outer membrane vesicles derived from *Bordetella parapertussis* as an acellular vaccine against *Bordetella parapertussis* and *Bordetella pertussis* infection. *Vaccine.* (2013) 31:5262–8. doi: 10.1016/j.vaccine.2013.08.059
294. Gaillard ME, Bottero D, Castuma CE, Basile LA, Hozbor D. Laboratory adaptation of *Bordetella pertussis* is associated with the loss of type three secretion system functionality. *Infect Immun.* (2011) 79:3677–82. doi: 10.1128/IAI.00136-11
295. Roberts R, Moreno G, Bottero D, Gaillard ME, Fingermann M, Graieb A, et al. Outer membrane vesicles as acellular vaccine against pertussis. *Vaccine.* (2008) 26:4639–46. doi: 10.1016/j.vaccine.2008.07.004
296. Raeven RH, Brummelman J, Pennings JLA, van der Maas L, Helm K, Tilstra WA, et al. Molecular and cellular signatures underlying superior immunity against *Bordetella pertussis* upon pulmonary vaccination. *Mucosal Immunol.* (2018) 11:979–93. doi: 10.1038/mi.2017.81
297. Raeven RH, van der Maas L, Tilstra W, Uittenbogaard JP, Bindels TH, Kuipers BA, et al. Immunoproteomic profiling of *Bordetella pertussis* outer membrane vesicle vaccine reveals broad and balanced humoral immunogenicity. *J Proteome Res.* (2015) 14:2929–42. doi: 10.1021/acs.jproteome.5b00258
298. Raeven RH, Brummelman J, Pennings JL, van der Maas L, Tilstra W, Helm K, et al. *Bordetella pertussis* outer membrane vesicle vaccine confers equal efficacy in mice with milder inflammatory responses compared to a whole-cell vaccine. *Sci Rep.* (2016) 6:38240. doi: 10.1038/srep38240
299. Raeven RHM, Brummelman J, Pennings JLA, van der Maas L, Helm K, Tilstra WA, et al. Molecular and cellular signatures underlying superior immunity against *Bordetella pertussis* upon pulmonary vaccination. *Mucosal Immunol.* (2018) 11:979–93. doi: 10.1038/mi.2017.110
300. Kanojia G, Raeven RHM, van der Maas L, Bindels THE, van Riet E, Metz B, et al. Development of a thermostable spray dried outer membrane vesicle pertussis vaccine for pulmonary immunization. *J Control Release.* (2018) 286:167–78. doi: 10.1016/j.jconrel.2018.07.035
301. Weiss AA, Patton AK, Millen SH, Chang SJ, Ward JI, Bernstein DI. Acellular pertussis vaccines and complement killing of *Bordetella pertussis*. *Infect Immun.* (2004) 72:7346–51. doi: 10.1128/IAI.72.12.7346-7351.2004
302. Coutte L, Locht C. Investigating pertussis toxin and its impact on vaccination. *Future Microbiol.* (2015) 10:241–54. doi: 10.2217/fmb.14.123
303. Isbrucker RA, Bliu A, Prior F. Modified binding assay for improved sensitivity and specificity in the detection of residual pertussis toxin in vaccine preparations. *Vaccine.* (2010) 28:2687–92. doi: 10.1016/j.vaccine.2010.01.040
304. Quentin-Millet MJ, Arminjon F, Danve B, Cadoz M, Armand J. Acellular pertussis vaccines: evaluation of reversion in a nude mouse model. *J Biol Stand.* (1988) 16:99–108. doi: 10.1016/0092-1157(88)90037-6
305. Kilár A, Dörnyei Á, Kocsis B. Structural characterization of bacterial lipopolysaccharides with mass spectrometry and on- and off-line separation techniques. *Mass Spectrom Rev.* (2013) 32:90–117. doi: 10.1002/mas.21352
306. Higgs R, Higgins SC, Ross PJ, Mills KH. Immunity to the respiratory pathogen *Bordetella pertussis*. *Mucosal Immunol.* (2012) 5:485–500. doi: 10.1038/mi.2012.54
307. Mahon BP, Ryan MS, Griffin F, Mills KH. Interleukin-12 is produced by macrophages in response to live or killed *Bordetella pertussis* and enhances the efficacy of an acellular pertussis vaccine by promoting induction of Th1 cells. *Infect Immun.* (1996) 64:5295–301.
308. Kubler-Kielb J, Vinogradov E, Lagergård T, Ginzberg A, King JD, Preston A, et al. Oligosaccharide conjugates of *Bordetella pertussis* and bronchiseptica induce bactericidal antibodies, an addition to pertussis vaccine. *Proc Natl Acad Sci USA.* (2011) 108:4087–92. doi: 10.1073/pnas.1100782108
309. Niedziela T, Letowska I, Lukasiewicz J, Kaszowska M, Czarnecka A, Kenne L, et al. Epitope of the vaccine-type *Bordetella pertussis* strain 186 lipooligosaccharide and antiendotoxin activity of antibodies directed against the terminal pentasaccharide-tetanus toxoid conjugate. *Infect Immun.* (2005) 73:7381–9. doi: 10.1128/IAI.73.11.7381-7389.2005
310. Koj S, Ługowski C, Niedziela T. [*Bordetella pertussis* lipooligosaccharide-derived neoglycoconjugates - new components of pertussis vaccine]. *Postepy Hig Med Dosw (Online)* (2015) 69:1013–30.
311. Ernst K, Eberhardt N, Mittler AK, Sonnabend M, Anastasia A, Freisinger S, et al. Pharmacological cyclophilin inhibitors prevent intoxication of mammalian cells with *Bordetella pertussis* toxin. *Toxins.* (2018) 10:E181. doi: 10.3390/toxins10050181
312. Kaiser E, Pust S, Kroll C, Barth H. Cyclophilin A facilitates translocation of the *Clostridium botulinum* C2 toxin across membranes of acidified endosomes into the cytosol of mammalian cells. *Cell Microbiol.* (2009) 11:780–95. doi: 10.1111/j.1462-5822.2009.01291.x
313. Lang AE, Ernst K, Lee H, Papatheodorou P, Schwan C, Barth H, et al. The chaperone Hsp90 and PPIases of the cyclophilin and FKBP families facilitate membrane translocation of *Photorhabdus luminescens* ADP-ribosyltransferases. *Cell Microbiol.* (2014) 16:490–503. doi: 10.1111/cmi.12228
314. Shitara Y, Takeuchi K, Nagamatsu Y, Wada S, Sugiyama Y, Horie T. Long-lasting inhibitory effects of cyclosporin A, but not tacrolimus, on OATP1B1- and OATP1B3-mediated uptake. *Drug Metab Pharmacokinet.* (2012) 27:368–78. doi: 10.2133/dmpk.DMPK-11-RG-096
315. Fabre I, Fabre G, Lena N, Cano JP. Kinetics of uptake and intracellular binding of Cyclosporine A in RAJI cells, *in vitro*. *Biochem Pharmacol.* (1986) 35:4261–6. doi: 10.1016/0006-2952(86)90704-5
316. Bertault-Pérès P, Maraninchi D, Carcassonne Y, Cano JP, Barbet J. Clinical pharmacokinetics of ciclosporin A in bone marrow transplantation patients. *Cancer Chemother Pharmacol.* (1985) 15:76–81. doi: 10.1007/BF00257300

Conflict of Interest: The authors declare that the research was conducted in the absence of any commercial or financial relationships that could be construed as a potential conflict of interest.

frontiers in Immunology

MINI REVIEW
published: 10 January 2020
doi: 10.3389/fimmu.2019.02997

Recombinant Influenza Vaccines: Saviors to Overcome Immunodominance

*Nimitha R. Mathew and Davide Angeletti**

Department of Microbiology and Immunology, Institute of Biomedicine, University of Gothenburg, Gothenburg, Sweden

It has been almost a decade since the 2009 influenza A virus pandemic hit the globe causing significant morbidity and mortality. Nonetheless, annual influenza vaccination, which elicits antibodies mainly against the head region of influenza hemagglutinin (HA), remains as the mainstay to combat and reduce symptoms of influenza infection. Influenza HA is highly antigenically variable, thus limiting vaccine efficacy. In addition, the variable HA head occupies the upper strata of the immunodominance hierarchy, thereby clouding the antibody response toward subdominant epitopes, which are usually conserved across different influenza strains. Isolation of monoclonal antibodies from individuals recognizing such epitopes has facilitated the development of recombinant vaccines that focus the adaptive immune response toward conserved, protective targets. Here, we review some significant leaps in recombinant vaccine development, which could possibly help to overcome B cell and antibody immunodominance and provide heterosubtypic immunity to influenza A virus.

Keywords: influenza A virus, immunodominance, vaccines, B cells, antibodies

OPEN ACCESS

Edited by:
Giuseppe Andrea Sautto,
University of Georgia, United States

Reviewed by:
Ali Ellebedy,
Washington University in St. Louis, United States
Gene Tan,
J. Craig Venter Institute, United States

****Correspondence:***
Davide Angeletti
davide.angeletti@gu.se

Specialty section:
This article was submitted to Vaccines and Molecular Therapeutics, a section of the journal Frontiers in Immunology

Received: *18 October 2019*
Accepted: *06 December 2019*
Published: *10 January 2020*

Citation:
Mathew NR and Angeletti D (2020) Recombinant Influenza Vaccines: Saviors to Overcome Immunodominance. Front. Immunol. 10:2997. doi: 10.3389/fimmu.2019.02997

INTRODUCTION

Influenza viruses belong to the family of Orthomyxoviridae and consists of A, B, C, and D types. Types A and B are currently circulating among humans (1–4). Influenza causes significant morbidity (30–50 million cases yearly) and mortality, with infection-associated respiratory deaths in the range of 4–8.8 per 100,000 individuals, posing heavy socioeconomic burden to society (5). Annual vaccination remains as the mainstay to prevent influenza infection, but, according to Centers for Disease Control and Prevention, it is effective only in 20–70% of the population, depending on season (6). Based on antigenic and phylogenetic properties of influenza surface glycoproteins, hemagglutinin (HA), and neuraminidase (NA), there are 18 HA (H1–H18), and 11 NA (N1–N11) Influenza A virus (IAV) serotypes and two influenza B of B/Victoria and B/Yamagata lineages (7, 8). HA is further divided into two phylogenetic groups. The current seasonal flu vaccines are either trivalent or quadrivalent containing HA from circulating H1N1, H3N2, and B/Victoria lineage or both influenza B lineages (9). IAV possess an error prone RNA polymerase, which results in mutations in surface antigens, leading to antigenic drift and antibodies being no longer effective. Therefore, it is necessary to update and administer vaccines every year by forecasting the drifted strains. In addition, the annual vaccination becomes ineffective during pandemic outbreaks, in which a new viral strain of zoonotic origin acquires the ability to replicate in humans (10, 11).

HA is the most abundant glycoprotein on the influenza virion surface and is crucial for host viral entry by binding to the terminal sialic acid residues on epithelial cells, resulting in fusion of viral and host cell membranes. HA is a trimer consisting of a globular head, harboring the receptor binding site, and an elongated stem region (12). Even though stem-specific B cells and antibodies are generated during infection and vaccination, the HA head is the main target of neutralizing antibodies. However, possibly due to its immunodominance (13), the head is subjected to higher rate of evolution (2.2–4.4 times) than the stem (14, 15). Intriguingly, while in animals, at least 12 mutations are necessary to drive full escape from immune sera (16), in humans, it appears that the polyclonal response can be extremely focused on one antigenic site (17–19). For example, in a circulating span of 35 years in humans, a single amino acid substitution at only seven sites in HA head beside the receptor binding site (RBS) was enough to drive major antigenic change in H3N2 (17, 20). HA stem, as a target for universal influenza vaccine, has gained enormous traction in recent years. One could argue that the stem region is inaccessible to B cells and antibodies (21). However, a study using a broad neutralizing antibody showed that nearly 75% of the HA on pandemic H1N1 is bound by a stem-specific mAb (22). There is an urgent need to introduce universal vaccines, targeting conserved regions and providing lifelong protection. This review focuses on possible strategies for developing universal influenza vaccines, mainly based on HA. Such strategies are summarized in **Figure 1**.

HEMAGGLUTININ STEM—A PROMISING UNIVERSAL VACCINE TARGET

HA stem has been an important candidate for development of universal vaccines because the stalk region is relatively conserved and evolves much slower and accommodate less amino acid substitutions as compared to the head domain. This could be due to minimal antibody pressure from low amount of circulating anti-stem antibodies (23, 24) and low tolerance to mutations in the stalk domain, which can lead to loss of viral fitness (25, 26), even though partial escape mutations in the stem can be generated (27). However, amino acid substitutions in the stalk have been reported to minimally affect the neutralization capacity of human cross-reactive, anti-stalk monoclonal antibodies (14, 28).

HA stem antibodies protect by (i) preventing viral entry by blocking the fusion of host cell membrane and viral membrane (29), (ii) reducing viral egress by blocking neuraminidase activity through steric hindrance (30–32), and (iii) FcR-mediated induction of antibody-dependent cellular cytotoxicity (ADCC), antibody-dependent cellular phagocytosis and reactive oxygen species production (33–35). Several human-derived broadly neutralizing anti-stem antibodies have been identified against either influenza group 1 (36–39) or group 2 (38, 40–42) or both groups (40, 43–50) or even against both influenza A and B subtypes (51). The identification of these antibodies was an incentive to develop vaccines, which are discussed below.

HEMAGGLUTININ STEM—HUMAN IMMUNE RESPONSES

In humans, memory B cells (Bmem), and antibodies against HA stem are subdominant and present in low levels. Analysis of serum samples from 202 healthy individuals collected between 2004 and 2010 revealed that anti-stem antibodies of group 1 specificity is found in 84% of the population (52); however, their level, as measured in human Intravenous Immunoglobulin preparations, is very low (23).

Ellebedy and colleagues (53) found that immunization with H5N1, which is not currently circulating in humans, boosted cross-reactive antibody response toward HA stem, when compared to seasonal vaccines. Because of the existence of lower levels of H5 head-specific Bmem as compared to stem-specific Bmem, H5N1 vaccination led to recruitment of stem-specific Bmem, their expansion, and antibody production. On the contrary, boosting with the same HA favors anti-head responses (53). Another study found that nearly 6 out of 10 individuals have Bmem specific between group 1 and 2 HA (50). Indeed, it appears that baseline levels of H5–H1 cross-reactive Bmem and H1-specific Bmem are no more than 2-fold different (54). However, after priming with an H5 DNA plasmid vaccine and boosting with A/Indonesia/05/2005 monovalent-inactivated virus, both head and stem Bmem were expanded but only head-specific Bmem persisted, while stem-specific Bmem expanded and contracted rapidly (50, 54). Finally, Andrews et al. observed that immunization with group 1 virus (H5N1) elicited anti-stem memory responses exclusively against group 1, while group 2 (H7N9) induced high levels of cross-protective anti-stem memory B cell responses with diverse repertoire despite a lower overall response. This study in humans suggests the potential of group 2 based vaccines to provide a broader protection as compared to group 1 (55). While all these studies highlight the ability of individuals to generate stem-specific Bmem and plasmablasts, they all note a rapid contraction of stem-specific cells. This disconnect between cell numbers, longevity, and serum antibodies highlight the complexity of B-cell fate decision. Understanding how antigen specificity can influence cell differentiation is a crucial challenge for next generation vaccines.

SITES OF VULNERABILITY IN HEMAGGLUTININ HEAD

Although HA stem is an excellent candidate for the development of universal vaccines, anti-HA stem titers in human correlates only with reduced viral shedding but do not predict the severity of influenza infection (56, 57). A recent study in humans indicated that a 2-fold increase in hemagglutination inhibition titer gave a 23.4% reduction in H1N1 infection risk, while the same increase in HA-stem-specific antibodies conferred only 14.2% reduction (58).

The globular head of the HA is target for most of the neutralizing antibodies, which prevents the viral entry by

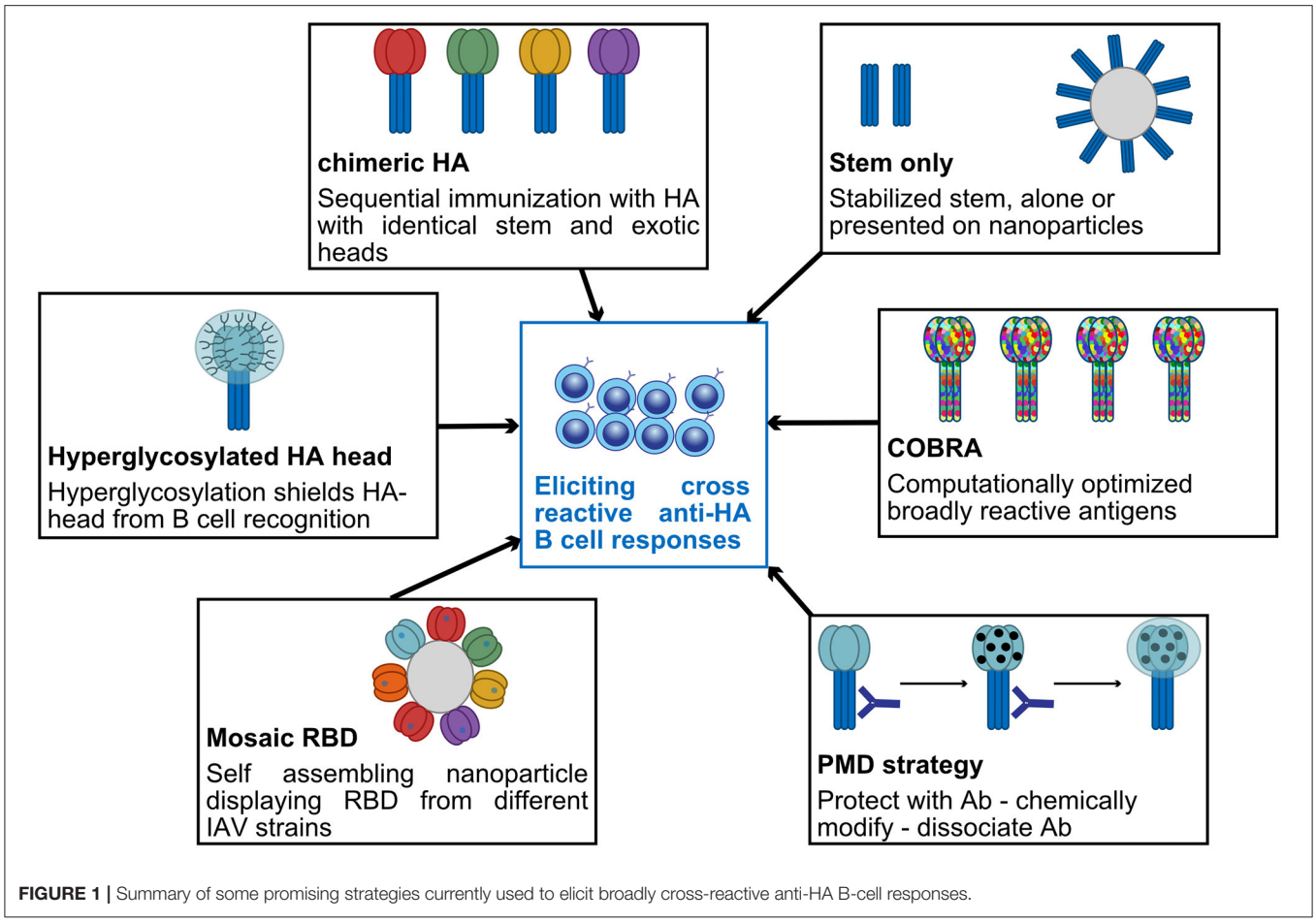

FIGURE 1 | Summary of some promising strategies currently used to elicit broadly cross-reactive anti-HA B-cell responses.

blocking the binding of RBS to sialic acid residues on host cell membrane (59). RBS is a shallow depression on HA head and consists of 130 loop, 150 loop, 190 helix, which are relatively conserved, and 220 loop, which is diverse among IAV subtypes (60, 61). Amino acid substitutions in the RBS determine host tropism, and specific substitutions are connected to altered receptor binding within subtype (62). Some RBS binding, broadly neutralizing antibodies have been identified, such as C05, S139/1, and F045-092, which neutralize within groups; CH65, 5J8, 2G1, and H5.3, which neutralize within subtype (63–71); and C12G6 and CR8033, which neutralize both influenza B lineages (51, 72).

Apart from RBS, broadly neutralizing antibodies have been identified against other conserved sites on HA head (73). An antibody (F005-126) which neutralizes 12 H3N2 subtypes by occupying the cleft formed by two HA head monomers and cross-linking them is known to prevent viral entry by blocking pH-induced HA conformational change (74). Bajic et al. found that subdominant antibodies can target an occluded epitope located on the lateral surface on HA head between two monomers using an H3 immunogen, hyperglycosylated on dominant epitopes. These antibodies protected against H3N2 challenge in an Fc-dependent manner (75). Similarly, two independent studies identified broadly neutralizing antibody, which bind hidden epitopes at HA trimer interface. These antibodies do not neutralize the virus but are suspected to disrupt the HA trimer integrity. Passive transfer experiments revealed that they protect mice from groups 1 and 2 viruses by preventing cell-to-cell viral spread or by FcγR or complement mediated effector mechanism (76, 77). HA exhibits "breathing" phenomenon at neutral or low pH where reversible separation of HA monomers exposes hidden epitopes to these specific antibodies (78–80). Vestigeal esterase domain is another possible HA target; it is located at the base of the HA head and can be target of broadly protective antibodies, which protect within subtypes (81, 82) and both lineages of influenza B virus (83). Like stem-directed antibodies, they protect through various mechanisms such as blocking viral egress, fusion, or by ADCC.

For most of the epitopes described above, we are just at the first step of the reverse vaccinology pipeline. However, there is hope that using some advanced *de novo* protein design tools, we will be able to create effective immune-focusing antigens (84, 85).

BIOENGINEERING ANTIGENS TO REFOCUS IMMUNE RESPONSES

Headless Hemagglutinins

One of the obvious ways to increase the anti-stem antibody response is to remove HA head to circumvent

its immunodominance (13, 86). Even though this sounds simple, removing the head and the transmembrane domain may cause conformational changes in the stem leading to loss of recognition by anti-stem antibodies (87). One of many successful attempts was achieved by creating stable trimeric mini-HA from H1N1, which retained similar binding affinity to two broadly neutralizing antibodies, CR9114 and CR6261, as that of full-length HA. When used to immunize non-human primates, the elicited antibodies competed with CR9114, induced ADCC, and neutralized H5N1 virus (88). Another study used H1HA10-Foldon and H3HA10-Foldon mini-HA, which generated neutralizing antibodies cross-reactive to both groups 1 and 2 IAV *in vitro* but with limited cross-group protection *in vivo* (89, 90). In contrast to these mini-HAs, an H5-based mini-HA produced and purified from *Escherichia coli* elicited anti-stem antibody responses and protection against both IAV subtypes (91). Pre-existing immunity plays a role in subsequent immune response to viral infection and vaccination (92). When tested in non-human primates who have been exposed to flu infection, mini-HA were shown to induce higher cross-protective antibody response as compared to seasonal trivalent inactivated vaccine, indicating their potential as a universal vaccine (93).

Ferritin is an iron storage protein which self-assembles into a nanoparticle consisting of 24 repetitive polypeptides, which can induce strong immune response and antigen presentation (94). Based on this, Yassine et al. engineered a nanoparticle containing intact HA stem from H1 (H1-ss-np), which generated anti-stem response almost 2-fold higher than that of trivalent inactivated vaccine. When immunized with H1-ss-np, mice and ferrets elicited broad antibody response against group 1 IAV as well as group 2 IAV, demonstrating heterosubtypic protection (95). Based on this, influenza H1 stabilized stem ferritin vaccine (H1ssF_3928) has entered a phase I ongoing clinical trial to evaluate its tolerability and immunogenicity in healthy adults. However, a thermostable and immunogenic nanoparticle vaccine containing group 2 H3 and H7 stem conferred only protection against homosubtypic viral challenge. Given the fact that these stem immunogens activates IgM BCR of unmutated common ancestor of the cross-reactive human anti-stem antibodies, the authors speculate that the lack of cross-group protection *in vivo* might be due to difference in BCR repertoire in mice and human (96).

Chimeric Hemagglutinin

Chimeric HAs (cHA) are full-length HA with stem derived from human viruses and globular head from distinct, exotic HAs. Based on this concept, repeated immunization with cHA with head from different flu subtype and same H1 HA stem induced high titers of stem-reactive antibodies against homologous and heterologous viruses (97). Several such cHA constructs, which confer protection by eliciting stem Abs, have been developed for group 1, group 2, and Influenza B viruses, with some inducing long-lasting antibodies (98–105). An interim report on a clinical trial using a cHA prime boost strategy was recently released (106). In this study, healthy volunteers, with measurable baseline H1-stalk antibody levels, were boosted with cHAs. The sharpest stem-antibody level increase was obtained when challenging with cH8/1N1 in AS03 adjuvant intramuscularly. However, further immunization with other cHA did not additionally boost stem responses. To build upon these promising findings, more studies are needed to assess the longevity of these responses and their stability upon natural infection or seasonal immunization.

Immune-Focusing Strategies

N-linked glycosylation on HA has been known to stabilize HA and shield virus from host immune response (107). Creating monoglycosylated HA or unmasking HA-stem of N-glycans could induce cross-strain neutralizing anti-stem antibodies (108, 109). Conversely, hyperglycosylating the HA head can also refocus response on stem (110). A recent study used "protect, modify, and deprotect" method to focus antibody response toward a stem epitope. In this strategy, after masking target epitope on stem with a monoclonal antibody, the surrounding undesired epitopes are chemically modified to reduce their antigenicity (111). On the other hand, other residues, outside stem, can also influence the neutralizing sensitivity to anti-stem antibodies by affecting HA-stalk stability and antibody access to stem epitopes (112).

Vaccine Engineering for Cross-Protection

Kanekiyo et al. used a ferritin nanoparticle displaying a repetitive array of HA hyper variable receptor binding domains (RBD from different H1N1 strains). Using this, they could subvert B cell response from strain-specific immunodominant epitopes to conserved, shared epitopes. Since cross-reactive B cells can recognize conserved epitope from an heterogenous array of RBD, these cells get preferentially activated due to avidity advantage and could selectively activate pre-existing cross-reactive Bmem. One of the antibodies generated after immunization, 441D6, binds to a conserved epitope, which lies opposite to RBS and protects against H1N1 strains spanning from 1977 to 2009 (113, 114). Anderson et al. generated cross-reactive antibody responses by injecting a mix of DNA vaccines containing HA genes from six members of group 1 IAV, which was further enhanced by inclusion of an antigen presenting cell targeting unit specific for MHCII, thus favoring BCR cross-linking (115). Another strategy to elicit broadly reactive antibodies within IAV subtypes is to use computationally optimized broadly reactive antigens (COBRA), which are displayed on virus like particles or expressed in live attenuated influenza vaccine. This approach uses multiple rounds of consensus generation to aggregate HA epitopes of IAV from different time periods. Such vaccines elicit polyclonal B cell responses and was shown to protect within subtypes (116–123). Combining several COBRA vaccines could confer heterosubtypic protection.

M2e-Based Vaccines

M2 is an ion channel with its ectodomain (M2e) exposed on virion and infected cell surfaces (124). M2e is quite

TABLE 1 | Characteristics of antibody responses to current universal vaccine targets and ability of seasonal vaccination to recall memory B cells and specific antibodies.

	Antibodies			Seasonal vaccination	
	Broadly cross reactive	**Neutralizing**	**Act via effector functions**	**Recall memory B cells**	**Elicit antibodies**
HA head	–	+	– (33)	+	+
HA head conserved targets	+	+/–[a]	+/–[b]	?[c] (73, 143)	?[d] (143)
HA stem	+	+	+ (33)	–/+[e] (21, 144)	–/+[e] (21)
NA	+	+/–[f] (141)	+ (145)	–[g] (136)	+/–[g] (146, 147)
M2e	+	– (148)	+ (149)	–	–

[a] *HA head conserved targets comprise lot of different targets. Neutralization ability depends on the target.*
[b] *See in the body of this review for references, depending on the target.*
[c] *Not many studies address this question. It appears that vaccination with newly introduced viruses might recall these B cells.*
[d] *Not many studies are addressing this issue, which is probably dependent on the target.*
[e] *Stem-specific memory B cells are mainly recalled and antibodies induced when new viruses are introduced (for example with H1N1/pdm2009).*
[f] *NA antibodies usually have NA-inhibition activity, which correlates well with plaque reduction but are not neutralizing, by definition.*
[g] *NA-B cells and antibodies are most likely not properly boosted, after seasonal vaccination, due to poor vaccine formulation, with variable/low NA amount.*

conserved across IAV; therefore, it has historically been considered as an ideal universal vaccine candidate (125). The mechanism of M2e-mediated protection is debated with both antibodies and T cells being important players (126–128). Several approaches have been undertaken to increase M2e immunogenicity, using VLP or different adjuvants (129–131). Of note, it appears that M2e antibodies act via effector functions and thus are infection permissive, making M2e vaccines more suitable when used in combination with others.

NEURAMINIDASE—THE EMERGING PLAYER

IAV NA as vaccine target has been neglected for decades, despite early discovery of potent anti-viral activity of NA antibodies (132). Even more surprisingly, NA amount in licensed vaccines varies enormously and is not checked by manufactures or regulatory authorities (133). Exciting new studies strongly point to a major role for anti-NA antibodies in protecting from disease and as the best correlates of protection (56, 134, 135). Critically, Chen et al. identified a number of human NA antibodies that cross-protected mice in therapeutic and prophylactic setting (136). Even more promising, several broadly neutralizing anti-NA mAbs have been isolated from an infected patient. These mAbs, directed to NA active site, demonstrated an unusual breadth in binding several IAV and IBV NA and mediating cross-neutralization and cross-protection *in vivo* (137). Still, despite some early studies, we do not know enough about NA antigenicity and the immunodominance of its antigenic sites (138–141). By applying some of the methods that allowed us to study in detail anti-HA responses, we should be able to break down anti-NA responses and identify promising universal vaccine candidates.

CONCLUSIONS—KNOW WHAT WE DO NOT KNOW

Bioengineering and design of epitope-focused immunogens is proceeding at an incredible speed in influenza and other fields. Several promising immunogens are now in clinical trials and, hopefully, will be available to the public soon, as long-lasting universal vaccines. It is, however, crucial to understand more about the basics of B cell responses to interpret results and inform on vaccination policies.

Introduction of pandemic H1N1 2009 virus showed that most individuals, with low serological anti-stem antibodies, were able to mount a stem-directed response, but repeated vaccinations skewed the immune response back to the immunodominant head (21). It will be critical to understand when, in which order and how often give universal vaccines to appropriately boost stem response. Andrews et al. demonstrated that novel B cells specific for variable epitopes have a different phenotype compared to reactivated Bmem specific for stem (142). To maximize success, efforts will need to be put in understanding how B-cell specificity can influence their programming and differentiation. Furthermore, it is still unclear how much of stem-specific antibodies are required for optimal protection from a drifted or heterologous virus. **Table 1** summarizes what we know about antibody responses to the major targets on IAV and how seasonal vaccination is able to boost those responses.

Finally, but not less important, new vaccines platforms are constantly being tested. RNA-based vaccines have shown exciting results when expressing influenza proteins, at least in animals [reviewed in (150)]. Some of the engineered vaccines discussed in this review could be delivered as RNA vaccines, alone or in combination, possibly avoiding clearance from pre-existing antibodies. Other novel, slow-release, vaccine formulations could help refocusing immune responses to subdominant targets (151–153).

We are just entering an exciting season of clinical trials, and while expectations are really high, we should not be discouraged

if some of the early attempts fail but rather persevere in the quest for a universal and long-lasting vaccine.

AUTHOR CONTRIBUTIONS

NM and DA researched the literature and wrote the manuscript.

FUNDING

This work was supported by the Swedish Research Council, Vetenskapsrådet (2017-01439), the Jeanssons Foundations (JS2018-0011), and the Institute of Biomedicine at the University of Gothenburg.

REFERENCES

1. Paules C, Subbarao K. Influenza. *Lancet*. (2017) 390:697–708. doi: 10.1016/S0140-6736(17)30129-0
2. Hause BM, Ducatez M, Collin EA, Ran Z, Liu R, Sheng Z, et al. Isolation of a novel swine influenza virus from Oklahoma in 2011 which is distantly related to human influenza C viruses. *PLoS Pathog.* (2013) 9:e1003176. doi: 10.1371/journal.ppat.1003176
3. Collin EA, Sheng Z, Lang Y, Ma W, Hause BM, Li F. Cocirculation of two distinct genetic and antigenic lineages of proposed influenza D virus in cattle. *J Virol.* (2015) 89:1036–42. doi: 10.1128/JVI.02718-14
4. Jackson D, Elderfield RA, Barclay WS. Molecular studies of influenza B virus in the reverse genetics era. *J Gen Virol.* (2011) 92(Pt 1):1–17. doi: 10.1099/vir.0.026187-0
5. Iuliano AD, Roguski KM, Chang HH, Muscatello DJ, Palekar R, Tempia S, et al. Estimates of global seasonal influenza-associated respiratory mortality:a modelling study. *Lancet*. (2018) 391:1285–300. doi: 10.1016/S0140-6736(17)33293-2
6. Belongia EA, Skowronski DM, McLean HQ, Chambers C, Sundaram ME, De Serres G. Repeated annual influenza vaccination and vaccine effectiveness:review of evidence. *Exp Rev Vaccines*. (2017) 16:1–14. doi: 10.1080/14760584.2017.1334554
7. Hutchinson EC. Influenza Virus. *Trends Microbiol.* (2018) 26:809–810. doi: 10.1016/j.tim.2018.05.013
8. Rota PA, Wallis TR, Harmon MW, Rota JS, Kendal AP, Nerome K. Cocirculation of two distinct evolutionary lineages of influenza type B virus since 1983. *Virology*. (1990) 175:59–68. doi: 10.1016/0042-6822(90)90186-U
9. Grohskopf LA, Alyanak E, Broder KR, Walter EB, Fry AM, Jernigan DB. Prevention and control of seasonal influenza with vaccines:recommendations of the advisory committee on immunization practices - United States, 2019–20 influenza season. *MMWR Recomm Rep*. (2019) 68:1–21. doi: 10.15585/mmwr.rr6803a1
10. Krammer F, Palese P. Advances in the development of influenza virus vaccines. *Nat Rev Drug Discov*. (2015) 14:167–82. doi: 10.1038/nrd4529
11. Past Pandemics. *Centers for Disease Control and Prevention, National Center for Immunization and Respiratory Diseases (NCIRD)*. (2018). Available online at: https://www.cdc.gov/flu/pandemic-resources/basics/past-pandemics.html
12. Gaymard A, Le Briand N, Frobert E, Lina B, Escuret V. Functional balance between neuraminidase and haemagglutinin in influenza viruses. *Clin Microbiol Infect*. (2016) 22:975–83. doi: 10.1016/j.cmi.2016.07.007
13. Angeletti D, Gibbs JS, Angel M, Kosik I, Hickman HD, Frank GM, et al. Defining B cell immunodominance to viruses. *Nat Immunol*. (2017) 18:456–63. doi: 10.1038/ni.3680
14. Kirkpatrick E, Qiu X, Wilson PC, Bahl J, Krammer F. The influenza virus hemagglutinin head evolves faster than the stalk domain. *Sci Rep*. (2018) 8:10432. doi: 10.1038/s41598-018-28706-1
15. Angeletti D, Yewdell JW. Understanding and manipulating viral immunity:antibody immunodominance enters center stage. *Trends Immunol*. (2018) 39:549–61. doi: 10.1016/j.it.2018.04.008
16. Das SR, Hensley SE, Ince WL, Brooke CB, Subba A, Delboy MG, et al. Defining influenza A virus hemagglutinin antigenic drift by sequential monoclonal antibody selection. *Cell Host Microbe*. (2013) 13:314–23. doi: 10.1016/j.chom.2013.02.008
17. Chambers BS, Parkhouse K, Ross TM, Alby K, Hensley SE. Identification of hemagglutinin residues responsible for H3N2 antigenic drift during the 2014–2015 influenza season. *Cell Rep*. (2015) 12:1–6. doi: 10.1016/j.celrep.2015.06.005
18. Huang KY, Rijal P, Schimanski L, Powell TJ, Lin TY, McCauley JW, et al. Focused antibody response to influenza linked to antigenic drift. *J Clin Invest*. (2015) 125:2631–45. doi: 10.1172/JCI81104
19. Lee JM, Eguia R, Zost SJ, Choudhary S, Wilson PC, Bedford T, et al. Mapping person-to-person variation in viral mutations that escape polyclonal serum targeting influenza hemagglutinin. *Elife*. (2019) 8:e49324. doi: 10.7554/eLife.49324
20. Koel BF, Burke DF, Bestebroer TM, van der Vliet S, Zondag GC, Vervaet G, et al. Substitutions near the receptor binding site determine major antigenic change during influenza virus evolution. *Science*. (2013) 342:976–9. doi: 10.1126/science.1244730
21. Andrews SF, Huang Y, Kaur K, Popova LI, Ho IY, Pauli NT, et al. Immune history profoundly affects broadly protective B cell responses to influenza. *Sci Transl Med*. (2015) 7:316ra192. doi: 10.1126/scitranslmed.aad0522
22. Harris AK, Meyerson JR, Matsuoka Y, Kuybeda O, Moran A, Bliss D, et al. Structure and accessibility of HA trimers on intact 2009 H1N1 pandemic influenza virus to stem region-specific neutralizing antibodies. *Proc Natl Acad Sci USA*. (2013) 110:4592–7. doi: 10.1073/pnas.12149 13110
23. Sui J, Sheehan J, Hwang WC, Bankston LA, Burchett SK, Huang CY, et al. Wide prevalence of heterosubtypic broadly neutralizing human anti-influenza A antibodies. *Clin Infect Dis*. (2011) 52:1003–9. doi: 10.1093/cid/cir121
24. Hoa LNM, Mai LQ, Bryant JE, Thai PQ, Hang NLK, Yen NTT, et al. Association between Hemagglutinin Stem-Reactive Antibodies and Influenza A/H1N1 Virus Infection during the 2009 Pandemic. *J Virol*. (2016) 90:6549–56. doi: 10.1128/JVI.00093-16
25. Doud MB, Bloom JD, Accurate measurement of the effects of all amino-acid mutations on influenza hemagglutinin. *Viruses*. (2016) 8:155. doi: 10.3390/v8060155
26. Heaton NS, Sachs D, Chen CJ, Hai R, Palese P. Genome-wide mutagenesis of influenza virus reveals unique plasticity of the hemagglutinin and NS1 proteins. *Proc Natl Acad Sci USA*. (2013) 110:20248–53. doi: 10.1073/pnas.1320524110
27. Anderson CS, Ortega S, Chaves FA, Clark AM, Yang H, Topham DJ, et al. Publisher correction:natural and directed antigenic drift of the H1 influenza virus hemagglutinin stalk domain. *Sci Rep*. (2018) 8:276. doi: 10.1038/s41598-017-17926-6
28. Shafieyan Y, Hinz B, Doud MB, Lee JM, Bloom JD. How single mutations affect viral escape from broad and narrow antibodies to H1 influenza hemagglutinin. *Nat Commun*. (2018) 9:1386. doi: 10.1038/s41467-018-03665-3
29. Varecková E, Mucha V, Wharton SA, Kostolanský F. Inhibition of fusion activity of influenza A haemagglutinin mediated by HA2-specific monoclonal antibodies. *Arch Virol*. (2003) 148:469–86. doi: 10.1007/s00705-002-0932-1
30. Chen YQ, Lan LY, Huang M, Henry C, Wilson PC. Hemagglutinin stalk-reactive antibodies interfere with influenza virus neuraminidase activity by steric hindrance. *J Virol*. (2019) 93:e01526–18. doi: 10.1128/JVI.01 526-18
31. Kosik I, Angeletti D, Gibbs JS, Angel M, Takeda K, Kosikova M, et al. Neuraminidase inhibition contributes to influenza A virus neutralization by anti-hemagglutinin stem antibodies. *J Exp Med*. (2019) 216:304–16. doi: 10.1084/jem.20181624
32. Wohlbold TJ, Chromikova V, Tan GS, Meade P, Amanat F, Comella P, et al. Hemagglutinin stalk- and neuraminidase-specific monoclonal antibodies protect against Lethal H10N8 influenza virus infection in mice. *J Virol*. (2016) 90:851–61. doi: 10.1128/JVI.02275-15

33. DiLillo DJ, Tan GS, Palese P, Ravetch JV. Broadly neutralizing hemagglutinin stalk-specific antibodies require FcgammaR interactions for protection against influenza virus *in vivo*. *Nat Med*. (2014) 20:143–51. doi: 10.1038/nm.3443
34. DiLillo DJ, Palese P, Wilson PC, Ravetch JV, DiLillo DJ. Broadly neutralizing anti-influenza antibodies require Fc receptor engagement for in vivo protection. *J Clin Invest*. (2016) 126:605–10. doi: 10.1172/JCI84428
35. Mullarkey CE, Bailey MJ, Golubeva DA, Tan GS, Nachbagauer R, He W, et al. Broadly neutralizing hemagglutinin stalk-specific antibodies induce potent phagocytosis of immune complexes by neutrophils in an Fc-dependent manner. *MBio*. (2016) 7:e01624–16. doi: 10.1128/mBio.01624-16
36. Sui J, Hwang WC, Perez S, Wei G, Aird D, Chen LM, et al. Structural and functional bases for broad-spectrum neutralization of avian and human influenza A viruses. *Nat Struct Mol Biol*. (2009) 16:265–73. doi: 10.1038/nsmb.1566
37. Ekiert DC, Bhabha G, Elsliger MA, Friesen RH, Jongeneelen M, Throsby M, et al. Antibody recognition of a highly conserved influenza virus epitope. *Science*. (2009) 324:246–51. doi: 10.1126/science.1171491
38. Nachbagauer R, Shore D, Yang H, Johnson SK, Gabbard JD, Tompkins SM, et al. Broadly reactive human monoclonal antibodies elicited following pandemic H1N1 influenza virus exposure protect mice against highly pathogenic H5N1 challenge. *J Virol*. (2018) 92:e00949–18. doi: 10.1128/JVI.00949-18
39. De Marco D, Clementi N, Mancini N, Solforosi L, Moreno GJ, Sun X, et al. A non-VH1–69 heterosubtypic neutralizing human monoclonal antibody protects mice against H1N1 and H5N1 viruses. *PLoS ONE*. (2012) 7:e34415. doi: 10.1371/journal.pone.0034415
40. Henry Dunand CJ, Leon PE, Kaur K, Tan GS, Zheng NY, Andrews S, et al. Preexisting human antibodies neutralize recently emerged H7N9 influenza strains. *J Clin Invest*. (2015) 125:1255–68. doi: 10.1172/JCI74374
41. Ekiert DC, Friesen RH, Bhabha G, Kwaks T, Jongeneelen M, Yu W, et al. A highly conserved neutralizing epitope on group 2 influenza A viruses. *Science*. (2011) 333:843–50. doi: 10.1126/science.1204839
42. Friesen RH, Lee PS, Stoop EJ, Hoffman RM, Ekiert DC, Bhabha G, et al. A common solution to group 2 influenza virus neutralization. *Proc Natl Acad Sci USA*. (2014) 111:445–50. doi: 10.1073/pnas.1319058110
43. Sakabe S, Iwatsuki-Horimoto K, Horimoto T, Nidom CA, Le Mt, Takano R, et al. A cross-reactive neutralizing monoclonal antibody protects mice from H5N1 and pandemic (H1N1) 2009 virus infection. *Antiviral Res*. (2010) 88:249–55. doi: 10.1016/j.antiviral.2010.09.007
44. Kallewaard NL, Corti D, Collins PJ, Neu U, McAuliffe JM, Benjamin E, et al. Structure and function analysis of an antibody recognizing all influenza A subtypes. *Cell*. (2016) 166:596–608. doi: 10.1016/j.cell.2016.05.073
45. Fu Y, Zhang Z, Sheehan J, Avnir Y, Ridenour C, Sachnik T, et al. A broadly neutralizing anti-influenza antibody reveals ongoing capacity of haemagglutinin-specific memory B cells to evolve. *Nat Commun*. (2016) 7:12780. doi: 10.1038/ncomms12780
46. Tharakaraman K, Subramanian V, Viswanathan K, Sloan S, Yen HL, Barnard DL, et al. A broadly neutralizing human monoclonal antibody is effective against H7N9. *Proc Natl Acad Sci USA*. (2015) 112:10890–5. doi: 10.1073/pnas.1502374112
47. Marjuki H, Mishin VP, Chai N, Tan MW, Newton EM, Tegeris J, et al. Human monoclonal antibody 81.39a effectively neutralizes emerging influenza A viruses of group 1 and 2 hemagglutinins. *J Virol*. (2016) 90:10446–58. doi: 10.1128/JVI.01284-16
48. Wyrzucki A, Bianchi M, Kohler I, Steck M, Hangartner L, et al. Heterosubtypic antibodies to influenza A virus have limited activity against cell-bound virus but are not impaired by strain-specific serum antibodies. *J Virol*. (2015) 89:3136–44. doi: 10.1128/JVI.03069-14
49. Clementi N, De Marco D, Mancini N, Solforosi L, Moreno GJ, Gubareva LV, et al. A human monoclonal antibody with neutralizing activity against highly divergent influenza subtypes. *PLoS ONE*. (2011) 6:e28001. doi: 10.1371/journal.pone.0028001
50. Joyce MG, Wheatley AK, Thomas PV, Chuang GY, Soto C, Bailer RT, et al. Vaccine-induced antibodies that neutralize group 1 and group 2 influenza A viruses. *Cell*. (2016) 166:609–23. doi: 10.1016/j.cell.2016.06.043
51. Dreyfus C, Laursen NS, Kwaks T, Zuijdgeest D, Khayat R, Ekiert DC, et al. Highly conserved protective epitopes on influenza B viruses. *Science*. (2012) 337:1343–8. doi: 10.1126/science.1222908
52. Yassine HM, McTamney PM, Boyington JC, Ruckwardt TJ, Crank MC, Smatti MK, et al. Use of hemagglutinin stem probes demonstrate prevalence of broadly reactive group 1 influenza antibodies in human sera. *Sci Rep*. (2018) 8:8628. doi: 10.1038/s41598-018-26538-7
53. Ellebedy AH, Krammer F, Li GM, Miller MS, Chiu C, Wrammert J, et al. Induction of broadly cross-reactive antibody responses to the influenza HA stem region following H5N1 vaccination in humans. *Proc Natl Acad Sci USA*. (2014) 111:13133–8. doi: 10.1073/pnas.1414070111
54. Wheatley AK, Whittle JR, Lingwood D, Kanekiyo M, Yassine HM, Ma SS, et al. H5N1 Vaccine-elicited memory B cells are genetically constrained by the IGHV locus in the recognition of a neutralizing epitope in the hemagglutinin stem. *J Immunol*. (2015) 195:602–10. doi: 10.4049/jimmunol.1402835
55. Andrews SF, Joyce MG, Chambers MJ, Gillespie RA, Kanekiyo M, Leung K, et al. Preferential induction of cross-group influenza A hemagglutinin stem-specific memory B cells after H7N9 immunization in humans. *Sci Immunol*. (2017) 2:eaan2676. doi: 10.1126/sciimmunol.aan2676
56. Park JK, Han A, Czajkowski L, Reed S, Athota R, Bristol T, et al. Evaluation of preexisting anti-hemagglutinin stalk antibody as a correlate of protection in a healthy volunteer challenge with influenza A/H1N1pdm virus. *MBio*. (2018) 9:e02284–17. doi: 10.1128/mBio.02284-17
57. Memoli MJ, Shaw PA, Han A, Czajkowski L, Reed S, Athota R, et al. Evaluation of antihemagglutinin and antineuraminidase antibodies as correlates of protection in an influenza A/H1N1 virus healthy human challenge model. *MBio*. (2016) 7:e00417–16. doi: 10.1128/mBio.00417-16
58. Christensen SR, Toulmin SA, Griesman T, Lamerato LE, Petrie JG, Martin ET, et al. Assessing the protective potential of H1N1 influenza virus hemagglutinin head and stalk antibodies in humans. *J Virol*. (2019) 93:e02134–18. doi: 10.1128/JVI.02134-18
59. Weis W, Brown JH, Cusack S, Paulson JC, Skehel JJ, Wiley DC. Structure of the influenza virus haemagglutinin complexed with its receptor, sialic acid. *Nature*. (1988) 333:426–31. doi: 10.1038/333426a0
60. Skehel JJ, Wiley DC. Receptor binding and membrane fusion in virus entry:the influenza hemagglutinin. *Annu Rev Biochem*. (2000) 69:531–69. doi: 10.1146/annurev.biochem.69.1.531
61. Wu NC, Xie J, Zheng T, Nycholat CM, Grande G, Paulson JC, et al. Diversity of functionally permissive sequences in the receptor-binding site of influenza hemagglutinin. *Cell Host Microbe*. (2017) 21:742–53.e8. doi: 10.1016/j.chom.2017.05.011
62. Shi Y, Wu Y, Zhang W, Qi J, Gao GF. Enabling the 'host jump':structural determinants of receptor-binding specificity in influenza A viruses. *Nat Rev Microbiol*. (2014) 12:822–31. doi: 10.1038/nrmicro3362
63. Ekiert DC, Kashyap AK, Steel J, Rubrum A, Bhabha G, Khayat R, et al. Cross-neutralization of influenza A viruses mediated by a single antibody loop. *Nature*. (2012) 489:526–32. doi: 10.1038/nature11414
64. Lee PS, Ohshima N, Stanfield RL, Yu W, Iba Y, Okuno Y, et al. Receptor mimicry by antibody F045–092 facilitates universal binding to the H3 subtype of influenza virus. *Nat Commun*. (2014) 5:3614. doi: 10.1038/ncomms4614
65. Whittle JR, Zhang R, Khurana S, King LR, Manischewitz J, Golding H, et al. Broadly neutralizing human antibody that recognizes the receptor-binding pocket of influenza virus hemagglutinin. *Proc Natl Acad Sci USA*. (2011) 108:14216–21. doi: 10.1073/pnas.1111497108
66. Hong M, Lee PS, Hoffman RM, Zhu X, Krause JC, Laursen NS, et al. Antibody recognition of the pandemic H1N1 Influenza virus hemagglutinin receptor binding site. *J Virol*. (2013) 87:12471–80. doi: 10.1128/JVI.01388-13
67. Krause JC, Tsibane T, Tumpey TM, Huffman CJ, Basler CF, Crowe JE. A broadly neutralizing human monoclonal antibody that recognizes a conserved, novel epitope on the globular head of the influenza H1N1 virus hemagglutinin. *J Virol*. (2011) 85:10905–8. doi: 10.1128/JVI.00700-11
68. Lee PS, Yoshida R, Ekiert DC, Sakai N, Suzuki Y, Takada A, et al. Heterosubtypic antibody recognition of the influenza virus hemagglutinin receptor binding site enhanced by avidity. *Proc Natl Acad Sci USA*. (2012) 109:17040–5. doi: 10.1073/pnas.1212371109

69. Yoshida R, Igarashi M, Ozaki H, Kishida N, Tomabechi D, Kida H, et al. Cross-protective potential of a novel monoclonal antibody directed against antigenic site B of the hemagglutinin of influenza A viruses. *PLoS Pathog.* (2009) 5:e1000350. doi: 10.1371/journal.ppat.1000350
70. Krause JC, Tsibane T, Tumpey TM, Huffman CJ, Albrecht R, Blum DL, et al. Human monoclonal antibodies to pandemic 1957 H2N2 and pandemic 1968 H3N2 influenza viruses. *J Virol.* (2012) 86:6334–40. doi: 10.1128/JVI.07158-11
71. Winarski KL, Thornburg NJ, Yu Y, Sapparapu G, Crowe JE, Spiller BW. Vaccine-elicited antibody that neutralizes H5N1 influenza and variants binds the receptor site and polymorphic sites. *Proc Natl Acad Sci USA.* (2015) 112:9346–51. doi: 10.1073/pnas.1502762112
72. Shen C, Chen J, Li R, Zhang M, Wang G, Stegalkina S, et al. A multimechanistic antibody targeting the receptor binding site potently cross-protects against influenza B viruses. *Sci Transl Med.* (2017) 9:eaam5752. doi: 10.1126/scitranslmed.aam5752
73. Raymond DD, Bajic G, Ferdman J, Suphaphiphat P, Settembre EC, Moody MA, et al. Conserved epitope on influenza-virus hemagglutinin head defined by a vaccine-induced antibody. *Proc Natl Acad Sci USA.* (2018) 115:168–73. doi: 10.1073/pnas.1715471115
74. Iba Y, Fujii Y, Ohshima N, Sumida T, Kubota-Koketsu R, Ikeda M, et al. Conserved neutralizing epitope at globular head of hemagglutinin in H3N2 influenza viruses. *J Virol.* (2014) 88:7130–44. doi: 10.1128/JVI.00420-14
75. Bajic G, Maron MJ, Adachi Y, Onodera T, McCarthy KR, McGee CE, et al. Influenza antigen engineering focuses immune responses to a subdominant but broadly protective viral epitope. *Cell Host Microbe.* (2019) 25:827–35.e6. doi: 10.1016/j.chom.2019.04.003
76. Bangaru S, Lang S, Schotsaert M, Vanderven HA, Zhu X, Kose N, et al. A site of vulnerability on the influenza virus hemagglutinin head domain trimer interface. *Cell.* (2019) 177:1136–52.e18. doi: 10.1016/j.cell.2019.04.011
77. Watanabe A, McCarthy KR, Kuraoka M, Schmidt AG, Adachi Y, Onodera T, et al. Antibodies to a conserved influenza head interface epitope protect by an IgG subtype-dependent mechanism. *Cell.* (2019) 177:1124–35.e16. doi: 10.1016/j.cell.2019.03.048
78. Das DK, Govindan R, Nikić-Spiegel I, Krammer F, Lemke EA, Munro JB. Direct visualization of the conformational dynamics of single influenza hemagglutinin trimers. *Cell.* (2018) 174:926–37.e12. doi: 10.1016/j.cell.2018.05.050
79. Adachi Y, Tonouchi K, Nithichanon A, Kuraoka M, Watanabe A, Shinnakasu R, et al. Exposure of an occluded hemagglutinin epitope drives selection of a class of cross-protective influenza antibodies. *Nat Commun.* (2019) 10:3883. doi: 10.1038/s41467-019-11821-6
80. Yewdell JW, Taylor A, Yellen A, Caton A, Gerhard W, Bächi T. et al. Mutations in or near the fusion peptide of the influenza virus hemagglutinin affect an antigenic site in the globular region. *J Virol.* (1993) 67:933–42.
81. Bangaru S, Zhang H, Gilchuk IM, Voss TG, Irving RP, Gilchuk P, et al. A multifunctional human monoclonal neutralizing antibody that targets a unique conserved epitope on influenza. *Nat Commun.* (2018) 9:2669. doi: 10.3410/f.733623822.793548444
82. Paul SS, Mok CK, Mak TM, Ng OW, Aboagye JO, Wohlbold TJ, et al. A cross-clade H5N1 influenza A virus neutralizing monoclonal antibody binds to a novel epitope within the vestigial esterase domain of hemagglutinin. *Antiviral Res.* (2017) 144:299–310. doi: 10.1016/j.antiviral.2017.06.012
83. Chai N, Swem LR, Park S, Nakamura G, Chiang N, Estevez A, et al. A broadly protective therapeutic antibody against influenza B virus with two mechanisms of action. *Nat Commun.* (2017) 8:14234. doi: 10.1038/ncomms14234
84. Sesterhenn F, Bonet J, Correia BE. Structure-based immunogen design-leading the way to the new age of precision vaccines. *Curr Opin Struct Biol.* (2018) 51:163–9. doi: 10.1016/j.sbi.2018.06.002
85. Sesterhenn F, Yang C, Cramer JT, Bonet J, Wen X, Abriata LA, et al. Trivalent cocktail of *de novo* designed immunogens enables the robust induction and focusing of functional antibodies *in vivo*. *bioRxiv*. (2019) 685867. doi: 10.1101/685867
86. Angeletti D, Yewdell JW. Is it possible to develop a "Universal" Influenza virus vaccine? outflanking antibody immunodominance on the road to universal influenza vaccination. *Cold Spring Harb Perspect Biol.* (2018) 10:a028852. doi: 10.1101/cshperspect.a028852
87. Cohen J. Immunology. A once-in-a-lifetime flu shot? *Science*. (2013) 341:1171. doi: 10.1126/science.341.6151.1171
88. Impagliazzo A, Milder F, Kuipers H, Wagner MV, Zhu X, Hoffman RM, et al. A stable trimeric influenza hemagglutinin stem as a broadly protective immunogen. *Science.* (2015) 349:1301–6. doi: 10.1126/science.aac7263
89. Mallajosyula VV, Citron M, Ferrara F, Lu X, Callahan C, Heidecker GJ, et al. Influenza hemagglutinin stem-fragment immunogen elicits broadly neutralizing antibodies and confers heterologous protection. *Proc Natl Acad Sci USA.* (2014) 111:E2514–23. doi: 10.1073/pnas.1402766111
90. Mallajosyula VV, Citron M, Ferrara F, Temperton NJ, Liang X, Flynn JA, et al. Hemagglutinin sequence conservation guided stem immunogen design from influenza A H3 subtype. *Front Immunol.* (2015) 6:329. doi: 10.3389/fimmu.2015.00329
91. Valkenburg SA, Mallajosyula VV, Li OT, Chin AW, Carnell G, Temperton N, et al. Stalking influenza by vaccination with pre-fusion headless HA mini-stem. *Sci Rep.* (2016) 6:22666. doi: 10.1038/srep22666
92. Vatti A, Monsalve DM, Pacheco Y, Chang C, Anaya JM, Gershwin ME. Original antigenic sin: a comprehensive review. *J Autoimmun.* (2017) 83:12–21. doi: 10.1016/j.jaut.2017.04.008
93. van der Lubbe JEM, Huizingh J, Verspuij JWA, Tettero L, Schmit-Tillemans SPR, Mooij P, et al. Mini-hemagglutinin vaccination induces cross-reactive antibodies in pre-exposed NHP that protect mice against lethal influenza challenge. *NPJ Vaccines.* (2018) 3:25. doi: 10.1038/s41541-018-0063-7
94. Lee LA, Wang Q. Adaptations of nanoscale viruses and other protein cages for medical applications. *Nanomedicine.* (2006) 2:137–49. doi: 10.1016/j.nano.2006.07.009
95. Yassine HM, Boyington JC, McTamney PM, Wei CJ, Kanekiyo M, Kong WP, et al. Hemagglutinin-stem nanoparticles generate heterosubtypic influenza protection. *Nat Med.* (2015) 21:1065–70. doi: 10.1038/nm.3927
96. Corbett KS, Moin SM, Yassine HM, Cagigi A, Kanekiyo M, Boyoglu-Barnum S, et al. Design of nanoparticulate group 2 influenza virus hemagglutinin stem antigens that activate unmutated ancestor B cell receptors of broadly neutralizing antibody lineages. *MBio.* (2019) 10:e02810–18. doi: 10.1128/mBio.02810-18
97. Hai R, Krammer F, Tan GS, Pica N, Eggink D, Maamary J, et al. Influenza viruses expressing chimeric hemagglutinins:globular head and stalk domains derived from different subtypes. *J Virol.* (2012) 86:5774–81. doi: 10.1128/JVI.00137-12
98. Krammer F, Pica N, Hai R, Margine I, Palese P. Chimeric hemagglutinin influenza virus vaccine constructs elicit broadly protective stalk-specific antibodies. *J Virol.* (2013) 87:6542–50. doi: 10.1128/JVI.00641-13
99. Nachbagauer R, Miller MS, Hai R, Ryder AB, Rose JK, Palese P, et al. Hemagglutinin stalk immunity reduces influenza virus replication and transmission in ferrets. *J Virol.* (2015) 90:3268–73. doi: 10.1128/JVI.02481-15
100. Nachbagauer R, Kinzler D, Choi A, Hirsh A, Beaulieu E, Lecrenier N, et al. A chimeric haemagglutinin-based influenza split virion vaccine adjuvanted with AS03 induces protective stalk-reactive antibodies in mice. *NPJ Vaccines.* (2016) 1:16015. doi: 10.1038/npjvaccines.2016.15
101. Krammer F, Hai R, Yondola M, Tan GS, Leyva-Grado VH, Ryder AB, et al. Assessment of influenza virus hemagglutinin stalk-based immunity in ferrets. *J Virol.* (2014) 88:3432–42. doi: 10.1128/JVI.03004-13
102. Ryder AB, Nachbagauer R, Buonocore L, Palese P, Krammer F, Rose JK. Vaccination with vesicular stomatitis virus-vectored chimeric hemagglutinins protects mice against divergent influenza virus challenge strains. *J Virol.* (2015) 90:2544–50. doi: 10.1128/JVI.02598-15
103. Margine I, Krammer F, Hai R, Heaton NS, Tan GS, Andrews SA, et al. Hemagglutinin stalk-based universal vaccine constructs protect against group 2 influenza A viruses. *J Virol.* (2013) 87:10435–46. doi: 10.1128/JVI.01715-13
104. Ermler ME, Kirkpatrick E, Sun W, Hai R, Amanat F, Chromikova V, et al. Chimeric hemagglutinin constructs induce broad protection against influenza B virus challenge in the mouse model. *J Virol.* (2017) 91:e00286–17. doi: 10.1128/JVI.00286-17
105. Isakova-Sivak I, Korenkov D, Smolonogina T, Kotomina T, Donina S, Matyushenko V, et al. Broadly protective anti-hemagglutinin stalk antibodies induced by live attenuated influenza vaccine expressing chimeric hemagglutinin. *Virology.* (2018) 518:313–23. doi: 10.1016/j.virol.2018.03.013

106. Bernstein DI, Guptill J, Naficy A, Nachbagauer R, Berlanda-Scorza F, Feser J, et al. Immunogenicity of chimeric haemagglutinin-based, universal influenza virus vaccine candidates:interim results of a randomised, placebo-controlled, phase 1 clinical trial. *Lancet Infect Dis.* 20:80–91 (2020). doi: 10.1016/S1473-3099(19)30393-7.
107. Tate MD, Job ER, Deng YM, Gunalan V, Maurer-Stroh S, Reading PC. Playing hide and seek:how glycosylation of the influenza virus hemagglutinin can modulate the immune response to infection. *Viruses.* (2014) 6:1294–316. doi: 10.3390/v6031294
108. Tseng YC, Wu CY, Liu ML, Chen TH, Chiang WL, Yu YH, et al. Egg-based influenza split virus vaccine with monoglycosylation induces cross-strain protection against influenza virus infections. *Proc Natl Acad Sci USA.* (2019) 116:3935–7. doi: 10.1073/pnas.1819197116
109. Liu WC, Jan JT, Huang YJ, Chen TH, Wu SC. Unmasking Stem-specific neutralizing epitopes by abolishing N-linked glycosylation sites of influenza virus hemagglutinin proteins for vaccine design. *J Virol.* (2016) 90:8496–508. doi: 10.1128/JVI.00880-16
110. Eggink D, Goff PH, Palese P. Guiding the immune response against influenza virus hemagglutinin toward the conserved stalk domain by hyperglycosylation of the globular head domain. *J Virol.* (2014) 88:699–704. doi: 10.1128/JVI.02608-13
111. Weidenbacher PA, Kim PS. Protect, modify, deprotect (PMD):A strategy for creating vaccines to elicit antibodies targeting a specific epitope. *Proc Natl Acad Sci USA.* (2019) 116:9947–52. doi: 10.1073/pnas.1822062116
112. Wang W, Song HS, Keller PW, Alvarado-Facundo E, Vassell R, Weiss CD. Conformational stability of the hemagglutinin of H5N1 influenza a viruses influences susceptibility to broadly neutralizing stem antibodies. *J Virol.* (2018) 92:e00247–18. doi: 10.1128/JVI.00247-18
113. Kanekiyo M, Joyce MG, Gillespie RA, Gallagher JR, Andrews SF, Yassine HM, et al. Mosaic nanoparticle display of diverse influenza virus hemagglutinins elicits broad B cell responses. *Nat Immunol.* (2019) 20:362–72. doi: 10.1038/s41590-018-0305-x
114. Krammer F. Fighting influenza through hemagglutinin diversity. *Nat Immunol.* (2019) 20:246–47. doi: 10.1038/s41590-019-0317-1
115. Anderson AM, Baranowska-Hustad M, Braathen R, Grodeland G, Bogen B. Simultaneous targeting of multiple hemagglutinins to APCs for induction of broad immunity against influenza. *J Immunol.* (2018) 200:2057–66. doi: 10.4049/jimmunol.1701088
116. Carter DM, Darby CA, Lefoley BC, Crevar CJ, Alefantis T, Oomen R, et al. Design and characterization of a computationally optimized broadly reactive hemagglutinin vaccine for H1N1 influenza viruses. *J Virol.* (2016) 90:4720–34. doi: 10.1128/JVI.03152-15
117. Giles BM, Ross TM. Computationally optimized antigens to overcome influenza viral diversity. *Exp Rev Vaccines.* (2012) 11:267–9. doi: 10.1586/erv.12.3
118. Sautto GA, Kirchenbaum GA, Ecker JW, Bebin-Blackwell AG, Pierce SR, Ross TM. Elicitation of broadly protective antibodies following infection with influenza viruses expressing H1N1 computationally optimized broadly reactive hemagglutinin antigens. *Immunohorizons.* (2018) 2:226–37. doi: 10.4049/immunohorizons.1800044
119. Giles BM, Crevar CJ, Carter DM, Bissel SJ, Schultz-Cherry S, Wiley CA, et al. A computationally optimized hemagglutinin virus-like particle vaccine elicits broadly reactive antibodies that protect nonhuman primates from H5N1 infection. *J Infect Dis.* (2012) 205:1562–70. doi: 10.1093/infdis/jis232
120. Giles BM, Ross TM. A computationally optimized broadly reactive antigen (COBRA) based H5N1 VLP vaccine elicits broadly reactive antibodies in mice and ferrets. *Vaccine.* (2011) 29:3043–54. doi: 10.1016/j.vaccine.2011.01.100
121. Wong TM, Allen JD, Bebin-Blackwell AG, Carter DM, Alefantis T, DiNapoli J, et al. Computationally optimized broadly reactive hemagglutinin elicits hemagglutination inhibition antibodies against a panel of H3N2 influenza virus cocirculating variants. *J Virol.* (2017) 91:e01581–17. doi: 10.1128/JVI.01581-17
122. Allen JD, Owino SO, Carter DM, Crevar CJ, Reese VA, Fox CB, et al. Broadened immunity and protective responses with emulsion-adjuvanted H5 COBRA-VLP vaccines. *Vaccine.* (2017) 35:5209–16. doi: 10.1016/j.vaccine.2017.07.107
123. Crevar CJ, Carter DM, Lee KY, Ross TM. Cocktail of H5N1 COBRA HA vaccines elicit protective antibodies against H5N1 viruses from multiple clades. *Hum Vaccin Immunother.* (2015) 11:572–83. doi: 10.1080/21645515.2015.1012013
124. Pinto LH, Lamb RA, The M2 proton channels of influenza A and B viruses. *J Biol Chem.* (2006) 281:8997–9000. doi: 10.1074/jbc.R500020200
125. Neirynck S, Deroo T, Saelens X, Vanlandschoot P, Jou WM, Fiers W. A universal influenza A vaccine based on the extracellular domain of the M2 protein. *Nat Med.* (1999) 5:1157–63. doi: 10.1038/13484
126. De Filette M, Ramne A, Birkett A, Lycke N, Löwenadler B, Min Jou W, et al. The universal influenza vaccine M2e-HBc administered intranasally in combination with the adjuvant CTA1-DD provides complete protection. *Vaccine.* (2006) 24:544–51. doi: 10.1016/j.vaccine.2005.08.061
127. Eliasson DG, Omokanye A, Schön K, Wenzel UA, Bernasconi V, Bemark M, et al. M2e-tetramer-specific memory CD4 T cells are broadly protective against influenza infection. *Mucosal Immunol.* (2018) 11:273–89. doi: 10.1038/mi.2017.14
128. Fu TM, Freed DC, Horton MS, Fan J, Citron MP, Joyce JG, et al. Characterizations of four monoclonal antibodies against M2 protein ectodomain of influenza A virus. *Virology.* (2009) 385:218–26. doi: 10.1016/j.virol.2008.11.035
129. Bernasconi V, Bernocchi B, Ye L, Lê MQ, Omokanye A, Carpentier R, et al. Porous nanoparticles with self-adjuvanting M2e-fusion protein and recombinant hemagglutinin provide strong and broadly protective immunity against influenza virus infections. *Front Immunol.* (2018) 9:2060. doi: 10.3389/fimmu.2018.02060
130. Eliasson DG, El Bakkouri K, Schön K, Ramne A, Festjens E, Löwenadler B, et al. CTA1-M2e-DD:a novel mucosal adjuvant targeted influenza vaccine. *Vaccine.* (2008) 26:1243–52. doi: 10.1016/j.vaccine.2007.12.027
131. McMichael AJ, Picker LJ.Schepens B, De Vlieger D, Saelens X. Vaccine options for influenza:thinking small. *Curr Opin Immunol.* (2018) 53:22–9. doi: 10.1016/j.coi.2018.03.024
132. Kilbourne ED, Laver WG, Schulman JL, Webster RG. Antiviral activity of antiserum specific for an influenza virus neuraminidase. *J Virol.* (1968) 2:281–8.
133. Kosik I, Yewdell JW. Influenza Hemagglutinin and Neuraminidase:Yin(-)Yang proteins coevolving to thwart immunity. *Viruses.* (2019) 11:346. doi: 10.3390/v11040346
134. Maier HE, Nachbagauer R, Kuan G, Ng S, Lopez R, Sanchez N, et al. Pre-existing anti-neuraminidase antibodies are associated with shortened duration of influenza A (H1N1)pdm virus shedding and illness in naturally infected adults. *Clin Infect Dis.* (2019) 2019:ciz639. doi: 10.1093/cid/ciz639
135. Ng S, Nachbagauer R, Balmaseda A, Stadlbauer D, Ojeda S, Patel M, et al. Novel correlates of protection against pandemic H1N1 influenza A virus infection. *Nat Med.* (2019) 25:962–7. doi: 10.1038/s41591-019-0463-x
136. Chen YQ, Wohlbold TJ, Zheng NY, Huang M, Huang Y, Neu KE, et al. Influenza infection in humans induces broadly cross-reactive and protective neuraminidase-reactive antibodies. *Cell.* (2018) 173:417–29.e10. doi: 10.1016/j.cell.2018.03.030
137. Stadlbauer D, Zhu X, McMahon M, Turner JS, Wohlbold TJ, Schmitz AJ, et al. Broadly protective human antibodies that target the active site of influenza virus neuraminidase. *Science.* (2019) 366:499–504. doi: 10.1126/science.aay0678
138. Laver WG, Air GM, Webster RG, Markoff LJ. Amino acid sequence changes in antigenic variants of type A influenza virus N2 neuraminidase. *Virology.* (1982) 122:450–60. doi: 10.1016/0042-6822(82)90244-6
139. Webster RG, Hinshaw VS, Laver WG. Selection and analysis of antigenic variants of the neuraminidase of N2 influenza viruses with monoclonal antibodies. *Virology.* (1982) 117:93–104. doi: 10.1016/0042-6822(82)90510-4
140. Air GM, Els MC, Brown LE, Laver WG, Webster RG. Location of antigenic sites on the three-dimensional structure of the influenza N2 virus neuraminidase. *Virology.* (1985) 145:237–48. doi: 10.1016/0042-6822(85)90157-6
141. Jiang L, Fantoni G, Couzens L, Gao J, Plant E, Ye Z, et al. Comparative efficacy of monoclonal antibodies that bind to different epitopes of the 2009 pandemic H1N1 influenza virus neuraminidase. *J Virol.* (2016) 90:117–28. doi: 10.1128/JVI.01756-15

142. Andrews SF, Chambers MJ, Schramm CA, Plyler J, Raab JE, Kanekiyo M, et al. Activation dynamics and immunoglobulin evolution of pre-existing and newly generated human memory B cell responses to influenza hemagglutinin. *Immunity*. (2019) 51:398–410.e5. doi: 10.1016/j.immuni.2019.06.024
143. Schmidt AG, Therkelsen MD, Stewart S, Kepler TB, Liao HX, Moody MA, et al. Viral receptor-binding site antibodies with diverse germline origins. *Cell*. (2015) 161:1026–34. doi: 10.1016/j.cell.2015.04.028
144. Li GM, Chiu C, Wrammert J, McCausland M, Andrews SF, Zheng NY, et al. Pandemic H1N1 influenza vaccine induces a recall response in humans that favors broadly cross-reactive memory B cells. *Proc Natl Acad Sci USA*. (2012) 109:9047–52. doi: 10.1073/pnas.1118979109
145. Job ER, Ysenbaert T, Smet A, Van Hecke A, Meuris L, Kleanthous H, et al. Fcgamma receptors contribute to the antiviral properties of influenza virus neuraminidase-specific antibodies. *MBio*. (2019) 10:e01667–19. doi: 10.1128/mBio.01667-19
146. Couch RB, Atmar RL, Keitel WA, Quarles JM, Wells J, Arden N, et al. Randomized comparative study of the serum antihemagglutinin and antineuraminidase antibody responses to six licensed trivalent influenza vaccines. *Vaccine*. (2012) 31:190–5. doi: 10.1016/j.vaccine.2012.10.065
147. Laguio-Vila MR, Thompson MG, Reynolds S, Spencer SM, Gaglani M, Naleway A, et al. Comparison of serum hemagglutinin and neuraminidase inhibition antibodies after 2010–2011 trivalent inactivated influenza vaccination in healthcare personnel. *Open Forum Infect Dis*. (2015) 2:ofu115. doi: 10.1093/ofid/ofu115
148. Schotsaert M, Ysenbaert T, Neyt K, Ibañez LI, Bogaert P, Schepens B, et al. Natural and long-lasting cellular immune responses against influenza in the M2e-immune host. *Mucosal Immunol*. (2013) 6:276–87. doi: 10.1038/mi.2012.69
149. El Bakkouri K, Descamps F, De Filette M, Smet A, Festjens E, Birkett A, et al. Universal vaccine based on ectodomain of matrix protein 2 of influenza A:Fc receptors and alveolar macrophages mediate protection. *J Immunol*. (2011) 186:1022–31. doi: 10.4049/jimmunol.0902147
150. Scorza FB, Pardi N. New kids on the block:RNA-based influenza virus vaccines. *Vaccines*. (2018) 6:20. doi: 10.3390/vaccines6020020
151. Angeletti D, Kosik I, Santos JJS, Yewdell WT, Boudreau CM, Mallajosyula VVA, et al. Outflanking immunodominance to target subdominant broadly neutralizing epitopes. *Proc Natl Acad Sci USA*. (2019) 116:13474–9. doi: 10.1073/pnas.1816300116
152. Cirelli KM, Carnathan DG, Nogal B, Martin JT, Rodriguez OL, Upadhyay AA, et al. Slow delivery immunization enhances HIV neutralizing antibody and germinal center responses via modulation of immunodominance. *Cell*. (2019) 177:1153–71.e28. doi: 10.1016/j.cell.2019.04.012
153. Moyer TJ, Zmolek AC, Irvine DJ. Beyond antigens and adjuvants:formulating future vaccines. *J Clin Invest*. (2016) 126:799–808. doi: 10.1172/JCI81083

Conflict of Interest: The authors declare that the research was conducted in the absence of any commercial or financial relationships that could be construed as a potential conflict of interest.

frontiers in Immunology

REVIEW
published: 21 January 2020
doi: 10.3389/fimmu.2019.03155

Humoral Immunity vs. *Salmonella*

Akiko Takaya[1], *Tomoko Yamamoto*[2] *and Koji Tokoyoda*[3]*

[1] Laboratory of Microbiology and Molecular Genetics, Graduate School of Pharmaceutical Sciences, Chiba University, Chiba, Japan, [2] Department of Infectious Diseases, Medical Mycology Research Center, Chiba University, Chiba, Japan, [3] Deutsches Rheuma-Forschungszentrum Berlin (DRFZ), A Leibniz Institute, Berlin, Germany

In primary infection with *Salmonella*, it has been reported—without consideration of *Salmonella*'s functions—that humoral immunity plays no role in the clearance of bacteria. In fact, *Salmonella* targets and suppresses several aspects of humoral immunity, including B cell lymphopoiesis, B cell activation, and IgG production. In particular, the suppression of IgG-secreting plasma cell maintenance allows the persistence of *Salmonella* in tissues. Therefore, the critical role(s) of humoral immunity in the response to *Salmonella* infection, especially at the late phase, should be re-investigated. The suppression of IgG plasma cell memory strongly hinders vaccine development against non-typhoidal *Salmonella* (NTS) because *Salmonella* can also reduce humoral immune memory against other bacteria and viruses, obtained from previous vaccination or infection. We propose a new vaccine against *Salmonella* that would not impair humoral immunity, and which could also be used as a treatment for antibody-dependent autoimmune diseases to deplete pathogenic long-lived plasma cells, by utilizing the *Salmonella*'s own suppression mechanism of humoral immunity.

Keywords: humoral immunity, antibody, plasma cells, IgG, *Salmonella*

OPEN ACCESS

Edited by:
Giuseppe Andrea Sautto, University of Georgia, United States

Reviewed by:
Carl De Trez, Vrije University Brussel, Belgium
Mark L. Lang, University of Oklahoma Health Sciences Center, United States

***Correspondence:**
Koji Tokoyoda
tokoyoda@drfz.de

Specialty section:
This article was submitted to Vaccines and Molecular Therapeutics, a section of the journal Frontiers in Immunology

Received: *25 October 2019*
Accepted: *30 December 2019*
Published: *21 January 2020*

Citation:
Takaya A, Yamamoto T and Tokoyoda K (2020) Humoral Immunity vs. Salmonella. Front. Immunol. 10:3155. doi: 10.3389/fimmu.2019.03155

INTRODUCTION

The immune system, i.e., innate and adaptive immunity, can overcome many types of bacterial infections. The frontline against infection with bacteria such as *Salmonella* is innate immunity. *Salmonella* infection leads to enteric fever or diarrhea, often resulting in death of humans and animals. The pathogenesis of infection should be separately considered as two dynamics of the immune system vs. *Salmonella*: firstly, bacterial growth within 1 week after infection and, secondly, if protected from death, bacterial clearance after 1 week after infection. Early bacterial growth in mice is controlled by the Nramp gene, expressed in macrophages (1), and is suppressed by a T-cell-independent host response which requires granuloma formation and production of nitric oxide and cytokines such as tumor necrosis factor α (TNFα), interleukin 12 (IL-12) and interferon γ (IFNγ) (2–6). For clearance of the bacteria, innate immunity, namely the complement system and phagocytosis by macrophages, neutrophils and dendritic cells, are the most critical responses against the bacterial pathogens, while IFNγ and antibodies resulting from adaptive immunity also dramatically enhance the innate immune response. It has been thought that adaptive immunity itself dominantly works for secondary infection except for IFNγ from T cells. However, it remains enigmatic how adaptive immunity contributes to the clearance of *Salmonella* in the primary infection. We herein discuss the roles of humoral immunity against *Salmonella* for the clearance of the bacteria.

DEVELOPING A VACCINE AGAINST *SALMONELLA*

Salmonella enterica is a Gram-negative intracellular bacterium with over 2,500 different serovars identified until now. *Salmonella* Typhi (*S.* Typhi) and *S.* Paratyphi cause typhoid fever, a systemic febrile illness only affecting humans. The other numerous NTS serovars such as *S.* Typhimurium and *S.* Enteritidis infect many different hosts and results in diarrheal disease. NTS also causes severe, extra-intestinal, invasive bacteremia, referred to as invasive NTS (iNTS) disease (7). Immunocompromised individuals, including those infected with human immunodeficiency virus (HIV) or malaria, and infants are particularly at risk of acquiring iNTS disease (8–12). iNTS disease is estimated to cause 3.4 million cases of illness and 681,316 deaths annually, with 63.7% of all cases occurring in children under the age of five (8). Thus, infection with NTS is still a serious health concern. Moreover, the emergence of multidrug-resistant strains of *Salmonella* calls into question the future use of antibiotics to treat infection and further emphasizes the need for the development of the safer and more effective vaccines. While a vaccine against NTS is not currently available, it has been reported that naturally acquired antibodies against NTS reduce the risk of iNTS disease (13, 14). In contrast, infection with *S.* Typhi can be prevented by vaccination with attenuated strains, e.g., Ty21a. However, effective vaccines preventing iNTS disease are likely to differ from those protecting against *S.* Typhi infections. Furthermore, it is known that *Salmonella* generates chronic carriers; a chronic carrier state has been identified in 2.2% of patients with reported NTS, lasting from 30 days to 8.3 years (15). Although *Salmonella* invades myeloid cells and escapes phagocytosis, it is unclear why humoral immunity does not contribute to the clearance of *Salmonella* which continuously transfers among short-lived myeloid cells. Overall, the lack of a vaccine and the presence of chronic carriers suggests that NTS suppresses long-lasting humoral immunity, i.e., humoral memory.

THE IMMUNE SYSTEM VS. *SALMONELLA*

Infection of susceptible Nramp^{-} mice with *S.* Typhimurium provides a murine model for typhoid fever which bears many similarities to human *S.* Typhi infection. This *S.* Typhi model is ultimately fatal due to the inability of such mice to restrict bacterial growth *in vivo*. Administration of attenuated strains of *S.* Typhimurium as a model of vaccination resulted in the generation of immune memory against *Salmonella* and protection against death from challenge with a virulent strain of the bacteria (16, 17). The murine model infected with virulent *S.* Typhimurium showed similar pathogenesis on the early growth of bacteria. However, it seems unclear whether the model with attenuated *S.* Typhimurium really mimics the clearance of *Salmonella*, i.e., whether *S.* Typhi and *S.* Typhimurium are excluded from their hosts in a similar way. Many studies have discussed typhoidal disease using NTS strains based on the assumption that *S.* Typhi and *S.* Typhimurium utilize the same invasion system in the hosts. However, it is impossible to compare the mechanism on the clearance of *Salmonella in vivo*, because *S.* Typhi is not infectious in mice. If *S.* Typhi and *S.* Typhimurium are excluded by distinct bacterial clearances, the difference may affect the ability to generate vaccines against *S.* Typhi and *S.* Typhimurium.

Innate cells can have several roles to play during the early stage of an infection, including controlling bacterial replication and producing cytokines and chemokines that activate and recruit inflammatory cells to the site of infection. Macrophages, neutrophils and dendritic cells increase in number early after *Salmonella* infection and produce cytokines that are important for host survival, such as TNFα. All three phagocytic cell types also harbor bacteria during infection. IFNγ from natural killer cells at the very early infection phase and from T cells at the late infection phase can activate macrophages and promote phagocytosis (18). In addition to innate cells, the clearance of bacteria from the tissues also requires functional CD4 T cells (19), resulting in long-lasting specific immunity to re-challenge infection (20). Susceptible mice can resolve a primary infection with attenuated *Salmonella* strains which requires a functioning immune system that can develop a T-bet-dependent Th1 cell response and IFNγ production to activate infected macrophages (19, 21). Similarly, mice lacking IL-12, IFNγ, reactive oxygen species, or inducible nitric oxide, all have deficiencies in primary clearance of *Salmonella* (22, 23). In contrast, mice lacking B cells resolve primary infection with attenuated bacterial strains with similar kinetics to wildtype mice (24, 25), indicating that B-cell responses do not participate in the primary clearance of the bacteria. CD8 T cells are generally not thought to contribute to the primary clearance of attenuated *Salmonella*, based on studies using β2-microglobulin-deficient mice that lack class I-restricted CD8 T cells (19, 26). However, recent experiments in mice lacking classical MHC class Ia genes, perforin, or granzyme, show that CD8 T cells make a modest contribution to *Salmonella* clearance during the later stages of the primary response (27). Overall, these data suggest a primary role for CD4 Th1 cells, a modest role for CD8 T cells and no role for B cells in primary immunity to *Salmonella*. However, the roles of adaptive immunity were considered from the viewpoint of how the lymphocytes respond to the infection, without any consideration of how *Salmonella* may purposefully subvert the immune response for its own advantage.

HUMORAL IMMUNITY VS. *SALMONELLA*

Immunization and infection with *Salmonella* greatly affects hematopoiesis in a TNFα- and CXCL12-dependent manner (28, 29). *Salmonella* is known to activate myelopoiesis and suppress B lymphopoiesis (30). Interestingly, the disruption of B lymphopoiesis has been also reported on *Plasmodium* infection in mice (31), suggesting the similar mechanism to *Salmonella*. This dramatic change in cellular commitment/differentiation is very reasonable, because in the early phase of infection, the immune system requires as many innate cells as possible to fight against the infection. Expanded myeloid cells are able to kill a

lot of *Salmonella*, but some become the host cells for *Salmonella* without phagocytosis. Furthermore, the provision of B cells to the periphery is impaired due to death of B cell precursors in the bone marrow (BM), resulting in an indirect advantage to *Salmonella* for their long-term persistence.

In general, antibodies can protect against bacteria mainly by facilitating the uptake of the pathogen by phagocytic cells, which then destroy the ingested bacteria. Antibodies do this in two ways: one is to coat the pathogen to be recognized by Fc receptors on phagocytic cells, which is called opsonization. Alternatively, antibodies binding to the surface of a pathogen can activate the proteins of the complement system. Complement activation results in opsonization of the pathogen by binding complement receptors on phagocytes. Other complement components recruit phagocytic cells to the site of infection, and the terminal components of complement can lyse certain microorganisms directly by forming pores in their membranes. Most intracellular pathogens spread by moving from cell to cell through the extracellular fluids. The extracellular spaces are protected by humoral immunity. Antibodies produced by plasma cells cause the destruction of extracellular microorganisms and therefore prevent the spread of intracellular infections. Phagocytes, *Salmonella*'s hosts, are short-lived and survive for 0.75 days (neutrophils, lifespan) (32), 18–20 h (phagocytic monocytes, half-life) (33), 1.5–2.9 days (dendritic cells, half-life) (34), and <7 days (peripheral macrophages, lifespan) (35). Therefore, in order to survive, *Salmonella* has to transfer into new host cells every 1–7 days passing through extracellular fluids containing antibodies. It is unknown how and why *Salmonella* can escape from antibodies in extracellular spaces when transferring into new host cells. In secondary immune responses, anti-S*almonella* IgG are critical for the enhancement of phagocytosis. However, anti-*Salmonella* IgG in the late phase of the primary immune response does not contribute to the clearance of the bacteria (23). This raises the following questions: what is the difference of anti-*Salmonella* antibodies in the primary and secondary immune responses? Is the affinity and/or amount of antibodies important? What other functions of *Salmonella* have to be also considered in the subversion of the immune response?

The activation of B cells and their differentiation into long-lived plasma cells is triggered by antigen and usually requires CD4 T cell help, presenting antigen on MHC class II. Bayer-Santos and his colleagues showed that a *Salmonella* protein, SteD depletes surface MHC class II and inhibits T cell activation (36). SteD localized in the Golgi network and vesicles containing the E3 ubiquitin ligase MARCH8 and MHC class II causing MARCH8-dependent ubiquitination and depletion of surface MHC class II and B7-2. A subset of effector CD4 T cells, known as T follicular helper cells, also control isotype switching and have a role in initiating somatic hypermutation of antibody variable V-region genes for affinity maturation mainly in germinal centers (GCs) of the spleen. Cunningham et al. indicated that GC formation is delayed when infected with *Salmonella* (37). However, GC-lacking CD40L (CD154)-deficient mice can normally induce the clearance of *Salmonella* in tissues. The formation of GCs and the affinity of antibodies do not affect the clearance of the bacteria. Di Niro et al. showed that *Salmonella* induces random activation, generating only a small fraction (0.5–2%) of *Salmonella*-specific plasma cells, and somatic hypermutation occurred efficiently at extrafollicular sites (38). Although it should be investigated how the abnormal induction consequently affects the immune responses, it is very intriguing why *Salmonella* does not allow immune cells to utilize the standard immune activation/maturation pathways. Following GC formation, B cells can differentiate into either short-lived plasma cells, memory B cells, or long-lived plasma cells. Memory B cells persist and are important for secondary immune responses against the same pathogen. Short-lived plasma cells temporally provide IgG, but do not survive for long periods of time. In contrast, long-lived plasma cells, or their precursors, migrate into the BM and persist in CXCL12-expressing stromal cells (39, 40). In general, IgG is the most critical antibody isotype for the clearance of bacteria and greatly contributes to the clearance of bacteria at least in the late phase of infection. In contrast, in the clearance of *Salmonella*, no role of B cells which has a potential to differentiate into IgG-secreting plasma cells has been reported. The distinction led to a possibility of *Salmonella*-specific suppression of humoral immunity, in particular IgG production as described below.

SALMONELLA ATTACKS THE MAIN SOURCE OF IGG

McSorley and Jenkins showed (i) that *Salmonella* can similarly survive in the tissues of naive wild-type and B cell-deficient mice until day 35 after infection, suggesting that antibodies and B cells are not necessary for the clearance of *Salmonella*, and (ii) that injection of heat-killed *Salmonella* induces a provision of anti-*Salmonella* IgG from day 20, although data of anti-*Salmonella* IgG titers in mice infected with live *Salmonella* are lacking (24). However, if *Salmonella* actively suppresses B cell functions, the necessity of B cells for fighting the infection therefore fails to be evaluated by these studies. Very recently, we have shown that *Salmonella* inhibits the persistence of IgG-secreting plasma cells in the BM of mice, which are the main source of serum IgG, by secreting a *Salmonella* protein known as SiiE (41) (**Figure 1**). Mice infected with a SiiE-deficient strain markedly enhanced the provision of anti-*Salmonella* IgG and promoted the clearance of *Salmonella,* even in the primary infection. Given these results, the roles of antibodies and B/plasma cells therefore have to be re-evaluated.

SiiE is known as an adhesin, binding to carbohydrates in a lectin-like manner, thereby promoting attachment of *Salmonella* to polarized epithelial cells and enabling colonization (42, 43). SiiE is secreted by *Salmonella* and remains surface-associated during bacterial invasion (44). SiiE mediates the first direct contact to the host cell through binding to glycostructures containing N-acetyl-glucosamine and/or α2, 3-linked sialic acid (45). Recently, Li et al. suggested that MUC1, the transmembrane mucin that is highly expressed at mucosal surfaces including the stomach and the intestinal tract, is a receptor for SiiE that enables apical invasion into enterocytes (46).

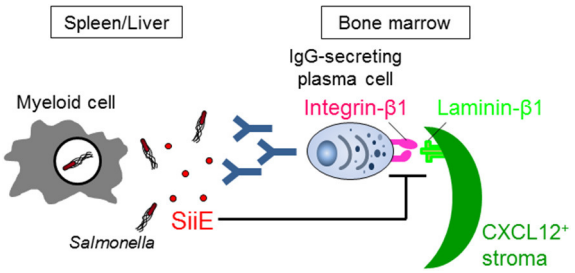

FIGURE 1 | *Salmonella* SiiE suppresses the retention of IgG-secreting plasma cells in BM survival niches by competing with laminin β1. SiiE secreted by *Salmonella* competes with laminin β1 to interact with integrin β1. The competition induces the detachment and then deletion of IgG-secreting plasma cells from laminin $\beta1^{+}CXCL12^{+}$ survival niches of the BM.

SiiE is a large protein with a molecular weight of 595 kDa. It has 53 highly similar repeats of bacterial immunoglobulin (BIg) domains that determine the length and only short protein moieties of distinct structure at the very N- and C-terminal parts (43). The amino acid sequence from 129 to 168 in the short N-terminal moiety has high homology to murine laminin β1. The 236 amino acid residues in the short N-terminal moiety consist of eight heptad repeats with a coiled-coil structure that are flanked by regions with a predominantly β-sheet structure (43). The integrity of the coiled-coil structure is required for the proper retention of SiiE and thereby affects invasion of polarized cells, while the β-sheet domains appear to be essential for the control of release of SiiE. The central part of the coiled-coil structure, including amino acids 129–168, plays an especially essential role in the retention of SiiE (43). The homologous region in the C-terminal region of laminin β1 also has a coiled-coil structure, which is involved in the assembly of a laminin molecule (47). The C-terminal region also modulates the integrin binding affinities of laminins (48). We showed that SiiE can bind to integrin β1, a laminin receptor, on BM IgG-secreting plasma cells and competes with their adhesion to laminin (41). Only the SiiE-derived peptide which has high homology to murine laminin β1 was able to reduce the number of BM IgG-secreting plasma cells. Moreover, the attenuated SiiE-deficient *Salmonella* enhanced both the production of high titers of protective IgG against *Salmonella* and the memory response, suggesting that it may be a novel and efficient vaccine against *Salmonella*. Histological analyses of the BM revealed that IgG- but not IgM-secreting plasma cells bind to laminin β1. Thus, laminin $\beta1^{+}CXCL12^{+}$ stromal cells are an integral part of the survival niche for IgG-secreting plasma cells in the BM, a lesson learnt from *Salmonella*.

ROLES OF HUMORAL IMMUNITY AGAINST *SALMONELLA* AND NEW GENERATION OF VACCINES

Salmonella SiiE reduces the number of BM IgG-secreting plasma cells (41). This reduction may have led to the underestimation of the roles of B cells, especially antibodies, in the late phase of the primary infection with *Salmonella*. If IgG production is not suppressed by *Salmonella* SiiE, humoral immunity, in particular IgG, is required for the clearance of *Salmonella* in the late phase of the primary infection (41). Infection with SiiE-deficient strain into B cell-deficient and wildtype mice should be examined in order to determine the precise role of humoral immunity in the late phase of primary infection with *Salmonella*. Since vaccines against NTS are not yet available, SiiE-deficient *Salmonella* may be the first efficient vaccine against NTS. It still remains unclear why vaccines against *S.* Typhi, but not NTS are available. Intriguingly, the *siiE* gene in *S.* Typhi has been reported as two distinct ORFs, suggesting that it is a pseudogene (49). The presence of a functional SiiE gene may be a reason for the differences in availability of vaccines against the two strains of *Salmonella*. Furthermore, SiiE impairs the persistence of all IgG-secreting plasma cells in an antigen-specific independent manner. This non-specific depletion of IgG-secreting plasma cells may result in the loss of long-lived plasma cells secreting IgG against many kinds of bacteria and viruses generated by previous vaccination or infection. Therefore, generating vaccines against NTS may be essential to avoid such a loss of vital of humoral memory. Other pathogens may also have an ability to suppress humoral immunity. Recent studies indicated that respiratory syncytial virus (RSV) infection fails to induce in IgA^{+} memory B cells (50) and that measles causes elimination of 11–73% of the antibody repertoire and depletion of previously expanded B memory clones after infection (51, 52). However, cellular and molecular mechanisms on their suppression are still unknown and should be investigated, then comparing with the case of *Salmonella*.

TREATMENT OF ANTIBODY-MEDIATED DISEASES USING A *SALMONELLA*-DERIVED PEPTIDE

The SiiE peptide homologous to laminin β1 significantly reduced the number of anti-DNA IgG-secreting plasma cells in the BM in the NZB/W murine model of lupus nephritis (41). This property could therefore be further exploited for the treatment of autoimmune diseases. Autoimmune diseases with a substantial contribution of pathogenic IgG autoantibodies, like systemic lupus erythematosus, can be refractory to conventional treatment e.g., immunosuppressive drugs and anti-CD20 antibodies, because BM plasma cells secreting these autoantibodies are protected in their BM niches (53–55). Multiple myeloma is caused by redundant titers of antibodies generated from plasma cell myeloma in the BM. It has already been reported that myeloma cell lines preferentially contact laminin *in vitro* (56, 57), suggesting that targeting of adhesion molecules including laminin should be considered as novel therapy (58). The depletion of BM plasma cell myeloma by SiiE may directly ameliorate disease. SiiE peptide and the related products may contribute to a recovery for these antibody-mediated diseases without relapse.

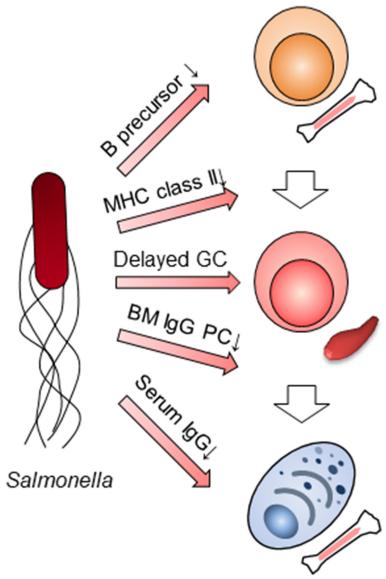

FIGURE 2 | Multilayer suppression of humoral immunity by *Salmonella* infection. *Salmonella* impairs humoral immunity at multiple stages; B cell lymphopoiesis, the expression of MHC class II in myeloid cells, germinal center (GC) formation, the persistence of BM IgG-secreting plasma cells (PC) and IgG titers in serum.

CONCLUSIONS AND PERSPECTIVES

Humoral immunity in the late phase of primary infection with *Salmonella* had been thought not to participate in the clearance of the bacteria. However, when taking into consideration *Salmonella*'s functions, it is clear that several aspects of humoral immunity, in particular the suppression of IgG production, does indeed contribute to the clearance of bacteria in the late phase of the primary infection (**Figure 2**). Using SiiE-deficient *Salmonella*, the collaboration between humoral immunity and other immune systems should be also re-evaluated. The function of other immune cells may be overestimated or underestimated due to the suppression of humoral immunity. Furthermore, the previous candidates of vaccines against NTS should be re-investigated by adding a mutation of SiiE. The combined mutations of *Salmonella* factors which interfere with immune systems may result in the development of the best vaccines against NTS. As infection with NTS may delete all IgG plasma cell memory gained by vaccination obtained from infancy, we therefore also alert to this danger and propose an obligatory use of vaccination against NTS in infancy.

AUTHOR CONTRIBUTIONS

AT and KT wrote the paper. TY supervised the work.

FUNDING

This work was supported by grants from the Leibniz Association (International Leibniz Research Cluster ImmunoMemory, KT), the German Research Council (DFG, TO944/2-1 and TO944/3-1, KT), the Institute for Global Prominent Research in Chiba University (AT), KAKENHI (18K07102, AT).

ACKNOWLEDGMENTS

We thank Mairi A. McGrath for your editing and scientific comments.

REFERENCES

1. Vidal SM, Malo D, Vogan K, Skamene E, Gros, P. Natural resistance to infection with intracellular parasites: isolation of a candidate for Bcg. *Cell.* (1993) 73:469–85. doi: 10.1016/0092-8674(93)90135-D
2. Umezawa K, Akaike T, Fujii S, Suga M, Setoguchi K, Ozawa A, et al. Induction of nitric oxide synthesis and xanthine oxidase and their roles in the antimicrobial mechanism against *Salmonella typhimurium* infection in mice. *Infect Immun.* (1997) 65:2932–40.
3. Kagaya K, Watanabe K, Fukazawa, Y. Capacity of recombinant gamma interferon to activate macrophages for *Salmonella*-killing activity. *Infect Immun.* (1989) 57:609–15.
4. Tite JP, Dougan G, Chatfield, SN. The involvement of tumor necrosis factor in immunity to *Salmonella* infection. *J Immunol.* (1991) 147:3161–4.
5. Kincy-Cain T, Clements JD, Bost KL. Endogenous and exogenous interleukin-12 augment the protective immune response in mice orally challenged with *Salmonella dublin*. *Infect Immun.* (1996) 64:1437–40.
6. Muotiala A, Makela PH. The role of IFN-γ in murine *Salmonella typhimurium* infection. *Microb Pathog.* (1990) 8:135–41. doi: 10.1016/0882-4010(90)90077-4
7. Feasey NA, Dougan G, Kingsley RA, Heyderman RS, Gordon MA. Invasive non-typhoidal salmonella disease: an emerging and neglected tropical disease in Africa. *Lancet.* (2012) 379:2489–99. doi: 10.1016/S0140-6736(11)61752-2
8. Ao TT, Feasey NA, Gordon MA, Keddy KH, Angulo FJ, Crump JA. Global burden of invasive nontyphoidal *Salmonella* disease, 2010. *Emerg Infect Dis.* (2015) 21:941–9. doi: 10.3201/eid2106.140999
9. Majowicz SE, Musto J, Scallan E, Angulo FJ, Kirk M, O'Brien SJ, et al. The global burden of nontyphoidal *Salmonella* gastroenteritis. *Clin Infect Dis.* (2010) 50:882–9. doi: 10.1086/650733
10. Crump JA, Heyderman RS. A perspective on invasive *Salmonella* disease in Africa. *Clin Infect Dis.* (2015) 61:S235–40. doi: 10.1093/cid/civ709
11. Uche IV, MacLennan CA, Saul A. A systematic review of the incidence, risk factors and case fatality rates of invasive nontyphoidal *Salmonella* (iNTS) disease in Africa (1966 to 2014). *PLoS Negl Trop Dis.* (2017) 11:e0005118. doi: 10.1371/journal.pntd.0005118
12. Park SE, Pak GD, Aaby P, Adu-Sarkodie Y, Ali M, Aseffa A, et al. The relationship between invasive nontyphoidal *Salmonella* disease, other bacterial bloodstream infections, and malaria in Sub-Saharan Africa. *Clin Infect Dis.* (2016) 62(Suppl. 1):S23–31. doi: 10.1093/cid/civ893
13. Gordon MA. Invasive nontyphoidal *Salmonella* disease: epidemiology, pathogenesis and diagnosis. *Curr Opin Infect Dis.* (2011) 24:484–9. doi: 10.1097/QCO.0b013e32834a9980
14. MacLennan CA, Gondwe EN, Msefula CL, Kingsley RA, Thomson NR, White SA, et al. The neglected role of antibody in protection against bacteremia caused by nontyphoidal strains of *Salmonella* in African children. *J Clin Invest.* (2008) 118:1553–62. doi: 10.1172/JCI33998

15. Marzel A, Desai PT, Goren A, Schorr YI, Nissan I, Porwollik S, et al. Persistent infections by nontyphoidal *Salmonella* in humans: epidemiology and genetics. *Clin Infect Dis.* (2016) 62:879–86. doi: 10.1093/cid/civ1221
16. Hoiseth SK, Stocker BA. Aromatic-dependent *Salmonella typhimurium* are non-virulent and effective as live vaccines. *Nature.* (1981) 291:238–9. doi: 10.1038/291238a0
17. Tennant SM, Levine MM. Live attenuated vaccines for invasive *Salmonella* infections. *Vaccine.* (2015) 33(Suppl. 3):C36–41. doi: 10.1016/j.vaccine.2015.04.029
18. Ingram JP, Brodsky IE, Balachandran, S. Interferon-γ in *Salmonella* pathogenesis: new tricks for an old dog. *Cytokine.* (2017) 98:27–32. doi: 10.1016/j.cyto.2016.10.009
19. Hess J, Ladel C, Miko D, Kaufmann SH. *Salmonella typhimurium* aroA$^-$ infection in gene-targeted immunodeficient mice: major role of CD4$^+$ TCR-αβcells and IFN-γin bacterial clearance independent of intracellular location. *J Immunol.* (1996) 156:3321–6.
20. Mastroeni P, Harrison JA, Hormaeche CE. Natural resistance and acquired immunity to *Salmonella*. *Fundam Clin Immunol.* (1994) 2:83–95.
21. Ravindran R, Foley J, Stoklasek T, Glimcher LH, McSorley SJ. Expression of T-bet by CD4 T cells is essential for resistance to *Salmonella* infection. *J Immunol.* (2005) 175:4603–10. doi: 10.4049/jimmunol.175.7.4603
22. Mastroeni P, Vazquez-Torres A, Fang FC, Xu Y, Khan S, Hormaeche CE, et al. Antimicrobial actions of the NADPH phagocyte oxidase and inducible nitric oxide synthase in experimental salmonellosis. II. Effects on microbial proliferation and host survival *in vivo*. *J Exp Med.* (2000) 192:237–48. doi: 10.1084/jem.192.2.237
23. Lehmann J, Bellmann S, Werner C, Schroder R, Schutze N, Alber G. IL-12p40-dependent agonistic effects on the development of protective innate and adaptive immunity against *Salmonella enteritidis*. *J Immunol.* (2001) 167:5304–15. doi: 10.4049/jimmunol.167.9.5304
24. McSorley SJ, Jenkins MK. Antibody is required for protection against virulent but not attenuated *Salmonella enterica* serovar Typhimurium. *Infect Immun.* (2000) 68:3344–8. doi: 10.1128/IAI.68.6.3344-3348.2000
25. Mastroeni P, Simmons C, Fowler R, Hormaeche CE, Dougan, G. *Igh-6*$^{-/-}$ (B-cell-deficient) mice fail to mount solid acquired resistance to oral challenge with virulent *Salmonella enterica* serovar Typhimurium and show impaired Th1 T-cell responses to *Salmonella* antigens. *Infect Immun.* (2000) 68:46–53. doi: 10.1128/IAI.68.1.46-53.2000
26. Lo WF, Ong H, Metcalf ES, Soloski MJ. T cell responses to Gram-negative intracellular bacterial pathogens: a role for CD8$^+$ T cells in immunity to *Salmonella* infection and the involvement of MHC class Ib molecules. *J Immunol.* (1999) 162:5398–406.
27. Lee SJ, Dunmire S, McSorley SJ. MHC class-I-restricted CD8 T cells play a protective role during primary *Salmonella* infection. *Immunol Lett.* (2012) 148:138–43. doi: 10.1016/j.imlet.2012.10.009
28. Ueda Y, Yang K, Foster SJ, Kondo M, Kelsoe G. Inflammation controls B lymphopoiesis by regulating chemokine CXCL12 expression. *J Exp Med.* (2004) 199:47–58. doi: 10.1084/jem.20031104
29. Ulich TR, del Castillo J, Ni RX, Bikhazi N. Hematologic interactions of endotoxin, tumor necrosis factor alpha (TNF alpha), interleukin 1, and adrenal hormones and the hematologic effects of TNF alpha in Corynebacterium parvum-primed rats. *J Leukoc Biol.* (1989) 45:546–57. doi: 10.1002/jlb.45.6.546
30. Slocombe T, Brown S, Miles K, Gray M, Barr TA, Gray D. Plasma cell homeostasis: the effects of chronic antigen stimulation and inflammation. *J Immunol.* (2013) 191:3128–38. doi: 10.4049/jimmunol.1301163
31. Bockstal V, Geurts N, Magez S. Acute disruption of bone marrow B lymphopoiesis and apoptosis of transitional and marginal zone B cells in the spleen following a blood-stage *Plasmodium chabaudi* infection in mice. *J Parasitol Res.* (2011) 2011:534697. doi: 10.1155/2011/534697
32. Pillay J, den Braber I, Vrisekoop N, Kwast LM, de Boer RJ, Borghans JA, et al. *In vivo* labeling with 2H2O reveals a human neutrophil lifespan of 5.4 days. *Blood.* (2010) 116:625–7. doi: 10.1182/blood-2010-01-259028
33. Italiani P, Boraschi D. From monocytes to M1/M2 macrophages: phenotypical vs. functional differentiation. *Front Immunol.* (2014) 5:514. doi: 10.3389/fimmu.2014.00514
34. Kamath AT, Henri S, Battye F, Tough DF, Shortman K. Developmental kinetics and lifespan of dendritic cells in mouse lymphoid organs. *Blood.* (2002) 100:1734–41. doi: 10.1182/blood.V100.5.1734.h81702001734_1734_1741
35. van Furth R. Origin and turnover of monocytes and macrophages. *Curr Top Pathol.* (1989) 79:125–50. doi: 10.1007/978-3-642-73855-5_6
36. Bayer-Santos E, Durkin CH, Rigano LA, Kupz A, Alix E, Cerny O, et al. The *Salmonella* effector SteD mediates MARCH8-dependent ubiquitination of MHC II molecules and inhibits T cell activation. *Cell Host Microbe.* (2016) 20:584–95. doi: 10.1016/j.chom.2016.10.007
37. Cunningham AF, Gaspal F, Serre K, Mohr E, Henderson IR, Scott-Tucker A, et al. *Salmonella* induces a switched antibody response without germinal centers that impedes the extracellular spread of infection. *J Immunol.* (2007) 178:6200–7. doi: 10.4049/jimmunol.178.10.6200
38. Di Niro R, Lee SJ, Vander Heiden JA, Elsner RA, Trivedi N, Bannock JM, et al. *Salmonella* infection drives promiscuous B cell activation followed by extrafollicular affinity maturation. *Immunity.* (2015) 43:120–31. doi: 10.1016/j.immuni.2015.06.013
39. Moser K, Tokoyoda K, Radbruch A, MacLennan I, Manz RA. Stromal niches, plasma cell differentiation and survival. *Curr Opin Immunol.* (2006) 18:265–70. doi: 10.1016/j.coi.2006.03.004
40. Tokoyoda K, Egawa T, Sugiyama T, Choi BI, Nagasawa, T. Cellular niches controlling B lymphocyte behavior within bone marrow during development. *Immunity.* (2004) 20:707–18. doi: 10.1016/j.immuni.2004.05.001
41. Manne C, Takaya A, Yamasaki Y, Mursell M, Hojyo S, Wu TY, et al. *Salmonella* SiiE prevents an efficient humoral immune memory by interfering with IgG$^+$ plasma cell persistence in the bone marrow. *Proc Natl Acad Sci USA.* (2019) 116:7425–30. doi: 10.1073/pnas.1818242116
42. Gerlach RG, Claudio N, Rohde M, Jackel D, Wagner C, Hensel M. Cooperation of *Salmonella* pathogenicity islands 1 and 4 is required to breach epithelial barriers. *Cell Microbiol.* (2008) 10:2364–76. doi: 10.1111/j.1462-5822.2008.01218.x
43. Wagner C, Polke M, Gerlach RG, Linke D, Stierhof YD, Schwarz H, et al. Functional dissection of SiiE, a giant non-fimbrial adhesin of *Salmonella enterica*. *Cell Microbiol.* (2011) 13:1286–301. doi: 10.1111/j.1462-5822.2011.01621.x
44. Morgan E, Bowen AJ, Carnell SC, Wallis TS, Stevens MP. SiiE is secreted by the *Salmonella enterica* Serovar Typhimurium Pathogenicity Island 4-encoded secretion system and contributes to intestinal colonization in cattle. *Infect Immun.* (2007) 75:1524–33. doi: 10.1128/IAI.01438-06
45. Wagner C, Barlag B, Gerlach RG, Deiwick J, Hensel M. The *Salmonella enterica* giant adhesin SiiE binds to polarized epithelial cells in a lectin-like manner. *Cell Microbiol.* (2014) 16:962–75. doi: 10.1111/cmi.12253
46. Li X, Bleumink-Pluym NMC, Luijkx Y, Wubbolts RW, van Putten JPM, Strijbis K. MUC1 is a receptor for the *Salmonella* SiiE adhesin that enables apical invasion into enterocytes. *PLoS Pathog.* (2019) 15:e1007566. doi: 10.1371/journal.ppat.1007566
47. Hohenester E. Structural biology of laminins. *Essays Biochem.* (2019) 63:285–95. doi: 10.1042/EBC20180075
48. Taniguchi Y, Ido H, Sanzen N, Hayashi M, Sato-Nishiuchi R, Futaki S, et al. The C-terminal region of laminin βchains modulates the integrin binding affinities of laminins. *J Biol Chem.* (2009) 284:7820–31. doi: 10.1074/jbc.M809332200
49. Main-Hester KL, Colpitts KM, Thomas GA, Fang FC, Libby SJ. Coordinate regulation of *Salmonella* pathogenicity island 1 (SPI1) and SPI4 in Salmonella enterica serovar Typhimurium. *Infect Immun.* (2008) 76:1024–35. doi: 10.1128/IAI.01224-07
50. Habibi MS, Jozwik A, Makris S, Dunning J, Paras A, DeVincenzo JP, et al. Impaired antibody-mediated protection and defective IgA B-cell memory in experimental infection of adults with respiratory syncytial virus. *Am J Respir Crit Care Med.* (2015) 191:1040–9. doi: 10.1164/rccm.201412-2256OC
51. Mina MJ, Kula T, Leng Y, Li M, de Vries RD, Knip M, et al. Measles virus infection diminishes preexisting antibodies that offer protection from other pathogens. *Science.* (2019) 366:599–606. doi: 10.1126/science.aay6485
52. Petrova VN, Sawatsky B, Han AX, Laksono BM, Walz L, Parker E, et al. Incomplete genetic reconstitution of B cell pools contributes to prolonged immunosuppression after measles. *Sci Immunol.* (2019) 4:aay6125. doi: 10.1126/sciimmunol.aay6125

53. Cheng Q, Mumtaz IM, Khodadadi L, Radbruch A, Hoyer BF, Hiepe F. Autoantibodies from long-lived 'memory' plasma cells of NZB/W mice drive immune complex nephritis. *Ann Rheum Dis.* (2013) 72:2011–7. doi: 10.1136/annrheumdis-2013-203455
54. Hoyer BF, Moser K, Hauser AE, Peddinghaus A, Voigt C, Eilat D, et al. Short-lived plasmablasts and long-lived plasma cells contribute to chronic humoral autoimmunity in NZB/W mice. *J Exp Med.* (2004) 199:1577–84. doi: 10.1084/jem.20040168
55. Hiepe F, Dorner T, Hauser AE, Hoyer BF, Mei H, Radbruch A. Long-lived autoreactive plasma cells drive persistent autoimmune inflammation. *Nat Rev Rheumatol.* (2011) 7:170–8. doi: 10.1038/nrrheum.2011.1
56. Kibler C, Schermutzki F, Waller HD, Timpl R, Muller CA, Klein G. Adhesive interactions of human multiple myeloma cell lines with different extracellular matrix molecules. *Cell Adhes Commun.* (1998) 5:307–23. doi: 10.3109/15419069809040300
57. Vande Broek I, Vanderkerken K, De Greef C, Asosingh K, Straetmans N, Van Camp B, et al. Laminin-1-induced migration of multiple myeloma cells involves the high-affinity 67 kD laminin receptor. *Br J Cancer.* (2001) 85:1387–95. doi: 10.1054/bjoc.2001.2078
58. Neri P, Bahlis NJ. Targeting of adhesion molecules as a therapeutic strategy in multiple myeloma. *Curr Cancer Drug Targets.* (2012) 12:776–96. doi: 10.2174/156800912802429337

Conflict of Interest: The authors declare that the research was conducted in the absence of any commercial or financial relationships that could be construed as a potential conflict of interest.

frontiers in Immunology

ORIGINAL RESEARCH
published: 23 January 2020
doi: 10.3389/fimmu.2019.03132

Enhanced Delivery of Rituximab Into Brain and Lymph Nodes Using Timed-Release Nanocapsules in Non-Human Primates

Meng Qin[1,2], Lan Wang[1,2], Di Wu[3], Christopher K. Williams[4], Duo Xu[3], Emiko Kranz[2,5], Qi Guo[2,6], Jiaoqiong Guan[7], Harry V. Vinters[4], YooJin Lee[1,2], Yiming Xie[1,2], Yun Luo[8], Guibo Sun[8], Xiaobo Sun[8], Zhanlong He[7], Yunfeng Lu[3], Masakazu Kamata[2,5†], Jing Wen[1,2*] and Irvin S. Y. Chen[1,2*]*

[1] Department of Microbiology, Immunology and Molecular Genetics, David Geffen School of Medicine at University of California, Los Angeles, Los Angeles, CA, United States, [2] UCLA AIDS Institute, Los Angeles, CA, United States, [3] Department of Chemical and Biomolecular Engineering, School of Engineering, UCLA, Los Angeles, CA, United States, [4] Departments of Pathology & Laboratory Medicine (Neuropathology) and Neurology, David Geffen School of Medicine at UCLA, Los Angeles, CA, United States, [5] Division of Hematology-Oncology, David Geffen School of Medicine at UCLA, Los Angeles, CA, United States, [6] School of Nursing, UCLA, Los Angeles, CA, United States, [7] Institute of Medical Biology, Peking Union Medical College, Chinese Academy of Medical Sciences, Kunming, China, [8] Institute of Medicinal Plant Development, Peking Union Medical College, Chinese Academy of Medical Sciences, Beijing, China

Tumor metastasis into the central nervous system (CNS) and lymph nodes (LNs) is a major obstacle for effective therapies. Therapeutic monoclonal antibodies (mAb) have revolutionized tumor treatment; however, their efficacy for treating metastatic tumors-particularly, CNS and LN metastases-is poor due to inefficient penetration into the CNS and LNs following intravenous injection. We recently reported an effective delivery of mAb to the CNS by encapsulating the anti-CD20 mAb rituximab (RTX) within a thin shell of polymer that contains the analogs of choline and acetylcholine receptors. This encapsulated RTX, denoted as n-RTX, eliminated lymphoma cells systemically in a xenografted humanized mouse model using an immunodeficient mouse as a recipient of human hematopoietic stem/progenitor cells and fetal thymus more effectively than native RTX; importantly, n-RTX showed notable anti-tumor effect on CNS metastases which is unable to show by native RTX. As an important step toward future clinical translation of this technology, we further analyzed the properties of n-RTX in immunocompetent animals, rats, and non-human primates (NHPs). Our results show that a single intravenous injection of n-RTX resulted in 10-fold greater levels in the CNS and 2-3-fold greater levels in the LNs of RTX, respectively, than the injection of native RTX in both rats and NHPs. In addition, we demonstrate the enhanced delivery and efficient B-cell depletion in lymphoid organs of NHPs with n-RTX. Moreover, detailed hematological analysis and liver enzyme activity tests indicate n-RTX treatment is safe in NHPs. As this nanocapsule platform can be universally applied to other therapeutic mAbs, it holds great promise for extending mAb therapy to poorly accessible body compartments.

Keywords: monoclonal antibody, central nervous system delivery, LNs delivery, non-human primate, nanocapsules

OPEN ACCESS

Edited by:
Giuseppe Andrea Sautto, University of Georgia, United States

Reviewed by:
Sean Lim, University of Southampton, United Kingdom
Maria J. Alonso, University of Santiago de Compostela, Spain

***Correspondence:**
Masakazu Kamata
masa3k@uab.edu
Jing Wen
wjjulia@ucla.edu
Irvin S. Y. Chen
syuchen@mednet.ucla.edu

†Present address:
Masakazu Kamata, Department of Microbiology, University of Alabama at Birmingham, Birmingham, AL, United States

Specialty section:
This article was submitted to Vaccines and Molecular Therapeutics, a section of the journal Frontiers in Immunology

Received: *23 October 2019*
Accepted: *23 December 2019*
Published: *23 January 2020*

Citation:
Qin M, Wang L, Wu D, Williams CK, Xu D, Kranz E, Guo Q, Guan J, Vinters HV, Lee Y, Xie Y, Luo Y, Sun G, Sun X, He Z, Lu Y, Kamata M, Wen J and Chen ISY (2020) Enhanced Delivery of Rituximab Into Brain and Lymph Nodes Using Timed-Release Nanocapsules in Non-Human Primates. Front. Immunol. 10:3132. doi: 10.3389/fimmu.2019.03132

INTRODUCTION

Therapeutic monoclonal antibodies (mAbs) such as rituximab (RTX, anti-CD20 for B-cell lymphomas) and trastuzumab (anti-HER2 for breast cancer) have revolutionized treatment for various types of cancers. However, their benefit in treating metastasized tumors of the central nervous system (CNS) or through lymphatic vessels into lymph nodes (LNs) (1, 2), is transient and limited, increasing life expectancy by only a few months. A major mechanism that renders metastasis more resistant to mAb treatment than primary tumors is limited antibody delivery into the CNS and lymphatic vessels (3, 4). Intraventricular or intrathecal administration of mAbs allows for bypass of the blood-brain barrier (BBB), resulting in relative effectiveness of antibody therapy in treating brain tumor metastases (5, 6); however, neurotoxicity and rapid efflux are known to hinder mAb application for brain tumor treatment (7). Subcutaneous administration of mAb targeting metastatic tumors shows the advantages of entering lymphatic vessels and binding to metastases in lymph nodes (LNs) (8). However, the restriction to regional nodes, toxicity at injection sites, and limited reach to organs without lymphatic vessels are major obstacles to using subcutaneous administration of mAb in treating systemic metastases (9). Therefore, a systemic intravenous injection route is the ideal means for administration of mAb treatment against metastatic tumors.

To improve BBB penetration for mAb delivery to the brain, modifications with various chemicals or biological components, such as lipidation or molecular targeting ligands, have been attempted (10, 11). Another strategy uses colloidal carriers such as liposomes, micelles, and nanoparticles, which transport cargos across the BBB by endocytosis and/or transcytosis (12–14). Improved therapeutic efficacy of these approaches has been demonstrated in rodents with brain tumors, Alzheimer's disease, acute ischemic stroke, and Parkinson's disease (15–17); however, non-specific tissue accumulation—including in liver, spleen, and kidney—is known to mediate acute toxicity and further decrease the effective amount of mAbs in the CNS (18). Moreover, none of those approaches achieved improvement of both LN and brain delivery at the same time.

Our nanotechnology platform utilizes "nanocapsules" which form a thin polymer shell that encapsulates individual macromolecules, protein, RNA, or DNA inside and protects them from the physiological environment (19–27). The shell is formed by *in situ* polymerization of monomers and stabilized by environmentally-responsive crosslinkers; cargoes can be released only through cleavage of these crosslinkers. We tailored these nanocapsules for CNS delivery with zwitterionic properties imbued by polymer shells composed of 2-methacryloyloxyethyl phosphorylcholine (MPC), which is clinically approved for use in coatings on implanted medical devices. MPC renders the polymer shells of nanocapsules highly biocompatible and efficacious due to low protein adsorption, improved circulation times, and minimal immunogenicity (28, 29). Moreover, such nanocapsules can effectively penetrate the BBB and deliver encapsulated macromolecules to the CNS via nicotinic acetylcholine receptors and choline transporters (30). This technology has demonstrated efficacy for neural regeneration in mice with spinal cord injuries (31) and antibody therapies for primary brain tumors (32) in mice.

Rituximab (RTX), a chimeric anti-CD20 monoclonal antibody, is used for treatment of B-cell malignancies such as non-Hodgkin's lymphomas (NHL) as well as chronic lymphocytic leukemia (CLL) (33). RTX administration contributes significant advancements toward systemic CD20+ NHL control, but treatment of primary and relapsed CNS lymphomas is inefficient due to poor penetration through the BBB (4). We recently demonstrated clearance of human B-cell tumors with brain metastases in xenograft humanized NOD-SCID-IL2receptor γ^{null} (NSG) mouse models by RTX nanocapsules (n-RTX) (34). Though these results are promising, further studies are limited by the challenge in collecting successive samples of cerebrospinal fluid (CSF) from the same mouse for analysis; moreover, the delivery into LNs, which are highly atrophic, cannot be confirmed in NSG mice. To address these limitations, we designed studies of n-RTX in both rats and non-human primates (NHPs) to further investigate delivery and biodistribution in both lymphatic tissues and CNS, and B-cell ablation in NHPs. Following a single IV dose of n-RTX, encapsulated RTX is released and maintained in blood for weeks resulting in effective B-cell ablation in blood and lymphatic tissues of NHPs. Importantly, we show significantly improved RTX delivery to the CNS and lymph nodes with no notable adverse effects.

RESULTS

Formulation of Nanocapsules With Hydrolysable Crosslinkers to Release mAbs

A formulation of nanocapsules with timed-release capabilities *in vivo* was synthesized based on previously published nanocapsules (19). We screened and selected two crosslinkers to sustain release at physiological conditions *in vivo*: hydrolysable crosslinker—poly (lactide-co-glycolide)-b-poly(ethylene glycol)-b-poly(lactide-co-glycolide) (PLA-PEG-PLA) and non-hydrolysable crosslinker—glycerol dimethacrylate (GDMA), which degrade rapidly and slowly, respectively, at physiological pH conditions. The ratios between and GDMA impact the release kinetics. With a higher PLA-PEG-PLA ratio, the crosslinkers will degrade in a shorter time. As the crosslinkers degrade, the shells of nanocapsules will loosen, swell, and dissociate resulting in the release of encapsulated mAbs. As shown in **Figure 1A**, nanocapsules encapsulating mAbs are synthesized through the following processes: first, the zwitterionic monomer (MPC) and two crosslinkers, PLA-PEG-PLA and GDMA, are enriched around the surface of the mAb (in this case, RTX) through hydrogen bonding (Step 1). Subsequent polymerization in an aqueous solution at 4°C wraps each molecule with a thin shell of polymer through *in situ* free-radical polymerization (Step 2). Finally, crosslinkers stabilize the polymer structure and release mAbs upon hydrolysis (Step 3). Transmission

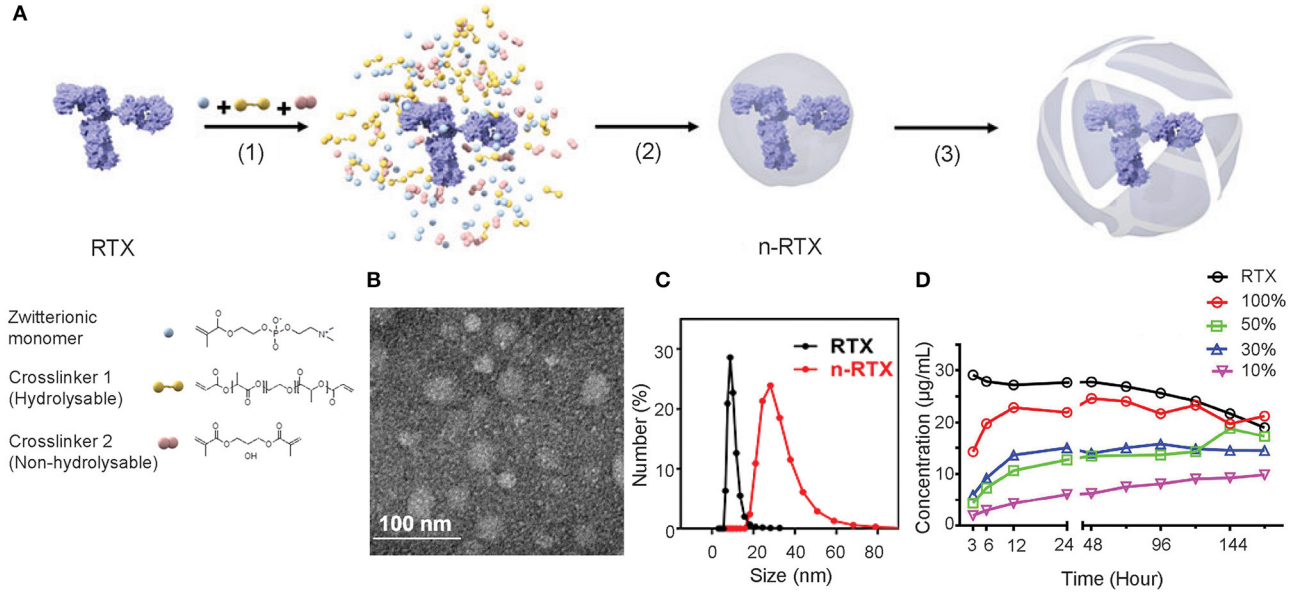

FIGURE 1 | Developing timed-release nanocapsules of RTX. **(A)** Scheme of the synthesis of and release by timed-release RTX nanocapsules (n-RTX) by (1) enriching zwitterionic monomer (MPC), hydrolysable crosslinker 1 (PLA-PEG-PLA) and non-hydrolysable crosslinker 2 (GDMA) around a RTX molecule, (2) *in-situ* polymerization of the monomer and crosslinkers forming a thin shell of polymer around an RTX molecule, and (3) releasing RTX when polymer shells are degraded under physiological condition. **(B)** Transmission Electron Microscopy image of n-RTX. **(C)** Size distribution of n-RTX measured by dynamic light scattering measurement. **(D)** Nanocapsules with mixed hydrolysable crosslinkers achieve timed release of RTX in rhesus macaque plasma. The nanocapsules synthesized with mixed PLA-PEG-PLA and GDMA crosslinkers at different ratios. Release kinetics of n-RTX with 100, 50, 30, 10, and 0% of PLA-PEG-PLA were tested. Thirty micrograms of nanocapsules were incubated in 1 mL of rhesus macaque plasma at 37°C. The concentration of released RTX was determined by ELISA.

electron microscopy (TEM) and dynamic light scattering (DLS) measurements show that these nanocapsules form a spherical morphology of 20–30 nm encasing mAb molecules inside (**Figures 1B,C**). Dependent on the ratios between PLA-PEG-PLA and GDMA, nanocapsules release RTX at different rates when incubated in rhesus macaque plasma *in vitro* (**Figure 1D**). The RTX concentration was detected by enzyme-linked immunosorbent assay (ELISA) using anti-RTX (anti-idiotype) antibody, which can only detect the free RTX released from nanocapsules since nanocapsules shields the epitopes of encapsulated antibodies by the polymer shells. The n-RTX with 50 and 30% PLA-PEG-PLA crosslinkers showed an intermediate level of release over 6 days. We already demonstrated improved CNS delivery of n-RTX with 50% PLA nanocapsules in mice in our published work (35), so the same formulation for following *in vivo* studies in rats and NHPs was used. We also demonstrated that improvement of CNS delivery with this nanocapsules formulation is applicable to other therapeutic mAbs. To prove this point, we tested Herceptin (anti-Her2) for breast cancer; similarly to n-RTX, Herceptin nanocapsules (n-Hercepin) show increased delivery to the CNS (**Figure S1**).

Improved Delivery to CNS and LNs of Rats by RTX Nanocapsules

We demonstrated the improved delivery to CNS and LNs by n-RTX using rats where greater amounts of CSF facilitate serial sampling within the same animals and mature LN formation enables clear visualization and detection in the lymphatic system. Native RTX and n-RTX, normalized with of the same amount of RTX for a single IV dose, showed comparable RTX level in plasma (**Figure 2A**). Whereas, native RTX in CSF was <0.1% of plasma levels, RTX released from n-RTX was 1%, and was maintained this level to days 14 and 21 when native antibody was barely detectable at day 4 (**Figure 2B**). At the endpoint, RTX levels in brain tissue were consistent with the CSF results; higher levels of RTX were observed in the n-RTX treated animals (**Figure 2C**). These results provide proof of concept for improved antibody delivery in the CNS compared to the native form. Improved levels of RTX from n-RTX are also observed in lymphatic-tissues, which include organs such as spleen, LNs in different locations, and three sections of the small intestine (**Figure 2C**). Tissue imaging shows clear biodistribution of fluorescently labeled native RTX and n-RTX on day 1 post-injection (**Figure 2D**). Compared to native RTX, n-RTX shows an improved distribution in lymphatic-tissues containing organs including LNs and spleen and, importantly, reduced accumulation in lung, liver, and kidney—major organs involved with clearance of recombinant antibodies. The decreased accumulation in lung, liver, and kidney is due to the superior anti-fouling property of n-RTX, which decrease the uptake by immune surveillance cells. The difference in biodistribution between RTX and n-RTX is further confirmed by quantifying the relative fluorescence units of the fluorescence label from each organ (**Figure 2E**).

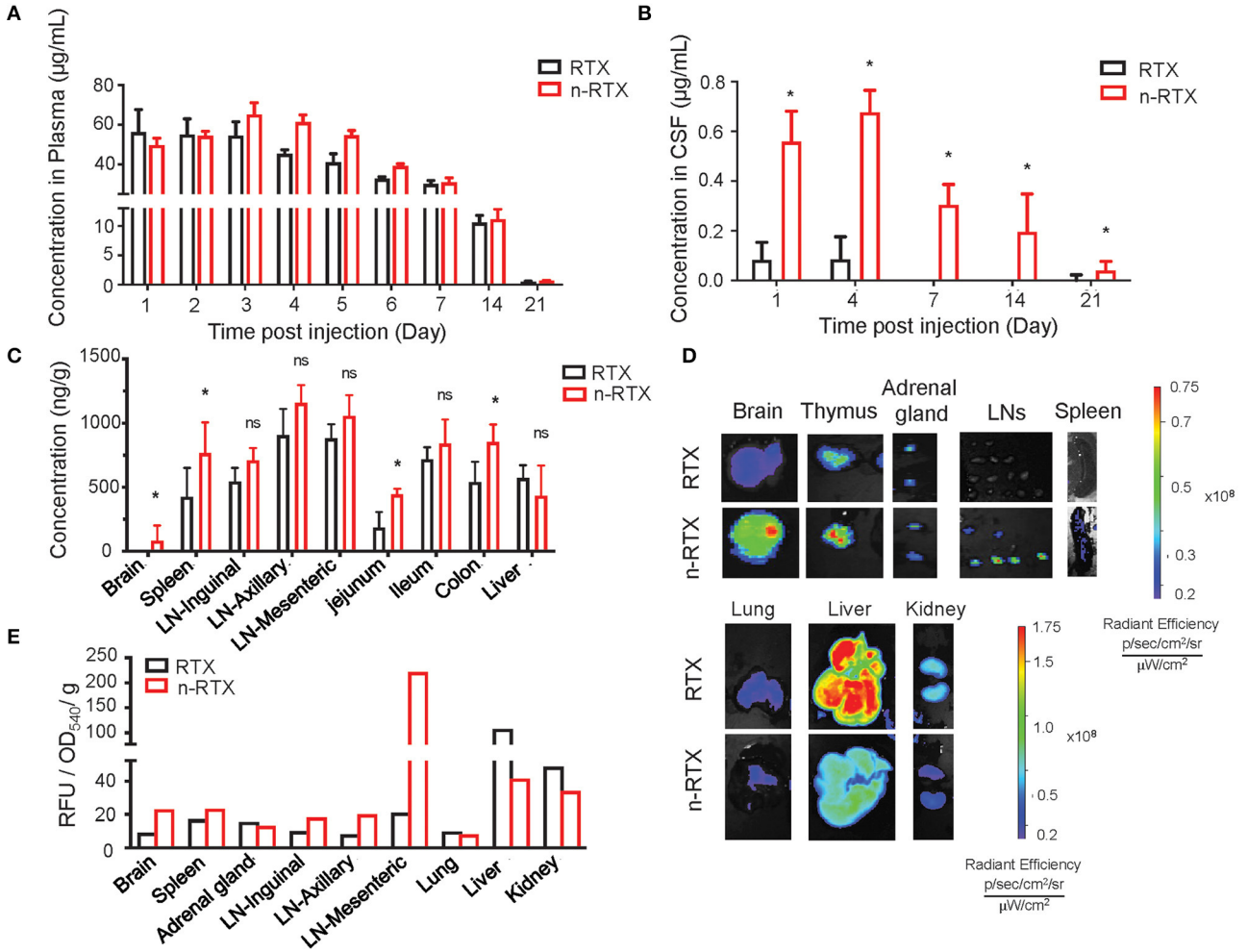

FIGURE 2 | Nanocapsulation of RTX improves levels of its tissue penetration, including CNS, in rats. A single dose (5 mg/kg) of native RTX or n-RTX was administered in rats through IV (intravenous) injection ($n = 3$). **(A–C)** The concentrations of free RTX in plasma **(A)** on Days 1, 2, 3, 4, 5, 6, 7, 14, and 21 and CSF **(B)** on Days 1, 4, 7, 14, and 21 were determined by ELISA. **(C)** Tissues, including LNs at three different locations, jejunum, ileum, colon, spleen, liver, and brain, were harvest at necropsy after perfusion on Day 22. Tissues were homogenized in PBS (1 mg tissue in 100 μl PBS), and tested by ELISA for RTX concentrations. A higher single dose (15 mg/kg) of fluorescent labeled native RTX or n-RTX was administered in rats through IV injection ($n = 1$) and monitored on IVIS *in vivo* imaging **(D,E)**. Organs were isolated and monitored by IVIS imaging on Day7 after injection. **(E)** Signal intensity from free RTX in each organ was quantified by software Living Image. Data were generated from $n = 3$ rats. Data are shown as means ± s.d. of biological triplicate. Statistical significance between native and nanocapsules was determined by one-tailed Mann–Whitney–Wilcoxon test. *Significant, $p < 0.1$; ns, not significant.

Enhanced Delivery of RTX Nanocapsules to the Brain of Rhesus Macaques

As an essential step toward future clinical translation of nanocapsules, we further analyzed the properties of n-RTX in non-human primates (NHPs). The study design is summarized in **Figure 3**. Four rhesus macaques were intravenously infused with a single dose (5 mg/kg, normalized for the RTX amount) of native RTX or n-RTX and processed for necropsy on Day 21 (Group I, #12025 and #13029) or Day 63 (Group II, #12069 and 12019). Blood samples were collected on Days 1, 3, 5, and 7 in the first week, and every 7 days after that (**Figure 3**, Stars). CSF sample collection started before infusion as a baseline (**Figure 3**, Day-12), on Day 3 post-infusion, and continued every 7 days until Day 21 for Group I; for Group II, CSF collection was initiated on Day 1 post-infusion and continued every week until Day 63. Lymph node (LN) biopsies were performed on Days 3 and 14 in Group I and on Days 3, 17, 28, and 42 in Group II (**Figure 3**, Double triangles). Eight tissues, including brain, thymus, lung, liver, spleen, kidney, intestine, and LNs, were harvested at necropsy following perfusion. LNs from different locations (inguinal LN, axillary LN, and mesenteric LN), and three pieces (3 × 3 cm) from each of other tissues were collected and used for ELISA assays. Brain and LN samples were also used for immunohistochemical (IHC) analysis.

We successfully demonstrated the enhanced CNS delivery of n-RTX in rhesus macaques (**Figure 4**). The levels of RTX released from n-RTX in rhesus macaque plasma was slightly lower on Day 1 compared to that of native RTX, probably due to the controlled

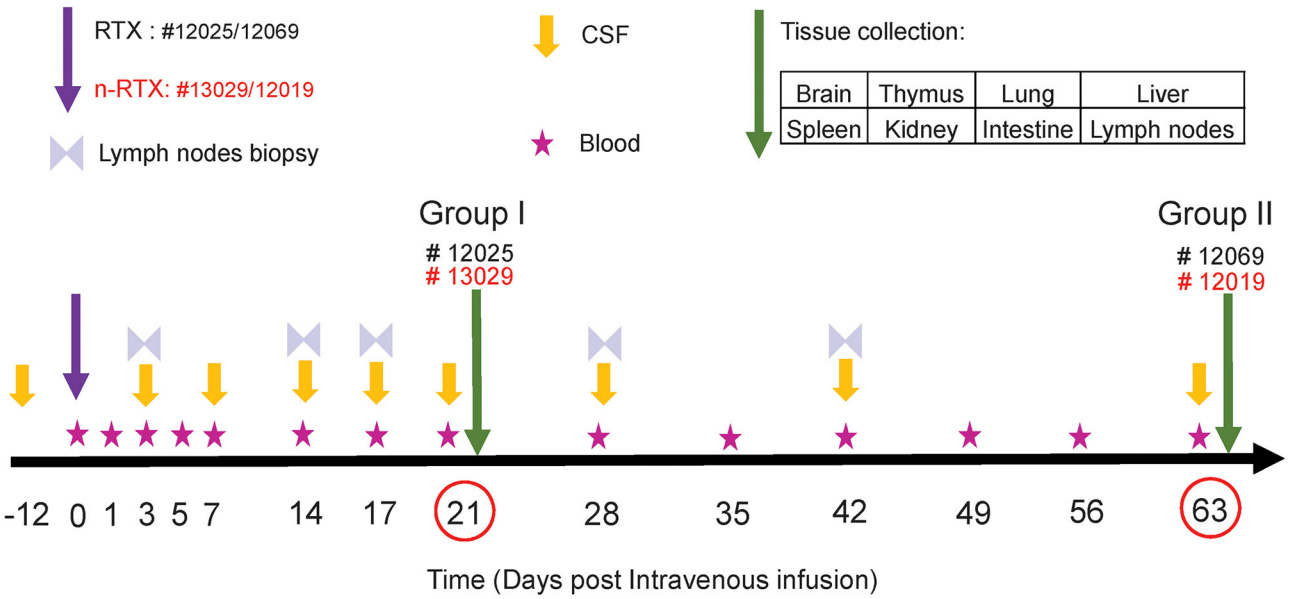

FIGURE 3 | Experimental schedule of RTX brain delivery in non-human primates. Four rhesus macaques were administered with a single 5 mg/kg dose of native RTX (Monkey ID #12025 and #12069) and n-RTX (Monkey ID #13029 and 12019) via IV infusion. Peripheral blood, CSF, and Inguinal lymph nodes were collected as scheduled. Other tissues were harvested at necropsy on Days 21 or 63 after perfusion.

RTX release from n-RTX in plasma (**Figure 4A**). The plasma level remained stable for 1 week, followed by a gradual decreased over time. Two animals treated with n-RTX (#13029 and 12019) showed 5- and 2.5-fold greater levels of free RTX in the CSF compared to those in native RTX-treated animals (#12025 and 12069), respectively, within the first week (**Figure 4B**). Native RTX fell below detection limits by Day 14, whereas free RTX released from n-RTX persisted until Day 21 in both groups. RTX concentration in the tissue homogenates was also assessed by ELISA (**Figure 4C**). In Group I, the animal treated with n-RTX (#13029) showed significantly higher levels of RTX in all tissues than that treated with native RTX (#12025) in all tissues. A similar trend was confirmed with animals in Group II, but the difference between those two treatments was less significant. Five regions of the brain, including the frontal, parietal, temporal occipital lobes, as well as cerebellum, were homogenized separately for ELISA. RTX was only detectable in Group I. RTX released from n-RTX was observed at approximately 4-fold levels in all brain regions than that in the brain tissues from the RTX-treated animal (**Figure 4D**).

Liver toxicity is a major concern for use of nanomedicines *in vivo* (35). Thus, liver damage is the one of the indexes of nanomedicine safety. In order to show that this nanocapsule platform improves brain delivery efficiency of therapeutic antibodies through systemic injection without inducing liver toxicity, three liver enzymes indicating acute liver toxicity were closely measured over the course of experiments: alanine aminotransferase (ALT), aspartate aminotransferase (AST), and alkaline phosphatase (ALP) (**Figure 5A**). As we confirmed in mice previously (34), no notable differences exist in levels between animals treated with RTX or n-RTX. Neither a complete liver function assay including serum globulin (GLB), indirect bilirubin (IBIL), gamma-glutamyl transferase (γ-GT), total protein (TP), and albumin (ALB), nor a blood chemistry test for white blood cell (WBC) count, lymphocyte count, monocyte count, neutrophil count, hemoglobin (HGB), hematocrit (HCT), and platelet counts (PLT), showed major differences between those animals (**Figure S2**). We have hereby concluded that n-RTX increases antibody delivery into the CNS by 4–10-fold with no detectable level of acute systemic toxicity.

We further showed no potential neurotoxicity caused by n-RTX treatment. Two well-known neurotoxicity markers were used in this test: glial fibrillary acidic protein (GFAP), of which levels increase with reactive gliosis (36), and ionized calcium-binding adapter molecule (IBA-1), of which levels increase upon mediating neuroinflammation (37). Compared to native RTX-treated animals, brain tissues of n-RTX treated animals showed normal morphology and no elevated expressions of those two markers (**Figures 5B,C**).

Comparison of Effector Activity Mediated by Native RTX and n-RTX

Lastly, we observed comparable B cell depletion by RTX and n-RTX in peripheral blood of NHPs. CD20 can be internalized by the binding of RTX (38, 39), so single staining for cell surface CD20 may underestimate total B cell levels. To more accurately measure B cell levels, we stained cells with both CD19 and CD20 antibodies. To minimize CD20 epitope masking by RTX, we used the CD20 antibody clone L26, which recognizes different epitope on rhesus CD20 molecules not blocked by RTX (40). Analysis by single staining for CD19+ showed similar results to double staining for CD19+/CD20+ cells (data not shown).

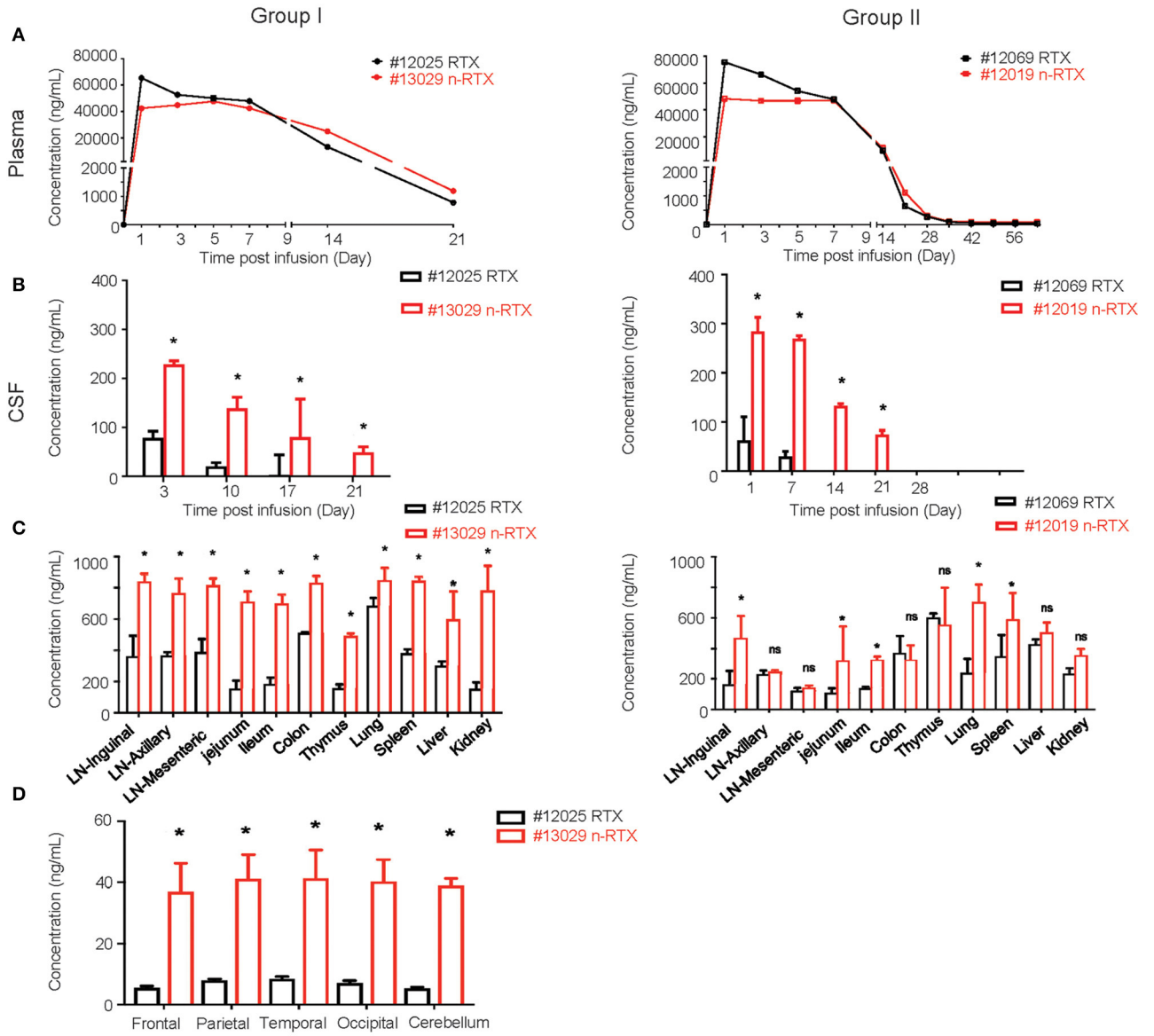

FIGURE 4 | Nanocapsulation of RTX improves levels of its tissue penetration in non-human primates. A single dose (5 mg/kg) of native RTX or n-RTX was administered in rhesus macaques through IV infusion **(A,B)**. The concentrations of free RTX in plasma **(A)** and CSF **(B)** were determined by ELISA. **(C)** At the endpoint of Group I (Day 21) and Group II (Day 63), LNs at three different locations, jejunum, ileum, colon, thymus, lung, spleen, liver, kidney, and brain were harvest after perfusion. Whole LNs and three pieces (3 × 3 cm) of other tissues were homogenized in PBS (1 mg tissue in 100 μl PBS) for ELISA test. **(D)** Five different regions of the brain (frontal, parietal, temporal occipital lobes, and cerebellum) were homogenized in PBS (1 mg tissue in 100 μl PBS) for ELISA test. Data are shown as means ± s.d. of biological triplicate. Statistical significance between native and nanocapsules was determined by one-tailed Mann–Whitney–Wilcoxon test. *Significant, $p < 0.1$, ns, not significant.

CD19+/CD20+ B cell levels dropped ∼80–90% within the first 7 days after treatment by both RTX and n-RTX (**Figure 6A**). Aside from the expected drop in B cells, the numbers of total WBCs, neutrophils, lymphocytes, and monocytes were relatively stable (**Figure S3**), indicating B-cell specific depletion by RTX in both forms. Levels of total CD3+ cells, CD3+/CD4+ T cells, and CD3+/CD8+ T cells were also stable over the course of treatment (**Figures 6B–D**).

To assess the specificity of depletion and accessibility to B cells in lymphoid tissues, we analyzed levels of B-cell depletion in LNs at three different localities: axillary, mesenteric and inguinal, by IHC analysis. Antibodies for CD20+, CD3+, and Bcl-6 were included to distinguish three different types of cells, B cells, T cells, and T follicular helper cells (**Figure 7A**). By further quantitative analysis of IHC staining results, CD20+ B cells showed a lower density in all three LNs of animals treated with n-RTX compared to that of native RTX on Day 21 (**Figure 7B**). Ratios of B cell against T cell (B/T ratio) detected by flow cytometry in inguinal LN indicated that n-RTX mediated prolonged B cell depletion over the course of treatment compared

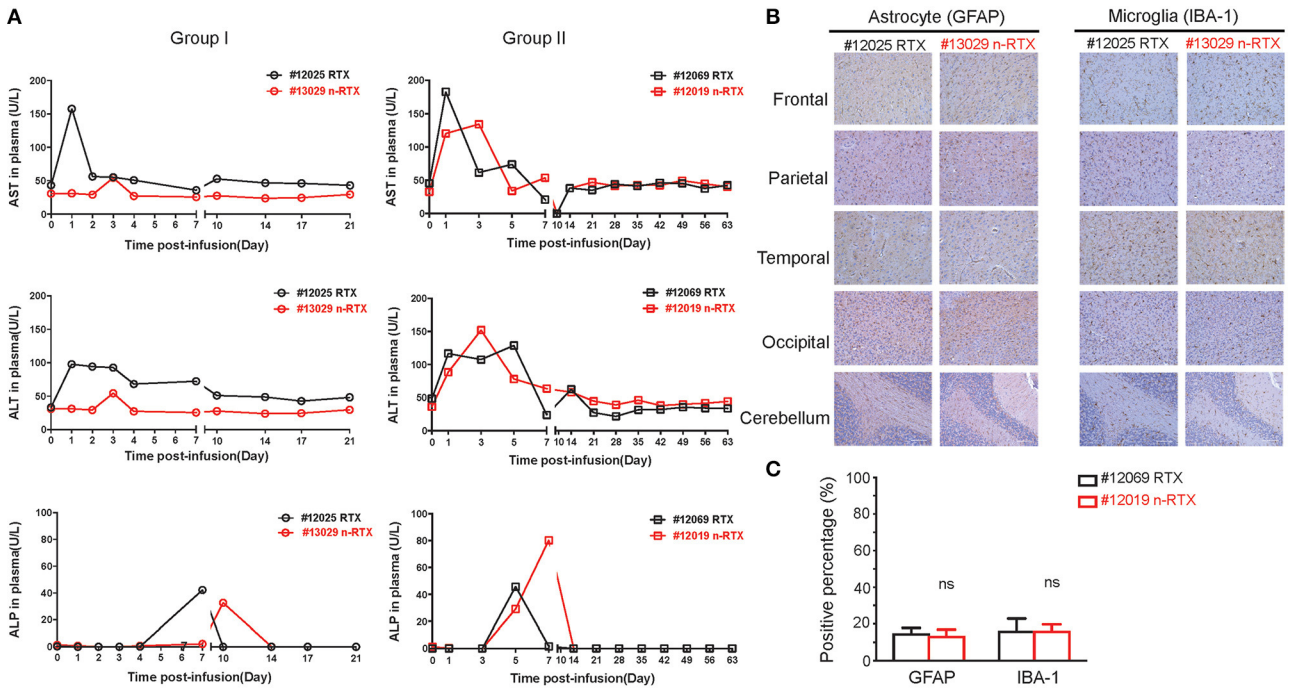

FIGURE 5 | RTX nanocapsules do not mediate notable levels of acute toxicity in the liver and brain. **(A)** Rhesus macaques were administrated with a single dose (5 mg/kg) of native RTX or n-RTX. Plasma samples were collected as scheduled and served for measuring levels of aspartate transaminase (AST), alanine transaminase (ALT), and alkaline phosphatase (ALP) by ELISA. **(B)** Brain tissues obtained from five different parts were fixed by 4% paraformaldehyde and processed for IHC analysis. Representative images of immunohistochemical staining for GFAP (astrocyte marker) and IBA-1 (microglial marker) were shown. Scale bar = 100 μm. **(C)** A positive pixel count in images (4 mm^2) from five different brain parts was quantified using Aperio ScanScope slide scanner. Positive pixel calculation for GFAP used the following variables: hue width = 0.371 and color saturation threshold = 9.7e-002. Positive pixel calculation for IBA-1 used the following variables: hue width = 0.5 and color saturation threshold = 4.0e-007. % positivity was calculated by total number of positive pixels divided by the total number of pixels. Data are shown as means ± s.d. of biological triplicate. Statistical significance, compared with the native RTX group, was determined by one-tailed *t*-test with Welch's correction. ns, not significant.

to native RTX (**Figure S4**). In contrast, no significant difference in levels of CD3+ T cells was confirmed between LNs treated with native RTX or n-RTX. The level of Bcl-6 expression in LNs, a marker of germinal center B cells and T follicular helper cells, showed no difference between two animals.

DISCUSSION

We utilized a platform wherein single mAbs are encapsulated within a thin polymer shell, called a "nanocapsule," to improve delivery of anti-tumor antibodies to the brain. Formulations were modified to utilize neutral polymers with zwitterionic properties (MPC polymers) and crosslinkers that hold the shell together which are later gradually hydrolyzed for timed release of mAb in a suitable microenvironment. This successful nanocapsule design sustains RTX in circulation, allows penetration into the brain, reaches deep tissues including LNs, and releases RTX in a controlled fashion. Our results detail the first test of a zwitterionic nanocarrier—nanocapsule—for therapeutic mAb delivery in NHPs. Importantly, the data clearly show efficient and prolonged delivery of RTX into both the CNS and LNs by a single dose of intravenous injection with no notable acute liver toxicity nor neurotoxicities.

Therapeutic mAbs are effective for treating several tumors; however, their performance is limited in the treatment of metastases in CNS and LNs, where the physical barriers are considered as one of the major obstacles to achieve effective mAbs delivery. Although subcutaneous administration is considered as an effective route for LN delivery through the absorption by lymphatic capillaries, the delivery into the lymphatic system is delayed due to the limitation of the absorption rate (41, 42). Moreover, the brain delivery of mAbs through subcutaneous administration is challenging due to the low concentration of mAbs in plasma. Therefore, intravenous injection is still a commonly used administration route for mAb therapy. However, achieving a high plasma concentration is insufficient for treatment of brain cancers due to poor delivery through the BBB. While multiple strategies have been attempted to facilitate greater antibody penetration through the BBB, the potential risks outweigh most benefits. One approach is to disrupt the tight junctions, allowing for passage, however, this approach raises safety concerns for the brain environment (43). Other approaches are the modification and engineering of mAbs to improve brain delivery; attaching charged or lipophilic moieties to mAbs to enhance absorptive-mediated transport, but those modifications are known to result in unexpected biodistribution, low sustainability, and insufficient

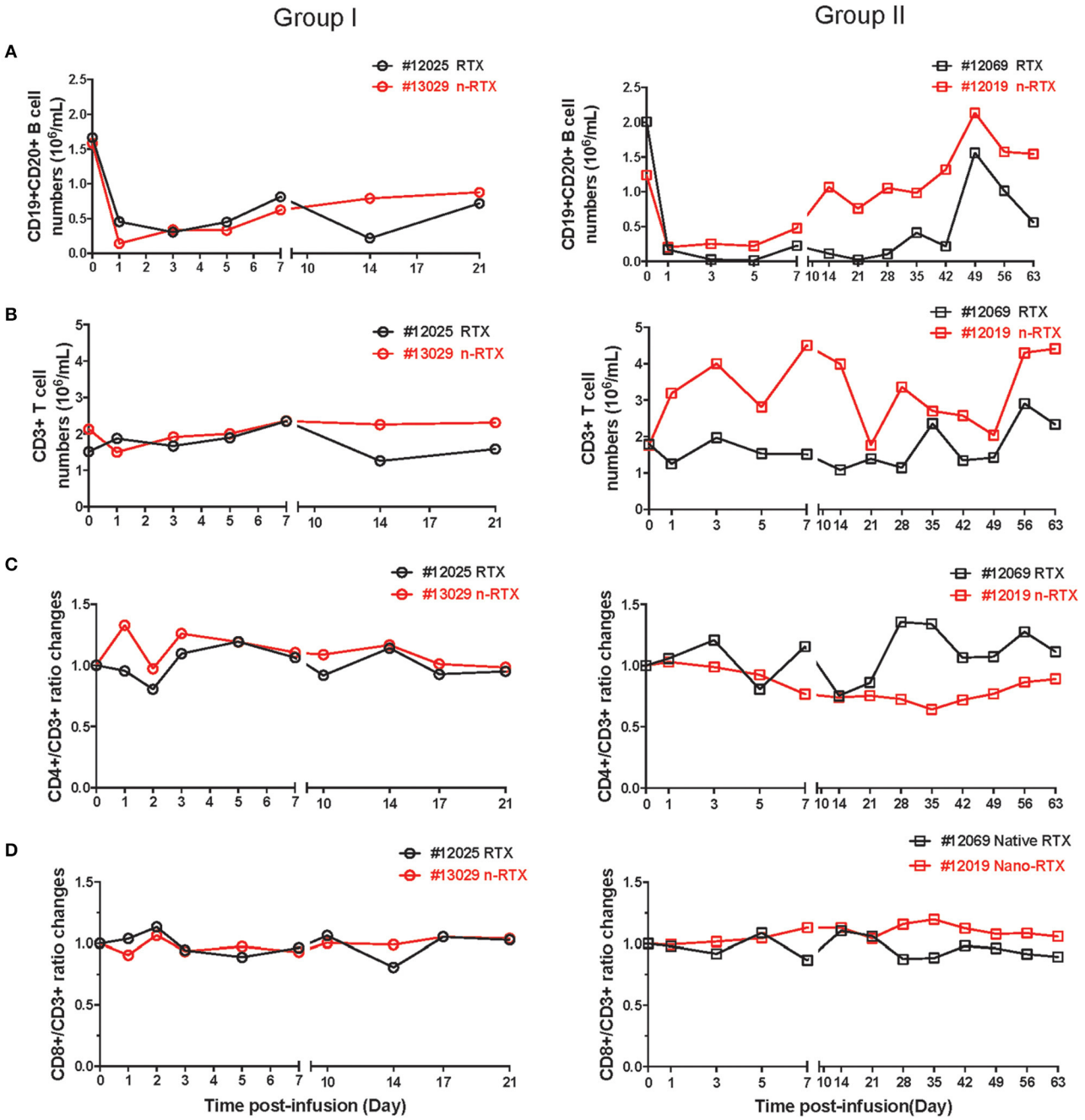

FIGURE 6 | Both native and nanocapsulated RTXs mediate similar levels of peripheral blood B cell depletion in rhesus macaques. Whole blood was collected as scheduled and processed for monitoring immunophenotyping by flow cytometry. **(A)** CD19+CD20+ B cells, **(B)** CD3+ total T cells, **(C)** CD4+T cells, and **(D)** CD8+T cells. **(A,B)** CD19+CD20 B cells and CD3+ T cells were showed by absolute numbers per 1 mL of blood. **(C,D)** The percentages of CD4+ T cells and CD8+ T cells in CD3+ T cells were normalized over baseline.

efficacy (44, 45). mAbs have also been encapsulated or conjugated with nanoparticles or liposomes to induce receptor-mediated transcytosis on the BBB (46, 47), but the efficacy, safety, and stability in NHPs are still unknown. Thus, despite decades of effort, effective delivery of mAbs to the both LNs and the CNS remains challenging.

We used the nanocapsule platform to achieve systemic delivery of RTX into both the CNS and LNs in both rodents and NHPs with single intravenous injection. The choline and acetylcholine analogous structures on the MPC polymer chains of nanocapsules, which can induce transcytosis through the BBB via nicotinic acetylcholine receptors and choline transporters,

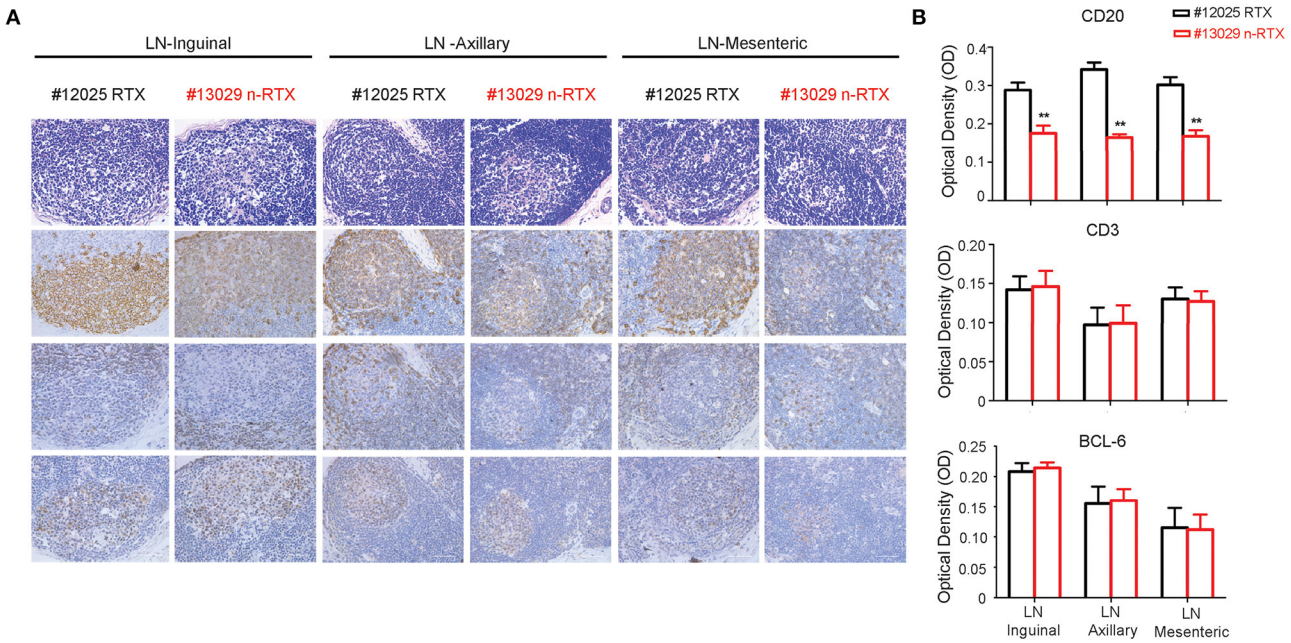

FIGURE 7 | Nanocapsulated RTX mediates superior B-cell depletion in LNs of rhesus macaques. LNs from three different locations (inguinal, axillary, and mesenteric) were collected at necropsy on Day 21 from Group I rhesus macaques with a single dose (5 mg/kg) of native RTX or n-RTX via IV and processed for immunohistochemical (IHC) analyses. **(A)** H&E (top) and IHC staining of CD20 (B cell, second), CD3 (T cell, third), and Bcl-6 (Germinal center, bottom) were performed on serial sections. Panels from left to right show the expression level in axillary, mesentery, and inguinal LNs, respectively. Scale bar = 50 μm. **(B)** 6.8 × 5 cm of each CD20 and CD3 positive staining ($n = 7$), and 3.4 × 4.2 cm of Bcl-6 ($n = 4$) were randomly selected and gray pixel values were measured by Image J software. Each bar indicates the mean inverse gray value ± standard deviation (mean ± SD). One-tailed *t*-test with Welch's correction was used for the statistical analysis. $^{**}p < 0.01$. H&E, hematoxylin and eosin stain.

play an important role to accomplish CNS penetration (30). In NHPs treated with nanoencapsulated RTX, levels of RTX in the CSF were 100 to 300 ng/mL over 14 days, which are 4–10-fold greater than that observed for native RTX in the CSF. It indicates that our nanocapsule platform achieved higher brain delivery compared to animals treated with native RTX. Moreover, similar to animals treated with native RTX, those treated with nanocapsules exhibited no notable blood, liver, or neuronal toxicities. These studies were conducted in immune competent rats and outbred NHP more closely modeling human therapy than in our previous studies utilizing immunodeficient mice. While these levels of RTX in the CNS were sufficient to clear xenografted B cell lymphomas in the immunodeficient mice, it is unclear whether these levels are high enough to have therapeutic efficacy in humans. Our results on biodistribution and safety profiles provide a rationale for further assessing efficacy and safety in human clinical studies.

CONCLUSION

Our studies suggest a non-invasive facile solution suitable for human application to address this critical issue of poor anti-cancer mAb deliverance to both LNs and the CNS. To date, similar results are obtained with one additional clinically approved anti-cancer mAb, anti-Her2 (Herceptin), as well as other non-therapeutic mAbs such as anti-CD4 (OKT4) (unpublished data). The platform is highly versatile, with biodistribution and pharmacokinetics being readily adjustable by rational choice of chemical formulation of the polymer shell. In addition to timed-release functionality via hydrolysis of crosslinkers under physiological pH conditions, mAb release can be further controlled by crosslinkers sensitive to environmental factors such as endosomal low pH and proteases (21). Our study supports the translation of therapy from animals to human clinical studies. Further enhancements of the platform may produce therapeutic delivery options for other diseases requiring mAbs delivery into the CNS and/or LNs.

MATERIALS AND METHODS

Materials

All chemicals were purchased from Sigma-Aldrich (St. Louis, MO, USA) unless otherwise noted. All cell culture reagents were purchased from ThermoFisher Scientific (Waltham, MA) unless otherwise noted. Hydrolysable crosslinker Poly(DL-lactide)-b-Poly(ethylene glycol)-b-Poly(DL-lactide)-diacrylate triblock (PLA-PEG-PLA) was purchased from PolySciTech Akina, Inc. (West Lafeyette, IN). Capture antibody for ELISA against rituximab was purchased from Bio-Rad Laboratories (HCA0620, Hercules, CA). Anti-CD19, anti-CD20, anti-CD3, anti-CD4, and anti-CD8 for flow cytometry were purchased from BioLegend, Inc (San Diego, CA, USA). Antibodies for

IHC staining were purchased from different vendors, identifying separately in Immunohistochemistry section. Rituximab, RITUXAN (Genentech, Inc.) was purchased from the UCLA hospital pharmacy.

Synthesis of Nanocapsules

The mAbs (RTX and Herceptin) were encapsulated via *in-situ* polymerization technology. The mAb solution (2.2 mg/mL in PBS) was mixed with MPC as monomer (40% m/v in PBS) and AI102 (PLA-PEG-PLA, 10% m/v in PBS) as well as glycerol dimethacrylate (GDMA, 10% m/v in DMSO) as degradable crosslinkers. Then the polymerization was initiated by adding ammonium persulfate (APS, 10% m/v in PBS) and N, N, N′, N′-tetramethylethylenediamine (TEMED) solution. Synthesized nanocapsules were dialyzed against PBS and purified by passing through a hydrophobic interaction column (Phenyl-Sepharose 4BCL). Since the nanocapsules possess a super-hydrophilic surface, their binding affinity to the column is much weaker than the native mAb. Thus, encapsulated protein will be eluted out with a high salt concentration buffer (10xPBS), whereas the native mAb binds on the column. Purification is confirmed by DLS and ELISA to show no free mAbs. Detailed parameters of the synthesis are provided in the **Table S1**.

Transmission Electron Microscopy (TEM) and Dynamic Light Scattering (DLS) Measurements of the Nanocapsules

The nanocapsule solution (0.2 mg/mL) 10 μL was dropped onto a carbon–coated copper grid. After 45 s incubation, excess amount of the samples was removed. The samples are stained with 1% phosphotungstic acid (PTA) at pH 7.0 after being rinsed with distilled water for three times. To investigate the size and zeta potential of the nanocapsules, DLS measurements were taken under the concentration of 0.5 mg/mL.

Pharmacokinetics and Bio-Distribution Studies

Four male rhesus macaques were single administered with 5 mg/kg of RTX and n-RTX via intravenous infusion in 30 mL sterile saline through femoral vein. 2–3 mL peripheral blood was collected in EDTA anticoagulant tubes and centrifuged at 5000 rpm/min for 2 min, the plasma was separated and freeze down in −80°C for further purposes. 300–500 μL CSF with no apparent blood contamination continually collected through 3–4th lumbar spine by 1 mL syringe and frozen in −80°C for ELISA test. All animals were anesthetized with an intraperitoneal injection of FFM mix (2.5 mg Fluanisone, 0.105 mg Fentanylcitrate, and 1.25 mg Midozalam HCl/kg in distilled water). On Days 21 and 64 post-injection, animals were euthanized; tissues were removed following heart perfusion with ice-cold saline and fixed in 4% paraformaldehyde for further analyses.

Flow Cytometry

Five hundred microliters peripheral blood was used for staining following the plasma separation. Cells was rinsed by cold PBS (pH7.4) once, counted, and then suspended in FACS buffer (2% FBS/PBS), followed by blocking with 2 μL Human Trustain FcX (BioLegend, US) at room temperature for 10 min. Following the staining of dead cells with LIVE/DEAD Fixable Violet Dead cell staining kit, cells were incubated with PerCP-CY5.5-conjugated mouse anti-human CD3, FITC-conjugated mouse anti-human CD8, BV605-conjugated mouse anti-human CD4, PE-conjugated mouse anti-human CD19, APC-CY7-conjugated mouse anti-human CD20 in dark at 4°C for 30 min. Cells were then rinsed with PBS for two times and fixed by 2% paraformaldehyde in PBS. Expression levels were assessed by BD LSRFortessa™ (BD Biosciences, Inc.), and analyzed with FlowJo (FlowJo, LLC).

Preparation of Fluorescence Labeled RTX

Rhodamine-B-labeled RTX was prepared by following the protocol provided by the manufacturer of fluorescence dyes. Fluorescent dyes, Rhodamine-B (RhB), were first dissolved in anhydrous DMSO to get 10 mg/mL stock solution, respectively. Then 50 μL of dye solutions were added gradually into 2 mL enzyme solutions (10 mg protein/mL, pH = 8.2, sodium carbonate, 100 mM). The reactions were carried out overnight at 4°C. Labeled RTX were then dialyzed against phosphate buffer (20 mM, pH = 7), condensed by centrifugal filtration (MWCO = 10 kDa) and stored at 4°C for further use. The concentration and dye/mAb ratio (D/P) were determined by the extinction coefficients of 2,101,000 M^{-1} cm^{-1} at 280 nm (RTX) and 108,000 M^{-1} cm^{-1} at 555 nm (RhB).

Tissue Imaging

The bioluminescence imaging of organs was performed with IVIS Spectrum imager (PerkinElmer, Waltham, MA). Rats were injected through IV with 15 mg/kg of fluorescent labeled native RTX or n-RTX and scarified at Day 7 post-injection. The tissue images present the total photon flux *per second* within each organ with rainbow color scales. To further quantifiably compare the fluorescent intensity, and the fluorescent intensity from tissue homogenates was quantified as Relative Fluorescence Unit (RFU) per g.

Immunohistochemistry

Axillary, mesenteric, and inguinal lymph nodes, frontal, parietal, temporal, occipital lobes, and cerebellum, were collected separately and fixed in formaldehyde. Four micrometers thickness section were cut serially post paraffin embedding. For staining, slides were first heated at 60°C for 1 h, then deparaffinized in xylene twice and rehydrated in an ethanol gradient. For antigen retrieval, LNs and brain lobes were treated with citrate buffer (Vector Laboratories and Biocare Medical, respectively) for 25 min at 100°C and for 50 min in pressure cooker post ddH_2O rinse, respectively. Sections were incubated with BLOXALL endogenous peroxidase (Vector Laboratories) and alkaline phosphatase blocking solution (Vector Laboratories) for 10 min at room temperature, followed with PBST (0.1% Tween-20) wash and serum blocking at room temperature for 1 h. Primary mouse anti-human CD20 (1:200, clone L26, Santa Cruz Biotechnology), which recognizes different

epitopes on rhesus CD20 molecules not covered by RTX to minimize CD20 epitope masking by rituximab, rabbit anti-human CD3 (1:100, cloneSP7, Invitrogen), and mouse anti-human Bcl-6 (1:100, cloneD8, Santa Cruz Biotechnology), were incubated overnight at 4°C, separately. Rabbit anti-human glia fibrillary acidic protein (GFAP) (1:200, Biocare Medical), mouse anti-human ionized calcium-binding adapter molecule 1 (IBA-1) (1:100, clone 20A12.1, Millipore) were separately used to identify astrocyte and microglia, respectively in brain lobes. After rinsed in PBST, the slides were incubated with ImmPRESS HRP universal secondary antibody at room temperature for 30 min. Followed with PBST wash, 3,3′-diaminobenzidine (DAB) staining, nucleus counterstaining, graded ethanol dehydration, xylene clear, the sections were covered with mounting medium (Thermo Fisher). Images were captured by inverted microscope (DMi1, Leica), brown staining was considered as positive signal, otherwise was considered as negative. Slides of lymph nodes were analyzed with Image J (NIH); slides of brain lobes were scanned by Aperio ScanScope slide scanner by 4 × 4 grid (20×).

For analysis of lymph nodes, 6.8 × 5 cm of each 40 magnified CD20 and CD3 positive staining ($n = 7$) and 3.4 × 4.2 cm of Bcl6 ($n = 4$), was randomly selected and their optical density (OD) numbers were calculated with the following formula: OD = log (max intensity/Mean intensity), where max intensity = 255 for 8-bit images. Brain slides were performed with the Aperio Positive Pixel Count v9 algorithm. Positive pixel calculation for GFAP used the following variables: hue width = 0.371 and color saturation threshold = 9.7e-002. Positive pixel calculation for IBA-1 used the following variables: hue width = 0.5 and color saturation threshold = 4.0e-007. Positivity was calculated by total number of positive pixels divided by the total number of pixels. The value was then multiplied by 100 to give a percentage for positive pixels. Total area analyzed for both GFAP and IBA is 4 mm^2. One-way ANOVA from SPSS software (IBM) was used for the analysis of statistical significance ($^{**}P < 0.01$), the inversed gray value of positive stained tissue was showed in histogram (mean ± SD).

MAb Detection by Enzyme-Linked Immunosorbent Assays (ELISA)

The concentration of RTX in animal body fluids and tissue homogenates was measured by ELISA against RTX. RTX levels were measured by ELISA using a monoclonal antibody (HCA062, clone#AbD02844, Bio-Rad, Hercules, CA), which specifically recognizes the idiotypic determinants of RTX. The 96-well plates were coated with 1 μg/mL of anti-RTX antibody (diluted in sodium carbonate–bicarbonate buffer), followed by blocking with 1% BSA/PBS for 2 h at room temperature. Diluted samples of RTX in PBST from 0 to 500 ng/mL were then added and incubated for 1 h at room temperature to obtain calibration curves. Animal body fluids and tissue homogenates containing encapsulated RTX in non-degradable nanocapsules were treated with 100 mM sodium acetate buffer (pH 5.4) at 4°C overnight and used for ELISA measurement. Released RTX from hydrolysable nanocapsules was directly measured with animal body fluids and tissue homogenates. All animal samples were added and incubated for an additional hour at room temperature. After washing with PBST for five times, peroxidase-conjugated anti-human Fc antibody was added and incubated for a further hour at room temperature. The substrate 3,3′,5,5′-Tetramethylbenzidine (TMB) solution was added and incubated until the appropriate color developed. The reaction was stopped and absorbance at 450 nm was measured with a plate reader (FLUOstar OPTIMA).

Animal Care and Ethics Statements

All research involving animals was conducted according to relevant national and international guidelines. Male SD rats (weighting 180–220 g, 6–8 weeks old) were provided by the Experimental Animal Center of Medical Department of Peking University. All interventions and animal care procedures were performed in accordance with the Guidelines and Policies for Anima l Surgery provided by our collaborator institute (Chinese Academy of Medical Sciences & Peking Union Medical College, Beijing, China) and were approved by the Institutional Animal Use and Care Committee. The rats were maintained in a temperature-controlled facility (temperature: 22 ± 1°C, humidity: 60%) with a 14 h light/10 h dark photoperiod and free access to food and water. Male rhesus macaques (weighing 4.8–5.2 kg, 4–5 years old) were purchased from the Medical Primate Research Center of the Institute of Medical Biology, Chinese Academy of Medical Sciences, and housed and bred according to the guidelines. The experimental protocols were reviewed and approved by the Yunnan Province Experimental Animal Management Association (SYXK-YN 2010-0009) and the Experimental Animal Ethic Committee of the Institute, which complied with the humane regulations of replacement, refinement, and reduction.

DATA AVAILABILITY STATEMENT

The datasets generated for this study are available on request to the corresponding author.

ETHICS STATEMENT

The animal study was reviewed and approved by 1. Institutional Animal Use and Care Committee, Chinese Academy of Medical Sciences and Peking Union Medical College, Beijing, China. 2. Yunnan Province Experimental Animal Management Association (SYXK-YN 2010-0009) and the Experimental Animal Ethic Committee of the Institute.

AUTHOR CONTRIBUTIONS

MQ, MK, and JW designed studies. MQ, LW, DW, CW, DX, QG, JG, EK, YLuo, YLee, and YX performed experiments. HV, GS, XS,

ZH, YLu, MK, JW, and IC discussed and interpreted data. MQ, JW, MK, and IC wrote the paper.

FUNDING

This work was supported in part by NIH grants R01AI110297 (IC), R01HL125030 (IC), R21AI114433 (IC), RO1AI110200 (MK), RO1CA232015 (MK), the UCLA AIDS Institute, UCLA CFAR Grant AI028697, the James B. Pendleton Charitable Trust and the McCarthy Family Foundation.

ACKNOWLEDGMENTS

We thank Kathy Situ for editing the manuscript, Rina Lee-Cha for providing editorial assistance.

SUPPLEMENTARY MATERIAL

The Supplementary Material for this article can be found online at: https://www.frontiersin.org/articles/10.3389/fimmu.2019.03132/full#supplementary-material

REFERENCES

1. Stacker SA, Achen MG, Jussila L, Baldwin ME, Alitalo K. Lymphangiogenesis and cancer metastasis. *Nat Rev Cancer*. (2002) 2:573–83. doi: 10.1038/nrc863
2. Tobler NE, Detmar M. Tumor and lymph node lymphangiogenesis–impact on cancer metastasis. *J Leukoc Biol*. (2006) 80:691–6. doi: 10.1189/jlb.1105653
3. Muldoon L, Soussain C, Jahnke K, Johanson C, Siegal T, Smith Q, et al. Chemotherapy delivery issues in central nervous system malignancy: a reality check. *J Clin Oncol*. (2007) 25:2295–305. doi: 10.1200/JCO.2006.09.9861
4. Rubenstein JL, Combs D, Rosenberg J, Levy A, McDermott M, Damon L, et al. Rituximab therapy for CNS lymphomas: targeting the leptomeningeal compartment. *Blood*. (2003) 101:466–8. doi: 10.1182/blood-2002-06-1636
5. Owonikoko T, Arbiser J, Zelnak A, Shu H, Shim H, Robin A, et al. Current approaches to the treatment of metastatic brain tumours. *Nat Rev Clin Oncol*. (2014) 11:203–22. doi: 10.1038/nrclinonc.2014.25
6. Komori M, Lin Y, Cortese I, Blake A, Ohayon J, Cherup J, et al. Insufficient disease inhibition by intrathecal rituximab in progressive multiple sclerosis. *Ann Clin Transl Neurol*. (2016) 3:166–79. doi: 10.1002/acn3.293
7. Groothuis D. The blood-brain and blood-tumor barriers: a review of strategies for increasing drug delivery. *Neuro Oncol*. (2000) 2:45–59. doi: 10.1093/neuonc/2.1.45
8. Weinstein JN, Steller MA, Keenan AM, Covell DG, Key ME, Sieber SM, et al. Monoclonal antibodies in the lymphatics: selective delivery to lymph node metastases of a solid tumor. *Science*. (1983) 222:423–6. doi: 10.1126/science.6623082
9. Weinstein JN, Parker RJ, Holton OD 3rd, Keenan AM, Covell DG, Black CD, et al. Lymphatic delivery of monoclonal antibodies: potential for detection and treatment of lymph node metastases. *Cancer Invest*. (1985) 3:85–95. doi: 10.3109/07357908509040610
10. Chacko A, Li C, Pryma D, Brem S, Coukos G, Muzykantov V. Targeted delivery of antibody-based therapeutic and imaging agents to CNS tumors: crossing the blood-brain barrier divide. *Expert Opin Drug Deliv*. (2013) 10:907–26. doi: 10.1517/17425247.2013.808184
11. Georgieva JV, Hoekstra D, Zuhorn IS. Smuggling drugs into the brain: an overview of ligands targeting transcytosis for drug delivery across the blood-brain barrier. *Pharmaceutics*. (2014) 6:557–83. doi: 10.3390/pharmaceutics6040557
12. Yang H. Nanoparticle-mediated brain-specific drug delivery, imaging, and diagnosis. *Pharmaceutical Res*. (2010) 27:1759–71. doi: 10.1007/s11095-010-0141-7
13. Zara G, Cavalli R, Fundaro A, Bargoni A, Caputo O, Gasco M. Pharmacokinetics of doxorubicin incorporated in solid lipid nanospheres (SLN). *Pharmacol Res*. (1999) 40:281–6. doi: 10.1006/phrs.1999.0509
14. Costantino L, Tosi G, Ruozi B, Bondioli L, Vandelli MA, Forni F. Chapter 3 - Colloidal systems for CNS drug delivery. *Progr Brain Res*. (2009) 180:35–69. doi: 10.1016/S0079-6123(08)80003-9
15. Garcion E, Lamprecht A, Heurtault B, Paillard A, Aubert-Pouessel A, Denizot B, et al. A new generation of anticancer, drug-loaded, colloidal vectors reverses multidrug resistance in glioma and reduces tumor progression in rats. *Mol Cancer Ther*. (2006) 5:1710–22. doi: 10.1158/1535-7163.MCT-06-0289
16. Lu C, Zhao Y, Wong H, Cai J, Peng L, Tian X. Current approaches to enhance CNS delivery of drugs across the brain barriers. *Int J Nanomed*. (2014) 9:2241–57. doi: 10.2147/IJN.S61288
17. Wong H, Wu X, Bendayan R. Nanotechnological advances for the delivery of CNS therapeutics. *Adv Drug Deliv Rev*. (2012) 64:686–700. doi: 10.1016/j.addr.2011.10.007
18. Scott A, Wolchok J, Old L. Antibody therapy of cancer. *Nat Rev Cancer*. (2012) 12:278–87. doi: 10.1038/nrc3236
19. Liang S, Liu Y, Jin X, Liu G, Wen J, Zhang LL, et al. Phosphorylcholine polymer nanocapsules prolong the circulation time and reduce the immunogenicity of therapeutic proteins. *Nano Res*. (2016) 9:1022–31. doi: 10.1007/s12274-016-0991-3
20. Yan M, Du J, Gu Z, Liang M, Hu Y, Zhang W, et al. A novel intracellular protein delivery platform based on single-protein nanocapsules. *Nat Nanotechnol*. (2010) 5:48–53. doi: 10.1038/nnano.2009.341
21. Wen J, Anderson SM, Du J, Yan M, Wang J, Shen M, et al. Controlled protein delivery based on enzyme-responsive nanocapsules. *Adv Mater*. (2011) 23:4549–53. doi: 10.1002/adma.201101771
22. Wen J, Yan M, Liu Y, Li J, Xie Y, Lu Y, et al. Specific elimination of latently HIV-1 infected cells using HIV-1 protease-sensitive toxin nanocapsules. *PLoS ONE*. (2016) 11:e0151572. doi: 10.1371/journal.pone.0151572
23. Tian H, Du J, Wen J, Liu Y, Montgomery SR, Scott TP, et al. Growth-factor nanocapsules that enable tunable controlled release for bone regeneration. *ACS Nano*. (2016) 10:7362–9. doi: 10.1021/acsnano.5b07950
24. Liu C, Wen J, Meng Y, Zhang K, Zhu J, Ren Y, et al. Efficient delivery of therapeutic miRNA nanocapsules for tumor suppression. *Adv Mater*. (2015) 27:292–7. doi: 10.1002/adma.201403387
25. Liu Y, Du JJ, Yan M, Lau MY, Hu J, Han H, et al. Biomimetic enzyme nanocomplexes and their use as antidotes and preventive measures for alcohol intoxication. *Nat Nanotechnol*. (2013) 8:187–92. doi: 10.1038/nnano.2012.264
26. Gu Z, Yan M, Hu B, Joo KI, Biswas A, Huang Y, et al. Protein nanocapsule weaved with enzymatically degradable polymeric network. *Nano Lett*. (2009) 9:4533–8. doi: 10.1021/nl902935b
27. Yan M, Wen J, Liang M, Lu YF, Kamata M, Chen ISY. Modulation of gene expression by polymer nanocapsule delivery of DNA cassettes encoding small RNAs. *PLoS ONE*. (2015) 10:e127986. doi: 10.1371/journal.pone.0127986
28. Chen S, Li L, Zhao C, Zheng J. Surface hydration: principles and applications toward low-fouling/nonfouling biomaterials. *Polymer*. (2010) 51:5283–93. doi: 10.1016/j.polymer.2010.08.022
29. Young G, Bowers R, Hall B, Port M. Six month clinical evaluation of a biomimetic hydrogel contact lens. *CLAO J*. (1997) 23:226–36.
30. Wu D, Qin M, Xu D, Wang L, Liu C, Ren J, et al. A bioinspired platform for effective delivery of protein therapeutics to the central nervous system. *Adv Mater*. (2019) 31:e1807557. doi: 10.1002/adma.201970127
31. Xu D, Wu D, Qin M, Nih LR, Liu C, Cao Z, et al. Efficient Delivery of nerve growth factors to the central nervous system for neural regeneration. *Adv Mater*. (2019) 31:e1900727. doi: 10.1002/adma.201900727
32. Han L, Liu C, Qi H, Zhou J, Wen J, Wu D, et al. Systemic delivery of monoclonal antibodies to the central nervous system for brain tumor therapy. *Adv Mater*. (2019) 31:e1805697. doi: 10.1002/adma.201805697
33. Rezvani AR, Maloney DG. Rituximab resistance. *Best Pract Res Cl Ha*. (2011) 24:203–16. doi: 10.1016/j.beha.2011.02.009
34. Wen J, Wu D, Qin M, Liu C, Wang L, Xu D, et al. Sustained delivery and molecular targeting of a therapeutic monoclonal antibody to metastases

in the central nervous system of mice. *Nat Biomed Eng*. (2019) 3:706–16. doi: 10.1038/s41551-019-0434-z
35. Shi J, Kantoff P, Wooster R, Farokhzad O. Cancer nanomedicine: progress, challenges and opportunities. *Nat Rev Cancer*. (2017) 17:20–37. doi: 10.1038/nrc.2016.108
36. Eng LF, Ghirnikar RS. GFAP and astrogliosis. *Brain Pathol*. (1994) 4:229–37. doi: 10.1111/j.1750-3639.1994.tb00838.x
37. Ito D, Imai Y, Ohsawa K, Nakajima K, Fukuuchi Y, Kohsaka S. Microglia-specific localisation of a novel calcium binding protein, Iba1. *Brain Res Mol Brain Res*. (1998) 57:1–9. doi: 10.1016/S0169-328X(98)00040-0
38. Lim SH, Vaughan AT, Ashton-Key M, Williams EL, Dixon SV, Chan HT, et al. Fc gamma receptor IIb on target B cells promotes rituximab internalization and reduces clinical efficacy. *Blood*. (2011) 118:2530–40. doi: 10.1182/blood-2011-01-330357
39. Boross P, Leusen JH. Mechanisms of action of CD20 antibodies. *Am J Cancer Res*. (2012) 2:676–90.
40. Mason DY, Comans-Bitter WM, Cordell JL, Verhoeven MA, van Dongen JJ. Antibody L26 recognizes an intracellular epitope on the B-cell-associated CD20 antigen. *Am J Pathol*. (1990) 136:1215–22.
41. McLennan DN, Porter CJ, Charman SA. Subcutaneous drug delivery and the role of the lymphatics. *Drug Discov Today Technol*. (2005) 2:89–96. doi: 10.1016/j.ddtec.2005.05.006
42. Richter WF, Jacobsen B. Subcutaneous absorption of biotherapeutics: knowns and unknowns. *Drug Metab Dispos*. (2014) 42:1881–9. doi: 10.1124/dmd.114.059238
43. Carman AJ, Mills JH, Krenz A, Kim DG, Bynoe MS. Adenosine receptor signaling modulates permeability of the blood-brain barrier. *J Neurosci*. (2011) 31:13272–80. doi: 10.1523/JNEUROSCI.3337-11.2011
44. Triguero D, Buciak JB, Yang J, Pardridge WM. Blood-brain barrier transport of cationized immunoglobulin G: enhanced delivery compared to native protein. *Proc Natl Acad Sci USA*. (1989) 86:4761–5. doi: 10.1073/pnas.86.12.4761
45. Yesilyurt V, Ramireddy R, Azagarsamy MA, Thayumanavan S. Accessing lipophilic ligands in dendrimer-based amphiphilic supramolecular assemblies for protein-induced disassembly. *Chemistry*. (2012) 18:223–9. doi: 10.1002/chem.201102727
46. Barar J, Rafi MA, Pourseif MM, Omidi Y. Blood-brain barrier transport machineries and targeted therapy of brain diseases. *Bioimpacts*. (2016) 6:225–48. doi: 10.15171/bi.2016.30
47. Tang X, Sun J, Ge T, Zhang K, Gui Q, Zhang S, et al. PEGylated liposomes as delivery systems for Gambogenic acid: characterization and *in vitro*/*in vivo* evaluation. *Colloids Surf B Biointerfaces*. (2018) 172:26–36. doi: 10.1016/j.colsurfb.2018.08.022

Conflict of Interest: IC has a financial interest in CSL Behring and Calimmune Inc. No funding was provided by these companies to support this work.

The remaining authors declare that the research was conducted in the absence of any commercial or financial relationships that could be construed as a potential conflict of interest.

frontiers in Immunology

REVIEW
published: 18 February 2020
doi: 10.3389/fimmu.2020.00188

The Use of Both Therapeutic and Prophylactic Vaccines in the Therapy of Papillomavirus Disease

Anna Rosa Garbuglia[1], Daniele Lapa[1], Catia Sias[1], Maria Rosaria Capobianchi[1] and Paola Del Porto[2]*

[1] Laboratory of Virology, "Lazzaro Spallanzani" National Institute for Infectious Diseases, IRCCS, Rome, Italy, [2] Department of Biology and Biotechnology "C. Darwin," Sapienza University, Rome, Italy

Human papillomavirus (HPV) is the most common sexually transmitted virus. The high-risk HPV types (i.e., HPV16, 18, 31, 33, 35, 39, 45, 51, 52, 56, 58, 59) are considered to be the main etiological agents of genital tract cancers, such as cervical, vulvar, vaginal, penile, and anal cancers, and of a subset of head and neck cancers. Three prophylactic HPV vaccines are available that are bivalent (vs. HPV16, 18), tetravalent (vs. HPV6, 11, 16, 18), and non-avalent (vs. HPV6, 11, 16, 18, 31, 33,45, 52, 58). All of these vaccines are based on recombinant DNA technology, and they are prepared from the purified L1 protein that self-assembles to form the HPV type-specific empty shells (i.e., virus-like particles). These vaccines are highly immunogenic and induce specific antibodies. Therapeutic vaccines differ from prophylactic vaccines, as they are designed to generate cell-mediated immunity against transformed cells, rather than neutralizing antibodies. Among the HPV proteins, the E6 and E7 oncoproteins are considered almost ideal as targets for immunotherapy of cervical cancer, as they are essential for the onset and evolution of malignancy and are constitutively expressed in both premalignant and invasive lesions. Several strategies have been investigated for HPV therapeutic vaccines designed to enhance $CD4^+$ and $CD8^+$ T-cell responses, including genetic vaccines (i.e., DNA/ RNA/virus/ bacterial), and protein-based, peptide-based or dendritic-cell-based vaccines. However, no vaccine has yet been licensed for therapeutic use. Several studies have suggested that administration of prophylactic vaccines immediately after surgical treatment of CIN2 cervical lesions can be considered as an adjuvant to prevent reactivation or reinfection, and other studies have described the relevance of prophylactic vaccines in the management of genital warts. This review summarizes the leading features of therapeutic vaccines, which mainly target the early oncoproteins E6 and E7, and prophylactic vaccines, which are based on the L1 capsid protein. Through an analysis of the specific immunogenic properties of these two types of vaccines, we discuss why and how prophylactic vaccines can be effective in the treatment of HPV-related lesions and relapse.

Keywords: human papillomavirus, immune response, cancer, prophylactic vaccine, therapeutic vaccine

OPEN ACCESS

Edited by:
Roberta Antonia Diotti, Vita-Salute San Raffaele University, Italy

Reviewed by:
Bryce Chackerian, University of New Mexico, United States
Edward Rybicki, University of Cape Town, South Africa

****Correspondence:***
Anna Rosa Garbuglia
argarbuglia@iol.it

Specialty section:
This article was submitted to Vaccines and Molecular Therapeutics, a section of the journal Frontiers in Immunology

Received: *18 November 2019*
Accepted: *24 January 2020*
Published: *18 February 2020*

Citation:
Garbuglia AR, Lapa D, Sias C, Capobianchi MR and Del Porto P (2020) The Use of Both Therapeutic and Prophylactic Vaccines in the Therapy of Papillomavirus Disease. Front. Immunol. 11:188. doi: 10.3389/fimmu.2020.00188

INTRODUCTION

Despite the introduction of prophylactic vaccines, the incidence of human papillomavirus (HPV)-related tumors remains high (1), particularly in developing countries of the sub-Saharan region. The current HPV prophylactic vaccines have indications for use in women up to the age of 45 years, but they are predominantly administered to adolescent of 9–15 years. As most cancers develop decades after an initial HPV infection, the impact of this vaccination program will be seen in the long-term. Therefore, setting-up a therapeutic vaccine that can provide results similar to surgical treatment or chemotherapy represents a challenge for the eradication of HPV-induced tumors. However, therapeutic vaccines are not yet available for clinical practice.

Several studies have suggested that administration of HPV prophylactic vaccines after surgical treatment of high-grade cervical intraepithelial neoplasia (CIN2-3) can be considered as an adjuvant to prevent HPV reactivation or reinfection. The relevance of prophylactic vaccines has also been demonstrated in the management of genital warts, although clinical studies have not delivered univocal results to date.

In this review, the HPV-related tumors and the life cycle of HPV are described, to better understand the characteristics of the different viral proteins that are targeted by prophylactic and therapeutic vaccines. Then, we summarize the leading features of prophylactic and therapeutic vaccines that target the L1 and E6, E7 oncoproteins, respectively. Finally, through an analysis of the specific immunogenic properties of these two types of vaccines, we discuss how prophylactic vaccines can be effective for the treatment of HPV-related lesions, and for prevention of HPV-related relapse.

HPV PREVALENCE

Human papillomavirus is the main agent of sexually transmitted diseases, and it can cause cancer in different anatomical districts with different prevalences (2). The highest proportion of HPV attribution as responsible for a cancer is for the cervix, where >99% of specimens are HPV-positive. In 2012, HPV-invasive cervical cancers reached >500,000 cases, which resulted in ∼250,000 deaths around the world[1]. HPV-related cancers are differently distributed across genders: among women, 8.6% of cancers are linked to HPV infections, while in men, <1% of cancers are attributable to HPV[2,3]. Differences are also observed in the geographic distributions of invasive cervical cancers: more than 85% occur in developing countries, where cervical screening programs and HPV vaccination campaigns are rarely available[4] (3, 4). HPV infection in a cervical site is frequently asymptomatic, and >90% of these resolve within 2 years without medical intervention (5), apparently through rapid immune clearance. However, the protective power of natural anti-HPV antibodies and the duration of immunity after infection are not fully understood. Also, only 50–60% of women show detectable anti-HPV antibodies after infection (6).

There are 15 high-risk (HR)-HPV genotypes that can lead to cancers of the cervix, anus, penis, vagina, vulva, and oropharynx (i.e., HPV16, 18, 3, 33, 35, 39, 45, 51, 52, 56, 58, 68, 73, 82) (7). The relevance of HPV to each of these individual cancers is now considered.

Cervical Cancer

Overall, 90% of cervical cancers are attributed to HR-HPV types. HPV16 and HPV18 are the most prevalent in invasive cervical cancer, where they account for 62.5 and 15.7% of cases, respectively (8). HPV-associated cancers include cervical squamous cell carcinoma (70%), cervical adenocarcinoma (25%), and mixed histology tumors (7)[5]. An immunocompromised status represents a risk factor for cervical dysplasia, as well as for latent reactivation of HPV at genital sites. Patients with human immunodeficiency virus (HIV) infection have a 5-fold greater risk of acquiring HPV-associated cervical cancer than those without HIV infection. Precancerous (squamous) intraepithelial lesions are categorized as low-grade (LSIL) and high-grade (HSIL) (9).

Anal Cancer

Anal intraepithelial neoplasia (AIN1-3) represents the precursor of invasive anal cancers, where 65% are cervical squamous cell carcinomas. For both sexes, 88–94% of these cancerous lesions are positive for HPV DNA, with HPV16 as the most commonly detected (∼87% of HPV-positive tumors), while only 9% of these anal cancers harbors HR-HPV18[6].

Annually, about 18,000 women are diagnosed with anal cancer worldwide, and this cancer is more frequent in women than in men (10). Furthermore, anal cancer incidence is increasing, which appears to be due to changes in sexual risk factors for HPV transmission (11). Persistent anal HPV infection is the major cause of anal cancer[7] (12). Women with a history of cervical cancer and cervical intraepithelial neoplasia grade 3 (HSIL) are also at increased risk of anal cancer. Cervical HR-HPV–positivity is associated with anal HR-HPV prevalence. In a study carried out by Lin, anal HR-HPV prevalence was significantly higher in cervical HR-HPV–positive women (43%) vs. cervical HR-HPV–negative women (9%) (13). These associations were even stronger for HPV16-positivity: in cervical HPV16-positive women, anal HPV16 prevalence was 41%, while in the HPV16-negative cervical group, anal HPV16 prevalence was 2%.

In men, the risk of anal cancer development is strictly related to sexual behavior and HIV immune status (14).

Penile Cancer

Approximately 50% of penile cancers can be attributed to HPV infections, although HPV also infects healthy subjects without progressing to neoplasia. In a British study carried out among 43 couples, 69% of the men were HPV-positive in the uro-genital tract (15). Another study in the USA showed similar high levels of

[1]https://gco.iarc.fr/
[2]https://publications.iarc.fr/108
[3]https://monographs.iarc.fr/wp-content/uploads/2018/06/mono100B-11.pdf
[4]http://globocan.iarc.fr/old/FactSheets/cancers/cervix-new.asp
[5]https://seer.cancer.gov/archive/csr/1975_2004/
[6]https://monographs.iarc.fr/wp-content/uploads/2018/06/mono90.pdf
[7]https://monographs.iarc.fr/wp-content/uploads/2018/06/mono100B.pdf

HPV prevalence, with 65.5% of the men HPV-positive: 51.2% of them harbored at least one typed HPV, and 14.3% of them were positive for an unclassified HPV infection (16). HPV clearance is observed in 75% of cases within 1 year (17). HPV-positivity is greater in penile intraepithelial neoplasia (PIN 1,2,3), which is considered the precursor of penile cancer, and in basaloid histological neoplasia (range, 75–80%) than in invasive cervical squamous cell carcinoma (range, 30–60%). HPV16 and HPV18 are the HPV types that are most frequently associated with all types of penile cancers[2].

Vulvar Cancer

It is estimated that 40–50% of vulvar cancers are associated with HPV. Overall, vulvar cancers represented 3% of gynecologic cancers in 2002 (18), and 60% of were observed in developed countries (18, 19)[8]. Vulvar intraepithelial neoplasia (VIN) is considered a precursor of vulvar squamous cell carcinoma, which represents >90% of vulvar cancers (20). The World Health Organization recognizes a three-grade system of VIN (i.e., VIN1-3), and VIN3 is considered as a precursor of invasive vulvar cancer. However, until recently, VIN2-3 had been considered as HSIL, and VIN1 (or LSIL) is no longer used, as there is misclassification of these low-grade lesions: these are often actually condilomata acuminata with transient HPV infection, or an inflammatory status of the vulva (21). VIN can be caused by two distinct etiological agents: HPV, which is linked to the usual form of VIN (uVIN), and differentiated VIN (dVIN) is associated with lichen sclerosus (22, 23). Generally, uVIN is common among young women, while dVIN is frequently seen for post-menopausal women. In VIN3/HSIL lesions, HPV16 had been detected in >91% of cases (24).

Vaginal Cancer

Cancer of the vagina is rare, and it accounts for only 2% of gynecological neoplasia. Nevertheless, from 2000 to 2015 there was an increase in vaginal cancer, which corresponded to 0.4% of vulvar carcinomas in the USA[9]. Vaginal intraepithelial neoplasia (VAIN) is considered a pre-malignant lesion. Previously, a three-tiered classified was used (VAIN1-3) according to epithelial involvement. In 2014, the World Health Organization revised this classification by substituting VAIN2-3 with HSIL, and VAIN1 with LSIL (25). About 82% of high-grade lesions (i.e., vaginal intraepithelial lesions, VAIN3, HSIL) and 91% of invasive vaginal carcinomas test positive for HPV DNA and/or HPV antibodies. HPV16 is the most prevalent HPV type in HSIL and vaginal cancers[2] (26–29).

Head and Neck Cancer

The most common head and neck cancers are squamous cell carcinomas (HNC) and they include neoplasia of the oral cavity, tongue, tonsils, oropharynx, hypopharynx, and larynx. The HR-HPV types most frequently detected in head and neck cancers are HPV16, followed by HPV18[2] (30, 31). Head and neck cancers are frequent in southern-central Asia (32); however, an increase in head and neck cancer incidence has been seen over recent years in developed countries (33) and among Caucasian men (34). Tonsillectomies can increase the overall survival rates of patients with diagnosis of tonsil carcinoma (35), but it does not influence the overall risk of oropharyngeal cancer (36).

A reduction in HPV-positive oropharyngeal cancer is observed in people with a specific genetic locus in the human leukocyte antigen region (HLA-DRB1*1301-HLA-DQA1*0103-HLA-DQB1*0603) (37). This protective effect might involve increased immune targeting of HPV-infected cells through the major histocompatibility complex haplotype binding to HPV peptides, resulting in a strong $CD4^+$ T-cell response (38).

Respiratory Papillomatosis

Different annual incidences of respiratory papillomatosis have been reported in different countries. For example, in Denmark, similar incidence has been reported in children (juvenile onset) (3.6/100,000 children) and in adults (3.9/100,000 adults) (38), while in the USA the annual respiratory papillomatosis incidence is 3-fold higher in children than in adults (4.6 vs. 3.9/100,000 children/adults) (39).

HPV6 and HPV11 are the main genotypes detected in respiratory papillomatosis. As spontaneous regression is rarely observed, surgical treatment is necessary to prevent progression of the lesions. Moreover, recurrence of papillomatosis is often observed, and retreatment is needed in most cases, which comes at a high economic burden (40). Although no structured trials have been carried out to date, HPV vaccine administration prior to the onset of sexual behavior might have a positive impact on prevention of respiratory papillomatosis in adulthood.

Genital Warts

Human papillomavirus infection can not only cause cancer, but also benign genital warts. These are very diffuse in the young and in adults, with prevalence from 4 to 11% (41–43). Treatment of genital warts includes therapies with imiquimod and podophyllotoxin, or surgical procedures, or cryotherapy and tricloroacetic acid. These medical interventions represent high costs for both private insurance (44) and health systems (45).

Condylomas were classically considered a benign lesion, with the exception of Buscke-Lowenstein tumors. This large tumor can undergo local invasion and can transform into anal cervical squamous cell carcinoma (46).

VIRAL CHARACTERISTICS AND IMMUNE RESPONSES

Life Cycle of HPV

Human papillomaviruses are non-enveloped icosahedral viruses that consist of 72 capsomers and are 55 nm in diameter. The viral genome is a circular double stranded DNA of ∼8,000 bp in length.

According to the time-regulated expression of proteins during the viral cycle, three functional genome regions can be distinguished: (i) the early region that encodes the E1, E2, E4, E5, E6, E7, E8 viral proteins that have regulatory functions in infected epithelial cells; (ii) the late region that encodes the two

[8]https://www.ncbi.nlm.nih.gov/books/NBK12354/
[9]http://www.seer.cancer.gov

viral capsid proteins L1 and L2; and (iii) the long control regions (also known as upstream regulatory regions) that contain *cis*-acting regulatory sequences that are involved in the control of viral replication and post-transcriptional phases (**Figure 1**).

Different viral proteins are expressed in different layers of the epithelium. The early proteins are expressed in basal epithelial cells, while the late proteins are expressed in the granular layer that includes more differentiated cells, and from where the virus is assembled and released. E1 is an ATPase helicase that is involved with E2 in viral replication and transcription regulation. The E1 and E2 complex interacts with the long control region ori site, which is considered to be the origin of HPV DNA replication (47–53). In the initial phase of infection, the HPV DNA genome is in the episomal form. It shows low amplification activity and there are ∼100 copies/cell (54). E2 ensures episomal maintenance of the HPV genome through interactions with other cellular factors. For example, Bromo-domain protein 4 (BRD4) is a mitotic chromosome-associated protein that is a critical binding partner for E2 for this activity (55). BRD4 and E2 co-localize on condensed mitotic chromosomes, and mediate episome segregation (55). E2 also regulates transcription of the E6 and E7 oncoproteins, the expression of which depends on an early promoter. E1 to E4 are encoded by a spliced RNA, and along with E5, they are translated under early promoter control in undifferentiated cells, and they appear to facilitate efficient productive replication in differentiating cells (56, 57).

E6 and E7 are small proteins of about 150 and 100 amino acids, respectively. The E6 oncoprotein acts through its PDZ-binding motif, which promotes its interactions with PDZ domains in multidomain proteins, to alter their functionality. These PDZ domains are present in many multidomain proteins that regulate key steps in the cellular processes of apoptosis, adhesion, and polarity (37–43, 58). E6 also impairs the activity of the p53 protein, which prevents DNA damage accumulation through induction of DNA repair, cell-cycle arrest, or apoptosis, which leads to transformation of HPV chronically infected cells.

The main targets of E7 are the pRB, p107, and p130 proteins, which are components of a complex that can repress the E2F transcription factor (59, 60). When E7 interacts with pRB, p107, and p130, it induces their degradation, and so E2F is free to activate genes such as cyclins A and E, to promote transition from G1 to S-phase of the cell cycle (61). The productive viral cycle also includes the synthesis of the late proteins L1 and L2 in the suprabasal epithelial cell layers, and this step is characterized by a change in mRNA splicing (62, 63). Icosahedral virions are composed of 360 L1 proteins that are organized in pentamers, each of which is associated with one monomer of L2. The productive life cycle is completed when the virions self-assemble, after packaging of the amplified HPV DNA genome, with the viral particles then shed from the epithelial cell layers (64).

Natural Immune Response

The immune response has an important role in clearing most HPV infections, although sometime the virus cannot be eliminated and can persist for several years, which represents a risk factor for neoplasia development (65). HPV-associated neoplastic progression is linked to dysregulated expression of the early viral genes. Specifically, increased expression of the E6 and E7 proteins in the basal epithelium leads to increased cell-cycle entry and loss of differentiation across the epithelium. The main cause of dysregulated HPV gene expression is integration of the viral genome into the host chromosomes (66). HPV DNA integrates randomly into the host DNA. During this process, the viral DNA can often be broken at any position within the E1-E2 region, with the loss of E2 function, and the consequent overexpression of E6 and E7 that promotes cellular transformation (67–69). However, a proportion of cervical cancers are associated with episomal DNA only. In such cases, the E2 open reading frame integrity is maintained, and this protein is expressed throughout the progression of the malignancy.

In natural infections, both humoral- and cell-mediated immune responses are induced. Genital infection with oncogenic HPV is common, but only a minority of infected patients develop epithelial lesions or cancer (70). Spontaneous clearance of an established infection is likely to be mediated by the cellular immune responses. Indeed, strong Th1 $CD4^+$ T-cell responses that are specific for HPV16 E6, E7, and E2 have been frequently detected in peripheral blood mononuclear cells of healthy individuals (71). In contrast, responses against HPV16 E6, E7, and E2 have rarely been detected in patients with HPV16-positive genital lesions or antigen-specific proliferative responses that show a non-inflammatory cytokine profile (72, 73).

Similarly, effective HPV18-specific T-cell responses are only seen in healthy controls, and not in HPV18-positive patients (74). For the role of $CD8^+$ T-cells in disease regression, a comparison of $CD8^+$ T-cell responses to E6 and E7 using enzyme-linked immunospot assays in individuals with incident or prevalent HPV 16 or 18 infections did not show any significant difference in the frequency of positivity between these two patient groups (33 vs. 40%) (75). At variance with this, in CIN2/3 lesions, more $CD8^+$ T-cells were seen for the epidermis of tissues that went on to regress (76). Also, large numbers of intraepithelial $CD8^+$ tumor-infiltrating lymphocytes have been associated with an absence of lymph-node metastases in patients with large early stage cervical cancer (76). Taken together, these findings indicate that the development of high-risk HPV-positive cervical cancer is associated with failure of HPV-specific T-cell responses.

The humoral immune response to HPV infection is mainly directed against conformational epitopes in the variable regions of the major coat protein L1 (77). This develops slowly, and is usually weak. Indeed, seroconversion appears to occur 6–18 months after infection, and type-specific antibodies to L1 are detected in 60–70% of women who acquire HPV infection (6, 78). HPV-seroprevalence is considerably lower in men than women, and it has been suggested that HPV-seropositive women might have higher antibody levels than HPV-seropositive men (79).

IgG and IgA are the most abundant isotypes in sera from natural infections. Other HPV antigens (e.g., E1, E2, E6, L2) do not commonly induce antibody responses in patients with acute or persistent HPV infections.

Studies that have investigated whether naturally acquired HPV antibodies can protect against subsequent HPV infections

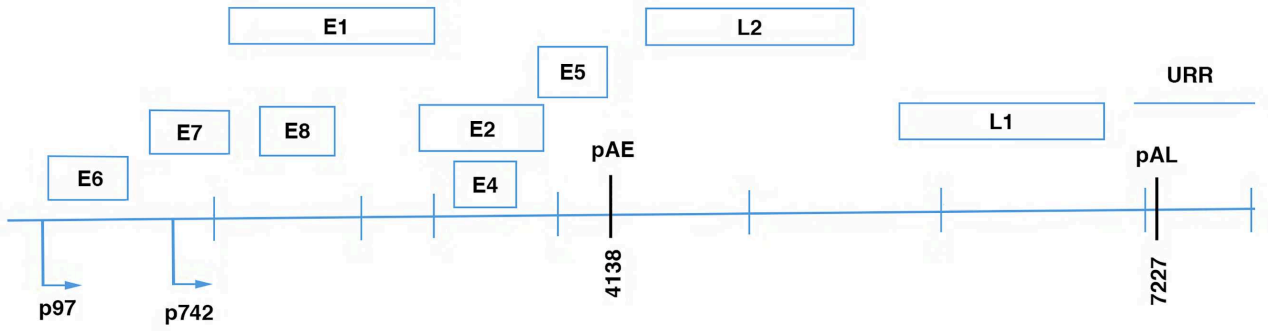

FIGURE 1 | Linear diagram of HPV16 genome showing the eight open reading frames (ORFs), the early (pAE), and the late (pAL) polyadenilation sites; p97, promoter of E6 and E7 viral oncoproteins; p670, promoter of the late proteins.

have reported mixed results (80–82). More recently a systematic review and meta-analysis that included >24,000 individuals showed that natural HPV antibodies provide protection against subsequent type-specific genital HPV infections in females. However, given that the antibody titers in natural immunity are considerably lower than those observed with vaccination, and that antibody responses are preferentially induced in women and are not induced in all infected individuals, it is likely that protection through the development of natural immunity is inferior to protection obtained from HPV vaccination (83).

HPV VACCINES

Prophylactic Vaccines

Three prophylactic vaccines for prevention of HPV infection are available at present: a bivalent vaccine against HPV16 and HPV18 (Cervarix) that was approved in 2007; a tetravalent vaccine against HPV6, 11, 16, and 18 (Gardasil) that was approved in 2006; and a nonavalent vaccine against HPV6, 11, 18, 31, 33, 45, 52, 58 (Gardasil 9) that was approved in 2016. However, the non-avalent vaccine is the only HPV vaccine that is currently available in the USA, and it was approved for males and females from 9 to 45 years by the US Food and Drug Administration in late 2018.

Initially, the administration of the HPV vaccines was in three doses, with the more recent change to a two-dose schedule driven by evaluation of girls aged 9–13 years who had received either two or three doses. The antibody responses of the young women (aged 16–26 years) who had followed a two-dose schedule were similar to those who received all three doses (84). Therefore, in 2016, the Advisory Committee on Immunization Practice declared that there was only the need for two doses of vaccine for those under 15 years of age. However, for females who start the vaccination between 15 and 45 years old, a three-dose schedule is recommended (at 0, 1–2, and 6 months) (84, 85)[10]. Also immunocompromised patients should follow the three-dose schedule regardless of sex and age at vaccination (86).

[10]https://www.cdc.gov/hpv/dowloads/9vhpv-guidance.pdf

All three of these vaccines use recombinant DNA technology and are prepared from the purified L1 protein, which self-assembles to form HPV type-specific empty shells (virus-like particles; VLPs). Only intact VLPs can generate protective antibodies, which supports the evidence that conformational epitopes of L1 are required to generate neutralizing antibodies (87).

The evidence that HPV VLP vaccines protect against high viral challenges through induction of neutralizing anti-L1 antibodies was obtained in preclinical studies in animals, which thus provided the strong rationale for development of VLP-based vaccines. In particular, in a canine model of experimentally induced oral papillomas, it was demonstrated that dogs vaccinated with the major capsid protein, L1, of canine oral papillomavirus developed antibodies against canine oral papillomavirus and became completely resistant to the viral challenge (88). Similarly, vaccination of rabbits with L1 VLPs protected them against papillomas induced by cottontail rabbit papillomavirus (89). In addition, in both of these animal models, passive transfer of immune serum protected the dogs and rabbits against the canine oral papillomavirus and cottontail rabbit papillomavirus challenges, respectively.

In humans, analysis of vaccine-induced antibody responses measured by several methods has demonstrated that almost 100% of vaccinated individuals generate a strong type-restricted serum antibody response to L1 VLP. These methods have included conventional enzyme-linked immunosorbent assays, competitive radioimmunoassays, competitive Luminex-based immunoassays, and pseudovirion-based neutralization assays.

Initial and follow-up studies that assessed the immunogenicity of the HPV 16/18 AS04-adjuvant vaccine in 15- to 25-year-old women showed that after vaccination, anti-HPV16 and anti-HPV18 total IgG antibodies peaked at month 7, reached a plateau between months 18 and 24, and remained constant for up to 76 months (90). Measurement of the neutralizing antibodies using pseudovirion-based neutralization assays confirmed high levels of functional antibodies as well. Then evaluation of long-term immunogenicity of the HPV16/18 vaccine in the serum of 15- to 55-year-old females revealed that the seropositivity for anti-HPV16 remained high in all of the age groups 10 years after the

first vaccination. For anti-HPV18, there were more seropositive females in the 15- to 25-year-old group (99.2%) than for the 26- to 45-year-olds (93.7%) and 46- to 55-year-olds (83.8%) (90). In these studies, the anti-HPV16 and anti-HPV18 titers remained above natural infection levels in all of the age groups, and more interestingly, they were predicted to persist for more than 30 years after vaccination (91).

Comparisons of the immunogenicities of the HPV16/18 and HPV6/11/16/18 vaccines in healthy women aged 18–45 years revealed that 7 months after vaccination, the serum neutralizing antibody responses elicited by the bivalent vaccine were significantly higher than those for the HPV6/11/16/18 vaccine. The differences in these responses for HPV16 and HPV18 were maintained at month 24, and also up to month 60 in women aged 18–45 years.

Antibody titers induced by vaccination are higher than those produced by natural infection[11]. Responses to HPV vaccination is weakly influenced by gender, with higher seroconversion in males than females (99 vs. 93%), and by age, with higher antibody titers in women aged 9–15 years (92, 93). The FUTURE I trial demonstrated that the efficacy of the tetravalent HPV vaccine was 100% against condyloma in HPV-naïve women, and 70% (vaginal condyloma) to 78% (vulvar condyloma) in the overall population. The efficacy of the non-avalent vaccine is comparable to that of the tetravalent vaccine against condyloma (94). Prophylactic HPV vaccines show excellent protection against high-grade CIN (i.e., CIN2, CIN3) and adenocarcinoma *in situ* for HR-HPV–naïve women. In particular, the non-avalent vaccine showed the highest efficacy for prevention of onset of CIN1 (relative risk reduction, 98.9%), CIN2 (97.1%), and CIN3 (100%) neoplasia (95).

Data for vaccine prevention against AIN are more limited. In the Guanacaste study, the tetravalent HPV vaccine prevented HPV16/18 infection in anal anatomic sites in 84% of women who were HPV-seronegative at baseline (96). Palefsky reported 77.5% prevention of AIN among HPV-naïve men aged 16–26 years who had sex with men (MSM) (97). The tetravalent vaccine also protects heterosexual naïve men from both anogenital HPV infections and HPV lesions, with an efficacy against infections and associated lesions of >90% (98). Also a Finnish randomized trial reported significant reduction of genital HPV infections in men following HPV16/18 vaccine administration (99).

For oropharyngeal cancer prevention, a risk reduction of 93.3% for precursor lesions of HPV-induced oral cancer was reported for the Guanacaste study (96). However, further studies are needed to demonstrate the efficacy of these vaccines on oropharyngeal cancer development.

Therapeutic Vaccines

The therapeutic vaccines differ from the prophylactic vaccines as they are aimed at the generation of cell-mediated immunity, rather than neutralizing antibodies. Although prophylactic vaccines can prevent HPV infections in 100% of cases, and precancerous cervical lesions (i.e., CIN) caused by the HPV genotypes included in the vaccine, HPV-related lesions remain a public problem worldwide for several reasons: (i) only 8% of low and middle income countries have introduced HPV vaccination programs[12]; (ii) HPV types that are not included in vaccines might be responsible for cancers (100); (iii) the cost of requirements for a cold chain and the absence of sanitary infrastructure limits HPV vaccine deployment in developing countries; and (iv) HPV vaccines are recommended for young women (9–26 years old), and as women older than 26 years are not vaccinated, they can develop cancers. It is also estimated that the impact of HPV vaccination on cancer incidence might not be appreciated for at least 20 years from any mass vaccination.

TABLE 1 | Conventional treatment of HPV-related cancers.

Cancer HPV related lesion	Conventional treatment
High-grade CIN	1. Loop electrosurgical excision procedure. 2. Cold knife. 3. Cone biopsy. 4. Electrofulgaration. 5. Cold-coagulation. 6. Cryotherapy.
Cervical cancer	1. Conization. 2. Radical hysterectomy. 3. Chemotherapy.
Vulvar intraepithelial neoplasia (VIN) and vulvar cancer	1. Surgical excision. 2. Topical agents (imiquimod). 3. Photodynamic therapy.
AIN and anal cancer	1. Ablative. 2. Chemotherapy (5-fluoracil, imiquimod, cidofovir).
PeIN and penile cancer	1. Surgical treatment. 2. Cisplatinum-based regimen.

CIN, cervical intraepithelial neoplasia; AIN, anal intraepithelial neoplasia; PeIN, penile intraepithelial neoplasia.

Currently, the treatment of high-grade disease (CIN2-3) includes electrosurgical excision of the transformation zone, with carbon dioxide lasers or knives used to perform conization, where the entire transformation zone is removed (101, 102) (**Table 1**). Incomplete excision, however, can occur, and HPV transformed cells can remain, which will facilitate recurrent neoplasia. Hence, there is the need for a therapeutic vaccine that can fully eliminate malignant cells.

The aim of a therapeutic vaccine against HPV is to induce *in-vivo* virus-specific T-cell responses against established HPV infections and lesions. For therapeutic vaccination to deliver unequivocal clinical benefits, improvements must be achieved at two levels: by maximizing the induction of T-cell responses with optimal amplitude, specificity and effector profile; and by ensuring that vaccine-induced T-cells can reach the tumor site and perform their functions without restraint (103).

Among the HPV proteins, the E6 and E7 oncoproteins are considered to be almost ideal targets for immunotherapy of cervical cancer, as these proteins are essential for the onset and

[11]http://www.rho.org/files/WHO_HPV_tech_info_nocover_2007.pdf

[12]https://apps.who.int/iris/bitstream/handle/10665/251810/WER9148.pdf;jsessionid=12D591BAA8A2E02CEB5223020DFC3526?sequence=1

evolution of malignancy, and are constitutively expressed in both premalignant and invasive lesions, while being absent in healthy cells (104). E6 and E7 have therefore been included in most therapeutic vaccines developed to date. Usually, a DNA sequence that encodes a fusion protein of E6 and E7 is inserted into a vector, and mutations are introduced into the regions that are responsible for the E6 interactions with p53, and the E7 interactions with pRB, to reduce their oncogenic power. The E1 and E2 viral proteins are also attractive candidates for therapeutic vaccines that target early viral infections, as they are highly expressed before viral genome integration (105).

Several strategies have been investigated for HPV therapeutic vaccines designed to enhance $CD4^+$ and $CD8^+$ T-cell responses, including genetic vaccines (e.g., DNA/ RNA/ virus/ bacterial), and protein-based, peptide-based or dendritic-cell-based vaccines. Among the bacterial vectors, live attenuated *Listeria monocytogenes* has been used to generate a promising HPV therapeutic vaccine. *L. monocytogenes* is considered a potent vaccine vector because it enters professional antigen-presenting cells and induces antigen-presenting cell maturation, and strong innate and adaptive immunity (106). In addition, *L. monocytogenes* grows very efficiently *in vitro* and lacks lipopolysaccharides, which are a major toxicity factor with Gram-negative bacteria (104). The safety of a recombinant live attenuated *L. monocytogenes* secreting E7 as a fusion protein joined to non-hemolytic listeriolysin O (*Lm*-LLO-E7) was demonstrated in a phase I clinical study that was conducted with 15 patients with late-stage metastatic cervical cancer (107). Evaluation of the efficacy of *Lm*-LLO-E7 (also known as ADXS11-001) in a prospective phase II clinical trial as second-line and third line for patients with recurrent metastatic cervical cancer showed that 12-month overall survival was 38%, which exceeded the historical overall survival of such patients, of 25%. A phase III clinical trial of *Lm*-LLO-E7 for high-grade cervical cancer is being conducted at the time of writing (see NCT02853604).

Encouraging data have also been obtained in clinical studies that have tested DNA-based vaccines. DNA vaccination consists of direct introduction into tissues of a plasmid that contains the DNA sequence that encodes the antigen(s) against which an immune response is sought. This relies on *in-situ* production of the antigen(s) as a result of the transfection of antigen-presenting cells and non-antigen-presenting cells, with the presentation of the expressed antigen(s) by both MHC class I and class II molecules. Furthermore, this results in activation of all three arms of the adaptive immune response (i.e., helper T cells, cytotoxic T cells, antibodies).

However, although DNA vaccines have been shown to induce balanced $CD4^+$ and $CD8^+$ T cells as well as humoral immune responses in small animal models, clinical data from multiple studies have demonstrated that they induce poor T-cell responses (108).

Many strategies to facilitate antigen processing and presentation, and also antigen delivery, have been adopted to ameliorate the immunogenicity of DNA vaccines against HPV (109–111).

A phase I study was carried out using the DNA vaccine VGX-3100 that consists of a mixture of two plasmids that encode the optimized consensus of the E6 and E7 genes of HPV genotypes 16 and 18. These were delivered via intramuscular injection, followed by electroporation, with 18 patients who had been previously treated for cervical intraepithelial neoplasia (CIN2/3). This study showed that 78% of the patients developed CD8+ T-cell responses, and 100% showed antibody positivity to at least two vaccine antigens (112). Notably, the peripheral blood T-cell responses elicited by VGX-3100 were an order of magnitude greater than naturally occurring responses, and a log unit greater than those previously reported for HPV therapeutic vaccines (112).

In 2015, the efficacy, safety, and immunogenicity of VGX-3100 was assessed in a phase II clinical trial in patients with CIN2/3. In the per-protocol analysis, 30.6% of the placebo recipients and 49.5% of the VGX-3100 recipients showed histological regression. Concomitant histopathological regression and viral clearance occurred in 14.3% of placebo recipients compared with 40.2% of vaccinated recipients (113). *Post-hoc* immunological analysis here demonstrated that VGX-3100 elicited significantly increased frequency of T-cell responses against HPV16/18 E6 and E7, and that the magnitude of the T-cell response against E6 was associated with clinical outcome. Humoral immune responses were also lower in placebo recipients than in VGX-3100 recipients, and the antibody responses against HPV16, HPV18, and E7 were significantly higher in the patients who had concomitant histopathological regression and viral clearance, compared to those who did not (113). A phase III clinical trial of VGX-3100 for women with CIN was initiated in 2017, and it is expected to end in 2021 (see NCT03185013).

Viral vectors including adenoviruses, adeno-associated viruses, alphaviruses, and vaccinia viruses (e.g., modified vaccinia Ankara virus; MVA) can be used to express the E2, E6, and E7 oncoproteins, and they can stimulate $CD4^+$ and $CD8^+$ T-cell responses. A MVA vector was used to produce the Tipapkinogen Sovacivec vaccine, which includes three exogenous genes that encode the human cytokine interleukin-2, and non-oncogenic E6 and E7. This vaccinia virus can induce interferon-α production and express HPV16 E6 and E7, which are presented by dendritic cells to activate naïve T cells in lymph nodes. At a follow-up of 2.5 years, compared to the placebo cohort at 10% viral clearance, the administration of Tipapkinogen Sovacivec vaccine provided complete resolution for 24% of patients with CIN2/3, irrespective of their HR-HPV baseline infection (i.e., HPV16, 18, 31, 33, 35, 39, 45, 52, 56, 58, 59, or 68). However, despite this significantly improved HPV viral clearance with this vaccine, it has still not been licensed for clinical use because of the modest efficacy (104).

Finally, a vaccine designed on recombinant MVA that contained the bovine papillomavirus E2 protein (MVA E2) was used to treat HPV-induced ano-genital intraepithelial lesions. A phase III study showed that 90% of female patients had complete elimination of lesions after treatment with MVA E2, with 100% seen for men. All of these patients treated with MVA E2 developed antibodies against the MVA E2 vaccine and

generated a specific cytotoxic response against the papilloma-transformed cells (114).

Interestingly, novel vaccination strategies aimed to maximize systemic as well as genital resident memory T cell responses to treat sexually transmitted infections and human papilloma virus neoplasia are being developed. In this context several studies have investigated the effect of either the topical delivery of host and pathogen derived immunomodulatory molecules or the delivery route of immunization in the induction of cervicovaginal long lived CD8+ T cell responses (115).

HPV PROPHYLACTIC VACCINES USED AS THERAPEUTIC VACCINES

The treatment of premalignant lesions (CIN2,3) by LLEP or conization sometimes fails to prevent lesion recurrence (116–118). This is often linked to incomplete excision of transformation zone consciously carried out by gynecologists. In fact, evidence shows that large excision of the cervix can compromise cervix integrity and can cause adverse neonatal outcome with preterm risk (119, 120). Moreover, recurrence risk is greater in presence of HR HPV infection (116, 121).

A systematic review of studies of the treatment of high-grade lesions (HSIL/ CIN2-3) reported that a median of 28% of the women remained positive for oncogenic HPV types 3 months after treatment. A decrease in this HPV persistence was seen during follow-up, as it fell to 21% after 6 months (102). Also, higher risks for the development of cervical and vaginal neoplasia have been reported for women who had previously been treated for CIN3, in comparison to the general female population, with this higher risk persisting for 20–25 years, and possibly longer (122). The risk of cervical cancer after treatment also increases with age. A large study with long-term follow-up for women treated for CIN3 reported standard incidence and mortality ratios (i.e., treated vs. placebo) for cervical and vaginal cancers of 10.58 and 7.60, respectively, for women aged 60–69 years, and 2.03 and 1.52, respectively, for women aged 30–39 years (123). Also, women who had previously reported CIN3 lesions showed greater probability of developing other HPV-related neoplasia of the genital tract (e.g., vaginal, vulvar, anal) or the oropharyngeal district (124).

As no vaccine has yet been licensed for therapeutic use, the prophylactic vaccines have been tested in several trials to determine their effectiveness for prevention of HPV disease recurrence or reinfection after CIN2-3 treatment. The recurrence for MSM who undergo treatment for high-grade anal intraepithelial neoplasia (HGAIN) is particularly high, as 50% show recurrence within 1 year (123). This makes it essential to find a treatment that can reduce the development of high-grade lesions in treated patients. In 2011, the effectiveness of the tetravalent HPV vaccine for the prevention of recurrent HGAIN was evaluated in HIV-negative, self-identified MSM with a history of biopsy-proven and treated HGAIN. In the 340.4 person-years of follow-up, 30.7% of the non-vaccinated patients developed recurrent HGAIN, compared to 13.6% of the vaccinated patients. Among these patients who were infected with HR-HPV types, the tetravalent vaccine was associated with significantly decreased risk of recurrent HGAIN at 2 years from study entry (hazard ratio, 0.47). To explain the partial effectiveness of the tetravalent vaccine in this study, it was speculated that some of these patients might have developed diseases that were related to the HPV genotypes not covered by the tetravalent vaccine or to multiple HPV infections. Further, some HGAIN might not have been identified and treated before the vaccinations, or the viral integration into the host genome had already occurred. Unfortunately, these aspects were not investigated.

In 2013, Kang et al. investigated the effectiveness of the tetravalent HPV vaccine to prevent recurrence of CIN2-3 in patients with high-grade CIN treated by the loop electrosurgical excision procedure (125). Recurrence was seen for 7.2% of the non-vaccinated patients and by 2.5% of the vaccinated patients. In patients infected with HPV16 and/or HPV18, 8.5% of the non-vaccinated patients and 2.5% of the vaccinated patients developed recurrent disease related to these HPV types. Although encouraging, these data indicate that the prophylactic HPV vaccine had weak activity against such HPV16/18-related high-grade lesions. Recently, a prospective clinical project, the SPERANZA study, was carried out to determine the effectiveness of the tetravalent vaccine for reduction of the risk of clinical relapse in women treated for CIN2 (126). Overall, 344 women were included in the study, and 6.4% of the non-vaccinated women showed clinical disease recurrence, while for the vaccinated women, there was only 1.2% recurrence. Vaccination here was associated with significantly reduced risk of subsequent HPV-related high-grade CIN after cervical surgery, at 81.2%. For the non-vaccinated women, the recurrent clinical disease was attributed to HPV11, 16, 18, 31, 33, 45, 53, 82, while for the vaccinated women, the two cases of clinical disease recurrence were associated with HPV33 and HPV82. In this study, about 40% of the patients enrolled were >36 years old, although neither the age range nor the age of women with recurrent clinical disease were reported, and thus it cannot be determined if the efficacy of the tetravalent HPV vaccine was influenced by the age of the patients at the time of their vaccination. At variance with this, a study by Hildesheim et al. included 1,711 women with carcinogenic human HPV infection and 311 women who received loop electrosurgical excision for cervical precancer. Here, there was no evidence that HPV16/18 vaccination alters the fate of an HPV infection present at the time of vaccination, or the rates of cervical infections and lesions after loop electrosurgical excision. For these HPV16/18 infections, in the cohort of women with HPV infection but without precancer, the efficacy of clearance was 5.4%, with progression to CIN1 seen for 15.5%, and to CIN2, for 0.3%. Moreover, after the loop electrosurgical excision, the vaccination had no significant effects on HPV16/18 infections and/or HPV16/18-associated cytological and histological lesions (127).

The data obtained on the efficacy of the tetravalent HPV vaccine for the prevention of anal condylomas are, however, more encouraging (128). Three hundred and thirteen MSM (mean age, 42 years) were enrolled for a median of 981 days. During

the follow-up, condyloma developed in 18.8% of non-vaccinated patients, and in 8.6% of vaccinated patients. Moreover, several clinical studies have demonstrated activity for HPV vaccination in the treatment of genital warts (129–131).

Altogether, these data suggest that there is possibility that prophylactic vaccines reduce the risk of HSIL recurrence in previously infected patients, although the exact protective mechanisms in infected individuals is not understood. The high risk of recurring infections is consistent with either auto-inoculation across anatomic sites or new inoculation or episodic reactivation of latent infection. As HPV vaccines prevent infection by induction of L1-specific antibodies that block viral entry, and L1 is not generally expressed during the oncogenic process, it is expected that these vaccines will be effective in the prevention of auto-inoculation or new infections.

The greater effectiveness obtained with prophylactic vaccines in the prevention and regression of genital warts might be related to the integration state of the HPV genome. In genital warts, the virus is not generally integrated into the host genome, and therefore viral particles are produced. In this case, the prophylactic vaccines that block viral entry through induction of L1-specific antibodies can prevent reinfections, which will favor the elimination of the virus. Conversely, in high-grade lesions, the virus genome is often integrated into the host genome, and infected cells do not express L1 and do not produce viral particles. Thus, as transformed cells are frequently in the basal layer of the derma, they will not be recognized by vaccine-induced antibodies, which are ineffective in the control of the disease course.

Furthermore, there are some cases in the treatment of HPV-related cancers where the use of prophylactic vaccines might not be recommended:

(1) Anal and cervical cancers that are not attributable to the HPV types that are included in the non-avalent HPV vaccine. Several studies have demonstrated that half of the HPV infections in MSM are caused by HPV types that are not included in the non-avalent HPV vaccine (132, 133) (**Table 2**). Here, over 2 years of observation, only about 30% of HIV-positive MSM had incidents of HR-HPV infections that were covered by the non-avalent vaccine (134). This situation can be also observed for women (**Table 2**).

(2) HPV DNA-negative cervical tumors. Over recent decades, several studies have reported that some cervical cancers are HPV-negative (135–139). Often, HPV DNA negativity is due to the sensitivity of the methods used in the HPV DNA detection, and so samples that have tested as HPV-negative might show as HPV-positive when retested with more sensitive assays (e.g., nested PCR) (136). The Cancer Genome and Molecular Characterization of Cervical Cancer Study used next-generation sequencing to characterize primary cervical cancers, and it established that 5% of the specimens were HPV-negative. This subset of HPV DNA-negative cancers is mainly observed among adenocarcinoma cancers, and predominantly in gastric-type adenocarcinomas. The pattern of immunostaining of gastric-type adenocarcinomas shows strong and diffuse positivity for MUC-6 and HIK1083 antibodies, which recognize epitopes of gastric pyloric glycoproteins, although they are p16 negative, which is a cell-cycle regulatory protein (140). Gastric-type adenocarcinomas have significantly higher rates of recurrence and mortality than HPV-positive cancers (141, 142). Furthermore, progression and regression of gastric-type adenocarcinomas are independent of HPV infection, and thus HPV vaccine administration here would be inappropriate.

TABLE 2 | Detail of cervical and anal samples from HIV positive patients with squamous intraepithelial lesions and HPV DNA negative or positive for HPV types that are not included in nonavalent vaccine.

		N. of cases (%) Pt HPV- 9v Neg	N. of cases (%) Pt HPV DNA Neg
Cervical samples	LSIL ($n = 231$)	72 (31.2)	70 (30.3)
	HSIL ($n = 55$)	17 (30.9)	6 (10.9)
Anal samples	AIN 1 ($n = 18$)	9 (50)	3 (16.7)
	AIN 2 ($n = 7$)	5 (71.4)	0
	AIN 3 ($n = 1$)	1	0

Pt, patient; LSIL, Low Grade Squamous Intraepithelial Lesion; HSIL, High Grade Squamous Intraepithelial Lesion; AIN, Anal intraepithelial neoplasia; 9v, nonavalent vaccine. These data are partially presented in CME event "Novità nel campo dell'infezione da HPV," Rome, 20th June 2018 INMI L Spallanzani IRCCS.

CONCLUSIONS

The data reported in this review highlight the significant efforts that have been carried out to set-up therapeutic vaccines against HPV-related malignancies. Although several approaches to produce an effective vaccine have been attempted, including the use of proteins, synthetic peptides, and viral proteins expressed in different vectors, and although some of the data appear encouraging, no therapeutic vaccines have been licensed in clinical practice yet. Recently, prophylactic vaccines have been used for treatment of recurrent forms or reinfections in subjects who have previously undergone surgical resection. However, the trials here have offered conflicting results, and vaccination did not guarantee 100% effectiveness. This is probably due to a residual burden of transformed cells that can persist after the surgical treatment, and that are not targeted by the humoral L1-specific immune response induced by the prophylactic vaccines. Although it cannot be excluded that the therapeutic potential of prophylactic vaccines could be improved by using different adjuvants or route of immunization, an additional limit in using prophylactic vaccines for therapeutic purposes is seen by the evidence that the non-avalent vaccine does not include all of the HR-HPV types. As the real extent of protection given by the non-avalent vaccine against other HPV types is not known, its use in the treatment of tumors related to these other HR-HPV types is questionable. Furthermore, for endometrial adenocarcinomas, such as gastric-type adenocarcinomas, which are HPV DNA-negative, careful virological and histological diagnosis must be made before administration of HPV prophylactic vaccines to treat HPV recurrence or reinfection.

AUTHOR CONTRIBUTIONS

AG and PD wrote the original version and edited versions. MC edited versions. DL and CS prepared figures and tables.

FUNDING

This work was supported by *Ricerca Corrente* Funding from Italian Ministry of Health.

REFERENCES

1. Ferlay J, Colombet M, Soerjomataram I, Mathers C, Parkin DM, Piñeros M, et al. Estimating the global cancer incidence and mortality in 2018: GLOBOCAN sources and methods. *Int J Cancer*. (2019) 144:1941–53. doi: 10.1002/ijc.31937
2. Plummer M, de Martel C, Vignat J, Ferlay J, Bray F, Franceschi S. Global burden of cancers attributable to infections in 2012: a synthetic analysis. *Lancet Glob Health*. (2016) 4:e609–16. doi: 10.1016/S2214-109X(16)30143-7
3. Crosbie EJ, Einstein MH, Franceschi S, Kitchener HC. Human papillomavirus and cervical cancer. *Lancet*. (2013) 382:889–99. doi: 10.1016/S0140-6736(13)60022-7
4. Vaccarella S, Franceschi S, Engholm G, Lönnberg S, Khan S, Bray F. 50 years of screening in the Nordic countries: quantifying the effects on cervical cancer incidence. *Br J Cancer*. (2014) 111:965–9. doi: 10.1038/bjc.2014.362
5. Moscicki AB, Schiffman M, Kjaer S, Villa LL. Chapter 5: updating the natural history of HPV and anogenital cancer. *Vaccine*. (2006) 24 (Suppl. 3):S3/42–51. doi: 10.1016/j.vaccine.2006.06.018
6. Carter JJ, Koutsky LA, Hughes JP, Lee SK, Kuypers J, Kiviat N, et al. Comparison of human papillomavirus types 16, 18, and 6 capsid antibody responses following incident infection. *J Infect Dis*. (2000) 181:1911–9. doi: 10.1086/315498
7. Cutts FT, Franceschi S, Goldie S, Castellsague X, de Sanjose S, Garnett G, et al. Human papillomavirus and HPV vaccines: a review. *Bull World Health Organ*. (2007) 85:719–26. doi: 10.2471/BLT.06.038414
8. Guan P, Howell-Jones R, Li N, Bruni L, de Sanjosé S, Franceschi S, et al. Human papillomavirus types in 115,789 HPV-positive women: a meta-analysis from cervical infection to cancer. *Int J Cancer*. (2012) 131:2349–59. doi: 10.1002/ijc.27485
9. Nayar R, Solomon D. Second edition of 'wfhe Bethesda System for reporting cervical cytology' - atlas, website, and Bethesda interobserver reproducibility project. *Cytojournal*. (2004)1:4. doi: 10.1007/978-1-4612-2042-8
10. de Martel C, Plummer M, Vignat J, Franceschi S. Worldwide burden of cancer attributable to HPV by site, country and HPV type. *Int J Cancer*. (2017) 141:664–70. doi: 10.1002/ijc.30716
11. Daling JR, Madeleine MM, Johnson LG, Schwartz SM, Shera KA, Wurscher MA, et al. Human papillomavirus, smoking, and sexual practices in the etiology of anal cancer. *Cancer*. (2004) 101:270–80. doi: 10.1002/cncr.20365
12. Lin C, Franceschi S, Clifford GM. Human papillomavirus types from infection to cancer in the anus, according to sex and HIV status: a systematic review and meta-analysis. *Lancet Infect Dis*. (2018) 18:198–206. doi: 10.1016/S1473-3099(17)30653-9
13. Lin C, Slama J, Gonzalez P, Goodman MT, Xia N, Kreimer AR, et al. Cervical determinants of anal HPV infection and high-grade anal lesions in women: a collaborative pooled analysis. *Lancet Infect Dis*. (2019) 19:880–91. doi: 10.1016/S1473-3099(19)30164-1
14. Garbuglia AR, Gentile M, Del Nonno F, Lorenzini P, Lapa D, Lupi F, et al. An anal cancer screening program for MSM in Italy: prevalence of multiple HPV types and vaccine-targeted infections. *J Clin Virol*. (2015) 72:49–54. doi: 10.1016/j.jcv.2015.09.001
15. Dunne EF, Nielson CM, Stone KM, Markowitz LE, Giuliano AR. Prevalence of HPV infection among men: a systematic review of the literature. *J Infect Dis*. (2006) 194:1044–57. doi: 10.1086/507432
16. Nielson CM, Flores R, Harris RB, Abrahamsen M, Papenfuss MR, Dunne EF, et al. Human papillomavirus prevalence and type distribution in male anogenital sites and semen. *Cancer Epidemiol Biomarkers Prev*. (2007) 16:1107–14. doi: 10.1158/1055-9965.EPI-06-0997
17. Nielson CM, Harris RB, Dunne EF, Abrahamsen M, Papenfuss MR, Flores R, et al. Risk factors for anogenital human papillomavirus infection in men. *J Infect Dis*. (2007) 196:1137–45. doi: 10.1086/521632
18. Giuliano AR, Tortolero-Luna G, Ferrer E, Burchell AN, de Sanjose S, Kjaer SK, et al. Epidemiology of human papillomavirus infection in men, cancers other than cervical and benign conditions. *Vaccine*. (2008) 26 (Suppl. 10):K17–28. doi: 10.1016/j.vaccine.2008.06.021
19. Sankaranarayanan R, Ferlay J. Worldwide burden of gynaecological cancer: the size of the problem. *Best Pract Res Clin Obstet Gynaecol*. (2006) 20:207–25. doi: 10.1016/j.bpobgyn.2005.10.007
20. de Sanjosé S, Alemany L, Ordi J, Tous S, Alejo M, Bigby SM, et al. Worldwide human papillomavirus genotype attribution in over 2000 cases of intraepithelial and invasive lesions of the vulva. *Eur J Cancer*. (2013) 49:3450–61. doi: 10.1016/j.ejca.2013.06.033
21. Hoang LN, Park KJ, Soslow RA, Murali R. Squamous precursor lesions of the vulva: current classification and diagnostic challenges. *Pathology*. (2016) 48:291–302. doi: 10.1016/j.pathol.2016.02.015
22. Bornstein J, Bogliatto F, Haefner HK, Stockdale CK, Preti M, Bohl TG, et al. The 2015 International society for the study of vulvovaginal disease (ISSVD) terminology of vulvar squamous intraepithelial lesions. *J Low Genit Tract Dis*. (2016) 20:11–4. doi: 10.1097/LGT.0000000000000169
23. van der Avoort IA, Shirango H, Hoevenaars BM, Grefte JM, de Hullu JA, de Wilde PC, et al. Vulvar squamous cell carcinoma is a multifactorial disease following two separate and independent pathways. *Int J Gynecol Pathol*. (2006) 25:22–9. doi: 10.1097/01.pgp.0000177646.38266.6a
24. Srodon M, Stoler MH, Baber GB, Kurman RJ. The distribution of low and high-risk HPV types in vulvar and vaginal intraepithelial neoplasia (VIN and VaIN). *Am J Surg Pathol*. (2006) 30:1513–8. doi: 10.1097/01.pas.0000213291.96401.48
25. Reich O, Regauer S, Marth C, Schmidt D, Horn LC, Dannecker C, et al. Precancerous lesions of the cervix, vulva and vagina according to the 2014 WHO classification of tumors of the female genital tract. *Geburtshilfe Frauenheilkd*. (2015) 75:1018–20. doi: 10.1055/s-0035-1558052
26. Hildesheim A, Han CL, Brinton LA, Kurman RJ, Schiller JT. Human papillomavirus type 16 and risk of preinvasive and invasive vulvar cancer: results from a seroepidemiological case-control study. *Obstet Gynecol*. (1997) 90:748–54. doi: 10.1016/S0029-7844(97)00467-5
27. Daling JR, Madeleine MM, Schwartz SM, Shera KA, Carter JJ, McKnight B, et al. A population-based study of squamous cell vaginal cancer: HPV and cofactors. *Gynecol Oncol*. (2002) 84:263–70. doi: 10.1006/gyno.2001.6502
28. Carter JJ, Madeleine MM, Shera K, Schwartz SM, Cushing-Haugen KL, Wipf GC, et al. Human papillomavirus 16 and 18 L1 serology compared across anogenital cancer sites. *Cancer Res*. (2001) 61:1934–40.
29. Lamos C, Mihaljevic C, Aulmann S, Bruckner T, Domschke C, Wallwiener M, et al. Detection of human papillomavirus infection in patients with vaginal intraepithelial neoplasia. *PLoS ONE*. (2016) 11:e0167386. doi: 10.1371/journal.pone.0167386
30. Parkin DM, Bray F. Chapter 2: The burden of HPV-related cancers. *Vaccine*. (2006) 24 (Suppl. 3):S3/11–25. doi: 10.1016/j.vaccine.2006.05.111
31. Kreimer AR, Clifford GM, Boyle P, Franceschi S. Human papillomavirus types in head and neck squamous cell carcinomas worldwide: a systematic review. *Cancer Epidemiol Biomarkers Prev*. (2005) 14:467–75. doi: 10.1158/1055-9965.EPI-04-0551
32. Pintos J, Black MJ, Sadeghi N, Ghadirian P, Zeitouni AG, Viscidi RP, et al. Human papillomavirus infection and oral cancer: a case-control study in Montreal, Canada. *Oral Oncol*. (2008) 44:242–50. doi: 10.1016/j.oraloncology.2007.02.005
33. Bosch FX, Broker TR, Forman D, Moscicki AB, Gillison ML, Doorbar J, et al. Comprehensive control of human papillomavirus

infections and related diseases. *Vaccine*. (2013) 31 (Suppl. 7):H1–31. doi: 10.1016/j.vaccine.2013.07.026
34. Herrero R, Quint W, Hildesheim A, Gonzalez P, Struijk L, Katki HA, et al. Reduced prevalence of oral human papillomavirus (HPV) 4 years after bivalent HPV vaccination in a randomized clinical trial in Costa Rica. *PLoS ONE*. (2013) 8:e68329. doi: 10.1371/journal.pone.0068329
35. Vokes EE, Agrawal N, Seiwert TY. HPV-associated head and neck cancer. *J Natl Cancer Inst*. (2015) 107:djv344. doi: 10.1093/jnci/djv344
36. Fakhry C, Andersen KK, Christensen J, Agrawal N, Eisele DW. The impact of tonsillectomy upon the risk of oropharyngeal carcinoma diagnosis and prognosis in the danish cancer registry. *Cancer Prev Res*. (2015) 8:583–9. doi: 10.1158/1940-6207.CAPR-15-0101
37. Lesseur C, Diergaarde B, Olshan AF, Wünsch-Filho V, Ness AR, Liu G, et al. Genome-wide association analyses identify new susceptibility loci for oral cavity and pharyngeal cancer. *Nat Genet*. (2016) 48:1544–50. doi: 10.1038/ng.3685
38. Bomholt A. Juvenile laryngeal papillomatosis. an epidemiological study from the Copenhagen region. *Acta Otolaryngol*. (1988) 105:367–71. doi: 10.3109/00016488809097020
39. Dickens P, Srivastava G, Loke SL, Larkin S. Human papillomavirus 6, 11, and 16 in laryngeal papillomas. *J Pathol*. (1991) 165:243–6. doi: 10.1002/path.1711650308
40. Derkay CS, Darrow DH. Recurrent respiratory papillomatosis. *Ann Otol Rhinol Laryngol*. (2006) 115:1–11. doi: 10.1177/00034894061150010 1
41. Fenton KA, Korovessis C, Johnson AM, McCadden A, McManus S, Wellings K, et al. Sexual behaviour in Britain: reported sexually transmitted infections and prevalent genital Chlamydia trachomatis infection. *Lancet*. (2001) 358:1851–4. doi: 10.1016/S0140-6736(01)06886-6
42. Grulich AE, de Visser RO, Smith AM, Rissel CE, Richters J. Sex in Australia: knowledge about sexually transmissible infections and blood-borne viruses in a representative sample of adults. *Aust N Z J Public Health*. (2003) 27:230–3. doi: 10.1111/j.1467-842X.2003.tb0 0813.x
43. Kjaer SK, Tran TN, Sparen P, Tryggvadottir L, Munk C, Dasbach E, et al. The burden of genital warts: a study of nearly 70,000 women from the general female population in the 4 Nordic countries. *J Infect Dis*. (2007) 196:1447–54. doi: 10.1086/522863
44. Insinga RP, Dasbach EJ, Myers ER. The health and economic burden of genital warts in a set of private health plans in the United States. *Clin Infect Dis*. (2003) 36:1397–403. doi: 10.1086/375074
45. Insinga RP, Dasbach EJ, Elbasha EH. Assessing the annual economic burden of preventing and treating anogenital human papillomavirus-related disease in the US: analytic framework and review of the literature. *Pharmacoeconomics*. (2005) 23:1107–22. doi: 10.2165/00019053-200523110-00004
46. Albuquerque A, Sarmento J, Rios E, Macedo G. Gastrointestinal: anal buschke loewenstein tumor. J *Gastroenterol Hepatol*. (2012) 27:1537. doi: 10.1111/j.1440-1746.2012.07204.x
47. Kasukawa H, Howley PM, Benson JD. A fifteen-amino-acid peptide inhibits human papillomavirus E1-E2 interaction and human papillomavirus DNA replication *in vitro*. *J Virol*. (1998) 72:8166–73. doi: 10.1128/JVI.72.10.8166-8173.1998
48. Stanley MA, Browne HM, Appleby M, Minson AC. Properties of a non-tumorigenic human cervical keratinocyte cell line. *Int J Cancer*. (1989) 43:672–6. doi: 10.1002/ijc.2910430422
49. Bedell MA, Hudson JB, Golub TR, Turyk ME, Hosken M, Wilbanks GD, et al. Amplification of human papillomavirus genomes *in vitro* is dependent on epithelial differentiation. *J Virol*. (1991) 65:2254–60. doi: 10.1128/JVI.65.5.2254-2260.1991
50. Parish JL, Bean AM, Park RB, Androphy EJ. ChlR1 is required for loading papillomavirus E2 onto mitotic chromosomes and viral genome maintenance. *Mol Cell*. (2006) 24:867–76. doi: 10.1016/j.molcel.2006.11.005
51. McBride AA. Replication and partitioning of papillomavirus genomes. *Adv Virus Res*. (2008) 72:155–205. doi: 10.1016/S0065-3527(08)00404-1
52. Van Tine BA, Dao LD, Wu SY, Sonbuchner TM, Lin BY, Zou N, et al. Human papillomavirus (HPV) origin-binding protein associates with mitotic spindles to enable viral DNA partitioning. *Proc Natl Acad Sci USA*. (2004) 101:4030–5. doi: 10.1073/pnas.0306848101
53. Bergvall M, Melendy T, Archambault J. The E1 proteins. *Virology*. (2013) 445:35–56. doi: 10.1016/j.virol.2013.07.020
54. Groves IJ, Coleman N. Pathogenesis of human papillomavirus-associated mucosal disease. *J Pathol*. (2015) 235:527–38. doi: 10.1002/path.4496
55. You J, Srinivasan V, Denis GV, Harrington WJ Jr, Ballestas ME, Kaye KM, et al. Kaposi's sarcoma-associated herpesvirus latency-associated nuclear antigen interacts with bromodomain protein Brd4 on host mitotic chromosomes. *J Virol*. (2006) 80:8909–19. doi: 10.1128/JVI.00502-06
56. Egawa N, Wang Q, Griffin HM, Murakami I, Jackson D, Mahmood R, et al. HPV16 and 18 genome amplification show different E4-dependence, with 16E4 enhancing E1 nuclear accumulation and replicative efficiency via its cell cycle arrest and kinase activation functions. *PLoS Pathog*. (2017) 13:e1006282. doi: 10.1371/journal.ppat.1006282
57. Hladik F, Liu H, Speelmon E, Livingston-Rosanoff D, Wilson S, Sakchalathorn P, et al. Combined effect of CCR5-Delta32 heterozygosity and the CCR5 promoter polymorphism−2459 A/G on CCR5 expression and resistance to human immunodeficiency virus type 1 transmission. *J Virol*. (2005) 79:11677–84. doi: 10.1128/JVI.79.18.11677-11684.2005
58. Suarez I, Trave G. Structural insights in multifunctional papillomavirus oncoproteins. *Viruses*. (2018) 10:37. doi: 10.3390/v10010037
59. Huh K, Zhou X, Hayakawa H, Cho JY, Libermann TA, Jin J, et al. Human papillomavirus type 16 E7 oncoprotein associates with the cullin 2 ubiquitin ligase complex, which contributes to degradation of the retinoblastoma tumor suppressor. *J Virol*. (2007) 81:9737–47. doi: 10.1128/JVI.00881-07
60. Zhang B, Chen W, Roman A. The E7 proteins of low- and high-risk human papillomaviruses share the ability to target the pRB family member p130 for degradation. *Proc Natl Acad Sci USA*. (2006) 103:437–42. doi: 10.1073/pnas.0510012103
61. Moody CA, Laimins LA. Human papillomavirus oncoproteins: pathways to transformation. *Nat Rev Cancer*. (2010) 10:550–60. doi: 10.1038/nrc2886
62. Bernard HU. Regulatory elements in the viral genome. *Virology*. (2013) 445:197–204. doi: 10.1016/j.virol.2013.04.035
63. Schwartz S. Papillomavirus transcripts and post-transcriptional regulation. *Virology*. (2013) 445:187–96. doi: 10.1016/j.virol.2013.04.034
64. Johansson C, Schwartz S. Regulation of human papillomavirus gene expression by splicing and polyadenylation. *Nat Rev Microbiol*. (2013) 11:239–51. doi: 10.1038/nrmicro2984
65. zur Hausen H. Papillomavirus infections–a major cause of human cancers. *Biochim Biophys Acta*. (1996) 1288:F55–78. doi: 10.1016/0304-419X(96)00020-0
66. Pett M, Coleman N. Integration of high-risk human papillomavirus: a key event in cervical carcinogenesis? *J Pathol*. (2007) 212:356–67. doi: 10.1002/path.2192
67. Stanley M. Immunobiology of HPV and HPV vaccines. *Gynecol Oncol*. (2008) 109 (Suppl. 2):S15–21. doi: 10.1016/j.ygyno.2008.02.003
68. Liaw KL, Hildesheim A, Burk RD, Gravitt P, Wacholder S, Manos MM, et al. A prospective study of human papillomavirus (HPV) type 16 DNA detection by polymerase chain reaction and its association with acquisition and persistence of other HPV types. *J Infect Dis*. (2001) 183:8–15. doi: 10.1086/317638
69. Woodman CB, Collins S, Winter H, Bailey A, Ellis J, Prior P, et al. Natural history of cervical human papillomavirus infection in young women: a longitudinal cohort study. *Lancet*. (2001) 357:1831–6. doi: 10.1016/S0140-6736(00)04956-4
70. van der Burg SH, de Jong A, Welters MJ, Offringa R, Melief CJ. The status of HPV16-specific T-cell reactivity in health and disease as a guide to HPV vaccine development. *Virus Res*. (2002) 89:275–84. doi: 10.1016/S0168-1702(02)00196-X
71. de Jong A, van Poelgeest MI, van der Hulst JM, Drijfhout JW, Fleuren GJ, Melief CJ, et al. Human papillomavirus type 16-positive cervical cancer is associated with impaired CD4+ T-cell immunity against early antigens E2 and E6. *Cancer Res*. (2004) 64:5449–55. doi: 10.1158/0008-5472.CAN-04-0831

72. van Poelgeest MI, Nijhuis ER, Kwappenberg KM, Hamming IE, Wouter Drijfhout J. Distinct regulation and impact of type 1 T-cell immunity against HPV16 L1, E2 and E6 antigens during HPV16-induced cervical infection and neoplasia. *Int J Cancer*. (2006) 118:675–83. doi: 10.1002/ijc.21394
73. van Poelgeest MI, van Seters M, van Beurden M, Kwappenberg KM, Heijmans-Antonissen C, Drijfhout JW, et al. Detection of human papillomavirus (HPV) 16-specific CD4+ T-cell immunity in patients with persistent HPV16-induced vulvar intraepithelial neoplasia in relation to clinical impact of imiquimod treatment. *Clin Cancer Res*. (2005) 11:5273–80. doi: 10.1158/1078-0432.CCR-05-0616
74. Welters MJ, van der Logt P, van den Eeden SJ, Kwappenberg KM, Drijfhout JW, Fleuren GJ, et al. Detection of human papillomavirus type 18 E6 and E7-specific CD4+ T-helper 1 immunity in relation to health versus disease. *Int J Cancer*. (2006) 118:950–6. doi: 10.1002/ijc.21459
75. Coleman HN, Moscicki AB, Farhat SN, Gupta SK, Wang X, Nakagawa M. CD8 T-cell responses in incident and prevalent human papillomavirus types 16 and 18 infections. *ISRN Obstet Gynecol*. (2012) 2012:854237. doi: 10.5402/2012/854237
76. Piersma SJ, Jordanova ES, van Poelgeest MI, Kwappenberg KM, van der Hulst JM, Drijfhout JW, et al. High number of intraepithelial CD8+ tumor-infiltrating lymphocytes is associated with the absence of lymph node metastases in patients with large early-stage cervical cancer. *Cancer Res*. (2007) 67:354–61. doi: 10.1158/0008-5472.CAN-06-3388
77. Carter JJ, Koutsky LA, Wipf GC, Christensen ND, Lee SK, Kuypers J, et al. The natural history of human papillomavirus type 16 capsid antibodies among a cohort of university women. *J Infect Dis*. (1996) 174:927–36. doi: 10.1093/infdis/174.5.927
78. Tong Y, Ermel A, Tu W, Shew M, Brown DR. Association of HPV types 6, 11, 16, and 18 DNA detection and serological response in unvaccinated adolescent women. *J Med Virol*. (2013) 85:1786–93. doi: 10.1002/jmv.23664
79. Beachler DC, Viscidi R, Sugar EA, Minkoff H, Strickler HD, Cranston RD, et al. A longitudinal study of human papillomavirus 16 L1, e6, and e7 seropositivity and oral human papillomavirus 16 infection. *Sex Transm Dis*. (2015) 42:93–7. doi: 10.1097/OLQ.0000000000000236
80. Safaeian M, Porras C, Schiffman M, Rodriguez AC, Wacholder S, Gonzalez P, et al. Epidemiological study of anti-HPV16/18 seropositivity and subsequent risk of HPV16 and−18 infections. *J Natl Cancer Inst*. (2010) 102:1653–62. doi: 10.1093/jnci/djq384
81. Franceschi S, Baussano I. Naturally acquired immunity against human papillomavirus (HPV): why it matters in the HPV vaccine era. *J Infect Dis*. (2014) 210:507–9. doi: 10.1093/infdis/jiu143
82. Castellsagué X, Naud P, Chow SN, Wheeler CM, Germar MJ, Lehtinen M, et al. Risk of newly detected infections and cervical abnormalities in women seropositive for naturally acquired human papillomavirus type 16/18 antibodies: analysis of the control arm of PATRICIA. *J Infect Dis*. (2014) 210:517–34. doi: 10.1093/infdis/jiu139
83. Beachler DC, Jenkins G, Safaeian M, Kreimer AR, Wentzensen N. Natural acquired immunity against subsequent genital human papillomavirus infection: a systematic review and meta-analysis. *J Infect Dis*. (2016) 213:1444–54. doi: 10.1093/infdis/jiv753
84. Dobson SR, McNeil S, Dionne M, Dawar M, Ogilvie G, Krajden M, et al. Immunogenicity of 2 doses of HPV vaccine in younger adolescents vs 3 doses in young women: a randomized clinical trial. *JAMA*. (2013) 309:1793–802. doi: 10.1001/jama.2013.1625
85. Meites E, Kempe A, Markowitz LE. Use of a 2-dose schedule for human papillomavirus vaccination - updated recommendations of the advisory committee on immunization practices. *MMWR Morb Mortal Wkly Rep*. (2016) 65:1405–8. doi: 10.15585/mmwr.mm6549a5
86. Markowitz LE, Dunne EF, Saraiya M, Chesson HW, Curtis CR, Gee J, et al. Human papillomavirus vaccination: recommendations of the advisory committee on immunization practices (ACIP). *MMWR Recomm Rep*. (2014) 63:1–30.
87. Stanley M, Pinto LA, Trimble C. Human papillomavirus vaccines—immune responses. *Vaccine*. (2012) 30 (Suppl. 5):F83–7. doi: 10.1016/j.vaccine.2012.04.106
88. Suzich JA, Ghim SJ, Palmer-Hill FJ, White WI, Tamura JK, Bell JA, et al. Systemic immunization with papillomavirus L1 protein completely prevents the development of viral mucosal papillomas. *Proc Natl Acad Sci USA*. (1995) 92:11553–7. doi: 10.1073/pnas.92.25.11553
89. Roden RB, Hubbert NL, Kirnbauer R, Breitburd F, Lowy DR, Schiller JT. Papillomavirus L1 capsids agglutinate mouse erythrocytes through a proteinaceous receptor. *J Virol*. (1995) 69:5147–51. doi: 10.1128/JVI.69.8.5147-5151.1995
90. GlaxoSmithKline Vaccine HPV-007 Study Group, Romanowski B, de Borba PC, Naud PS, Roteli-Martins CM, De Carvalho NS, et al. Sustained efficacy and immunogenicity of the human papillomavirus (HPV)-16/18 AS04-adjuvanted vaccine: analysis of a randomised placebo-controlled trial up to 6.4 years. *Lancet*. (2009) 374:1975–85. doi: 10.1016/S0140-6736(09)61567-1
91. Schwarz TF, Galaj A, Spaczynski M, Wysocki J, Kaufmann AM, Poncelet S, et al. Ten-year immune persistence and safety of the HPV-16/18 AS04-adjuvanted vaccine in females vaccinated at 15-55 years of age. *Cancer Med*. (2017) 6:2723–31. doi: 10.1002/cam4.1155
92. Garland SM, Hernandez-Avila M, Wheeler CM, Perez G, Harper DM, Leodolter S, et al. Quadrivalent vaccine against human papillomavirus to prevent anogenital diseases. *N Engl J Med*. (2007) 356:1928–43. doi: 10.1056/NEJMoa061760
93. Pedersen C, Petaja T, Strauss G, Rumke HC, Poder A, Richardus JH, et al. Immunization of early adolescent females with human papillomavirus type 16 and 18 L1 virus-like particle vaccine containing AS04 adjuvant. *J Adolesc Health*. (2007) 40:564–71. doi: 10.1016/j.jadohealth.2007.02.015
94. Joura EA, Giuliano AR, Iversen OE, Bouchard C, Mao C, Mehlsen J, et al. A 9-valent HPV vaccine against infection and intraepithelial neoplasia in women. *N Engl J Med*. (2015) 372:711–23. doi: 10.1056/NEJMoa1405044
95. Arbyn M, Xu L. Efficacy and safety of prophylactic HPV vaccines. A Cochrane review of randomized trials. *Expert Rev Vaccines*. (2018) 17:1085–91. doi: 10.1080/14760584.2018.1548282
96. Hildesheim A, Wacholder S, Catteau G, Struyf F, Dubin G, Herrero R, et al. Efficacy of the HPV-16/18 vaccine: final according to protocol results from the blinded phase of the randomized Costa Rica HPV-16/18 vaccine trial. *Vaccine*. (2014) 32:5087–97. doi: 10.1016/j.vaccine.2014.06.038
97. Palefsky JM, Giuliano AR, Goldstone S, Moreira ED Jr, Aranda C, Jessen H, et al. HPV vaccine against anal HPV infection and anal intraepithelial neoplasia. *N Engl J Med*. (2011) 365:1576–85. doi: 10.1056/NEJMoa1010971
98. Giuliano AR, Palefsky JM, Goldstone S, Moreira ED Jr, Penny ME, Aranda C, et al. Efficacy of quadrivalent HPV vaccine against HPV Infection and disease in males. *N Engl J Med*. (2011) 364:401–11. doi: 10.1056/NEJMoa0909537
99. Lehtinen T, Söderlund-Strand A, Petäjä T, Eriksson T, Jokiranta S, Natunen K, et al. Human Papillomavirus (HPV) Prevalence in Male Adolescents 4 Years After HPV-16/18 Vaccination. *J Infect Dis*. (2017) 216:966–8. doi: 10.1093/infdis/jix415
100. Safaeian M, van Doorslaer K, Schiffman M, Chen Z, Rodriguez AC, Herrero R, et al. Lack of heterogeneity of HPV16 E7 sequence compared with HPV31 and HPV73 may be related to its unique carcinogenic properties. *Arch Virol*. (2010) 155:367–70. doi: 10.1007/s00705-009-0579-2
101. Marth C, Landoni F, Mahner S, McCormack M, Gonzalez-Martin A, Colombo N, et al. Cervical cancer: ESMO Clinical Practice Guidelines for diagnosis, treatment and follow-up. *Ann Oncol*. (2017) 28(Suppl. 4):iv72-iv83. doi: 10.1093/annonc/mdx220
102. Hoffman SR, Le T, Lockhart A, Sanusi A, Dal Santo L, Davis M, et al. Patterns of persistent HPV infection after treatment for cervical intraepithelial neoplasia (CIN): a systematic review. *Int J Cancer*. (2017) 141:8–23. doi: 10.1002/ijc.30623
103. Vermaelen K. Vaccine strategies to improve anti-cancer cellular immune responses. *Front Immunol*. (2019) 10:8. doi: 10.3389/fimmu.2019.00008
104. Chabeda A, Yanez RJR, Lamprecht R, Meyers AE, Rybicki EP, Hitzeroth II. Therapeutic vaccines for high-risk HPV-associated diseases. *Papillomavirus Res*. (2018) 5:46–58. doi: 10.1016/j.pvr.2017.12.006
105. Yang L, Mohr I, Fouts E, Lim DA, Nohaile M, Botchan M. The E1 protein of bovine papilloma virus 1 is an ATP-dependent DNA helicase. *Proc Natl Acad Sci USA*. (1993) 90:5086–90. doi: 10.1073/pnas.90.11.5086
106. Flickinger JC Jr, Rodeck U, Snook AE. Listeria monocytogenes as a vector for cancer immunotherapy: current understanding and progress. *Vaccines*. (2018) 6:E48. doi: 10.3390/vaccines6030048
107. Maciag PC, Radulovic S, Rothman J. The first clinical use of a live-attenuated Listeria monocytogenes vaccine: a Phase I safety study of Lm-LLO-E7 in

patients with advanced carcinoma of the cervix. *Vaccine*. (2009) 27:3975–83. doi: 10.1016/j.vaccine.2009.04.041
108. Ferraro B, Morrow MP, Hutnick NA, Shin TH, Lucke CE, Weiner DB. Clinical applications of DNA vaccines: current progress. *Clin Infect Dis*. (2011) 53:296–302. doi: 10.1093/cid/cir334
109. Kim TJ, Jin HT, Hur SY, Yang HG, Seo YB, Hong SR, et al. Clearance of persistent HPV infection and cervical lesion by therapeutic DNA vaccine in CIN3 patients. *Nat Commun*. (2014) 5:5317. doi: 10.1038/ncomms6317
110. Samuels S, Marijne Heeren A, Zijlmans HJMAA, Welters MJP, van den Berg JH, Philips D, et al. HPV16 E7 DNA tattooing: safety, immunogenicity, and clinical response in patients with HPV-positive vulvar intraepithelial neoplasia. *Cancer Immunol Immunother*. (2017) 66:1163–73. doi: 10.1007/s00262-017-2006-y
111. Trimble CL, Peng S, Kos F, Gravitt P, Viscidi R, Sugar E, et al. A phase I trial of a human papillomavirus DNA vaccine for HPV16+ cervical intraepithelial neoplasia 2/3. *Clin Cancer Res*. (2009) 15:361–7. doi: 10.1158/1078-0432.CCR-08-1725
112. Bagarazzi ML, Yan J, Morrow MP, Shen X, Parker RL, Lee JC, et al. Immunotherapy against HPV16/18 generates potent TH1 and cytotoxic cellular immune responses. *Sci Transl Med*. (2012) 4:155ra138. doi: 10.1126/scitranslmed.3004414
113. Trimble CL, Morrow MP, Kraynyak KA, Shen X, Dallas M, Yan J, et al. Safety, efficacy, and immunogenicity of VGX-3100, a therapeutic synthetic DNA vaccine targeting human papillomavirus 16 and 18 E6 and E7 proteins for cervical intraepithelial neoplasia 2/3: a randomised, double-blind, placebo-controlled phase 2b trial. *Lancet*. (2015) 386:2078–88. doi: 10.1016/S0140-6736(15)00239-1
114. Rosales R, López-Contreras M, Rosales C, Magallanes-Molina JR, Gonzalez-Vergara R, Arroyo-Cazarez JM, et al. Regression of human papillomavirus intraepithelial lesions is induced by MVA E2 therapeutic vaccine. *Hum Gene Ther*. (2014) 25:1035–49. doi: 10.1089/hum.2014.024
115. Çuburu N, Kim R, Guittard GC, Thompson CD, Day PM, Hamm DE, et al. A prime-pull-amplify vaccination strategy to maximize induction of circulating and genital-resident intraepithelial CD8+ memory T cells. *J Immunol*. (2019) 202:1250–64. doi: 10.4049/jimmunol.1800219
116. Arbyn M, Redman CWE, Verdoodt F, Kyrgiou M, Tzafetas M, Ghaem-Maghami S, et al. Incomplete excision of cervical precancer as a predictor of treatment failure: a systematic review and meta-analysis. *Lancet Oncol*. (2017) 18:1665–79. doi: 10.1016/S1470-2045(17)30700-3
117. Ghaem-Maghami S, Sagi S, Majeed G, Soutter WP. Incomplete excision of cervical intraepithelial neoplasia and risk of treatment failure: a meta-analysis. *Lancet Oncol*. (2007) 8:985–93. doi: 10.1016/S1470-2045(07)70283-8
118. Ghaem-Maghami S, De-Silva D, Tipples M, Lam S, Perryman K, Soutter W. Determinants of success in treating cervical intraepithelial neoplasia. *BJOG*. (2011) 118:679–84. doi: 10.1111/j.1471-0528.2010.02770.x
119. Arbyn M, Kyrgiou M, Simoens C, Raifu AO, Koliopoulos G, Martin-Hirsch P, et al. Perinatal mortality and other severe adverse pregnancy outcomes associated with treatment of cervical intraepithelial neoplasia: meta-analysis. *BMJ*. (2008) 18:a1284. doi: 10.1136/bmj.a1284
120. Kyrgiou M, Athanasiou A, Paraskevaidi M, Mitra A, Kalliala I, Martin-Hirsch P, et al. Adverse obstetric outcomes after local treatment for cervical preinvasive and early invasive disease according to cone depth: systematic review and meta-analysis. *BMJ*. (2016) 28:i3633. doi: 10.1097/01.ogx.0000508341.95858.c5
121. Bruno MT, Cassaro N, Garofalo S, Boemi S. HPV16 persistent infection and recurrent disease after LEEP. *Virol J*. (2019) 16:148. doi: 10.1186/s12985-019-1252-3
122. Strander B, Hällgren J, Sparén P. Effect of ageing on cervical or vaginal cancer in Swedish women previously treated for cervical intraepithelial neoplasia grade 3: population based cohort study of long term incidence and mortality. *BMJ*. (2014) 348:f7361. doi: 10.1136/bmj.f7361
123. Ebisch RMF, Rutten DWE, IntHout J, Melchers WJG, Massuger LFAG, Bulten J, et al. Long-lasting increased risk of human papillomavirus-related carcinomas and premalignancies after cervical intraepithelial neoplasia grade 3: a population-based cohort study. *J Clin Oncol*. (2017) 35:2542–50. doi: 10.1200/JCO.2016.71.4543
124. Swedish KA, Factor SH, Goldstone SE. Prevention of recurrent high-grade anal neoplasia with quadrivalent human papillomavirus vaccination of men who have sex with men: a nonconcurrent cohort study. *Clin Infect Dis*. (2012) 54:891–8. doi: 10.1093/cid/cir1036
125. Kang WD, Choi HS, Kim SM. Is vaccination with quadrivalent HPV vaccine after loop electrosurgical excision procedure effective in preventing recurrence in patients with high-grade cervical intraepithelial neoplasia (CIN2-3)? *Gynecol Oncol*. (2013) 130:264–8. doi: 10.1016/j.ygyno.2013.04.050
126. Ghelardi A, Parazzini F, Martella F, Pieralli A, Bay P, Tonetti A, et al. SPERANZA project: HPV vaccination after treatment for CIN2. *Gynecol Oncol*. (2018) 151:229–34. doi: 10.1016/j.ygyno.2018.08.033
127. Hildesheim A, Gonzalez P, Kreimer AR, Wacholder S, Schussler J, Rodriguez AC, et al. Impact of human papillomavirus (HPV) 16 and 18 vaccination on prevalent infections and rates of cervical lesions after excisional treatment. *Am J Obstet Gynecol*. (2016) 215:212.e1–5. doi: 10.1016/j.ajog.2016.02.021
128. Swedish KA, Goldstone SE. Prevention of anal condyloma with quadrivalent human papillomavirus vaccination of older men who have sex with men. *PLoS ONE*. (2014) 9:e93393. doi: 10.1371/journal.pone.0093393
129. Kreuter A, Waterboer T, Wieland U. Regression of cutaneous warts in a patient with WILD syndrome following recombinant quadrivalent human papillomavirus vaccination. *Arch Dermatol*. (2010) 146:1196–7. doi: 10.1001/archdermatol.2010.290
130. Moscato GM, Di Matteo G, Ciotti M, Di Bonito P, Andreoni M, Moschese V. Dual response to human papilloma virus vaccine in an immunodeficiency disorder: resolution of plantar warts and persistence of condylomas. *J Eur Acad Dermatol Venereol*. (2016) 30:1212–3. doi: 10.1111/jdv.13133
131. Lee HJ, Kim JK, Kim DH, Yoon MS. Condyloma accuminatum treated with recombinant quadrivalent human papillomavirus vaccine (types 6, 11, 16, 18). *J Am Acad Dermatol*. (2011) 64:e130–2. doi: 10.1016/j.jaad.2010.12.032
132. Petry KU, Bollaerts K, Bonanni P, Stanley M, Drury R, Joura E, et al. Estimation of the individual residual risk of cervical cancer after vaccination with the nonavalent HPV vaccine. *Hum Vaccin Immunother*. (2018) 14:1800–6. doi: 10.1080/21645515.2018.1450125
133. Poynten IM, Tabrizi SN, Jin F, Templeton DJ, Machalek DA, Cornall A, et al. Vaccine-preventable anal human papillomavirus in Australian gay and bisexual men. *Papillomavirus Res*. (2017) 3:80–4. doi: 10.1016/j.pvr.2017.02.003
134. Ong JJ, Walker S, Grulich A, Hoy J, Read TRH, Bradshaw C, et al. Incidence, clearance, and persistence of anal human papillomavirus in men who have sex with men living with human immunodeficiency virus: implications for human papillomavirus vaccination. *Sex Transm Dis*. (2019) 46:229–33. doi: 10.1097/OLQ.0000000000000958
135. Rodríguez-Carunchio L, Soveral I, Steenbergen RD, Torné A, Martinez S, Fusté P, et al. HPV-negative carcinoma of the uterine cervix: a distinct type of cervical cancer with poor prognosis. *BJOG*. (2015) 122:119–27. doi: 10.1111/1471-0528.13071
136. Tao X, Zheng B, Yin F, Zeng Z, Li Z, Griffith CC, et al. Polymerase chain reaction human papillomavirus (HPV) detection and HPV genotyping in Invasive cervical cancers with prior negative HC2 test results. Am *J Clin Pathol*. (2017) 147:477–83. doi: 10.1093/ajcp/aqx027
137. Petry KU, Liebrich C, Luyten A, Zander M, Iftner T. Surgical staging identified false HPV-negative cases in a large series of invasive cervical cancers. *Papillomavirus Res*. (2017) 4:85–9. doi: 10.1016/j.pvr.2017.10.003
138. Tjalma W. HPV negative cervical cancers and primary HPV screening. *Facts Views Vis Obgyn*. (2018) 10:107–13.
139. Pirog EC, Lloveras B, Molijn A, Tous S, Guimerà N, Alejo M, et al. HPV prevalence and genotypes in different histological subtypes of cervical adenocarcinoma, a worldwide analysis of 760 cases. *Mod Pathol*. (2014) 27:1559–67. doi: 10.1038/modpathol.2014.55
140. Pirog EC. Cervical adenocarcinoma: diagnosis of human papillomavirus-positive and human papillomavirus-negative tumors. *Arch*

Pathol Lab Med. (2017) 141:1653–67. doi: 10.5858/arpa.2016-0356-RA

141. Kusanagi Y, Kojima A, Mikami Y, Kiyokawa T, Sudo T, Yamaguchi S, et al. Absence of high-risk human papillomavirus (HPV) detection in endocervical adenocarcinoma with gastric morphology and phenotype. *Am J Pathol*. (2010) 177:2169–75. doi: 10.2353/ajpath.2010.100323
142. Park KJ, Kiyokawa T, Soslow RA, Lamb CA, Oliva E, Zivanovic O, et al. Unusual endocervical adenocarcinomas: an immunohistochemical analysis with molecular detection of human papillomavirus. *Am J Surg Pathol*. (2011) 35:633–46. doi: 10.1097/PAS.0b013e31821534b9

Conflict of Interest: The authors declare that the research was conducted in the absence of any commercial or financial relationships that could be construed as a potential conflict of interest.

Advantages of publishing in Frontiers

OPEN ACCESS
Articles are free to read for greatest visibility and readership

FAST PUBLICATION
Around 90 days from submission to decision

HIGH QUALITY PEER-REVIEW
Rigorous, collaborative, and constructive peer-review

TRANSPARENT PEER-REVIEW
Editors and reviewers acknowledged by name on published articles

Frontiers
Avenue du Tribunal-Fédéral 34
1005 Lausanne | Switzerland

Visit us: www.frontiersin.org
Contact us: info@frontiersin.org | +41 21 510 17 00

REPRODUCIBILITY OF RESEARCH
Support open data and methods to enhance research reproducibility

DIGITAL PUBLISHING
Articles designed for optimal readership across devices

FOLLOW US
@frontiersin

IMPACT METRICS
Advanced article metrics track visibility across digital media

EXTENSIVE PROMOTION
Marketing and promotion of impactful research

LOOP RESEARCH NETWORK
Our network increases your article's readership